

©Copyright 2015

Lori C. Berman

Properties of Stellar Clusters and their Relation to Molecular Gas in the Andromeda Galaxy

Lori C. Beerman

A dissertation submitted in partial fulfillment of the
requirements for the degree of

Doctor of Philosophy

University of Washington

2015

Reading Committee:

Julianne J. Dalcanton, Chair

Tom Quinn

Ben Williams

Program Authorized to Offer Degree:
Astronomy

University of Washington

Abstract

Properties of Stellar Clusters and their Relation to Molecular Gas in the Andromeda Galaxy

Lori C. Beerman

Chair of the Supervisory Committee:
Professor Julianne J. Dalcanton
Astronomy

The apparent age and mass of a stellar cluster can be strongly affected by stochastic sampling of the stellar initial mass function, when inferred from the integrated color of low mass clusters ($\lesssim 10^4 M_\odot$). I use simulated star clusters to show that these effects are minimized when the brightest, rapidly evolving stars in a cluster can be resolved, and the light of the fainter, more numerous unresolved stars can be analyzed separately. I show the success of this technique first using simulated clusters, and then with a stellar cluster in M31. This method represents one way of accounting for the discrete, stochastic sampling of the stellar initial mass function in less massive clusters and can be leveraged in studies of clusters throughout the Local Group and other nearby galaxies.

Next I present results for the Panchromatic Hubble Andromeda Treasury (PHAT) cluster sample, which is the largest uniformly derived extragalactic cluster sample to date, containing 2753 clusters. I determine the ages, masses, and extinctions of this cluster sample and demonstrate their accuracy through the use of synthetic clusters. The parameter estimates were done using two methods: CMD fitting of the resolved stars and integrated light fitting using discrete population models. I summarize the most accurate estimates for each cluster, and find that the distributions in age and mass are similar to the cluster distributions in other Local Group Galaxies.

Finally, I combine several astronomical data sets to investigate the life cycle of molecular clouds in the Andromeda Galaxy. The primary data sets I use are the PHAT cluster sample and a molecular cloud catalogue that is constructed from new high spatial/spectral

resolution (20 pc, 1 km/s) CARMA observations. Several ancillary data sets, including $H\alpha$ and Spitzer IR emission maps are also used, taking advantage of broad wavelength coverage to search for indicators of star formation with different timescales. The distribution of the youngest clusters shows a strong correlation with the molecular cloud distribution, while no correlation is evident for clusters greater than 30 Myr. Each molecular cloud in the sample is classified as a star-forming cloud or a non-star forming cloud, based on the presence of any one of several star formation indicators. About 60% of the clouds in the sample were found to be associated with massive star formation. Based on the comparison between these observations and the results from a Monte Carlo simulation, I will estimate a total lifetime of 13-30 Myr for molecular clouds in M31

TABLE OF CONTENTS

	Page
List of Figures	ii
Chapter 1: Introduction	1
1.1 Overview of Star (Cluster) Formation	1
1.2 Importance of Studying Star Clusters	3
1.3 Outline	7
Chapter 2: Measuring Ages and Masses of Partially Resolved Stellar Clusters	9
2.1 Stochastic Fluctuations	11
2.2 Method	14
2.3 Tests on Simulated Clusters	21
2.4 Application to a Real Cluster	25
2.5 Discussion	28
2.6 Conclusions	30
Chapter 3: PHAT Clusters	31
3.1 Cluster Sample	33
3.2 Determining Cluster Properties	39
3.3 Analysis of Results	55
3.4 Conclusions	67
Chapter 4: Investigating the Life Cycle of Molecular Clouds in the Andromeda Galaxy	69
4.1 Cloud Lifetimes	69
4.2 Data: Clouds and Star Formation Indicators	75
4.3 Classifying Clouds by their Star Formation Indicators	79
4.4 Conclusions	101
Chapter 5: Conclusions	103
Bibliography	190

LIST OF FIGURES

Figure Number	Page
1.1	caption: Color-magnitude diagram showing the location of theoretical isochrones for four unreddened clusters of ages: 10 Myr (blue), 100 Myr (purple), 1 Gyr (green), 10 Gyr (red). 4
2.1	Simulated color-magnitude diagrams for two 10 Myr old, $10^3 M_{\odot}$ clusters at solar metallicity. Due to stochastic sampling of the initial mass function, the cluster in the left panel does not contain any evolved stars, while the cluster on the right has one evolved red giant. Integrated colors are included for each panel, along with a 10 Myr isochrone, and a horizontal line showing the magnitude of the main sequence turnoff. 12
2.2	Examples of the variation in cluster resolution with distance. The left panel shows the M31 cluster PC1017, at a distance of 0.785 Mpc (Johnson et al., 2012). The middle and right panels show image simulations of this cluster at roughly twice and four times the distance of M31 (1.57 and 3.14 Mpc). The image is in the F814W filter, and has been smoothed and rebinned to simulate the two further distances. 14
2.3	Color-magnitude diagrams in two of the PHAT survey filters for solar metallicity clusters at four fiducial ages. Horizontal lines indicate three possible values for M_{lim} : -2.0 , -3.0 , and -4.0 . Stars fainter than these lines are considered part of the unresolved component. The black clusters have no extinction, while the red clusters have $A_V = 2.0$ mag. 16
2.4	Absolute magnitudes in the F814W filter as a function of age for simulated solar metallicity clusters at four fiducial masses. The left panel shows the total integrated flux, while the right panel shows only the unresolved flux contained in stars fainter than the magnitude cutoff at $M_{\text{lim}} = -3$. 30 clusters are plotted for each age. The clusters in the right panel exhibit much less spread in magnitude at a given age and mass, since the most luminous, rapidly evolving stars are excluded. 18

2.5	Colors as a function of age for simulated solar metallicity clusters at four fiducial masses. The left panel shows the total integrated color, while the right panel shows only the unresolved color (excluding stars with F814W magnitudes brighter than $M_{\text{lim}} = -3$). 30 clusters are plotted for each age. The discontinuity in the right panel between $\log(t/\text{yr}) = 8$ and 8.4 is a result of where M_{lim} is in relation to the main sequence turnoff (see Figure 2.3) and the age step size used. For clarity, all the $10^6 M_{\odot}$ clusters were shifted to the left by 0.06 dex, the $10^5 M_{\odot}$ clusters were shifted to the left by 0.02 dex, the $10^4 M_{\odot}$ clusters were shifted to the right by 0.02 dex, and the $10^3 M_{\odot}$ clusters were shifted to the right by 0.06 dex. The black curve shows the colors predicted from continuously populated Padova SSP models (Marigo et al., 2008; Girardi et al., 2010).	20
2.6	Recovered vs input age of the simulated test clusters, color coded by the difference in recovered vs input extinction, for four values of M_{lim} in the F814W filter. To clearly see the distribution of recovered values, Gaussian noise with a dispersion of $\sigma = 0.05$ dex in each direction was added in the upper panels. The bottom panels show the median for the residuals in $\log(t)$ for all clusters at each input age, along with the 16 th and 84 th percentile of the residuals.	22
2.7	Recovered vs input age (left plots) and mass (right plots) of the simulated test clusters, color coded by the variation in recovered extinction. The top row shows the results from using unresolved light with $M_{\text{lim}} = -3$, while the bottom row shows the results from using integrated light. We added Gaussian noise with a dispersion of $\sigma = 0.05$ dex in each direction for clarity. The bottom panels show the median (dot) along with the 16 th and 84 th percentile (bar) values of the residuals in $\log(t)$ and $\log(M)$, respectively. At each age time step, the age residuals are shown for each input mass, where the more massive clusters' residuals are shifted slightly to the left and the less massive clusters are shifted slightly to the right. The mass residuals are shown for four age groups (limits of 7.0, 7.5, 8.0, 8.5, 9.0), where the older clusters' residuals are shifted slightly to the left and the younger clusters' residuals are shifted slightly to the right.	24
2.8	Test cluster PC1017 in M31, as observed with the PHAT survey (Johnson et al., 2012). Left panel is the image shown with the photometric aperture. Right panel shows the color-magnitude diagram for this same cluster. The best-fit isochrone (20 Myr, $A_V = 0.9$) from fitting the resolved stars is shown in black. The stars excluded in the unresolved fitting are shown in red. The unresolved method gives an age of 40 Myr and $A_V = 0.42$. The blue isochrone (80 Myr, $A_V = 0.28$ mag) that was obtained using traditional integrated light fitting is a poor fit to the resolved stars.	26
3.1	Background GALEX NUV image of M31 showing the locations of the stellar clusters (blue points) in the PHAT _{cluster} sample.	34

3.2	Two example HST/ACS optical images of clusters in the PHAT sample. AP81, a typical young cluster is shown in the left panel, and AP71, an older cluster is shown on the right panel. The clusters are clearly resolved into stars. However, the stellar background is complex, which complicates both interpretation of the CMD and measurement of the integrated light.	36
3.3	Spatial completeness maps for the dense stellar cluster AP2023. The left panel shows the spatial distribution of the 50% completeness magnitude and the right panel shows the completeness percentage at a fixed magnitude of 24.47 (corresponding to an absolute magnitude of 0). The completeness varies sharply with radius, changing from nearly zero completeness to > 80% completeness over a change in radius of < 1".	38
3.4	Original CMD for AP2023 (left panel) and after crowding cut using a surface brightness cutoff of 18 mag/arcsec ² (right panel). This cut successfully eliminated bad photometry due to extreme crowding in the center of the cluster, leaving a CMD that shows a clear blue horizontal branch, characteristic of old metal poor globular clusters.	38
3.5	Results from running 866 synthetic clusters through MATCH. Top panels show each input parameter versus the Match recovered parameter, color-coded by input mass. A small amount of Gaussian scatter was added for clarity to avoid overplotting points at discrete values of mass and age. The middle panels show each input parameter versus the difference between input and recovered parameter, also color-coded by input mass. The RMS deviation in $\log(t)$ is 0.43 yr, the deviation in $\log(M)$ is 0.34 M_{\odot} and is 0.32 magnitudes in A_V . Clusters above $10^3 M_{\odot}$ are recovered especially well. The bottom panels show input and recovered histograms for each parameter.	42
3.6	Top left panel shows the difference in input and recovered $\log(t)$ versus the difference in input and recovered $\log(M)$. Top right panel shows the difference in input and recovered $\log(t)$ versus the difference in input and recovered A_V . Top left panel shows the difference in input and recovered $\log(M)$ versus the difference in input and recovered A_V . It is clear that failures in one parameter correlate with failures in the other parameters.	43
3.7	Color-magnitude diagram for PHAT cluster AP3219 in the left panel and the background population on the right panel. The blue isochrone corresponds to the best fit age and extinction from CMD fitting, while the green isochrone corresponds to the expected age and extinction from integrated light fitting.	44
3.8	Color magnitude diagram for PHAT cluster AP3320 in the left panel and the background population on the right panel. The blue isochrone corresponds to the best fit age and extinction from CMD fitting, while the green isochrone corresponds to the expected age and extinction from integrated light fitting.	46

3.9	Comparison of MATCH best fit results to integrated light expectation value. Top left panel is age, top right is mass, bottom is A_V . All plots have uncertainties in the PDFs incorporated by Monte Carlo sampling of the PDF.	48
3.10	MATCH versus integrated $\log(t)$ where the size of the points represents the amount of variation in the cluster color when the brightest stars are removed. A small amount of Gaussian scatter was added in the x -direction for clarity. Older clusters show noticeably more stable colors.	50
3.11	MATCH versus integrated $\log(t)$ where flagged clusters with unacceptable fits in both methods are shown in red, and clusters where the non default fit is better are shown in green. Histograms on sides show distributions of each. A small amount of Gaussian scatter was added in the x -direction for clarity.	53
3.12	Integrated $\log(M)$ versus the number of filter detections where all flagged clusters are shown in red. Histograms on sides show distributions of each. A small amount of Gaussian scatter was added in the y -direction for clarity.	55
3.13	Age versus mass for the final cluster results, color-coded by extinction.	56
3.14	PHAT cluster locations shown on the GALEX NUV image, where the clusters are color-coded by age. The youngest clusters (blue) lie mostly along the 10 kpc star-forming ring.	57
3.15	PHAT cluster locations shown on the GALEX NUV image, where the clusters are color-coded by mass. The massive clusters (red) lie mostly in the bulge, while lower mass clusters are spread throughout the disk.	58
3.16	PHAT cluster locations shown on the dust map (Draine et al., 2007) image, where the clusters are color-coded by extinction. The more reddened clusters (red) are mostly coincident with dusty regions.	59
3.17	Present day age distribution (top panel) and mass distribution (bottom panel) as a function of cluster mass for the entire cluster sample. Orange shaded regions represent uncertainties that arise from uncertainties in the parameter fits, and the green shaded regions represent the uncertainties from the bootstrap resampling as described in the text.	60
3.18	Present day age distribution as a function of cluster age for several slices in cluster mass. Orange shaded regions represent uncertainties that arise from uncertainties in the parameter fits, and the green shaded regions represent the uncertainties from bootstrap resampling.	61
3.19	Present day mass distribution as a function of cluster age for several slices in cluster age. Orange shaded regions represent uncertainties that arise from uncertainties in the parameter fits, and the green shaded regions represent the uncertainties from the bootstrap resampling as described in the text.	62

3.20	Present day age distribution (top panel) and mass distribution (bottom panel) as a function of cluster mass using only the results of the integrated light fitting. Orange shaded regions represent uncertainties that arise from uncertainties in the parameter fits, and the green shaded regions represent the uncertainties from the bootstrap resampling as described in the text.	64
3.21	Present day age distribution as a function of cluster age for several slices in cluster mass using the results of the integrated light fitting. Orange shaded regions represent uncertainties that arise from uncertainties in the parameter fits, and the green shaded regions represent the uncertainties from the bootstrap resampling as described in the text.	65
3.22	Present day mass distribution as a function of cluster mass for several slices in cluster age using the results of the integrated light fitting. Orange shaded regions represent uncertainties that arise from uncertainties in the parameter fits, and the green shaded regions represent the uncertainties from the bootstrap resampling as described in the text.	66
3.23	Difference (optimal - integrated) in the number density between our fiducial results for the cluster sample and the integrated light results in the age-mass parameter space, where red is where there are more of the fiducial clusters in that bin and blue is where there are more integrated clusters in that bin.	67
4.1	The evolutionary stages in the life cycle of a star forming molecular cloud: pre-stellar, embedded star formation, exposed star formation - HII regions, and exposed star formation - HII regions and young clusters.	70
4.2	CO integrated intensity map (signal masked) from the CARMA Survey of Andromeda, overplotted with points identifying the clouds in the catalog.	77
4.3	CO integrated intensity map from the CARMA survey of Andromeda, overplotted with circles showing the locations of the clusters in the CO footprint, for four cluster age bins.	80
4.4	Frequency distributions of the deprojected distance for clusters to the nearest molecular cloud, in four age bins. The blue histograms represent the entire cluster sample, while the green histograms are for clusters $> 10^{3.2} M_{\odot}$, where the cluster sample is complete. The red line shows the expected distribution for randomly located clusters. The youngest clusters show a spatial correlation with the clouds, while clusters older than 30 Myr are consistent with a random distribution.	83
4.5	Example of a cloud that was classified as star forming. Each image was clipped at 36 arcsec in RA and Dec (or 135pc x 636pc along major or minor axis) in RA and Dec from the center of each cloud. Magenta contours show the CO emission, with a spacing of 4.0 K*km/s. The circles show locations of young clusters, where blue are < 10 Myr.	85

4.6	Example of a cloud that was classified as non star forming. Each image was clipped at 36 arcsec in RA and Dec (or 135pc x 636pc along major or minor axis) in RA and Dec from the center of each cloud. Magenta contours show the CO emission, with a spacing of 4.0 K*km/s.	86
4.7	Example of a cloud that has strong evidence of embedded star formation, as seen by the strong emission in the IR images. Each image was clipped at 36 arcsec in RA and Dec (or 135pc x 636pc along major or minor axis) in RA and Dec from the center of each cloud. Magenta contours show the CO emission, with a spacing of 4.0 K*km/s.	87
4.8	Classification of molecular clouds based on star formation activity. 39% clouds do not show signs of star formation, which are shown in black. Clouds with possible IR emission are in red (12%) and definite IR emitting clouds are in magenta (6%). Clouds with definite IR and possible H α emission are in orange (4%), and those with definite H α and IR are in green (19%). Cyan clouds are those with a H α and IR (3.7%), and a possible young cluster (4%), and the blue clouds are those with a young cluster, H α , and IR emission (16%).	88
4.9	Fraction of molecular clouds in each elliptical region for the three main cloud states. Top left is the fraction of quiescent clouds, top right is the fraction of clouds showing embedded star formation (IR-only emission), bottom is the fraction of clouds showing exposed star formation (H α and/or young clusters). Darker ellipses represent regions where there is a higher fraction of that type, while lighter ellipses represent regions where there is a lower fraction of that type of cloud.	89
4.10	The distribution of the mass (top left panel), radius (top right panel), velocity dispersion (bottom left), and virial parameter (bottom right) of molecular clouds with different star forming properties, including all 'definite' and 'possible' classifications. The stars indicate the median values in each category, the dots indicate the following percentiles: 2, 16, 84, and 98. The inner box indicates the inner quartiles of the data, and the yellow region is a kernel density estimate of the distribution of each parameter. There is no statistically significant difference in the properties of the molecular clouds among the different populations, except for the H α emitting clouds, which have a slightly larger average mass and radius	90
4.11	Results from the simulations that drew random distributions for three timescales for simulated molecular clouds. This plot shows the mean pre-stellar lifetime vs the mean disruption time, for several slices of the mean post-stellar lifetime. Lighter colors indicate a larger percentage of clouds had associated star formation; darker colors indicate a smaller percentage of clouds had associated star formation.	97

4.12 Results from the simulations that drew random distributions for three timescales for simulated molecular clouds. These plot shows the mean pre-stellar lifetime for star-forming clouds vs the mean disruption time. The left panel shows the values in the mean post-stellar lifetime for star-forming clouds that match the observational estimate (7-15 Myr, as calculated in Section 4.3.4. The right panel shows the mean post-stellar timescales that match the results for the LMC and M33, about 16-24 Myr. The black dots indicate the values of the percentage of star forming clouds and mean pre-stellar timescale that match the values found in the LMC (Kawamura et al., 2009), while the blue values match those for M33 (Miura et al., 2012). . . . 98

ACKNOWLEDGMENTS

Lori is incredibly grateful to her husband, her stepdaughter, and her mom for all their love and support throughout this journey. She would also like to thank her advisor, Prof. Julianne Dalcanton for her mentorship throughout grad school. Lori would also like to acknowledge the welcoming and supportive environment of the entire UW Astronomy community.

Chapter 1

INTRODUCTION

Stellar population studies have been key to the progress in a large range of astrophysical fields from star formation to galactic evolution and cosmology. Previous work on resolved stellar populations was limited to the Milky Way, where distance uncertainties and dust obscuration make it challenging to form a complete sample. The Hubble Space Telescope (HST) has transformed the study of resolved stellar populations in nearby galaxies. Observing the stellar populations of a nearby galaxy with HST allows us to avoid some of these disadvantages to studying galactic clusters, while enabling a uniform sample of spatially resolved clusters down to fairly low cluster masses. Obtaining a uniform cluster sample with precise age and mass determinations will be of great use to many areas of research.

1.1 Overview of Star (Cluster) Formation

Since an understanding of the process of stellar cluster formation is important to this thesis, I will begin with a background overview of star formation, focusing on the observational signatures of each stage.

1.1.1 Molecular Gas

The molecular phase of the ISM represents about less than one percent and is usually confined to the plane of the disk in spiral galaxies, yet molecular clouds are the exclusive sites of star formation. Molecular clouds are made up predominantly of molecular Hydrogen, along with a small amount of dust and other molecules such as CO and its isotopes, NH₃, H₂CO, and CS. Molecular clouds range from 10 - 100 pc in size and $10^2 - 10^6 M_{\odot}$ in mass (Ferrière, 2001).

Star formation occurs in the coldest densest part of clouds at high optical extinction. Typical densities are $100 - 1000 \text{ cm}^{-3}$ and temperatures are about 10 K. Star formation is

a very inefficient process; for most clouds, their efficiency (the ratio of molecular gas mass that gets turned into stars) is only a few percent (e.g., Evans et al., 2009). There is no consensus on why this efficiency is so low, however turbulence and feedback from young stars are thought to be main causes.

Even though molecular clouds are predominantly Hydrogen, the H₂ molecule does not produce emission at the typical temperature of the molecular gas. However, CO has its lowest rotational emission line at only 5K, therefore it typically does emit at the temperature of a molecular clouds, and is often used as a tracer for molecular gas (e.g., Dame et al., 2001). When computing total molecular gas mass, a constant conversion factor from CO to molecular Hydrogen is assumed. However, there is some evidence that this conversion factor varies with respect to environment (Blitz et al., 2007; Hughes et al., 2010).

Though we often treat these clouds as individual objects, most molecular gas is part of a filamentary structure that is hierarchical. Large associations of clouds are referred to as Giant Molecular Associations (GMAs) and are a few hundred pc in size and have masses $> 10^6 M_{\odot}$.

1.1.2 Stages of Star Formation

Once a region of a molecular cloud becomes unstable to gravitationally collapse, it forms stars. Clusters form in clumps, which are of the order 0.3 - 5 pc and density $10^3 - 10^4 \text{ cm}^{-3}$. Individual stars form in cores, which are < 0.1 pc with densities $> 10^5 \text{ cm}^{-3}$. Up to 80 percent of stars are thought to form as part of clusters (Lada & Lada, 2003), however a large percentage of these clusters will not stay as gravitationally bound objects for more than ~ 10 Myr.

When stars begin to form, they do so deep within the molecular cloud. These star forming regions suffer from high extinction in optical and UV and are often only observable at long wavelengths. Dust absorbs UV radiation and re-emits in the infrared (IR). IR (from $\sim 2 - 24 \mu\text{m}$) and radio continuum emission are common ways to search for embedded star clusters that is not visible at optical wavelengths (Lada & Lada, 2003).

As stars begin to form feedback on the cloud becomes important. $H\alpha$ emission, which

is created from a recombination in ionized gas, traces hot young stars of 3-10 Myr that emit enough high energy photons to ionize the surrounding gas. Photoionization, radiation pressure, and stellar winds from massive stars cause the gas still left around the young stars to become dispersed (e.g., Murray, 2011). As gas becomes dispersed, we can then observe young cluster in optical wavelengths.

1.2 Importance of Studying Star Clusters

Star clusters are often referred to as simple stellar populations (SSP) since they consist of stars that are born from same cloud of gas, therefore they are all a common distance away from us and have the same age and chemical composition. These common characteristics of star clusters make them a widely used tool in many areas of astrophysics.

The Hertzsprung-Russell Diagram, and its observational counterpart the color-magnitude diagram (CMD), aid us in determining the ages and metallicities for star clusters. Since the stars are all born at the same age and are the same distance from us, we can fit isochrones (lines of constant time) to the cluster's CMD to derive properties such as age, mass, metallicity, and extinction if there are enough resolved stars in the cluster. It is much easier to get these properties from clusters rather than individual stars.

While stars are burning Hydrogen in their core, they are located along the main sequence, where massive, hot luminous stars are at the upper left and low mass, cool stars are at the bottom right. When a star runs out of Hydrogen it expands and become more luminous, leaving the main sequence. This location is known as the main sequence turn-off. Since lifetime on the main sequence is inversely correlated with stellar mass and all stars in a cluster have a common age, observing the turn-off point for a cluster allows us to identify the age of the cluster. An example CMD showing the locations of isochrones at four fiducial ages is shown in Figure 1.1.

1.2.1 Application of Star Clusters to Astrophysics

1.2.1.a Lifetimes of Molecular Clouds

Kennicutt & Evans (2012) identify robust constraints on the ages and lifetimes of star-

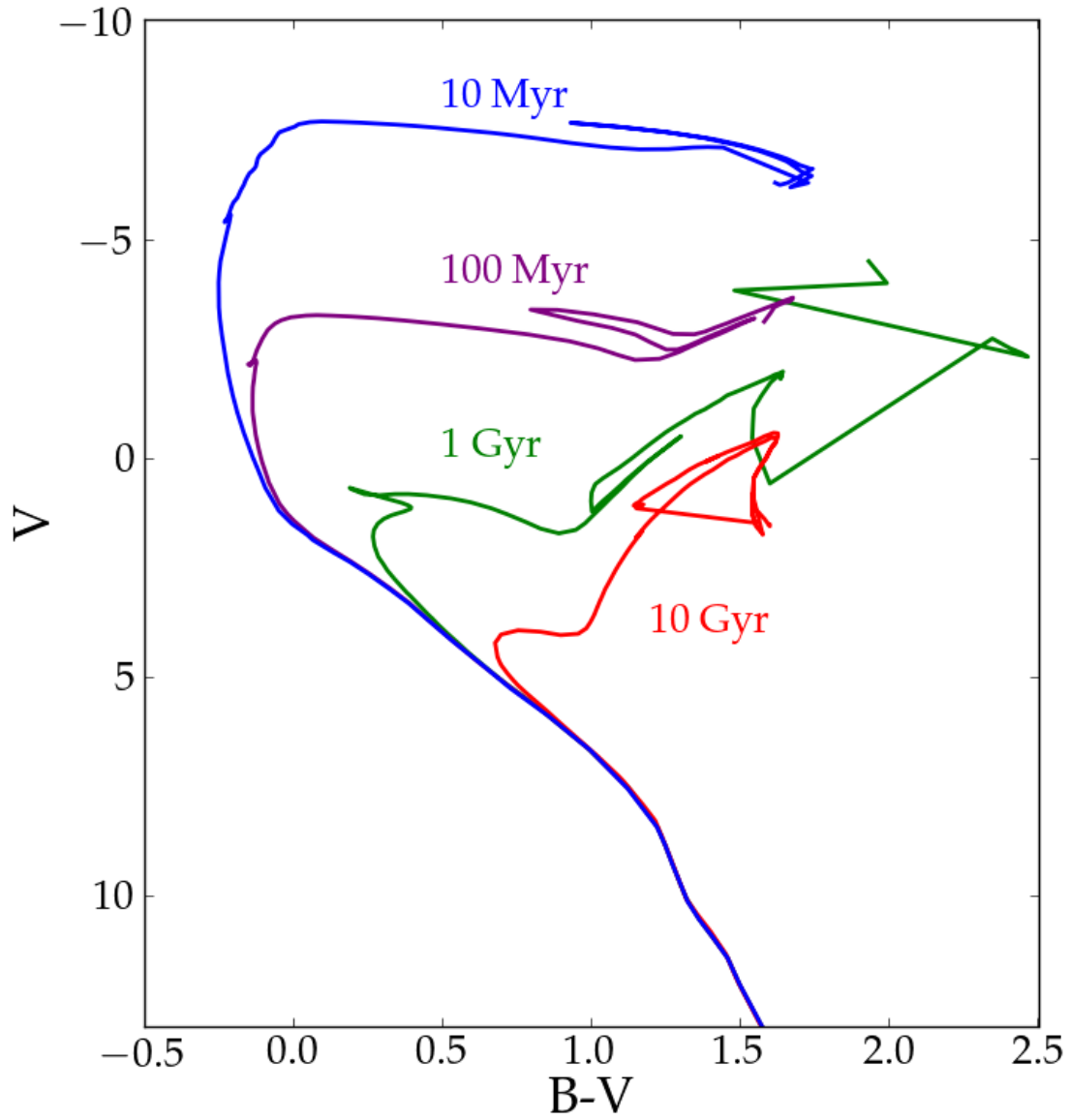


Figure 1.1 caption: Color-magnitude diagram showing the location of theoretical isochrones for four unreddened clusters of ages: 10 Myr (blue), 100 Myr (purple), 1 Gyr (green), 10 Gyr (red).

forming clouds as a key unknown in the subject of star formation in the Milky Way and nearby galaxies. While there is general agreement on the overall lifetimes of molecular clouds, the timescales associated with individual phases of star formation are still uncertain. Analysis of a population of spatially resolved molecular clouds along with equally well resolved star formation indicators is required for progress in this area. This subject will be explored in detail in a later chapter.

1.2.1.b The Initial Mass Function

The initial mass function (IMF) refers to the number of stars of a given mass that are born. The first seminal work in this field was done by Salpeter (1955) who found that the IMF obeys a power law $dN/dM \propto M^{-\alpha}$ where $\alpha = 2.35$. Later studies found generally agreement with this slope, however Kroupa (2001) argued for a broken power law, and Chabrier (2003) used a lognormal for the peak of the distribution, combined with a power law tail at the high mass end.

The form and universality of the IMF has far reaching impact from the understanding of star formation to galaxy evolution throughout time. Most studies agree that the IMF peaks between 0.1 and 1 M_{\odot} , however, at present there is still much debate regarding variations from the IMF and whether or not claimed variations are statistically significant or not. To go from the observed present day mass function to the initial mass function requires accounting for mass loss due to stellar evolution. This correction is much smaller when only looking at young clusters than it is for a range of individual stars, and provides a more accurate measurement of the high mass IMF slope. Clusters in an extragalactic system are also useful since they are all the same distance, age, and metallicity, which reduces the uncertainties in the light to mass conversion. Therefore, studying the IMF for a large uniform sample of clusters provides the most direct way to distinguish among different IMFs.

1.2.1.c Cluster Dissolution and the Fraction of Clustered Stars

Only a small fraction of bound clusters remain after 10-100 Myr, however it is not known if this is primarily due to a low overall fraction of stars born in clusters versus looser

associations or if there is a strong infant mortality, where most clusters are dissolved at very young ages. There is some debate in the literature over the importance of disruption processes relative to formation in clusters (e.g., Silva-Villa et al., 2013; Fall & Chandar, 2012; Bastian et al., 2011). Some of these studies are clouded by cluster definition inconsistencies. This is an area that needs a large sample of young clusters to accurately measure the fraction of stars formed in bound clusters, as opposed to in loose associations or no associations.

A related issue is cluster dissolution: how do clusters dissolve as a function of time, and which ones live to be bound objects for a long period of time? Though most stars form as part of a cluster, not many of them survive in clusters until old age. We need greater cluster samples in order to learn more about the process of cluster dissolution, such as whether cluster dissolution depends on the mass of the cluster.

The present day mass function for clusters that do remain bound over at least tens of Myr provides information about both cluster formation and dissolution. While there is large agreement over the mass distributions in a large range of galactic environments (Zhang & Fall, 1999; Bastian et al., 2011; Fall & Chandar, 2012), it is still unknown whether this is universal, and how the combinations of IMF, cluster dissolution, and observational selection effects contribute to the form of the mass distribution.

1.2.1.d Stellar Evolution Models

While there has been much progress in creating stellar evolution models, there are still certain rare phases which are not well constrained, especially rare and rapid phases in the later stages of stellar evolution such as thermally pulsating AGB stars and horizontal branch stars. A large sample of stellar clusters with known ages will allow calibration of these models to better understand the process of star formation (Soderblom, 2010). These models are also used heavily in other areas of astrophysics, such as galaxy evolution and predicting habitability of exoplanets.

1.2.1.e Galaxy Evolution and Cosmology

Star clusters are the building blocks of galaxies. Studying their formation history helps us understand how the galaxies themselves formed and evolved. Large samples of stellar clusters in extragalactic systems are key in understanding the chemical and dynamical evolution of galaxies. Star clusters help us determine when various components (i.e. bulge, disk, halo) of a galaxy formed as well as when major events such as mergers occurred.

In addition to studying relatively nearby galaxies, star clusters are a necessary tool in cosmological studies as well. Since nearby galaxies are the endpoints of cosmological simulations, understanding the components of these galaxies in a resolved manner allows us to compare to simulations.

1.3 Outline

In subsequent chapters of this thesis, I will address several key outstanding questions related to star clusters and star formation. My thesis consisted of two major parts: deriving the properties of stellar clusters in M31, and using these properties along with other star formation tracers to investigate their relationship with molecular clouds on sub-kiloparsec scales.

First, I discuss a new method to determine the properties of star clusters by analyzing the unresolved component of a cluster's light. Utilizing a suite of synthetic clusters, I show that by subtracting off the bright evolved stars from a cluster whose light is partially resolved, we can obtain more accurate age determinations than from looking at the total integrated light. The improvements over traditional integrated light fitting are most evident for lower mass clusters where the effects of stochasticity are greatest. This method was also applied to an M31 cluster, and results using the unresolved method were comparable to the properties determined spectroscopically, from discrete models, and isochrone fitting.

Next, I utilize the largest extragalactic spiral galaxy cluster sample to date, containing over 2700 clusters, which were identified from images in the Panchromatic Hubble Andromeda Treasury (Dalcanton et al., 2012; Johnson et al., 2015). This clusters span a large range of ages and masses, as well as location throughout the disk of M31. I derive the

cluster properties by fitting their color-magnitude diagrams to modeled CMDs, and then I compare the results from CMD fitting to those from a method using integrated light along with discrete probabilistic models. I determine in which areas of parameter space each method is more accurate, and then comment on how the distributions of ages and masses would change if only integrated light measurements were available.

Finally, I use this cluster sample with known ages and study the distribution of clusters with that of molecular clouds from the CARMA Survey of Andromeda (Schruba et al, in prep). After investigating the relationships between the clouds and several star formation indicators, I assign each cloud to a specific evolutionary state and determine a statistical lifetime for each phase in the cloud's life. I then compare these results with that of a simulation which provides constraints on the disruption timescales for molecular clouds.

Chapter 2

**MEASURING AGES AND MASSES OF PARTIALLY RESOLVED
STELLAR CLUSTERS**

This chapter has been published as Beerman et al. 2012, ApJ, 760, 2, and is reproduced by permission of the AAS.

Stellar clusters are used as tools in the study of star formation, stellar evolution, and galactic evolution because they contain numerous stars of the same age, distance, and metallicity. Their scientific utility rests on our ability to accurately measure their ages, masses, and metallicities.

Resolved observations of individual stars provide the most direct way of measuring the properties of clusters. By resolving individual stars, one can analyze the resulting color-magnitude diagrams (CMDs) by comparing them to isochrones, allowing one to derive the age, extinction, metallicity, and distance of an individual cluster (e.g., Hodge, 1983; Elson & Fall, 1988; Piatti et al., 2007). An additional advantage is that one can obtain an estimate of extinction that is independent of model colors. However, this approach is limited by the angular resolution of the available images. If a cluster is too distant, there will not be enough individual stars resolved to use isochrone fitting. The distance limit for analyzing clusters through resolved stars varies with the surface brightness of the cluster and the resolution of the telescope, but in practice isochrone fitting has rarely been used beyond a few Mpc, even with the Hubble Space Telescope (HST).

If the stars in a cluster are unresolved, then the properties of the cluster can only be derived from the integrated light of the entire cluster (e.g., Larsen, 2009). Such studies have less stringent requirements for angular resolution, and can be carried out at larger distances (up to ~ 50 Mpc; Adamo et al. 2010). Thus, analysis of the integrated light of unresolved star clusters will remain the method of choice for deriving ages and masses of clusters in more distant galaxies, which span the largest possible range of environments and

star formation modes.

There is growing awareness of the potential limitations of unresolved cluster studies. One of the most severe is stochastic sampling of the stellar initial mass function (IMF), which strongly affects the integrated colors and fluxes of low mass clusters. Discrete sampling of the IMF affects the present day mass function, altering a cluster’s color and luminosity from what would be expected if the IMF were continuously populated up to the highest possible stellar mass, and causes potentially rapid changes in color and magnitude throughout the lives of the cluster (Piskunov et al., 2011). Clusters with masses less than a few $10^4 M_{\odot}$ are subject to the effects of small number statistics at the upper end of their mass function, and thus their light can be dominated by just a few post-main sequence stars. A small variation in their number or evolutionary state can cause two otherwise similar clusters to have drastically different integrated colors (up to five magnitudes) (e.g., Barbaro & Bertelli, 1977; Girardi & Bica, 1993; Girardi et al., 1995; Santos & Frogel, 1997; Brocato et al., 1999; Lançon & Mouhcine, 2000; Bruzual, 2002; Anders et al., 2004; Raimondo et al., 2005; Cerviño & Luridiana, 2006; Deveikis et al., 2008; Popescu & Hanson, 2010b, see also Figure 2.1 in §2.1). This spread in colors leads to large systematic errors when deriving the clusters’ properties. Stochastic effects have been shown to be the largest source of error when deriving masses and ages for unresolved clusters (e.g., Lançon & Mouhcine, 2000; Cerviño & Luridiana, 2004; Maíz Apellániz, 2009; Piskunov et al., 2009; Popescu & Hanson, 2010a; Fouesneau & Lançon, 2010).

New techniques have been developed to more accurately age-date low mass clusters, by taking stochastic sampling into account. These improvements are imperative, given that current surveys are delving more deeply into the low mass regime. Specifically, recent studies such as Deveikis et al. (2008), Fouesneau & Lançon (2010), and Popescu & Hanson (2010b,a) have moved away from the traditional population synthesis models towards discrete population models, where the mass function is explicitly considered as a discrete distribution of stars. The main ingredients of such techniques are large collections of discretely sampled synthetic clusters from Monte-Carlo simulations (e.g., da Silva et al., 2012), which can be compared with the observed photometry. Alternatively, individual filters can be down-weighted to reflect the degree of stochasticity (Maíz Apellániz, 2009).

The growing body of literature on stochastic fluctuations of clusters has clearly shown that these fluctuations are due to the random presence of massive upper main sequence and evolving stars within a population. There is also evidence that the flux from the main sequence is fairly stable in comparison (within a few tens of percent; Lançon et al. 2008). As the quality of the observations has improved, we are currently able to resolve the most massive cluster stars out to distances of about 4-5 Mpc. In many cases, one can explicitly identify the tiny subpopulation of rapidly evolving luminous stars, and exclude this small stochastically sampled population from analysis of the integrated light. Removing the post-main sequence stars from the analysis reduces the effect of stochasticity, offering a promising way forward for deriving accurate ages of low mass clusters.

In this paper, we explore a method for analyzing only the unresolved part of a young cluster’s light, which in the ideal case includes only stars up through the main sequence turnoff. This approach minimizes some of the troublesome effects related to the stochastically sampled upper end of a cluster’s stellar mass function. Since younger clusters are more susceptible to stochastic fluctuations and are found in abundance in nearby galaxies, we focus on minimizing errors for the younger clusters. We demonstrate the effectiveness of this method using synthetic clusters. We then apply this method to a cluster in M31 from the Panchromatic Hubble Andromeda Treasury (PHAT; Dalcanton et al. 2012).

This paper is organized as follows: In §2.1 we demonstrate the problem of stochastic fluctuations in the integrated colors of clusters. In §2.2 we describe our method of using only unresolved light to study partially resolved clusters. We show the results of a simultaneous derivation of age, mass, and extinction for simulated clusters in §2.3. In §2.4 we test our method on a cluster in the PHAT survey which has independent measurements of its parameters. We discuss practical aspects of using this method in §2.5 and state our conclusions in §2.6.

2.1 Stochastic Fluctuations

A cluster’s light is dominated by the brightest, most massive stars. A small stochastic difference in the number or evolutionary state of these stars can cause two otherwise similar clusters to have drastically different integrated colors. This effect is very pronounced in

young clusters (< 100 Myr), whose flux may be dominated by a small number of bright red giants or supergiants that bias the integrated color towards the red. To illustrate the effects of stochasticity in a young cluster, we created a synthetic example that shows the dramatic impact that one evolved star may have on a cluster’s integrated light, similar to the examples shown in Santos & Frogel (1997). For consistency with the PHAT survey, we will consider filters used in this survey, in particular F336W, F475W, F814W, and F160W.

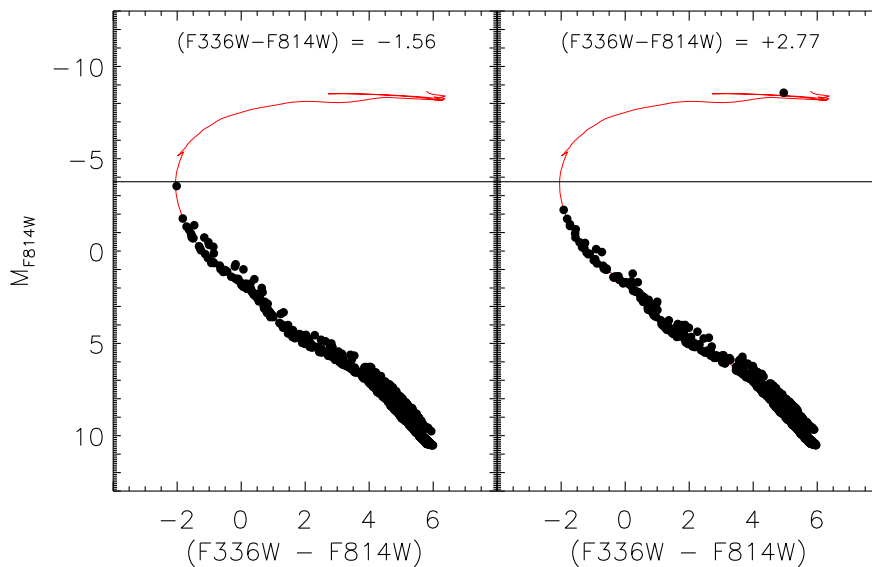


Figure 2.1 Simulated color-magnitude diagrams for two 10 Myr old, $10^3 M_{\odot}$ clusters at solar metallicity. Due to stochastic sampling of the initial mass function, the cluster in the left panel does not contain any evolved stars, while the cluster on the right has one evolved red giant. Integrated colors are included for each panel, along with a 10 Myr isochrone, and a horizontal line showing the magnitude of the main sequence turnoff.

Figure 2.1 shows two realizations of a 10 Myr old cluster with a mass of $10^3 M_{\odot}$, generated using the program `Fake` (Dolphin, 2002), which is described in detail in §2.2.1. Both of these clusters are generated assuming the same underlying isochrone, total mass, and initial mass function. The thickness of the main sequence is due to binarity, assuming a binary fraction of 0.35 and a Salpeter (1955) slope for the binary mass distribution.

In the realization in the left panel, the sampled population does not include any rapidly evolving post-main sequence stars. The integrated (F336W–F814W) color is -1.56 , and is dominated by the massive blue stars at the top of the main sequence. In the right panel, however, the cluster (again, with the same mass and age) happens to have one very massive, bright red giant, due to stochastic sampling of the initial mass function. This bright evolved star now dominates the total integrated color of this cluster, which is now $+2.77$ – a difference of more than four magnitudes. A 10 Myr old cluster could therefore potentially have the same integrated color as a 10 Gyr old cluster due to one evolved giant star. Although the effect is smaller, one might also expect stochastic variations in the blue flux due to variations in the sparsely populated upper main sequence. This can also be seen in Figure 2.1, where there is a 1 magnitude difference in the luminosity of the brightest main sequence star between the two cluster realizations. These effects make age and mass determinations based on integrated color extremely uncertain.

While Figure 2.1 shows large differences in the two cluster realizations brightward of $M_{F814W} = -2$, faintward of this limit the two clusters are populated quite similarly. This similarity suggests that if the single red giant could be excluded, the color and luminosity of the rest of the stellar population would be better behaved, and would share the same blue colors expected for a young cluster. This could in practice be done if the brightest one or several stars that correspond to the red giant and supergiant phases are resolved.

With HST’s high resolution imaging, there are a number of large nearby galaxies whose clusters are partially resolved into stars. Figure 2.2 demonstrates the variation in cluster resolution with distance. The left panel shows the M31 cluster PC1017, at a distance of 0.78 Mpc (Johnson et al., 2012). The middle and right panels show image simulations of this cluster at roughly twice and four times the distance of M31 (1.57 and 3.14 Mpc). Even at these distances, the cluster’s brightest stars can be resolved (in particular, the red evolved stars), while the majority of the more numerous main sequence stars remain unresolved. These fainter stars are blended together and fall below the detection limit, particularly in the center of the cluster, where the crowding and background level are high. Many older clusters at larger distances may also fall in this regime, because evaporation and cluster dissolution lead them to have lower surface densities, allowing individual bright stars to be

detected (Gieles et al., 2011).

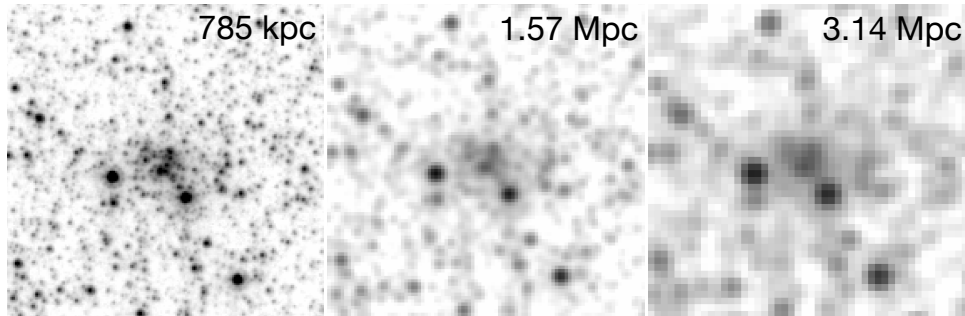


Figure 2.2 Examples of the variation in cluster resolution with distance. The left panel shows the M31 cluster PC1017, at a distance of 0.785 Mpc (Johnson et al., 2012). The middle and right panels show image simulations of this cluster at roughly twice and four times the distance of M31 (1.57 and 3.14 Mpc). The image is in the F814W filter, and has been smoothed and rebinned to simulate the two further distances.

2.2 Method

2.2.1 Simulated Clusters

To demonstrate the potential of analyzing the unresolved flux in a partially resolved cluster (rather than its fully integrated counterpart), we start by building a set of unresolved light models. This includes choosing a value for the magnitude cutoff, M_{lim} , which is described in §2.2.2. Then, based on this set of models, we show our method using simulated clusters and an M31 test cluster from the PHAT data set.

We utilized a variety of simulated clusters to test the degree to which stochastic effects are suppressed by restricting the light to the unresolved portion. We generated CMDs for simulated clusters using the program `Fake`, which is part of the CMD analysis suite `MATCH` (see Dolphin 2002). This program generates CMDs for synthetic stellar populations using theoretical isochrones. We used the Padova models (Marigo et al., 2008) for the isochrone set, with updated AGB tracks from Girardi et al. 2010, along with a Salpeter initial mass function (Salpeter, 1955). The Salpeter IMF produces more low-mass stars and a higher mass-to-light ratio than the Kroupa IMF (Kroupa, 2001). The simulations were done using HST filters, since we plan to apply this technique to M31 clusters observed with HST. We

chose to study clusters at four fiducial masses: $M_{cl} / M_{\odot} = 10^3, 10^4, 10^5, \text{ and } 10^6$. This range is representative of the various masses of clusters we expect to be able to detect in nearby galaxies with HST. At the lower mass end, the clusters experience a high level of stochasticity, while at the high mass end, clusters fully populate their isochrones, and suffer few color and luminosity variations due to stochasticity. The simulated clusters' ages t ranged from $\log(t/\text{yr}) = 7$ to $\log(t/\text{yr}) = 10$, in increments of $\Delta \log(t/\text{yr}) = 0.3 - 0.4$. Thirty clusters at each age and mass were produced at solar metallicity, and another thirty at subsolar metallicity ($Z = 0.1 Z_{\odot}$). Solar metallicity clusters are mainly used throughout this paper since this is appropriate for young clusters in nearby large spirals like M31.

Fake generates clusters by randomly drawing masses from the initial mass function until the desired cluster mass is reached. However, if a massive star is drawn which will put the cluster over the given limit, this star is discarded in favor of lower mass stars. This approach leads to a bias in the resulting cluster's mass function, which will include more low mass main sequence stars. This is a known effect of the cluster simulation, and should be kept in mind when analyzing resulting cluster fluxes and colors. However, we are not studying the clusters' mass functions, and this does not affect the self-consistent analysis on synthetic models that we conduct in this paper. Alternate methods exist to sample the cluster mass function, including those found in (Maíz Apellániz, 2009; Weidner & Kroupa, 2006, 2004; Popescu & Hanson, 2009), some of which produce better sampling of the mass function of very low mass clusters. However, the differences between our method and a proper filling of the cluster mass function are small for the mass range we are considering ($M_{cl} \gtrsim 10^3 M_{\odot}$).

2.2.2 Selection of Magnitude Cutoff

To study the broad behavior of partially resolved clusters, we chose a simple magnitude cutoff M_{lim} that defines the threshold below which the cluster stars are treated as unresolved. This threshold does not necessarily have to be assigned to the actual magnitude limit of the data, and should be far from the completeness limit. Such an approach can compensate for the strong radial variation in the detection limit, which tends to be significantly brighter in a cluster's crowded inner regions. Ideally, we would like our value of M_{lim} to be at a

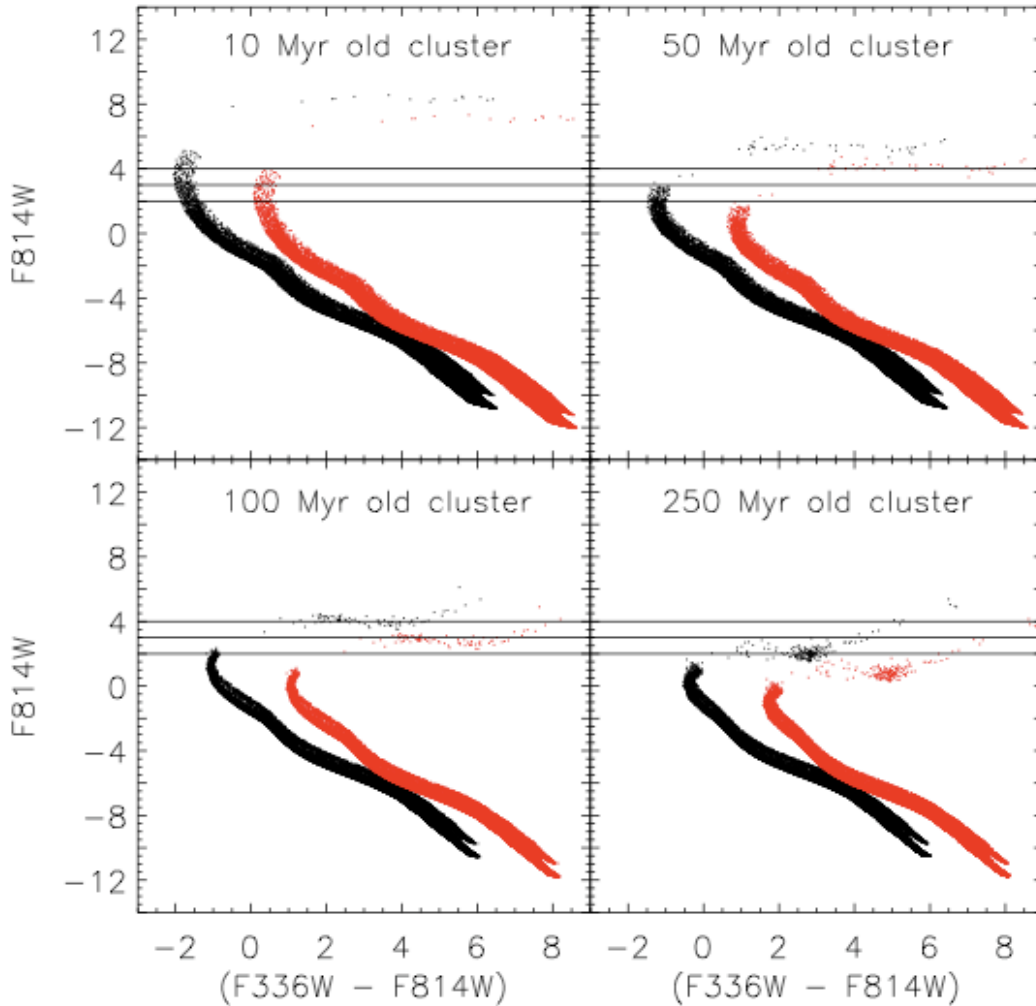


Figure 2.3 Color-magnitude diagrams in two of the PHAT survey filters for solar metallicity clusters at four fiducial ages. Horizontal lines indicate three possible values for M_{lim} : -2.0 , -3.0 , and -4.0 . Stars fainter than these lines are considered part of the unresolved component. The black clusters have no extinction, while the red clusters have $A_V = 2.0$ mag.

level that excludes all the luminous evolved stars, and that leaves stars up through the main sequence turnoff. If our M_{lim} is too faint, the main sequence turnoff will not be included, thus excluding the source of the age information. If our imposed M_{lim} is too bright, we will include more post-main sequence stars, which will not be as effective in reducing stochasticity. In this section we examine the best choice of M_{lim} for the PHAT

data set. A similar exercise should be done when applying this method to other data sets.

Figure 2.3 shows the CMDs of simulated clusters at four fiducial ages, along with three values of M_{lim} : -2.0 , -3.0 , and -4.0 . These values of M_{lim} were chosen to be above the detection thresholds of individual stars in M31. The black points are for stars in a cluster with no extinction, and the red points are for $A_V = 2.0$ mag (assuming $R_V = 3.1$ and a Cardelli et al. (1989) extinction law, which we use throughout this paper). The number of stars being counted as part of the unresolved light clearly depends upon the age, extinction, and value of M_{lim} . Clusters younger than 25 Myr have all evolved stars cut off, regardless of M_{lim} and extinction. For heavily extinguished 50 Myr old clusters, some evolved stars remain below the less stringent values of M_{lim} , and are therefore not removed from the unresolved component. For clusters with little to no extinction, the age at which evolved stars begin to fall below the brightest M_{lim} is 100 Myr. We therefore expect that this method will offer the most improvements when estimating the ages of younger clusters, which have F814W turnoff magnitudes of -2 and -3 for ages of 35 Myr and 18 Myr, respectively (Girardi et al., 2010). Since younger clusters also suffer more from stochastic effects, we therefore focus on minimizing errors for younger clusters. The tests described in §2.3 show reduced errors for $M_{\text{lim}} = -2$ and -3 . For our analysis, since $M_{\text{lim}} = -2$ and -3 are both effective at reducing stochastic effects in the young clusters, we choose to use the brighter $M_{\text{lim}} = -3$ to ensure that all the stars brighter than this will be well resolved.

The clusters in the PHAT survey are an excellent application for this method since they are observed in six filters with HST, and the completeness is high even at $M_{814} = 0$. At larger distances, this method can be used in galaxies that meet this resolution limit, but do not have enough resolved cluster stars to do isochrone fitting. It is also important to note that the cluster photometry needs to be complete at or brighter than M_{lim} . This condition may be difficult to achieve for very dense clusters.

2.2.3 *Simulating the Unresolved Light*

Figure 2.4 shows the relationship between a cluster’s absolute magnitude and mass, for the integrated F814W magnitude of both the entire cluster (left panel) and the unresolved light

below the magnitude threshold of $M_{\text{lim}} = -3$ (right panel). For a given cluster mass, the variance in absolute magnitude depends on the cluster’s age and number of evolved stars. For the youngest, least massive clusters, the spread is almost five magnitudes, while the unresolved light spans less than 1.2 magnitudes. This large magnitude dispersion is consistent with previous work on stochastic fluctuations (e.g., Santos & Frogel, 1997; Piskunov et al., 2009; Popescu & Hanson, 2010b). If a young low mass cluster contains only one or two bright, evolved giants or supergiants, that cluster’s brightness can increase by several magnitudes, and it may appear as a more massive cluster. In contrast, the clusters with no evolved stars have much fainter magnitudes. This causes the bimodal distribution seen for the young low mass clusters, as previously pointed out by Chiosi et al. (1988); Lançon & Mouhcine (2000); Cerviño & Valls-Gabaud (2003); Popescu & Hanson (2010b,a); Fouesneau & Lançon (2010).

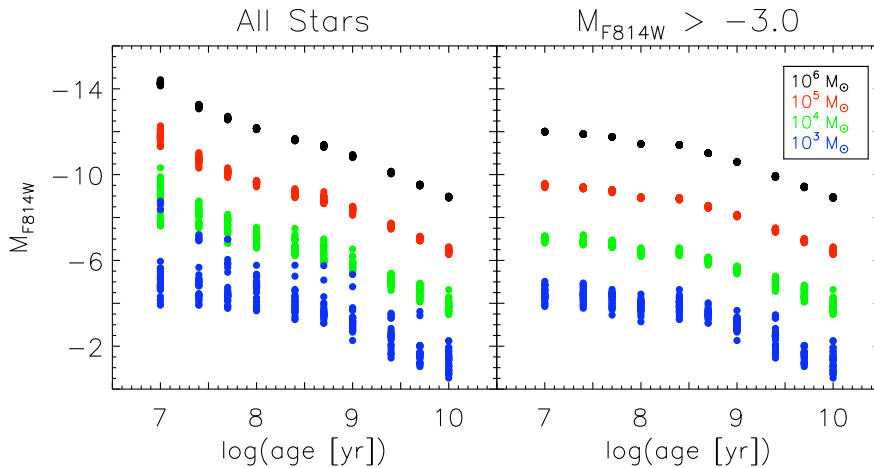


Figure 2.4 Absolute magnitudes in the F814W filter as a function of age for simulated solar metallicity clusters at four fiducial masses. The left panel shows the total integrated flux, while the right panel shows only the unresolved flux contained in stars fainter than the magnitude cutoff at $M_{\text{lim}} = -3$. 30 clusters are plotted for each age. The clusters in the right panel exhibit much less spread in magnitude at a given age and mass, since the most luminous, rapidly evolving stars are excluded.

The stochastic effects visible in Figures 2.1 and 2.4 make age determinations using integrated colors challenging. Theoretically, it is possible to obtain much better results by

looking only at colors derived from the unresolved light. To test this, in Figure 2.5 we compare the colors derived from either the integrated light (left) or the unresolved light (right) to the simulated clusters' input ages, again restricting the unresolved light to stars fainter than $M_{\text{lim}} = -3$ in the F814W filter.

Figure 2.5 shows that the spread in colors becomes small (less than 0.5 magnitudes) as the cluster mass approaches $10^6 M_{\odot}$ and the cluster's mass function becomes less subject to stochastic sampling. Even for clusters of $10^5 M_{\odot}$, the colors of the youngest clusters span a range of 0.9 mag, which can lead to significant errors (more than 100 Myr) when deriving ages from these colors. These uncertainties can cause significant problems in studies of more distant galaxies, for which clusters like these are the only clusters detected, and for which no individual stars can be resolved.

At even lower masses ($\lesssim 10^4 M_{\odot}$), stochasticity has an even larger effect, for the younger clusters especially. The youngest clusters exhibit a range in colors from (F336W–F814W) = -2 to $+3$, a spread of five magnitudes. At red colors, the $10^3 M_{\odot}$ clusters have only one or two red giants or supergiants that are responsible for biasing the overall color. The bluer clusters have no red (super)giants, such that their light is dominated by the O and B stars on the main sequence. This again causes the bimodal distribution in color seen for the young low mass clusters.

In contrast, when only the unresolved light is considered (right panel of Figure 2.5), the variation in color decreases to less than one magnitude for clusters with ages less than 100 Myr, even for the least massive clusters. Thus, using only unresolved light reduces variation in color by four magnitudes. For older clusters, the variation in color for the least massive clusters increases to almost two magnitudes, since not as many of the red evolved stars' light are excluded. However, in practice, old low mass clusters are rare since most have already dispersed. Ignoring the older (> 100 Myr), least massive clusters, the color variations are on the order of one magnitude or less for all clusters of the same age and mass when only their unresolved light is considered.

In addition to much smaller dispersion, the unresolved colors show several differences when compared to the traditional simple stellar population (SSP) models (shown as the black curve). The unresolved colors are in general bluer than the colors given by the SSP

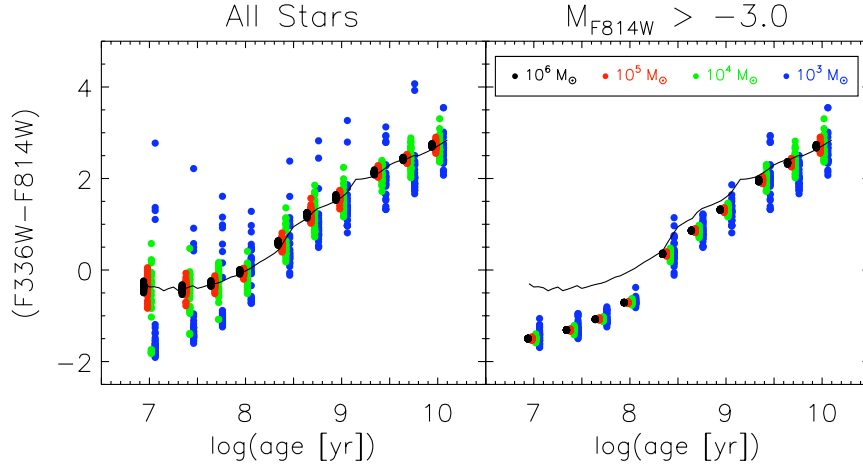


Figure 2.5 Colors as a function of age for simulated solar metallicity clusters at four fiducial masses. The left panel shows the total integrated color, while the right panel shows only the unresolved color (excluding stars with F814W magnitudes brighter than $M_{\text{lim}} = -3$). 30 clusters are plotted for each age. The discontinuity in the right panel between $\log(t/\text{yr}) = 8$ and 8.4 is a result of where M_{lim} is in relation to the main sequence turnoff (see Figure 2.3) and the age step size used. For clarity, all the $10^6 M_{\odot}$ clusters were shifted to the left by 0.06 dex, the $10^5 M_{\odot}$ clusters were shifted to the left by 0.02 dex, the $10^4 M_{\odot}$ clusters were shifted to the right by 0.02 dex, and the $10^3 M_{\odot}$ clusters were shifted to the right by 0.06 dex. The black curve shows the colors predicted from continuously populated Padova SSP models (Marigo et al., 2008; Girardi et al., 2010).

models, since not all of the evolved, red (super)giant stars' light is included. The unresolved colors also show a smooth variation for ages less than $\log(t/\text{yr}) = 8$, while there is a modest discontinuity in unresolved colors seen between $\log(t/\text{yr}) = 8$ and 8.4. This effect is a result of where M_{lim} is in relation to the main sequence turnoff (see Figure 2.3) and the age step size used. For clusters younger than $\log(t/\text{yr}) = 8.4$, the unresolved component excludes all evolved stars, while for older clusters, the choice of M_{lim} leaves some evolved stars in the unresolved component. The colors of the older clusters, therefore, match more closely with those predicted by the SSP models.

Similar tests conducted at a metallicity of $Z = 0.1 Z_{\odot}$ yielded qualitatively similar results to the solar metallicity case presented above.

2.3 Tests on Simulated Clusters

In practice, determining a cluster’s properties is often done through a simultaneous derivation of age, mass, and extinction determined using χ^2 minimization compared to a set of fiducial models, (e.g., Pasquali et al., 2003; Hancock et al., 2008). The value of χ_k^2 for comparing data to a set of k model parameters is given by

$$\chi_k^2(M) = \sum_{i=1}^N \frac{(D_i - M \times \theta_{ik})^2}{\sigma_i^2} \quad (2.1)$$

where D_i is the data flux in the i th filter, θ_{ik} is the k th model flux in the i th filter, σ_i is the variance in the i th filter, M is the mass, and the summation is over the available filters. The parameters of the model k are then varied until χ_k^2 is at a global minimum.

A χ^2 minimization was used to simultaneously recover the age and extinction for a set of test clusters to a set of model clusters, while optimizing for the mass, using only their unresolved flux. The test clusters were drawn from the clusters used in the analysis in §2.2.3, with additional clusters between the ages 10 Myr and 100 Myr added to better probe the rapidly evolving stellar populations of young clusters. Thirty clusters at each age were chosen as test clusters, for a total of 540 test clusters. The test clusters’ masses ranged from $M_{cl} / M_{\odot} = 10^3 - 10^6$. We looked at four HST filters that are being used in the PHAT survey: F336W, F475W, F814W, and F160W. Each test cluster was then given a random value of foreground extinction between $A_V = 0$ to $A_V = 3.0$ mag; no differential extinction was included for this initial test. A small amount of random Gaussian noise ($\sigma = 0.05$ mag) was also added to these clusters to simulate observational errors, which we assume are Gaussian. This noise value was used for the variance, σ_i , through the conversion $\sigma_{flux} = flux \times (1 - 10^{-0.4 \sigma_{mag}})$.

The set of clusters that were used as models were taken from the most massive clusters at each age. These model clusters were massive enough for their main sequence to be considered fully populated ($> 10^5 M_{\odot}$). Altogether, we used model clusters at eighteen different ages from $\log(t/\text{yr}) = 7$ to 10.

The models used were normalized as the unresolved flux per unit mass and, assuming that light scales as mass, the test clusters’ unresolved fluxes were scaled to match the model

clusters' fluxes. Therefore, mass is a parameter solved for during the minimization by calculating the scale factor between the fluxes of the test clusters and the model clusters. Extinction was recovered by including these same models at 50 values of extinction between $A_V = 0$ to 3.5 mag.

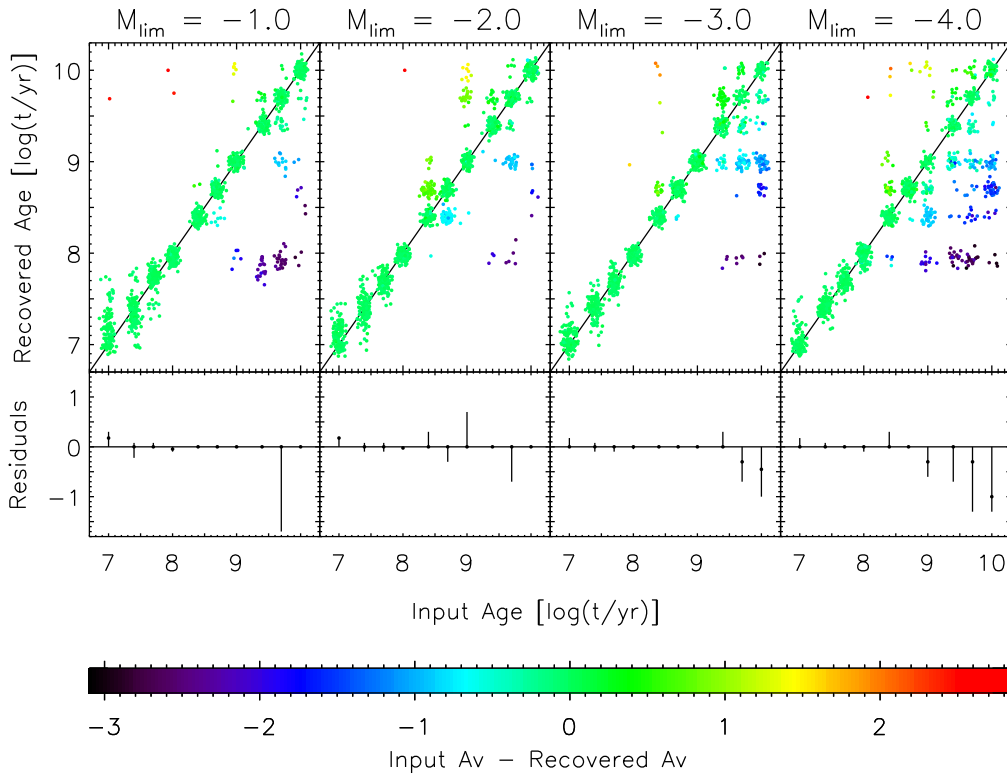


Figure 2.6 Recovered vs input age of the simulated test clusters, color coded by the difference in recovered vs input extinction, for four values of M_{lim} in the F814W filter. To clearly see the distribution of recovered values, Gaussian noise with a dispersion of $\sigma = 0.05$ dex in each direction was added in the upper panels. The bottom panels show the median for the residuals in $\log(t)$ for all clusters at each input age, along with the 16th and 84th percentile of the residuals.

Figure 2.6 shows the recovered ages for four different values of M_{lim} , color coded by the difference in recovered and input extinction. For $M_{\text{lim}} = -2$, the bias in recovered ages is close to 0, and the average error is 0.09 dex. The average error in mass is 0.05 dex, and there is a slight bias toward underestimating the mass. The average error in A_V is 0.12

mag. The errors were calculated by taking the mean of the absolute differences in input – output. These values represent a lower limit, since the calculated errors are in many cases dominated by the grid size. 54% of the clusters’ ages are recovered to better than the resolution of the grid of models, and 96% are recovered within 0.5 dex. $M_{\text{lim}} = -3$ has similar errors, while $M_{\text{lim}} = -1$ has a slightly larger error in age. $M_{\text{lim}} = -4$ does not offer as large an improvement, and shows a large number of outliers. With this brighter limit, evolved stars are still included in the unresolved light at most ages, so the stochastic effects are not as reduced. For fainter magnitude limits ($M_{\text{lim}} \geq -1$), the age sensitivity is reduced since all of the evolved stars and some of the bright main sequence stars are being removed for clusters younger than 50 Myr with low extinction, as seen in Figure 2.3. For the least massive clusters ($<10^3 M_{\odot}$), the average error in age is 0.17 dex. The feature seen at a recovered age of $\log(t/\text{yr}) = 8$ consists mostly of low mass clusters that are not well recovered. This occurs because, due to the shape of the continuous SSP models, when the minimization routine searches for the closest match to the models, certain age models are more attractive to a wider variety of clusters, which was pointed out in Section 4.3 of Foesneau & Lançon 2010.

Figure 2.7 compares the results of the χ^2 minimization for $M_{\text{lim}} = -3$ (top panel), with the results for traditional fitting to integrated light models (bottom panel). The left plots show recovered ages and the right plots are the recovered masses, color coded by the difference in recovered and input extinction. In addition to the feature seen at a recovered age of $\log(t/\text{yr}) = 8$, explained above, there is an additional feature at $\log(t/\text{yr}) = 10$. This feature results from the finite range of model properties. For clusters that are redder than the age-extinction range covered by the models, they are always fit to the oldest age in the models. This effect can also be seen in Foesneau et al. 2012. The large feature at a recovered age of $\log(t/\text{yr}) = 10$ is not seen in the results from using the unresolved light (top panel). The feature at $\log(t/\text{yr}) = 8$ is also significantly reduced compared to the integrated light results. Due to the monotonic variation in unresolved color, as seen in Figure 2.5, many of the sources of color degeneracies in integrated light are not present for the unresolved light. This leads to greater accuracy in deriving the cluster ages and masses.

For the fits to integrated light, there is a bias of 0.09 dex toward older ages, and the

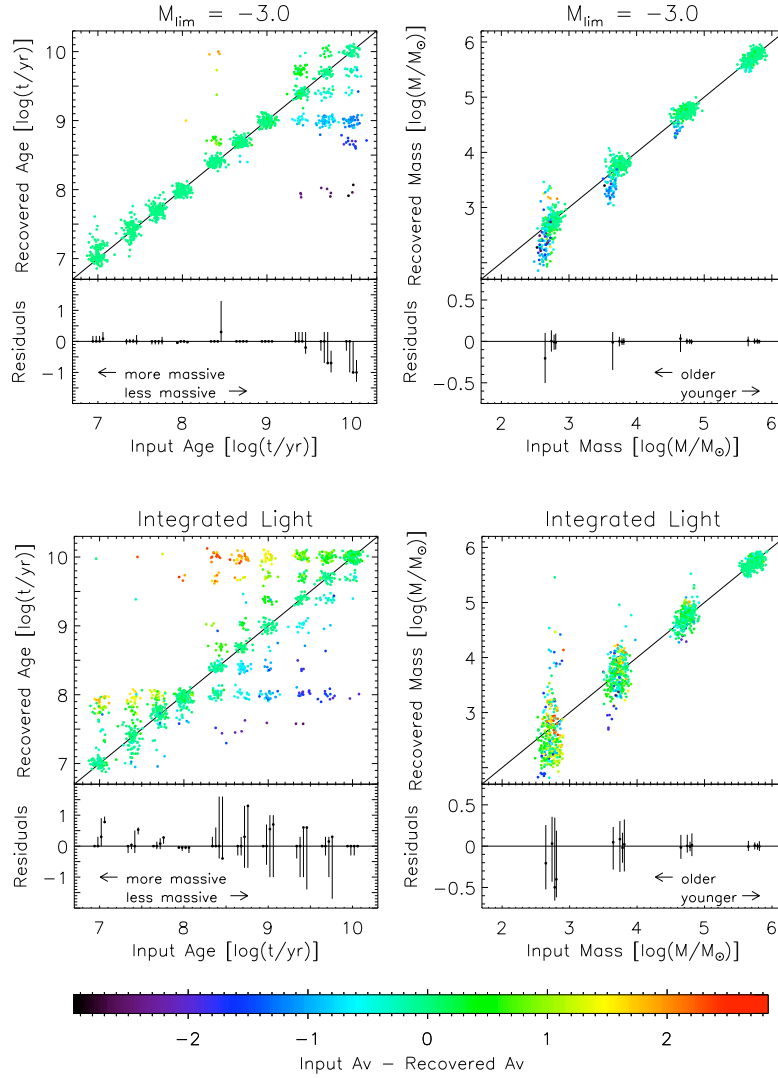


Figure 2.7 Recovered vs input age (left plots) and mass (right plots) of the simulated test clusters, color coded by the variation in recovered extinction. The top row shows the results from using unresolved light with $M_{\text{lim}} = -3$, while the bottom row shows the results from using integrated light. We added Gaussian noise with a dispersion of $\sigma = 0.05$ dex in each direction for clarity. The bottom panels show the median (dot) along with the 16th and 84th percentile (bar) values of the residuals in $\log(t)$ and $\log(M)$, respectively. At each age time step, the age residuals are shown for each input mass, where the more massive clusters' residuals are shifted slightly to the left and the less massive clusters are shifted slightly to the right. The mass residuals are shown for four age groups (limits of 7.0, 7.5, 8.0, 8.5, 9.0), where the older clusters' residuals are shifted slightly to the left and the younger clusters' residuals are shifted slightly to the right.

average error for all test clusters is 0.26 dex in age. 36% of the clusters' ages are recovered to better than the resolution of the grid of models, and 83% are recovered within 0.5 dex. Some clusters' recovered ages can be as much as 3 dex away from their input age. The mass estimates are more robust and have an average error of 0.19 dex. However, significant scatter exists for the integrated light fits for the lower mass clusters, which violate the assumption that mass scales monotonically with luminosity (see Figure 2.4), as we have implicitly assumed in our fitting process. The average error for A_V is 0.45 mag, and recovered values of A_V are biased by 0.16 mag toward lower extinctions. This extinction bias explains the age bias, since young, highly extinguished clusters are being recovered as older, less extinguished clusters. When considering only clusters whose masses are $\leq 10^3 M_\odot$, the average error in age is 0.51 dex, considerably higher than the error for low mass clusters when using unresolved light.

In this analysis we explored clusters with a range of extinction up to $A_V = 3.0$ mag, which is appropriate for most M31 clusters. If independent constraints on A_V are available, the age-extinction degeneracy is lifted, and the errors will be reduced even further. For example, for $M_{\text{lim}} = -2$, if A_V is known to within 1 magnitude, the error in age decreases from 0.09 to 0.03 dex. Also, using additional filters would improve the accuracy of the age and mass determination (Maíz Apellániz, 2009), while providing greater constraints on extinction. The metallicity of all of our clusters was fixed at solar, however this analysis could be extended to varying metallicities. Allowing the metallicity to vary would cause further degeneracies with age and extinction. A full characterization of errors and systematics is beyond the scope of this paper and is postponed to a further publication.

2.4 Application to a Real Cluster

In this section we extend the χ^2 fitting to an observed cluster from the PHAT cluster catalog (Johnson et al., 2012), PC1017. Figure 2.8 shows the CMD for cluster PC1017 which we use as a test cluster to demonstrate our unresolved method.

The challenge of using a real cluster to test this method is that we do not know its intrinsic properties. We chose this cluster as our test cluster because there are good independent estimates of its parameters. Caldwell et al. (2009) used spectroscopy to age-date this cluster

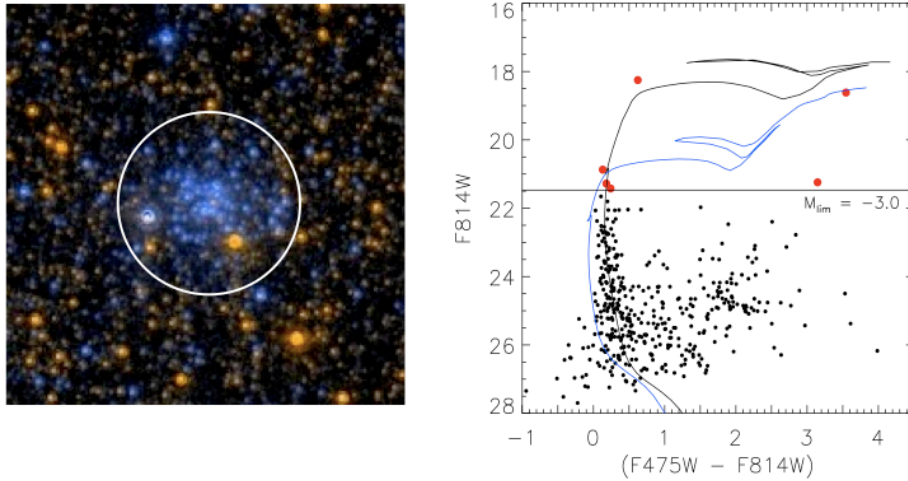


Figure 2.8 Test cluster PC1017 in M31, as observed with the PHAT survey (Johnson et al., 2012). Left panel is the image shown with the photometric aperture. Right panel shows the color-magnitude diagram for this same cluster. The best-fit isochrone (20 Myr, $A_V = 0.9$) from fitting the resolved stars is shown in black. The stars excluded in the unresolved fitting are shown in red. The unresolved method gives an age of 40 Myr and $A_V = 0.42$. The blue isochrone (80 Myr, $A_V = 0.28$ mag) that was obtained using traditional integrated light fitting is a poor fit to the resolved stars.

as 33 Myr, with a factor of 2 uncertainty. Its mass was found to be $\log(M_{cl} / M_{\odot}) = 3.88$, and A_V was 0.68 mag. Stochasticity can however affect these spectroscopic estimates as well. Another prediction given by the discrete models from Fouesneau & Lançon 2010 gives an age of 41 Myr, $\log(M_{cl} / M_{\odot}) = 3.9$, and $A_V = 0.3$ mag. Additionally, since this cluster has many resolved stars, we were able to make determinations by isochrone matching the best fit age and extinction with the CMD analysis suite MATCH (Dolphin, 2002). This gives an age of 20 Myr ($\log(t/\text{yr}) = 7.3 \pm 0.1$), $\log(M_{cl}) = 3.8 \pm 0.3$, and an $A_V = 0.9 \pm 0.15$ mag.

We measure the unresolved flux for the cluster using a three step process. Due to large photometric errors in F160W, we use only F336W, F475W, and F814W. For each of the six images, we sum the light within the photometric aperture (2.19") and within a background annulus (2.63" - 7.45"). Next, we identify all stars with F814W magnitudes brighter than $M_{\text{lim}} = -3$ within the two measurement regions. This removes the flux from

the six brightest stars in Figure 2.8. We subtract the flux contribution from these bright stars from the cluster and background flux totals. Finally, we subtract the remaining background flux (representing the summed light of field stars with $F814W > M_{\text{lim}}$) and obtain our final unresolved fluxes for the cluster.

The cluster's properties were determined through χ^2 minimization using the unresolved flux values. For PC1017, the unresolved light analysis gives a best fit age of 40 Myr, with $\log(M_{cl}) = 3.62 M_{\odot}$ and $A_V = 0.42$ mag. All models with $\chi^2 < 1 \pm (1 / \sqrt{n})$ were considered good fits, where n represents the degrees of freedom, 3 in this case. From the distribution of good fits, the 68% confidence interval gives an age range of 16 - 64 Myr, a mass range of $\log(M_{cl}) = 3.56 - 3.67 M_{\odot}$, and an extinction between 0.20 and 0.64 mag. These values are consistent with both the spectroscopically determined properties, as well as those predicted by the discrete models.

We have also analyzed this cluster using traditional integrated light fitting. This method gives a best fit age of 80 Myr, $\log(M_{cl})$ of $3.86 M_{\odot}$, and A_V of 0.28 mag. The 68% confidence intervals were 64 - 96 Myr, with a $\log(M_{cl})$ between 3.81 and $3.90 M_{\odot}$, and an extinction between 0.17 and 0.39 mag. Fitting the total integrated light therefore gives a derived age that is too old, due to the presence of the luminous red giant. In contrast, the unresolved flux results in an age that is more consistent with the ages determined spectroscopically, by the discrete models, and from isochrone fitting.

We find that the mass estimated by the unresolved method is lower by ~ 0.2 dex compared to the other three methods, which is of the same order as the bias towards low masses found in §2.3. However, the unresolved mass estimate is still within the error bars determined by the isochrone fitting as well. The underestimate of the cluster's mass could indicate that the mass-to-light scaling needs to be recalibrated for use with unresolved light.

Though there are differences in the derived ages, masses, and extinctions for the different methods, the properties determined by the unresolved method agree well with those determined by the independent estimates. The differences in extinction can mostly be attributed to the age-extinction degeneracy. The age determined by isochrone fitting was the youngest, and it also had the highest extinction. Alternately, this cluster could be slightly older, with a lower extinction, as estimated by the discrete and unresolved models.

2.5 Discussion

2.5.1 Applicability

Analyzing the unresolved component of a cluster’s light shows promise for reducing some of the stochastic effects associated with deriving the properties of star clusters. This method is best suited for low mass clusters, where stochastic issues make normal integrated light methods fail, and where there are small numbers of bright stars that we wish to subtract. The dispersion is still significant for clusters of $10^3 M_{\odot}$, but this method can produce more accurate results for these lower mass clusters than traditional integrated light fitting. It can be used for clusters in galaxies from $\sim 1\text{-}3$ Mpc, where full CMD fitting is not possible, but a small number of bright stars can be individually resolved. The value of M_{lim} should be optimized for the targeted clusters’ age range.

2.5.2 Best Choice of M_{lim}

The choice of cutoff magnitude M_{lim} was based on trying to achieve stability in the unresolved component of the clusters’ light, while preserving a strong correlation of flux with age. The values of M_{lim} discussed in this paper were chosen to work well with the PHAT data set. Several things should be kept in mind when trying to decide what value of M_{lim} should be used. At distances greater than a few Mpc, even HST imaging will make it difficult to resolve stars down to moderately bright magnitudes (e.g., $M_{814} = -3$). However, in these cases, the method should be adjusted to use a brighter M_{lim} at the expense of limiting the age range one can probe. A brighter cutoff would be better suited to younger and/or less extincted clusters, while a fainter cutoff would yield better results for older and/or more extincted clusters.

One difficulty associated with subtracting the resolved star fluxes is that completeness of resolved photometry can vary greatly as a function of radius within the cluster. M_{lim} should be above the completeness limit of the data since accurate stellar photometry of the resolved stars is needed to subtract off their flux. If M_{lim} is bright enough and the number of bright stars we wish to subtract is small enough, then resolving these few bright objects should be possible in most cases. This will be the case for lower mass clusters, for which

this method is most useful. To optimize this method for a general use, M_{lim} could be a parameter that is solved for during the χ^2 minimization as well. This would allow the value of M_{lim} to be optimized for the age of each cluster, and to reduce stochastic effects for older clusters as well as younger clusters.

2.5.3 Field/Foreground Contamination

Another benefit to this method not previously discussed is that it minimizes bright field/foreground star contamination. As long as the star in question is brighter than the chosen M_{lim} , its flux is not included in the analysis. Therefore, the determination of cluster membership does not affect the derived cluster's properties.

2.5.4 Model Uncertainties

Our analysis depends on the accuracy of the models used and the assumption that dust attenuation acts in a predictable way. These factors may cause the actual uncertainties in derived properties to be higher. One advantage of looking at the unresolved light is that this will be less sensitive to model uncertainties for massive post-main sequence stars, which are quite substantial. One potential complication, however, is that the separation between main sequence and post-main sequence stars is not always as clean as the models predict (Larsen et al., 2011), which again complicates the choice of M_{lim} .

2.5.5 Future Work

Eventually the best way to study a cluster is to combine the study of the unresolved and resolved portions of its light. The resolved stars can be analyzed using isochrone fitting, and the unresolved color could be analyzed separately. Then the results from these two methods can be compared to ensure consistency.

A more complete study of a variety of clusters is needed to further show the applicability of this method. This would include optimizing the value of M_{lim} to be solved for during the fitting process, investigating the effects of crowding and blending, further comparisons with other age-dating methods, and extending this method out to larger distances.

2.6 Conclusions

We investigated the properties of partially resolved stellar clusters using simulations and found that stochastic variations in color can be greatly decreased when considering only flux below a limiting magnitude M_{lim} . This unresolved light component utilizes the stability of the main sequence light along with the age information in the main sequence turnoff but eliminates the often stochastically sampled upper end of the stellar mass function. By using only this unresolved component of the flux, we have shown that we can derive accurate age, mass, and extinction determinations with a variety of simulated clusters. The improvements over traditional integrated light fitting are most evident for lower mass clusters where the effects of stochasticity are greatest. This method was also applied to an M31 cluster, and results using the unresolved method were comparable to the properties determined spectroscopically, from discrete models, and isochrone fitting.

This new technique will be especially useful for lower mass clusters (less than a few $10^4 M_{\odot}$), crowded clusters, and clusters in nearby galaxies with only a few resolved stars. This method can also be used as a sanity check for clusters whose age and mass determinations come from isochrone fitting. It also allows for the potential of obtaining reliable property determination for clusters too far away to be analyzed with isochrone fitting methods. In this situation, the unresolved technique provides greater accuracy while still utilizing continuous models, without needing spectroscopy or computationally intensive discrete models.

Chapter 3

PHAT CLUSTERS

Stellar clusters are widely used out to ~ 50 Mpc to investigate star formation, stellar evolution, and the formation histories and evolution of galaxies. At these distances, integrated light measurements are routinely used to analyze the ages and masses of clusters. These methods fit multi-wavelength flux measurements (usually including the UV) with predictions from models of single age stellar populations and foreground dust. This is a mature field, with many catalogs of clusters with ages and masses derived from integrated light measurements, such as those for M83 (Bastian et al., 2012), M33 (San Roman et al., 2010), the Large Magellanic Cloud (LMC; Hunter et al., 2003; Popescu et al., 2012), M51 (Chandar et al., 2011), and the Antennae Galaxies (Whitmore et al., 2010).

Most advanced methods include discrete models, which attempt to reduce the stochastic effects that are inherent in integrated light studies. Integrated light determinations of the cluster properties are generally fairly accurate for clusters above a few $10^4 M_{\odot}$ mass. However, for lower mass clusters, this method suffers greatly from stochastic effects due to the clusters' luminosity being dominated by a very small number of stars, rather than by a well populated stellar mass function. The effects of stochasticity are particularly severe at young cluster ages due to individual stars rapidly evolving off the main sequence (e.g., Lançon & Mouhcine, 2000; Cerviño & Luridiana, 2004; Maíz Apellániz, 2009; Piskunov et al., 2009; Popescu & Hanson, 2010b; Fouesneau & Lançon, 2010; Beerman et al., 2012). Older than a few 100 Myr, the integrated light of the cluster is dominated by more numerous lower mass stars, and thus reduces the effects of stochasticity. While current studies that treat the mass function as a discrete distribution of stars (Fouesneau et al., 2012; Popescu et al., 2012) do a much better job than traditional integrated light age determinations, problems remain, such as sensitivity to stellar models for rapidly evolving massive stars, and uncertain photometry due to the effects of crowding, spatially variable complex backgrounds, and dust.

New surveys such as LEGUS (Calzetti et al., 2015), will vastly increase the samples of integrated multi-wavelength measurements of clusters in extragalactic systems. This sample offers tremendous potential for investigating areas such as star formation histories and environmental variations of star and cluster formation over a much wider range of galaxy properties than are represented in the very local universe. However it is important to test the validity of these integrated light derived properties, and to understand their biases and potential failure modes before the reliability of these studies can be firmly established.

Deriving cluster properties using color-magnitude diagrams (CMDs) of resolved stars has been the gold standard. With resolved stars, we can fit stellar models to their CMD to derive the age and extinction, and using mass-to-light ratios or stellar models, we can derive their mass as well with a greater accuracy. These resolved studies do not suffer from stochastic effects like the integrated studies do and generally lead to more accurate results. However, such studies can only be used in clusters that are sufficiently close that their individual stars can be resolved from one another.

The Local Group is currently the only place where large populations of clusters can be resolved into individual stars. It is therefore the ideal place to compare cluster property determination methods. Such a test is possible using ground based data in the Magellanic Clouds, but these low metallicity dwarf systems are not representative of the metal-rich disk dominated systems that we observe out to further distances. M31, however, is the perfect system for this kind of comparison study, since it is near enough that we can obtain both resolved measurements of individual stars within the clusters (using HST) and integrated light measurements of the clusters as a whole. We can therefore compare the results from both methods and determine in what environments and for what types of clusters the methods agree and where integrated light fitting is biased or fails completely. This comparison will ensure that surveys done at larger distances can optimize their age and mass results from integrated light fits.

The Panchromatic Hubble Andromeda Treasury (PHAT; Dalcanton et al., 2012) survey of M31 has the exceptional resolution and broad wavelength coverage that is required for this comparison. The PHAT survey imaged 1/3 of M31's disk in six filters (Williams et al., 2014) and has been used to construct a large well-characterized sample of clusters (Johnson

et al., 2015). We can resolve many individual stars within the clusters, enabling us to accurately derive their properties. We can also identify clusters down to very low masses, guaranteeing high completeness, and a large number of clusters where the effectiveness of stochastic models can be tested. This sample allows us to investigate both methods of determining cluster parameters and how that accuracy depends on parameter space.

The organization of this chapter is as follows: In Section 3.1 we describe the PHAT cluster sample used in this chapter. In Section 3.2 we describe our two methods for determining cluster properties. Section 3.2.1 describes the CMD fitting technique and Section 3.2.2 describes the integrated light technique. We present the results in Section 3.2.3, with broad comparisons between the methods in Section 3.2.3.a and common failure modes investigated in Section 3.2.3.b. We do a by-eye check of all results in Section 3.2.3.c and present a table of our final results. We explore the age and mass distribution for our cluster sample in Section 3.3.1 and investigate how this would change for integrated light only studies in Section 3.3.2. Finally, we present our conclusions in Section 3.4.

3.1 Cluster Sample

We use the cluster sample from the PHAT survey (Johnson et al., 2015). The Panchromatic Hubble Andromeda Treasury (PHAT; Dalcanton et al., 2012) was a four year HST survey that imaged $\sim 1/3$ of M31’s star-forming disk and resolved over 100 million stars (Williams et al., 2014). The survey was done in six filters, covering UV to near-IR: F275W, F336W, F475W, F814W, F110W, and F160W. Photometry was done for individual stars brighter than ~ 27.9 in the F475W band (for a S/N ratio of 4).

From these images, in collaboration with the Zooniverse citizen science team, Johnson et al. (2015), compiled a catalog of 2753 clusters using the results of a by-eye search of all the optical PHAT images. The final cluster catalog includes many faint and sparse clusters, and increases the number of known clusters within the PHAT footprint by a factor of six. The integrated magnitudes of clusters range over three magnitudes in the F475W band, and the luminosity function probes two orders of magnitude deeper than previous studies done in the LMC, M33, and M83. While some of the objects in the catalog may not be bound objects, this catalog does not include larger scale (> 10 pc) associations of stars.

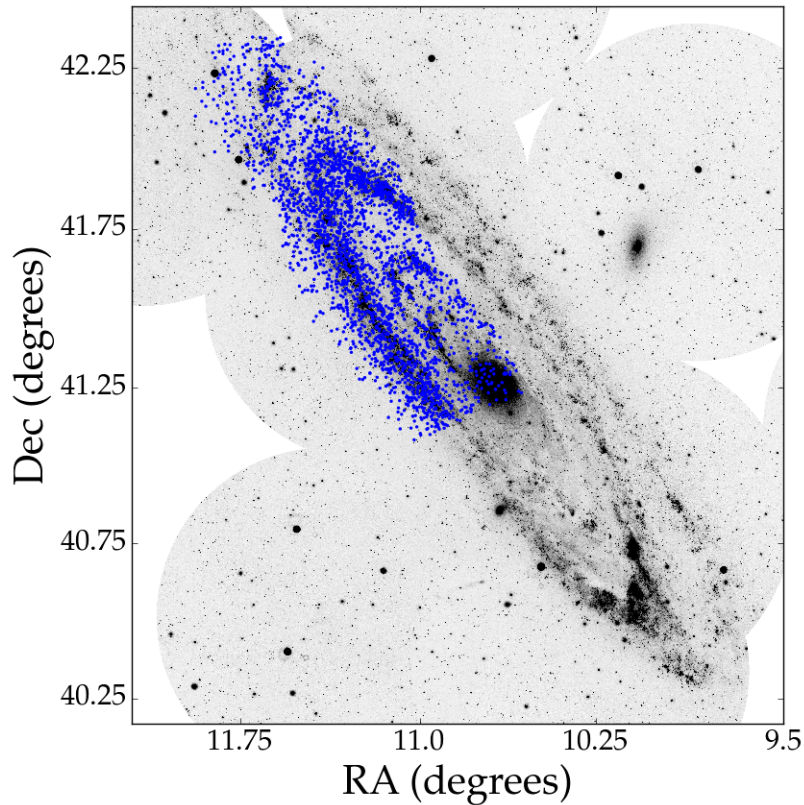


Figure 3.1 Background GALEX NUV image of M31 showing the locations of the stellar clusters (blue points) in the PHAT cluster sample.

To assess the completeness of the cluster sample, artificial clusters, with a range of ages and masses, were inserted into the images used in the by-eye search and their recovery rate was measured. As expected, the catalog completeness is a function of both age and mass, where the sample is highly complete at $M > 10^{3.2} M_{\odot}$ and $t > 10$ Myr. At ages < 10 Myr, many clusters may still be embedded within molecular gas, and would not have been identified by the optical image search. Completeness is also a function of galactic environment, where clusters in the crowded inner region of M31 are more likely to be missed. Additionally, completeness is higher for clusters < 100 Myr, since there are more stars on the main sequence, making the clusters more easily identifiable. Artificial cluster tests show

that the cluster sample is 50 percent complete down to $500 M_{\odot}$ for clusters younger than 100 Myr. For a complete description of the completeness of the cluster sample, see Johnson et al. (2015).

3.1.1 Cluster Photometry: Individual Stars

In this chapter we use optical photometry for the cluster CMD fitting. CMD fitting requires two bands, and the PHAT survey filters F475W and F814W provide the deepest photometry of the stars within each cluster. These two filters have about 50% more detections than in the UV or IR bands, since the UV images are about two magnitudes shallower than the optical images, and the IR suffers more from crowding due to the lower angular resolution of the WFC3/IR camera.

Johnson et al. (2015) defined circular apertures for each cluster which ranged from $0.7''$ (2.7 pc) to $6.4''$ (24.2 pc) in radius. The apertures were chosen by first centroiding on the smoothed F475W image, then visually inspecting the curves of growth for each cluster. Each cluster's aperture is set to be the point where the cluster light profile drops below the background noise. This choice of aperture size allows the maximum possible cluster stars included while minimizing contamination from background sources. The same aperture size was used in each filter.

Photometry for individual cluster stars was performed with DOLPHOT, which is a version of HSTPHOT with HST specific modules (Dolphin, 2000). We also generated a "background only" CMD, by extracting photometry from within an annulus from $1.2 - 3.4 \times$ the aperture radius, covering $10 \times$ the cluster's area.

In Figure 3.2 we show two example images and CMDs of clusters in the PHAT sample. With HST, the individual cluster stars can be readily resolved.

Artificial star tests (ASTs) were used to assess completeness and photometric bias within each cluster. The ASTs were generated by inserting the PSF of each AST into the photometry for that cluster and then redoing the photometry with and without that AST, then measuring the stars' recovered properties in each optical filter. 50,000 artificial stars were created for each cluster, with the stars being distributed both spatially as a function of their

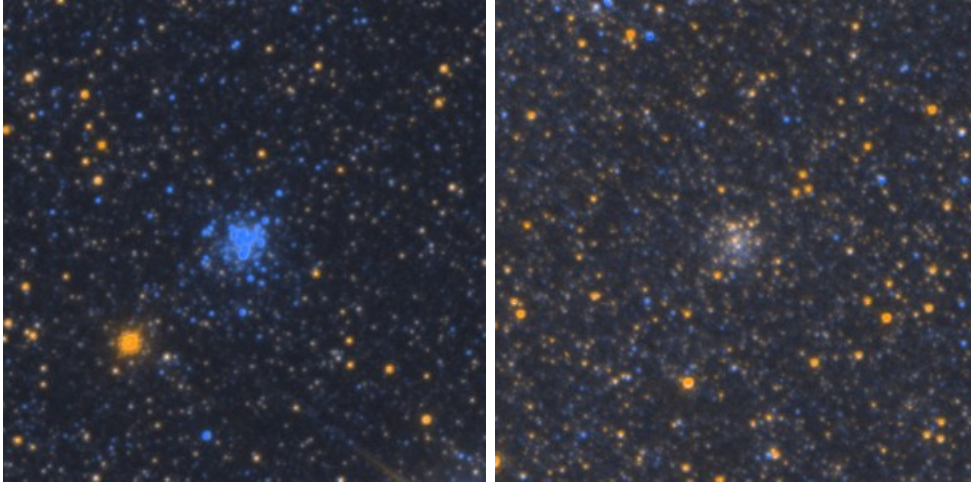


Figure 3.2 Two example HST/ACS optical images of clusters in the PHAT sample. AP81, a typical young cluster is shown in the left panel, and AP71, an older cluster is shown on the right panel. The clusters are clearly resolved into stars. However, the stellar background is complex, which complicates both interpretation of the CMD and measurement of the integrated light.

light profile and uniformly on the CMD. Since we had to generate over 150 million ASTs for the optical bands alone, adding the other four bands would have led to an exorbitant amount of computation time being spent on AST creation.

3.1.1.a Crowding

For some crowded clusters, crowding and blending of the central stars can significantly affect the CMD. Inspecting the images and integrated light results show that this is a significant problem in the very crowded central regions of globular clusters. This effect can be seen in Figure 3.3, which plots the spatial distribution of the 50% completeness magnitude (left panel) and the completeness percentage at 24.47 magnitude (right panel, corresponding to an absolute magnitude of 0) for a crowded cluster. The completeness percentage is clearly very low in the central region. Due to this high crowding, in these low completeness regions, the small numbers of detected stars blend together and appear to be brighter than they are, and the majority of fainter stars are undetected. When this happens, it creates a false "main sequence" on the CMD which can produce a much younger fit in age than the

actual cluster’s age.

We tried to limit the effects of severe central crowding by removing the central regions from the CMDs of the most crowded clusters and doing the MATCH analysis on the remaining stars. Of the dense, older clusters in our sample, 118 have been previously observed by Caldwell et al (in prep). Many of these are globular clusters that have severe crowding. Caldwell et al (in prep) did a by-eye annulus fit to these clusters to attempt to define spatial regions that were not hampered by crowding effects. We use his defined annuli for these clusters and only kept the stars and ASTs that were within the uncrowded annuli as defined by his by-eye annuli.

To extend this method to the entire cluster sample, we found the surface brightness that corresponded to the inner radii for the clusters in the Caldwell sample. There are a few extremely crowded clusters that need a more strict surface brightness cut, but most of the clusters had a radial cut at about 18 mag/arcsec^2 in the F814W band. We adopted this as our surface brightness cut for the rest of the cluster sample. We then found the corresponding radius for each cluster, and removed all stars both from the photometry and ASTs that are interior to this radius. In Figure 3.4 we show an example of the cluster CMD before (left panel) and after (right panel) the removal of interior stars. For this cluster, the surface brightness cut removed mostly stars above $F475W = 23.5$, and the resulting best fit age changed from $\log(\text{age} / \text{yr}) = 6.6$ to 8.8.

This surface brightness cut affected 290 clusters. Inclusion of this cut changed the ages of 25% of these clusters, and eliminated the worst problems with crowding mimicking a young main sequence. However, as we show below in Section 3.2.3.a, there are a small number of crowded clusters that still appear to have artificially young ages.

3.1.2 Cluster Photometry: Integrated Photometry

For integrated photometry, Johnson et al. (2015) performed integrated aperture photometry for each cluster in each of the six PHAT filters, using the apertures described in Section 3.1.1 for both the clusters and the background. The background annulus for each cluster was divided into ten equal area annuli, and the integrated flux was measured in each. To avoid

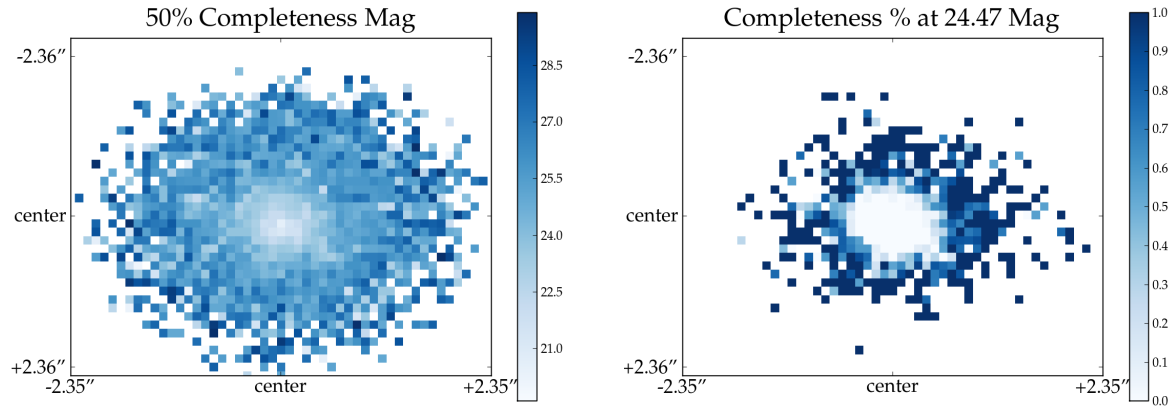


Figure 3.3 Spatial completeness maps for the dense stellar cluster AP2023. The left panel shows the spatial distribution of the 50% completeness magnitude and the right panel shows the completeness percentage at a fixed magnitude of 24.47 (corresponding to an absolute magnitude of 0). The completeness varies sharply with radius, changing from nearly zero completeness to $> 80\%$ completeness over a change in radius of $< 1''$.

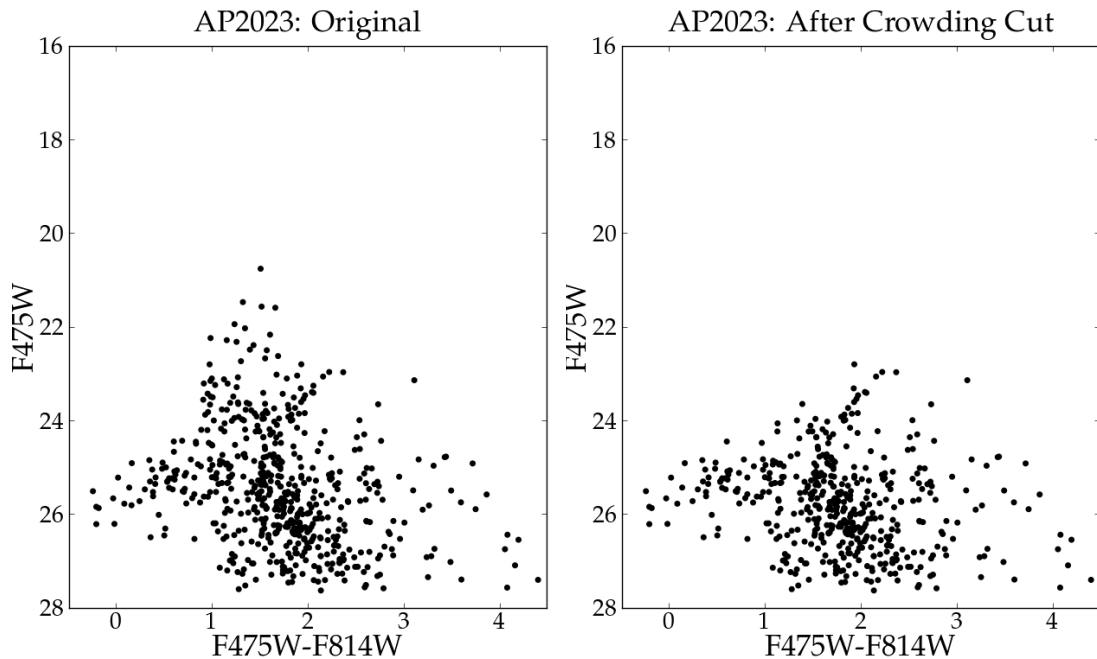


Figure 3.4 Original CMD for AP2023 (left panel) and after crowding cut using a surface brightness cutoff of 18 mag/arcsec^2 (right panel). This cut successfully eliminated bad photometry due to extreme crowding in the center of the cluster, leaving a CMD that shows a clear blue horizontal branch, characteristic of old metal poor globular clusters.

sources that are not representative of typical background sources, two sigma outliers were rejected. The mean flux of the non-rejected annuli are used as the background flux level, which is subtracted from the flux within the cluster aperture. A signal over the background of at least 3 was set to be the minimum detection threshold in a given band. For consistency with the stellar photometry, all flux measurements used the Vega magnitude system as reference, and the magnitudes were kept in the native HST filters. A complete description of how the integrated cluster photometry was done can be found in Section 4 of Johnson et al. (2012).

Associated measurement uncertainties are lower than 0.2 magnitudes for most clusters. Uncertainties in the background represent the largest source of uncertainty in the integrated photometric measurements. Background uncertainties are calculated from the standard deviation of all the non-rejected annuli used in the background flux measurement. To determine how much light falls outside the aperture, radial flux profiles are fit to each cluster, and the resulting fits are used to make aperture corrections. Based on synthetic cluster tests, between 0.1 - 0.3 mag of light is lost from each cluster that is outside the aperture. Aperture corrections are made by fitting a King (1962) profile to the cluster light and extrapolating out past the aperture. Uncertainties in the measured aperture flux are less than 0.01 magnitudes.

3.2 Determining Cluster Properties

In this chapter we use two methods for determining cluster properties. The first method is modeling the CMD fitting of the individual resolved stars in each cluster. The second is fitting the integrated light (including upper limits) in six bandpasses to discrete probabilistic models. In this section we describe each method and their corresponding strengths and limitations.

3.2.1 CMD Fitting

For Milky Way clusters and those in nearby galaxies (out to ~ 2 Mpc), Modeling the CMD of the clusters' resolved stellar population provides the most robust determination of the clusters' properties. CMD fitting allows us to take advantage of all the information in

the main sequence and evolved stellar populations, including their colors, magnitudes, and relative numbers. Modeling the entire CMD therefore provides the most accurate age, mass, and extinction determination for clusters with significant numbers of resolved stars above the completeness limit of the observations.

We performed CMD fitting to the resolved stars of each cluster using a modified version of the MATCH fitting program (Dolphin, 2002), optimized for fitting a single age population plus a background model. MATCH takes the following parameters as inputs: IMF, binary fraction, extinction, distance, and stellar evolution library. For a range of age and metallicity combinations, MATCH generates model CMDs using the given stellar evolution library for bins in CMD space. Artificial star tests (ASTs) are used to model the completeness and photometric errors, which are then convolved with the model CMD. The background is statistically modeled and added to the model CMD.

The best fit age and extinction model is found using the minimum of the Poisson likelihood \mathcal{L} , since the number counts of stars in a CMD is Poisson distributed. The mass is not a model parameter but is found by a normalization to the number of stars, assuming the appropriate mass-to-light ratio. The goodness of fit parameter that comes out of the Poisson likelihood is used to infer the reported uncertainties. The fit parameter is equal to $-2 \ln(\mathcal{L})$, meaning that the difference in the fit parameter of a given model relative to that of the best fit model goes as σ^2 . Thus, all fit values less than 1 away from the minimum fit value are within one standard deviation of the best fit. This method produces a full probability distribution function (PDF) for each cluster. When reporting uncertainties in a single parameter, we calculate the minimum and maximum values that are within one standard deviation of the best fit.

We ran each cluster through MATCH in the single stellar population mode. We considered 36 age bins distributed in $\log t$ between 6.6 and 10.1 with 0.1 dex spacing, and a single bin from 10.1 to 10.15 at the oldest ages. Tests at finer age bins of 0.05 dex spacing showed no difference in results, and substantially longer computation times. Since the disk of M31 has approximately solar-like metallicity (e.g., Sanders et al., 2012; Zurita & Bresolin, 2012), we chose to only fit around solar metallicity (-0.2 to 0.1 solar Z_{\odot} with 0.1 dex spacing) to limit computation time. This assumption is not valid for the small population of old, low

metallicity clusters, but these clusters are well fit by the integrated light measurements. We used a Salpeter (1955) IMF, along with a binary fraction of 0.35. The extinction was allowed to vary from 0 to 3.0 in steps of 0.05. The distance modulus used was 24.47 (McConnachie et al., 2005). We used the stellar evolution models from Padova (Marigo et al., 2008) with updated AGB tracks from Girardi et al. (2010).

3.2.1.a Reliability of CMD Fitting

To investigate how well MATCH recovers cluster properties, we tested MATCH’s performance using a set of artificial clusters with known properties. These synthetic clusters were created with a range of ages and masses, although we focused on ages less than 1 Gyr, where we expect to rely on CMD fitting rather than integrated light fitting. These synthetic clusters were inserted into the PHAT images at various locations within the footprint, and then run through the photometry pipeline in a similar manner to the real clusters. We also ran artificial stars for each of these synthetic clusters, in the same manner as the real clusters.

In Figure 3.5 we plot the input parameter (x -axis) vs the best fit result from MATCH (y -axis) for the 866 synthetic clusters. The top panels are color coded by input mass. A small amount of Gaussian scatter was added for clarity to avoid overplotting points at discrete values of mass and age. There is good general agreement between the input and recovered parameters. Fewer than 5% of the best fit ages are more than 1 dex away from the input age, and only 12% are more than half a dex away. The RMS deviation in $\log(t)$ is 0.43 yr. The cluster masses are generally more accurately recovered, with only 4.4% of best fit masses being more than 1 dex away from the input mass; 8.3% are more than half a dex away. The RMS deviation in $\log(M)$ is $0.34 M_{\odot}$ and 0.32 magnitudes in A_V .

To illustrate that failures in one parameter cause failures in another parameter, in Figure 3.6 we plot the difference between each parameter’s input and recovered value. In the top left panel we see that clusters with incorrect ages also tend to have incorrect extinctions. The top right panel shows that failures in recovering age also tend to have failures in recovering mass. The bottom shows that the same is true for mass and extinction.

The failure cases are mostly confined to low mass, young clusters that have been fit as

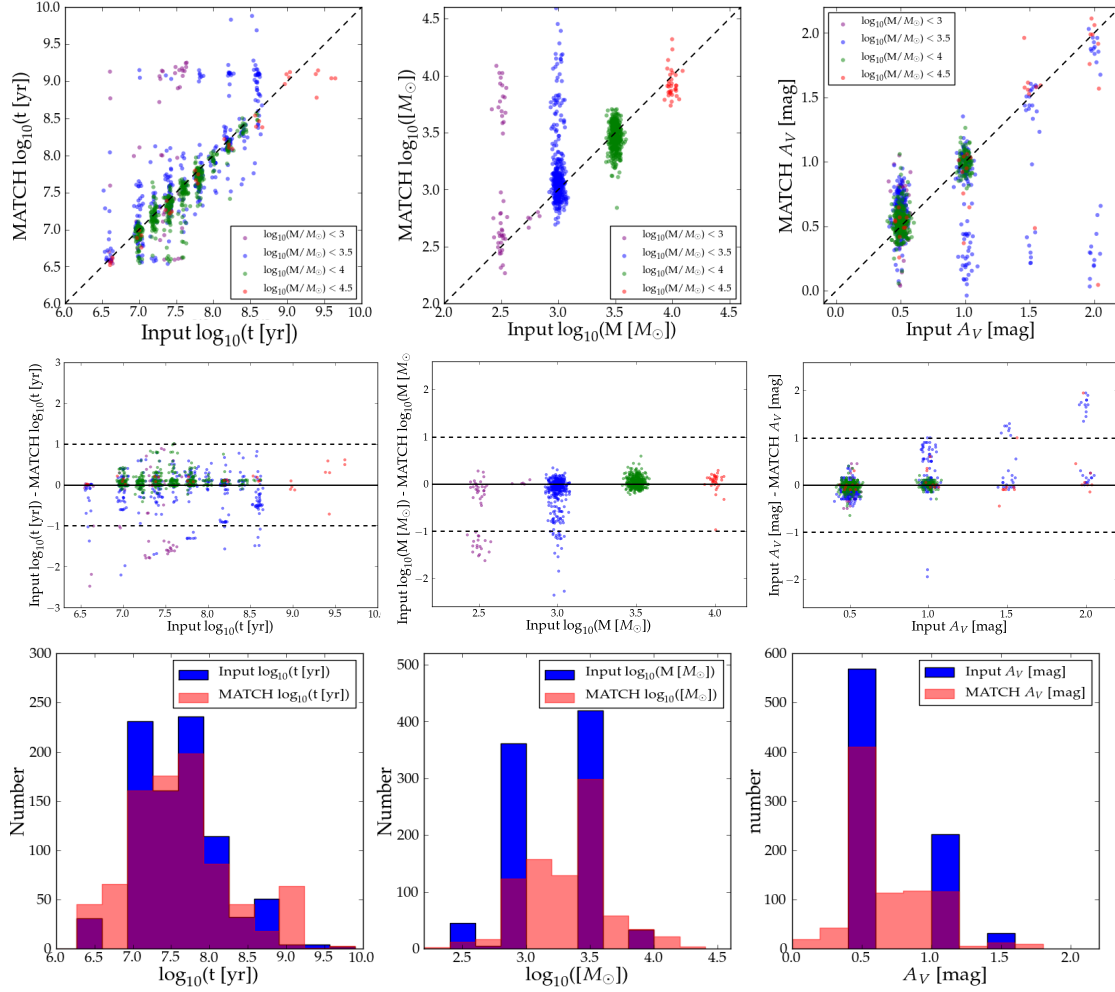


Figure 3.5 Results from running 866 synthetic clusters through MATCH. Top panels show each input parameter versus the Match recovered parameter, color-coded by input mass. A small amount of Gaussian scatter was added for clarity to avoid overplotting points at discrete values of mass and age. The middle panels show each input parameter versus the difference between input and recovered parameter, also color-coded by input mass. The RMS deviation in $\log(t)$ is 0.43 yr, the deviation in $\log(M)$ is $0.34 M_{\odot}$ and is 0.32 magnitudes in A_V . Clusters above $10^3 M_{\odot}$ are recovered especially well. The bottom panels show input and recovered histograms for each parameter.

older clusters due to sparse main sequences. In these clusters, there are not enough stars on the main sequence for MATCH to reliably derive a young age. The MATCH results are generally very accurate for clusters that are at least $10^3 M_{\odot}$, since these clusters have

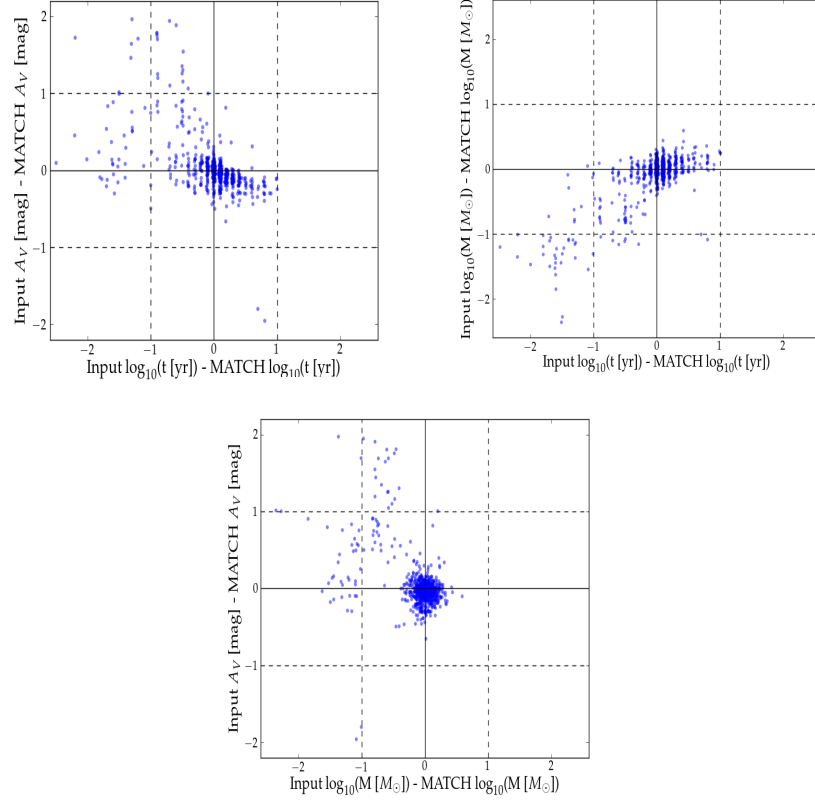


Figure 3.6 Top left panel shows the difference in input and recovered $\log(t)$ versus the difference in input and recovered $\log(M)$. Top right panel shows the difference in input and recovered $\log(t)$ versus the difference in input and recovered A_V . Top left panel shows the difference in input and recovered $\log(M)$ versus the difference in input and recovered A_V . It is clear that failures in one parameter correlate with failures in the other parameters.

enough of a main sequence to be properly fitted by the CMD fitting technique. Looking at just these clusters, only 1% had best fit ages more than 1 dex away from their input age, and only 9.7% were more than 0.5 dex away.

When there are not enough cluster stars above our completeness limit (about $2-3 M_{\odot}$), MATCH fits to the turnoff of the background stars, which is usually at 1 Gyr. Figure 3.7 shows an example of a $10^{3.4} M_{\odot}$ cluster for which MATCH derived an age of 1 Gyr (blue isochrone), but the likely age from integrated light fitting (green isochrone) is much older. The blue isochrone is clearly going through stars that are likely to be associated with the

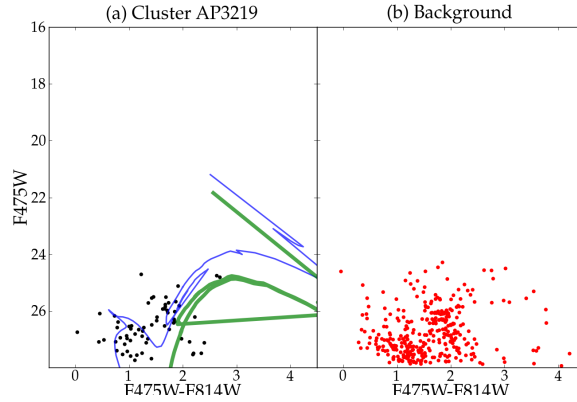


Figure 3.7 Color-magnitude diagram for PHAT cluster AP3219 in the left panel and the background population on the right panel. The blue isochrone corresponds to the best fit age and extinction from CMD fitting, while the green isochrone corresponds to the expected age and extinction from integrated light fitting.

background. We expect to see this feature in the PHAT cluster results for older and very sparse clusters that do not have many stars above the completeness limit.

3.2.2 Integrated Light Fitting

Beyond ~ 2 Mpc, individual cluster stars can no longer be resolved and integrated light measurements must be used to derive the clusters' properties. More recent techniques that use integrated light now attempt to account for stochasticity by treating the mass function as a discrete distribution of stars (Fouesneau & Lançon, 2010; Popescu & Hanson, 2010b; Deveikis et al., 2008; da Silva et al., 2012). These methods use discrete models generated from Monte Carlo simulations of clusters and compare the integrated properties of these to clusters integrated photometry to determine the clusters properties. These methods perform better than traditional integrated light fitting. However they still do not have the leverage available when modeling the distributions of individual resolved stars.

In this chapter we use the results from the Pegase.2n models that were described in Fouesneau et al. (2014), which was based on Pegase (Fioc & Rocca-Volmerange, 1997).

Fouesneau et al. (2014) published properties for the Johnson et al. (2012) "Year 1" PHAT cluster sample containing 601 clusters. We now extend that probabilistic fitting of the integrated cluster photometry to the entire PHAT cluster sample. This method uses discrete models made from Monte Carlo simulations of clusters from low ($50 M_{\odot}$) to high ($5 \times 10^5 M_{\odot}$) masses, where stochastic sampling of the IMF is taken into account. Above this mass the cluster's full mass function is being sampled, and continuous models are used instead. The cluster spectral energy distributions (SEDs) in six filters are then compared to the discrete models and the full Bayesian posterior probability distributions are calculated in age-mass-extinction space, assuming power-law distributions of age and mass, and a uniform distribution of A_V as priors.

For our integrated light fits, model clusters ranged in age from 1 Myr to 20 Gyr, and their extinctions ranged from 0 to $3 A_V$. Metallicity was kept at solar for all discrete models, then a grid of metallicities from $Z = 0.004$ to $0.05 Z_{\odot}$ was used for the continuous models, since these massive clusters are likely to be globular clusters with lower metallicities. We marginalize over metallicity in the posterior probability distributions. This technique is described in detail in Fouesneau & Lançon (2010) and Fouesneau et al. (2014). We adopt ages and masses for each cluster by calculating the mean of each PDF. The uncertainties are calculated from the percentiles of the posterior distribution, and we report the 16th and 84th percentiles as our one sigma uncertainties.

3.2.2.a Reliability of Integrated Light Fitting

Even though discrete models do a much better job at predicting cluster colors in stochastic regimes, the problem of stochasticity still exists, especially when considering the issue of cluster membership. If a background star is within the aperture, the integrated fit will include this star without considering whether there are enough other stars at the appropriate locations in IMF space to make the star a likely cluster member. For many of these clusters, MATCH does not attempt to fit this bright star and treats it as a background star, since one would expect more stars slightly lower on the main sequence than are observed, if this truly were a cluster member. Therefore, including a bright background star in the aperture may

result in integrated light measurements that are too young for these clusters. In Figure 3.8 we show the CMD of a cluster that has one bright star that is causing the integrated fit (green isochrone) to be much younger than the MATCH fit (blue isochrone).

In addition, stochastic models are extremely sensitive to models of stellar evolution for rapidly evolving massive stars. In stochastically sampled clusters, the integrated light is extremely sensitive to the presence of even one luminous star. If stellar models do not predict the correct colors, magnitudes, and lifetimes of such stars, then the stochastic models cannot accurately capture the behavior of real clusters. For example, stellar evolution models do not accurately predict the correct ratio of blue to red evolved core-Helium burning stars. The models predict too few blue supergiants with respect to red supergiants, which leads to the integrated fitting predicting too young ages when a blue supergiant is present (Dohm-Palmer & Skillman, 2002; McQuinn et al., 2011). This effect will be explored fully in Johnson et al (in prep).

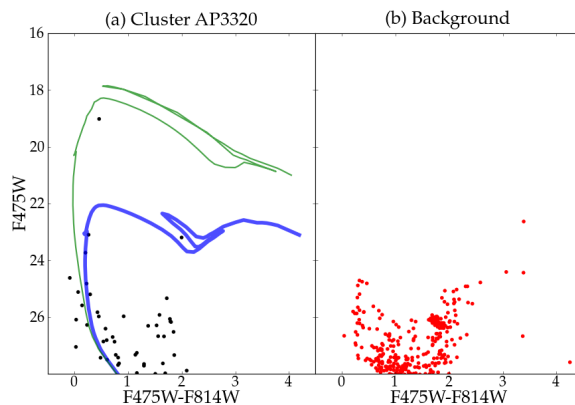


Figure 3.8 Color magnitude diagram for PHAT cluster AP3320 in the left panel and the background population on the right panel. The blue isochrone corresponds to the best fit age and extinction from CMD fitting, while the green isochrone corresponds to the expected age and extinction from integrated light fitting.

3.2.3 Merged Cluster Parameters

We have two completely independent techniques for determining the cluster parameters. We can use these both for mutual verification and for identifying failure modes inherent in either technique. We also use this comparison to decide which fiducial values to adopt for the age, mass, and extinction in subsequent analyses with this sample.

3.2.3.a Broad Sample-Wide Comparisons

Ages: In Figure 3.9 we compare the age that results from CMD fitting with MATCH to the age from integrated light fitting. We account for uncertainties in their PDFs using Monte Carlo sampling of the PDF of each cluster 1000 times for both the MATCH and the integrated light PDFs.

Overall there is a good agreement between the two methods. 60.71% of the two ages are within 0.5 dex of each other, while 85.0% are within 1 dex of each other. The median one sigma uncertainty in age is 0.3 for MATCH, and 0.33 for the integrated light fitting, so there are comparable levels of reported uncertainty in the two methods. The distribution is roughly symmetric about the 1:1 line, therefore there are no significant biases in either method with respect to each other.

While the overall agreement in age between the two methods is good, there are a few areas of differences. Almost all the clusters whose integrated-fitted age is older than in MATCH, also have lower integrated extinctions, and vice versa. Either the cluster is intrinsically red, thus older, or it is younger and heavily reddened.

We also see a clear feature at 1 Gyr for the MATCH age results as described in Section 3.2.1.a. The vertical overdensity is a byproduct of CMD fitting failing when there are few cluster stars higher than the completeness limit. This failure tends to occur when clusters are low mass, when the background is high, or when the main sequence turnoff is below the cluster completeness limit. For our cluster sample, this means that the CMD ages will be less accurate for clusters older than a few hundred Myr.

Masses: In Figure 3.9 we also plot the MATCH mass vs integrated mass. Note that MATCH computes the present day mass of the cluster while the integrated light fitting gives

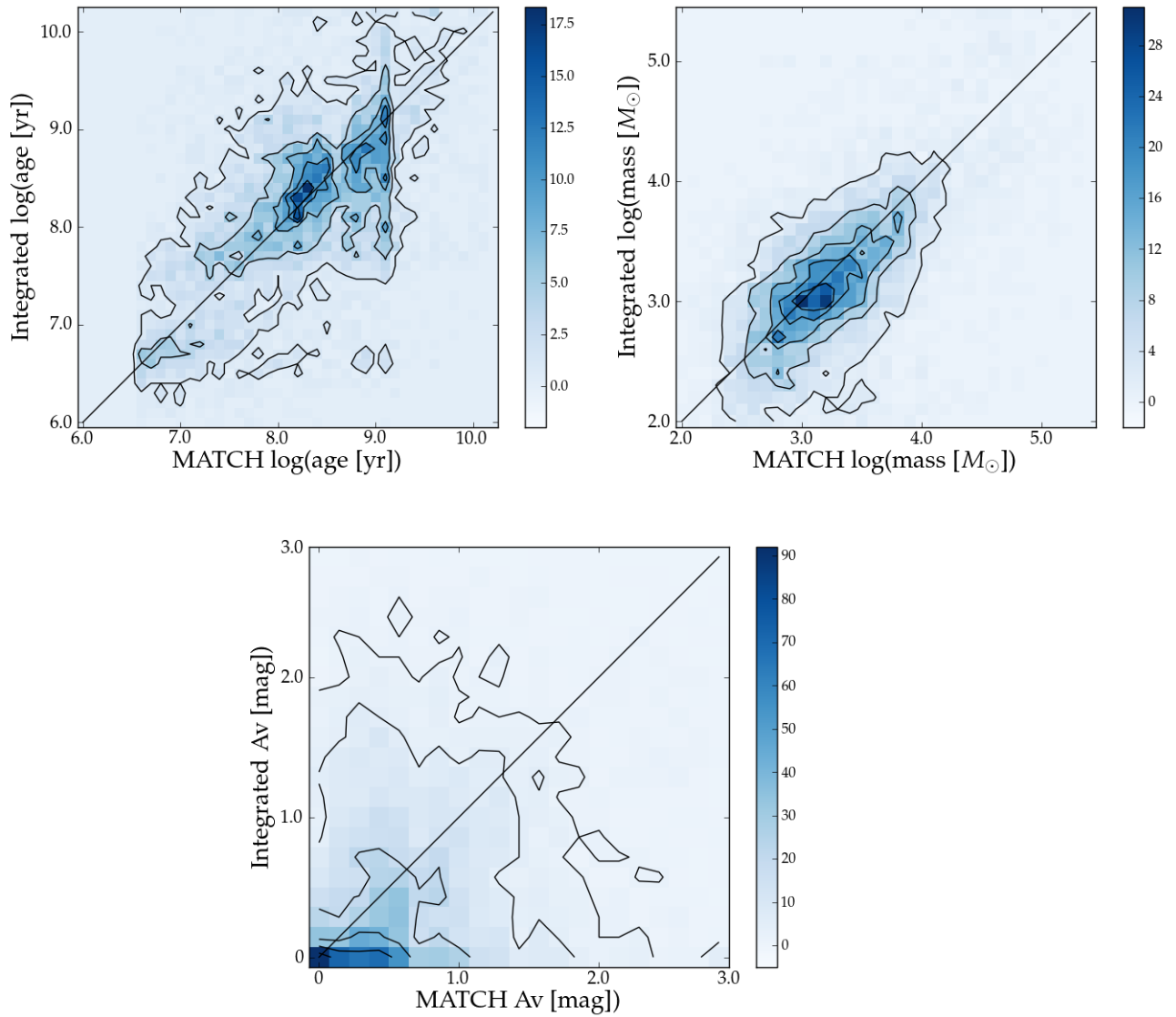


Figure 3.9 Comparison of MATCH best fit results to integrated light expectation value. Top left panel is age, top right is mass, bottom is A_V . All plots have uncertainties in the PDFs incorporated by Monte Carlo sampling of the PDF.

the initial mass. The cluster masses from the two methods agree very well overall. 76.2% of clusters have masses within 0.5 dex of each other, and 94.0% of masses are within 1 dex.

3.2.3.b Assessing Disagreements

We know from earlier sections that neither method is expected to work well in all regimes. There are three main categories of failure modes that might result in inaccurate fits. First, even though we attempted to address crowding by applying a surface brightness cut and removing the centermost stars (as described in Section 3.1.1.a), there are about 100 clusters that are most likely Gyr or older clusters, based on their integrated colors and appearances, but that have crowding issues in the CMD, that have led MATCH to fit these clusters as younger.

The second situation that causes inaccurate fits is when a cluster has one or a few bright stars that contribute significantly to the integrated luminosity and drive the integrated light fits to younger ages, as seen in Section 3.2.2.a. We can get a sense of which clusters may experience this issue by calculating the cluster’s ”unresolved” magnitude and color, similar to what is done in Beerman et al. (2012). Briefly, we derive the ”unresolved” flux by subtracting flux from stars brighter than a cutoff magnitude from the integrated flux, which can then be converted into magnitudes and colors. This correction diminishes the stochasticity while preserving a strong dependence of color on the cluster age. However, because the integrated light measurements have already had background light subtracting off, subtracting off the flux of the brightest stars can leave a cluster with a negative flux, since we are ”double subtracting” off the background component associated with the bright stars. For our analysis here, we are only examining clusters whose integrated flux is greater than the ”unresolved” flux. To do a proper measurement of the ”unresolved” flux, we would need to statistically add back the flux from background stars that are included in the aperture.

To identify clusters that may be affected by background contamination, in Figure 3.10 we plot the MATCH age versus integrated age, where the size of the points represents the magnitude difference between the ”unresolved” magnitudes and the integrated magnitudes.

We used a cutoff magnitude of $F814W = -3$ mag to compute the "unresolved" magnitudes, as in Beerman et al. (2012). As expected, there is great variability in the magnitudes of young clusters, since these have been shown to suffer greatly from stochastic effects. A high fraction of the clusters that the integrated light fits as young but MATCH identifies as old also show large variations in integrated – "unresolved" magnitude relative to the other older clusters. These are clusters where the MATCH ages are likely to be correct, but where a single bright foreground star has biased the integrated light results to young ages.

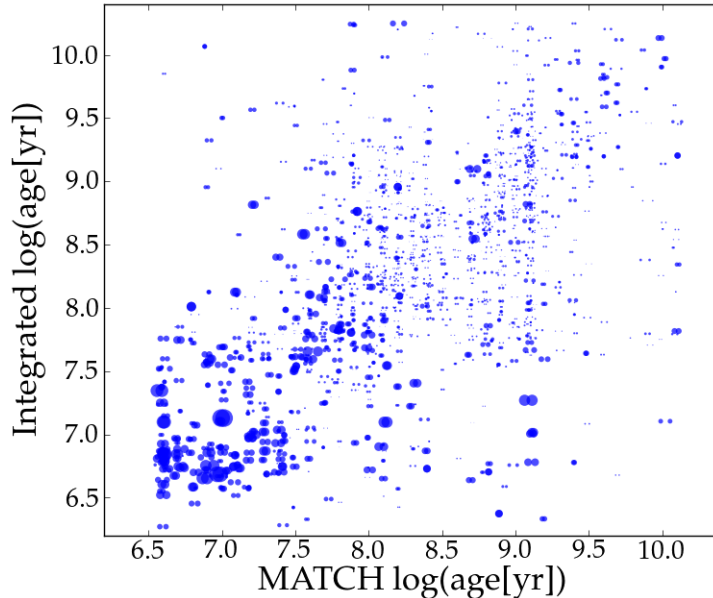


Figure 3.10 MATCH versus integrated $\log(t)$ where the size of the points represents the amount of variation in the cluster color when the brightest stars are removed. A small amount of Gaussian scatter was added in the x -direction for clarity. Older clusters show noticeably more stable colors.

The third category of failure mode is when a cluster has too few resolved stars brighter than our completeness limit. In these cases, MATCH will fit to the background stars, dominated by stars whose main sequence turn off is just above the completeness, since there are not enough cluster stars to provide significant age constraints, which was discussed in Section 3.2.1.a.

3.2.3.c *Assigning Parameters to the Cluster Sample*

To carry out analyses of the PHAT cluster sample, we need to adopt a single "best" age, mass, and extinction for each cluster. This step involves choosing the result from one of the two analysis methods. We have argued that each method has a preferred regime, with CMD fitting expected to perform best at ages < 300 Myr where large numbers of turnoff stars are above the completeness limit. Integrated light fits are expected to perform better at older ages where the effects of stochasticity are less, as shown in (Figure 3.10, where the size of the points corresponds to the amount of variation in the cluster color when the brightest stars are removed). However, we also know that neither method performs flawlessly, and have identified several possible failure modes.

To pick the "best" fit for each cluster, we first adopt a default as MATCH providing the "best" fits for clusters < 300 Myr (in MATCH age), and integrated light as being the "best" fit for clusters older than this. We visually inspect each cluster using its color cutout image and optical. On each CMD we plot the isochrone corresponding to the best fit MATCH age and the isochrone for the expectation from the integrated light fit. We looked through all of these and identified cases where the default best fit was a notably poorer match to the CMD, utilizing the image to help identify cases where crowding is a problem. Clusters for which neither method produced an acceptable fit were flagged. Out of the 1649 young clusters, 91% were acceptably fit by the default MATCH fit. Out of the 1062 older clusters, 81% were acceptably fit by the default integrated light. Overall, only 1% of the clusters were not well fit by either method. When neither method is acceptable, we report the MATCH fit as best if the MATCH result is < 300 Myr, and the integrated fit when the MATCH results is older.

Our by-eye method of comparing fits resulted in a trusted value for the parameters of each cluster. In Table 1 we show a stub table of the parameters for each cluster based on this evaluation. A full table is shown in the Appendix. These are the cluster parameters that we use for the rest of our analysis.

In general the by-eye evaluation confirmed what we suspected from the plots in the previous sections. Namely, that CMD fitting provides more robust parameter estimates for

Table 3.1. Cluster Parameters

AP ID ^a	CMD Best Fit Parameters ^b			Integrated Best Fit Parameters ^c			Best ^d Flag ^e	R _{ap} ^f	N _{stars} ^g	N _{bg} ^h	
	log(<i>t</i> [Myr])	log(<i>M</i> [<i>M</i> _⊙])	<i>A_V</i> [mag]	log(<i>t</i> [Myr])	log(<i>M</i> [<i>M</i> _⊙])	<i>A_V</i> [mag]					
AP1	8.80 ^{+0.00} _{-0.00}	4.04 ^{+0.03} _{-0.03}	0.05 ^{+0.10} _{-0.05}	8.97 ^{+0.05} _{-0.05}	4.13 ^{+0.05} _{-0.05}	0.08 ^{+0.09} _{-0.08}	I	0	2.19	408	229
AP2	8.40 ^{+0.00} _{-0.00}	3.98 ^{+0.00} _{-0.03}	1.15 ^{+0.00} _{-0.05}	8.73 ^{+0.10} _{-0.07}	3.52 ^{+0.07} _{-0.07}	0.15 ^{+0.12} _{-0.15}	I	0	1.86	255	169
AP3	8.80 ^{+0.00} _{-0.10}	3.48 ^{+0.05} _{-0.00}	0.00 ^{+0.30} _{-0.00}	8.57 ^{+0.08} _{-0.09}	3.09 ^{+0.08} _{-0.07}	0.11 ^{+0.13} _{-0.11}	I	0	1.95	197	113

^aAndromeda Project ID (Johnson et al., 2015)

^bBest fit parameter results from CMD fitting using the MATCH package (Dolphin, 2002).

^cWeighted mean of the PDF results from fitting the integrated light using Pegase.2n (Fouesneau et al., 2014).

^dMethod that produces the most accurate results. The default is CMD fitting for clusters < 300 Myr and integrated fitting for clusters older than 300 Myr, but in individual cases the alternative method is adopted based on a by-eye quality check.

^eFlag set to 1 indicates best fit is not acceptable based on by eye quality check.

^fAperture radius in arcseconds.

^gNumber of stars in the cluster CMD.

^hNumber of predicted background stars in the aperture.

younger (< 300 Myr) clusters that still have multiple stars on their upper main sequence. Integrated light determinations yield more accurate estimates for older clusters whose main sequence stars have already evolved.

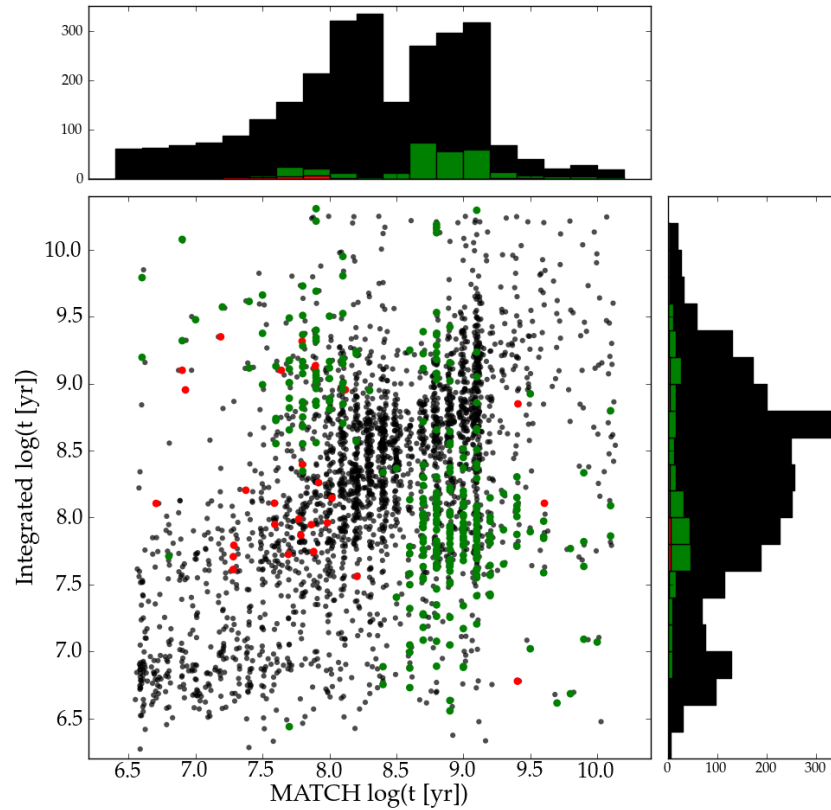


Figure 3.11 MATCH versus integrated $\log(t)$ where flagged clusters with unacceptable fits in both methods are shown in red, and clusters where the non default fit is better are shown in green. Histograms on sides show distributions of each. A small amount of Gaussian scatter was added in the x -direction for clarity.

In Figure 3.11 we plot the MATCH ages vs the integrated ages, along with the projected histograms on each axis, where all clusters in the sample are plotted in black, and the clusters that were flagged as having neither the integrated nor the MATCH fits appear to be acceptable based on the CMD are shown in red. The green points are those clusters for which the non default value is a better fit than the default fit (i.e., a young cluster whose

integrated light fit is better than the MATCH fit). From this, we can see that most clusters that were flagged had disagreements between their CMD and integrated ages. In these cases the default method is not providing an accurate age for that cluster.

The group of clusters that are likely older globulars that have crowding issues on their CMDs as described in Section 3.1.1.a can be seen in Figure 3.11 as the group of flagged clusters that have young MATCH ages and older integrated ages. These clusters that have drastically younger integrated fits due to one bright possible background star are evident in the bottom right of Figure 3.11, at older MATCH ages and younger integrated ages.

We note that the histograms also show a larger fraction of clusters that have been flagged in the bins around a MATCH age of 1 Gyr, indicating poor fits likely due to MATCH fitting to the background stars when there are not enough cluster stars above our completeness limit, as described in Section 3.2.1.a.

We can also investigate how the number of filters in which a cluster was detected correlates with the flagged clusters. In Figure 3.12 we show the integrated $\log(M)$ versus the number of filter detections where all flagged clusters are shown in red. A cluster was considered detected in a given passband if it had signal to noise (S/N) > 3 with respect to the variation in the background (Johnson et al., 2015). Naturally the more massive clusters tend to be detected in more filters. It is interesting that clusters with detections in five and six filters have a larger percentage of flagged clusters than those with only three or four detections. One possible explanation for this is that given more data points along with imperfect models may force some clusters into unusual places in the age-mass-extinction parameter space, where having fewer data points gives a greater degree of freedom to allow the models to fit the light in those filters.

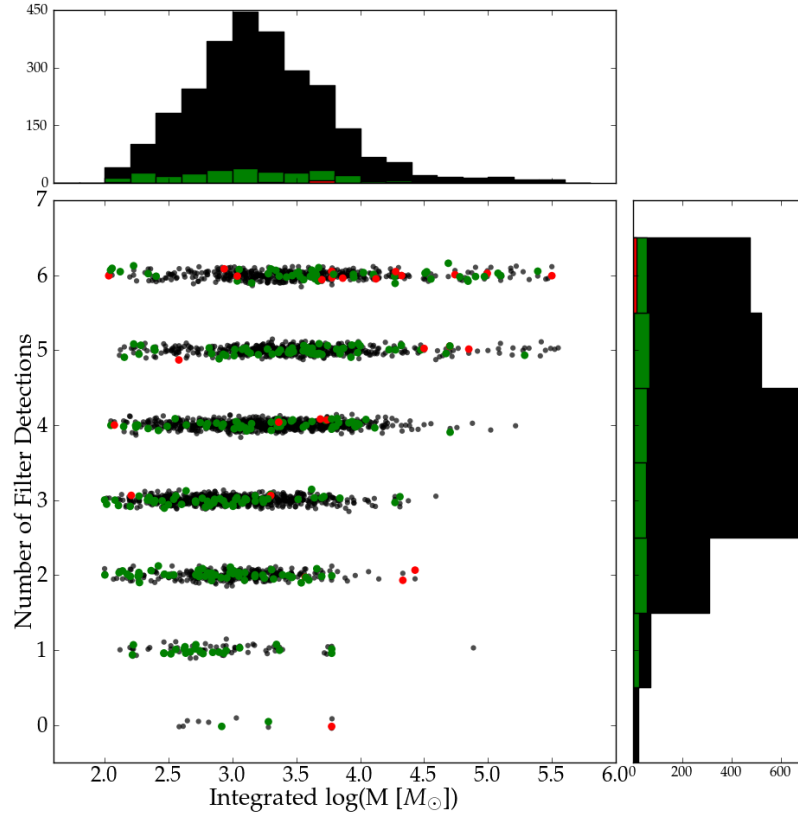


Figure 3.12 Integrated $\log(M)$ versus the number of filter detections where all flagged clusters are shown in red. Histograms on sides show distributions of each. A small amount of Gaussian scatter was added in the y -direction for clarity.

3.3 Analysis of Results

From here forward, we use the final adopted ages and masses in Table 1 to investigate properties of the cluster distributions. We first characterize the broad properties of the cluster sample. We then consider how these properties would change if only integrated measurements were available, as is the case for studies of more distant cluster populations.

3.3.1 Age and Mass Distributions

Now that we have ages and masses assigned to each cluster, we can look at the global distributions of these properties. In Figure 3.13 we show the final results for age versus

mass, color-coded by A_V . There is a large range in both age and mass for our cluster sample, getting down to a few hundred solar masses, much lower than in other extragalactic cluster samples. We see that there are no old, low mass clusters as expected from models of cluster dissolution (e.g., Bastian & Goodwin, 2006), and even if they do exist, they would likely fall below our detection limit. We also find no old highly reddened clusters, whereas young clusters have large range of extinction, which is consistent with them often being located in gas rich regions with active star formation. Additionally, we do not observe any young massive clusters, which we should have detected if they actually exist. This could indicate M31 was more efficient at forming massive clusters in the past.

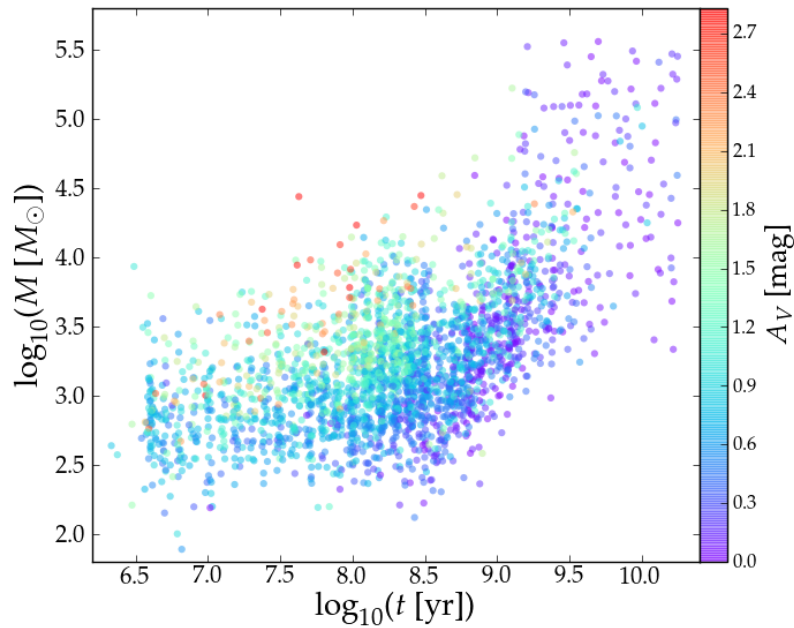


Figure 3.13 Age versus mass for the final cluster results, color-coded by extinction.

In Figure 3.14 we show the cluster locations on a background GALEX NUV image,

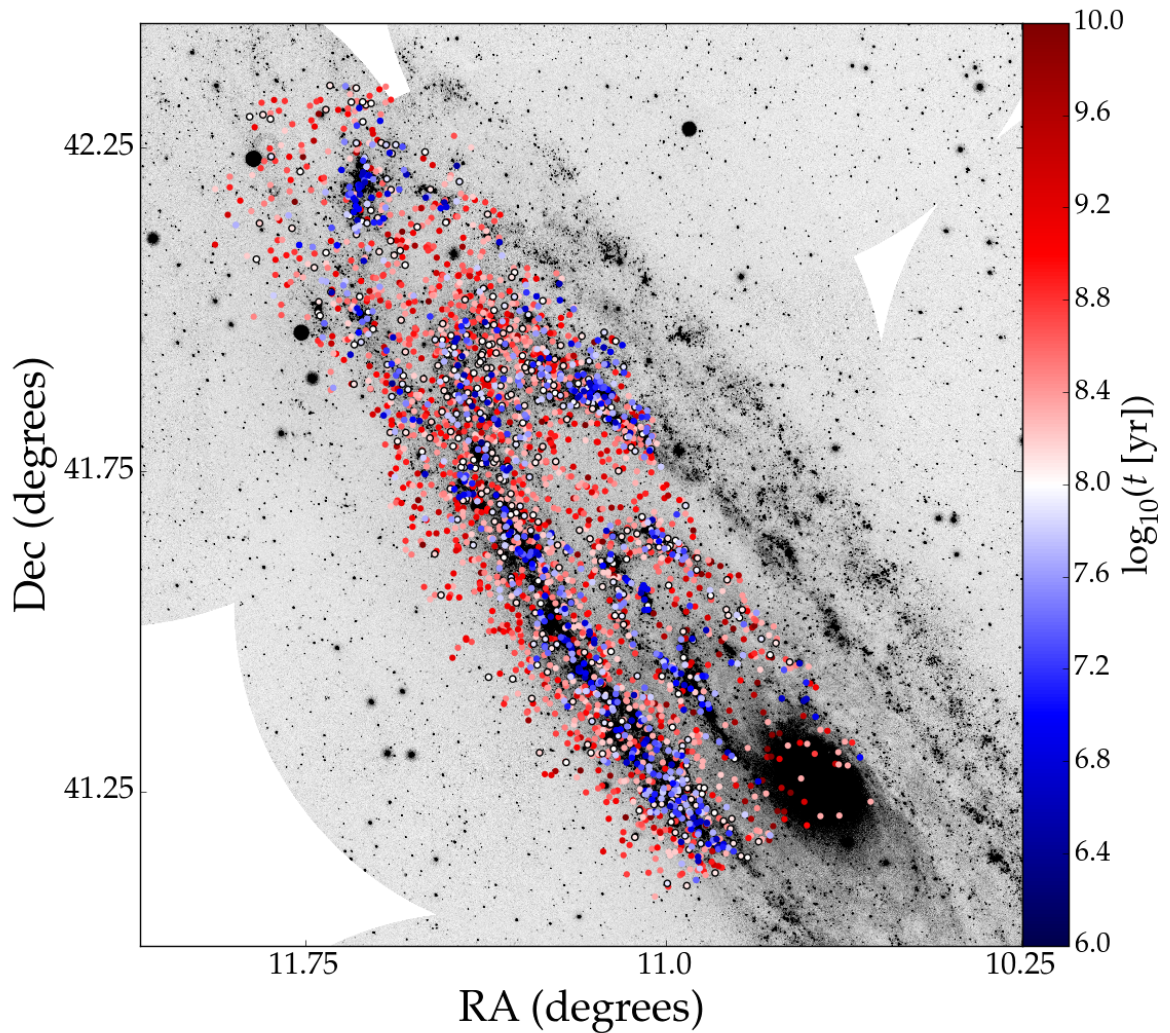


Figure 3.14 PHAT cluster locations shown on the GALEX NUV image, where the clusters are color-coded by age. The youngest clusters (blue) lie mostly along the 10 kpc star-forming ring.

where the clusters are color-coded by age. The youngest clusters, shown in blue, trace the 10 kpc star-forming ring, while clusters found in the bulge region are older. Figure 3.15 shows the cluster locations color-coded by mass, where more massive clusters are in red. The massive clusters lie predominantly in the bulge, while lower mass clusters are spread

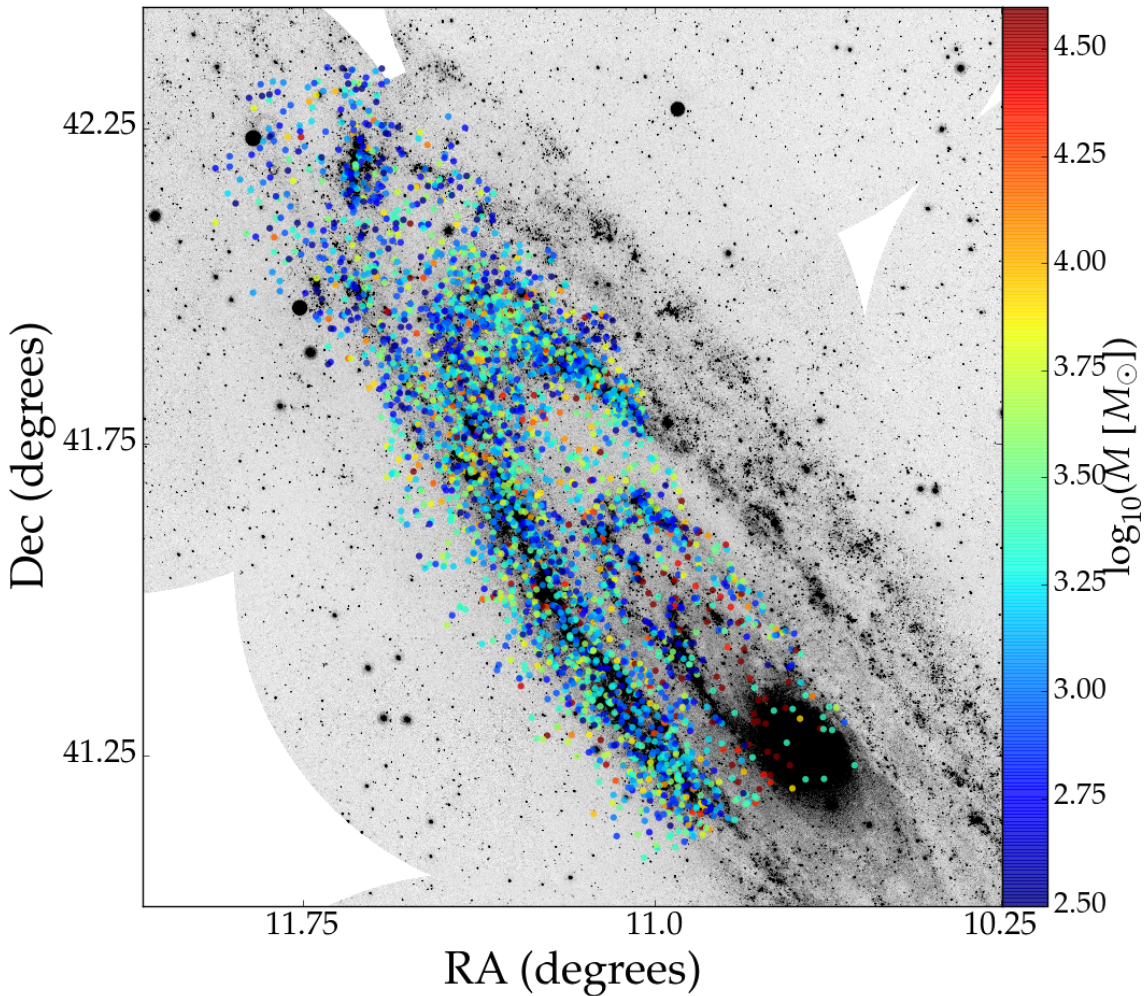


Figure 3.15 PHAT cluster locations shown on the GALEX NUV image, where the clusters are color-coded by mass. The massive clusters (red) lie mostly in the bulge, while lower mass clusters are spread throughout the disk.

throughout the disk. Figure 3.16 shows the cluster locations color-coded by extinction, over the M31 dust map. The more reddened clusters, shown as darker red, are mostly coincident with dusty regions, as expected.

In Figure 3.17 we plot the present day age distribution (top panel - number of clusters

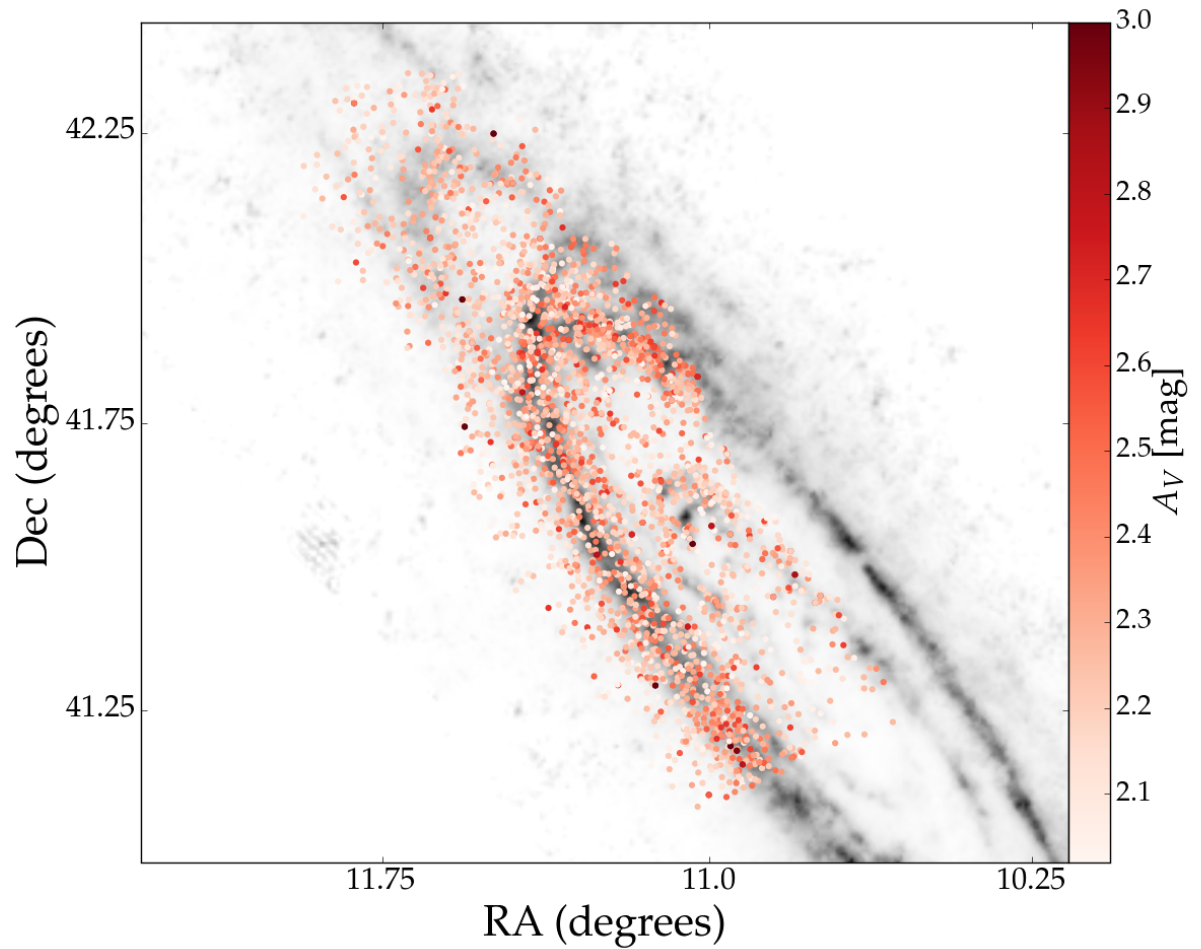


Figure 3.16 PHAT cluster locations shown on the dust map (Draine et al., 2007) image, where the clusters are color-coded by extinction. The more reddened clusters (red) are mostly coincident with dusty regions.

per age bin, scaled by the width of each bin) and mass distribution (bottom panel - number of clusters per mass bin, scaled by the width of each bin). Figure 3.18 shows the age distribution for several slices in cluster mass, and Figure 3.19 shows the mass distribution for several slices in cluster age. These are marginal distributions, meaning that the age distribution is summed up over all masses and extinctions, and the mass distribution is

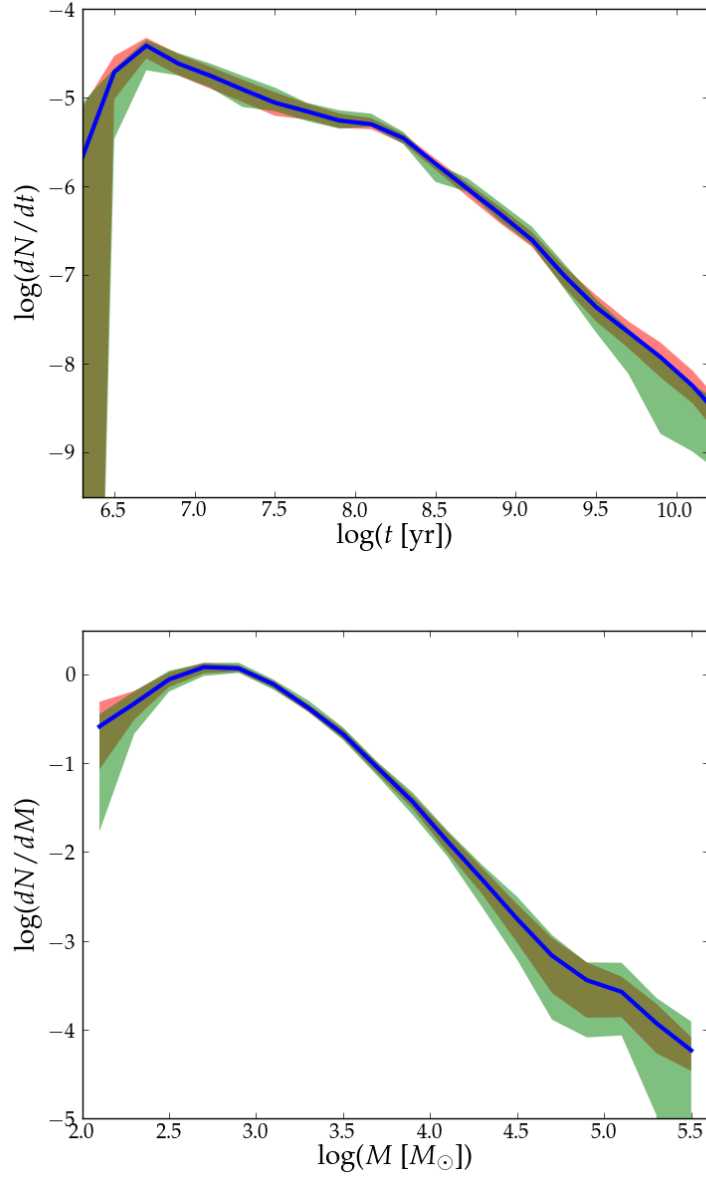


Figure 3.17 Present day age distribution (top panel) and mass distribution (bottom panel) as a function of cluster mass for the entire cluster sample. Orange shaded regions represent uncertainties that arise from uncertainties in the parameter fits, and the green shaded regions represent the uncertainties from the bootstrap resampling as described in the text.

summed up over all ages and extinctions.

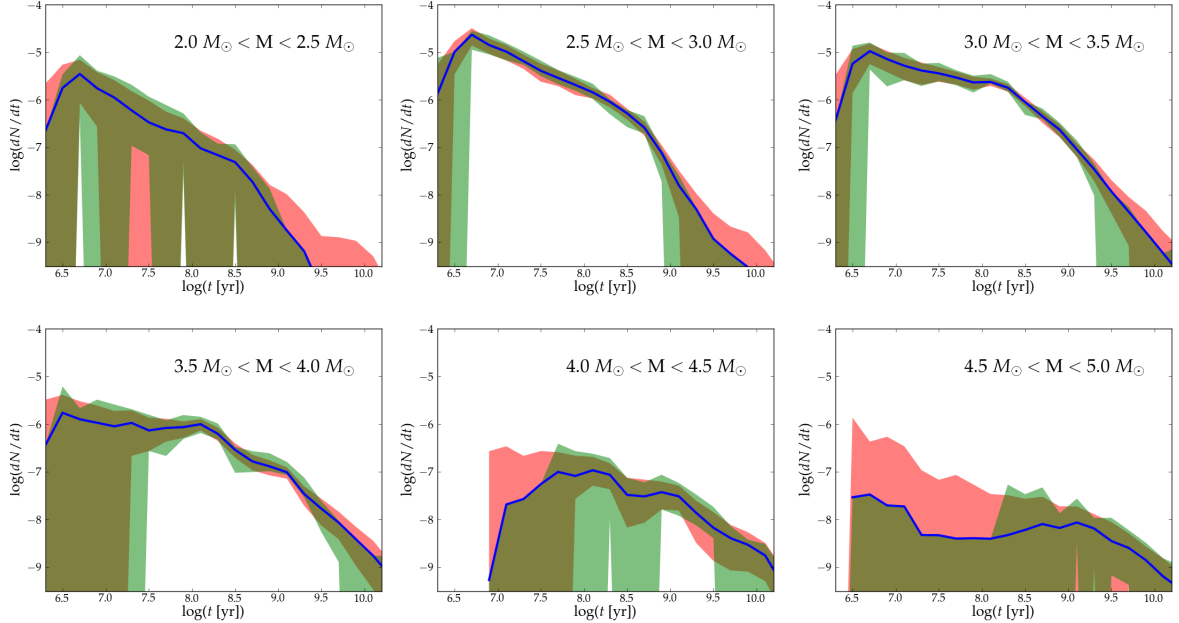


Figure 3.18 Present day age distribution as a function of cluster age for several slices in cluster mass. Orange shaded regions represent uncertainties that arise from uncertainties in the parameter fits, and the green shaded regions represent the uncertainties from bootstrap resampling.

There are two main sources of uncertainty when calculating these distributions: uncertainty in the fitting procedure and uncertainty in the random sampling of clusters. To account for the first, we make use of the information in the PDFs of each cluster. Using only a best fit value would not yield an accurate global distribution since many clusters have wide or multiple peaked PDFs. Additionally, summing the PDFs for each individual cluster assumes the PDFs are Gaussian, which is often not accurate. Instead, we draw 1000 Monte Carlo samples from the PDF of each cluster. We then calculate the mean and the standard deviation of the Monte Carlo draws for each cluster. These means are binned in equal log spacing in age and mass to come up with the distributions shown, where the binned value for the means are represented by the blue lines, and the minimum and maximum values, representing the fitting uncertainties, are shown as the red regions. These fitting uncertain-

ties are shown as the red regions in the distribution plots and tend to be lower than the sampling uncertainties.

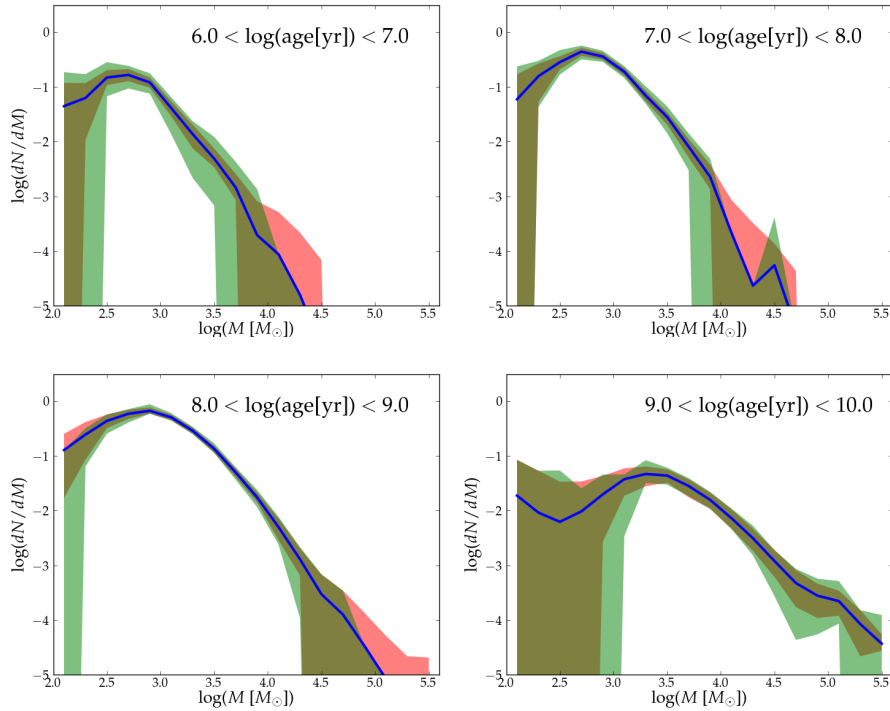


Figure 3.19 Present day mass distribution as a function of cluster age for several slices in cluster age. Orange shaded regions represent uncertainties that arise from uncertainties in the parameter fits, and the green shaded regions represent the uncertainties from the bootstrap resampling as described in the text.

To assess the sampling uncertainties due to the finite number of clusters, we perform bootstrap resampling, where we draw a random realization of the cluster sample 1000 times (e.g., Fouesneau et al., 2014). We derive the age and mass distributions for each of these realizations, and we take the minimum and maximum of these distributions as the sampling uncertainties, which are shown as the green shaded regions. The sampling uncertainties are largest where there are fewer clusters, namely at older ages and at the high and low mass ends. For the mass distribution, sampling uncertainty dominates the parameter uncertainty for the whole distribution, since the mass determinations are fairly well constrained as

compared to the age determinations.

For the the age distribution, we see that uncertainties in the parameter fits dominate at the youngest ages, while sampling uncertainties dominate at the oldest ages, where there are few clusters. Sampling uncertainties also dominate at the poorly populated high mass end, while the two sources of uncertainty are similar in scale for the lower mass clusters.

The present day age distribution depends on several physical effects: the cluster formation history, cluster dissolution, and selection effects. The decline in the number of clusters at older ages is most likely a combination of these effects. These distributions are largely power laws, and are broadly consistent with expectations and results of the smaller Foesneau et al. (2014) sample. There is a roll over to low masses/ages consistent with sample incompleteness. Distributions will be analyzed completely in Foesneau et al (in prep). Note that these are the complete observed distributions, and are not corrected for completeness, which also explains the large sampling uncertainties. The sample is highly complete for $M < 10^{3.2} M_{\odot}$ and $t > 10$ Myr. The turnover seen at lower masses and ages is in incomplete region, therefore the validity of this turnover is inconclusive. A full analysis of cluster dissolution will be presented in Foesneau (in prep).

3.3.2 Using Integrated Cluster Photometry at Larger Distances

Most extragalactic systems are too distant for us to resolve their individual stars, and thus only have integrated photometry available. Now we revisit the results from the previous section and investigate how they would have changed had we only used integrated photometry.

In Figure 3.20 we show the overall marginalized age and mass distributions for the integrated fits only. Figure 3.21 shows the integrated age distribution for several slices in cluster mass, and Figure 3.22 shows the integrated mass distribution for several slices in cluster age. The uncertainties were calculated as described in Section 3.3.1.

We can compare these figures directly with Figures 3.17, 3.18, and 3.19 to see how the inferred distributions would change given only integrated fitting results. The overall age distributions both show evidence for a turnover at the youngest ages, although this is in an

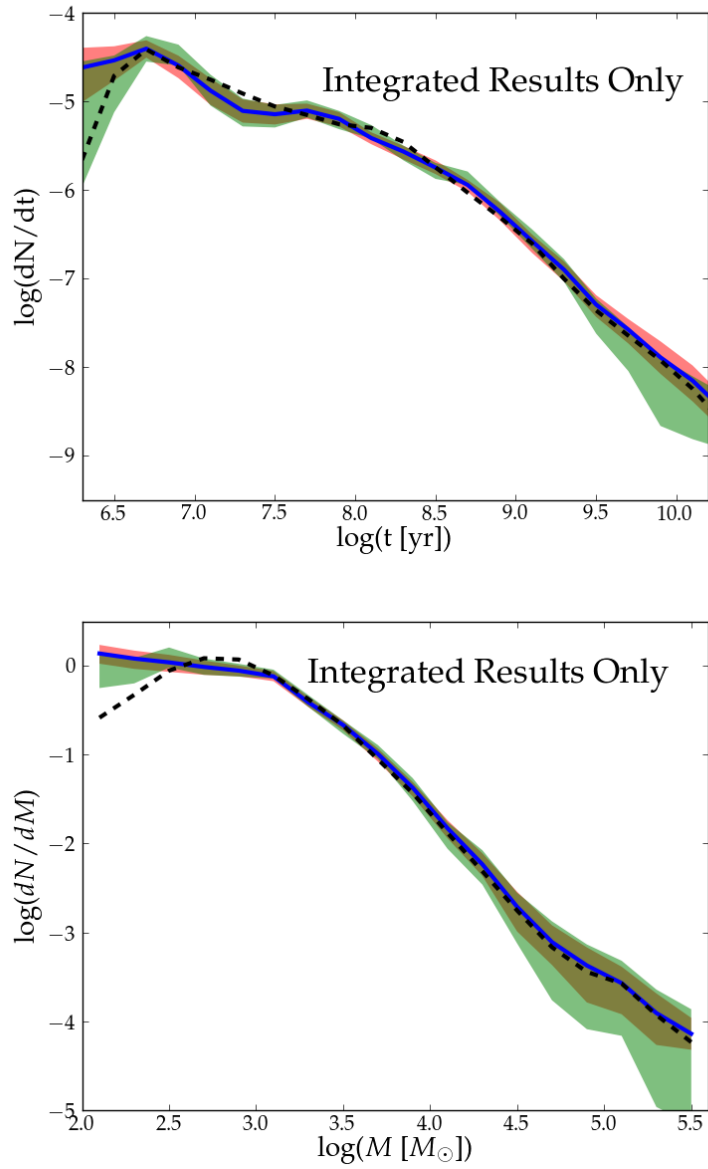


Figure 3.20 Present day age distribution (top panel) and mass distribution (bottom panel) as a function of cluster mass using only the results of the integrated light fitting. Orange shaded regions represent uncertainties that arise from uncertainties in the parameter fits, and the green shaded regions represent the uncertainties from the bootstrap resampling as described in the text.

incomplete region. The integrated age distribution shows a dip around 20-30 Myr that the age distribution in Section 3.3.1 does not show. In Figure 3.21 we see that the dip in the age distribution between 10 and 100 Myr is primarily from clusters $< 10^3 M_\odot$. These young low mass clusters are strongly affected by stochasticity. However, such clusters will be too faint to be detected in more distant samples.

The overall mass distributions are similar to each other in the region where we are complete (above $10^{3.2} M_\odot$), however the mass distribution in Section 3.3.1 shows a turnover at the lowest masses, while the integrated mass distribution appears flat for the mass range below $\sim 10^{3.2} M_\odot$. Figure 3.22 shows that the mass distribution for the youngest clusters appears to turn over at low masses, similar to what is seen in the overall distribution for the fiducial distribution. However for ages between 10 Myr and 1 Gyr the distributions appear to be flat at the lowest masses.

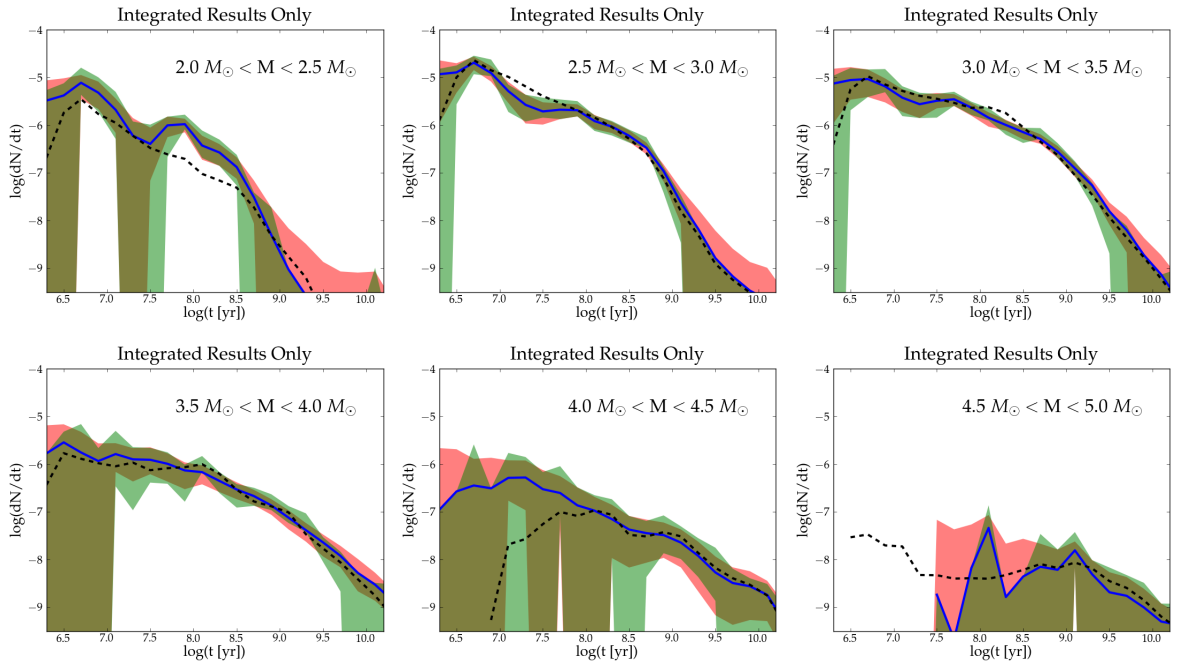


Figure 3.21 Present day age distribution as a function of cluster age for several slices in cluster mass using the results of the integrated light fitting. Orange shaded regions represent uncertainties that arise from uncertainties in the parameter fits, and the green shaded regions represent the uncertainties from the bootstrap resampling as described in the text.

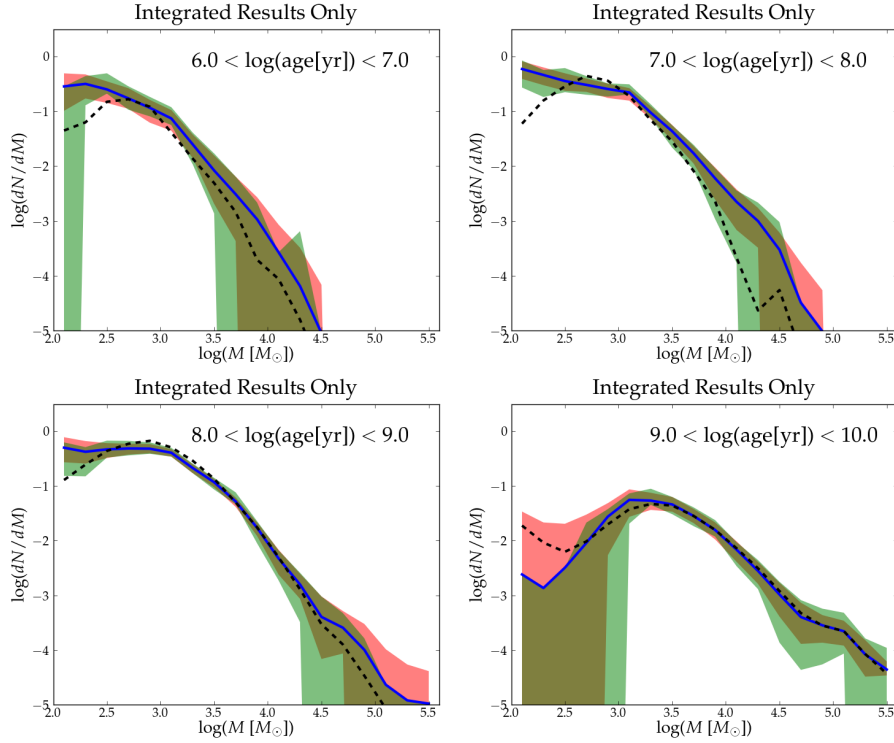


Figure 3.22 Present day mass distribution as a function of cluster mass for several slices in cluster age using the results of the integrated light fitting. Orange shaded regions represent uncertainties that arise from uncertainties in the parameter fits, and the green shaded regions represent the uncertainties from the bootstrap resampling as described in the text.

In Figure 3.23 we show the difference in density between our fiducial results for the cluster sample and the integrated light results in each age-mass bin scaled by the square root of the number of clusters in each bin. From this plot we can investigate which regions of parameter space change when we have only integrated light measurements. At older ages, there is not much difference between the integrated results and the results from Section 3.2.3.c since we used the integrated results for most clusters older than 300 Myr. At younger ages, the integrated results under predicts the number of intermediate mass clusters at 100 Myr. It also predicts fewer clusters of $\sim 1000 M_\odot$ overall, and a slightly larger number of very low mass ($\sim 200 M_\odot$) clusters.

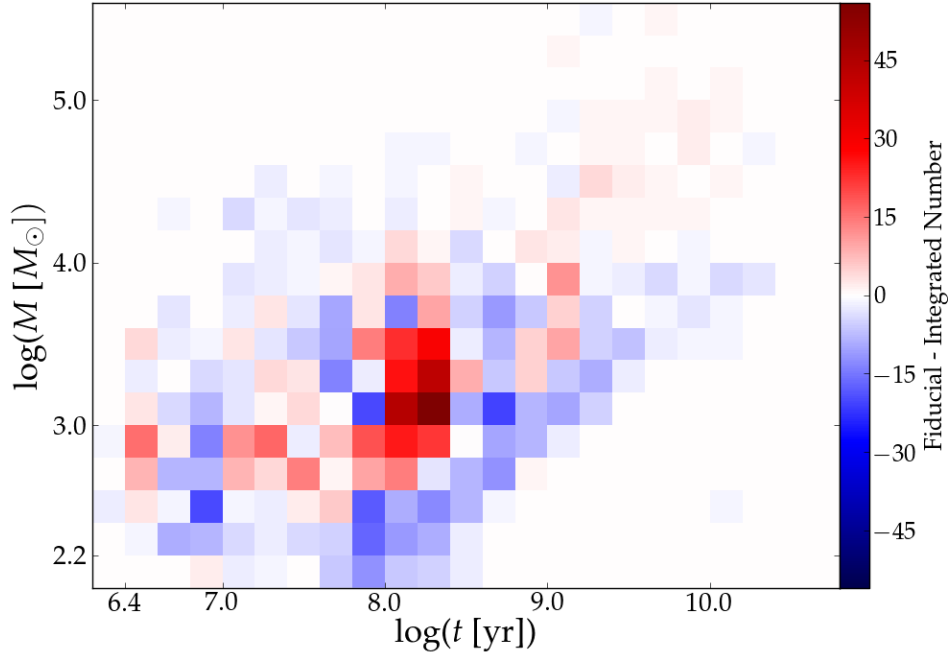


Figure 3.23 Difference (optimal - integrated) in the number density between our fiducial results for the cluster sample and the integrated light results in the age-mass parameter space, where red is where there are more of the fiducial clusters in that bin and blue is where there are more integrated clusters in that bin.

3.4 Conclusions

We calculate ages, masses, and extinctions for 2753 clusters in the PHAT cluster sample using two methods: CMD fitting and fitting integrated photometry to discrete models. Tests on synthetic clusters show that the CMD fitting method recovers the parameters well for most clusters. We did a by-eye check of which method is most accurate for each cluster and used this as our determination for the parameters. Clusters in the sample range from a few hundred to $10^5 M_{\odot}$, 6 Myr - 10.2 Gyr, and 0 - 3 A_V . This represents a large range in cluster properties, and allows us to use this sample for many studies of clusters that require completeness over a large mass range.

In general, we find that for clusters less than about 300 Myr, the CMD fitting method

is most accurate. For clusters older than this, many of their stars have evolved off the main sequence, and the turnoff falls below our detection limit, making it difficult to accurately fit models to the CMD. In contrast, integrated models do a better job when clusters are older and stochastic effects are not as drastic.

We plot the present day age and mass distributions for the cluster sample, utilizing Monte Carlo techniques to account for uncertainties in the parameter determinations as well as the sampling. These distributions show a lack of young massive clusters as well as old, low mass clusters. Comparison to the integrated light only distributions shows that the general trends are recovered well, while there may be some differences in incomplete regions of parameter space.

Chapter 4

INVESTIGATING THE LIFE CYCLE OF MOLECULAR CLOUDS IN THE ANDROMEDA GALAXY

In this chapter I use the ages of the PHAT cluster sample found in the previous chapter as an age tracer to determine the timescales of each evolutionary phase for molecular clouds in M31.

Molecular clouds are the precursors to stars, which are the building blocks of galaxies. Understanding the life cycle of molecular clouds is important in understanding the physics of star formation, the dynamics of the ISM, the evolution of galaxies, and the origin of low star formation efficiencies. However, in their recent review of star formation in the Milky Way and nearby galaxies, Kennicutt & Evans (2012) identify robust constraints on the ages and lifetimes of star forming clouds as a key unknown in the subject of star formation in the Milky Way and nearby galaxies. Answering this question is challenging, and requires both a large sample of clouds at a high resolution and a suite of equally high resolution resolved star formation indicators.

4.1 Cloud Lifetimes

There have been attempts to quantify the total lifetime of giant molecular clouds (GMC, mass: $10^4 - 6 \times 10^6 M_{\odot}$, radius: 10 - 100 pc) in terms of their internal dynamical timescales. The lifetime could be a single dynamical time, as suggested by Elmegreen (2000), or several dynamical times, as proposed by Tan et al. (2006). Observationally, most estimates of cloud lifetimes have been in the 20-30 Myr range, which is much longer than the free fall time for a GMC. In the Milky Way (MW), several studies have led to an estimate for the cloud lifetime of $\sim 17-40$ Myr (Blitz & Shu, 1980; McKee & Ostriker, 2007; Murray, 2011). Estimates of cloud lifetimes in extragalactic studies in the LMC, M33, and M51 have also agreed well with the MW estimates and range from 20-40 (Kawamura et al., 2009; Blitz et al., 2007; Mizuno et al., 2001; Yamaguchi et al., 2001; Fukui et al., 1999; Miura et al., 2012; Meidt

et al., 2015). Additionally, these timescales may not be universal as there is some evidence that more molecular rich galaxies have longer lasting GMCs (Koda et al., 2009) and smaller molecular clouds have shorter lived clouds (Murray, 2011).

Beyond these global timescale estimates, there have been further efforts to determine the timescales for the various evolutionary phases through which a cloud passes. In Figure 4.1 we show an illustration of these evolutionary phases. The first phase is the pre-stellar phase, where a molecular cloud exists before it forms stars. In this phase the molecular gas will be observed but no star formation indicators seen. Next, star formation begins deep within the cloud and suffers from heavy extinction in the optical. Infrared (IR) and radio continuum emission are typical indicators of embedded star formation. The young stars emit lots of radiation ionizes the surrounding gas which we see as $H\alpha$ emission. The stars become exposed and for a time we can observe both the young stars and their parent cloud coincidentally. Once a molecular cloud forms massive stars, these stars are very destructive to their host clouds. After feedback from these stars disrupts the cloud, we only observe the young stars not surrounded by any gas.

Molecular Cloud Life Cycle

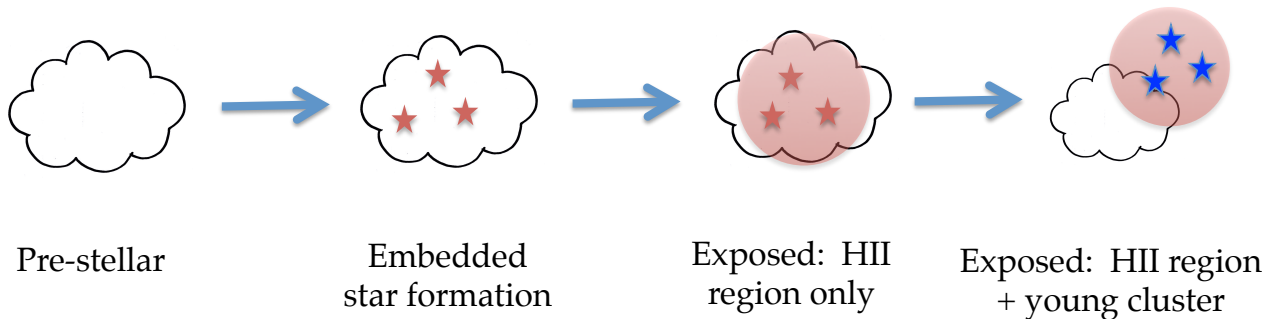


Figure 4.1 The evolutionary stages in the life cycle of a star forming molecular cloud: pre-stellar, embedded star formation, exposed star formation - HII regions, and exposed star formation - HII regions and young clusters.

To determine the timescales of these evolutionary phases, several extragalactic studies have looked at large samples of molecular clouds within a galaxy and associated them with star formation indicators. They assume an evolutionary process where all giant molecular clouds form stars, and consist of several evolutionary phases. Some of the studies then infer the time of each phase by assuming that the number of clouds in each state is proportional to the time spent in that state and comparing to clusters with age determinations. Different studies have slightly different definitions of each phase and different star formation tracers they are using which leads to some additional uncertainty.

4.1.1 Embedded Star-Forming Phase

Observing the percentage of clouds that do not show any signs of star formation gives us some indications of the length of the clouds' pre-stellar phase. Estimates of this first stage of a cloud's life still remain uncertain and this has prompted some debate (e.g., Elmegreen, 2000; Hartmann et al., 2001; Tassis & Mouschovias, 2004). Several Milky Way (MW) studies have shown that it is rare to observe a giant molecular cloud that is not currently forming massive stars (e.g., Maddalena & Thaddeus, 1985; Blitz, 1991, 1993; Williams & McKee, 1997), which implies a very short pre-stellar lifetime, <3 Myr. However, additional observations have shown that the temperatures of many MW molecular clouds indicate that they are not star-forming, therefore non star-forming clouds in the Milky Way may not be as rare as once thought (Chiar et al., 1994; Longmore et al., 2013).

Since a global catalog of MW clouds is difficult due to velocity crowding, we need to look externally to get an accurate total age of star forming clouds. Extragalactic studies that quantify the percentage of molecular clouds in a galaxy that are not forming stars vary from 1% up to 26% with calculated pre-stellar lifetimes from 1 to 6 Myr (Kawamura et al., 2009; Mizuno et al., 2001; Yamaguchi et al., 2001; Fukui et al., 1999; Gratier et al., 2012; Miura et al., 2012) . This seems to depend on the resolution of the study, where studies that resolve individual clouds (tens of parsec resolution) have the larger percentage of non star forming clouds.

The next evolutionary stage is the embedded star forming phase. This phase is generally

thought to be very short, less than 3 Myr (Lada & Lada, 2003). In the LMC, Kawamura et al. (2009) find no evidence for embedded star formation, indicating a very short timescale. However, in M33, as much as 33% of the sample was classified as having embedded star formation (Gratier et al., 2012), which would indicate a more substantial fraction of a clouds life is spent in this stage. These studies used different tracers (radio continuum in the LMC and mid IR in M33), which could explain some of the difference in amount of embedded star formation.

4.1.2 Exposed Star Formation Phase

The exposed star forming lifetime can be split up into two categories: clouds with only HII regions, and those with both HII regions and young clusters. This first exposed phase is more uncertain than the previous phases, where extragalactic studies have found the percentage of clouds in a population with only HII regions ranging from 20% - 50% and estimates of this timescale are from 3-13 Myr. Some of this uncertainty could be due to how this evolutionary phase is defined in various studies, since some studies only count small HII regions for this phase (Fukui et al., 1999; Kawamura et al., 2009) while others include any HII region (Miura et al., 2012) and others also include UV emission as an indicator of this phase (Gratier et al., 2012).

The second category of the exposed star formation phase is when molecular clouds have associated young star clusters/associations, many times along with HII regions. The estimates for this timescale are somewhat uncertain, and range from 5 Myr to 30 Myr (e.g., Leisawitz et al., 1989; Hartmann et al., 2001; Bastian & Strader, 2014). Population studies in extragalactic systems find a large range in the percentage of clouds in this phase from 26% to 45% when including clusters up to 10 Myr (Kawamura et al., 2009; Miura et al., 2012). Additionally, Miura et al. (2012) included a category for clouds with clusters from 10-30 Myr old that also had HII regions, and found 45% of all clouds in this category, indicating that clouds can live up to 30 Myr after forming a cluster.

4.1.3 GMC Dependence

Another open question is how star formation depends on various GMC properties. There is some evidence for preferential star formation in more massive clouds, clouds with smaller line widths, and those closer to virial equilibrium in IC342 (Hirota et al., 2011). However, these effects were not seen in the LMC, where the only difference between non star forming and star forming clouds was that the non star forming GMCs showed lower peak CO brightness Hughes et al. (2010).

While there is general agreement for an overall lifetime of 20-30 Myr, the timescales of individual phases remain uncertain. The fraction of clouds that are observed as star forming, and in turn the respective phases, may be dependent on resolution and/or galactic environment. Higher resolution studies find a longer pre-stellar timescale, although there is agreement that this timescales is less than 10 Myr. The embedded timescale is thought to be short, <3 Myr. The exposed phases are a bit more uncertain while some studies indicate clusters do not spend much time associated with their parent cloud (<5 Myr), others find clusters and HII regions up to 30 Myr old still associated with molecular gas. Additional high resolution studies of molecular clouds and star formation tracers are needed to make further progress in this area.

4.1.4 Molecular Clouds in M31

M31 is an ideal environment in which to study the relationship between molecular clouds and star formation since it is the closest large spiral galaxy to our own, at a distance of 785 kpc (McConnachie et al., 2005). We can obtain a less biased sample than in the Milky Way, where distances can be very uncertain and dust blocks many clouds from our sight, but in a regime that is similar to the MW in metallicity, gas content, and current star formation rate. M31 is also quite different from the other extragalactic systems that have been studied in detail. It has a higher metallicity and lower star formation rate efficiency than the LMC and M33, and will allow us to extend our knowledge of molecular cloud timescales to this regime.

Traditionally surveys of molecular gas have not had the angular resolution to resolve

Table 4.1. LMC and M33 Cloud Classifications and Timescales

Star Formation Indicators	LMC ^a		M33 ^b		M33 ^c
	Percentage	Timescale	Percentage	Timescale	Percentage
No indicators	24%	6 Myr	1%	1 Myr	17%
IR emission only	–	–	–	–	33%
HII region only	50%	13 Myr	20%	3-7 Myr	48%
HII region and <10 Myr cluster	26%	7 Myr	45%	5-10 Myr	–
HII region and 10 Myr < cluster < 30 Myr	–	–	34%	8-17 Myr	–

^a(Kawamura et al., 2009). Did not look for tracers in the IR but did look for embedded clusters in the radio continuum, and found no evidence for this phase.

^b(Miura et al., 2012). Included 24 μm emitting clouds in the second classification rather than separating these out. Did note that most 24 μm emitting sources also had HII regions.

^c(Gratier et al., 2012). Searched for embedded star formation in 8 μm and 24 μm images. Searched for exposed star formation in FUV and H α images. Did not look for associated young clusters or calculate statistical lifetimes.

individual clouds. With modern telescopes such as CARMA and ALMA, high resolution studies of extragalactic molecular clouds are now possible. Previous cloud studies in M31 include Nieten et al. (2006), which had a resolution of ~ 90 pc, and therefore could not resolve individual molecular clouds, and Rosolowsky (2007), which had a higher resolution (25 pc) but did not look at the relation between the clouds and clusters or other star formation indicators. More recently the Herschel Exploitation of Local Galaxy Andromeda (HELGA) (Kirk et al., 2013) used a dendrogram analysis of Herschel 350 μm maps to identify 236 GMCs in M31, although they indicate that the Herschel resolution is probably picking up giant molecular associations (larger scale compositions of several GMCs), rather than clouds, since their resolution is 93 pc.

To associate individual clouds with their star formation properties, we require a survey at the resolution of individual clouds (< 40 pc). With its resolution of ~ 20 pc, the CARMA Survey of Andromeda (Schruba et al, in prep) allows us to identify individual molecular clouds, rather than just giant clouds or associations, and investigate their properties to

derive timescales for each phase.

In M31 we take advantage of several other high resolution data sets that allow us to classify each cloud with a particular evolutionary phase depending on which tracers are associated with it. The Massey Local Group survey has high resolution $H\alpha$ imaging which allow us to see HII regions of massive star formation (Massey et al., 2006). Additionally, high resolution Spitzer IRAC and MIPS data for several IR passbands allows us to identify clouds that have potentially embedded star formation (Barmby et al., 2006; Gordon et al., 2006). Finally, the PHAT survey has extremely high resolution and large spatial area (covers 1/3 of M31’s star forming disk) in six broadband filters allowing over 100 million stars to be resolved (Dalcanton et al., 2012). From this, the largest uniform extragalactic cluster sample (about 3000 clusters) was identified (Johnson et al., 2015).

In this chapter, we combine the molecular cloud sample from the CARMA Survey of Andromeda with a variety of star formation tracers to measure the fraction of molecular clouds in each evolutionary phase. In Section 4.2 we describe the molecular cloud and PHAT cluster samples, along with the other data used as star formation indicators. We compare the distributions of the cloud and cluster samples in Section 4.3.1. In Section 4.3.2 we calculate the percentages of clouds that are in each phase by observing the molecular cloud distribution and its relation to star formation indicators. We investigate the distributions of molecular cloud properties in Section 4.3.3. Next we calculate statistical lifetimes for each evolutionary phase in Section 4.3.4. Then, in Section 4.3.5, we compare our observational results to a Monte Carlo simulation of molecular clouds and star formation, which puts constraints on the characteristic cloud disruption time. Finally, we discuss uncertainties and biases in Section 4.3.6 and then compare this study to the LMC and M33 studies in Section 4.3.7.

4.2 Data: Clouds and Star Formation Indicators

4.2.1 Cloud Catalog

We use the molecular cloud catalog from the CARMA survey of Andromeda (Schruba et al, in prep) in the ^{12}CO ($J = 1-0$) line at 2.6 mm. The resolution of the CARMA data is 5.5

arcsec (~ 20 pc at the distance of M31), and 2.5 km/s, which is sufficient to resolve individual GMCs. Clouds were identified using the CPROPS routine, which first locates peaks in the CO emission, then associates neighboring voxels to the local peaks down to an intensity at which the voxel brightness isocontour merges with the one of a neighboring peak, and finally determined the properties of those connected sets of voxels (i.e., the clouds). For a detailed description of CPROPS, see Rosolowsky & Leroy (2006). The range of cloud masses in the sample is $\sim 10^4 - 10^6 M_\odot$. About 1/3 of the total CO emission is contained within the catalog, while 1/3 is contained within 50 pc of the edge of the clouds and the remaining 1/3 is diffuse.

4.2.2 Cluster Sample

To age-date stellar populations that may be associated with molecular clouds, we use stellar clusters from the PHAT survey (Johnson et al., 2015). Since many young clusters are disrupted within a short amount of time after forming (Lada & Lada, 2003), they may not be the ideal star formation tracer if molecular clouds are long-lived. For the likely timescales of < 30 Myr, we would expect many star forming molecular clouds to potentially host a clustered stellar population. However, if cluster disruption occurs extremely quickly with respect to the clouds, this may not be the ideal tracer to use, which is why we also include H α images, as described in the next section.

PHAT was a four year HST survey of M31 in 6 filters, covering the UV, optical, and NIR (Dalcanton et al., 2012). From these data, clusters were identified as part of a citizen science program, where users performed a by-eye search of all the optical PHAT images to identify potential clusters. The final sample extends to very low masses ($< 10^3 M_\odot$), and is 50 percent complete down to $500 M_\odot$ for clusters younger than 100 Myr. Many of these clusters may not be gravitationally bound, but they are all smaller than typical large OB associations, which are > 10 pc (Johnson et al., 2015).

The PHAT cluster catalog has a well-characterized completeness function. It is highly complete at $M > 10^{3.2} M_\odot$, $t > 10$ Myr, but there are some issues at low masses and young ages that must be considered when associating the sample with molecular clouds. First, the

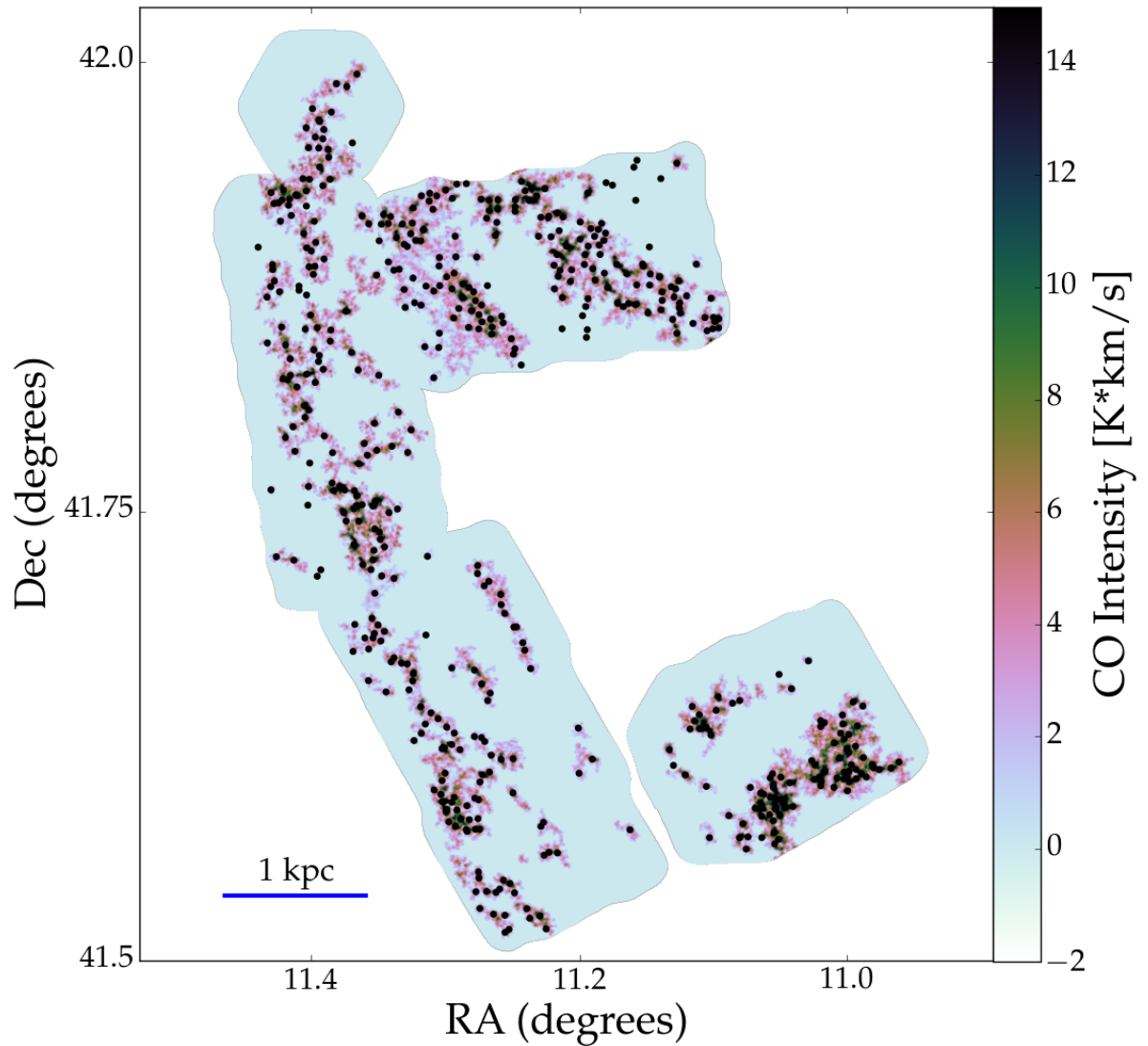


Figure 4.2 CO integrated intensity map (signal masked) from the CARMA Survey of Andromeda, overplotted with points identifying the clouds in the catalog.

youngest (<10 Myr) clusters may be deeply embedded within their molecular cloud, and thus may not be visible in the optical images used for cluster selection. Second, clusters are more likely to be missed in the crowded inner regions of the galaxy. Third, for ages

<100 Myr, completeness is high to lower masses for younger clusters, due to there being more stars on the main sequence, making the cluster easier to identify. For the youngest (<10 Myr) clusters especially, completeness becomes an issue since many of these are still embedded within their molecular gas clouds and identification of clusters was done with optical images. See Johnson et al. (2015) for further analysis of cluster completeness.

We determined cluster ages from color magnitude diagram (CMD) fitting of the resolved stars within each cluster (Beerman et al, in prep). The CMD fitting was done using the MATCH program (Dolphin, 2002), which simultaneously fits a grid of models in age, mass, and extinction to the CMD. We used the Padova models (Marigo et al., 2008) for the theoretical isochrones, with updated AGB tracks from Girardi et al. (2010), along with a Salpeter initial mass function (Salpeter, 1955) and a binary fraction of 0.35. We allowed values up to 3.0 mag for extinction, $\log(\text{age/yr})$ from 6.6 to 10.15, and metallicity Z from -0.2 to 0.1 Z_{\odot} .

4.2.3 Additional Star Formation Indicators

Since we are likely missing both dust-embedded young clusters, and extended star forming regions such as in OB associations, we need other reliable tracers of star formation, such as $H\alpha$ and IR emission.

$H\alpha$ is an excellent tracer of recent ($\lesssim 5\text{-}10$ Myr) high mass star formation ($M > 10M_{\odot}$), since these young massive stars emit copious amounts of ionizing radiation. We identified HII regions using the $H\alpha$ image from the Local Group Galaxy Survey (Massey et al., 2006, resolution $\sim 1'' \sim 3.8$ pc). We expect that the $H\alpha$ emission should correlate with the molecular clouds from which the stars were born, if the clouds are still surviving.

In addition to visible massive star formation, we would like to account for possible embedded star formation. Embedded star formation can be very difficult to detect since stars form in the densest part of the molecular cloud, which has the highest extinction. Since embedded star formation would not be evident in the wavelengths of the PHAT filters, we must look at other data sets which are better able to detect embedded star formation, such as the mid-IR.

We used imaging in several IR passbands to search for embedded star formation. We first used Spitzer IRAC images from Barmby et al. (2006), centered at wavelengths of: 3.6, 4.5, 5.6, and 8.0 μm and with resolutions of $\sim 2''$ (~ 7.6 pc). In these images, we look for non stellar point-like sources, which are indicative of embedded star formation, rather than diffuse dust emission that is caused by the reprocessing of the general UV background. The bluest of these filters contains starlight, hot dust emission, and some polycyclic aromatic hydrocarbon (PAH) emission associated with HII regions, whereas the reddest is dominated by PAH emission, presumably heated by the young stars.

24 μm emission is also often used as a star formation indicator, since this also contains reprocessed UV starlight. We obtained the 24 μm Spitzer MIPS image of M31 (Gordon et al., 2006), with a resolution of 6'' (23 pc), to use as a possible indicator for embedded star formation. We classify a cloud as having embedded star formation if there is emission in 24 μm and at least one of the shorter wavelength IRAC images. Note however, that the 24 μm band has contributions from evolved AGB stars, so identifying bright 24 μm emission sources may overestimate the number of star forming regions.

4.3 Classifying Clouds by their Star Formation Indicators

4.3.1 Initial CO-Cluster Comparisons

Before carrying out a full statistical analysis using all of the star formation indicators, we can qualitatively investigate the spatial relationship between the youngest stellar clusters and the molecular cloud population. We would expect to find the youngest clusters near a molecular cloud, since they were recently formed (e.g., Bica et al., 1996; Kawamura et al., 2009). Figure 4.3 shows the CO moment 0 map along with the clusters identified by PHAT, color-coded by their age. The molecular gas is mainly confined to the 10 kpc ring and the inner disk, while the clusters appear to be more uniformly distributed throughout the CO footprint. There are areas where young clusters are spatially associated with a cloud; however, there is also a prominent gap where no clusters are found, near the bottom right of the image. This region is also coincident with strong CO emission. It is possible that there are clusters forming in this area, but they are still embedded within the gas cloud; we

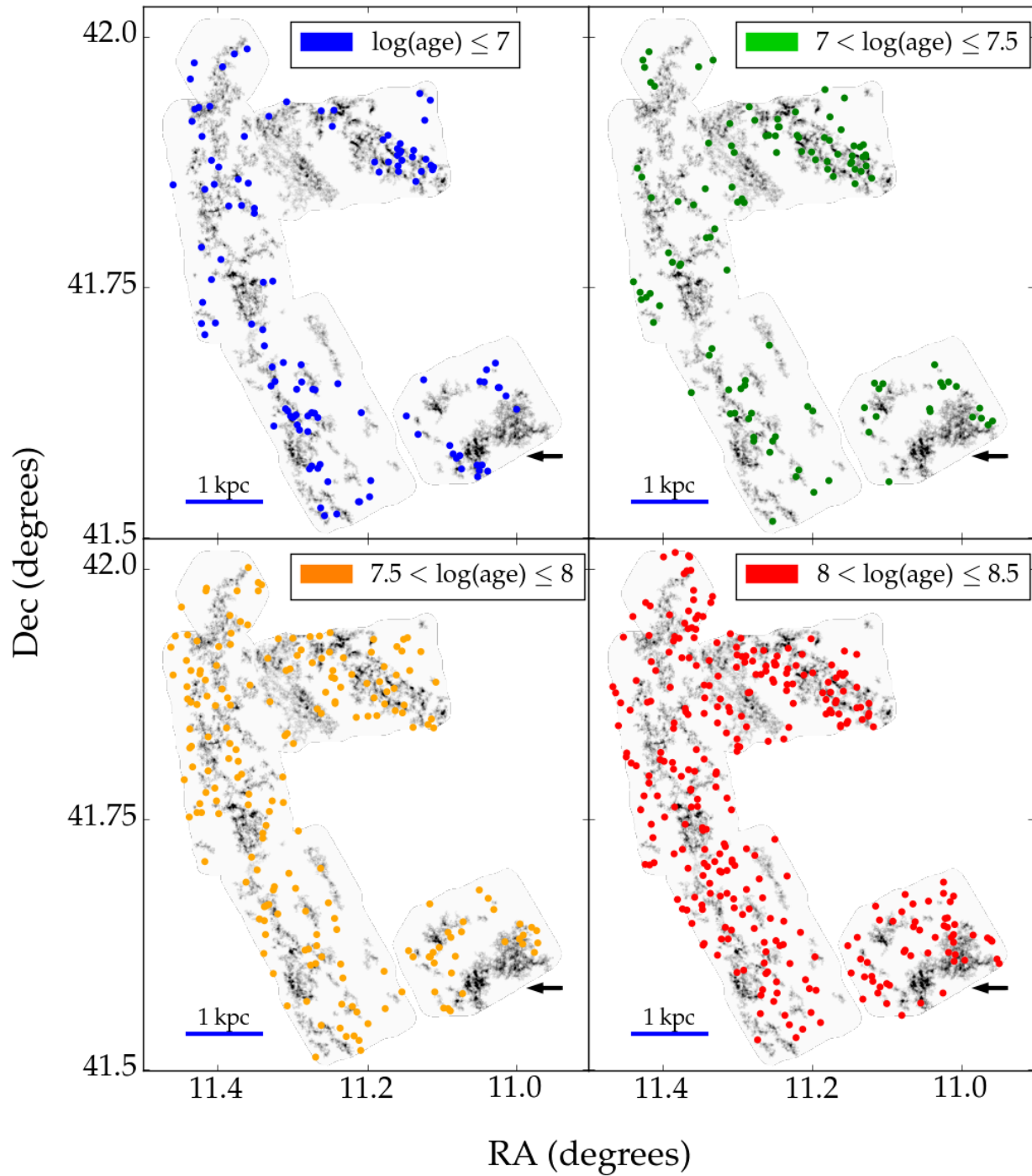


Figure 4.3 CO integrated intensity map from the CARMA survey of Andromeda, overplotted with circles showing the locations of the clusters in the CO footprint, for four cluster age bins.

explore this possibility more in the following section.

To investigate the spatial relationship between the clusters and clouds as a function of cluster age, we measured the distance between each cluster and the nearest molecular cloud, for four different age bins. The distances were deprojected in 2d using $d_{physical}^2 = d_{majoraxis}^2 + (d_{minoraxis}/\cos(i))^2$, with an inclination of $i = 77.7$ degrees and a position angle of 37.7 degrees (Corbelli et al., 2010). Fig 4.4 shows the resulting frequency distributions, with spatial bins of 25 pc, similar to the figures shown in Fukui et al. (1999) and Kawamura et al. (2009). The red line shows the distances to the clusters if the same number of clusters were randomly distributed within the CO footprint. The youngest clusters (<10 Myr) show an enhanced spatial correlation with the clouds, indicating that there are more clusters near molecular clouds than what the random distribution predicts. We find that 69% of young (<10 Myr) clusters are within 100 pc of a cloud, similar to what is seen in the LMC, where 71% of the youngest clusters and associations are within 100 pc of a molecular cloud.

We performed a Kolmogorov-Smirnov (K-S) test for each distribution as compared to the random distribution. Both the youngest ($t < 10$ Myr) age bin and the second youngest ($10 \text{ Myr} < t < 30 \text{ Myr}$) are inconsistent with the expectation for a random distribution at a 95% confidence level (p-value = 1.88×10^{-5} for the youngest age bin and 0.017 for the second youngest age bin). In contrast, the two oldest age bins (with $t > 30$ Myr) are consistent with a random distribution, showing that the spatial correlation disappears for clusters older than ~ 30 Myr.

Because the cluster ages used in Figures 4.3 and 4.4 have associated uncertainties, we have considered whether errors in the age estimates could have affected our results. For example, the second youngest age bin has 118 clusters from 10-32 Myr, and 37% of these have one sigma level uncertainties that could put them into the youngest age bin. To test if possible scattering of clusters from the youngest age bin into the second age bin could have caused the correlation in the second age bin, we removed all clusters from the second age bin whose one sigma uncertainties overlapped with the first bin. When we recalculated the K-S test with just these reliable clusters, the distribution in the second age bin was consistent with a random distribution at a 95% confidence level (p-value = 0.171). It is therefore possible that the second age bin shows a deviation from a random distribution by

containing younger clusters with uncertain ages. Thus, it appears that the spatial correlation between clouds and clusters is erased on 10-30 Myr timescales.

Since these histograms include all clusters (not only massive ones where our cluster sample is complete) we wanted to test for differences when including only clusters in the mass range where our sample is complete. Unfortunately even with a large cluster sample we do not have many young clusters that are more massive than our mass completeness limit of $10^{3.2}$. We plot this as the green histograms over the full sample in each bin. While the results appear consistent with the full sample results, the sample sizes in the two youngest bins are too small to determine whether or not there is a mass dependence.

While the existence of a correlation is quite clear, it is not immediately obvious how it should be interpreted. Clouds themselves are spatially correlated, thus stellar clusters that formed out of one (now dissipated) cloud may be correlated with another cloud with which it does not actually share an evolutionary connection. In light of this, the disappearance of a correlation for $t > 10\text{-}30$ Myr places an upper bound on the cloud lifetimes as well as the lifetimes on which molecular clouds are correlated with each other.

Given the strong correlation of $t < 10$ Myr clusters with molecular clouds, we will use the existence of such clusters as an indicator of star formation for the molecular cloud sample.

4.3.2 Classification of Molecular Clouds Based on Star Formation Indicators

To inspect each of the 478 molecular clouds for signs of star formation, we created postage stamp plots from the following images: CO, H α , 3.6 μm , 5.8 μm , 8 μm , 24 μm , and the F336W, F475W, F814W PHAT images. We clipped each postage stamp image at 36" (or 135pc \times 636pc along major or minor axis) from the center of each cloud, and overplotted contours of the CO emission.

We visually inspected these postage stamp plots and classified each cloud as being a star forming cloud or not, similar to the analysis from Kawamura et al. (2009) in the LMC and Gratier et al. (2012) in M33. We further classified the star forming clouds by which indicators had a local peak of emission that also overlapped with the minimum CO contour based on a by eye detection. It can be difficult to associate emission for a particular

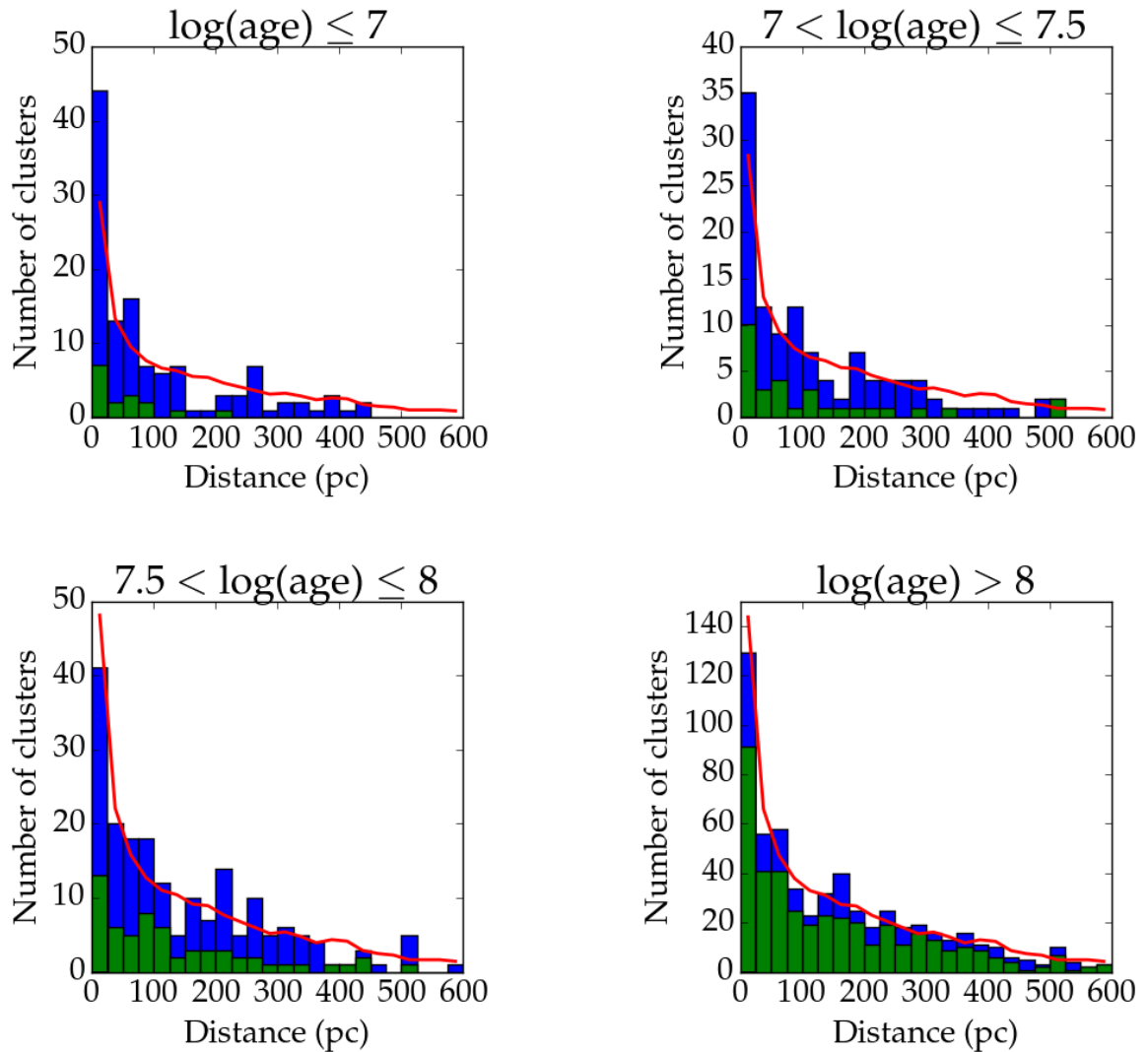


Figure 4.4 Frequency distributions of the deprojected distance for clusters to the nearest molecular cloud, in four age bins. The blue histograms represent the entire cluster sample, while the green histograms are for clusters $> 10^{3.2} M_{\odot}$, where the cluster sample is complete. The red line shows the expected distribution for randomly located clusters. The youngest clusters show a spatial correlation with the clouds, while clusters older than 30 Myr are consistent with a random distribution.

cloud in crowded regions, where emission could be attributed to more than one cloud. In several cases, it was unclear whether emission or a young cluster should be associated with a particular cloud or one of its neighbors, or whether IR emission was due to the underlying

stellar population or not. For these cases, we classified the clouds as possibly having the particular indicator.

We use four classifications for each of the clouds dependent on which star formation tracers they exhibit: no tracer of star formation, IR emission only, $H\alpha$ + IR emission, and young cluster along with $H\alpha$ and/or IR emission. The results from this classification are shown in Table 4.2. 49% of clouds showed at least one definite indicator of star formation; an additional 12% were classified as possibly having IR emission. 16% of the star forming clouds were coincident with a young (< 10 Myr) cluster, and also had IR and/or $H\alpha$ emission, and 4% of the clouds with definite $H\alpha$ emission had a possible related young cluster. An additional 19% had definite $H\alpha$ and IR emission. A further 4% of clouds had definite IR emission and possible $H\alpha$.

In Figure 4.5 we show an example cloud that is definitely forming stars. It has three young clusters, shown by the blue circles, along with strong $H\alpha$ emission, and emission in the four IR images.

Figure 4.6 shows an example cloud that was classified as non star forming. It does not show strong emission in $H\alpha$, any of the IR bands, and it does not coincide with any young clusters. We found that 39 - 51% of the clouds do not show any signs of star formation, depending on whether we include the clouds with only possible emission in one of the star formation indicators. Note that these are upper limits on the fraction of quiescent clouds since this IR emission can come from other sources as well as from star formation.

There are several clouds without $H\alpha$ emission that show strong coincident 5.8 and 8 μm emission, and are bright in 24 μm . These clouds are good candidates for containing deeply embedded star clusters. Figure 4.7 shows an example. 12% of clouds showed possible IR emission as their only indicator, and only 6% had definite IR emission.

Figure 4.8 shows that the presence of star formation indicators seems to be spatially associated on larger scales with cloud associations. Each cloud was looked at on an individual basis, yet we can observe these large spatial correlations, such as the region at the lower right where most of the molecular clouds are non star forming. Many of the clouds along the 10 kpc star forming ring, not surprisingly, show evidence of star formation.

To illustrate the properties of clouds on larger spatial scales, in Figure 4.9 we define

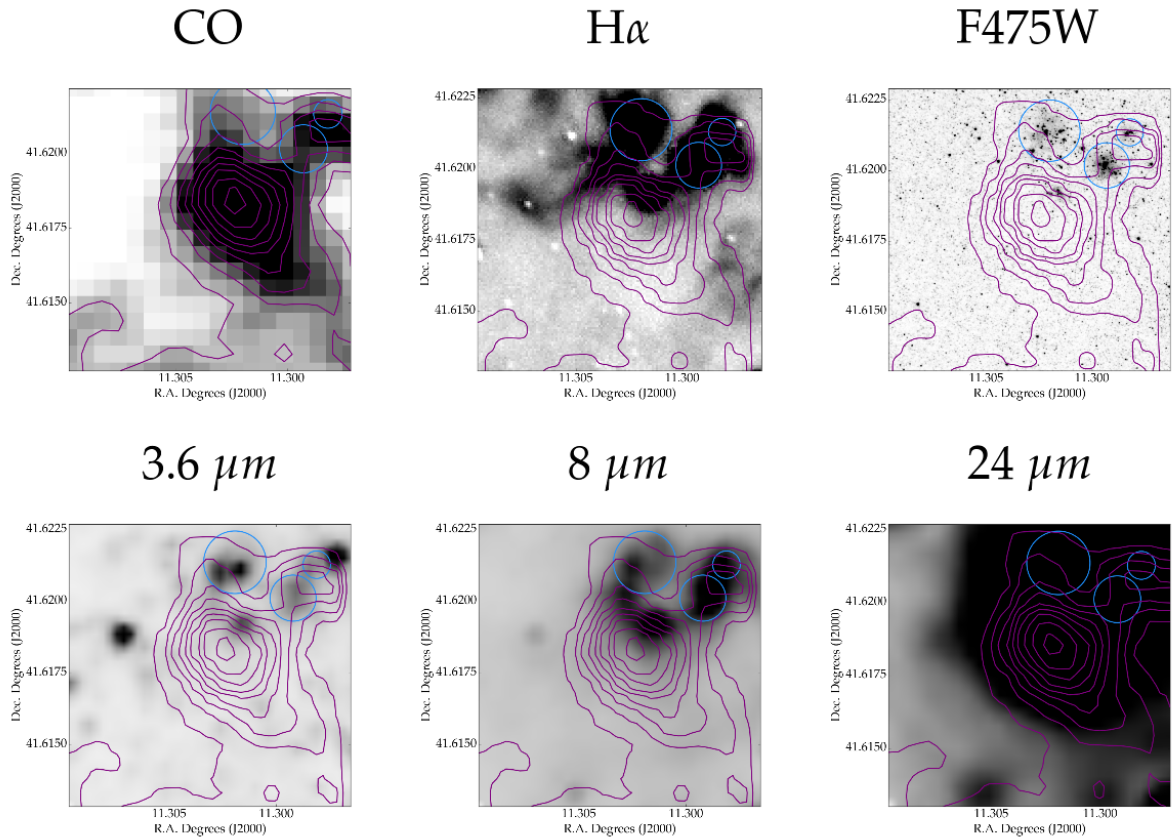


Figure 4.5 Example of a cloud that was classified as star forming. Each image was clipped at 36 arcsec in RA and Dec (or 135pc x 636pc along major or minor axis) in RA and Dec from the center of each cloud. Magenta contours show the CO emission, with a spacing of 4.0 K*km/s. The circles show locations of young clusters, where blue are <10 Myr.

ellipses throughout the CO footprint that contain regions of coherent molecular gas structures. We then calculate the fraction of clouds within each elliptical region that belong to the three main classifications of clouds: quiescent, containing embedded star formation (including the possible IR, IR, and IR with possible H α classifications from Figure 4.8), and containing exposed star formation (including the H α , H α with IR and possible cluster, and clusters with H α and IR classifications from Figure 4.8). This again shows that the inner disk at the bottom right of the panels contains mostly quiescent clouds, while the 10 kpc ring has much more star formation activity. The top of the 10 kpc ring (the middle two

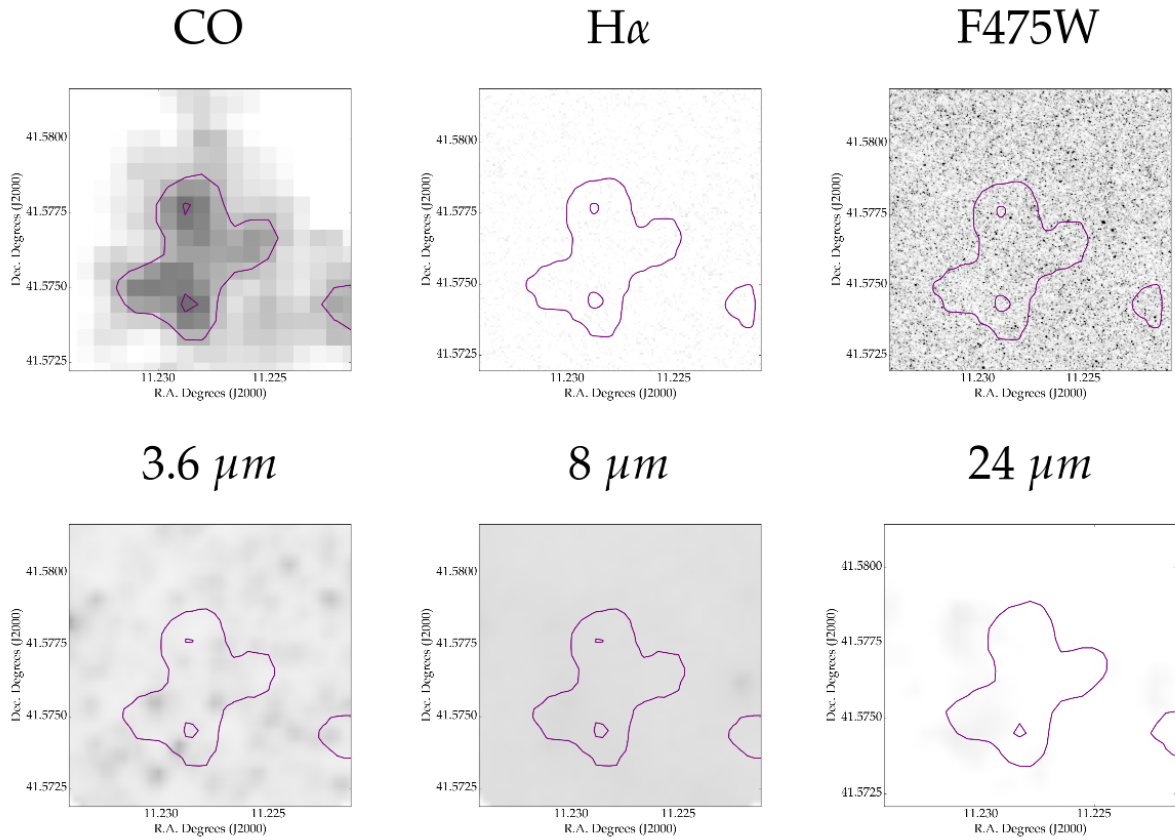


Figure 4.6 Example of a cloud that was classified as non star forming. Each image was clipped at 36 arcsec in RA and Dec (or 135pc x 636pc along major or minor axis) in RA and Dec from the center of each cloud. Magenta contours show the CO emission, with a spacing of 4.0 K*km/s.

ellipses in the upper region of Figure 4.9) seems to contain more embedded star formation than the rest of the ring, which is mostly dominated by exposed star formation.

4.3.3 The Distribution of Molecular Cloud Properties

Given the clear coherent variations in the star forming properties of M31's molecular clouds, it is worth exploring if the origin lies in variations in cloud properties. In Figure 4.10 we plot the distribution of molecular cloud masses (top left panel), radii (top right panel), velocity dispersions (bottom left panel) and virial parameter (bottom right panel) of the

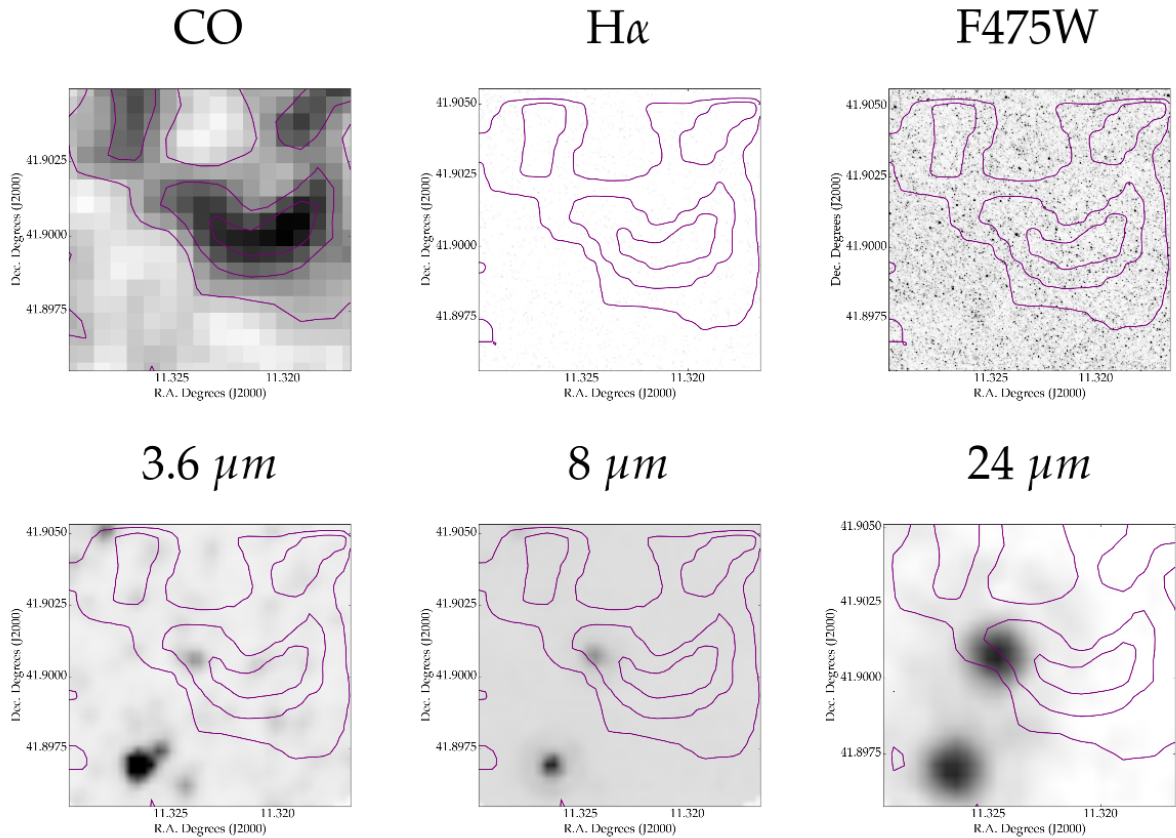


Figure 4.7 Example of a cloud that has strong evidence of embedded star formation, as seen by the strong emission in the IR images. Each image was clipped at 36 arcsec in RA and Dec (or 135pc x 636pc along major or minor axis) in RA and Dec from the center of each cloud. Magenta contours show the CO emission, with a spacing of 4.0 K*km/s.

different classifications of molecular clouds. For these plots, we merge 'possible' classifications together with 'definite' classifications. If a cloud has multiple indicators present, we categorize it using the most evolved indicator (i.e. if a cluster has both a young cluster and H α emission, it is classified as a cloud with a young cluster). These distributions, 'violin plots', are shown as a combination of a box plot and a kernel density plot.

The mass distributions of the molecular clouds are broadly similar, with no statistically significant difference between the quiescent (non star forming) clouds, the embedded star forming (IR emitting) clouds, and the clouds with young clusters as judged by the K-S

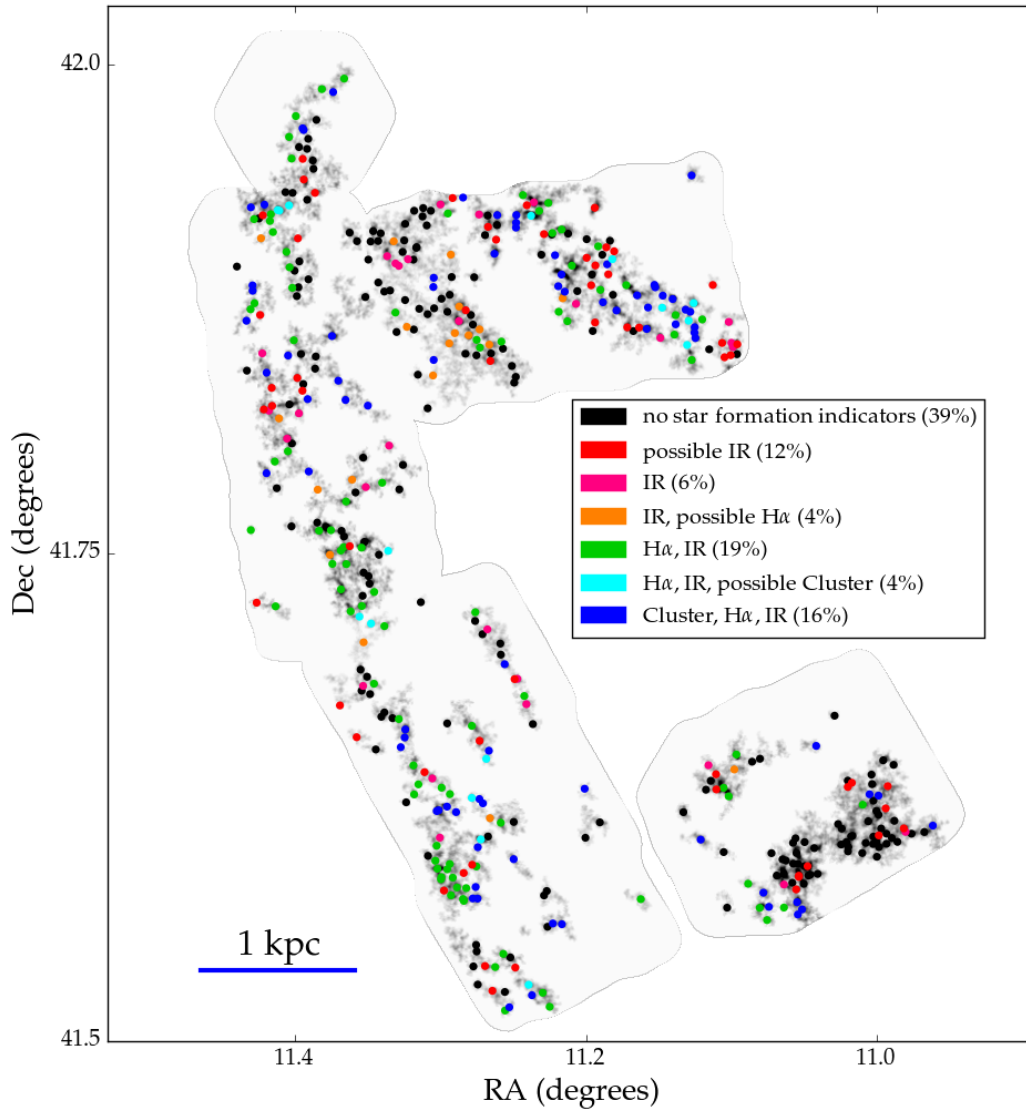


Figure 4.8 Classification of molecular clouds based on star formation activity. 39% clouds do not show signs of star formation, which are shown in black. Clouds with possible IR emission are in red (12%) and definite IR emitting clouds are in magenta (6%). Clouds with definite IR and possible H α emission are in orange (4%), and those with definite H α and IR are in green (19%). Cyan clouds are those with a H α and IR (3.7%), and a possible young cluster (4%), and the blue clouds are those with a young cluster, H α , and IR emission (16%).

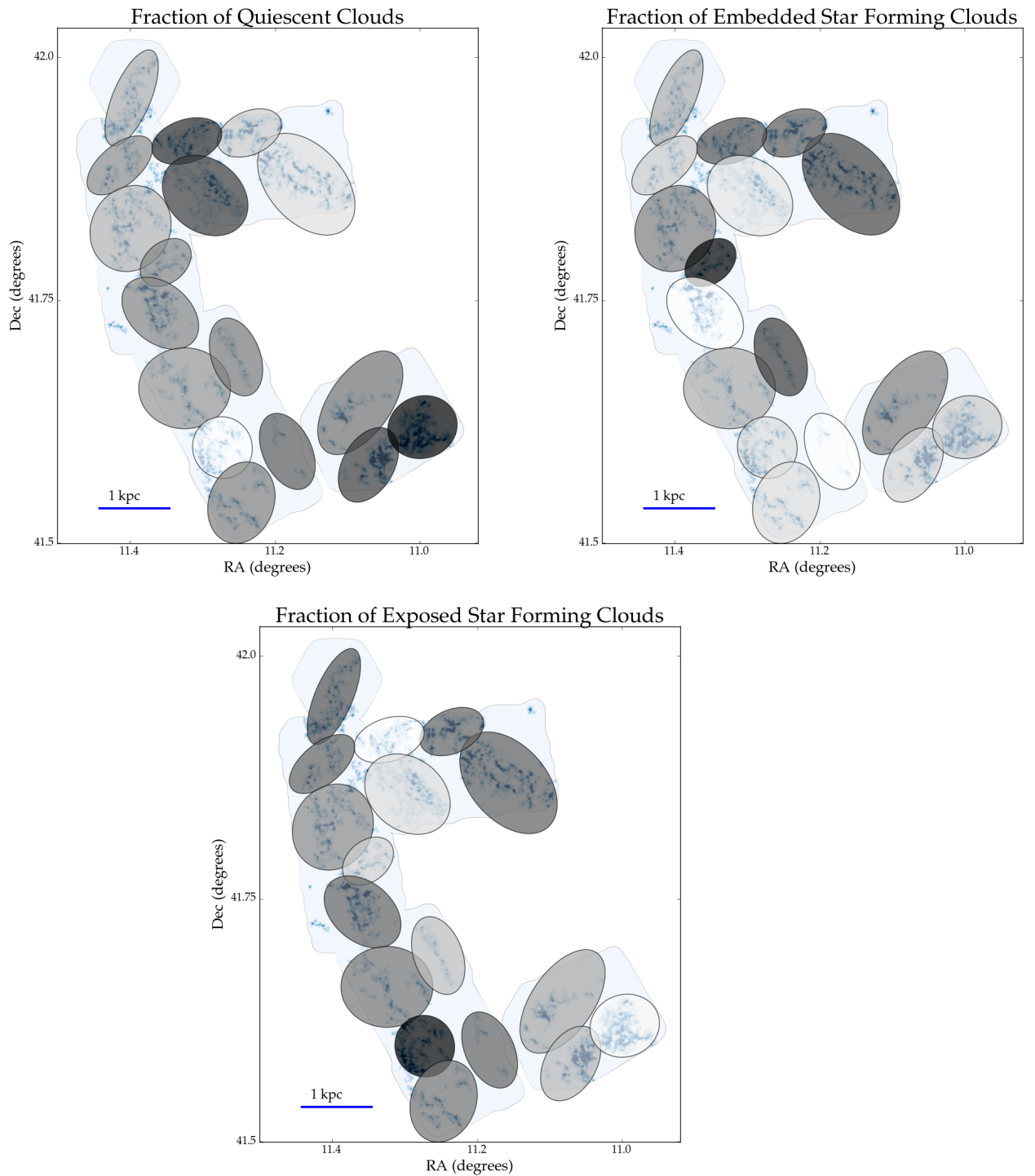


Figure 4.9 Fraction of molecular clouds in each elliptical region for the three main cloud states. Top left is the fraction of quiescent clouds, top right is the fraction of clouds showing embedded star formation (IR-only emission), bottom is the fraction of clouds showing exposed star formation ($H\alpha$ and/or young clusters). Darker ellipses represent regions where there is a higher fraction of that type, while lighter ellipses represent regions where there is a lower fraction of that type of cloud.

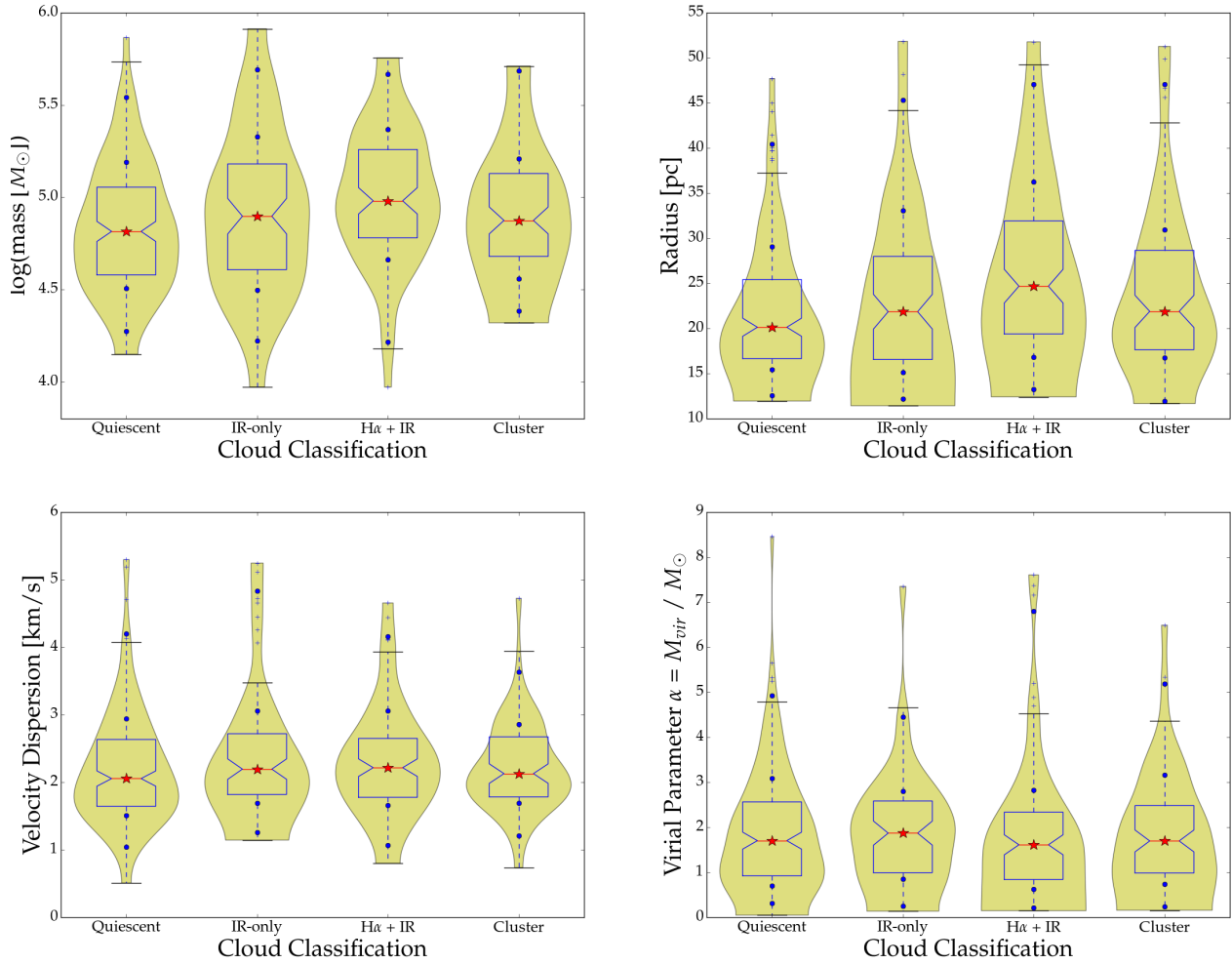


Figure 4.10 The distribution of the mass (top left panel), radius (top right panel), velocity dispersion (bottom left), and virial parameter (bottom right) of molecular clouds with different star forming properties, including all 'definite' and 'possible' classifications. The stars indicate the median values in each category, the dots indicate the following percentiles: 2, 16, 84, and 98. The inner box indicates the inner quartiles of the data, and the yellow region is a kernel density estimate of the distribution of each parameter. There is no statistically significant difference in the properties of the molecular clouds among the different populations, except for the H α emitting clouds, which have a slightly larger average mass and radius

test (at a 95% confidence level with p-value = 0.0772 and 0.2663, respectively). There are differences between the clouds associated with H α and the other groups. The H α emitting clouds have the highest mass (median = $9.56 \times 10^4 M_\odot$, compared to $6.52 \times 10^4 M_\odot$ for the lowest median mass, seen in the quiescent clouds). The K-S test shows that the H α emitting clouds are statistically different than the quiescent clouds (p-value = 0.0002). The IR-only emitting clouds have a notably higher dispersion in mass (standard deviation = $1.4 \times 10^5 M_\odot$ for the IR-only emitting clouds vs 9.5×10^4 , 1.1×10^5 , and $9.8 \times 10^4 M_\odot$ for the other categories).

The radius shows similar trends as the mass, where the quiescent clouds have the lowest (median = 20.13 pc) and the H α emitting clouds the largest (median = 24.68 pc). Again, only the H α clouds show a statistically significant difference from the quiescent clouds (p-value = 3.25×10^{-5}). The IR-only emitting and young cluster clouds both have indistinguishable distributions of radii.

The mass and radius distributions in Figure 4.10 are broadly compatible with an evolutionary sequence where lower mass clouds gain additional mass, become more dense, form stars, and then the cloud disperses. In this model, the largest masses will be seen right before the cloud begins to disrupt, in the H α emitting stage. This general picture is also compatible with the fact that the distributions for all classifications remain unchanged if we only consider clouds in the 'definite' category and exclude the 'possible' classifications; however clouds with definite IR emission are larger (median mass = $1.05 \times 10^5 M_\odot$, median radius = 25.96 pc) than the clouds with possible emission (median mass = $6.26 \times 10^4 M_\odot$, radius = 19.23 pc, similar to quiescent clouds). This behavior makes sense since the clouds with possible IR emission are closer to the previous evolutionary stage (i.e., the quiescent clouds), and the clouds with definite IR emission are similar to the following stage (i.e., the H α and IR emitting stage), where clouds are observed to be larger and more massive.

The bottom left panel of Figure 4.10 shows the distributions of the velocity dispersion, which traces the amount of turbulence within a cloud (top panel). The median velocity dispersion for the different types is very similar (2.05, 2.19, 2.22, and 2.13 km/s for quiescent, IR, H α , and young cluster classifications, respectively) and does not show statistically significant difference with a K-S test. However, the quiescent clouds have a larger range in

velocity dispersion than the other classifications.

In the bottom right panel of Figure 4.10 we show the distribution of the virial parameter α , which measures the boundedness of a cloud, where values less than one means the cloud is gravitationally bound and values above one represent an unbounded cloud. Most of the clouds in the sample do not seem to be gravitationally bound as a whole. The median virial parameter for the different molecular cloud categories is also similar to each other, although the quiescent clouds have a slightly larger range (median = 1.70, 1.87, 1.61, and 1.70 for non star forming, IR, H α , young cluster, respectively). Excluding the 'possible' classifications again, the only significantly change is the IR emitting clouds, as was the case for mass and radius. The 'definite' IR emitting clouds show a slightly higher median α (1.87) and a higher velocity dispersion (2.33 km/s); only the latter is statistically different than the quiescent clouds, with a p -value of 0.031. This could be indicative of the IR-only emitting clouds still accreting material, since that may increase the clouds' virial parameter as well as velocity dispersion.

4.3.4 *Statistical Lifetimes of Molecular Cloud Phases*

With the cloud classifications in Table 4.2, we can assign timescales for the different stages of star formation that are shown in Figure 4.1. This statistical lifetime calculation assumes that both cloud and clusters are formed steadily over the last 10 Myr. We find that out of 120 young clusters (<10 Myr), 30% were associated with a molecular cloud; including the possible cluster associations brings the total to 43%. This implies that on average, the time for a cloud to disrupt after the cluster becomes exposed is about 3-4 Myr. This agrees with the timescale for physical disruption processes such as supernovae, winds, and photoionization, which are thought to occur on timescales <5 Myr after the onset of star formation.

If we further assume that all clouds that we observe eventually form stars, we can compare the relative number of clouds in each evolutionary stage to assign a timescale for that stage. Using the relative number of clouds in each classification, taking into account both the definite and possible classifications, gives a timescale of 6-15 Myr before a cloud

begins to form stars, followed by a timescale of 1-4 Myr stage of embedded (IR emitting) star formation, and then a 3-7 Myr phase of $H\alpha$ emission, as the young stars photoionize the surrounding molecular cloud. Adding these phases together gives a total estimate for a cloud's lifetime of 13-30 Myr.

We have also explored possible environmental variations in the lifetimes of these phases. The two major environments observed in the CO footprint are the 10 kpc star forming ring, and the inner disk at 5-6 kpc. The overall star formation rate surface density over the last 400 Myr for the inner disk is a factor of 2-3 lower than for the 10 kpc star forming ring (Lewis et al., 2015), so we might expect differences in the percentage of star forming clouds in these two regions. We separated out the inner disk from the rest of the sample (the clouds along the 10 kpc ring) and redid the cloud classification percentages. For the inner disk, which contains 92 clouds, the percentage of quiescent clouds went up to 64%, while the quiescent population of the ring (386 clouds) decreased to 33.2%. The inner disk clearly contains clouds that either have a much longer pre-stellar lifetime and/or contains clouds which will never form stars.

4.3.5 Estimating Cloud Lifetime by Comparison to Simulations

The traditional statistical lifetime estimates presented in the previous section are predicated on the assumption that every quiescent cloud will someday form stars. However, it is also possible that some fraction of molecular clouds will be disrupted by turbulence and/or galactic shear before star formation begins. In this case, the simple argument above will break down, because the time a star-forming cloud spends in the pre-stellar phase will not be directly proportional to the number of clouds observed without star formation, since this also includes the total lifetime of clouds that will never form stars. This may lead to estimates of the pre-stellar lifetime that are too high.

We took a more sophisticated approach to this problem by simulating a population of clouds that includes "inert" clouds that will never participate in star formation. We then investigate what lifetimes and fractions of inert clouds would be consistent with the observed percentages in Table 4.2.

Table 4.2. M31 Cloud Classifications and Timescales

Classification ^a	Percentage ^b	Timescale ^c
No Star Formation Indicators		
Definite only	39%	6 Myr
Definite + Possible	51%	15 Myr
IR Emission		
Definite only	6%	1 Myr
Definite + Possible	22%	4 Myr
H α and IR Emission		
Definite only	19%	3 Myr
Definite + Possible	27%	7 Myr
Young Cluster, H α and IR Emission		
Definite only	16%	3 Myr
Definite + Possible	20%	4 Myr

^aStar formation indicators that are coincident with a molecular cloud.

^bPercentage of clouds that show evidence of the indicator. Possible cases are whether it is uncertain if emission is from a particular cloud.

^cTimescale estimates from the relative percentage of clouds in each classification and comparing with young (< 10 Myr) clusters.

Each run of the simulation created 10,000 clouds, with each cloud given a random age drawn uniformly between 1 and 100 Myr. This maximum age is large enough that the range does not affect the results of the simulation.

For each cloud, we use Poisson rate statistics to calculate three different hypothetical timescales: t_{sf} , the mean pre-stellar time, t_{psf} , the mean post-stellar time (including embedded star formation, $H\alpha$ emitting, and young cluster phases), and the disruption time, t_d which represents the mean time for a cloud to disrupt due to non star formation forces such as galactic shear. These three timescales were all randomly drawn from exponential functions, which is the expectation for a Poisson process of some fixed rate. Each cloud can only form stars once during its lifetime; all star formation is instantaneous. We then use these three timescales to set an evolution path for each cloud.

Once the population's timescales were all randomly generated, we compared each cloud's timescales to each other to decide the fate of the cloud. There are three possible outcomes: First, if t_d is less than t_{sf} , the cloud is disrupted before it can form stars, and so it is in a dormant state for its whole lifetime. The cloud's total lifetime is then just t_d . Second, if the cloud becomes disrupted after forming stars but before the completion of the post-stellar lifetime, it dies prematurely by external forces, and the lifetime is again equal to the disruption timescale t_d . These clouds are counted as star forming. Finally, a cloud's disruption timescale can be longer than both its pre-stellar and post-stellar lifetimes, in this case, the cloud dies naturally after completing its star formation. The total lifetime for these clouds is $t_{sf} + t_{psf}$. We carry out this process for every simulated cloud, and then examine the statistics of the clouds at the end of the simulation, measuring the fraction of clouds that have formed stars.

To get steady state results, we sampled the cloud population at a random time at least 25 Myr after the first possible birth time. We measured the fraction of clouds that are star forming at this time (the latter two categories above). We end up with a grid of mean timescales and the resulting fraction of star forming clouds at each grid point; we can compare this with our observational results from the previous section.

Figure 4.11 shows the resulting percentage of clouds with star formation after running the simulation over the grid of values for the three timescales. We plot the results of

the simulation for several slices in the post-stellar lifetime parameter, color-coded by the resulting fraction of clouds that are star forming. For populations of clouds where the star formation fraction is higher than 0.5, the disruption timescale must be longer than the pre-stellar timescale so that the clouds have time to form their stars before being disrupted. For lower fractions of star forming clouds, the mean disruption timescale is short compared with the mean pre-stellar timescale, allowing the clouds to disrupt before they are able to form stars.

We now use two of our observational results from the previous section to constrain the simulation results. We can fix the mean post-stellar lifetime to be the total lifetime of the IR emitting phase, the $H\alpha$ emitting phase, and the young cluster phase, which was calculation in Section 4.3.4 as being 7-15 Myr. This result should not depend on our previous assumption that all clouds formed stars since the post-stellar lifetime applies only to star-forming clouds. This assumption selects only the simulation runs where t_{psf} is between 7 and 15 Myr. We can then ask what region of the grid produces the observed fraction of star forming clouds of 49-61% (including only 'definite' or 'definite' and 'possible' cases, respectively) for M31.

Additionally, we can investigate where the LMC and M33 would fall in our simulations results plot. Both the LMC and M33 clouds have similar mean post-stellar lifetimes (20 Myr in the LMC (Kawamura et al., 2009) and 16-34 Myr in M33 (Miura et al., 2012)). We select the simulation runs where t_{psf} is between 16 and 24 Myr to show the results for these galaxies.

In Figure 4.12 we show the locations where the simulation results match the results for M31 presented in Section 4.3.4 (left panel) as well as for the LMC and M33 (right panel, black and blue point, respectively). The points show where the fraction of star forming clouds matches with the observations for each galaxy (49-61% for M31, 76% for the LMC, and 99% for M33). For both M31 and the LMC, the mean disruption time has to be about the same as the pre-stellar timescale. There can still be some dormant clouds with longer lifetimes, but the mean time to disrupt is fairly short, $\lesssim 15$ Myr. For M33, since the observed fraction of star forming clouds is so high, the mean disruption timescale must be greater than the mean pre-stellar lifetime to allow time for most of the clouds to form stars.

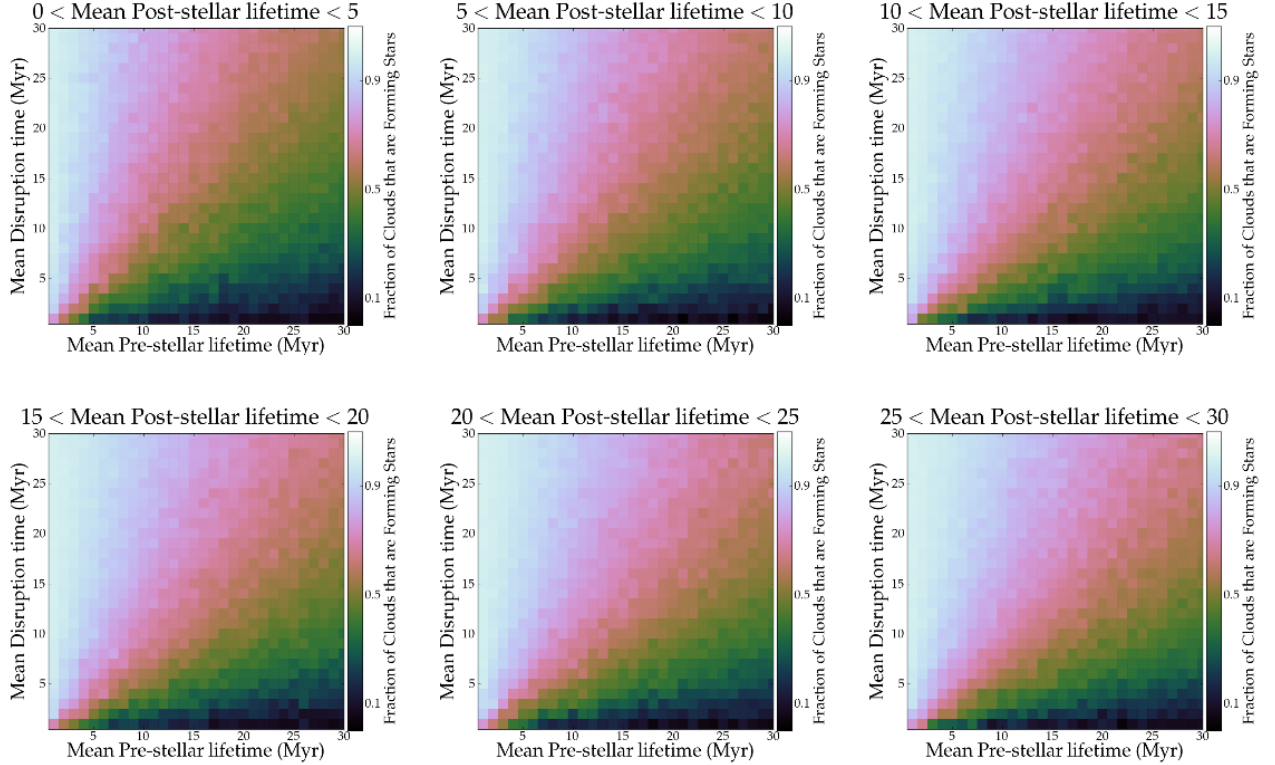


Figure 4.11 Results from the simulations that drew random distributions for three timescales for simulated molecular clouds. This plot shows the mean pre-stellar lifetime vs the mean disruption time, for several slices of the mean post-stellar lifetime. Lighter colors indicate a larger percentage of clouds had associated star formation; darker colors indicate a smaller percentage of clouds had associated star formation.

4.3.6 Uncertainties and Biases

To interpret our results, we must first quantify our selection bias, completeness, and parameter uncertainties. The resolution and sensitivity of the CO survey may have a strong effect on the number of detectable clouds and their properties, which in turn affects the total percentage of star forming clouds and the derived timescales. The relative numbers of star forming vs non star forming clouds will also depend on the mass range of the detected clouds and on the spatial resolution. Measurements that are averaged over larger areas

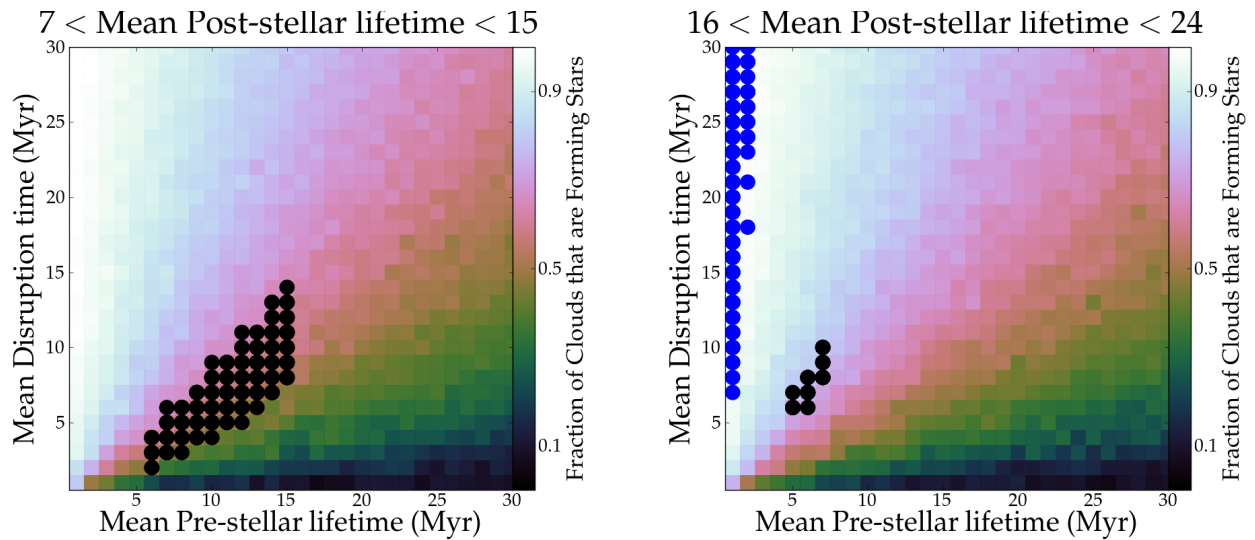


Figure 4.12 Results from the simulations that drew random distributions for three timescales for simulated molecular clouds. These plot shows the mean pre-stellar lifetime for star-forming clouds vs the mean disruption time. The left panel shows the values in the mean post-stellar lifetime for star-forming clouds that match the observational estimate (7-15 Myr, as calculated in Section 4.3.4). The right panel shows the mean post-stellar timescales that match the results for the LMC and M33, about 16-24 Myr. The black dots indicate the values of the percentage of star forming clouds and mean pre-stellar timescale that match the values found in the LMC (Kawamura et al., 2009), while the blue values match those for M33 (Miura et al., 2012).

or associations of clouds are not able to detect which individual clouds are forming stars. Often large associations are comprised of several clouds, and sometime star formation is only occurring in part of the association, so increasing the size of our 'clouds' would result in more clouds showing signs of star formation. Indeed, if we decrease the resolution of the CO data, many of our smaller clouds would be considered as one large cloud. This effect could explain why lower resolution studies find a larger percentage of star-forming clouds.

Our inferred fraction of star forming clouds may also be affected by uncertainty in identifying embedded star formation. We have assumed the IR emission is associated with heating of dust by young stars, but some IR emission may be due to dust heated by evolved stars instead, leading us to overestimate the amount of embedded star formation. On the other hand, embedded star formation may be occurring that is below the detection and/or confusion limit of the IR images used, which would cause the opposite effect of missing some embedded star formation. There is also uncertainty in which cloud contains emission in crowded regions, due to the relatively poor IR resolutions. However, even including all the uncertain cases, embedded star formation makes up no more than 36% of all the star forming clouds, so even significant errors will have a smaller effect on the overall star forming fraction.

Another possible limitation is that our star formation indicators generally trace only massive star formation. We are restricted to identifying star forming clouds using clusters of masses greater than a few hundred solar masses, or through individual star-forming regions that are capable of ionizing and/or heating their surrounding gas. There therefore may be lower mass star formation occurring in clouds that we are not detecting. However, based on a Salpeter IMF, clouds with mass of at least $M > 10^4 M_{\odot}$ have a large probability of forming at least one massive star if star formation has occurred (Zasov & Kasparova, 2014). Similar studies (Kawamura et al., 2009; Miura et al., 2012) are also affected by this same limitation.

Finally, M31 has a high inclination which may affect our association of objects, both through projection effects and through additional clusters possibly being hidden behind the dust. Additionally, it is possibly that clusters could drift substantially far away from their birth cloud over 10 Myr, then the cloud would survive and not be associated with the cluster

any more.

4.3.7 Comparison with Other Galaxies

We have found that about 60% of M31's molecular clouds show signs of star formation, and comparison with young clusters leads to a statistical lifetime between 13-30 Myr. There are two main studies that are very similar to ours, Kawamura's study of the LMC and Miura's study of M33. Both this study and the LMC study by Kawamura et al. (2009) used the age of the youngest clusters, 10 Myr. All assumed a steady state of cloud and cluster formation. While the total lifetime found for M31 agrees with the results from the LMC and M33, the percentage of star forming clouds, and thus the relative time spent in the various phases, that we have found for M31 is quite different.

In all three studies, the inferred total cloud lifetimes are about the same, but the M31 clouds spend more of their lifetime in the pre-stellar phase and less time in the post star formation stage. One possible explanation for this difference is that these two studies also included OB associations as part of their cluster sample (about 1/6 of the total cluster sample in the LMC studies), thus increasing the number of "clusters" that could be associated with molecular clouds. Performing a separate search through the PHAT sample for these OB associations could potentially increase the number of clouds that are classified as star forming. However, any OB association would also likely produce H α or IR emission that we have already taken into account, and thus this difference seems unlikely to be the primary cause of M31's lower fraction of star forming clouds. Additionally, the fraction of clusters in M31 is about a factor of two lower than in LMC (Johnson, in prep), which could explain why we are seeing more clouds with only H α emission rather than H α along with a young cluster.

Given that the low fraction of star forming clouds appears to be real, it must reflect other underlying differences between M31 and the other systems. M31 is quite a different environment than the LMC and M33, which could explain the differences in the cloud populations. M31 is much more massive, and has a high metallicity, compared to the LMC and M33 ($Z = 1/2 Z_{\odot}$; Fukui & Kawamura, 2010). Molecular clouds in the SMC also

show evidence for larger H_2 reserves surrounding the CO bright molecular gas (Leroy et al., 2007), indicating that studies in low metallicity galaxies may be missing some of the non SF molecular clouds. This would be consistent with the evidence that clouds in the LMC and M33 may be more strongly bound than those in M31 (Fukui et al., 2001; Wong et al., 2011; Engargiola et al., 2003; Rosolowsky, 2005). In contrast, M31's more weakly bound clouds might be more easily disrupted in a more diffuse medium, which could explain why fewer clouds are forming stars. However, given the similar overall cloud lifetimes in all three galaxies, faster disruption in M31 appears unlikely. In low metallicity galaxies the CO emission can be observed only in regions of higher column density (Israel et al., 1993; Bolatto et al., 2013), which may be expected to have higher star formation rate efficiencies. Additionally, in the M33 study, the tracer used was CO($J = 3-2$) which detects higher column density gas, therefore this study was not as sensitive to more diffuse clouds.

Aside from metallicity, one of the major differences between M31 and the LMC and M33 is M31's much lower star formation rate efficiency (SFE). M31's SFE over the past 100 Myr is less than 10% (Lewis et al., 2015), while estimates for M33's SFE range from 15% (Gratier et al., 2012) to 30% (Tabatabaei & Berkhuijsen, 2010). M31 also is known to have a lower massive star formation rate than M33 and the LMC (Humphreys et al., 1990). The Kennicutt-Schmidt law states that the star formation rate efficiency drops with decreasing star formation rate intensity. Since M33 has been about $1.5 - 3 \times$ more efficient at forming stars over the past 100 Myr, this could explain why we observe a lower fraction of star forming clouds in M31.

4.4 Conclusions

We utilized the molecular cloud catalog from the CARMA Survey of Andromeda (M31) and compared it with the PHAT cluster catalog, $\text{H}\alpha$ map, and several IR emission maps to study the star-forming properties of the molecular clouds. We found that 61% of the clouds showed indications of massive star formation, which is lower than what is found in other studies of the LMC and M33. 43% of clouds had visible signs of star formation, and 18% had only signs of embedded star formation. Based on number of clouds in a given evolutionary stage, we estimate a statistical cloud lifetime of 13-30 Myr assuming all clouds

eventually form stars. We then compared our observational results with a Monte Carlo simulation, removing the assumption that all clouds form stars. We found that the mean time disruption time is fairly short, $\lesssim 15$ Myr for both M31 and the LMC. For M33, the mean disruption timescale must be greater than the mean pre-stellar lifetime to allow time for the majority of molecular clouds to form stars.

Chapter 5

CONCLUSIONS

This thesis explored different techniques for determining the properties of stellar clusters. I began by introducing a new method that can be used for stellar clusters at a distance of 1-3 Mpc whose light is comprised of both a few resolved stars and unresolved starlight. By eliminating the few brightest evolved stars which are responsible for drastic changes in color due to stochasticity, the unevolved light is much more stable and can be used to accurately determine the ages, masses, and extinctions of clusters. Synthetic tests show that using only unevolved light accurately recovers the ages, masses, and extinctions for young, low mass clusters, where integrated light is less accurate. The unevolved light method has potential to improve on integrated light fitting techniques for clusters whose light is partially resolved.

I used CMD fitting to determine age, mass, and extinction for the largest extragalactic cluster sample to date. I also compared these results to those determined by integrated light fitting using discrete models. I found that there is a good overall agreement between the methods, and the CMD fitting technique works better for younger clusters, while the integrated light method works better for older clusters who do not have many stars above our completeness limit. Clusters in the sample range from a few hundred to $10^5 M_{\odot}$, 6 Myr - 10.2 Gyr, and 0 - 3 A_V . I noted a lack of young, massive clusters as well as old lower mass clusters. The age and mass distributions agree with those found in other extragalactic studies. For future work, I will be determining these cluster properties using the unevolved light technique as well.

With these accurate properties of clusters, I compared the PHAT cluster sample along with additional star formation indicators, to the CARMA survey of molecular gas in M31. I found that the the spatial correlation between clouds and clusters is erased on 10-30 Myr timescales. By associated each evolutionary phase in a molecular cloud's life with the appropriate star formation indicator, I found that almost 40% of clouds are in a quiescent,

non star-forming phase, greater than what is observed in other nearby galaxies. This difference could be due to resolution effects or an intrinsic difference in the star formation rate intensities of M31 as compared to the other galaxies that have been studied. I also calculated a statistical lifetime for the molecular clouds between 13-30 Myr. Finally, I compared these observational results to a Monte Carlo simulation which did not assume that all clouds eventually form stars. This simulation led to an estimate of $\lesssim 15$ Myr for the mean disruption time of molecular clouds in M31.

A

Table 1. Appendix: Cluster Parameters

AP ID ^a	CMD Best Fit Parameters ^b			Integrated Best Fit Parameters ^c			Best ^d	Flag ^e	R _{ap} ^f	N _{stars} ^g	N _{bg} ^h
	log(<i>t</i> [Myr])	log(<i>M</i> [<i>M</i> _⊙])	<i>A_V</i> [mag]	log(<i>t</i> [Myr])	log(<i>M</i> [<i>M</i> _⊙])	<i>A_V</i> [mag]					
AP1	8.80 ^{+0.00} _{-0.00}	4.04 ^{+0.03} _{-0.03}	0.05 ^{+0.10} _{-0.05}	8.97 ^{+0.05} _{-0.05}	4.13 ^{+0.05} _{-0.05}	0.08 ^{+0.09} _{-0.08}	I	0	2.19	408	229
AP2	8.40 ^{+0.00} _{-0.00}	3.98 ^{+0.00} _{-0.03}	1.15 ^{+0.00} _{-0.05}	8.73 ^{+0.10} _{-0.07}	3.52 ^{+0.07} _{-0.07}	0.15 ^{+0.12} _{-0.15}	I	0	1.86	255	169
AP3	8.80 ^{+0.00} _{-0.10}	3.48 ^{+0.05} _{-0.00}	0.00 ^{+0.30} _{-0.00}	8.57 ^{+0.08} _{-0.09}	3.09 ^{+0.08} _{-0.07}	0.11 ^{+0.13} _{-0.11}	I	0	1.95	197	113
AP4	8.80 ^{+0.00} _{-0.00}	4.14 ^{+0.00} _{-0.03}	0.00 ^{+0.00} _{-0.00}	8.97 ^{+0.05} _{-0.05}	4.13 ^{+0.05} _{-0.05}	0.05 ^{+0.09} _{-0.05}	I	0	2.87	530	281
AP5	8.40 ^{+0.00} _{-0.10}	3.41 ^{+0.04} _{-0.01}	0.45 ^{+0.20} _{-0.01}	8.67 ^{+0.05} _{-0.05}	3.37 ^{+0.06} _{-0.06}	0.07 ^{+0.09} _{-0.07}	I	0	1.46	208	166
AP6	8.50 ^{+0.00} _{-0.10}	3.83 ^{+0.00} _{-0.02}	0.50 ^{+0.15} _{-0.00}	8.39 ^{+0.12} _{-0.12}	3.63 ^{+0.11} _{-0.10}	0.26 ^{+0.27} _{-0.25}	I	0	2.23	351	214
AP7	8.20 ^{+0.00} _{-0.30}	3.16 ^{+0.00} _{-0.04}	0.45 ^{+0.10} _{-0.05}	8.20 ^{+0.13} _{-0.12}	3.21 ^{+0.13} _{-0.13}	0.45 ^{+0.29} _{-0.30}	I	0	1.86	124	55
AP9	8.70 ^{+0.00} _{-0.06}	4.26 ^{+0.00} _{-0.00}	0.25 ^{+0.00} _{-0.00}	8.85 ^{+0.07} _{-0.06}	4.17 ^{+0.05} _{-0.05}	0.12 ^{+0.11} _{-0.11}	I	0	2.87	724	427
AP11	8.90 ^{+0.00} _{-0.00}	3.58 ^{+0.02} _{-0.00}	0.00 ^{+0.05} _{-0.00}	8.84 ^{+0.27} _{-0.29}	3.41 ^{+0.16} _{-0.13}	0.18 ^{+0.21} _{-0.18}	I	0	1.77	137	43
AP12	9.00 ^{+0.00} _{-0.00}	4.25 ^{+0.01} _{-0.05}	0.40 ^{+0.00} _{-0.10}	9.07 ^{+0.35} _{-0.20}	4.02 ^{+0.12} _{-0.10}	0.50 ^{+0.24} _{-0.35}	I	0	2.26	343	182
AP13	8.70 ^{+0.00} _{-0.00}	4.07 ^{+0.02} _{-0.00}	0.10 ^{+0.05} _{-0.00}	8.74 ^{+0.06} _{-0.07}	4.06 ^{+0.05} _{-0.05}	0.09 ^{+0.11} _{-0.09}	I	0	2.49	510	289
AP14	8.20 ^{+0.10} _{-0.00}	4.08 ^{+0.05} _{-0.00}	1.25 ^{+0.00} _{-0.10}	8.08 ^{+0.19} _{-0.14}	3.85 ^{+0.09} _{-0.08}	0.69 ^{+0.26} _{-0.26}	I	0	2.50	509	225
AP15	8.50 ^{+0.00} _{-0.00}	3.87 ^{+0.01} _{-0.00}	0.30 ^{+0.05} _{-0.05}	8.56 ^{+0.05} _{-0.05}	3.71 ^{+0.05} _{-0.05}	0.03 ^{+0.07} _{-0.03}	I	0	2.75	592	490
AP16	8.40 ^{+0.00} _{-0.00}	3.57 ^{+0.03} _{-0.03}	0.75 ^{+0.05} _{-0.00}	8.07 ^{+0.14} _{-0.13}	3.68 ^{+0.12} _{-0.10}	0.95 ^{+0.27} _{-0.29}	I	0	2.06	311	205
AP17	8.80 ^{+0.00} _{-0.00}	3.57 ^{+0.02} _{-0.01}	0.05 ^{+0.05} _{-0.05}	7.75 ^{+0.03} _{-0.03}	2.20 ^{+0.03} _{-0.03}	0.30 ^{+0.07} _{-0.07}	I	0	2.12	264	158
AP18	8.30 ^{+0.00} _{-0.80}	3.49 ^{+0.00} _{-0.09}	0.45 ^{+0.35} _{-0.05}	8.39 ^{+0.19} _{-0.22}	3.44 ^{+0.13} _{-0.12}	0.35 ^{+0.45} _{-0.35}	I	0	1.97	304	259
AP19	9.20 ^{+0.00} _{-0.00}	3.82 ^{+0.06} _{-0.00}	0.15 ^{+0.10} _{-0.00}	7.90 ^{+1.16} _{-1.34}	3.47 ^{+0.33} _{-0.39}	1.39 ^{+0.90} _{-1.00}	I	0	2.00	155	38
AP23	8.40 ^{+0.00} _{-0.00}	3.85 ^{+0.02} _{-0.00}	0.55 ^{+0.05} _{-0.05}	8.58 ^{+0.06} _{-0.06}	3.63 ^{+0.06} _{-0.06}	0.04 ^{+0.07} _{-0.04}	I	0	2.30	366	206
AP24	7.20 ^{+0.10} _{-0.10}	3.12 ^{+0.01} _{-0.02}	0.70 ^{+0.05} _{-0.05}	7.73 ^{+0.05} _{-0.06}	3.17 ^{+0.06} _{-0.06}	0.35 ^{+0.12} _{-0.11}	I	0	1.60	183	159
AP25	8.50 ^{+0.10} _{-0.00}	3.44 ^{+0.02} _{-0.02}	0.50 ^{+0.05} _{-0.15}	8.36 ^{+0.32} _{-0.22}	3.47 ^{+0.12} _{-0.13}	0.84 ^{+0.41} _{-0.68}	I	0	1.95	156	53
AP26	9.00 ^{+0.00} _{-0.10}	3.90 ^{+0.03} _{-0.05}	0.00 ^{+0.15} _{-0.00}	8.55 ^{+0.14} _{-0.13}	3.95 ^{+0.08} _{-0.08}	1.36 ^{+0.23} _{-0.23}	I	0	2.02	297	168
AP27	7.40 ^{+0.00} _{-0.70}	3.18 ^{+0.00} _{-0.07}	0.55 ^{+0.05} _{-0.05}	7.46 ^{+0.13} _{-0.10}	3.80 ^{+0.08} _{-0.08}	0.54 ^{+0.16} _{-0.17}	I	0	2.25	306	303
AP28	8.30 ^{+0.00} _{-0.00}	3.86 ^{+0.01} _{-0.02}	0.85 ^{+0.05} _{-0.05}	8.60 ^{+0.08} _{-0.08}	3.71 ^{+0.05} _{-0.05}	0.19 ^{+0.15} _{-0.15}	I	0	1.98	274	142
AP29	8.80 ^{+0.00} _{-0.00}	4.02 ^{+0.00} _{-0.03}	0.10 ^{+0.00} _{-0.05}	7.69 ^{+0.14} _{-0.16}	3.37 ^{+0.17} _{-0.20}	0.33 ^{+0.20} _{-0.20}	I	0	2.66	448	215
AP30	8.10 ^{+0.10} _{-0.00}	3.84 ^{+0.03} _{-0.04}	1.75 ^{+0.00} _{-0.15}	9.25 ^{+0.11} _{-0.10}	4.01 ^{+0.07} _{-0.07}	0.21 ^{+0.13} _{-0.13}	I	0	1.89	237	47
AP31	8.20 ^{+0.10} _{-0.00}	3.52 ^{+0.01} _{-0.01}	0.30 ^{+0.05} _{-0.05}	8.40 ^{+0.07} _{-0.08}	3.44 ^{+0.09} _{-0.09}	0.22 ^{+0.17} _{-0.18}	I	0	2.30	274	160
AP32	8.20 ^{+0.00} _{-0.00}	3.92 ^{+0.00} _{-0.04}	1.10 ^{+0.00} _{-0.05}	8.23 ^{+0.15} _{-0.11}	3.68 ^{+0.11} _{-0.11}	0.48 ^{+0.22} _{-0.29}	I	0	2.42	462	323
AP33	8.20 ^{+0.00} _{-0.00}	3.50 ^{+0.03} _{-0.00}	0.35 ^{+0.05} _{-0.00}	8.10 ^{+0.09} _{-0.09}	3.70 ^{+0.08} _{-0.09}	0.75 ^{+0.20} _{-0.19}	I	0	1.76	158	45
AP34	8.80 ^{+0.00} _{-0.00}	3.53 ^{+0.02} _{-0.03}	0.05 ^{+0.05} _{-0.05}	8.57 ^{+0.15} _{-0.14}	3.51 ^{+0.10} _{-0.09}	0.66 ^{+0.24} _{-0.24}	I	0	1.78	221	138
AP35	8.80 ^{+0.00} _{-0.00}	3.84 ^{+0.02} _{-0.00}	0.00 ^{+0.05} _{-0.00}	8.53 ^{+0.23} _{-0.24}	3.90 ^{+0.13} _{-0.12}	0.50 ^{+0.47} _{-0.45}	I	0	2.27	247	160
AP36	8.30 ^{+0.00} _{-0.00}	3.41 ^{+0.00} _{-0.02}	0.50 ^{+0.05} _{-0.05}	8.31 ^{+0.12} _{-0.00}	3.02 ^{+0.17} _{-0.03}	0.03 ^{+0.07} _{-0.03}	I	0	1.64	204	168
AP44	8.30 ^{+0.00} _{-0.10}	4.01 ^{+0.02} _{-0.02}	1.30 ^{+0.10} _{-0.00}	8.67 ^{+0.11} _{-0.11}	3.75 ^{+0.07} _{-0.05}	0.49 ^{+0.18} _{-0.17}	I	0	1.84	295	156
AP45	8.40 ^{+0.00} _{-0.00}	3.96 ^{+0.02} _{-0.01}	0.60 ^{+0.05} _{-0.05}	8.56 ^{+0.12} _{-0.11}	3.95 ^{+0.07} _{-0.06}	0.47 ^{+0.19} _{-0.20}	I	0	2.65	538	414

Table 1 (cont'd)

AP ID ^a	CMD Best Fit Parameters ^b			Integrated Best Fit Parameters ^c			Best ^d Flag ^e	R _{ap} ^f	N _{stars} ^g	N _{bg} ^h	
	log(<i>t</i> [Myr])	log(<i>M</i> [<i>M</i> _⊙])	<i>A_V</i> [mag]	log(<i>t</i> [Myr])	log(<i>M</i> [<i>M</i> _⊙])	<i>A_V</i> [mag]					
AP46	8.20 ^{+0.00} _{-0.50}	3.39 ^{+0.02} _{-0.08}	0.65 ^{+0.15} _{-0.00}	7.32 ^{+0.88} _{-0.72}	3.13 ^{+0.23} _{-0.18}	0.75 ^{+0.37} _{-0.58}	I	0	1.56	118	56
AP47	8.20 ^{+0.00} _{-0.10}	4.10 ^{+0.00} _{-0.03}	1.35 ^{+0.05} _{-0.00}	8.84 ^{+0.05} _{-0.06}	3.87 ^{+0.05} _{-0.05}	0.04 ^{+0.08} _{-0.04}	I	0	2.06	393	207
AP48	8.20 ^{+0.00} _{-0.00}	3.95 ^{+0.00} _{-0.02}	0.55 ^{+0.00} _{-0.05}	8.24 ^{+0.08} _{-0.07}	4.10 ^{+0.06} _{-0.06}	0.36 ^{+0.14} _{-0.14}	I	0	2.46	475	279
AP49	8.80 ^{+0.00} _{-0.30}	3.95 ^{+0.00} _{-0.03}	0.15 ^{+0.00} _{-0.10}	0.00 ^{+0.00} _{-0.00}	0.00 ^{+0.00} _{-0.00}	0.00 ^{+0.00} _{-0.00}	I	0	4.14	692	817
AP50	8.40 ^{+0.30} _{-0.10}	3.90 ^{+0.01} _{-0.06}	1.00 ^{+0.10} _{-0.75}	8.84 ^{+0.15} _{-0.16}	3.87 ^{+0.09} _{-0.08}	0.28 ^{+0.25} _{-0.23}	I	0	2.05	381	228
AP52	8.10 ^{+0.00} _{-0.00}	4.14 ^{+0.00} _{-0.00}	0.70 ^{+0.00} _{-0.00}	8.29 ^{+0.07} _{-0.08}	4.36 ^{+0.06} _{-0.05}	0.49 ^{+0.15} _{-0.15}	I	0	3.31	842	625
AP53	8.00 ^{+0.00} _{-0.10}	3.70 ^{+0.00} _{-0.04}	1.45 ^{+0.00} _{-0.05}	7.64 ^{+0.00} _{-0.11}	2.70 ^{+0.01} _{-0.09}	0.66 ^{+0.20} _{-0.31}	I	0	2.02	270	128
AP55	8.90 ^{+0.00} _{-0.00}	4.08 ^{+0.02} _{-0.00}	0.00 ^{+0.08} _{-0.00}	8.81 ^{+0.07} _{-0.07}	3.86 ^{+0.06} _{-0.06}	0.13 ^{+0.14} _{-0.13}	I	0	2.39	490	223
AP56	8.50 ^{+0.00} _{-0.20}	3.78 ^{+0.02} _{-0.04}	0.35 ^{+0.30} _{-0.00}	8.74 ^{+0.05} _{-0.05}	3.71 ^{+0.05} _{-0.05}	0.01 ^{+0.07} _{-0.01}	I	0	1.83	295	183
AP58	9.10 ^{+0.00} _{-0.00}	3.81 ^{+0.04} _{-0.05}	0.30 ^{+0.15} _{-0.00}	7.89 ^{+1.13} _{-1.34}	3.46 ^{+0.33} _{-0.38}	1.39 ^{+0.88} _{-0.97}	I	0	1.99	172	54
AP59	8.20 ^{+0.00} _{-0.00}	3.74 ^{+0.01} _{-0.01}	1.10 ^{+0.00} _{-0.05}	8.71 ^{+0.08} _{-0.08}	3.49 ^{+0.07} _{-0.07}	0.17 ^{+0.13} _{-0.14}	I	0	2.45	334	237
AP60	8.50 ^{+0.00} _{-0.00}	3.68 ^{+0.03} _{-0.00}	0.45 ^{+0.10} _{-0.00}	8.71 ^{+0.05} _{-0.05}	3.43 ^{+0.06} _{-0.06}	0.04 ^{+0.08} _{-0.04}	I	0	1.80	237	155
AP61	8.50 ^{+0.10} _{-0.00}	3.56 ^{+0.02} _{-0.03}	0.40 ^{+0.05} _{-0.15}	8.50 ^{+0.11} _{-0.09}	3.16 ^{+0.11} _{-0.09}	0.16 ^{+0.18} _{-0.16}	I	0	1.79	195	148
AP63	8.50 ^{+0.00} _{-0.00}	3.75 ^{+0.06} _{-0.00}	0.65 ^{+0.10} _{-0.00}	8.35 ^{+0.06} _{-0.06}	3.40 ^{+0.08} _{-0.07}	0.14 ^{+0.15} _{-0.14}	I	0	2.26	255	111
AP64	9.00 ^{+0.00} _{-0.20}	3.58 ^{+0.05} _{-0.05}	0.00 ^{+0.65} _{-0.05}	8.65 ^{+0.11} _{-0.11}	3.09 ^{+0.09} _{-0.09}	0.36 ^{+0.23} _{-0.25}	I	0	1.46	141	71
AP65	8.60 ^{+0.10} _{-0.30}	3.67 ^{+0.01} _{-0.09}	0.45 ^{+0.35} _{-0.20}	8.79 ^{+0.05} _{-0.04}	3.48 ^{+0.06} _{-0.06}	0.05 ^{+0.09} _{-0.05}	I	0	1.84	268	200
AP66	8.30 ^{+0.00} _{-0.90}	3.28 ^{+0.02} _{-0.14}	0.55 ^{+0.20} _{-0.00}	8.27 ^{+0.13} _{-0.11}	3.23 ^{+0.09} _{-0.11}	0.49 ^{+0.28} _{-0.22}	I	0	1.85	153	95
AP68	9.10 ^{+0.00} _{-0.00}	4.20 ^{+0.03} _{-0.03}	0.35 ^{+0.00} _{-0.10}	9.48 ^{+0.19} _{-0.20}	4.21 ^{+0.08} _{-0.09}	0.19 ^{+0.23} _{-0.19}	I	0	1.83	279	137
AP69	7.90 ^{+0.40} _{-0.10}	3.97 ^{+0.00} _{-0.45}	2.65 ^{+0.05} _{-0.65}	7.95 ^{+1.19} _{-1.42}	3.57 ^{+0.35} _{-0.44}	1.38 ^{+0.87} _{-1.02}	I	1	1.86	207	78
AP70	8.80 ^{+0.00} _{-0.10}	3.57 ^{+0.00} _{-0.03}	0.20 ^{+0.20} _{-0.10}	8.48 ^{+0.10} _{-0.09}	3.09 ^{+0.09} _{-0.08}	0.20 ^{+0.17} _{-0.18}	I	0	2.51	183	64
AP71	9.30 ^{+0.30} _{-0.10}	4.40 ^{+0.14} _{-0.09}	0.35 ^{+0.15} _{-0.10}	9.23 ^{+0.57} _{-0.77}	3.93 ^{+0.15} _{-0.15}	0.85 ^{+0.81} _{-0.60}	I	0	1.43	126	64
AP72	8.10 ^{+0.10} _{-0.10}	3.97 ^{+0.00} _{-0.06}	1.50 ^{+0.00} _{-0.20}	8.73 ^{+0.09} _{-0.09}	4.03 ^{+0.06} _{-0.06}	0.66 ^{+0.14} _{-0.15}	I	0	1.92	293	180
AP74	8.10 ^{+0.00} _{-0.30}	3.38 ^{+0.02} _{-0.06}	1.55 ^{+0.20} _{-0.00}	7.66 ^{+0.91} _{-0.90}	3.13 ^{+0.21} _{-0.19}	1.04 ^{+0.63} _{-0.70}	I	0	1.43	134	67
AP77	9.00 ^{+0.00} _{-0.00}	4.12 ^{+0.06} _{-0.00}	0.00 ^{+0.00} _{-0.00}	9.11 ^{+0.11} _{-0.13}	4.18 ^{+0.07} _{-0.07}	0.18 ^{+0.15} _{-0.15}	I	0	3.01	681	430
AP80	8.80 ^{+0.00} _{-0.10}	4.00 ^{+0.04} _{-0.00}	0.30 ^{+0.35} _{-0.00}	8.86 ^{+0.10} _{-0.12}	3.74 ^{+0.07} _{-0.08}	0.18 ^{+0.16} _{-0.15}	I	0	2.25	400	256
AP81	7.30 ^{+0.10} _{-0.10}	3.50 ^{+0.00} _{-0.01}	0.70 ^{+0.00} _{-0.05}	7.61 ^{+0.17} _{-0.21}	3.30 ^{+0.17} _{-0.21}	0.30 ^{+0.12} _{-0.13}	I	0	1.91	175	54
AP83	8.70 ^{+0.00} _{-0.01}	3.57 ^{+0.03} _{-0.04}	0.20 ^{+0.10} _{-0.05}	8.36 ^{+0.14} _{-0.04}	2.94 ^{+0.17} _{-0.03}	0.04 ^{+0.09} _{-0.04}	I	0	1.71	253	187
AP84	8.20 ^{+0.00} _{-0.00}	3.88 ^{+0.00} _{-0.00}	0.90 ^{+0.00} _{-0.00}	8.35 ^{+0.06} _{-0.08}	4.03 ^{+0.07} _{-0.07}	0.67 ^{+0.19} _{-0.17}	I	0	1.80	269	153
AP85	8.00 ^{+0.00} _{-0.00}	3.64 ^{+0.01} _{-0.01}	0.60 ^{+0.05} _{-0.00}	8.15 ^{+0.09} _{-0.08}	3.62 ^{+0.09} _{-0.08}	0.37 ^{+0.17} _{-0.20}	I	0	2.58	266	97
AP86	8.50 ^{+0.10} _{-0.00}	3.61 ^{+0.02} _{-0.03}	0.50 ^{+0.05} _{-0.15}	8.14 ^{+0.11} _{-0.13}	3.62 ^{+0.12} _{-0.12}	1.09 ^{+0.30} _{-0.24}	I	0	2.00	237	139
AP87	8.60 ^{+0.10} _{-0.00}	3.60 ^{+0.02} _{-0.02}	0.15 ^{+0.00} _{-0.15}	8.03 ^{+0.11} _{-0.11}	3.74 ^{+0.08} _{-0.08}	1.09 ^{+0.19} _{-0.18}	I	0	2.20	383	299
AP88	8.50 ^{+0.10} _{-0.00}	3.79 ^{+0.03} _{-0.02}	0.60 ^{+0.05} _{-0.15}	8.11 ^{+1.47} _{-1.46}	3.78 ^{+1.25} _{-1.18}	1.45 ^{+1.03} _{-1.02}	I	0	2.59	519	260
AP89	8.80 ^{+0.00} _{-0.00}	4.10 ^{+0.03} _{-0.00}	0.20 ^{+0.05} _{-0.05}	8.80 ^{+0.03} _{-0.03}	3.60 ^{+0.04} _{-0.03}	0.00 ^{+0.07} _{-0.00}	I	0	1.93	361	244

Table 1 (cont'd)

AP ID ^a	CMD Best Fit Parameters ^b			Integrated Best Fit Parameters ^c			Best ^d Flag ^e	R _{ap} ^f	N _{stars} ^g	N _{bg} ^h	
	log(<i>t</i> [Myr])	log(<i>M</i> [<i>M</i> _⊙])	<i>A_V</i> [mag]	log(<i>t</i> [Myr])	log(<i>M</i> [<i>M</i> _⊙])	<i>A_V</i> [mag]					
AP90	8.30 ^{+0.00} _{-0.00}	3.75 ^{+0.00} _{-0.03}	1.35 ^{+0.00} _{-0.10}	8.24 ^{+0.07} _{-0.18}	3.78 ^{+0.13} _{-0.12}	1.30 ^{+0.38} _{-0.17}	I	0	1.54	177	65
AP91	7.50 ^{+0.20} _{-0.20}	3.43 ^{+0.02} _{-0.01}	1.00 ^{+0.10} _{-0.05}	7.52 ^{+0.08} _{-0.07}	3.86 ^{+0.06} _{-0.05}	0.18 ^{+0.10} _{-0.09}	I	0	2.21	339	319
AP93	7.70 ^{+0.10} _{-0.00}	3.83 ^{+0.03} _{-0.00}	1.20 ^{+0.00} _{-0.05}	8.06 ^{+0.08} _{-0.07}	4.23 ^{+0.06} _{-0.06}	0.81 ^{+0.13} _{-0.14}	I	0	2.18	336	254
AP94	7.20 ^{+0.10} _{-0.10}	3.75 ^{+0.00} _{-0.02}	0.95 ^{+0.00} _{-0.00}	7.92 ^{+0.12} _{-0.11}	4.07 ^{+0.08} _{-0.07}	0.38 ^{+0.19} _{-0.18}	I	0	2.53	469	324
AP95	8.50 ^{+0.00} _{-0.00}	4.34 ^{+0.00} _{-0.00}	0.65 ^{+0.00} _{-0.00}	8.74 ^{+0.08} _{-0.08}	4.35 ^{+0.05} _{-0.05}	0.21 ^{+0.17} _{-0.16}	I	0	3.55	1117	739
AP96	8.10 ^{+0.10} _{-0.00}	3.84 ^{+0.02} _{-0.00}	0.70 ^{+0.05} _{-0.05}	8.63 ^{+0.07} _{-0.07}	3.86 ^{+0.04} _{-0.05}	0.05 ^{+0.10} _{-0.05}	I	0	2.73	551	428
AP97	8.90 ^{+0.00} _{-0.10}	4.00 ^{+0.04} _{-0.04}	0.10 ^{+0.25} _{-0.05}	8.28 ^{+0.10} _{-0.09}	4.10 ^{+0.09} _{-0.08}	1.24 ^{+0.20} _{-0.20}	I	0	2.45	244	256
AP98	7.40 ^{+0.40} _{-0.00}	3.72 ^{+0.02} _{-0.02}	1.30 ^{+0.00} _{-0.15}	7.34 ^{+0.73} _{-0.27}	3.99 ^{+0.23} _{-0.16}	0.95 ^{+0.29} _{-0.49}	I	0	2.18	422	319
AP99	8.80 ^{+0.00} _{-0.20}	3.54 ^{+0.00} _{-0.04}	0.00 ^{+0.35} _{-0.00}	0.00 ^{+0.00} _{-0.00}	0.00 ^{+0.00} _{-0.00}	0.00 ^{+0.00} _{-0.00}	I	0	1.70	243	179
AP100	9.10 ^{+0.00} _{-0.00}	4.17 ^{+0.00} _{-0.06}	0.20 ^{+0.05} _{-0.05}	8.89 ^{+0.21} _{-0.31}	4.02 ^{+0.09} _{-0.09}	0.72 ^{+0.36} _{-0.32}	I	0	2.32	316	82
AP101	8.00 ^{+0.00} _{-0.50}	3.89 ^{+0.00} _{-0.07}	1.00 ^{+0.15} _{-0.00}	8.49 ^{+0.04} _{-0.04}	3.64 ^{+0.05} _{-0.04}	0.05 ^{+0.11} _{-0.05}	I	0	2.14	310	201
AP102	7.70 ^{+0.10} _{-0.00}	4.12 ^{+0.02} _{-0.00}	1.05 ^{+0.00} _{-0.00}	6.49 ^{+0.06} _{-0.07}	3.93 ^{+0.17} _{-0.14}	1.03 ^{+0.07} _{-0.09}	I	0	5.06	1550	1368
AP103	8.20 ^{+0.10} _{-0.10}	3.42 ^{+0.02} _{-0.08}	0.65 ^{+0.10} _{-0.15}	8.31 ^{+0.11} _{-0.11}	3.20 ^{+0.11} _{-0.10}	0.27 ^{+0.26} _{-0.24}	I	0	1.74	208	152
AP104	8.90 ^{+0.00} _{-0.00}	3.96 ^{+0.00} _{-0.03}	0.25 ^{+0.00} _{-0.05}	8.58 ^{+0.13} _{-0.13}	3.45 ^{+0.09} _{-0.08}	0.30 ^{+0.26} _{-0.26}	I	0	1.72	250	135
AP106	9.00 ^{+0.00} _{-0.00}	3.63 ^{+0.00} _{-0.00}	0.00 ^{+0.00} _{-0.00}	8.80 ^{+0.08} _{-0.07}	3.39 ^{+0.09} _{-0.08}	0.24 ^{+0.16} _{-0.15}	I	0	1.40	140	57
AP107	9.10 ^{+0.00} _{-0.00}	4.12 ^{+0.05} _{-0.03}	0.05 ^{+0.10} _{-0.00}	9.11 ^{+0.09} _{-0.09}	3.95 ^{+0.10} _{-0.09}	0.12 ^{+0.12} _{-0.12}	I	0	2.17	419	274
AP108	8.20 ^{+0.00} _{-0.00}	4.12 ^{+0.03} _{-0.00}	0.85 ^{+0.05} _{-0.00}	8.27 ^{+0.37} _{-1.03}	3.80 ^{+0.26} _{-0.68}	0.19 ^{+0.22} _{-0.19}	I	0	3.24	743	435
AP111	7.30 ^{+0.30} _{-0.10}	3.68 ^{+0.03} _{-0.02}	2.20 ^{+0.00} _{-0.10}	8.87 ^{+0.06} _{-0.05}	3.78 ^{+0.05} _{-0.06}	0.10 ^{+0.10} _{-0.10}	I	0	1.74	267	194
AP112	8.80 ^{+0.00} _{-0.10}	3.32 ^{+0.00} _{-0.04}	0.00 ^{+0.10} _{-0.00}	9.18 ^{+0.12} _{-0.09}	4.70 ^{+0.10} _{-0.09}	0.06 ^{+0.14} _{-0.06}	I	0	2.73	318	203
AP114	9.10 ^{+0.00} _{-0.00}	4.23 ^{+0.08} _{-0.00}	0.15 ^{+0.15} _{-0.00}	9.10 ^{+0.09} _{-0.11}	3.86 ^{+0.10} _{-0.10}	0.06 ^{+0.10} _{-0.06}	I	0	2.33	437	264
AP115	8.90 ^{+0.00} _{-0.00}	3.68 ^{+0.03} _{-0.01}	0.00 ^{+0.10} _{-0.00}	8.86 ^{+0.06} _{-0.05}	3.43 ^{+0.07} _{-0.07}	0.18 ^{+0.11} _{-0.12}	I	0	1.70	183	98
AP119	8.20 ^{+0.00} _{-0.00}	3.71 ^{+0.00} _{-0.02}	0.70 ^{+0.00} _{-0.05}	8.47 ^{+0.07} _{-0.07}	3.53 ^{+0.07} _{-0.07}	0.10 ^{+0.15} _{-0.10}	I	0	1.95	322	215
AP120	8.90 ^{+0.00} _{-0.00}	3.40 ^{+0.02} _{-0.02}	0.05 ^{+0.10} _{-0.05}	9.22 ^{+0.21} _{-0.19}	3.44 ^{+0.14} _{-0.15}	0.22 ^{+0.20} _{-0.20}	I	0	1.48	88	26
AP121	8.50 ^{+0.00} _{-0.00}	3.94 ^{+0.02} _{-0.00}	0.50 ^{+0.05} _{-0.00}	8.42 ^{+0.11} _{-0.11}	3.69 ^{+0.11} _{-0.11}	0.39 ^{+0.27} _{-0.25}	I	0	2.39	451	317
AP122	6.60 ^{+0.30} _{-0.00}	2.90 ^{+0.00} _{-0.04}	0.95 ^{+0.00} _{-0.10}	7.76 ^{+0.04} _{-0.04}	3.03 ^{+0.06} _{-0.06}	0.00 ^{+0.07} _{-0.00}	I	0	1.34	127	85
AP123	8.50 ^{+0.00} _{-0.00}	3.74 ^{+0.00} _{-0.03}	0.35 ^{+0.00} _{-0.10}	8.57 ^{+0.08} _{-0.08}	3.80 ^{+0.06} _{-0.06}	0.31 ^{+0.16} _{-0.16}	I	0	2.11	352	273
AP124	8.90 ^{+0.10} _{-0.00}	3.85 ^{+0.04} _{-0.03}	0.80 ^{+0.10} _{-0.25}	9.25 ^{+0.13} _{-0.13}	4.15 ^{+0.08} _{-0.08}	0.28 ^{+0.17} _{-0.17}	I	0	2.86	262	109
AP125	8.80 ^{+0.00} _{-0.00}	4.05 ^{+0.00} _{-0.03}	0.10 ^{+0.00} _{-0.05}	6.70 ^{+0.04} _{-0.05}	2.15 ^{+0.04} _{-0.05}	0.40 ^{+0.07} _{-0.07}	I	0	2.51	485	324
AP126	8.70 ^{+0.00} _{-0.00}	3.59 ^{+0.00} _{-0.00}	0.00 ^{+0.05} _{-0.00}	8.76 ^{+0.11} _{-0.10}	3.45 ^{+0.07} _{-0.07}	0.10 ^{+0.12} _{-0.10}	I	0	1.69	210	139
AP127	8.20 ^{+0.00} _{-0.10}	3.53 ^{+0.03} _{-0.02}	0.45 ^{+0.15} _{-0.00}	8.30 ^{+0.13} _{-0.12}	3.72 ^{+0.12} _{-0.11}	0.59 ^{+0.25} _{-0.26}	I	0	2.12	292	233
AP128	8.10 ^{+0.00} _{-0.10}	3.78 ^{+0.00} _{-0.04}	1.10 ^{+0.05} _{-0.00}	8.72 ^{+0.10} _{-0.10}	3.71 ^{+0.07} _{-0.06}	0.30 ^{+0.17} _{-0.17}	I	0	1.56	229	171
AP129	8.40 ^{+0.00} _{-0.10}	3.37 ^{+0.00} _{-0.03}	0.60 ^{+0.00} _{-0.05}	7.90 ^{+0.13} _{-0.17}	3.16 ^{+0.13} _{-0.11}	0.60 ^{+0.19} _{-0.18}	I	0	1.91	160	79
AP131	8.30 ^{+0.00} _{-0.00}	3.73 ^{+0.02} _{-0.00}	0.70 ^{+0.05} _{-0.00}	8.44 ^{+0.15} _{-0.15}	3.46 ^{+0.11} _{-0.11}	0.23 ^{+0.23} _{-0.21}	I	0	2.33	321	192

Table 1 (cont'd)

AP ID ^a	CMD Best Fit Parameters ^b			Integrated Best Fit Parameters ^c			Best ^d Flag ^e	R _{ap} ^f	N _{stars} ^g	N _{bg} ^h	
	log(<i>t</i> [Myr])	log(<i>M</i> [<i>M</i> _⊙])	<i>A_V</i> [mag]	log(<i>t</i> [Myr])	log(<i>M</i> [<i>M</i> _⊙])	<i>A_V</i> [mag]					
AP132	9.00 ^{+0.10} _{-0.00}	4.01 ^{+0.05} _{-0.02}	0.35 ^{+0.00} _{-0.25}	8.96 ^{+0.27} _{-0.25}	4.01 ^{+0.13} _{-0.12}	0.65 ^{+0.29} _{-0.39}	I	0	2.34	211	137
AP133	9.70 ^{+0.00} _{-0.20}	4.87 ^{+0.00} _{-0.17}	0.05 ^{+0.05} _{-0.05}	9.10 ^{+0.30} _{-0.22}	4.12 ^{+0.09} _{-0.09}	0.70 ^{+0.29} _{-0.36}	I	0	1.77	275	187
AP134	8.20 ^{+0.00} _{-0.00}	3.89 ^{+0.00} _{-0.00}	0.50 ^{+0.00} _{-0.00}	8.18 ^{+0.08} _{-0.08}	4.08 ^{+0.06} _{-0.06}	0.61 ^{+0.16} _{-0.16}	I	0	2.93	554	358
AP135	8.80 ^{+0.00} _{-0.20}	3.37 ^{+0.03} _{-0.04}	0.45 ^{+0.50} _{-0.05}	10.20 ^{+0.03} _{-0.03}	3.95 ^{+0.03} _{-0.03}	0.30 ^{+0.07} _{-0.07}	I	0	1.72	106	42
AP136	8.40 ^{+0.00} _{-0.00}	3.42 ^{+0.01} _{-0.02}	0.70 ^{+0.05} _{-0.05}	8.94 ^{+0.06} _{-0.07}	3.30 ^{+0.08} _{-0.07}	0.02 ^{+0.07} _{-0.02}	I	0	1.79	183	117
AP137	8.40 ^{+0.00} _{-0.00}	3.67 ^{+0.02} _{-0.00}	0.70 ^{+0.05} _{-0.00}	8.55 ^{+0.08} _{-0.08}	3.40 ^{+0.08} _{-0.08}	0.36 ^{+0.15} _{-0.16}	I	0	1.52	174	96
AP138	8.10 ^{+0.00} _{-0.00}	3.42 ^{+0.00} _{-0.02}	0.75 ^{+0.00} _{-0.05}	8.33 ^{+0.13} _{-0.12}	3.41 ^{+0.12} _{-0.10}	0.37 ^{+0.26} _{-0.27}	I	0	1.94	217	160
AP139	7.60 ^{+0.00} _{-0.00}	4.18 ^{+0.00} _{-0.00}	3.00 ^{+0.00} _{-0.00}	9.10 ^{+0.03} _{-0.03}	4.70 ^{+0.03} _{-0.03}	0.10 ^{+0.07} _{-0.07}	I	1	2.40	287	261
AP141	6.60 ^{+0.20} _{-0.00}	2.98 ^{+0.02} _{-0.09}	1.25 ^{+0.05} _{-0.25}	7.52 ^{+0.03} _{-0.05}	3.42 ^{+0.05} _{-0.05}	0.19 ^{+0.08} _{-0.07}	I	0	2.32	156	102
AP142	8.10 ^{+0.00} _{-0.00}	3.61 ^{+0.02} _{-0.00}	0.65 ^{+0.05} _{-0.00}	8.25 ^{+0.11} _{-0.10}	3.74 ^{+0.09} _{-0.08}	0.66 ^{+0.21} _{-0.22}	I	0	2.06	344	258
AP143	9.00 ^{+0.00} _{-0.20}	3.65 ^{+0.02} _{-0.06}	0.00 ^{+0.45} _{-0.00}	8.60 ^{+0.39} _{-0.46}	3.49 ^{+0.11} _{-0.09}	0.50 ^{+0.69} _{-0.50}	I	0	1.71	180	71
AP144	8.30 ^{+0.10} _{-0.00}	3.72 ^{+0.05} _{-0.00}	0.80 ^{+0.10} _{-0.00}	8.44 ^{+0.21} _{-0.17}	3.82 ^{+0.12} _{-0.13}	0.87 ^{+0.35} _{-0.43}	I	0	1.96	241	102
AP145	8.40 ^{+0.00} _{-0.00}	3.50 ^{+0.02} _{-0.00}	0.25 ^{+0.10} _{-0.00}	8.46 ^{+0.07} _{-0.05}	3.45 ^{+0.08} _{-0.05}	0.10 ^{+0.13} _{-0.10}	I	0	2.00	253	153
AP146	9.10 ^{+0.00} _{-0.00}	4.03 ^{+0.00} _{-0.10}	0.20 ^{+0.05} _{-0.10}	9.22 ^{+0.19} _{-0.19}	3.88 ^{+0.11} _{-0.12}	0.22 ^{+0.18} _{-0.18}	I	0	1.86	252	135
AP147	7.90 ^{+0.10} _{-0.20}	3.37 ^{+0.05} _{-0.05}	1.80 ^{+0.10} _{-0.10}	8.86 ^{+0.26} _{-0.27}	3.47 ^{+0.13} _{-0.13}	0.33 ^{+0.28} _{-0.26}	I	0	1.63	165	63
AP149	8.30 ^{+0.10} _{-0.00}	3.77 ^{+0.04} _{-0.01}	1.05 ^{+0.00} _{-0.10}	8.34 ^{+0.23} _{-0.17}	3.81 ^{+0.13} _{-0.16}	0.96 ^{+0.36} _{-0.50}	I	0	1.84	262	159
AP152	8.20 ^{+0.00} _{-0.00}	3.73 ^{+0.05} _{-0.00}	0.45 ^{+0.10} _{-0.00}	8.29 ^{+0.11} _{-0.12}	3.99 ^{+0.08} _{-0.08}	0.70 ^{+0.23} _{-0.22}	I	0	2.93	588	432
AP153	9.50 ^{+0.00} _{-0.20}	4.90 ^{+0.03} _{-0.11}	0.15 ^{+0.40} _{-0.00}	7.08 ^{+0.04} _{-0.04}	3.15 ^{+0.03} _{-0.03}	1.60 ^{+0.07} _{-0.07}	I	0	3.13	290	574
AP155	7.20 ^{+0.10} _{-0.40}	3.38 ^{+0.01} _{-0.01}	1.45 ^{+0.10} _{-0.00}	7.30 ^{+0.88} _{-0.74}	3.19 ^{+0.24} _{-0.23}	0.73 ^{+0.38} _{-0.57}	I	0	1.59	121	81
AP156	9.20 ^{+0.00} _{-0.00}	4.04 ^{+0.04} _{-0.05}	0.35 ^{+0.10} _{-0.05}	7.98 ^{+0.29} _{-0.31}	3.74 ^{+0.14} _{-0.10}	2.16 ^{+0.23} _{-0.23}	I	0	1.77	146	66
AP157	8.00 ^{+0.00} _{-0.10}	3.85 ^{+0.03} _{-0.07}	1.85 ^{+0.10} _{-0.10}	8.75 ^{+0.14} _{-0.01}	3.51 ^{+0.16} _{-0.02}	0.40 ^{+0.10} _{-0.10}	I	0	1.51	233	158
AP158	8.10 ^{+0.10} _{-0.00}	3.58 ^{+0.02} _{-0.02}	0.85 ^{+0.05} _{-0.05}	8.20 ^{+0.10} _{-0.11}	3.57 ^{+0.09} _{-0.10}	0.84 ^{+0.23} _{-0.22}	I	0	1.69	196	110
AP159	9.00 ^{+0.00} _{-0.10}	3.72 ^{+0.01} _{-0.06}	0.10 ^{+0.20} _{-0.05}	8.73 ^{+0.50} _{-0.65}	3.40 ^{+0.14} _{-0.13}	0.60 ^{+0.85} _{-0.60}	I	0	1.37	151	114
AP161	9.30 ^{+0.00} _{-0.20}	4.07 ^{+0.00} _{-0.22}	0.00 ^{+0.40} _{-0.00}	8.16 ^{+0.09} _{-0.13}	3.89 ^{+0.10} _{-0.09}	1.89 ^{+0.23} _{-0.18}	I	0	1.68	188	142
AP162	10.10 ^{+0.00} _{-2.60}	5.14 ^{+0.08} _{-5.14}	0.10 ^{+2.15} _{-0.00}	9.45 ^{+0.78} _{-0.76}	4.20 ^{+0.21} _{-0.18}	0.89 ^{+0.81} _{-0.80}	I	0	1.75	225	156
AP163	7.90 ^{+0.00} _{-0.00}	3.57 ^{+0.00} _{-0.02}	0.95 ^{+0.04} _{-0.05}	7.87 ^{+0.10} _{-0.09}	3.96 ^{+0.08} _{-0.08}	0.99 ^{+0.15} _{-0.15}	I	0	1.71	277	218
AP164	8.30 ^{+0.00} _{-0.00}	4.01 ^{+0.00} _{-0.01}	0.55 ^{+0.00} _{-0.05}	8.46 ^{+0.08} _{-0.08}	3.95 ^{+0.06} _{-0.06}	0.18 ^{+0.17} _{-0.17}	I	0	2.91	638	484
AP165	8.50 ^{+0.00} _{-0.30}	3.17 ^{+0.00} _{-0.11}	0.40 ^{+0.20} _{-0.10}	8.08 ^{+0.28} _{-0.25}	3.21 ^{+0.16} _{-0.16}	0.88 ^{+0.43} _{-0.48}	I	0	1.82	140	90
AP166	7.30 ^{+0.10} _{-0.00}	4.33 ^{+0.06} _{-0.00}	3.00 ^{+0.00} _{-0.00}	0.00 ^{+0.00} _{-0.00}	0.00 ^{+0.00} _{-0.00}	0.00 ^{+0.00} _{-0.00}	I	0	2.29	400	365
AP167	8.80 ^{+0.00} _{-0.00}	3.35 ^{+0.05} _{-0.02}	0.10 ^{+0.20} _{-0.05}	9.14 ^{+0.10} _{-0.11}	3.39 ^{+0.10} _{-0.10}	0.03 ^{+0.07} _{-0.03}	I	0	1.36	160	116
AP168	8.00 ^{+0.10} _{-0.10}	3.72 ^{+0.01} _{-0.04}	1.05 ^{+0.05} _{-0.10}	8.62 ^{+0.07} _{-0.08}	3.44 ^{+0.07} _{-0.07}	0.06 ^{+0.15} _{-0.06}	I	0	1.80	237	176
AP169	8.20 ^{+0.00} _{-0.30}	3.48 ^{+0.00} _{-0.06}	0.75 ^{+0.15} _{-0.05}	8.34 ^{+0.09} _{-0.09}	3.29 ^{+0.11} _{-0.11}	0.25 ^{+0.23} _{-0.23}	I	0	1.49	181	122
AP170	9.10 ^{+0.00} _{-0.00}	3.83 ^{+0.00} _{-0.04}	0.15 ^{+0.05} _{-0.05}	7.99 ^{+0.34} _{-0.39}	2.81 ^{+0.31} _{-0.35}	0.48 ^{+0.26} _{-0.39}	I	0	1.74	174	80

Table 1 (cont'd)

AP ID ^a	CMD Best Fit Parameters ^b			Integrated Best Fit Parameters ^c			Best ^d Flag ^e	R _{ap} ^f	N _{stars} ^g	N _{bg} ^h	
	log(<i>t</i> [Myr])	log(<i>M</i> [<i>M</i> _⊙])	<i>A_V</i> [mag]	log(<i>t</i> [Myr])	log(<i>M</i> [<i>M</i> _⊙])	<i>A_V</i> [mag]					
AP172	8.10 ^{+0.00} _{-0.30}	3.36 ^{+0.04} _{-0.13}	1.85 ^{+0.25} _{-0.05}	9.28 ^{+0.13} _{-0.11}	3.90 ^{+0.09} _{-0.09}	0.20 ^{+0.13} _{-0.17}	I	0	1.70	191	90
AP173	8.20 ^{+0.00} _{-0.00}	3.98 ^{+0.00} _{-0.02}	1.25 ^{+0.00} _{-0.00}	8.35 ^{+0.08} _{-0.09}	3.91 ^{+0.08} _{-0.07}	0.79 ^{+0.24} _{-0.16}	I	0	2.09	338	164
AP174	9.10 ^{+0.00} _{-0.00}	3.81 ^{+0.00} _{-0.00}	0.00 ^{+0.00} _{-0.00}	0.00 ^{+0.00} _{-0.00}	0.00 ^{+0.00} _{-0.00}	0.00 ^{+0.00} _{-0.00}	I	0	2.19	222	171
AP175	8.10 ^{+0.10} _{-0.00}	3.68 ^{+0.03} _{-0.01}	0.85 ^{+0.00} _{-0.05}	8.35 ^{+0.04} _{-0.04}	3.75 ^{+0.04} _{-0.04}	0.60 ^{+0.07} _{-0.07}	I	0	2.04	213	67
AP179	8.90 ^{+0.10} _{-0.00}	3.85 ^{+0.09} _{-0.03}	0.60 ^{+0.05} _{-0.15}	9.15 ^{+0.18} _{-0.14}	3.98 ^{+0.11} _{-0.11}	0.35 ^{+0.16} _{-0.19}	I	0	2.01	143	53
AP180	7.80 ^{+0.20} _{-0.30}	3.13 ^{+0.01} _{-0.03}	1.20 ^{+0.05} _{-0.10}	8.28 ^{+0.06} _{-0.06}	2.72 ^{+0.09} _{-0.09}	0.02 ^{+0.07} _{-0.02}	I	0	1.56	80	40
AP182	9.10 ^{+0.70} _{-0.00}	3.88 ^{+0.73} _{-0.05}	0.55 ^{+0.00} _{-0.45}	9.06 ^{+0.52} _{-0.80}	3.80 ^{+0.14} _{-0.14}	0.71 ^{+0.93} _{-0.59}	I	0	1.93	196	102
AP184	9.10 ^{+0.00} _{-0.00}	3.72 ^{+0.05} _{-0.04}	0.00 ^{+0.10} _{-0.00}	8.43 ^{+0.67} _{-0.39}	3.84 ^{+0.07} _{-0.05}	1.20 ^{+0.57} _{-0.83}	I	0	2.05	197	83
AP185	8.30 ^{+0.10} _{-0.10}	3.28 ^{+0.01} _{-0.02}	0.35 ^{+0.05} _{-0.10}	8.18 ^{+0.15} _{-0.08}	3.11 ^{+0.13} _{-0.10}	0.11 ^{+0.15} _{-0.11}	I	0	1.81	177	100
AP186	7.80 ^{+0.00} _{-0.00}	3.97 ^{+0.01} _{-0.00}	1.35 ^{+0.05} _{-0.00}	7.83 ^{+0.11} _{-0.13}	4.08 ^{+0.06} _{-0.07}	1.11 ^{+0.18} _{-0.18}	I	0	1.97	359	239
AP187	8.10 ^{+0.00} _{-0.00}	3.81 ^{+0.00} _{-0.02}	0.45 ^{+0.00} _{-0.05}	8.24 ^{+0.09} _{-0.08}	3.94 ^{+0.07} _{-0.07}	0.26 ^{+0.18} _{-0.17}	I	0	2.68	559	434
AP188	7.90 ^{+0.00} _{-0.40}	3.21 ^{+0.00} _{-0.06}	0.70 ^{+0.05} _{-0.05}	8.15 ^{+0.03} _{-0.03}	3.12 ^{+0.06} _{-0.05}	0.42 ^{+0.07} _{-0.08}	I	0	1.85	193	160
AP190	10.00 ^{+0.00} _{-1.00}	4.95 ^{+0.04} _{-0.49}	0.80 ^{+1.00} _{-0.05}	7.10 ^{+0.05} _{-0.05}	3.99 ^{+0.14} _{-0.16}	2.51 ^{+0.17} _{-0.17}	I	0	2.70	66	210
AP191	8.30 ^{+0.00} _{-0.00}	3.74 ^{+0.02} _{-0.00}	0.35 ^{+0.05} _{-0.00}	8.42 ^{+0.08} _{-0.08}	3.76 ^{+0.07} _{-0.07}	0.17 ^{+0.19} _{-0.16}	I	0	2.28	441	341
AP192	7.80 ^{+0.00} _{-0.20}	4.14 ^{+0.07} _{-0.00}	2.00 ^{+0.30} _{-0.00}	9.32 ^{+0.09} _{-0.09}	4.32 ^{+0.06} _{-0.06}	0.08 ^{+0.11} _{-0.08}	I	1	1.97	400	209
AP193	8.40 ^{+0.00} _{-0.00}	3.76 ^{+0.03} _{-0.00}	0.70 ^{+0.10} _{-0.00}	8.46 ^{+0.12} _{-0.11}	3.54 ^{+0.10} _{-0.09}	0.33 ^{+0.25} _{-0.24}	I	0	1.94	308	225
AP194	7.80 ^{+0.00} _{-0.80}	3.07 ^{+0.00} _{-0.09}	0.90 ^{+0.10} _{-0.00}	8.29 ^{+0.07} _{-0.07}	3.55 ^{+0.05} _{-0.05}	0.46 ^{+0.13} _{-0.14}	I	0	1.47	78	46
AP195	7.80 ^{+1.90} _{-0.00}	4.11 ^{+0.64} _{-0.05}	2.80 ^{+0.05} _{-2.75}	9.37 ^{+0.46} _{-0.37}	4.23 ^{+0.16} _{-0.13}	0.53 ^{+0.40} _{-0.41}	I	0	1.74	286	178
AP196	8.40 ^{+0.40} _{-0.00}	3.98 ^{+0.13} _{-0.00}	1.30 ^{+0.00} _{-0.80}	8.81 ^{+0.26} _{-0.33}	3.98 ^{+0.10} _{-0.10}	0.70 ^{+0.49} _{-0.39}	I	0	2.53	482	330
AP197	7.40 ^{+0.00} _{-0.10}	3.22 ^{+0.03} _{-0.03}	0.50 ^{+0.10} _{-0.05}	6.75 ^{+0.35} _{-0.35}	3.42 ^{+0.37} _{-0.35}	0.29 ^{+0.20} _{-0.25}	I	0	1.92	139	72
AP199	8.90 ^{+0.10} _{-0.00}	3.63 ^{+0.01} _{-0.06}	0.35 ^{+0.05} _{-0.30}	8.37 ^{+0.24} _{-0.21}	3.10 ^{+0.15} _{-0.14}	0.55 ^{+0.39} _{-0.43}	I	0	1.98	180	75
AP200	8.70 ^{+0.00} _{-0.00}	3.67 ^{+0.02} _{-0.02}	0.10 ^{+0.05} _{-0.05}	8.78 ^{+0.06} _{-0.06}	3.49 ^{+0.06} _{-0.06}	0.04 ^{+0.08} _{-0.04}	I	0	1.79	243	160
AP201	9.10 ^{+0.06} _{-0.00}	4.21 ^{+0.00} _{-0.02}	0.45 ^{+0.10} _{-0.00}	7.93 ^{+0.11} _{-0.16}	3.96 ^{+0.14} _{-0.11}	1.62 ^{+0.27} _{-0.23}	I	0	2.79	314	114
AP202	7.50 ^{+0.90} _{-0.20}	3.30 ^{+0.11} _{-0.03}	0.70 ^{+0.00} _{-0.25}	7.86 ^{+0.15} _{-0.17}	3.16 ^{+0.09} _{-0.09}	0.33 ^{+0.21} _{-0.21}	I	0	1.70	138	63
AP203	9.00 ^{+0.00} _{-0.00}	4.00 ^{+0.03} _{-0.00}	0.05 ^{+0.05} _{-0.00}	8.63 ^{+0.16} _{-0.12}	3.62 ^{+0.11} _{-0.04}	0.53 ^{+0.24} _{-0.24}	I	0	1.90	279	121
AP204	7.80 ^{+0.20} _{-0.20}	3.93 ^{+0.03} _{-0.04}	1.75 ^{+0.05} _{-0.10}	9.01 ^{+0.08} _{-0.09}	3.79 ^{+0.07} _{-0.07}	0.09 ^{+0.12} _{-0.09}	I	0	1.73	253	160
AP205	8.40 ^{+0.10} _{-0.00}	3.46 ^{+0.02} _{-0.02}	0.75 ^{+0.00} _{-0.20}	8.94 ^{+0.07} _{-0.08}	3.40 ^{+0.08} _{-0.08}	0.04 ^{+0.09} _{-0.04}	I	0	1.42	174	131
AP207	7.80 ^{+0.00} _{-0.10}	3.67 ^{+0.02} _{-0.02}	1.00 ^{+0.05} _{-0.00}	7.67 ^{+0.24} _{-0.10}	3.63 ^{+0.16} _{-0.07}	1.01 ^{+0.21} _{-0.20}	I	0	1.63	235	173
AP208	8.10 ^{+0.00} _{-0.10}	3.95 ^{+0.00} _{-0.03}	1.20 ^{+0.05} _{-0.05}	8.77 ^{+0.06} _{-0.06}	3.82 ^{+0.06} _{-0.06}	0.02 ^{+0.06} _{-0.02}	I	0	1.98	307	182
AP209	8.40 ^{+0.10} _{-0.10}	3.80 ^{+0.05} _{-0.00}	0.75 ^{+0.15} _{-0.10}	8.69 ^{+0.16} _{-0.15}	3.89 ^{+0.08} _{-0.07}	0.54 ^{+0.23} _{-0.24}	I	0	1.95	357	270
AP210	8.00 ^{+0.00} _{-0.00}	4.15 ^{+0.04} _{-0.00}	1.80 ^{+0.10} _{-0.00}	8.50 ^{+0.60} _{-0.39}	4.05 ^{+0.10} _{-0.11}	1.05 ^{+0.61} _{-0.89}	I	0	1.77	265	116
AP211	9.30 ^{+0.20} _{-0.10}	4.40 ^{+0.12} _{-0.11}	0.95 ^{+0.00} _{-0.25}	9.31 ^{+0.73} _{-0.76}	4.18 ^{+0.20} _{-0.17}	1.17 ^{+0.93} _{-0.65}	I	0	2.11	84	67
AP212	7.50 ^{+0.00} _{-0.00}	4.59 ^{+0.00} _{-0.00}	3.00 ^{+0.00} _{-0.00}	0.00 ^{+0.00} _{-0.00}	0.00 ^{+0.00} _{-0.00}	0.00 ^{+0.00} _{-0.00}	I	0	4.44	1082	1387

Table 1 (cont'd)

AP ID ^a	CMD Best Fit Parameters ^b			Integrated Best Fit Parameters ^c			Best ^d Flag ^e	R _{ap} ^f	N _{stars} ^g	N _{bg} ^h	
	log(<i>t</i> [Myr])	log(<i>M</i> [<i>M</i> _⊙])	<i>A_V</i> [mag]	log(<i>t</i> [Myr])	log(<i>M</i> [<i>M</i> _⊙])	<i>A_V</i> [mag]					
AP213	8.30 ^{+0.00} _{-0.20}	3.40 ^{+0.02} _{-0.05}	0.70 ^{+0.35} _{-0.05}	8.61 ^{+0.12} _{-0.11}	3.54 ^{+0.08} _{-0.08}	0.44 ^{+0.22} _{-0.24}	I	0	1.53	190	110
AP214	8.10 ^{+0.00} _{-0.00}	3.91 ^{+0.03} _{-0.02}	1.40 ^{+0.05} _{-0.05}	8.96 ^{+0.13} _{-0.15}	3.77 ^{+0.07} _{-0.07}	0.26 ^{+0.22} _{-0.22}	I	0	1.70	264	148
AP215	8.50 ^{+0.00} _{-0.10}	3.49 ^{+0.02} _{-0.03}	0.80 ^{+0.15} _{-0.00}	8.88 ^{+0.05} _{-0.05}	3.27 ^{+0.06} _{-0.06}	0.02 ^{+0.07} _{-0.02}	I	0	1.42	117	60
AP216	8.60 ^{+0.10} _{-0.00}	3.88 ^{+0.02} _{-0.03}	0.60 ^{+0.05} _{-0.25}	8.56 ^{+0.11} _{-0.11}	3.52 ^{+0.08} _{-0.08}	0.31 ^{+0.24} _{-0.24}	I	0	1.93	299	212
AP217	7.90 ^{+0.00} _{-0.10}	3.93 ^{+0.00} _{-0.01}	1.30 ^{+0.05} _{-0.05}	8.77 ^{+0.06} _{-0.06}	3.79 ^{+0.04} _{-0.03}	0.06 ^{+0.09} _{-0.06}	I	0	1.99	320	151
AP218	8.20 ^{+0.00} _{-0.60}	3.08 ^{+0.00} _{-0.07}	0.50 ^{+0.20} _{-0.05}	7.44 ^{+0.26} _{-0.20}	3.02 ^{+0.08} _{-0.08}	0.84 ^{+0.15} _{-0.15}	I	0	1.61	106	49
AP219	7.50 ^{+0.50} _{-0.10}	2.90 ^{+0.03} _{-0.01}	0.70 ^{+0.00} _{-0.15}	7.99 ^{+0.12} _{-0.13}	2.82 ^{+0.10} _{-0.09}	0.41 ^{+0.19} _{-0.20}	I	0	1.74	99	55
AP220	7.80 ^{+0.00} _{-0.00}	4.01 ^{+0.11} _{-0.00}	2.60 ^{+0.20} _{-0.00}	9.73 ^{+0.13} _{-0.11}	4.69 ^{+0.07} _{-0.06}	0.16 ^{+0.09} _{-0.08}	I	0	2.40	229	133
AP221	9.00 ^{+0.00} _{-0.00}	3.88 ^{+0.03} _{-0.05}	0.15 ^{+0.10} _{-0.05}	9.22 ^{+0.13} _{-0.11}	3.75 ^{+0.12} _{-0.10}	0.06 ^{+0.10} _{-0.06}	I	0	1.94	277	148
AP222	8.10 ^{+0.00} _{-0.00}	3.29 ^{+0.02} _{-0.01}	0.35 ^{+0.05} _{-0.05}	8.18 ^{+0.09} _{-0.08}	3.19 ^{+0.11} _{-0.10}	0.23 ^{+0.18} _{-0.19}	I	0	1.85	220	172
AP223	8.80 ^{+0.00} _{-0.10}	3.66 ^{+0.02} _{-0.01}	0.00 ^{+0.25} _{-0.00}	8.52 ^{+0.18} _{-0.19}	3.45 ^{+0.13} _{-0.13}	0.49 ^{+0.41} _{-0.37}	I	0	2.03	258	150
AP226	8.70 ^{+0.00} _{-0.00}	4.77 ^{+0.00} _{-0.00}	0.35 ^{+0.00} _{-0.00}	8.84 ^{+0.04} _{-0.03}	4.59 ^{+0.04} _{-0.03}	0.01 ^{+0.07} _{-0.01}	I	0	5.35	1956	915
AP227	8.80 ^{+0.00} _{-0.10}	3.49 ^{+0.05} _{-0.00}	0.00 ^{+0.40} _{-0.05}	7.94 ^{+0.00} _{-0.07}	2.05 ^{+0.01} _{-0.05}	0.19 ^{+0.08} _{-0.07}	I	0	1.52	132	71
AP228	8.50 ^{+0.10} _{-0.00}	3.57 ^{+0.02} _{-0.02}	0.70 ^{+0.00} _{-0.20}	8.56 ^{+0.10} _{-0.10}	3.28 ^{+0.09} _{-0.09}	0.26 ^{+0.20} _{-0.20}	I	0	1.76	188	96
AP229	9.00 ^{+0.00} _{-0.00}	4.03 ^{+0.04} _{-0.02}	0.15 ^{+0.10} _{-0.05}	7.87 ^{+0.02} _{-0.06}	2.49 ^{+0.05} _{-0.03}	0.02 ^{+0.06} _{-0.02}	I	0	2.05	358	246
AP230	8.70 ^{+0.00} _{-0.00}	4.40 ^{+0.03} _{-0.00}	0.40 ^{+0.10} _{-0.00}	8.23 ^{+0.11} _{-0.11}	4.29 ^{+0.06} _{-0.07}	1.13 ^{+0.19} _{-0.20}	I	0	3.64	973	574
AP231	9.00 ^{+0.10} _{-0.00}	4.04 ^{+0.03} _{-0.04}	0.40 ^{+0.10} _{-0.20}	8.09 ^{+0.36} _{-0.50}	3.18 ^{+0.45} _{-0.72}	0.70 ^{+0.37} _{-0.40}	I	0	2.33	356	218
AP232	8.30 ^{+0.00} _{-0.10}	3.81 ^{+0.04} _{-0.00}	0.75 ^{+0.15} _{-0.00}	8.68 ^{+0.05} _{-0.04}	3.62 ^{+0.05} _{-0.05}	0.01 ^{+0.07} _{-0.01}	I	0	2.45	463	374
AP233	9.00 ^{+0.00} _{-0.00}	3.72 ^{+0.03} _{-0.04}	0.10 ^{+0.10} _{-0.05}	10.03 ^{+0.05} _{-0.06}	4.14 ^{+0.06} _{-0.06}	0.00 ^{+0.07} _{-0.00}	I	0	1.71	179	88
AP234	8.30 ^{+0.00} _{-0.30}	3.33 ^{+0.01} _{-0.17}	0.65 ^{+0.10} _{-0.15}	8.17 ^{+0.14} _{-0.11}	3.64 ^{+0.13} _{-0.10}	0.99 ^{+0.25} _{-0.25}	I	0	1.79	213	164
AP235	9.40 ^{+0.00} _{-0.10}	4.50 ^{+0.00} _{-0.17}	0.00 ^{+0.05} _{-0.00}	9.13 ^{+0.15} _{-0.14}	4.04 ^{+0.09} _{-0.09}	0.22 ^{+0.17} _{-0.18}	I	0	2.06	387	248
AP238	8.30 ^{+0.00} _{-0.00}	4.10 ^{+0.02} _{-0.00}	0.95 ^{+0.05} _{-0.00}	8.49 ^{+0.09} _{-0.09}	4.10 ^{+0.06} _{-0.05}	0.63 ^{+0.17} _{-0.18}	I	0	2.08	383	195
AP239	8.90 ^{+0.00} _{-0.10}	3.74 ^{+0.09} _{-0.00}	0.00 ^{+0.35} _{-0.00}	8.73 ^{+0.09} _{-0.08}	3.64 ^{+0.06} _{-0.07}	0.12 ^{+0.14} _{-0.12}	I	0	3.19	747	606
AP242	8.90 ^{+0.00} _{-0.00}	3.98 ^{+0.00} _{-0.00}	0.05 ^{+0.00} _{-0.05}	8.90 ^{+0.05} _{-0.05}	3.62 ^{+0.06} _{-0.06}	0.07 ^{+0.10} _{-0.07}	I	0	2.31	398	256
AP243	8.70 ^{+0.00} _{-0.10}	3.69 ^{+0.02} _{-0.03}	0.15 ^{+0.30} _{-0.05}	8.84 ^{+0.04} _{-0.04}	3.52 ^{+0.06} _{-0.05}	0.00 ^{+0.07} _{-0.00}	I	0	1.88	297	208
AP244	7.70 ^{+0.00} _{-0.30}	3.65 ^{+0.00} _{-0.02}	0.60 ^{+0.10} _{-0.00}	7.34 ^{+0.38} _{-0.61}	3.63 ^{+0.29} _{-0.48}	0.52 ^{+0.35} _{-0.44}	I	0	2.61	412	238
AP245	9.90 ^{+0.10} _{-0.00}	4.55 ^{+0.07} _{-0.00}	0.20 ^{+0.00} _{-0.15}	7.68 ^{+0.07} _{-0.06}	2.86 ^{+0.08} _{-0.08}	0.10 ^{+0.08} _{-0.08}	I	0	1.91	181	89
AP246	8.40 ^{+0.00} _{-0.10}	3.63 ^{+0.02} _{-0.02}	0.85 ^{+0.10} _{-0.00}	8.32 ^{+0.38} _{-0.18}	3.62 ^{+0.12} _{-0.22}	0.89 ^{+0.36} _{-0.82}	I	0	1.69	184	126
AP249	7.30 ^{+0.10} _{-0.10}	3.25 ^{+0.02} _{-0.02}	1.25 ^{+0.05} _{-0.05}	7.25 ^{+0.04} _{-0.07}	3.58 ^{+0.07} _{-0.06}	1.34 ^{+0.14} _{-0.16}	I	0	1.91	235	182
AP250	9.00 ^{+0.00} _{-0.10}	3.56 ^{+0.03} _{-0.01}	0.00 ^{+0.20} _{-0.00}	8.87 ^{+0.08} _{-0.08}	3.34 ^{+0.09} _{-0.08}	0.44 ^{+0.16} _{-0.16}	I	0	1.73	152	77
AP251	8.90 ^{+0.00} _{-0.10}	3.40 ^{+0.03} _{-0.02}	0.00 ^{+0.15} _{-0.00}	8.82 ^{+0.07} _{-0.07}	3.20 ^{+0.06} _{-0.07}	0.00 ^{+0.07} _{-0.00}	I	0	1.59	180	123
AP252	9.30 ^{+0.40} _{-0.00}	4.75 ^{+0.27} _{-0.01}	0.65 ^{+0.10} _{-0.30}	8.72 ^{+0.20} _{-0.26}	4.45 ^{+0.07} _{-0.08}	1.99 ^{+0.35} _{-0.28}	I	0	2.00	313	164
AP253	7.90 ^{+0.00} _{-0.00}	4.40 ^{+0.00} _{-0.00}	1.80 ^{+0.00} _{-0.00}	9.10 ^{+0.03} _{-0.03}	4.85 ^{+0.03} _{-0.03}	0.10 ^{+0.07} _{-0.07}	I	1	3.30	832	729

Table 1 (cont'd)

AP ID ^a	CMD Best Fit Parameters ^b			Integrated Best Fit Parameters ^c			Best ^d Flag ^e	R _{ap} ^f	N _{stars} ^g	N _{bg} ^h	
	log(<i>t</i> [Myr])	log(<i>M</i> [<i>M</i> _⊙])	<i>A_V</i> [mag]	log(<i>t</i> [Myr])	log(<i>M</i> [<i>M</i> _⊙])	<i>A_V</i> [mag]					
AP254	8.20 ^{+0.10} _{-0.00}	3.34 ^{+0.02} _{-0.01}	0.55 ^{+0.05} _{-0.05}	8.59 ^{+0.06} _{-0.06}	3.39 ^{+0.06} _{-0.06}	0.05 ^{+0.10} _{-0.05}	I	0	1.88	272	223
AP255	6.80 ^{+0.10} _{-0.10}	3.17 ^{+0.00} _{-0.02}	1.05 ^{+0.00} _{-0.05}	6.81 ^{+0.06} _{-0.07}	3.15 ^{+0.18} _{-0.09}	0.82 ^{+0.07} _{-0.08}	I	0	2.70	272	247
AP256	9.10 ^{+0.00} _{-0.00}	3.71 ^{+0.05} _{-0.04}	0.35 ^{+0.05} _{-0.15}	9.39 ^{+0.20} _{-0.22}	3.85 ^{+0.12} _{-0.11}	0.20 ^{+0.22} _{-0.19}	I	0	2.10	235	123
AP257	8.20 ^{+0.00} _{-0.30}	3.73 ^{+0.03} _{-0.06}	1.80 ^{+0.30} _{-0.00}	9.61 ^{+0.21} _{-0.19}	3.92 ^{+0.14} _{-0.12}	0.12 ^{+0.16} _{-0.12}	I	0	1.49	211	150
AP258	9.50 ^{+0.20} _{-0.10}	4.17 ^{+0.10} _{-0.12}	0.00 ^{+0.20} _{-0.00}	9.35 ^{+0.39} _{-0.29}	3.99 ^{+0.13} _{-0.12}	0.58 ^{+0.30} _{-0.42}	I	0	1.93	191	115
AP260	9.10 ^{+0.00} _{-0.00}	4.02 ^{+0.04} _{-0.17}	0.15 ^{+0.15} _{-0.05}	7.63 ^{+0.06} _{-0.09}	2.23 ^{+0.15} _{-0.12}	0.06 ^{+0.09} _{-0.06}	I	0	1.85	288	195
AP261	9.00 ^{+0.00} _{-0.10}	3.66 ^{+0.00} _{-0.09}	0.00 ^{+0.05} _{-0.00}	8.11 ^{+1.47} _{-1.46}	3.77 ^{+1.25} _{-1.18}	1.45 ^{+1.02} _{-1.02}	I	0	1.85	191	94
AP263	8.60 ^{+0.10} _{-0.10}	3.44 ^{+0.02} _{-0.02}	0.40 ^{+0.15} _{-0.10}	8.06 ^{+0.11} _{-0.12}	3.46 ^{+0.11} _{-0.11}	1.14 ^{+0.24} _{-0.23}	I	0	1.71	204	152
AP266	6.90 ^{+0.10} _{-0.00}	3.61 ^{+0.00} _{-0.01}	0.85 ^{+0.00} _{-0.05}	7.39 ^{+0.05} _{-0.06}	4.01 ^{+0.05} _{-0.05}	0.06 ^{+0.09} _{-0.06}	I	0	4.59	659	389
AP267	8.80 ^{+0.00} _{-0.10}	4.12 ^{+0.03} _{-0.02}	0.55 ^{+0.30} _{-0.00}	8.07 ^{+0.12} _{-0.10}	3.64 ^{+0.10} _{-0.10}	0.99 ^{+0.20} _{-0.20}	I	0	2.33	376	215
AP269	8.80 ^{+0.00} _{-0.00}	3.69 ^{+0.01} _{-0.02}	0.10 ^{+0.00} _{-0.10}	8.63 ^{+0.56} _{-0.57}	4.21 ^{+0.12} _{-0.05}	0.58 ^{+0.74} _{-0.58}	I	0	2.52	338	204
AP271	8.40 ^{+0.00} _{-0.10}	3.68 ^{+0.00} _{-0.06}	0.45 ^{+0.10} _{-0.10}	8.75 ^{+0.06} _{-0.06}	3.74 ^{+0.05} _{-0.05}	0.00 ^{+0.07} _{-0.00}	I	0	2.08	354	285
AP272	8.10 ^{+0.00} _{-0.00}	3.68 ^{+0.00} _{-0.00}	1.00 ^{+0.00} _{-0.00}	8.56 ^{+0.18} _{-0.21}	3.40 ^{+0.11} _{-0.11}	0.26 ^{+0.38} _{-0.26}	I	0	2.05	264	172
AP274	7.90 ^{+0.00} _{-0.10}	4.44 ^{+0.00} _{-0.01}	1.95 ^{+0.05} _{-0.00}	9.07 ^{+0.07} _{-0.07}	4.52 ^{+0.06} _{-0.06}	0.20 ^{+0.12} _{-0.12}	I	0	3.17	792	270
AP275	8.60 ^{+0.00} _{-0.30}	3.23 ^{+0.00} _{-0.09}	0.35 ^{+0.30} _{-0.10}	8.36 ^{+0.10} _{-0.11}	2.96 ^{+0.12} _{-0.12}	0.54 ^{+0.26} _{-0.28}	I	0	1.39	101	72
AP276	8.50 ^{+0.00} _{-0.10}	3.31 ^{+0.02} _{-0.06}	0.45 ^{+0.20} _{-0.00}	8.79 ^{+0.06} _{-0.05}	3.24 ^{+0.05} _{-0.05}	0.05 ^{+0.08} _{-0.05}	I	0	1.26	120	88
AP278	9.30 ^{+0.20} _{-2.00}	4.31 ^{+0.03} _{-4.31}	0.65 ^{+1.75} _{-0.15}	10.24 ^{+0.01} _{-0.02}	4.99 ^{+0.04} _{-0.03}	0.41 ^{+0.06} _{-0.08}	I	0	1.72	104	212
AP283	9.10 ^{+0.00} _{-0.10}	3.65 ^{+0.08} _{-0.13}	0.45 ^{+0.25} _{-0.05}	10.05 ^{+0.04} _{-0.04}	4.45 ^{+0.04} _{-0.04}	0.01 ^{+0.07} _{-0.01}	I	0	2.95	144	111
AP284	8.30 ^{+0.00} _{-0.00}	3.58 ^{+0.01} _{-0.06}	0.75 ^{+0.05} _{-0.10}	8.49 ^{+0.09} _{-0.08}	3.24 ^{+0.09} _{-0.08}	0.16 ^{+0.17} _{-0.16}	I	0	1.87	200	126
AP285	6.60 ^{+0.00} _{-0.00}	3.49 ^{+0.00} _{-0.02}	1.00 ^{+0.00} _{-0.05}	6.60 ^{+0.17} _{-0.16}	3.46 ^{+0.29} _{-0.24}	0.41 ^{+0.07} _{-0.08}	I	0	4.27	1121	1071
AP286	8.20 ^{+0.00} _{-0.10}	3.72 ^{+0.00} _{-0.05}	0.95 ^{+0.10} _{-0.05}	8.76 ^{+0.08} _{-0.07}	3.73 ^{+0.08} _{-0.07}	0.34 ^{+0.15} _{-0.16}	I	0	1.97	346	273
AP287	7.80 ^{+0.20} _{-0.00}	3.65 ^{+0.03} _{-0.00}	1.00 ^{+0.05} _{-0.05}	7.75 ^{+0.18} _{-0.15}	3.70 ^{+0.17} _{-0.17}	0.93 ^{+0.30} _{-0.33}	I	0	2.16	354	281
AP288	9.60 ^{+0.10} _{-0.00}	5.06 ^{+0.08} _{-0.00}	0.00 ^{+0.00} _{-0.00}	8.11 ^{+1.47} _{-1.46}	3.78 ^{+1.25} _{-1.18}	1.45 ^{+1.02} _{-1.03}	I	1	2.16	318	184
AP289	8.10 ^{+0.00} _{-0.00}	3.59 ^{+0.00} _{-0.02}	0.70 ^{+0.00} _{-0.05}	8.10 ^{+0.13} _{-0.13}	3.29 ^{+0.11} _{-0.12}	0.24 ^{+0.24} _{-0.23}	I	0	1.82	222	169
AP290	8.40 ^{+0.10} _{-0.00}	3.66 ^{+0.00} _{-0.07}	0.60 ^{+0.05} _{-0.20}	8.37 ^{+0.12} _{-0.09}	3.69 ^{+0.08} _{-0.09}	0.50 ^{+0.23} _{-0.30}	I	0	1.64	249	206
AP291	8.80 ^{+0.00} _{-0.00}	3.43 ^{+0.01} _{-0.04}	0.05 ^{+0.00} _{-0.05}	0.00 ^{+0.00} _{-0.00}	0.00 ^{+0.00} _{-0.00}	0.00 ^{+0.00} _{-0.00}	I	0	2.47	261	204
AP292	9.60 ^{+0.10} _{-0.00}	4.80 ^{+0.09} _{-0.00}	0.00 ^{+0.00} _{-0.00}	9.68 ^{+0.13} _{-0.14}	4.88 ^{+0.07} _{-0.08}	0.07 ^{+0.10} _{-0.07}	I	0	2.77	247	145
AP294	7.60 ^{+0.00} _{-0.30}	3.98 ^{+0.00} _{-0.05}	1.55 ^{+0.05} _{-0.05}	7.68 ^{+0.12} _{-0.11}	3.99 ^{+0.07} _{-0.07}	1.23 ^{+0.17} _{-0.17}	I	0	2.31	449	360
AP295	8.10 ^{+0.00} _{-0.10}	3.22 ^{+0.00} _{-0.02}	0.45 ^{+0.05} _{-0.00}	8.17 ^{+0.11} _{-0.10}	3.48 ^{+0.12} _{-0.10}	0.49 ^{+0.23} _{-0.22}	I	0	1.92	174	131
AP296	8.00 ^{+0.00} _{-0.10}	3.53 ^{+0.00} _{-0.02}	0.65 ^{+0.05} _{-0.00}	8.03 ^{+0.16} _{-0.18}	3.24 ^{+0.14} _{-0.13}	0.30 ^{+0.28} _{-0.27}	I	0	2.98	438	326
AP297	8.40 ^{+0.10} _{-0.20}	3.28 ^{+0.02} _{-0.03}	0.50 ^{+0.10} _{-0.10}	8.29 ^{+0.09} _{-0.09}	2.95 ^{+0.12} _{-0.12}	0.20 ^{+0.21} _{-0.19}	I	0	1.82	128	52
AP299	8.00 ^{+0.10} _{-0.00}	3.36 ^{+0.01} _{-0.04}	0.90 ^{+0.00} _{-0.15}	8.51 ^{+0.19} _{-0.15}	3.69 ^{+0.10} _{-0.11}	0.82 ^{+0.32} _{-0.38}	I	0	2.01	244	186
AP300	8.70 ^{+0.00} _{-0.40}	3.51 ^{+0.00} _{-0.09}	0.20 ^{+0.60} _{-0.00}	8.51 ^{+0.08} _{-0.06}	3.04 ^{+0.09} _{-0.07}	0.08 ^{+0.11} _{-0.08}	I	0	1.76	214	162

Table 1 (cont'd)

AP ID ^a	CMD Best Fit Parameters ^b			Integrated Best Fit Parameters ^c			Best ^d Flag ^e	R _{ap} ^f	N _{stars} ^g	N _{bg} ^h	
	log(<i>t</i> [Myr])	log(<i>M</i> [<i>M</i> _⊙])	<i>A_V</i> [mag]	log(<i>t</i> [Myr])	log(<i>M</i> [<i>M</i> _⊙])	<i>A_V</i> [mag]					
AP301	8.30 ^{+0.00} _{-0.00}	3.64 ^{+0.00} _{-0.02}	1.15 ^{+0.00} _{-0.05}	8.38 ^{+0.10} _{-0.07}	3.37 ^{+0.14} _{-0.09}	0.72 ^{+0.25} _{-0.22}	I	0	1.75	138	45
AP302	7.10 ^{+0.00} _{-0.40}	2.93 ^{+0.02} _{-0.01}	0.45 ^{+0.10} _{-0.00}	6.84 ^{+0.24} _{-0.23}	2.82 ^{+0.20} _{-0.22}	0.66 ^{+0.12} _{-0.13}	I	0	1.76	266	271
AP303	9.20 ^{+0.00} _{-0.00}	4.28 ^{+0.00} _{-0.03}	0.65 ^{+0.10} _{-0.05}	8.28 ^{+1.28} _{-1.59}	3.82 ^{+0.35} _{-0.45}	1.39 ^{+0.93} _{-1.08}	I	0	2.25	245	104
AP304	8.70 ^{+0.00} _{-0.00}	3.48 ^{+0.03} _{-0.00}	0.45 ^{+0.10} _{-0.00}	8.64 ^{+0.10} _{-0.11}	3.32 ^{+0.07} _{-0.08}	0.63 ^{+0.17} _{-0.17}	I	0	1.93	169	108
AP305	8.20 ^{+0.20} _{-0.00}	3.43 ^{+0.03} _{-0.01}	1.20 ^{+0.05} _{-0.10}	8.91 ^{+0.08} _{-0.09}	3.08 ^{+0.09} _{-0.08}	0.16 ^{+0.16} _{-0.15}	I	0	1.46	157	114
AP307	9.00 ^{+0.00} _{-0.00}	3.90 ^{+0.04} _{-0.04}	0.30 ^{+0.10} _{-0.05}	8.78 ^{+0.08} _{-0.08}	3.45 ^{+0.07} _{-0.07}	0.43 ^{+0.15} _{-0.15}	I	0	2.17	264	127
AP309	8.20 ^{+0.10} _{-0.10}	3.38 ^{+0.01} _{-0.04}	0.65 ^{+0.10} _{-0.15}	8.37 ^{+0.17} _{-0.17}	3.21 ^{+0.13} _{-0.11}	0.29 ^{+0.29} _{-0.28}	I	0	2.00	288	232
AP311	7.60 ^{+0.00} _{-0.40}	3.19 ^{+0.01} _{-0.03}	0.50 ^{+0.05} _{-0.05}	7.92 ^{+0.08} _{-0.01}	3.09 ^{+0.06} _{-0.08}	0.27 ^{+0.08} _{-0.16}	I	0	1.80	157	109
AP313	8.30 ^{+0.00} _{-0.20}	3.07 ^{+0.01} _{-0.03}	0.30 ^{+0.05} _{-0.10}	8.22 ^{+0.11} _{-0.12}	3.04 ^{+0.09} _{-0.08}	0.33 ^{+0.23} _{-0.24}	I	0	1.65	133	108
AP314	8.40 ^{+0.10} _{-0.00}	3.56 ^{+0.03} _{-0.02}	0.90 ^{+0.10} _{-0.10}	8.65 ^{+0.33} _{-0.11}	3.39 ^{+0.06} _{-0.12}	0.44 ^{+0.14} _{-0.44}	I	0	1.60	191	131
AP315	8.20 ^{+0.00} _{-0.60}	3.38 ^{+0.00} _{-0.08}	0.40 ^{+0.20} _{-0.00}	8.29 ^{+0.09} _{-0.08}	3.26 ^{+0.09} _{-0.09}	0.20 ^{+0.18} _{-0.18}	I	0	1.51	214	148
AP317	9.20 ^{+0.00} _{-0.00}	4.36 ^{+0.03} _{-0.00}	0.35 ^{+0.05} _{-0.00}	8.63 ^{+0.16} _{-0.16}	4.32 ^{+0.08} _{-0.07}	1.77 ^{+0.23} _{-0.24}	I	0	3.14	437	188
AP318	8.20 ^{+0.30} _{-0.10}	3.43 ^{+0.11} _{-0.02}	1.25 ^{+0.05} _{-0.20}	8.32 ^{+0.10} _{-0.08}	3.35 ^{+0.13} _{-0.10}	0.73 ^{+0.23} _{-0.22}	I	0	1.67	163	82
AP319	8.40 ^{+0.00} _{-0.10}	3.24 ^{+0.00} _{-0.09}	0.65 ^{+0.05} _{-0.15}	8.17 ^{+0.13} _{-0.13}	2.95 ^{+0.12} _{-0.12}	0.37 ^{+0.23} _{-0.24}	I	0	1.70	178	129
AP322	7.80 ^{+0.30} _{-0.30}	3.00 ^{+0.04} _{-0.04}	0.90 ^{+0.05} _{-0.15}	8.29 ^{+0.10} _{-0.11}	2.75 ^{+0.12} _{-0.10}	0.18 ^{+0.18} _{-0.17}	I	0	1.52	89	50
AP323	7.30 ^{+0.00} _{-0.00}	3.75 ^{+0.00} _{-0.00}	1.35 ^{+0.05} _{-0.00}	7.47 ^{+0.17} _{-0.19}	4.29 ^{+0.10} _{-0.10}	1.26 ^{+0.26} _{-0.24}	I	0	2.47	389	195
AP324	9.00 ^{+0.60} _{-0.20}	4.38 ^{+0.37} _{-0.15}	1.40 ^{+0.60} _{-0.45}	9.26 ^{+0.96} _{-0.65}	4.12 ^{+0.30} _{-0.11}	1.21 ^{+0.75} _{-0.89}	I	0	1.69	196	94
AP325	8.30 ^{+0.00} _{-0.00}	3.35 ^{+0.03} _{-0.02}	0.45 ^{+0.10} _{-0.05}	8.65 ^{+0.04} _{-0.04}	3.29 ^{+0.06} _{-0.07}	0.02 ^{+0.07} _{-0.02}	I	0	1.56	184	138
AP326	8.50 ^{+0.00} _{-0.00}	3.76 ^{+0.00} _{-0.02}	0.30 ^{+0.05} _{-0.05}	8.57 ^{+0.06} _{-0.06}	3.55 ^{+0.04} _{-0.05}	0.02 ^{+0.07} _{-0.02}	I	0	2.15	364	250
AP327	8.70 ^{+0.10} _{-0.10}	3.65 ^{+0.04} _{-0.18}	1.65 ^{+0.20} _{-0.35}	9.09 ^{+0.40} _{-0.84}	3.36 ^{+0.21} _{-0.22}	0.52 ^{+0.68} _{-0.46}	I	0	1.42	99	42
AP329	8.20 ^{+0.00} _{-0.00}	3.48 ^{+0.02} _{-0.02}	0.85 ^{+0.05} _{-0.00}	7.90 ^{+0.33} _{-0.28}	3.10 ^{+0.34} _{-0.42}	0.41 ^{+0.27} _{-0.26}	I	0	2.26	333	235
AP330	9.50 ^{+0.00} _{-1.80}	4.56 ^{+0.00} _{-0.96}	0.00 ^{+2.85} _{-0.00}	8.95 ^{+0.44} _{-0.70}	4.67 ^{+0.07} _{-0.09}	0.86 ^{+0.89} _{-0.58}	I	0	2.75	643	346
AP331	9.00 ^{+0.00} _{-0.00}	3.58 ^{+0.06} _{-0.02}	0.15 ^{+0.15} _{-0.00}	7.91 ^{+0.18} _{-0.31}	3.67 ^{+0.17} _{-0.17}	1.81 ^{+0.53} _{-0.34}	I	0	1.71	120	40
AP332	7.30 ^{+0.10} _{-0.30}	3.20 ^{+0.00} _{-0.04}	0.70 ^{+0.05} _{-0.00}	7.77 ^{+0.39} _{-0.46}	3.53 ^{+0.19} _{-0.17}	0.72 ^{+0.65} _{-0.56}	I	0	1.90	363	335
AP335	8.30 ^{+0.00} _{-0.00}	3.97 ^{+0.00} _{-0.02}	0.55 ^{+0.00} _{-0.05}	8.50 ^{+0.08} _{-0.08}	3.91 ^{+0.07} _{-0.06}	0.14 ^{+0.16} _{-0.14}	I	0	2.71	614	459
AP339	9.80 ^{+0.20} _{-0.80}	5.05 ^{+0.12} _{-0.37}	1.15 ^{+0.60} _{-0.00}	9.53 ^{+0.69} _{-0.75}	4.12 ^{+0.36} _{-0.05}	1.24 ^{+0.86} _{-0.49}	I	0	1.49	138	102
AP340	8.40 ^{+0.00} _{-0.20}	3.64 ^{+0.02} _{-0.07}	1.40 ^{+0.15} _{-0.05}	8.45 ^{+0.11} _{-0.09}	2.99 ^{+0.12} _{-0.11}	0.43 ^{+0.22} _{-0.21}	I	0	1.51	165	99
AP341	8.70 ^{+0.10} _{-0.00}	4.02 ^{+0.00} _{-0.04}	0.35 ^{+0.05} _{-0.25}	8.08 ^{+0.10} _{-0.12}	3.97 ^{+0.06} _{-0.06}	1.10 ^{+0.19} _{-0.19}	I	0	2.49	392	201
AP342	9.00 ^{+0.00} _{-0.00}	3.62 ^{+0.03} _{-0.00}	0.05 ^{+0.05} _{-0.05}	8.78 ^{+0.22} _{-0.27}	3.51 ^{+0.09} _{-0.09}	0.66 ^{+0.34} _{-0.33}	I	0	1.47	155	78
AP343	8.90 ^{+0.00} _{-0.10}	3.74 ^{+0.04} _{-0.02}	0.20 ^{+0.30} _{-0.00}	9.11 ^{+0.58} _{-0.69}	3.97 ^{+0.16} _{-0.15}	0.64 ^{+0.77} _{-0.59}	I	0	1.69	197	98
AP344	8.50 ^{+0.00} _{-0.10}	3.62 ^{+0.06} _{-0.00}	0.65 ^{+0.25} _{-0.00}	8.81 ^{+0.30} _{-0.47}	3.61 ^{+0.11} _{-0.10}	0.31 ^{+0.58} _{-0.31}	I	0	1.99	312	206
AP345	8.80 ^{+0.00} _{-0.10}	3.19 ^{+0.08} _{-0.00}	0.00 ^{+0.50} _{-0.05}	8.31 ^{+0.03} _{-0.04}	3.07 ^{+0.05} _{-0.04}	1.07 ^{+0.10} _{-0.06}	I	0	1.25	91	47
AP346	9.40 ^{+0.00} _{-0.30}	4.41 ^{+0.00} _{-0.59}	0.15 ^{+0.20} _{-0.05}	8.23 ^{+1.29} _{-1.55}	3.76 ^{+0.34} _{-0.43}	1.36 ^{+0.96} _{-1.12}	I	0	2.47	271	147

Table 1 (cont'd)

AP ID ^a	CMD Best Fit Parameters ^b			Integrated Best Fit Parameters ^c			Best ^d Flag ^e	R _{ap} ^f	N _{stars} ^g	N _{bg} ^h	
	log(<i>t</i> [Myr])	log(<i>M</i> [<i>M</i> _⊙])	<i>A_V</i> [mag]	log(<i>t</i> [Myr])	log(<i>M</i> [<i>M</i> _⊙])	<i>A_V</i> [mag]					
AP349	8.70 ^{+0.10} _{-0.00}	3.51 ^{+0.04} _{-0.01}	0.30 ^{+0.15} _{-0.20}	8.58 ^{+0.13} _{-0.13}	3.28 ^{+0.09} _{-0.08}	0.20 ^{+0.20} _{-0.19}	I	0	1.96	170	61
AP350	8.20 ^{+0.10} _{-0.40}	3.63 ^{+0.03} _{-0.07}	0.75 ^{+0.15} _{-0.05}	8.37 ^{+0.07} _{-0.06}	3.31 ^{+0.08} _{-0.07}	0.08 ^{+0.11} _{-0.08}	I	0	2.44	403	333
AP351	8.40 ^{+0.10} _{-0.10}	3.42 ^{+0.04} _{-0.03}	0.90 ^{+0.15} _{-0.10}	8.49 ^{+0.15} _{-0.15}	2.96 ^{+0.11} _{-0.11}	0.21 ^{+0.26} _{-0.21}	I	0	1.64	175	121
AP352	8.00 ^{+0.00} _{-0.10}	3.85 ^{+0.08} _{-0.02}	1.75 ^{+0.30} _{-0.00}	8.60 ^{+0.15} _{-0.12}	3.69 ^{+0.10} _{-0.06}	0.76 ^{+0.23} _{-0.23}	I	0	1.63	257	121
AP353	8.90 ^{+0.00} _{-0.10}	3.59 ^{+0.03} _{-0.00}	0.00 ^{+0.25} _{-0.00}	8.54 ^{+0.08} _{-0.06}	2.60 ^{+0.10} _{-0.08}	0.00 ^{+0.07} _{-0.00}	I	0	1.55	157	87
AP354	8.80 ^{+0.00} _{-0.10}	3.39 ^{+0.06} _{-0.01}	0.20 ^{+0.40} _{-0.05}	8.76 ^{+0.06} _{-0.06}	3.09 ^{+0.07} _{-0.07}	0.02 ^{+0.07} _{-0.02}	I	0	1.70	190	147
AP358	8.40 ^{+0.00} _{-0.10}	3.58 ^{+0.02} _{-0.03}	0.45 ^{+0.10} _{-0.05}	7.20 ^{+0.82} _{-0.66}	3.16 ^{+0.27} _{-0.24}	0.65 ^{+0.36} _{-0.43}	I	0	2.45	466	392
AP363	8.30 ^{+0.00} _{-0.30}	3.98 ^{+0.00} _{-0.15}	1.70 ^{+0.15} _{-0.05}	8.90 ^{+0.07} _{-0.09}	3.64 ^{+0.07} _{-0.08}	0.06 ^{+0.10} _{-0.06}	I	0	2.16	400	278
AP364	9.30 ^{+0.20} _{-0.00}	4.26 ^{+0.11} _{-0.03}	0.15 ^{+0.10} _{-0.05}	9.29 ^{+0.26} _{-0.25}	3.81 ^{+0.14} _{-0.14}	0.26 ^{+0.23} _{-0.23}	I	0	1.69	216	116
AP366	6.70 ^{+0.00} _{-0.10}	2.98 ^{+0.01} _{-0.01}	0.70 ^{+0.05} _{-0.00}	6.63 ^{+0.07} _{-0.06}	2.55 ^{+0.24} _{-0.26}	0.53 ^{+0.08} _{-0.09}	I	0	2.62	248	166
AP367	8.10 ^{+0.00} _{-0.60}	3.17 ^{+0.00} _{-0.06}	0.45 ^{+0.20} _{-0.00}	9.10 ^{+0.03} _{-0.03}	3.15 ^{+0.03} _{-0.03}	0.10 ^{+0.07} _{-0.07}	I	0	1.75	188	155
AP368	9.10 ^{+0.00} _{-0.00}	4.01 ^{+0.06} _{-0.02}	0.10 ^{+0.15} _{-0.00}	8.90 ^{+0.41} _{-0.12}	3.74 ^{+0.22} _{-0.06}	0.61 ^{+0.27} _{-0.36}	I	0	2.06	370	248
AP369	8.10 ^{+0.10} _{-0.00}	3.45 ^{+0.03} _{-0.02}	1.20 ^{+0.10} _{-0.10}	8.47 ^{+0.13} _{-0.12}	3.33 ^{+0.11} _{-0.11}	0.46 ^{+0.27} _{-0.29}	I	0	1.89	203	154
AP371	9.10 ^{+0.00} _{-0.00}	3.47 ^{+0.03} _{-0.06}	0.15 ^{+0.10} _{-0.05}	8.16 ^{+1.23} _{-1.41}	3.36 ^{+0.28} _{-0.30}	1.54 ^{+1.09} _{-1.20}	I	0	1.35	83	36
AP372	8.20 ^{+0.00} _{-0.00}	3.55 ^{+0.00} _{-0.04}	0.70 ^{+0.00} _{-0.05}	7.92 ^{+0.89} _{-0.25}	2.48 ^{+1.03} _{-0.30}	0.10 ^{+0.07} _{-0.07}	I	0	1.45	161	102
AP374	9.00 ^{+0.00} _{-0.00}	4.02 ^{+0.02} _{-0.04}	0.05 ^{+0.05} _{-0.00}	8.40 ^{+0.06} _{-0.06}	3.52 ^{+0.07} _{-0.10}	0.48 ^{+0.14} _{-0.17}	I	0	2.05	355	210
AP375	7.70 ^{+0.20} _{-0.20}	3.19 ^{+0.02} _{-0.02}	0.75 ^{+0.10} _{-0.05}	8.08 ^{+0.08} _{-0.08}	3.65 ^{+0.07} _{-0.08}	0.48 ^{+0.16} _{-0.16}	I	0	1.72	177	142
AP378	8.70 ^{+0.00} _{-0.00}	3.68 ^{+0.04} _{-0.00}	0.60 ^{+0.05} _{-0.00}	8.86 ^{+0.14} _{-0.10}	3.39 ^{+0.07} _{-0.08}	0.27 ^{+0.11} _{-0.20}	I	0	1.80	193	82
AP379	8.80 ^{+0.10} _{-0.00}	3.77 ^{+0.04} _{-0.04}	0.25 ^{+0.05} _{-0.25}	9.05 ^{+0.12} _{-0.10}	3.72 ^{+0.10} _{-0.11}	0.08 ^{+0.08} _{-0.08}	I	0	1.87	264	150
AP380	9.20 ^{+0.00} _{-0.00}	3.97 ^{+0.05} _{-0.01}	0.00 ^{+0.10} _{-0.00}	8.04 ^{+1.19} _{-1.45}	3.66 ^{+0.34} _{-0.47}	1.38 ^{+0.89} _{-1.04}	I	0	2.09	255	86
AP384	9.10 ^{+0.10} _{-0.00}	3.80 ^{+0.19} _{-0.07}	0.20 ^{+0.15} _{-0.05}	8.66 ^{+0.11} _{-0.10}	3.51 ^{+0.10} _{-0.06}	1.05 ^{+0.19} _{-0.16}	I	0	1.71	206	137
AP387	9.10 ^{+0.00} _{-0.00}	3.88 ^{+0.04} _{-0.06}	0.00 ^{+0.15} _{-0.00}	7.68 ^{+0.94} _{-0.96}	3.23 ^{+0.24} _{-0.24}	1.10 ^{+0.68} _{-0.71}	I	0	1.71	175	85
AP388	9.40 ^{+0.20} _{-0.00}	4.71 ^{+0.11} _{-0.05}	0.05 ^{+0.15} _{-0.00}	9.20 ^{+0.15} _{-0.14}	4.26 ^{+0.10} _{-0.10}	0.31 ^{+0.18} _{-0.19}	I	0	2.28	443	288
AP389	8.30 ^{+0.40} _{-0.00}	3.46 ^{+0.05} _{-0.01}	0.80 ^{+0.00} _{-0.50}	8.83 ^{+0.06} _{-0.06}	3.32 ^{+0.07} _{-0.06}	0.05 ^{+0.09} _{-0.05}	I	0	1.49	164	84
AP390	7.00 ^{+0.40} _{-0.10}	3.54 ^{+0.03} _{-0.01}	0.50 ^{+0.05} _{-0.05}	7.69 ^{+0.12} _{-0.11}	4.09 ^{+0.08} _{-0.08}	0.21 ^{+0.16} _{-0.16}	I	0	2.45	573	555
AP391	7.80 ^{+0.10} _{-0.10}	3.13 ^{+0.02} _{-0.04}	0.60 ^{+0.05} _{-0.10}	8.16 ^{+0.23} _{-0.56}	3.06 ^{+0.29} _{-0.64}	0.09 ^{+0.11} _{-0.09}	I	0	1.60	223	176
AP393	9.10 ^{+0.00} _{-0.00}	3.91 ^{+0.00} _{-0.00}	0.00 ^{+0.00} _{-0.00}	0.00 ^{+0.00} _{-0.00}	0.00 ^{+0.00} _{-0.00}	0.00 ^{+0.00} _{-0.00}	I	0	2.64	288	469
AP394	7.50 ^{+0.00} _{-0.40}	3.58 ^{+0.00} _{-0.05}	1.35 ^{+0.10} _{-0.00}	7.69 ^{+1.01} _{-1.19}	3.69 ^{+0.36} _{-0.44}	1.05 ^{+0.64} _{-0.64}	I	0	1.91	250	162
AP395	8.30 ^{+0.00} _{-0.10}	3.35 ^{+0.01} _{-0.03}	0.70 ^{+0.05} _{-0.05}	8.53 ^{+0.13} _{-0.18}	3.25 ^{+0.13} _{-0.12}	0.24 ^{+0.41} _{-0.24}	I	0	1.54	171	136
AP398	8.80 ^{+0.00} _{-0.40}	3.68 ^{+0.02} _{-0.06}	0.40 ^{+0.80} _{-0.10}	9.14 ^{+0.15} _{-0.16}	3.50 ^{+0.13} _{-0.13}	0.17 ^{+0.15} _{-0.15}	I	0	1.61	162	102
AP400	7.10 ^{+0.20} _{-0.20}	2.82 ^{+0.00} _{-0.01}	0.80 ^{+0.05} _{-0.05}	6.83 ^{+0.06} _{-0.07}	2.54 ^{+0.21} _{-0.18}	0.30 ^{+0.09} _{-0.09}	I	0	1.80	83	54
AP402	8.50 ^{+0.20} _{-0.10}	3.34 ^{+0.07} _{-0.02}	0.85 ^{+0.05} _{-0.35}	8.36 ^{+0.20} _{-0.19}	3.10 ^{+0.14} _{-0.13}	0.43 ^{+0.41} _{-0.38}	I	0	1.84	173	116
AP403	6.90 ^{+0.10} _{-0.10}	3.64 ^{+0.00} _{-0.04}	1.80 ^{+0.00} _{-0.05}	6.65 ^{+0.10} _{-0.12}	4.20 ^{+0.16} _{-0.16}	0.96 ^{+0.10} _{-0.10}	I	0	2.65	405	415

Table 1 (cont'd)

AP ID ^a	CMD Best Fit Parameters ^b			Integrated Best Fit Parameters ^c			Best ^d Flag ^e	R _{ap} ^f	N _{stars} ^g	N _{bg} ^h	
	log(<i>t</i> [Myr])	log(<i>M</i> [<i>M</i> _⊙])	<i>A_V</i> [mag]	log(<i>t</i> [Myr])	log(<i>M</i> [<i>M</i> _⊙])	<i>A_V</i> [mag]					
AP404	9.00 ^{+0.00} _{-0.00}	3.94 ^{+0.00} _{-0.04}	0.20 ^{+0.05} _{-0.05}	8.95 ^{+0.12} _{-0.08}	3.49 ^{+0.10} _{-0.07}	0.27 ^{+0.16} _{-0.19}	I	0	1.83	220	111
AP405	8.20 ^{+0.00} _{-0.00}	3.45 ^{+0.00} _{-0.03}	0.95 ^{+0.00} _{-0.05}	7.85 ^{+0.12} _{-0.09}	3.30 ^{+0.11} _{-0.12}	0.76 ^{+0.14} _{-0.19}	I	0	2.06	281	175
AP406	9.10 ^{+0.00} _{-0.00}	3.95 ^{+0.01} _{-0.04}	0.60 ^{+0.05} _{-0.10}	9.26 ^{+0.19} _{-0.19}	3.54 ^{+0.12} _{-0.11}	0.36 ^{+0.22} _{-0.25}	I	0	1.31	111	33
AP407	9.10 ^{+0.00} _{-1.30}	3.59 ^{+0.00} _{-0.22}	0.10 ^{+2.15} _{-0.05}	8.00 ^{+0.13} _{-0.29}	2.77 ^{+0.33} _{-0.45}	0.80 ^{+0.58} _{-0.56}	I	0	1.38	119	72
AP409	8.00 ^{+0.10} _{-0.10}	3.56 ^{+0.03} _{-0.08}	1.35 ^{+0.05} _{-0.05}	7.90 ^{+0.11} _{-0.12}	3.99 ^{+0.08} _{-0.08}	1.87 ^{+0.21} _{-0.20}	I	0	1.50	200	156
AP410	9.10 ^{+0.00} _{-0.00}	3.79 ^{+0.06} _{-0.01}	0.10 ^{+0.00} _{-0.10}	9.03 ^{+0.30} _{-0.71}	3.82 ^{+0.11} _{-0.11}	0.42 ^{+0.92} _{-0.40}	I	0	1.70	218	111
AP412	8.20 ^{+0.00} _{-0.00}	3.52 ^{+0.02} _{-0.01}	0.45 ^{+0.05} _{-0.00}	8.07 ^{+0.11} _{-0.11}	3.52 ^{+0.10} _{-0.10}	0.54 ^{+0.22} _{-0.23}	I	0	2.29	419	358
AP413	9.20 ^{+0.00} _{-0.10}	3.64 ^{+0.00} _{-0.22}	0.05 ^{+0.20} _{-0.00}	7.99 ^{+0.08} _{-0.16}	3.24 ^{+0.16} _{-0.16}	1.52 ^{+0.35} _{-0.28}	I	0	1.66	59	37
AP414	8.80 ^{+0.00} _{-0.10}	3.83 ^{+0.01} _{-0.03}	0.20 ^{+0.35} _{-0.05}	8.60 ^{+0.17} _{-0.28}	3.62 ^{+0.17} _{-0.12}	0.30 ^{+0.58} _{-0.30}	I	0	1.95	315	213
AP416	8.90 ^{+0.10} _{-0.00}	3.51 ^{+0.04} _{-0.00}	0.10 ^{+0.10} _{-0.05}	8.60 ^{+0.13} _{-0.14}	3.24 ^{+0.11} _{-0.12}	0.53 ^{+0.30} _{-0.30}	I	0	1.57	143	66
AP417	7.50 ^{+0.10} _{-0.30}	3.24 ^{+0.00} _{-0.04}	1.30 ^{+0.05} _{-0.10}	6.74 ^{+0.08} _{-0.07}	2.73 ^{+0.17} _{-0.27}	1.17 ^{+0.09} _{-0.07}	I	0	2.30	134	72
AP418	8.00 ^{+0.20} _{-0.00}	3.20 ^{+0.01} _{-0.02}	0.60 ^{+0.05} _{-0.10}	8.32 ^{+0.06} _{-0.04}	2.73 ^{+0.09} _{-0.06}	0.00 ^{+0.07} _{-0.00}	I	0	1.57	157	103
AP419	8.20 ^{+0.10} _{-0.50}	2.90 ^{+0.01} _{-0.05}	0.40 ^{+0.25} _{-0.00}	8.00 ^{+0.07} _{-0.09}	3.16 ^{+0.08} _{-0.08}	0.98 ^{+0.11} _{-0.12}	I	0	1.57	68	35
AP420	9.10 ^{+0.00} _{-1.30}	3.81 ^{+0.00} _{-0.13}	0.00 ^{+2.05} _{-0.00}	8.66 ^{+0.11} _{-0.13}	3.36 ^{+0.07} _{-0.08}	0.33 ^{+0.21} _{-0.20}	I	0	1.70	176	84
AP422	7.80 ^{+0.60} _{-0.30}	3.03 ^{+0.11} _{-0.03}	0.90 ^{+0.10} _{-0.25}	8.09 ^{+0.16} _{-0.18}	2.60 ^{+0.19} _{-0.21}	0.17 ^{+0.17} _{-0.16}	I	0	1.50	104	68
AP423	8.40 ^{+0.00} _{-0.00}	3.68 ^{+0.02} _{-0.04}	0.55 ^{+0.05} _{-0.05}	8.61 ^{+0.05} _{-0.05}	3.45 ^{+0.06} _{-0.06}	0.03 ^{+0.07} _{-0.03}	I	0	2.34	431	353
AP425	9.40 ^{+0.00} _{-0.10}	4.22 ^{+0.04} _{-0.17}	0.00 ^{+0.10} _{-0.00}	8.06 ^{+0.06} _{-0.05}	4.55 ^{+0.04} _{-0.05}	1.45 ^{+0.10} _{-0.10}	I	0	1.80	135	182
AP426	8.80 ^{+0.00} _{-0.00}	3.47 ^{+0.03} _{-0.00}	0.35 ^{+0.10} _{-0.05}	8.08 ^{+0.07} _{-0.07}	2.54 ^{+0.14} _{-0.12}	0.03 ^{+0.07} _{-0.03}	I	0	1.52	130	74
AP428	8.70 ^{+0.10} _{-0.00}	3.16 ^{+0.03} _{-0.03}	0.35 ^{+0.05} _{-0.25}	9.25 ^{+0.09} _{-0.09}	3.20 ^{+0.11} _{-0.12}	0.06 ^{+0.10} _{-0.06}	I	0	1.52	79	33
AP429	8.50 ^{+0.20} _{-0.00}	3.88 ^{+0.03} _{-0.01}	0.75 ^{+0.05} _{-0.40}	8.24 ^{+0.08} _{-0.08}	3.95 ^{+0.08} _{-0.07}	1.05 ^{+0.18} _{-0.16}	I	0	2.27	332	197
AP431	7.20 ^{+0.00} _{-0.20}	3.21 ^{+0.00} _{-0.02}	0.45 ^{+0.05} _{-0.00}	6.97 ^{+0.24} _{-0.29}	3.69 ^{+0.33} _{-0.57}	0.64 ^{+0.10} _{-0.10}	I	0	2.82	480	474
AP432	9.10 ^{+0.00} _{-0.30}	3.46 ^{+0.04} _{-0.32}	0.10 ^{+0.50} _{-0.05}	8.47 ^{+0.77} _{-0.47}	3.34 ^{+0.21} _{-0.20}	0.96 ^{+0.71} _{-0.88}	I	0	1.50	97	37
AP433	8.40 ^{+0.10} _{-0.90}	3.12 ^{+0.00} _{-0.12}	0.30 ^{+0.35} _{-0.15}	7.12 ^{+0.22} _{-0.17}	2.94 ^{+0.16} _{-0.13}	0.82 ^{+0.15} _{-0.16}	I	0	1.32	141	123
AP434	8.20 ^{+0.10} _{-0.00}	3.27 ^{+0.03} _{-0.00}	0.30 ^{+0.10} _{-0.00}	8.14 ^{+0.12} _{-0.12}	3.40 ^{+0.10} _{-0.09}	0.65 ^{+0.25} _{-0.24}	I	0	2.08	283	246
AP435	7.70 ^{+0.10} _{-0.20}	2.75 ^{+0.02} _{-0.02}	0.50 ^{+0.10} _{-0.05}	7.85 ^{+0.03} _{-0.03}	2.25 ^{+0.03} _{-0.03}	0.00 ^{+0.07} _{-0.00}	I	0	1.39	80	51
AP436	8.90 ^{+0.00} _{-0.00}	3.61 ^{+0.02} _{-0.03}	0.15 ^{+0.10} _{-0.05}	8.88 ^{+0.33} _{-0.47}	3.43 ^{+0.12} _{-0.11}	0.45 ^{+0.54} _{-0.39}	I	0	1.71	172	97
AP437	8.00 ^{+0.00} _{-0.20}	3.55 ^{+0.05} _{-0.02}	2.30 ^{+0.25} _{-0.00}	9.50 ^{+0.26} _{-0.23}	3.91 ^{+0.11} _{-0.11}	0.44 ^{+0.28} _{-0.29}	I	0	1.54	135	49
AP438	9.50 ^{+0.00} _{-0.10}	4.35 ^{+0.02} _{-0.10}	0.00 ^{+0.10} _{-0.00}	9.32 ^{+0.24} _{-0.22}	4.24 ^{+0.09} _{-0.09}	0.61 ^{+0.25} _{-0.30}	I	0	2.12	87	226
AP439	7.60 ^{+0.40} _{-0.20}	3.08 ^{+0.03} _{-0.03}	0.65 ^{+0.05} _{-0.20}	7.63 ^{+0.20} _{-0.19}	3.13 ^{+0.08} _{-0.07}	0.59 ^{+0.20} _{-0.20}	I	0	1.48	163	136
AP440	7.80 ^{+0.00} _{-0.20}	3.78 ^{+0.00} _{-0.14}	2.75 ^{+0.10} _{-0.10}	8.56 ^{+0.52} _{-0.34}	3.86 ^{+0.12} _{-0.10}	1.52 ^{+0.51} _{-0.71}	I	0	1.63	182	101
AP443	7.70 ^{+1.10} _{-0.00}	4.09 ^{+0.00} _{-0.85}	3.00 ^{+0.00} _{-3.00}	7.72 ^{+1.14} _{-1.18}	4.33 ^{+0.41} _{-0.46}	1.21 ^{+0.59} _{-0.66}	I	1	2.36	196	136
AP444	8.40 ^{+0.20} _{-0.20}	3.43 ^{+0.03} _{-0.11}	1.10 ^{+0.05} _{-0.35}	8.73 ^{+0.06} _{-0.06}	3.19 ^{+0.07} _{-0.07}	0.02 ^{+0.07} _{-0.02}	I	0	1.62	189	138
AP445	9.10 ^{+0.10} _{-1.70}	3.50 ^{+0.65} _{-3.50}	0.15 ^{+2.05} _{-0.00}	0.00 ^{+0.00} _{-0.00}	0.00 ^{+0.00} _{-0.00}	0.00 ^{+0.00} _{-0.00}	I	0	2.85	139	737

Table 1 (cont'd)

AP ID ^a	CMD Best Fit Parameters ^b			Integrated Best Fit Parameters ^c			Best ^d Flag ^e	R _{ap} ^f	N _{stars} ^g	N _{bg} ^h	
	log(<i>t</i> [Myr])	log(<i>M</i> [<i>M</i> _⊙])	<i>A_V</i> [mag]	log(<i>t</i> [Myr])	log(<i>M</i> [<i>M</i> _⊙])	<i>A_V</i> [mag]					
AP446	7.60 ^{+0.20} _{-0.10}	3.07 ^{+0.02} _{-0.02}	0.50 ^{+0.00} _{-0.10}	7.78 ^{+0.18} _{-0.20}	3.16 ^{+0.09} _{-0.09}	0.65 ^{+0.24} _{-0.24}	I	0	2.13	222	170
AP447	8.30 ^{+0.70} _{-1.00}	3.01 ^{+0.05} _{-3.01}	1.55 ^{+0.45} _{-0.94}	7.22 ^{+0.15} _{-0.10}	3.89 ^{+0.06} _{-0.06}	1.00 ^{+0.16} _{-0.17}	I	0	1.80	120	186
AP448	9.10 ^{+0.00} _{-0.00}	3.93 ^{+0.02} _{-0.04}	0.30 ^{+0.05} _{-0.10}	9.50 ^{+0.14} _{-0.13}	3.86 ^{+0.10} _{-0.10}	0.11 ^{+0.16} _{-0.11}	I	0	1.86	185	79
AP449	8.60 ^{+0.00} _{-0.00}	3.62 ^{+0.03} _{-0.00}	0.05 ^{+0.05} _{-0.00}	8.69 ^{+0.07} _{-0.07}	3.45 ^{+0.06} _{-0.05}	0.11 ^{+0.12} _{-0.11}	I	0	1.82	227	125
AP450	6.70 ^{+0.10} _{-0.10}	3.26 ^{+0.01} _{-0.02}	1.35 ^{+0.10} _{-0.05}	6.60 ^{+0.06} _{-0.07}	2.51 ^{+0.26} _{-0.22}	1.08 ^{+0.08} _{-0.07}	I	0	1.58	157	129
AP451	7.10 ^{+0.20} _{-0.30}	2.85 ^{+0.03} _{-0.02}	1.85 ^{+0.10} _{-0.05}	7.84 ^{+0.11} _{-0.12}	3.07 ^{+0.06} _{-0.06}	1.05 ^{+0.13} _{-0.13}	I	0	1.19	66	41
AP452	7.30 ^{+0.20} _{-0.00}	3.57 ^{+0.01} _{-0.01}	0.70 ^{+0.00} _{-0.05}	8.21 ^{+0.11} _{-0.11}	3.65 ^{+0.09} _{-0.09}	0.23 ^{+0.26} _{-0.22}	I	0	2.18	360	247
AP453	8.90 ^{+0.10} _{-0.00}	3.87 ^{+0.03} _{-0.06}	0.20 ^{+0.05} _{-0.15}	8.72 ^{+0.16} _{-0.18}	3.50 ^{+0.09} _{-0.09}	0.32 ^{+0.28} _{-0.26}	I	0	1.63	263	183
AP454	6.60 ^{+0.40} _{-0.00}	2.82 ^{+0.00} _{-0.02}	0.80 ^{+0.00} _{-0.05}	6.82 ^{+0.10} _{-0.10}	2.97 ^{+0.23} _{-0.22}	0.55 ^{+0.10} _{-0.10}	I	0	2.57	131	104
AP455	9.00 ^{+0.10} _{-0.00}	3.35 ^{+0.07} _{-0.05}	0.20 ^{+0.10} _{-0.15}	8.71 ^{+0.22} _{-0.23}	3.12 ^{+0.12} _{-0.11}	0.63 ^{+0.33} _{-0.32}	I	0	1.51	87	32
AP457	8.30 ^{+0.00} _{-0.00}	4.02 ^{+0.00} _{-0.03}	1.60 ^{+0.00} _{-0.05}	8.17 ^{+0.16} _{-0.15}	3.62 ^{+0.15} _{-0.10}	1.01 ^{+0.27} _{-0.26}	I	0	1.66	236	129
AP458	8.90 ^{+0.00} _{-0.20}	4.03 ^{+0.05} _{-0.10}	0.85 ^{+0.65} _{-0.06}	8.26 ^{+0.13} _{-0.11}	3.78 ^{+0.11} _{-0.08}	1.48 ^{+0.24} _{-0.24}	I	0	1.98	295	189
AP459	8.40 ^{+0.10} _{-0.00}	3.84 ^{+0.00} _{-0.04}	0.80 ^{+0.00} _{-0.20}	8.74 ^{+0.14} _{-0.15}	3.77 ^{+0.07} _{-0.07}	0.33 ^{+0.20} _{-0.20}	I	0	2.10	316	214
AP461	8.40 ^{+0.10} _{-0.00}	3.23 ^{+0.05} _{-0.00}	0.40 ^{+0.15} _{-0.05}	8.14 ^{+0.13} _{-0.12}	3.21 ^{+0.14} _{-0.14}	0.79 ^{+0.27} _{-0.30}	I	0	1.56	82	25
AP462	7.40 ^{+0.10} _{-0.40}	3.45 ^{+0.00} _{-0.09}	1.65 ^{+0.05} _{-0.05}	6.80 ^{+0.02} _{-0.08}	3.23 ^{+0.16} _{-0.18}	1.57 ^{+0.10} _{-0.08}	I	0	1.94	229	213
AP463	9.10 ^{+0.00} _{-0.20}	3.76 ^{+0.05} _{-0.07}	0.35 ^{+0.55} _{-0.05}	8.94 ^{+0.60} _{-0.42}	3.65 ^{+0.12} _{-0.11}	0.93 ^{+0.48} _{-0.71}	I	0	1.54	158	72
AP464	9.10 ^{+0.00} _{-1.50}	3.52 ^{+0.07} _{-0.45}	0.10 ^{+1.85} _{-0.00}	9.63 ^{+0.21} _{-0.11}	3.83 ^{+0.16} _{-0.09}	0.03 ^{+0.05} _{-0.03}	I	0	1.52	169	102
AP468	8.50 ^{+0.00} _{-0.10}	3.83 ^{+0.00} _{-0.02}	0.35 ^{+0.05} _{-0.05}	8.66 ^{+0.13} _{-0.15}	3.80 ^{+0.08} _{-0.08}	0.17 ^{+0.20} _{-0.17}	I	0	2.37	482	341
AP469	8.10 ^{+0.00} _{-0.10}	3.26 ^{+0.00} _{-0.04}	0.40 ^{+0.00} _{-0.05}	7.99 ^{+0.11} _{-0.14}	2.99 ^{+0.10} _{-0.10}	0.16 ^{+0.16} _{-0.14}	I	0	1.59	137	86
AP471	8.90 ^{+0.00} _{-0.00}	3.90 ^{+0.03} _{-0.06}	0.25 ^{+0.05} _{-0.10}	8.96 ^{+0.10} _{-0.10}	3.53 ^{+0.09} _{-0.09}	0.15 ^{+0.14} _{-0.14}	I	0	1.75	257	168
AP475	8.90 ^{+0.00} _{-0.90}	3.45 ^{+0.04} _{-0.22}	0.15 ^{+1.25} _{-0.00}	8.94 ^{+0.17} _{-0.15}	3.32 ^{+0.12} _{-0.12}	0.23 ^{+0.19} _{-0.21}	I	0	1.54	205	139
AP476	8.20 ^{+0.00} _{-0.10}	2.92 ^{+0.05} _{-0.01}	0.30 ^{+0.25} _{-0.00}	8.35 ^{+0.10} _{-0.05}	2.89 ^{+0.13} _{-0.09}	0.11 ^{+0.12} _{-0.11}	I	0	1.27	105	80
AP477	8.00 ^{+0.00} _{-0.00}	3.30 ^{+0.00} _{-0.02}	0.45 ^{+0.00} _{-0.05}	8.13 ^{+0.10} _{-0.08}	3.32 ^{+0.11} _{-0.12}	0.47 ^{+0.20} _{-0.20}	I	0	1.86	178	95
AP478	8.90 ^{+0.10} _{-0.00}	3.46 ^{+0.02} _{-0.08}	0.45 ^{+0.05} _{-0.25}	8.80 ^{+0.15} _{-0.17}	3.21 ^{+0.11} _{-0.11}	0.24 ^{+0.22} _{-0.22}	I	0	1.39	128	85
AP480	9.10 ^{+0.00} _{-0.00}	3.97 ^{+0.05} _{-0.03}	0.20 ^{+0.10} _{-0.00}	9.22 ^{+0.13} _{-0.12}	3.79 ^{+0.10} _{-0.10}	0.13 ^{+0.14} _{-0.13}	I	0	2.10	315	190
AP481	9.00 ^{+0.00} _{-0.00}	3.91 ^{+0.03} _{-0.04}	0.15 ^{+0.05} _{-0.10}	8.76 ^{+0.21} _{-0.23}	3.57 ^{+0.08} _{-0.07}	0.53 ^{+0.32} _{-0.33}	I	0	1.90	249	145
AP482	8.20 ^{+0.00} _{-0.40}	3.08 ^{+0.02} _{-0.03}	0.35 ^{+0.20} _{-0.05}	8.31 ^{+0.09} _{-0.09}	2.96 ^{+0.11} _{-0.11}	0.23 ^{+0.19} _{-0.20}	I	0	1.34	123	74
AP483	8.80 ^{+0.00} _{-0.00}	3.64 ^{+0.03} _{-0.00}	0.05 ^{+0.05} _{-0.00}	0.00 ^{+0.00} _{-0.00}	0.00 ^{+0.00} _{-0.00}	0.00 ^{+0.00} _{-0.00}	I	0	3.69	491	297
AP484	8.10 ^{+0.00} _{-0.70}	3.46 ^{+0.00} _{-0.10}	1.40 ^{+0.30} _{-0.05}	8.52 ^{+0.25} _{-0.20}	3.61 ^{+0.13} _{-0.15}	0.85 ^{+0.42} _{-0.54}	I	0	1.32	148	100
AP485	8.90 ^{+0.00} _{-0.00}	3.80 ^{+0.03} _{-0.04}	0.25 ^{+0.10} _{-0.05}	7.68 ^{+0.92} _{-0.95}	3.24 ^{+0.25} _{-0.24}	1.11 ^{+0.68} _{-0.71}	I	0	1.75	243	146
AP486	8.90 ^{+0.00} _{-0.00}	3.55 ^{+0.05} _{-0.00}	0.00 ^{+0.10} _{-0.00}	8.50 ^{+0.12} _{-0.11}	3.27 ^{+0.11} _{-0.11}	0.53 ^{+0.23} _{-0.33}	I	0	1.64	183	109
AP487	8.40 ^{+0.10} _{-0.00}	3.86 ^{+0.05} _{-0.02}	1.30 ^{+0.10} _{-0.15}	8.57 ^{+0.14} _{-0.12}	3.60 ^{+0.09} _{-0.08}	0.56 ^{+0.25} _{-0.25}	I	0	2.26	383	251
AP488	8.40 ^{+0.10} _{-0.00}	3.75 ^{+0.03} _{-0.00}	1.05 ^{+0.05} _{-0.10}	7.75 ^{+0.03} _{-0.03}	2.12 ^{+0.04} _{-0.05}	0.30 ^{+0.07} _{-0.07}	I	0	2.08	282	188

Table 1 (cont'd)

AP ID ^a	CMD Best Fit Parameters ^b			Integrated Best Fit Parameters ^c			Best ^d Flag ^e	R _{ap} ^f	N _{stars} ^g	N _{bg} ^h	
	log(<i>t</i> [Myr])	log(<i>M</i> [<i>M</i> _⊙])	<i>A_V</i> [mag]	log(<i>t</i> [Myr])	log(<i>M</i> [<i>M</i> _⊙])	<i>A_V</i> [mag]					
AP489	8.90 ^{+0.00} _{-0.10}	3.67 ^{+0.03} _{-0.03}	0.25 ^{+0.30} _{-0.00}	8.86 ^{+0.07} _{-0.08}	3.13 ^{+0.08} _{-0.08}	0.09 ^{+0.11} _{-0.09}	I	0	1.57	139	63
AP493	8.20 ^{+0.10} _{-0.00}	3.73 ^{+0.04} _{-0.02}	1.40 ^{+0.05} _{-0.10}	8.90 ^{+0.24} _{-0.46}	3.51 ^{+0.11} _{-0.11}	0.30 ^{+0.51} _{-0.29}	I	0	1.42	157	101
AP494	8.40 ^{+0.00} _{-0.60}	2.93 ^{+0.01} _{-0.13}	0.15 ^{+0.25} _{-0.00}	7.98 ^{+0.17} _{-0.13}	2.58 ^{+0.15} _{-0.15}	0.09 ^{+0.13} _{-0.09}	I	0	1.68	144	103
AP498	8.00 ^{+0.00} _{-0.00}	3.89 ^{+0.02} _{-0.00}	1.55 ^{+0.05} _{-0.00}	8.72 ^{+0.07} _{-0.06}	3.82 ^{+0.06} _{-0.06}	0.50 ^{+0.15} _{-0.15}	I	0	1.86	343	256
AP499	9.10 ^{+0.00} _{-0.00}	4.72 ^{+0.05} _{-0.04}	1.55 ^{+0.00} _{-0.10}	8.52 ^{+1.48} _{-1.61}	4.11 ^{+1.07} _{-1.49}	2.00 ^{+0.66} _{-0.58}	I	0	1.66	179	102
AP500	8.30 ^{+0.00} _{-0.30}	3.10 ^{+0.00} _{-0.04}	0.30 ^{+0.20} _{-0.00}	8.29 ^{+0.29} _{-0.27}	3.16 ^{+0.18} _{-0.15}	0.41 ^{+0.38} _{-0.36}	I	0	1.70	154	142
AP501	9.40 ^{+0.00} _{-0.10}	4.21 ^{+0.03} _{-0.15}	0.00 ^{+0.15} _{-0.00}	8.11 ^{+1.47} _{-1.46}	3.78 ^{+1.25} _{-1.18}	1.45 ^{+1.02} _{-1.02}	I	0	1.66	125	54
AP503	7.80 ^{+0.00} _{-0.80}	3.80 ^{+0.00} _{-0.10}	1.85 ^{+0.25} _{-0.00}	8.54 ^{+0.48} _{-0.42}	3.66 ^{+0.14} _{-0.12}	0.64 ^{+0.63} _{-0.60}	I	0	1.70	229	178
AP504	7.80 ^{+0.30} _{-0.10}	3.23 ^{+0.04} _{-0.02}	0.70 ^{+0.00} _{-0.15}	7.95 ^{+0.16} _{-0.17}	3.18 ^{+0.09} _{-0.09}	0.61 ^{+0.25} _{-0.24}	I	0	1.73	242	206
AP505	9.20 ^{+0.10} _{-0.30}	3.64 ^{+0.23} _{-0.37}	0.00 ^{+0.34} _{-0.00}	7.87 ^{+1.04} _{-1.14}	3.27 ^{+0.26} _{-0.26}	1.40 ^{+0.85} _{-0.89}	I	0	1.53	111	46
AP508	8.60 ^{+0.10} _{-0.00}	3.40 ^{+0.00} _{-0.05}	0.35 ^{+0.00} _{-0.30}	7.56 ^{+0.16} _{-0.17}	3.63 ^{+0.20} _{-0.21}	2.12 ^{+0.21} _{-0.18}	I	0	1.78	196	152
AP509	8.50 ^{+0.00} _{-0.00}	3.40 ^{+0.03} _{-0.03}	0.30 ^{+0.05} _{-0.10}	8.15 ^{+0.14} _{-0.14}	3.37 ^{+0.11} _{-0.10}	0.77 ^{+0.28} _{-0.27}	I	0	1.46	150	79
AP511	7.80 ^{+0.20} _{-0.20}	3.15 ^{+0.02} _{-0.03}	0.45 ^{+0.10} _{-0.05}	8.06 ^{+0.09} _{-0.10}	3.36 ^{+0.08} _{-0.07}	0.38 ^{+0.16} _{-0.16}	I	0	1.49	136	79
AP514	8.10 ^{+0.00} _{-0.40}	3.29 ^{+0.01} _{-0.09}	0.45 ^{+0.15} _{-0.05}	8.28 ^{+0.08} _{-0.08}	3.28 ^{+0.08} _{-0.09}	0.15 ^{+0.18} _{-0.15}	I	0	1.47	183	119
AP516	8.30 ^{+0.00} _{-0.50}	3.46 ^{+0.00} _{-0.11}	0.85 ^{+0.20} _{-0.05}	8.35 ^{+0.09} _{-0.09}	3.41 ^{+0.11} _{-0.09}	0.68 ^{+0.22} _{-0.21}	I	0	1.58	180	135
AP518	8.20 ^{+0.10} _{-0.00}	3.65 ^{+0.04} _{-0.04}	1.50 ^{+0.00} _{-0.20}	7.85 ^{+0.03} _{-0.03}	2.21 ^{+0.03} _{-0.05}	0.09 ^{+0.07} _{-0.07}	I	0	1.76	203	130
AP521	10.00 ^{+0.10} _{-0.10}	5.25 ^{+0.36} _{-0.08}	0.10 ^{+0.15} _{-0.00}	9.64 ^{+0.33} _{-0.40}	4.46 ^{+0.11} _{-0.11}	0.49 ^{+0.40} _{-0.30}	I	0	2.69	442	288
AP522	6.60 ^{+0.10} _{-0.00}	3.25 ^{+0.00} _{-0.01}	0.80 ^{+0.00} _{-0.00}	6.52 ^{+0.13} _{-0.11}	3.26 ^{+0.28} _{-0.17}	0.45 ^{+0.10} _{-0.09}	I	0	3.35	341	196
AP523	7.50 ^{+0.40} _{-0.40}	2.97 ^{+0.01} _{-0.07}	1.00 ^{+0.05} _{-0.20}	7.74 ^{+0.19} _{-0.14}	3.63 ^{+0.09} _{-0.11}	1.15 ^{+0.22} _{-0.30}	I	0	1.56	102	50
AP524	7.80 ^{+0.40} _{-0.00}	3.06 ^{+0.04} _{-0.04}	1.75 ^{+0.00} _{-0.45}	8.04 ^{+0.08} _{-0.10}	3.32 ^{+0.15} _{-0.17}	1.67 ^{+0.27} _{-0.25}	I	0	1.39	54	16
AP527	8.20 ^{+0.10} _{-0.20}	3.34 ^{+0.03} _{-0.05}	1.20 ^{+0.10} _{-0.05}	8.36 ^{+0.09} _{-0.09}	2.49 ^{+0.15} _{-0.15}	0.11 ^{+0.14} _{-0.11}	I	0	1.30	131	107
AP529	8.10 ^{+0.10} _{-0.00}	3.56 ^{+0.03} _{-0.02}	1.75 ^{+0.05} _{-0.10}	8.88 ^{+0.11} _{-0.11}	3.17 ^{+0.11} _{-0.11}	0.11 ^{+0.14} _{-0.11}	I	0	1.49	164	139
AP530	9.10 ^{+0.00} _{-0.00}	3.79 ^{+0.06} _{-0.03}	0.30 ^{+0.15} _{-0.00}	9.22 ^{+0.33} _{-0.25}	3.71 ^{+0.14} _{-0.15}	0.42 ^{+0.25} _{-0.36}	I	0	1.74	187	118
AP531	8.50 ^{+0.10} _{-0.00}	3.38 ^{+0.02} _{-0.00}	0.35 ^{+0.09} _{-0.15}	8.27 ^{+0.09} _{-0.13}	3.52 ^{+0.11} _{-0.12}	0.90 ^{+0.29} _{-0.24}	I	0	1.53	128	51
AP532	9.10 ^{+0.00} _{-0.00}	3.81 ^{+0.05} _{-0.00}	0.20 ^{+0.10} _{-0.05}	8.97 ^{+0.28} _{-0.30}	3.74 ^{+0.11} _{-0.10}	0.46 ^{+0.37} _{-0.36}	I	0	2.13	264	117
AP533	9.10 ^{+0.00} _{-0.00}	3.70 ^{+0.01} _{-0.02}	0.00 ^{+0.05} _{-0.00}	8.39 ^{+0.47} _{-0.36}	3.42 ^{+0.20} _{-0.21}	1.20 ^{+0.68} _{-0.91}	I	0	1.46	121	61
AP534	7.50 ^{+0.00} _{-0.20}	2.80 ^{+0.01} _{-0.02}	0.85 ^{+0.10} _{-0.00}	7.90 ^{+0.15} _{-0.15}	2.76 ^{+0.10} _{-0.10}	0.39 ^{+0.21} _{-0.21}	I	0	1.42	64	35
AP535	8.50 ^{+0.00} _{-0.50}	3.41 ^{+0.00} _{-0.19}	0.65 ^{+0.30} _{-0.05}	8.69 ^{+0.09} _{-0.06}	3.28 ^{+0.08} _{-0.09}	0.27 ^{+0.14} _{-0.19}	I	0	1.34	133	82
AP538	8.40 ^{+0.00} _{-0.00}	3.18 ^{+0.03} _{-0.05}	0.45 ^{+0.05} _{-0.05}	8.42 ^{+0.09} _{-0.06}	2.87 ^{+0.12} _{-0.10}	0.07 ^{+0.12} _{-0.07}	I	0	1.46	168	139
AP539	8.50 ^{+0.00} _{-0.10}	3.72 ^{+0.01} _{-0.03}	0.65 ^{+0.05} _{-0.05}	8.79 ^{+0.09} _{-0.09}	3.48 ^{+0.06} _{-0.07}	0.12 ^{+0.14} _{-0.12}	I	0	2.28	455	379
AP540	7.70 ^{+0.10} _{-0.00}	4.56 ^{+0.06} _{-0.00}	2.95 ^{+0.00} _{-0.05}	0.00 ^{+0.00} _{-0.00}	0.00 ^{+0.00} _{-0.00}	0.00 ^{+0.00} _{-0.00}	I	0	3.74	602	306
AP541	8.10 ^{+0.00} _{-0.20}	3.66 ^{+0.02} _{-0.06}	1.55 ^{+0.15} _{-0.00}	7.70 ^{+0.03} _{-0.03}	2.20 ^{+0.03} _{-0.03}	0.30 ^{+0.07} _{-0.07}	I	0	1.66	206	139
AP542	8.20 ^{+0.00} _{-0.10}	3.56 ^{+0.02} _{-0.05}	1.55 ^{+0.05} _{-0.10}	9.33 ^{+0.08} _{-0.08}	3.69 ^{+0.07} _{-0.07}	0.03 ^{+0.07} _{-0.03}	I	0	1.49	182	112

Table 1 (cont'd)

AP ID ^a	CMD Best Fit Parameters ^b			Integrated Best Fit Parameters ^c			Best ^d Flag ^e	R _{ap} ^f	N _{stars} ^g	N _{bg} ^h	
	log(<i>t</i> [Myr])	log(<i>M</i> [<i>M</i> _⊙])	<i>A_V</i> [mag]	log(<i>t</i> [Myr])	log(<i>M</i> [<i>M</i> _⊙])	<i>A_V</i> [mag]					
AP543	8.80 ^{+0.00} _{-0.10}	3.50 ^{+0.03} _{-0.03}	0.15 ^{+0.30} _{-0.00}	8.05 ^{+0.09} _{-0.09}	3.67 ^{+0.10} _{-0.07}	1.49 ^{+0.20} _{-0.19}	I	0	1.52	198	161
AP544	9.10 ^{+0.00} _{-0.00}	3.59 ^{+0.04} _{-0.05}	0.25 ^{+0.10} _{-0.05}	9.21 ^{+0.62} _{-0.67}	3.87 ^{+0.19} _{-0.16}	0.75 ^{+0.74} _{-0.62}	I	0	1.95	97	64
AP545	9.40 ^{+0.00} _{-0.00}	4.57 ^{+0.00} _{-0.02}	0.00 ^{+0.00} _{-0.00}	0.00 ^{+0.00} _{-0.00}	0.00 ^{+0.00} _{-0.00}	0.00 ^{+0.00} _{-0.00}	I	0	2.94	404	324
AP547	8.30 ^{+0.00} _{-0.10}	3.12 ^{+0.01} _{-0.04}	0.55 ^{+0.10} _{-0.00}	6.90 ^{+1.03} _{-0.80}	2.97 ^{+0.26} _{-0.20}	0.84 ^{+0.36} _{-0.63}	I	0	1.44	138	112
AP548	7.50 ^{+0.00} _{-0.20}	3.27 ^{+0.00} _{-0.02}	1.15 ^{+0.05} _{-0.00}	7.18 ^{+0.19} _{-0.19}	2.96 ^{+0.19} _{-0.20}	1.09 ^{+0.18} _{-0.18}	I	0	1.83	158	138
AP549	9.10 ^{+0.40} _{-1.50}	3.61 ^{+0.18} _{-3.61}	0.40 ^{+2.00} _{-0.30}	8.84 ^{+0.52} _{-0.67}	3.49 ^{+0.18} _{-0.16}	0.68 ^{+0.84} _{-0.59}	I	0	1.43	151	86
AP551	8.00 ^{+0.00} _{-0.10}	3.44 ^{+0.00} _{-0.04}	0.90 ^{+0.05} _{-0.05}	7.57 ^{+0.19} _{-0.17}	3.65 ^{+0.09} _{-0.04}	1.41 ^{+0.19} _{-0.19}	I	0	1.83	247	193
AP552	6.70 ^{+0.00} _{-0.10}	3.56 ^{+0.00} _{-0.00}	0.40 ^{+0.00} _{-0.00}	6.67 ^{+0.12} _{-0.15}	3.23 ^{+0.29} _{-0.26}	0.02 ^{+0.07} _{-0.02}	I	0	3.55	991	956
AP554	8.10 ^{+0.10} _{-0.10}	3.04 ^{+0.00} _{-0.05}	0.45 ^{+0.00} _{-0.10}	8.16 ^{+0.16} _{-0.15}	3.09 ^{+0.09} _{-0.08}	0.70 ^{+0.28} _{-0.30}	I	0	1.48	132	107
AP556	8.20 ^{+0.00} _{-0.00}	3.92 ^{+0.00} _{-0.05}	1.45 ^{+0.00} _{-0.10}	8.82 ^{+0.20} _{-0.18}	3.79 ^{+0.11} _{-0.06}	0.51 ^{+0.32} _{-0.34}	I	0	1.95	360	275
AP557	8.90 ^{+0.00} _{-0.00}	3.86 ^{+0.01} _{-0.05}	0.55 ^{+0.05} _{-0.10}	8.65 ^{+0.21} _{-0.22}	2.96 ^{+0.13} _{-0.14}	0.40 ^{+0.31} _{-0.31}	I	0	1.33	120	65
AP562	9.10 ^{+0.00} _{-0.10}	3.63 ^{+0.04} _{-0.08}	0.15 ^{+0.20} _{-0.00}	9.14 ^{+0.33} _{-0.25}	3.46 ^{+0.15} _{-0.13}	0.36 ^{+0.29} _{-0.32}	I	0	1.57	131	62
AP563	7.60 ^{+0.10} _{-0.20}	3.27 ^{+0.01} _{-0.03}	0.60 ^{+0.05} _{-0.10}	6.33 ^{+0.19} _{-0.28}	2.97 ^{+0.35} _{-0.42}	0.89 ^{+0.19} _{-0.17}	I	0	1.46	189	149
AP564	8.40 ^{+0.00} _{-0.10}	3.45 ^{+0.00} _{-0.06}	0.70 ^{+0.10} _{-0.05}	8.67 ^{+0.10} _{-0.10}	3.40 ^{+0.08} _{-0.08}	0.27 ^{+0.20} _{-0.21}	I	0	1.69	199	132
AP565	10.00 ^{+0.10} _{-0.20}	4.78 ^{+0.38} _{-0.15}	0.05 ^{+0.20} _{-0.00}	8.67 ^{+0.96} _{-0.79}	3.81 ^{+0.15} _{-0.15}	1.35 ^{+0.96} _{-1.13}	I	0	1.81	205	136
AP566	8.50 ^{+0.00} _{-0.20}	3.44 ^{+0.01} _{-0.05}	0.50 ^{+0.25} _{-0.00}	8.84 ^{+0.10} _{-0.10}	3.47 ^{+0.08} _{-0.10}	0.11 ^{+0.14} _{-0.11}	I	0	1.81	206	162
AP568	9.10 ^{+0.00} _{-0.10}	3.49 ^{+0.05} _{-0.05}	0.05 ^{+0.40} _{-0.00}	8.78 ^{+0.75} _{-0.71}	3.57 ^{+0.19} _{-0.20}	1.07 ^{+0.91} _{-0.80}	I	0	1.65	130	68
AP569	8.40 ^{+0.00} _{-0.10}	3.33 ^{+0.00} _{-0.08}	0.70 ^{+0.05} _{-0.10}	8.60 ^{+0.14} _{-0.16}	3.15 ^{+0.11} _{-0.10}	0.28 ^{+0.32} _{-0.27}	I	0	1.65	177	138
AP570	8.30 ^{+0.00} _{-0.10}	3.58 ^{+0.07} _{-0.04}	1.50 ^{+0.25} _{-0.00}	8.23 ^{+0.07} _{-0.09}	3.71 ^{+0.12} _{-0.10}	1.50 ^{+0.23} _{-0.19}	I	0	1.66	169	92
AP571	8.00 ^{+0.10} _{-0.20}	3.57 ^{+0.01} _{-0.07}	1.95 ^{+0.05} _{-0.10}	8.41 ^{+0.12} _{-0.11}	3.17 ^{+0.15} _{-0.15}	0.48 ^{+0.31} _{-0.35}	I	0	1.49	139	58
AP572	9.00 ^{+0.00} _{-0.00}	3.54 ^{+0.04} _{-0.06}	0.00 ^{+0.10} _{-0.00}	9.37 ^{+0.05} _{-0.05}	3.61 ^{+0.07} _{-0.07}	0.00 ^{+0.07} _{-0.00}	I	0	1.39	138	78
AP573	8.80 ^{+0.00} _{-0.00}	3.59 ^{+0.00} _{-0.06}	0.45 ^{+0.00} _{-0.15}	8.16 ^{+0.36} _{-0.42}	2.62 ^{+0.42} _{-0.54}	0.31 ^{+0.21} _{-0.19}	I	0	1.90	227	163
AP576	8.40 ^{+0.10} _{-0.10}	3.13 ^{+0.03} _{-0.02}	0.40 ^{+0.10} _{-0.10}	8.11 ^{+0.16} _{-0.16}	3.21 ^{+0.16} _{-0.15}	0.92 ^{+0.29} _{-0.29}	I	0	1.43	178	156
AP577	7.90 ^{+0.10} _{-0.50}	2.88 ^{+0.02} _{-0.05}	0.65 ^{+0.15} _{-0.05}	7.81 ^{+0.19} _{-0.10}	3.18 ^{+0.15} _{-0.12}	1.08 ^{+0.27} _{-0.25}	I	0	1.39	135	100
AP578	8.30 ^{+0.00} _{-0.40}	3.70 ^{+0.02} _{-0.06}	0.95 ^{+0.20} _{-0.05}	8.31 ^{+0.07} _{-0.08}	3.92 ^{+0.07} _{-0.07}	0.79 ^{+0.18} _{-0.15}	I	0	2.05	358	206
AP580	9.10 ^{+0.00} _{-0.00}	3.87 ^{+0.02} _{-0.10}	0.50 ^{+0.05} _{-0.05}	8.58 ^{+0.71} _{-0.67}	3.35 ^{+0.22} _{-0.21}	0.97 ^{+0.85} _{-0.85}	I	0	1.70	125	72
AP583	9.10 ^{+0.00} _{-0.10}	3.74 ^{+0.05} _{-0.11}	0.05 ^{+0.20} _{-0.00}	7.77 ^{+0.10} _{-0.09}	3.06 ^{+0.09} _{-0.09}	0.58 ^{+0.18} _{-0.17}	I	0	1.89	239	168
AP587	8.30 ^{+0.00} _{-0.10}	3.65 ^{+0.03} _{-0.03}	0.75 ^{+0.10} _{-0.00}	8.14 ^{+0.11} _{-0.10}	3.84 ^{+0.07} _{-0.06}	1.11 ^{+0.18} _{-0.18}	I	0	1.73	238	158
AP588	7.70 ^{+0.10} _{-0.20}	4.09 ^{+0.00} _{-0.29}	2.80 ^{+0.05} _{-0.35}	9.15 ^{+0.16} _{-0.15}	4.03 ^{+0.09} _{-0.09}	0.53 ^{+0.22} _{-0.23}	I	0	1.65	206	156
AP592	8.40 ^{+0.20} _{-0.20}	3.15 ^{+0.07} _{-0.04}	0.50 ^{+0.25} _{-0.25}	8.44 ^{+0.13} _{-0.02}	2.89 ^{+0.16} _{-0.08}	0.28 ^{+0.17} _{-0.16}	I	0	1.34	145	108
AP593	8.50 ^{+0.10} _{-0.10}	3.45 ^{+0.03} _{-0.02}	0.55 ^{+0.15} _{-0.10}	8.49 ^{+0.08} _{-0.06}	2.75 ^{+0.13} _{-0.11}	0.08 ^{+0.11} _{-0.08}	I	0	2.11	252	192
AP595	8.70 ^{+0.10} _{-0.00}	3.57 ^{+0.08} _{-0.04}	0.80 ^{+0.25} _{-0.20}	8.85 ^{+0.51} _{-0.52}	3.80 ^{+0.13} _{-0.13}	1.29 ^{+0.85} _{-0.81}	I	0	1.48	140	72
AP597	7.70 ^{+0.10} _{-0.30}	3.38 ^{+0.00} _{-0.04}	0.65 ^{+0.10} _{-0.05}	7.63 ^{+0.17} _{-0.17}	3.33 ^{+0.07} _{-0.07}	0.52 ^{+0.19} _{-0.18}	I	0	1.59	171	126

Table 1 (cont'd)

AP ID ^a	CMD Best Fit Parameters ^b			Integrated Best Fit Parameters ^c			Best ^d Flag ^e	R _{ap} ^f	N _{stars} ^g	N _{bg} ^h	
	log(<i>t</i> [Myr])	log(<i>M</i> [<i>M</i> _⊙])	<i>A_V</i> [mag]	log(<i>t</i> [Myr])	log(<i>M</i> [<i>M</i> _⊙])	<i>A_V</i> [mag]					
AP598	9.00 ^{+0.10} _{-0.00}	3.64 ^{+0.04} _{-0.02}	0.10 ^{+0.10} _{-0.05}	9.13 ^{+0.09} _{-0.10}	3.37 ^{+0.11} _{-0.11}	0.06 ^{+0.10} _{-0.06}	I	0	1.62	142	78
AP599	9.40 ^{+0.00} _{-0.00}	4.70 ^{+0.00} _{-0.00}	0.00 ^{+0.00} _{-0.00}	9.22 ^{+0.07} _{-0.06}	5.19 ^{+0.04} _{-0.04}	0.10 ^{+0.10} _{-0.10}	I	0	3.50	521	567
AP600	8.80 ^{+0.10} _{-0.10}	3.42 ^{+0.06} _{-0.13}	0.30 ^{+0.20} _{-0.23}	8.75 ^{+0.08} _{-0.07}	2.86 ^{+0.09} _{-0.09}	0.08 ^{+0.11} _{-0.08}	I	0	1.29	109	73
AP601	9.10 ^{+0.00} _{-0.10}	3.92 ^{+0.02} _{-0.07}	0.25 ^{+0.10} _{-0.00}	9.43 ^{+0.40} _{-0.50}	3.74 ^{+0.18} _{-0.15}	0.28 ^{+0.50} _{-0.28}	I	0	2.29	222	119
AP604	8.80 ^{+0.00} _{-0.10}	3.43 ^{+0.04} _{-0.00}	0.00 ^{+0.35} _{-0.05}	8.48 ^{+0.14} _{-0.13}	3.05 ^{+0.09} _{-0.09}	0.31 ^{+0.27} _{-0.26}	I	0	1.62	145	93
AP606	8.90 ^{+0.00} _{-0.00}	3.82 ^{+0.07} _{-0.00}	0.30 ^{+0.15} _{-0.05}	8.81 ^{+0.26} _{-0.25}	3.27 ^{+0.17} _{-0.18}	0.20 ^{+0.24} _{-0.20}	I	0	1.52	178	110
AP607	6.60 ^{+0.30} _{-0.00}	2.96 ^{+0.00} _{-0.04}	0.75 ^{+0.00} _{-0.10}	6.78 ^{+0.10} _{-0.10}	2.79 ^{+0.33} _{-0.35}	0.23 ^{+0.10} _{-0.10}	I	0	2.30	293	271
AP608	8.90 ^{+0.00} _{-0.00}	4.17 ^{+0.00} _{-0.04}	0.05 ^{+0.00} _{-0.05}	8.90 ^{+0.06} _{-0.07}	3.96 ^{+0.05} _{-0.05}	0.10 ^{+0.10} _{-0.10}	I	0	2.62	575	361
AP609	7.20 ^{+0.10} _{-0.20}	3.35 ^{+0.00} _{-0.06}	1.75 ^{+0.00} _{-0.40}	7.42 ^{+0.11} _{-0.10}	4.33 ^{+0.07} _{-0.08}	1.50 ^{+0.13} _{-0.14}	I	0	1.77	185	136
AP611	7.90 ^{+0.00} _{-0.50}	3.78 ^{+0.04} _{-0.07}	2.15 ^{+0.45} _{-0.05}	7.96 ^{+1.20} _{-1.40}	3.90 ^{+0.37} _{-0.48}	1.36 ^{+0.79} _{-0.97}	I	0	1.95	316	172
AP612	8.20 ^{+0.00} _{-0.20}	3.61 ^{+0.00} _{-0.05}	0.80 ^{+0.10} _{-0.00}	8.18 ^{+0.40} _{-0.19}	3.73 ^{+0.12} _{-0.19}	0.97 ^{+0.39} _{-0.87}	I	0	1.81	229	112
AP614	9.10 ^{+0.10} _{-0.10}	3.79 ^{+0.30} _{-0.00}	0.20 ^{+0.15} _{-0.05}	8.72 ^{+0.25} _{-0.25}	3.61 ^{+0.10} _{-0.07}	0.63 ^{+0.32} _{-0.34}	I	0	2.44	285	150
AP615	8.20 ^{+0.20} _{-0.30}	3.00 ^{+0.03} _{-0.06}	0.55 ^{+0.15} _{-0.15}	8.59 ^{+0.15} _{-0.15}	2.77 ^{+0.14} _{-0.11}	0.25 ^{+0.23} _{-0.22}	I	0	1.52	119	87
AP616	9.10 ^{+0.00} _{-0.00}	3.60 ^{+0.04} _{-0.00}	0.00 ^{+0.15} _{-0.00}	9.17 ^{+0.16} _{-0.06}	3.39 ^{+0.13} _{-0.13}	0.16 ^{+0.03} _{-0.16}	I	0	1.35	99	42
AP617	8.40 ^{+0.10} _{-0.00}	3.51 ^{+0.04} _{-0.04}	1.05 ^{+0.05} _{-0.25}	8.56 ^{+0.13} _{-0.14}	3.24 ^{+0.10} _{-0.10}	0.18 ^{+0.23} _{-0.18}	I	0	1.52	139	79
AP620	7.30 ^{+0.20} _{-0.20}	3.26 ^{+0.01} _{-0.02}	0.70 ^{+0.05} _{-0.05}	7.60 ^{+0.18} _{-0.17}	3.34 ^{+0.07} _{-0.07}	0.43 ^{+0.18} _{-0.18}	I	0	1.80	131	61
AP622	9.00 ^{+0.00} _{-0.00}	3.45 ^{+0.02} _{-0.04}	0.00 ^{+0.05} _{-0.00}	9.27 ^{+0.11} _{-0.10}	3.46 ^{+0.10} _{-0.10}	0.06 ^{+0.10} _{-0.06}	I	0	1.32	95	27
AP624	8.10 ^{+0.00} _{-0.10}	3.88 ^{+0.04} _{-0.04}	2.35 ^{+0.10} _{-0.05}	9.19 ^{+0.17} _{-0.16}	3.52 ^{+0.12} _{-0.13}	0.25 ^{+0.19} _{-0.19}	I	0	1.56	149	85
AP626	7.20 ^{+0.10} _{-0.30}	4.24 ^{+0.04} _{-0.07}	2.85 ^{+0.05} _{-0.00}	9.35 ^{+0.03} _{-0.03}	5.50 ^{+0.03} _{-0.03}	0.00 ^{+0.07} _{-0.00}	I	1	3.22	699	792
AP627	8.80 ^{+0.00} _{-0.10}	3.76 ^{+0.04} _{-0.04}	0.25 ^{+0.35} _{-0.00}	8.81 ^{+0.04} _{-0.05}	3.32 ^{+0.06} _{-0.06}	0.00 ^{+0.07} _{-0.00}	I	0	1.63	181	88
AP629	9.10 ^{+0.00} _{-0.00}	4.06 ^{+0.07} _{-0.06}	0.15 ^{+0.05} _{-0.10}	9.49 ^{+0.18} _{-0.18}	4.38 ^{+0.09} _{-0.08}	0.13 ^{+0.22} _{-0.13}	I	0	1.96	400	330
AP630	8.00 ^{+0.00} _{-0.10}	3.64 ^{+0.02} _{-0.02}	1.25 ^{+0.10} _{-0.00}	8.15 ^{+0.12} _{-0.12}	3.71 ^{+0.13} _{-0.10}	1.13 ^{+0.28} _{-0.26}	I	0	1.50	193	130
AP632	9.00 ^{+0.00} _{-0.00}	3.58 ^{+0.02} _{-0.05}	0.00 ^{+0.10} _{-0.00}	8.69 ^{+0.11} _{-0.12}	3.34 ^{+0.08} _{-0.08}	0.69 ^{+0.19} _{-0.19}	I	0	1.29	104	37
AP633	9.10 ^{+0.00} _{-0.00}	3.77 ^{+0.02} _{-0.09}	0.30 ^{+0.10} _{-0.05}	8.45 ^{+0.75} _{-0.58}	3.31 ^{+0.12} _{-0.11}	1.07 ^{+0.87} _{-1.06}	I	0	1.17	114	61
AP634	8.90 ^{+0.10} _{-0.00}	3.33 ^{+0.02} _{-0.03}	0.25 ^{+0.05} _{-0.15}	9.22 ^{+0.29} _{-0.21}	3.57 ^{+0.16} _{-0.16}	0.36 ^{+0.21} _{-0.32}	I	0	1.57	129	50
AP636	8.00 ^{+0.30} _{-0.50}	2.83 ^{+0.05} _{-0.08}	0.50 ^{+0.10} _{-0.10}	8.24 ^{+0.11} _{-0.11}	2.65 ^{+0.15} _{-0.16}	0.17 ^{+0.19} _{-0.17}	I	0	1.22	117	96
AP637	7.40 ^{+0.20} _{-0.30}	3.06 ^{+0.02} _{-0.03}	0.60 ^{+0.05} _{-0.05}	8.03 ^{+0.07} _{-0.08}	3.08 ^{+0.07} _{-0.07}	0.30 ^{+0.14} _{-0.14}	I	0	1.76	154	113
AP638	9.00 ^{+0.10} _{-0.00}	3.85 ^{+0.02} _{-0.05}	0.10 ^{+0.15} _{-0.05}	9.40 ^{+0.08} _{-0.08}	3.91 ^{+0.07} _{-0.06}	0.06 ^{+0.10} _{-0.06}	I	0	1.56	159	57
AP639	8.90 ^{+0.10} _{-0.00}	3.60 ^{+0.03} _{-0.04}	0.25 ^{+0.10} _{-0.20}	7.94 ^{+0.11} _{-0.11}	3.59 ^{+0.13} _{-0.12}	1.62 ^{+0.32} _{-0.23}	I	0	1.56	170	86
AP642	8.70 ^{+0.00} _{-0.30}	3.65 ^{+0.04} _{-0.07}	0.35 ^{+0.50} _{-0.00}	8.61 ^{+0.31} _{-0.44}	3.33 ^{+0.20} _{-0.17}	0.48 ^{+0.78} _{-0.48}	I	0	1.55	170	135
AP643	8.90 ^{+0.00} _{-0.00}	3.87 ^{+0.04} _{-0.04}	0.30 ^{+0.15} _{-0.00}	8.92 ^{+0.06} _{-0.06}	3.28 ^{+0.07} _{-0.07}	0.08 ^{+0.11} _{-0.08}	I	0	1.83	254	161
AP644	8.80 ^{+0.00} _{-0.80}	3.50 ^{+0.08} _{-0.02}	0.05 ^{+1.35} _{-0.00}	8.38 ^{+0.13} _{-0.12}	3.03 ^{+0.09} _{-0.07}	0.32 ^{+0.23} _{-0.24}	I	0	1.36	128	80
AP645	8.00 ^{+0.10} _{-0.50}	3.44 ^{+0.00} _{-0.10}	0.90 ^{+0.10} _{-0.10}	8.72 ^{+0.07} _{-0.06}	3.45 ^{+0.05} _{-0.05}	0.07 ^{+0.10} _{-0.07}	I	0	1.48	183	118

Table 1 (cont'd)

AP ID ^a	CMD Best Fit Parameters ^b			Integrated Best Fit Parameters ^c			Best ^d Flag ^e	R _{ap} ^f	N _{stars} ^g	N _{bg} ^h	
	log(<i>t</i> [Myr])	log(<i>M</i> [<i>M</i> _⊙])	<i>A_V</i> [mag]	log(<i>t</i> [Myr])	log(<i>M</i> [<i>M</i> _⊙])	<i>A_V</i> [mag]					
AP646	9.10 ^{+0.00} _{-0.00}	4.32 ^{+0.00} _{-0.04}	0.30 ^{+0.05} _{-0.10}	8.60 ^{+0.21} _{-0.18}	4.34 ^{+0.06} _{-0.06}	1.36 ^{+0.28} _{-0.29}	I	0	2.79	290	228
AP647	7.70 ^{+0.00} _{-0.50}	3.13 ^{+0.01} _{-0.05}	0.75 ^{+0.10} _{-0.00}	8.13 ^{+0.08} _{-0.08}	3.71 ^{+0.07} _{-0.07}	0.64 ^{+0.16} _{-0.17}	I	0	1.71	97	47
AP648	8.40 ^{+0.10} _{-0.00}	3.30 ^{+0.04} _{-0.03}	0.40 ^{+0.05} _{-0.15}	8.01 ^{+0.10} _{-0.11}	3.70 ^{+0.09} _{-0.08}	0.85 ^{+0.21} _{-0.19}	I	0	2.08	337	267
AP649	7.40 ^{+0.10} _{-0.60}	3.05 ^{+0.00} _{-0.04}	0.70 ^{+0.10} _{-0.05}	7.68 ^{+0.09} _{-0.08}	3.28 ^{+0.08} _{-0.08}	0.83 ^{+0.14} _{-0.14}	I	0	1.94	239	175
AP650	7.60 ^{+0.20} _{-0.10}	3.81 ^{+0.00} _{-0.22}	3.00 ^{+0.00} _{-0.40}	8.61 ^{+0.15} _{-0.15}	3.07 ^{+0.09} _{-0.09}	0.31 ^{+0.27} _{-0.27}	I	0	1.42	131	78
AP651	7.00 ^{+0.10} _{-0.10}	3.04 ^{+0.01} _{-0.01}	0.50 ^{+0.05} _{-0.00}	7.10 ^{+0.20} _{-0.17}	3.06 ^{+0.13} _{-0.10}	0.42 ^{+0.13} _{-0.12}	I	0	1.90	123	81
AP653	9.00 ^{+0.00} _{-0.10}	3.53 ^{+0.03} _{-0.10}	0.25 ^{+0.15} _{-0.10}	8.72 ^{+0.22} _{-0.24}	3.22 ^{+0.12} _{-0.13}	0.80 ^{+0.35} _{-0.34}	I	0	1.54	115	62
AP654	9.10 ^{+0.00} _{-0.00}	3.77 ^{+0.01} _{-0.09}	0.50 ^{+0.15} _{-0.05}	8.03 ^{+1.13} _{-1.34}	3.37 ^{+0.27} _{-0.31}	1.48 ^{+1.01} _{-1.08}	I	0	2.06	136	48
AP656	9.10 ^{+0.80} _{-0.00}	4.63 ^{+0.69} _{-0.05}	1.10 ^{+0.05} _{-0.20}	9.43 ^{+0.58} _{-0.51}	4.20 ^{+0.25} _{-0.12}	0.84 ^{+0.57} _{-0.47}	I	0	1.91	240	120
AP659	8.80 ^{+0.00} _{-0.00}	3.37 ^{+0.02} _{-0.03}	0.30 ^{+0.05} _{-0.20}	8.52 ^{+0.11} _{-0.10}	3.09 ^{+0.11} _{-0.09}	0.64 ^{+0.22} _{-0.22}	I	0	1.47	106	50
AP660	9.50 ^{+0.20} _{-0.20}	4.79 ^{+0.14} _{-0.16}	0.70 ^{+0.05} _{-0.15}	9.55 ^{+0.54} _{-0.60}	4.61 ^{+0.17} _{-0.16}	1.46 ^{+0.63} _{-0.49}	I	0	1.79	290	256
AP661	9.10 ^{+0.90} _{-0.00}	4.00 ^{+0.86} _{-0.08}	0.55 ^{+0.05} _{-0.45}	9.21 ^{+0.92} _{-0.71}	4.05 ^{+0.22} _{-0.19}	1.07 ^{+0.80} _{-0.94}	I	0	1.66	209	130
AP662	6.60 ^{+0.70} _{-0.10}	2.73 ^{+0.03} _{-0.04}	0.80 ^{+0.00} _{-0.20}	7.17 ^{+0.04} _{-0.04}	3.61 ^{+0.06} _{-0.05}	0.49 ^{+0.08} _{-0.07}	I	0	1.89	247	341
AP663	8.80 ^{+0.00} _{-0.10}	3.79 ^{+0.03} _{-0.05}	0.30 ^{+0.30} _{-0.05}	9.01 ^{+0.10} _{-0.10}	3.45 ^{+0.09} _{-0.09}	0.07 ^{+0.10} _{-0.07}	I	0	1.65	226	169
AP664	8.50 ^{+0.00} _{-0.60}	3.35 ^{+0.00} _{-0.15}	0.80 ^{+0.30} _{-0.05}	7.35 ^{+0.53} _{-0.73}	3.35 ^{+0.27} _{-0.21}	1.57 ^{+0.67} _{-0.55}	I	0	2.18	285	222
AP665	10.10 ^{+0.10} _{-2.80}	4.86 ^{+0.56} _{-4.86}	0.05 ^{+2.10} _{-0.05}	8.79 ^{+0.30} _{-0.41}	3.59 ^{+0.11} _{-0.11}	0.94 ^{+0.62} _{-0.43}	I	0	1.57	119	40
AP666	8.00 ^{+0.00} _{-0.20}	3.96 ^{+0.03} _{-0.07}	2.00 ^{+0.10} _{-0.00}	9.27 ^{+0.20} _{-0.17}	4.00 ^{+0.09} _{-0.09}	0.29 ^{+0.19} _{-0.22}	I	0	1.63	191	63
AP668	8.40 ^{+1.10} _{-0.00}	3.79 ^{+0.80} _{-1.20}	2.70 ^{+0.15} _{-0.15}	8.71 ^{+1.06} _{-0.92}	3.71 ^{+0.31} _{-0.35}	1.67 ^{+0.92} _{-0.90}	I	0	1.63	131	67
AP669	9.00 ^{+0.00} _{-0.10}	3.53 ^{+0.06} _{-0.12}	0.30 ^{+0.30} _{-0.10}	8.00 ^{+1.14} _{-1.36}	3.39 ^{+0.29} _{-0.34}	1.44 ^{+0.98} _{-1.07}	I	0	1.50	144	69
AP671	8.00 ^{+0.10} _{-0.40}	3.59 ^{+0.06} _{-0.12}	2.15 ^{+0.25} _{-0.10}	6.69 ^{+0.05} _{-0.04}	2.43 ^{+0.17} _{-0.21}	1.97 ^{+0.09} _{-0.08}	I	0	1.42	147	78
AP673	8.20 ^{+0.00} _{-0.00}	3.12 ^{+0.03} _{-0.02}	1.00 ^{+0.10} _{-0.05}	7.89 ^{+0.74} _{-0.70}	3.19 ^{+0.35} _{-0.29}	1.41 ^{+1.20} _{-1.15}	I	0	1.61	175	138
AP674	7.80 ^{+0.10} _{-0.20}	3.34 ^{+0.03} _{-0.02}	1.40 ^{+0.10} _{-0.05}	7.88 ^{+0.06} _{-0.07}	3.10 ^{+0.10} _{-0.09}	0.97 ^{+0.16} _{-0.16}	I	0	1.45	141	93
AP675	7.90 ^{+0.10} _{-0.30}	2.84 ^{+0.02} _{-0.03}	0.50 ^{+0.10} _{-0.05}	8.18 ^{+0.06} _{-0.06}	2.68 ^{+0.10} _{-0.11}	0.08 ^{+0.10} _{-0.08}	I	0	1.50	64	35
AP676	8.20 ^{+0.00} _{-0.60}	3.40 ^{+0.01} _{-0.10}	0.90 ^{+0.20} _{-0.00}	8.84 ^{+0.05} _{-0.05}	3.36 ^{+0.06} _{-0.06}	0.04 ^{+0.09} _{-0.04}	I	0	1.45	183	136
AP677	8.00 ^{+0.00} _{-0.40}	3.58 ^{+0.00} _{-0.31}	2.10 ^{+0.15} _{-0.35}	9.08 ^{+0.18} _{-0.15}	3.67 ^{+0.11} _{-0.11}	0.26 ^{+0.18} _{-0.19}	I	0	1.93	252	157
AP679	9.00 ^{+0.00} _{-0.10}	3.76 ^{+0.06} _{-0.03}	0.10 ^{+0.25} _{-0.05}	8.75 ^{+0.14} _{-0.15}	3.09 ^{+0.09} _{-0.08}	0.21 ^{+0.20} _{-0.20}	I	0	1.45	142	78
AP680	9.20 ^{+0.40} _{-0.00}	4.70 ^{+0.24} _{-0.05}	0.80 ^{+0.00} _{-0.20}	9.43 ^{+0.35} _{-0.27}	4.55 ^{+0.12} _{-0.10}	0.85 ^{+0.27} _{-0.33}	I	0	2.24	403	295
AP681	6.70 ^{+0.50} _{-0.00}	2.83 ^{+0.03} _{-0.01}	0.90 ^{+0.00} _{-0.10}	7.63 ^{+0.25} _{-0.22}	2.80 ^{+0.12} _{-0.11}	0.30 ^{+0.24} _{-0.23}	I	0	1.57	168	151
AP682	8.90 ^{+0.00} _{-0.10}	4.07 ^{+0.00} _{-0.12}	0.70 ^{+0.25} _{-0.05}	8.40 ^{+1.36} _{-1.45}	3.28 ^{+0.85} _{-0.85}	1.51 ^{+1.01} _{-1.03}	I	0	2.15	395	143
AP683	9.20 ^{+0.10} _{-0.10}	3.75 ^{+0.10} _{-0.16}	0.20 ^{+0.20} _{-0.05}	8.73 ^{+0.30} _{-0.32}	3.28 ^{+0.14} _{-0.15}	0.67 ^{+0.43} _{-0.43}	I	0	1.80	176	98
AP690	7.90 ^{+0.10} _{-0.20}	3.24 ^{+0.02} _{-0.02}	0.90 ^{+0.10} _{-0.05}	7.00 ^{+0.67} _{-0.66}	3.17 ^{+0.26} _{-0.24}	1.69 ^{+0.44} _{-0.54}	I	0	2.27	292	267
AP691	8.90 ^{+0.10} _{-0.10}	3.13 ^{+0.06} _{-0.03}	0.10 ^{+0.30} _{-0.05}	8.91 ^{+0.56} _{-0.48}	3.31 ^{+0.19} _{-0.21}	0.84 ^{+0.58} _{-0.65}	I	0	1.42	63	26
AP693	7.00 ^{+0.00} _{-0.10}	3.18 ^{+0.00} _{-0.03}	1.00 ^{+0.05} _{-0.00}	7.13 ^{+0.14} _{-0.10}	4.25 ^{+0.11} _{-0.11}	0.73 ^{+0.12} _{-0.11}	I	0	3.09	551	560

Table 1 (cont'd)

AP ID ^a	CMD Best Fit Parameters ^b			Integrated Best Fit Parameters ^c			Best ^d Flag ^e	R _{ap} ^f	N _{stars} ^g	N _{bg} ^h	
	log(<i>t</i> [Myr])	log(<i>M</i> [<i>M</i> _⊙])	<i>A_V</i> [mag]	log(<i>t</i> [Myr])	log(<i>M</i> [<i>M</i> _⊙])	<i>A_V</i> [mag]					
AP694	7.80 ^{+0.00} _{-0.10}	4.12 ^{+0.00} _{-0.15}	2.45 ^{+0.05} _{-0.15}	9.19 ^{+0.49} _{-0.31}	4.51 ^{+0.13} _{-0.10}	0.76 ^{+0.36} _{-0.52}	I	0	2.12	313	152
AP696	6.90 ^{+0.00} _{-0.10}	3.36 ^{+0.01} _{-0.01}	1.35 ^{+0.05} _{-0.05}	6.82 ^{+0.14} _{-0.16}	3.05 ^{+0.33} _{-0.45}	1.06 ^{+0.12} _{-0.12}	I	0	2.40	310	300
AP697	9.00 ^{+0.00} _{-0.10}	3.59 ^{+0.03} _{-0.15}	0.30 ^{+0.25} _{-0.10}	8.11 ^{+0.23} _{-0.25}	2.79 ^{+0.22} _{-0.19}	0.51 ^{+0.49} _{-0.43}	I	0	1.56	154	114
AP699	8.00 ^{+0.30} _{-0.20}	3.43 ^{+0.06} _{-0.04}	1.20 ^{+0.05} _{-0.15}	8.32 ^{+0.12} _{-0.12}	3.07 ^{+0.12} _{-0.12}	0.35 ^{+0.29} _{-0.29}	I	0	1.62	189	140
AP700	8.30 ^{+0.10} _{-0.00}	3.37 ^{+0.01} _{-0.02}	1.35 ^{+0.00} _{-0.10}	8.73 ^{+0.14} _{-0.14}	2.91 ^{+0.11} _{-0.10}	0.21 ^{+0.19} _{-0.20}	I	0	1.37	89	28
AP701	7.40 ^{+0.00} _{-0.30}	3.07 ^{+0.00} _{-0.02}	0.90 ^{+0.10} _{-0.00}	8.40 ^{+0.07} _{-0.09}	3.71 ^{+0.06} _{-0.05}	0.11 ^{+0.17} _{-0.11}	I	0	2.09	318	306
AP702	9.10 ^{+0.00} _{-0.00}	3.84 ^{+0.00} _{-0.04}	0.10 ^{+0.05} _{-0.05}	9.09 ^{+0.07} _{-0.09}	3.47 ^{+0.09} _{-0.10}	0.02 ^{+0.07} _{-0.02}	I	0	1.61	173	59
AP708	9.10 ^{+0.00} _{-0.10}	4.26 ^{+0.05} _{-0.12}	0.20 ^{+0.15} _{-0.00}	7.76 ^{+0.03} _{-0.04}	2.15 ^{+0.20} _{-0.15}	0.15 ^{+0.10} _{-0.10}	I	0	2.34	390	203
AP709	8.20 ^{+0.00} _{-0.10}	3.27 ^{+0.00} _{-0.01}	0.55 ^{+0.05} _{-0.00}	8.47 ^{+0.07} _{-0.01}	3.05 ^{+0.09} _{-0.02}	0.03 ^{+0.07} _{-0.03}	I	0	1.69	137	71
AP710	8.40 ^{+0.00} _{-0.00}	3.18 ^{+0.01} _{-0.04}	0.65 ^{+0.00} _{-0.15}	8.32 ^{+0.11} _{-0.10}	3.03 ^{+0.12} _{-0.11}	0.58 ^{+0.24} _{-0.30}	I	0	1.48	104	67
AP711	8.00 ^{+0.00} _{-0.10}	3.33 ^{+0.00} _{-0.03}	0.60 ^{+0.00} _{-0.05}	6.72 ^{+0.06} _{-0.06}	3.00 ^{+0.20} _{-0.57}	1.37 ^{+0.09} _{-0.08}	I	0	2.33	335	251
AP712	8.30 ^{+0.00} _{-0.10}	3.47 ^{+0.00} _{-0.02}	0.35 ^{+0.05} _{-0.00}	8.31 ^{+0.10} _{-0.12}	3.67 ^{+0.09} _{-0.08}	0.34 ^{+0.24} _{-0.22}	I	0	1.59	225	185
AP713	8.80 ^{+0.00} _{-0.00}	3.24 ^{+0.02} _{-0.00}	0.05 ^{+0.15} _{-0.00}	8.39 ^{+0.12} _{-0.10}	3.11 ^{+0.16} _{-0.14}	0.81 ^{+0.31} _{-0.33}	I	0	1.37	73	26
AP714	8.40 ^{+0.00} _{-0.10}	3.42 ^{+0.00} _{-0.04}	0.70 ^{+0.10} _{-0.05}	8.81 ^{+0.08} _{-0.08}	3.28 ^{+0.07} _{-0.07}	0.08 ^{+0.10} _{-0.08}	I	0	1.31	145	109
AP715	8.70 ^{+0.10} _{-0.10}	3.45 ^{+0.00} _{-0.07}	0.70 ^{+0.10} _{-0.35}	8.85 ^{+0.43} _{-0.49}	3.22 ^{+0.24} _{-0.22}	0.31 ^{+0.50} _{-0.30}	I	0	1.57	155	108
AP716	8.90 ^{+0.10} _{-0.00}	3.45 ^{+0.06} _{-0.04}	0.45 ^{+0.05} _{-0.20}	8.92 ^{+0.52} _{-0.57}	3.38 ^{+0.17} _{-0.16}	0.75 ^{+0.66} _{-0.62}	I	0	1.35	93	44
AP717	7.50 ^{+0.00} _{-0.30}	3.30 ^{+0.00} _{-0.03}	1.30 ^{+0.10} _{-0.00}	7.77 ^{+0.12} _{-0.12}	3.23 ^{+0.08} _{-0.08}	0.91 ^{+0.16} _{-0.16}	I	0	1.61	167	108
AP721	8.70 ^{+0.00} _{-0.30}	3.30 ^{+0.01} _{-0.06}	0.05 ^{+0.35} _{-0.00}	8.42 ^{+0.13} _{-0.14}	3.16 ^{+0.12} _{-0.11}	0.31 ^{+0.31} _{-0.28}	I	0	1.45	166	112
AP722	7.80 ^{+0.00} _{-0.10}	3.82 ^{+0.00} _{-0.05}	2.20 ^{+0.10} _{-0.10}	8.69 ^{+0.15} _{-0.15}	3.51 ^{+0.08} _{-0.06}	0.64 ^{+0.22} _{-0.21}	I	0	1.31	154	80
AP723	6.60 ^{+0.40} _{-0.00}	3.13 ^{+0.05} _{-0.00}	1.45 ^{+0.05} _{-0.00}	7.15 ^{+0.15} _{-0.16}	3.60 ^{+0.08} _{-0.08}	1.25 ^{+0.12} _{-0.11}	I	0	1.93	203	142
AP725	7.80 ^{+0.00} _{-0.10}	4.14 ^{+0.02} _{-0.03}	2.70 ^{+0.15} _{-0.00}	9.47 ^{+0.14} _{-0.12}	3.95 ^{+0.08} _{-0.08}	0.13 ^{+0.15} _{-0.13}	I	0	1.64	240	157
AP726	9.00 ^{+0.00} _{-0.00}	3.56 ^{+0.03} _{-0.04}	0.15 ^{+0.05} _{-0.10}	7.85 ^{+0.03} _{-0.03}	2.35 ^{+0.04} _{-0.03}	0.40 ^{+0.07} _{-0.07}	I	0	1.67	159	85
AP727	7.60 ^{+0.20} _{-0.50}	3.14 ^{+0.01} _{-0.11}	1.20 ^{+0.10} _{-0.10}	8.37 ^{+0.07} _{-0.08}	2.92 ^{+0.12} _{-0.12}	0.26 ^{+0.20} _{-0.20}	I	0	1.28	99	63
AP728	9.00 ^{+0.10} _{-0.10}	3.49 ^{+0.17} _{-0.00}	0.00 ^{+0.35} _{-0.00}	8.96 ^{+0.10} _{-0.05}	3.36 ^{+0.08} _{-0.08}	0.05 ^{+0.03} _{-0.05}	I	0	1.57	176	116
AP729	9.00 ^{+0.00} _{-0.10}	3.75 ^{+0.02} _{-0.06}	0.35 ^{+0.25} _{-0.05}	9.01 ^{+0.10} _{-0.08}	3.77 ^{+0.09} _{-0.08}	0.00 ^{+0.07} _{-0.00}	I	0	1.73	147	115
AP732	9.50 ^{+0.10} _{-0.10}	4.68 ^{+0.10} _{-0.17}	0.00 ^{+0.20} _{-0.00}	8.35 ^{+0.16} _{-0.18}	4.15 ^{+0.08} _{-0.08}	1.63 ^{+0.28} _{-0.28}	I	0	1.71	284	171
AP733	8.90 ^{+0.00} _{-0.10}	3.49 ^{+0.08} _{-0.06}	0.25 ^{+0.40} _{-0.05}	8.96 ^{+0.35} _{-0.78}	3.35 ^{+0.16} _{-0.19}	0.34 ^{+1.01} _{-0.34}	I	0	1.72	194	130
AP734	9.80 ^{+0.00} _{-0.30}	5.08 ^{+0.00} _{-0.34}	0.20 ^{+0.05} _{-0.10}	8.95 ^{+0.48} _{-0.66}	4.39 ^{+0.10} _{-0.10}	1.09 ^{+0.80} _{-0.56}	I	0	1.81	287	218
AP735	8.50 ^{+0.00} _{-0.80}	3.75 ^{+0.00} _{-0.13}	1.05 ^{+0.95} _{-0.00}	8.50 ^{+0.09} _{-0.09}	3.29 ^{+0.10} _{-0.11}	0.53 ^{+0.23} _{-0.23}	I	0	1.31	143	112
AP737	8.40 ^{+0.00} _{-0.00}	3.44 ^{+0.00} _{-0.02}	1.30 ^{+0.05} _{-0.05}	10.01 ^{+0.08} _{-0.09}	3.92 ^{+0.07} _{-0.07}	0.01 ^{+0.07} _{-0.01}	I	0	1.45	102	52
AP738	8.90 ^{+0.00} _{-0.10}	3.83 ^{+0.03} _{-0.06}	0.05 ^{+0.25} _{-0.00}	8.70 ^{+0.27} _{-0.28}	3.66 ^{+0.10} _{-0.10}	0.57 ^{+0.37} _{-0.38}	I	0	1.64	230	131
AP741	7.60 ^{+0.00} _{-0.20}	3.84 ^{+0.06} _{-0.06}	2.65 ^{+0.15} _{-0.00}	8.11 ^{+1.47} _{-1.46}	3.78 ^{+1.25} _{-1.18}	1.45 ^{+1.02} _{-1.02}	I	1	1.44	157	58
AP742	7.60 ^{+0.00} _{-0.20}	3.18 ^{+0.02} _{-0.04}	1.00 ^{+0.10} _{-0.10}	8.10 ^{+0.03} _{-0.04}	3.85 ^{+0.03} _{-0.03}	0.50 ^{+0.07} _{-0.07}	I	0	1.63	199	184

Table 1 (cont'd)

AP ID ^a	CMD Best Fit Parameters ^b			Integrated Best Fit Parameters ^c			Best ^d Flag ^e	R _{ap} ^f	N _{stars} ^g	N _{bg} ^h	
	log(<i>t</i> [Myr])	log(<i>M</i> [<i>M</i> _⊙])	<i>A_V</i> [mag]	log(<i>t</i> [Myr])	log(<i>M</i> [<i>M</i> _⊙])	<i>A_V</i> [mag]					
AP747	8.80 ^{+0.00} _{-0.00}	3.73 ^{+0.03} _{-0.01}	0.20 ^{+0.10} _{-0.04}	8.96 ^{+0.08} _{-0.09}	3.32 ^{+0.07} _{-0.09}	0.01 ^{+0.07} _{-0.01}	I	0	1.51	154	112
AP748	7.50 ^{+0.00} _{-0.20}	3.50 ^{+0.01} _{-0.03}	0.80 ^{+0.05} _{-0.00}	6.65 ^{+0.92} _{-0.58}	3.44 ^{+0.46} _{-0.37}	0.97 ^{+0.18} _{-0.19}	I	0	2.06	322	231
AP749	9.00 ^{+0.00} _{-0.00}	3.58 ^{+0.02} _{-0.03}	0.15 ^{+0.10} _{-0.05}	8.65 ^{+0.30} _{-0.38}	3.14 ^{+0.18} _{-0.15}	0.32 ^{+0.56} _{-0.32}	I	0	1.66	109	42
AP750	8.10 ^{+0.00} _{-0.40}	2.83 ^{+0.02} _{-0.04}	0.30 ^{+0.18} _{-0.00}	6.79 ^{+0.95} _{-0.65}	3.10 ^{+0.35} _{-0.33}	1.59 ^{+0.30} _{-0.56}	I	0	1.46	129	101
AP751	8.40 ^{+0.00} _{-0.00}	3.55 ^{+0.02} _{-0.04}	1.00 ^{+0.05} _{-0.05}	8.26 ^{+0.62} _{-0.56}	2.85 ^{+0.82} _{-0.65}	0.43 ^{+0.28} _{-0.42}	I	0	1.68	229	137
AP752	8.00 ^{+0.10} _{-0.60}	2.79 ^{+0.01} _{-0.08}	0.50 ^{+0.10} _{-0.10}	9.35 ^{+0.03} _{-0.04}	3.55 ^{+0.03} _{-0.04}	0.00 ^{+0.07} _{-0.00}	I	0	1.55	54	28
AP756	7.90 ^{+0.00} _{-0.10}	3.57 ^{+0.01} _{-0.16}	2.30 ^{+0.10} _{-0.20}	9.13 ^{+0.05} _{-0.05}	4.99 ^{+0.06} _{-0.06}	0.17 ^{+0.14} _{-0.13}	I	1	2.37	233	414
AP757	7.60 ^{+0.00} _{-0.00}	4.21 ^{+0.02} _{-0.00}	2.85 ^{+0.05} _{-0.00}	0.00 ^{+0.00} _{-0.00}	0.00 ^{+0.00} _{-0.00}	0.00 ^{+0.00} _{-0.00}	I	0	2.88	327	429
AP758	8.20 ^{+0.10} _{-0.00}	3.18 ^{+0.01} _{-0.07}	0.60 ^{+0.05} _{-0.10}	8.82 ^{+0.26} _{-0.11}	3.37 ^{+0.26} _{-0.11}	0.02 ^{+0.07} _{-0.02}	I	0	1.56	181	136
AP759	8.90 ^{+0.00} _{-0.10}	3.29 ^{+0.01} _{-0.10}	0.10 ^{+0.30} _{-0.05}	9.15 ^{+0.09} _{-0.10}	3.27 ^{+0.12} _{-0.11}	0.11 ^{+0.09} _{-0.10}	I	0	1.38	104	68
AP761	8.40 ^{+0.30} _{-0.10}	3.67 ^{+0.09} _{-0.04}	1.40 ^{+0.15} _{-0.55}	8.54 ^{+0.20} _{-0.08}	3.18 ^{+0.20} _{-0.01}	0.50 ^{+0.17} _{-0.17}	I	0	1.80	242	166
AP764	7.80 ^{+0.10} _{-0.00}	3.33 ^{+0.01} _{-0.01}	0.95 ^{+0.00} _{-0.05}	7.57 ^{+0.98} _{-1.05}	3.35 ^{+0.30} _{-0.33}	0.95 ^{+0.66} _{-0.62}	I	0	1.59	199	109
AP767	7.20 ^{+0.00} _{-0.10}	3.19 ^{+0.01} _{-0.02}	1.60 ^{+0.05} _{-0.00}	7.02 ^{+0.43} _{-0.30}	2.96 ^{+0.71} _{-0.68}	1.45 ^{+0.18} _{-0.23}	I	0	2.76	368	338
AP768	8.50 ^{+0.00} _{-0.50}	2.95 ^{+0.00} _{-0.08}	0.35 ^{+0.35} _{-0.00}	8.41 ^{+0.07} _{-0.06}	2.40 ^{+0.14} _{-0.15}	0.03 ^{+0.07} _{-0.03}	I	0	1.45	111	75
AP771	7.40 ^{+0.00} _{-0.60}	3.27 ^{+0.00} _{-0.13}	1.95 ^{+0.05} _{-0.05}	6.50 ^{+0.91} _{-0.36}	3.18 ^{+0.52} _{-0.42}	1.84 ^{+0.18} _{-0.14}	I	0	1.58	137	112
AP773	8.30 ^{+0.10} _{-0.00}	3.28 ^{+0.02} _{-0.03}	0.60 ^{+0.05} _{-0.10}	8.63 ^{+0.06} _{-0.06}	3.16 ^{+0.07} _{-0.07}	0.04 ^{+0.08} _{-0.04}	I	0	1.81	269	238
AP774	7.40 ^{+0.10} _{-0.50}	3.18 ^{+0.00} _{-0.05}	0.90 ^{+0.05} _{-0.05}	7.79 ^{+0.29} _{-0.32}	3.24 ^{+0.18} _{-0.18}	0.57 ^{+0.49} _{-0.48}	I	0	1.96	237	160
AP776	7.70 ^{+0.00} _{-0.00}	3.50 ^{+0.01} _{-0.03}	1.80 ^{+0.05} _{-0.05}	7.80 ^{+0.14} _{-0.16}	3.65 ^{+0.14} _{-0.13}	1.51 ^{+0.26} _{-0.23}	I	0	1.60	195	162
AP777	9.10 ^{+0.00} _{-0.20}	3.43 ^{+0.02} _{-0.04}	0.20 ^{+0.39} _{-0.10}	8.03 ^{+1.16} _{-1.35}	3.37 ^{+0.28} _{-0.32}	1.48 ^{+0.99} _{-1.10}	I	0	1.57	130	54
AP778	8.20 ^{+0.10} _{-0.00}	3.51 ^{+0.04} _{-0.03}	1.65 ^{+0.05} _{-0.10}	7.83 ^{+0.05} _{-0.05}	2.20 ^{+0.10} _{-0.08}	0.58 ^{+0.27} _{-0.14}	I	0	1.42	162	110
AP779	9.10 ^{+0.00} _{-0.00}	3.74 ^{+0.04} _{-0.04}	0.30 ^{+0.10} _{-0.05}	8.92 ^{+0.36} _{-0.82}	3.41 ^{+0.17} _{-0.18}	0.45 ^{+1.23} _{-0.45}	I	0	1.48	109	26
AP780	8.00 ^{+0.00} _{-0.00}	3.58 ^{+0.02} _{-0.02}	0.50 ^{+0.05} _{-0.05}	8.00 ^{+0.25} _{-0.21}	3.52 ^{+0.12} _{-0.11}	0.43 ^{+0.36} _{-0.39}	I	0	2.14	200	76
AP781	8.10 ^{+0.10} _{-0.00}	2.98 ^{+0.01} _{-0.02}	0.55 ^{+0.00} _{-0.10}	7.90 ^{+0.15} _{-0.23}	3.03 ^{+0.29} _{-0.19}	0.49 ^{+0.62} _{-0.35}	I	0	1.53	80	34
AP782	7.90 ^{+0.10} _{-0.00}	3.95 ^{+0.02} _{-0.04}	2.45 ^{+0.05} _{-0.05}	7.75 ^{+0.15} _{-0.15}	3.86 ^{+0.12} _{-0.11}	2.19 ^{+0.27} _{-0.26}	I	1	1.84	251	172
AP783	8.10 ^{+0.00} _{-0.00}	3.74 ^{+0.03} _{-0.03}	1.50 ^{+0.05} _{-0.00}	8.54 ^{+0.16} _{-0.15}	3.48 ^{+0.10} _{-0.08}	0.47 ^{+0.26} _{-0.28}	I	0	1.57	167	104
AP784	9.10 ^{+0.00} _{-0.00}	3.67 ^{+0.10} _{-0.05}	0.15 ^{+0.25} _{-0.05}	8.82 ^{+0.38} _{-0.51}	3.30 ^{+0.17} _{-0.17}	0.49 ^{+0.66} _{-0.45}	I	0	1.30	120	72
AP785	7.70 ^{+0.00} _{-0.40}	3.01 ^{+0.01} _{-0.03}	0.90 ^{+0.10} _{-0.00}	7.97 ^{+0.07} _{-0.07}	2.39 ^{+0.13} _{-0.13}	0.16 ^{+0.11} _{-0.11}	I	0	1.36	63	28
AP787	8.80 ^{+0.00} _{-0.60}	3.52 ^{+0.03} _{-0.23}	0.45 ^{+1.00} _{-0.00}	8.24 ^{+0.06} _{-0.08}	3.42 ^{+0.11} _{-0.10}	1.33 ^{+0.21} _{-0.18}	I	0	1.53	159	104
AP788	9.10 ^{+0.00} _{-1.10}	3.44 ^{+0.05} _{-0.43}	0.30 ^{+1.80} _{-0.00}	7.80 ^{+0.10} _{-0.10}	3.01 ^{+0.23} _{-0.25}	1.32 ^{+0.37} _{-0.39}	I	0	1.63	86	31
AP789	8.10 ^{+0.10} _{-0.50}	2.97 ^{+0.00} _{-0.07}	0.65 ^{+0.10} _{-0.05}	8.16 ^{+0.05} _{-0.05}	2.12 ^{+0.10} _{-0.09}	0.00 ^{+0.07} _{-0.00}	I	0	1.67	82	48
AP790	9.10 ^{+0.10} _{-0.00}	3.62 ^{+0.23} _{-0.04}	0.25 ^{+0.10} _{-0.10}	8.76 ^{+0.23} _{-0.26}	3.06 ^{+0.12} _{-0.11}	0.72 ^{+0.37} _{-0.39}	I	0	1.30	79	30
AP791	8.40 ^{+0.00} _{-0.10}	3.37 ^{+0.01} _{-0.10}	1.65 ^{+0.15} _{-0.05}	8.71 ^{+0.15} _{-0.17}	3.07 ^{+0.09} _{-0.09}	0.69 ^{+0.27} _{-0.26}	I	0	1.23	83	35
AP792	8.50 ^{+0.00} _{-0.00}	3.47 ^{+0.03} _{-0.00}	0.50 ^{+0.10} _{-0.00}	8.60 ^{+0.19} _{-0.01}	3.03 ^{+0.18} _{-0.00}	0.10 ^{+0.08} _{-0.10}	I	0	1.19	127	78

Table 1 (cont'd)

AP ID ^a	CMD Best Fit Parameters ^b			Integrated Best Fit Parameters ^c			Best ^d Flag ^e	R _{ap} ^f	N _{stars} ^g	N _{bg} ^h	
	log(<i>t</i> [Myr])	log(<i>M</i> [<i>M</i> _⊙])	<i>A_V</i> [mag]	log(<i>t</i> [Myr])	log(<i>M</i> [<i>M</i> _⊙])	<i>A_V</i> [mag]					
AP793	8.20 ^{+0.10} _{-0.30}	3.16 ^{+0.02} _{-0.06}	0.85 ^{+0.20} _{-0.10}	9.07 ^{+0.06} _{-0.09}	3.31 ^{+0.07} _{-0.09}	0.00 ^{+0.07} _{-0.00}	I	0	1.20	95	56
AP794	8.40 ^{+0.10} _{-0.30}	3.41 ^{+0.02} _{-0.08}	0.65 ^{+0.15} _{-0.10}	8.17 ^{+0.49} _{-0.34}	2.46 ^{+0.61} _{-0.45}	0.11 ^{+0.08} _{-0.09}	I	0	1.46	190	151
AP795	7.40 ^{+0.00} _{-0.40}	2.98 ^{+0.01} _{-0.03}	0.55 ^{+0.10} _{-0.05}	7.10 ^{+0.54} _{-0.60}	2.97 ^{+0.20} _{-0.21}	0.41 ^{+0.24} _{-0.25}	I	0	1.64	143	114
AP796	7.70 ^{+0.20} _{-0.00}	3.77 ^{+0.03} _{-0.05}	2.90 ^{+0.05} _{-0.15}	9.06 ^{+0.07} _{-0.08}	4.27 ^{+0.08} _{-0.08}	0.00 ^{+0.07} _{-0.00}	I	0	1.66	77	173
AP798	8.90 ^{+0.00} _{-0.10}	3.31 ^{+0.02} _{-0.02}	0.00 ^{+0.30} _{-0.00}	8.98 ^{+0.23} _{-0.19}	3.30 ^{+0.10} _{-0.10}	0.46 ^{+0.25} _{-0.30}	I	0	1.24	107	64
AP799	8.20 ^{+0.00} _{-1.00}	3.45 ^{+0.04} _{-0.19}	0.95 ^{+0.30} _{-0.05}	8.70 ^{+0.06} _{-0.06}	3.41 ^{+0.06} _{-0.06}	0.07 ^{+0.11} _{-0.07}	I	0	1.35	173	129
AP800	9.20 ^{+0.00} _{-0.10}	3.52 ^{+0.05} _{-0.23}	0.10 ^{+0.10} _{-0.10}	8.19 ^{+0.15} _{-0.17}	3.41 ^{+0.14} _{-0.12}	1.66 ^{+0.35} _{-0.30}	I	0	1.43	79	29
AP801	9.40 ^{+0.10} _{-0.10}	4.43 ^{+0.06} _{-0.10}	0.25 ^{+0.05} _{-0.05}	9.44 ^{+0.22} _{-0.18}	3.95 ^{+0.13} _{-0.13}	0.26 ^{+0.20} _{-0.21}	I	0	1.56	192	113
AP802	7.70 ^{+0.60} _{-0.28}	3.17 ^{+0.11} _{-0.04}	1.00 ^{+0.05} _{-0.15}	8.74 ^{+0.45} _{-0.49}	3.48 ^{+0.15} _{-0.13}	0.63 ^{+0.66} _{-0.53}	I	0	1.41	144	98
AP805	8.20 ^{+1.10} _{-0.00}	3.30 ^{+0.60} _{-0.03}	1.75 ^{+0.05} _{-1.70}	9.14 ^{+0.54} _{-0.70}	3.64 ^{+0.18} _{-0.16}	0.61 ^{+0.71} _{-0.54}	I	0	1.41	104	66
AP806	8.80 ^{+0.00} _{-0.00}	3.49 ^{+0.03} _{-0.03}	0.15 ^{+0.10} _{-0.05}	8.57 ^{+0.12} _{-0.09}	2.84 ^{+0.12} _{-0.10}	0.20 ^{+0.19} _{-0.18}	I	0	1.41	117	64
AP808	6.80 ^{+0.30} _{-0.10}	2.55 ^{+0.01} _{-0.02}	0.45 ^{+0.05} _{-0.10}	6.85 ^{+0.12} _{-0.10}	2.57 ^{+0.29} _{-0.29}	0.45 ^{+0.10} _{-0.10}	I	0	1.37	133	113
AP809	8.10 ^{+0.00} _{-0.00}	3.57 ^{+0.00} _{-0.00}	0.95 ^{+0.00} _{-0.00}	8.42 ^{+0.16} _{-0.14}	3.49 ^{+0.10} _{-0.10}	0.41 ^{+0.27} _{-0.30}	I	0	2.71	423	334
AP811	8.70 ^{+0.00} _{-0.80}	2.79 ^{+0.06} _{-0.26}	0.05 ^{+0.45} _{-0.00}	7.71 ^{+0.43} _{-0.39}	3.00 ^{+0.14} _{-0.16}	1.43 ^{+0.52} _{-0.51}	I	0	1.48	102	86
AP812	8.20 ^{+0.10} _{-0.00}	3.17 ^{+0.02} _{-0.02}	0.80 ^{+0.05} _{-0.10}	8.66 ^{+0.07} _{-0.07}	2.98 ^{+0.07} _{-0.07}	0.06 ^{+0.10} _{-0.06}	I	0	1.40	125	99
AP813	9.10 ^{+0.10} _{-0.00}	3.85 ^{+0.15} _{-0.08}	0.35 ^{+0.05} _{-0.15}	8.73 ^{+0.16} _{-0.22}	3.64 ^{+0.10} _{-0.08}	1.06 ^{+0.30} _{-0.24}	I	0	1.64	155	92
AP814	9.10 ^{+0.00} _{-0.00}	3.82 ^{+0.03} _{-0.09}	0.25 ^{+0.00} _{-0.15}	9.02 ^{+0.17} _{-0.08}	3.54 ^{+0.12} _{-0.12}	0.22 ^{+0.07} _{-0.21}	I	0	1.61	207	107
AP818	6.60 ^{+0.10} _{-0.00}	3.09 ^{+0.01} _{-0.02}	0.60 ^{+0.00} _{-0.05}	6.90 ^{+0.16} _{-0.13}	3.07 ^{+0.24} _{-0.25}	0.14 ^{+0.12} _{-0.12}	I	0	3.49	567	432
AP819	7.80 ^{+0.10} _{-0.00}	3.33 ^{+0.02} _{-0.02}	1.10 ^{+0.05} _{-0.05}	8.08 ^{+0.10} _{-0.10}	3.25 ^{+0.07} _{-0.07}	0.58 ^{+0.16} _{-0.16}	I	0	1.52	179	141
AP820	8.90 ^{+0.00} _{-0.10}	3.64 ^{+0.02} _{-0.03}	0.20 ^{+0.30} _{-0.00}	7.73 ^{+0.39} _{-0.40}	2.64 ^{+0.12} _{-0.13}	0.15 ^{+0.18} _{-0.15}	I	0	1.58	199	134
AP821	8.50 ^{+0.10} _{-0.00}	3.57 ^{+0.02} _{-0.02}	0.35 ^{+0.05} _{-0.10}	8.44 ^{+0.09} _{-0.08}	3.20 ^{+0.09} _{-0.09}	0.15 ^{+0.19} _{-0.15}	I	0	1.76	279	218
AP822	9.10 ^{+0.00} _{-0.10}	3.61 ^{+0.01} _{-0.07}	0.05 ^{+0.05} _{-0.05}	8.33 ^{+0.18} _{-0.17}	3.29 ^{+0.16} _{-0.18}	0.88 ^{+0.39} _{-0.43}	I	0	1.62	172	100
AP827	9.00 ^{+0.00} _{-0.10}	3.34 ^{+0.06} _{-0.08}	0.00 ^{+0.25} _{-0.05}	8.07 ^{+0.25} _{-0.24}	2.88 ^{+0.16} _{-0.16}	0.89 ^{+0.42} _{-0.47}	I	0	1.30	78	38
AP828	7.90 ^{+0.00} _{-0.00}	3.38 ^{+0.02} _{-0.03}	1.25 ^{+0.05} _{-0.05}	7.73 ^{+0.41} _{-0.29}	3.59 ^{+0.30} _{-0.16}	1.61 ^{+0.53} _{-0.45}	I	0	1.66	159	119
AP830	8.40 ^{+0.00} _{-0.20}	3.09 ^{+0.00} _{-0.06}	0.35 ^{+0.05} _{-0.00}	9.11 ^{+0.07} _{-0.08}	3.50 ^{+0.08} _{-0.09}	0.02 ^{+0.07} _{-0.02}	I	0	1.68	189	156
AP831	7.30 ^{+0.40} _{-0.40}	2.81 ^{+0.03} _{-0.02}	1.05 ^{+0.10} _{-0.10}	7.87 ^{+0.05} _{-0.05}	2.79 ^{+0.08} _{-0.07}	0.48 ^{+0.11} _{-0.11}	I	0	1.89	78	46
AP833	7.90 ^{+0.10} _{-0.60}	3.06 ^{+0.00} _{-0.11}	1.15 ^{+0.15} _{-0.10}	6.93 ^{+0.12} _{-0.11}	2.36 ^{+0.20} _{-0.24}	0.60 ^{+0.11} _{-0.11}	I	0	1.52	143	123
AP834	7.70 ^{+0.10} _{-0.00}	3.98 ^{+0.07} _{-0.02}	2.75 ^{+0.05} _{-0.05}	7.88 ^{+0.10} _{-0.10}	4.29 ^{+0.07} _{-0.07}	1.66 ^{+0.18} _{-0.17}	I	0	1.67	123	182
AP835	9.00 ^{+0.10} _{-0.30}	3.67 ^{+0.05} _{-0.27}	0.25 ^{+0.75} _{-0.10}	9.01 ^{+0.51} _{-0.78}	3.83 ^{+0.15} _{-0.15}	0.70 ^{+0.97} _{-0.60}	I	0	1.81	251	178
AP837	9.30 ^{+0.00} _{-2.30}	4.77 ^{+0.01} _{-0.82}	0.00 ^{+3.00} _{-0.00}	9.96 ^{+0.06} _{-0.05}	5.42 ^{+0.04} _{-0.04}	0.03 ^{+0.07} _{-0.03}	I	0	1.84	279	358
AP839	8.50 ^{+0.00} _{-0.10}	3.56 ^{+0.04} _{-0.00}	0.80 ^{+0.20} _{-0.00}	8.70 ^{+0.09} _{-0.10}	3.20 ^{+0.09} _{-0.09}	0.19 ^{+0.19} _{-0.18}	I	0	1.53	130	69
AP840	8.80 ^{+0.00} _{-0.30}	3.33 ^{+0.04} _{-0.04}	0.00 ^{+0.70} _{-0.05}	7.85 ^{+0.03} _{-0.03}	2.18 ^{+0.05} _{-0.06}	0.20 ^{+0.07} _{-0.07}	I	0	1.79	199	173
AP841	8.30 ^{+0.00} _{-0.00}	3.54 ^{+0.03} _{-0.01}	1.00 ^{+0.05} _{-0.05}	8.71 ^{+0.05} _{-0.05}	3.14 ^{+0.07} _{-0.07}	0.02 ^{+0.07} _{-0.02}	I	0	1.42	149	105

Table 1 (cont'd)

AP ID ^a	CMD Best Fit Parameters ^b			Integrated Best Fit Parameters ^c			Best ^d Flag ^e	R _{ap} ^f	N _{stars} ^g	N _{bg} ^h	
	log(<i>t</i> [Myr])	log(<i>M</i> [<i>M</i> _⊙])	<i>A_V</i> [mag]	log(<i>t</i> [Myr])	log(<i>M</i> [<i>M</i> _⊙])	<i>A_V</i> [mag]					
AP842	8.60 ^{+0.00} _{-0.20}	3.27 ^{+0.03} _{-0.07}	0.40 ^{+0.35} _{-0.00}	8.68 ^{+0.22} _{-0.22}	3.36 ^{+0.12} _{-0.11}	0.53 ^{+0.30} _{-0.31}	I	0	1.64	196	158
AP843	8.30 ^{+0.00} _{-0.10}	3.60 ^{+0.03} _{-0.02}	0.80 ^{+0.10} _{-0.00}	8.80 ^{+0.06} _{-0.06}	3.56 ^{+0.06} _{-0.05}	0.02 ^{+0.07} _{-0.02}	I	0	1.77	260	203
AP844	7.10 ^{+0.50} _{-0.30}	2.54 ^{+0.16} _{-0.02}	0.85 ^{+0.60} _{-0.05}	7.51 ^{+0.13} _{-0.09}	3.56 ^{+0.08} _{-0.09}	0.78 ^{+0.15} _{-0.16}	I	0	1.50	163	156
AP845	9.10 ^{+0.00} _{-0.00}	4.14 ^{+0.04} _{-0.05}	0.75 ^{+0.15} _{-0.05}	9.36 ^{+0.68} _{-0.68}	4.01 ^{+0.19} _{-0.16}	1.16 ^{+0.81} _{-0.64}	I	0	1.66	150	64
AP846	6.80 ^{+0.00} _{-0.10}	3.12 ^{+0.01} _{-0.03}	0.80 ^{+0.05} _{-0.05}	6.70 ^{+0.14} _{-0.14}	3.15 ^{+0.43} _{-0.74}	0.55 ^{+0.13} _{-0.12}	I	0	1.84	244	205
AP848	9.10 ^{+0.00} _{-0.00}	3.69 ^{+0.06} _{-0.00}	0.25 ^{+0.10} _{-0.00}	8.37 ^{+0.20} _{-0.25}	2.90 ^{+0.37} _{-0.44}	0.73 ^{+0.59} _{-0.64}	I	0	1.59	117	43
AP849	9.10 ^{+0.00} _{-0.00}	3.60 ^{+0.03} _{-0.03}	0.20 ^{+0.00} _{-0.15}	8.77 ^{+0.13} _{-0.12}	3.09 ^{+0.11} _{-0.08}	0.48 ^{+0.24} _{-0.25}	I	0	1.59	123	52
AP850	8.20 ^{+0.00} _{-0.50}	3.34 ^{+0.01} _{-0.14}	1.25 ^{+0.25} _{-0.00}	8.55 ^{+0.20} _{-0.24}	3.16 ^{+0.14} _{-0.15}	0.33 ^{+0.45} _{-0.33}	I	0	1.59	178	138
AP855	7.40 ^{+0.00} _{-0.30}	3.13 ^{+0.01} _{-0.03}	0.55 ^{+0.10} _{-0.05}	6.87 ^{+0.32} _{-0.36}	3.20 ^{+0.17} _{-0.15}	0.61 ^{+0.15} _{-0.15}	I	0	3.00	638	594
AP857	7.10 ^{+0.50} _{-0.30}	2.82 ^{+0.05} _{-0.03}	0.95 ^{+0.10} _{-0.10}	8.10 ^{+0.12} _{-0.12}	3.28 ^{+0.13} _{-0.12}	0.45 ^{+0.26} _{-0.24}	I	0	1.40	79	49
AP859	9.60 ^{+0.00} _{-0.00}	4.72 ^{+0.01} _{-0.01}	0.00 ^{+0.00} _{-0.00}	9.59 ^{+0.08} _{-0.07}	5.18 ^{+0.05} _{-0.05}	0.06 ^{+0.09} _{-0.06}	I	0	2.14	173	219
AP864	9.10 ^{+0.00} _{-0.00}	3.85 ^{+0.10} _{-0.02}	0.05 ^{+0.15} _{-0.00}	9.85 ^{+0.17} _{-0.16}	4.08 ^{+0.11} _{-0.11}	0.10 ^{+0.13} _{-0.10}	I	0	1.87	279	225
AP867	7.30 ^{+0.10} _{-0.30}	3.39 ^{+0.02} _{-0.03}	1.50 ^{+0.10} _{-0.00}	6.76 ^{+0.24} _{-0.25}	3.42 ^{+0.20} _{-0.20}	1.87 ^{+0.14} _{-0.15}	I	0	1.95	177	82
AP869	8.10 ^{+0.00} _{-0.10}	3.73 ^{+0.02} _{-0.01}	0.35 ^{+0.05} _{-0.00}	8.00 ^{+0.15} _{-0.15}	3.78 ^{+0.08} _{-0.08}	0.42 ^{+0.26} _{-0.25}	I	0	2.07	316	194
AP870	7.60 ^{+0.40} _{-0.20}	3.15 ^{+0.04} _{-0.03}	1.00 ^{+0.05} _{-0.20}	7.72 ^{+0.20} _{-0.22}	3.28 ^{+0.09} _{-0.08}	1.34 ^{+0.24} _{-0.23}	I	0	1.49	148	112
AP872	9.10 ^{+0.70} _{-0.00}	3.73 ^{+0.40} _{-0.07}	0.60 ^{+0.05} _{-0.40}	9.65 ^{+0.38} _{-0.41}	3.78 ^{+0.18} _{-0.17}	0.48 ^{+0.32} _{-0.31}	I	0	1.51	104	54
AP873	8.20 ^{+0.10} _{-0.40}	3.15 ^{+0.01} _{-0.06}	0.60 ^{+0.15} _{-0.05}	8.28 ^{+0.19} _{-0.17}	2.97 ^{+0.11} _{-0.10}	0.46 ^{+0.33} _{-0.39}	I	0	1.55	107	72
AP875	8.80 ^{+0.10} _{-0.00}	3.63 ^{+0.10} _{-0.10}	0.30 ^{+0.20} _{-0.15}	8.70 ^{+0.06} _{-0.06}	3.21 ^{+0.07} _{-0.08}	0.06 ^{+0.10} _{-0.06}	I	0	1.46	152	98
AP879	7.70 ^{+0.00} _{-0.40}	3.30 ^{+0.02} _{-0.05}	0.80 ^{+0.15} _{-0.00}	7.67 ^{+0.16} _{-0.14}	3.48 ^{+0.08} _{-0.09}	0.53 ^{+0.18} _{-0.18}	I	0	1.61	166	138
AP880	8.30 ^{+0.00} _{-0.20}	3.32 ^{+0.00} _{-0.08}	0.70 ^{+0.10} _{-0.05}	7.79 ^{+0.21} _{-0.20}	3.37 ^{+0.11} _{-0.11}	1.37 ^{+0.29} _{-0.30}	I	0	1.58	186	144
AP881	9.30 ^{+0.00} _{-0.00}	4.58 ^{+0.00} _{-0.00}	0.00 ^{+0.00} _{-0.00}	0.00 ^{+0.00} _{-0.00}	0.00 ^{+0.00} _{-0.00}	0.00 ^{+0.00} _{-0.00}	I	0	3.80	670	880
AP882	7.40 ^{+0.00} _{-0.10}	4.17 ^{+0.00} _{-0.08}	2.85 ^{+0.00} _{-0.05}	8.20 ^{+0.57} _{-1.06}	3.36 ^{+0.09} _{-0.05}	0.66 ^{+1.30} _{-0.66}	I	1	1.70	306	235
AP884	7.40 ^{+0.00} _{-0.50}	2.71 ^{+0.01} _{-0.06}	0.95 ^{+0.10} _{-0.00}	7.04 ^{+0.11} _{-0.13}	2.57 ^{+0.20} _{-0.19}	0.56 ^{+0.11} _{-0.11}	I	0	1.13	81	71
AP887	8.10 ^{+0.10} _{-0.80}	2.85 ^{+0.08} _{-0.08}	0.90 ^{+0.45} _{-0.00}	8.51 ^{+0.62} _{-0.49}	3.29 ^{+0.24} _{-0.23}	0.76 ^{+0.77} _{-0.70}	I	0	1.48	151	108
AP889	9.10 ^{+0.00} _{-0.00}	3.59 ^{+0.11} _{-0.00}	0.20 ^{+0.20} _{-0.00}	8.02 ^{+1.06} _{-1.18}	3.18 ^{+0.26} _{-0.23}	1.47 ^{+0.94} _{-1.04}	I	0	1.49	110	69
AP890	8.30 ^{+0.30} _{-0.00}	3.16 ^{+0.08} _{-0.02}	0.55 ^{+0.15} _{-0.25}	8.78 ^{+0.08} _{-0.07}	3.29 ^{+0.08} _{-0.08}	0.05 ^{+0.09} _{-0.05}	I	0	1.84	270	246
AP893	9.00 ^{+0.00} _{-0.00}	3.61 ^{+0.05} _{-0.04}	0.20 ^{+0.15} _{-0.00}	8.78 ^{+0.44} _{-0.47}	3.26 ^{+0.24} _{-0.22}	0.48 ^{+0.54} _{-0.44}	I	0	1.31	107	56
AP896	8.90 ^{+0.10} _{-0.00}	3.77 ^{+0.04} _{-0.12}	0.30 ^{+0.10} _{-0.25}	10.06 ^{+0.12} _{-0.10}	4.15 ^{+0.09} _{-0.08}	0.09 ^{+0.11} _{-0.09}	I	0	1.62	206	144
AP897	8.90 ^{+0.00} _{-0.20}	3.59 ^{+0.03} _{-0.01}	0.00 ^{+0.60} _{-0.00}	7.55 ^{+0.13} _{-0.14}	3.33 ^{+0.07} _{-0.07}	0.79 ^{+0.15} _{-0.14}	I	0	1.52	177	113
AP898	8.80 ^{+0.00} _{-0.00}	3.60 ^{+0.03} _{-0.01}	0.30 ^{+0.10} _{-0.00}	9.38 ^{+0.15} _{-0.16}	3.54 ^{+0.12} _{-0.12}	0.09 ^{+0.12} _{-0.09}	I	0	1.63	180	114
AP900	8.10 ^{+0.00} _{-0.20}	3.08 ^{+0.01} _{-0.19}	1.90 ^{+0.20} _{-0.15}	9.02 ^{+0.25} _{-0.21}	3.28 ^{+0.16} _{-0.17}	0.35 ^{+0.19} _{-0.33}	I	0	1.36	81	34
AP901	9.40 ^{+0.00} _{-0.00}	4.51 ^{+0.00} _{-0.01}	0.00 ^{+0.00} _{-0.00}	9.20 ^{+0.08} _{-0.08}	4.82 ^{+0.05} _{-0.05}	0.20 ^{+0.10} _{-0.10}	I	0	2.23	208	257
AP902	8.10 ^{+0.00} _{-0.10}	3.60 ^{+0.00} _{-0.02}	1.05 ^{+0.10} _{-0.00}	8.40 ^{+0.10} _{-0.08}	3.37 ^{+0.11} _{-0.09}	0.41 ^{+0.21} _{-0.24}	I	0	1.86	260	181

Table 1 (cont'd)

AP ID ^a	CMD Best Fit Parameters ^b			Integrated Best Fit Parameters ^c			Best ^d Flag ^e	R _{ap} ^f	N _{stars} ^g	N _{bg} ^h	
	log(<i>t</i> [Myr])	log(<i>M</i> [<i>M</i> _⊙])	<i>A_V</i> [mag]	log(<i>t</i> [Myr])	log(<i>M</i> [<i>M</i> _⊙])	<i>A_V</i> [mag]					
AP903	8.20 ^{+1.20} _{-0.00}	3.24 ^{+0.94} _{-0.03}	1.35 ^{+0.00} _{-1.35}	0.00 ^{+0.00} _{-0.00}	0.00 ^{+0.00} _{-0.00}	0.00 ^{+0.00} _{-0.00}	I	0	2.35	145	498
AP906	8.90 ^{+0.00} _{-0.00}	3.73 ^{+0.00} _{-0.06}	0.60 ^{+0.00} _{-0.20}	8.60 ^{+0.26} _{-0.87}	3.42 ^{+0.30} _{-1.03}	0.20 ^{+0.13} _{-0.15}	I	0	1.35	89	30
AP908	8.90 ^{+0.10} _{-0.00}	3.84 ^{+0.05} _{-0.00}	0.30 ^{+0.10} _{-0.05}	9.23 ^{+0.44} _{-0.38}	3.91 ^{+0.17} _{-0.14}	0.44 ^{+0.42} _{-0.41}	I	0	2.30	338	256
AP910	9.10 ^{+0.00} _{-0.00}	4.09 ^{+0.00} _{-0.00}	0.00 ^{+0.00} _{-0.00}	9.20 ^{+0.14} _{-0.11}	3.86 ^{+0.10} _{-0.09}	0.11 ^{+0.12} _{-0.11}	I	0	3.05	474	258
AP911	8.80 ^{+0.00} _{-0.00}	3.38 ^{+0.02} _{-0.04}	0.15 ^{+0.10} _{-0.15}	8.18 ^{+0.16} _{-0.16}	2.97 ^{+0.13} _{-0.14}	0.57 ^{+0.34} _{-0.35}	I	0	1.32	109	63
AP912	8.70 ^{+0.10} _{-0.00}	3.12 ^{+0.03} _{-0.05}	0.50 ^{+0.00} _{-0.35}	8.14 ^{+0.11} _{-0.13}	2.99 ^{+0.14} _{-0.15}	1.34 ^{+0.30} _{-0.29}	I	0	1.10	63	32
AP914	7.80 ^{+0.20} _{-0.00}	3.05 ^{+0.02} _{-0.03}	0.60 ^{+0.05} _{-0.05}	8.07 ^{+0.09} _{-0.06}	3.11 ^{+0.06} _{-0.05}	0.41 ^{+0.15} _{-0.19}	I	0	1.42	111	84
AP915	9.00 ^{+0.00} _{-0.00}	3.75 ^{+0.09} _{-0.04}	0.10 ^{+0.20} _{-0.05}	8.40 ^{+0.37} _{-0.29}	3.45 ^{+0.18} _{-0.21}	0.86 ^{+0.58} _{-0.76}	I	0	1.71	235	155
AP918	8.10 ^{+0.00} _{-0.10}	3.96 ^{+0.04} _{-0.02}	2.20 ^{+0.15} _{-0.00}	9.98 ^{+0.05} _{-0.05}	4.47 ^{+0.06} _{-0.06}	0.04 ^{+0.08} _{-0.04}	I	0	1.86	136	117
AP919	8.10 ^{+0.00} _{-0.00}	3.30 ^{+0.00} _{-0.05}	0.80 ^{+0.00} _{-0.10}	8.26 ^{+0.12} _{-0.12}	3.21 ^{+0.13} _{-0.12}	0.38 ^{+0.29} _{-0.28}	I	0	1.38	164	140
AP920	8.20 ^{+0.00} _{-0.50}	3.58 ^{+0.03} _{-0.05}	1.60 ^{+0.45} _{-0.00}	7.57 ^{+0.03} _{-0.05}	2.34 ^{+0.04} _{-0.03}	0.09 ^{+0.08} _{-0.07}	I	0	1.62	147	100
AP921	8.30 ^{+0.00} _{-0.00}	3.09 ^{+0.04} _{-0.02}	0.25 ^{+0.10} _{-0.05}	7.79 ^{+0.07} _{-0.07}	3.46 ^{+0.07} _{-0.07}	1.28 ^{+0.14} _{-0.14}	I	0	1.43	138	106
AP923	9.00 ^{+0.00} _{-0.00}	3.80 ^{+0.07} _{-0.00}	0.10 ^{+0.05} _{-0.10}	9.39 ^{+0.16} _{-0.15}	3.78 ^{+0.08} _{-0.08}	0.20 ^{+0.20} _{-0.20}	I	0	1.56	170	114
AP925	7.60 ^{+0.00} _{-0.60}	3.18 ^{+0.00} _{-0.05}	0.95 ^{+0.15} _{-0.00}	6.94 ^{+0.84} _{-0.74}	3.33 ^{+0.38} _{-0.35}	1.23 ^{+0.45} _{-0.57}	I	0	1.65	190	145
AP927	8.20 ^{+0.10} _{-0.00}	3.53 ^{+0.02} _{-0.02}	1.25 ^{+0.05} _{-0.05}	8.47 ^{+0.13} _{-0.12}	3.21 ^{+0.12} _{-0.12}	0.31 ^{+0.27} _{-0.27}	I	0	1.78	252	199
AP929	6.60 ^{+0.30} _{-0.00}	3.23 ^{+0.00} _{-0.03}	0.60 ^{+0.00} _{-0.10}	6.88 ^{+0.16} _{-0.13}	3.38 ^{+0.31} _{-0.31}	0.42 ^{+0.08} _{-0.09}	I	0	3.82	366	225
AP930	9.00 ^{+0.00} _{-0.00}	3.70 ^{+0.09} _{-0.05}	0.20 ^{+0.05} _{-0.10}	9.92 ^{+0.09} _{-0.09}	4.09 ^{+0.07} _{-0.07}	0.04 ^{+0.08} _{-0.04}	I	0	1.31	59	84
AP932	10.10 ^{+0.10} _{-0.50}	5.48 ^{+0.38} _{-0.71}	0.25 ^{+0.40} _{-0.00}	10.25 ^{+0.00} _{-0.03}	4.59 ^{+0.06} _{-0.06}	0.45 ^{+0.10} _{-0.10}	I	0	1.85	274	196
AP933	7.70 ^{+0.20} _{-0.50}	3.01 ^{+0.03} _{-0.07}	0.90 ^{+0.00} _{-0.25}	7.94 ^{+0.11} _{-0.11}	3.02 ^{+0.07} _{-0.07}	0.49 ^{+0.14} _{-0.14}	I	0	1.24	58	15
AP935	8.00 ^{+0.30} _{-0.20}	2.95 ^{+0.03} _{-0.07}	0.65 ^{+0.05} _{-0.25}	8.35 ^{+0.09} _{-0.08}	2.86 ^{+0.12} _{-0.11}	0.16 ^{+0.16} _{-0.15}	I	0	1.37	126	101
AP937	8.70 ^{+0.00} _{-0.30}	2.89 ^{+0.03} _{-0.06}	0.25 ^{+0.50} _{-0.05}	7.92 ^{+0.24} _{-0.20}	2.46 ^{+0.15} _{-0.15}	0.25 ^{+0.24} _{-0.22}	I	0	1.23	47	29
AP938	8.20 ^{+0.00} _{-0.10}	3.04 ^{+0.01} _{-0.03}	0.70 ^{+0.05} _{-0.05}	8.08 ^{+0.17} _{-0.17}	3.41 ^{+0.16} _{-0.16}	1.26 ^{+0.37} _{-0.34}	I	0	1.39	150	125
AP939	7.70 ^{+0.10} _{-0.00}	4.11 ^{+0.06} _{-0.00}	3.00 ^{+0.00} _{-0.05}	9.08 ^{+0.12} _{-0.12}	3.70 ^{+0.10} _{-0.09}	0.13 ^{+0.14} _{-0.13}	I	0	2.14	293	224
AP942	7.80 ^{+0.20} _{-0.20}	3.20 ^{+0.03} _{-0.03}	0.75 ^{+0.08} _{-0.05}	7.82 ^{+0.27} _{-0.23}	2.72 ^{+0.19} _{-0.21}	0.33 ^{+0.31} _{-0.29}	I	0	1.95	235	189
AP945	8.80 ^{+0.00} _{-0.00}	3.66 ^{+0.00} _{-0.03}	0.05 ^{+0.05} _{-0.05}	8.99 ^{+0.15} _{-0.15}	3.55 ^{+0.12} _{-0.12}	0.14 ^{+0.14} _{-0.13}	I	0	2.10	330	252
AP946	9.40 ^{+0.00} _{-0.00}	4.45 ^{+0.03} _{-0.00}	0.00 ^{+0.00} _{-0.00}	9.96 ^{+0.10} _{-0.09}	5.11 ^{+0.05} _{-0.05}	0.23 ^{+0.12} _{-0.12}	I	0	1.85	119	253
AP948	7.90 ^{+0.20} _{-0.10}	3.47 ^{+0.05} _{-0.02}	1.05 ^{+0.10} _{-0.05}	8.31 ^{+0.05} _{-0.17}	2.98 ^{+0.03} _{-0.11}	0.14 ^{+0.13} _{-0.13}	I	0	1.73	189	126
AP950	8.30 ^{+0.00} _{-0.60}	3.46 ^{+0.00} _{-0.09}	0.80 ^{+0.35} _{-0.05}	8.52 ^{+0.13} _{-0.17}	3.20 ^{+0.06} _{-0.06}	0.23 ^{+0.31} _{-0.23}	I	0	1.49	177	117
AP951	8.30 ^{+0.00} _{-0.00}	3.44 ^{+0.03} _{-0.00}	0.65 ^{+0.05} _{-0.00}	8.22 ^{+0.16} _{-0.10}	3.48 ^{+0.17} _{-0.09}	0.73 ^{+0.24} _{-0.24}	I	0	2.02	293	242
AP954	8.90 ^{+0.00} _{-0.10}	3.94 ^{+0.04} _{-0.04}	0.45 ^{+0.30} _{-0.00}	8.33 ^{+0.26} _{-0.21}	3.47 ^{+0.15} _{-0.15}	0.77 ^{+0.42} _{-0.58}	I	0	1.80	260	168
AP955	6.60 ^{+0.40} _{-0.00}	3.46 ^{+0.03} _{-0.03}	1.40 ^{+0.00} _{-0.10}	7.41 ^{+0.20} _{-0.05}	3.84 ^{+0.12} _{-0.11}	0.45 ^{+0.14} _{-0.27}	I	0	2.60	427	365
AP956	9.10 ^{+0.00} _{-0.00}	4.16 ^{+0.02} _{-0.04}	0.20 ^{+0.05} _{-0.05}	8.99 ^{+0.11} _{-0.08}	3.57 ^{+0.08} _{-0.08}	0.09 ^{+0.09} _{-0.09}	I	0	2.20	355	233
AP957	8.90 ^{+0.00} _{-0.10}	3.51 ^{+0.03} _{-0.08}	0.30 ^{+0.25} _{-0.05}	8.89 ^{+0.07} _{-0.08}	3.17 ^{+0.08} _{-0.08}	0.02 ^{+0.07} _{-0.02}	I	0	1.66	197	152

Table 1 (cont'd)

AP ID ^a	CMD Best Fit Parameters ^b			Integrated Best Fit Parameters ^c			Best ^d Flag ^e	Rap ^f	N _{stars} ^g	N _{bg} ^h	
	log(<i>t</i> [Myr])	log(<i>M</i> [<i>M</i> _⊙])	<i>A_V</i> [mag]	log(<i>t</i> [Myr])	log(<i>M</i> [<i>M</i> _⊙])	<i>A_V</i> [mag]					
AP958	9.10 ^{+0.00} _{-0.10}	4.08 ^{+0.01} _{-0.07}	0.55 ^{+0.15} _{-0.05}	8.19 ^{+0.25} _{-0.59}	3.48 ^{+0.30} _{-0.47}	1.23 ^{+0.47} _{-0.55}	I	0	2.29	300	195
AP959	8.10 ^{+0.00} _{-0.00}	3.18 ^{+0.02} _{-0.00}	0.50 ^{+0.05} _{-0.00}	8.29 ^{+0.06} _{-0.07}	3.54 ^{+0.09} _{-0.08}	0.57 ^{+0.18} _{-0.16}	I	0	1.61	87	37
AP960	8.30 ^{+0.20} _{-0.00}	3.16 ^{+0.02} _{-0.07}	0.90 ^{+0.10} _{-0.20}	9.43 ^{+0.12} _{-0.11}	3.55 ^{+0.09} _{-0.09}	0.06 ^{+0.10} _{-0.06}	I	0	1.34	96	52
AP961	9.20 ^{+0.00} _{-0.00}	4.16 ^{+0.04} _{-0.08}	0.25 ^{+0.05} _{-0.05}	9.10 ^{+0.49} _{-0.93}	3.84 ^{+0.12} _{-0.13}	0.60 ^{+1.13} _{-0.57}	I	0	1.70	187	114
AP964	8.30 ^{+0.20} _{-0.10}	3.27 ^{+0.16} _{-0.02}	1.15 ^{+0.15} _{-0.20}	8.89 ^{+0.05} _{-0.05}	3.13 ^{+0.08} _{-0.08}	0.06 ^{+0.10} _{-0.06}	I	0	1.28	132	82
AP966	9.10 ^{+0.00} _{-0.00}	3.90 ^{+0.02} _{-0.06}	0.15 ^{+0.10} _{-0.05}	9.01 ^{+0.59} _{-0.80}	3.88 ^{+0.15} _{-0.15}	0.97 ^{+0.95} _{-0.67}	I	0	1.77	200	102
AP970	8.90 ^{+0.00} _{-0.10}	3.19 ^{+0.03} _{-0.04}	0.00 ^{+0.20} _{-0.00}	8.41 ^{+0.08} _{-0.08}	2.47 ^{+0.14} _{-0.15}	0.13 ^{+0.15} _{-0.13}	I	0	1.41	91	59
AP972	8.50 ^{+0.10} _{-0.10}	3.33 ^{+0.00} _{-0.11}	0.70 ^{+0.10} _{-0.15}	9.56 ^{+0.41} _{-0.51}	3.83 ^{+0.17} _{-0.17}	0.36 ^{+0.46} _{-0.35}	I	0	1.48	159	100
AP973	8.70 ^{+0.10} _{-0.00}	2.98 ^{+0.02} _{-0.06}	0.30 ^{+0.05} _{-0.20}	9.30 ^{+0.05} _{-0.04}	3.36 ^{+0.04} _{-0.04}	0.01 ^{+0.07} _{-0.01}	I	0	1.38	76	33
AP975	8.00 ^{+0.00} _{-0.40}	3.26 ^{+0.00} _{-0.04}	0.75 ^{+0.15} _{-0.00}	6.74 ^{+0.51} _{-0.54}	3.23 ^{+0.20} _{-0.21}	1.34 ^{+0.16} _{-0.16}	I	0	1.51	167	129
AP977	8.40 ^{+0.00} _{-0.30}	2.88 ^{+0.01} _{-0.11}	0.75 ^{+0.15} _{-0.05}	8.52 ^{+0.17} _{-0.17}	2.59 ^{+0.17} _{-0.17}	0.29 ^{+0.32} _{-0.28}	I	0	1.24	64	37
AP979	8.20 ^{+0.40} _{-0.10}	3.19 ^{+0.05} _{-0.09}	1.15 ^{+0.10} _{-0.50}	7.79 ^{+0.20} _{-0.13}	3.35 ^{+0.19} _{-0.19}	1.54 ^{+0.33} _{-0.29}	I	0	1.52	133	87
AP980	7.20 ^{+0.10} _{-0.10}	3.51 ^{+0.03} _{-0.01}	1.55 ^{+0.05} _{-0.00}	7.37 ^{+0.10} _{-0.10}	4.49 ^{+0.05} _{-0.05}	1.38 ^{+0.13} _{-0.13}	I	0	1.81	223	181
AP981	8.90 ^{+0.00} _{-0.00}	3.20 ^{+0.06} _{-0.01}	0.00 ^{+0.20} _{-0.00}	8.43 ^{+0.37} _{-0.36}	2.87 ^{+0.22} _{-0.20}	0.60 ^{+0.73} _{-0.60}	I	0	1.32	66	39
AP982	8.50 ^{+0.20} _{-0.10}	3.26 ^{+0.00} _{-0.19}	1.40 ^{+0.05} _{-0.35}	9.11 ^{+0.18} _{-0.16}	3.15 ^{+0.14} _{-0.13}	0.18 ^{+0.18} _{-0.17}	I	0	1.42	83	38
AP983	7.90 ^{+0.00} _{-0.50}	3.30 ^{+0.00} _{-0.06}	1.25 ^{+0.10} _{-0.00}	7.69 ^{+0.06} _{-0.06}	3.23 ^{+0.06} _{-0.07}	0.96 ^{+0.11} _{-0.12}	I	0	1.40	137	110
AP985	8.70 ^{+0.00} _{-0.20}	3.22 ^{+0.05} _{-0.05}	0.00 ^{+0.50} _{-0.05}	8.78 ^{+0.05} _{-0.04}	3.27 ^{+0.05} _{-0.05}	0.05 ^{+0.09} _{-0.05}	I	0	1.53	197	144
AP986	9.00 ^{+0.00} _{-1.40}	3.50 ^{+0.26} _{-0.00}	0.00 ^{+2.80} _{-0.00}	7.99 ^{+0.28} _{-0.34}	3.27 ^{+0.22} _{-0.20}	1.08 ^{+0.65} _{-0.53}	I	0	1.46	163	124
AP990	8.20 ^{+0.10} _{-0.10}	3.26 ^{+0.02} _{-0.03}	0.70 ^{+0.05} _{-0.10}	8.04 ^{+0.22} _{-0.26}	3.20 ^{+0.22} _{-0.17}	0.85 ^{+0.58} _{-0.43}	I	0	1.84	237	197
AP991	8.80 ^{+0.00} _{-0.10}	3.33 ^{+0.06} _{-0.00}	0.00 ^{+0.35} _{-0.00}	7.83 ^{+0.06} _{-0.06}	3.34 ^{+0.07} _{-0.07}	1.52 ^{+0.11} _{-0.11}	I	0	1.49	114	68
AP992	7.80 ^{+0.10} _{-0.40}	3.04 ^{+0.01} _{-0.05}	0.40 ^{+0.10} _{-0.10}	8.23 ^{+0.07} _{-0.06}	3.39 ^{+0.08} _{-0.07}	0.07 ^{+0.11} _{-0.07}	I	0	1.61	172	138
AP993	8.80 ^{+0.00} _{-0.10}	3.49 ^{+0.02} _{-0.05}	0.00 ^{+0.35} _{-0.00}	8.45 ^{+0.13} _{-0.17}	3.16 ^{+0.10} _{-0.10}	0.21 ^{+0.34} _{-0.21}	I	0	1.54	193	148
AP995	7.00 ^{+0.20} _{-0.30}	2.95 ^{+0.02} _{-0.04}	0.95 ^{+0.05} _{-0.10}	6.68 ^{+0.14} _{-0.18}	2.30 ^{+0.20} _{-0.21}	0.83 ^{+0.13} _{-0.13}	I	0	1.25	87	66
AP996	9.10 ^{+0.00} _{-0.10}	3.68 ^{+0.02} _{-0.17}	0.10 ^{+0.10} _{-0.05}	9.17 ^{+0.08} _{-0.08}	3.20 ^{+0.09} _{-0.10}	0.02 ^{+0.07} _{-0.02}	I	0	1.37	110	57
AP997	8.60 ^{+0.10} _{-0.00}	3.53 ^{+0.03} _{-0.06}	0.65 ^{+0.00} _{-0.25}	8.40 ^{+0.16} _{-0.15}	3.03 ^{+0.11} _{-0.12}	0.34 ^{+0.30} _{-0.29}	I	0	1.77	226	162
AP998	7.90 ^{+0.10} _{-0.80}	2.51 ^{+0.00} _{-0.11}	0.35 ^{+0.15} _{-0.10}	7.53 ^{+0.08} _{-0.08}	3.03 ^{+0.11} _{-0.14}	0.28 ^{+0.09} _{-0.07}	I	0	1.41	37	25
AP1001	8.40 ^{+0.00} _{-0.10}	3.77 ^{+0.00} _{-0.11}	1.35 ^{+0.10} _{-0.10}	8.73 ^{+0.20} _{-0.21}	3.43 ^{+0.09} _{-0.09}	0.49 ^{+0.29} _{-0.27}	I	0	1.60	164	128
AP1002	7.50 ^{+0.00} _{-0.20}	3.13 ^{+0.00} _{-0.04}	0.45 ^{+0.00} _{-0.05}	7.67 ^{+0.12} _{-0.11}	3.08 ^{+0.06} _{-0.07}	0.27 ^{+0.12} _{-0.13}	I	0	1.39	120	84
AP1003	7.70 ^{+0.20} _{-0.20}	3.19 ^{+0.04} _{-0.02}	0.75 ^{+0.10} _{-0.05}	8.14 ^{+0.19} _{-0.17}	3.23 ^{+0.16} _{-0.17}	0.53 ^{+0.36} _{-0.37}	I	0	1.84	245	192
AP1005	9.10 ^{+0.00} _{-0.00}	3.85 ^{+0.11} _{-0.03}	0.25 ^{+0.15} _{-0.05}	9.01 ^{+0.50} _{-0.47}	3.68 ^{+0.16} _{-0.15}	0.72 ^{+0.49} _{-0.51}	I	0	2.05	261	179
AP1006	7.10 ^{+0.40} _{-0.00}	3.42 ^{+0.01} _{-0.02}	1.40 ^{+0.00} _{-0.15}	7.65 ^{+0.15} _{-0.14}	3.74 ^{+0.08} _{-0.07}	0.81 ^{+0.18} _{-0.18}	I	0	1.42	181	135
AP1007	8.30 ^{+0.30} _{-0.10}	3.55 ^{+0.06} _{-0.05}	1.60 ^{+0.20} _{-0.50}	8.40 ^{+0.20} _{-0.18}	3.20 ^{+0.21} _{-0.17}	0.74 ^{+0.41} _{-0.40}	I	0	2.25	330	269
AP1008	9.00 ^{+0.00} _{-0.00}	4.23 ^{+0.03} _{-0.00}	0.50 ^{+0.10} _{-0.00}	9.15 ^{+0.67} _{-0.56}	4.89 ^{+0.46} _{-0.45}	1.34 ^{+1.03} _{-0.95}	I	0	3.41	615	193

Table 1 (cont'd)

AP ID ^a	CMD Best Fit Parameters ^b			Integrated Best Fit Parameters ^c			Best ^d Flag ^e	R _{ap} ^f	N _{stars} ^g	N _{bg} ^h	
	log(<i>t</i> [Myr])	log(<i>M</i> [<i>M</i> _⊙])	<i>A_V</i> [mag]	log(<i>t</i> [Myr])	log(<i>M</i> [<i>M</i> _⊙])	<i>A_V</i> [mag]					
AP1009	9.30 ^{+0.00} _{-0.00}	4.15 ^{+0.00} _{-0.05}	0.00 ^{+0.10} _{-0.00}	9.54 ^{+0.14} _{-0.14}	4.98 ^{+0.06} _{-0.06}	0.41 ^{+0.20} _{-0.18}	I	0	1.58	62	242
AP1012	8.20 ^{+0.00} _{-0.00}	3.79 ^{+0.04} _{-0.03}	2.15 ^{+0.05} _{-0.05}	9.25 ^{+0.88} _{-0.74}	3.98 ^{+0.18} _{-0.16}	1.30 ^{+0.91} _{-0.93}	I	0	1.45	115	68
AP1014	8.00 ^{+0.80} _{-0.70}	3.32 ^{+0.20} _{-0.46}	2.20 ^{+0.65} _{-1.25}	8.84 ^{+0.14} _{-0.12}	3.62 ^{+0.09} _{-0.09}	0.63 ^{+0.22} _{-0.23}	I	0	1.64	171	66
AP1015	9.10 ^{+0.00} _{-0.10}	3.54 ^{+0.03} _{-0.05}	0.25 ^{+0.25} _{-0.00}	10.22 ^{+0.03} _{-0.06}	3.82 ^{+0.07} _{-0.07}	0.05 ^{+0.10} _{-0.05}	I	0	1.05	66	20
AP1017	7.80 ^{+0.10} _{-0.10}	3.52 ^{+0.04} _{-0.07}	2.35 ^{+0.10} _{-0.05}	8.18 ^{+0.11} _{-0.42}	2.57 ^{+0.07} _{-0.47}	0.20 ^{+0.12} _{-0.11}	I	0	1.44	121	58
AP1018	9.00 ^{+0.10} _{-0.00}	3.47 ^{+0.04} _{-0.07}	0.20 ^{+0.05} _{-0.15}	9.42 ^{+0.40} _{-0.50}	3.71 ^{+0.16} _{-0.18}	0.42 ^{+0.37} _{-0.37}	I	0	1.42	112	59
AP1020	9.10 ^{+0.90} _{-0.00}	4.10 ^{+0.70} _{-0.07}	0.80 ^{+0.00} _{-0.50}	9.25 ^{+0.49} _{-0.35}	3.86 ^{+0.15} _{-0.13}	0.68 ^{+0.37} _{-0.51}	I	0	1.41	159	94
AP1023	8.40 ^{+0.10} _{-0.10}	3.36 ^{+0.04} _{-0.04}	0.95 ^{+0.20} _{-0.15}	8.77 ^{+0.07} _{-0.07}	3.05 ^{+0.07} _{-0.07}	0.18 ^{+0.15} _{-0.15}	I	0	1.32	119	77
AP1024	9.00 ^{+0.10} _{-0.00}	3.79 ^{+0.12} _{-0.04}	0.15 ^{+0.15} _{-0.05}	9.22 ^{+0.12} _{-0.12}	3.68 ^{+0.10} _{-0.10}	0.13 ^{+0.14} _{-0.13}	I	0	1.60	217	137
AP1026	7.00 ^{+0.40} _{-0.20}	2.78 ^{+0.02} _{-0.08}	0.75 ^{+0.05} _{-0.15}	7.27 ^{+0.17} _{-0.18}	3.43 ^{+0.10} _{-0.12}	0.96 ^{+0.11} _{-0.11}	I	0	1.61	170	146
AP1027	7.90 ^{+0.10} _{-0.20}	3.57 ^{+0.04} _{-0.02}	1.45 ^{+0.15} _{-0.05}	9.10 ^{+0.04} _{-0.04}	3.69 ^{+0.05} _{-0.05}	0.00 ^{+0.07} _{-0.00}	I	0	1.36	164	98
AP1028	8.80 ^{+0.00} _{-0.20}	3.84 ^{+0.01} _{-0.11}	0.55 ^{+0.55} _{-0.10}	8.73 ^{+0.28} _{-0.32}	3.50 ^{+0.10} _{-0.09}	0.60 ^{+0.42} _{-0.38}	I	0	1.60	191	112
AP1030	8.80 ^{+0.10} _{-0.00}	3.27 ^{+0.09} _{-0.03}	0.25 ^{+0.10} _{-0.19}	8.03 ^{+0.17} _{-0.18}	3.24 ^{+0.17} _{-0.16}	1.28 ^{+0.36} _{-0.36}	I	0	1.54	139	101
AP1031	8.00 ^{+0.10} _{-0.60}	2.96 ^{+0.05} _{-0.07}	1.55 ^{+0.25} _{-0.00}	8.95 ^{+0.17} _{-0.13}	2.89 ^{+0.14} _{-0.14}	0.11 ^{+0.11} _{-0.11}	I	0	1.42	71	41
AP1032	8.10 ^{+0.00} _{-0.00}	3.10 ^{+0.00} _{-0.07}	0.60 ^{+0.00} _{-0.10}	8.43 ^{+0.10} _{-0.09}	3.12 ^{+0.10} _{-0.09}	0.18 ^{+0.19} _{-0.18}	I	0	1.65	214	186
AP1033	8.80 ^{+0.00} _{-0.10}	3.46 ^{+0.03} _{-0.03}	0.05 ^{+0.30} _{-0.00}	8.90 ^{+0.08} _{-0.08}	3.23 ^{+0.07} _{-0.08}	0.18 ^{+0.14} _{-0.14}	I	0	1.24	122	80
AP1034	8.70 ^{+0.00} _{-0.20}	3.49 ^{+0.07} _{-0.01}	0.15 ^{+0.50} _{-0.05}	8.52 ^{+0.08} _{-0.08}	3.49 ^{+0.09} _{-0.08}	0.49 ^{+0.18} _{-0.18}	I	0	1.54	209	163
AP1035	8.70 ^{+1.00} _{-0.10}	6.45 ^{+0.61} _{-2.65}	3.00 ^{+0.05} _{-2.50}	7.63 ^{+0.16} _{-0.09}	4.44 ^{+0.11} _{-0.03}	2.83 ^{+0.07} _{-0.12}	I	0	1.75	188	152
AP1036	7.90 ^{+0.00} _{-0.30}	3.08 ^{+0.00} _{-0.08}	0.90 ^{+0.10} _{-0.05}	7.95 ^{+0.15} _{-0.11}	3.18 ^{+0.14} _{-0.13}	0.73 ^{+0.22} _{-0.29}	I	0	1.28	115	80
AP1037	8.10 ^{+0.10} _{-0.30}	3.15 ^{+0.00} _{-0.07}	0.65 ^{+0.05} _{-0.10}	8.25 ^{+0.08} _{-0.08}	2.94 ^{+0.09} _{-0.08}	0.13 ^{+0.13} _{-0.12}	I	0	1.64	171	129
AP1038	9.00 ^{+0.00} _{-0.20}	3.47 ^{+0.05} _{-0.21}	0.35 ^{+0.55} _{-0.00}	9.10 ^{+0.88} _{-0.58}	3.79 ^{+0.21} _{-0.16}	1.15 ^{+0.63} _{-0.85}	I	0	1.46	124	74
AP1041	7.20 ^{+0.00} _{-0.10}	3.59 ^{+0.01} _{-0.03}	1.60 ^{+0.05} _{-0.05}	6.57 ^{+0.15} _{-0.14}	2.83 ^{+0.50} _{-0.55}	1.10 ^{+0.13} _{-0.13}	I	0	2.27	270	250
AP1043	8.00 ^{+0.30} _{-0.20}	2.92 ^{+0.03} _{-0.03}	0.40 ^{+0.05} _{-0.20}	6.66 ^{+0.32} _{-0.45}	2.98 ^{+0.10} _{-0.08}	1.28 ^{+0.11} _{-0.13}	I	0	1.31	82	49
AP1044	8.30 ^{+0.10} _{-0.30}	3.10 ^{+0.04} _{-0.03}	0.35 ^{+0.25} _{-0.05}	8.96 ^{+0.07} _{-0.06}	3.40 ^{+0.07} _{-0.07}	0.00 ^{+0.07} _{-0.00}	I	0	1.63	165	122
AP1045	8.20 ^{+0.10} _{-0.30}	3.55 ^{+0.04} _{-0.11}	1.50 ^{+0.10} _{-0.05}	8.90 ^{+0.10} _{-0.10}	3.12 ^{+0.10} _{-0.10}	0.20 ^{+0.16} _{-0.16}	I	0	1.53	154	111
AP1047	9.30 ^{+0.10} _{-0.10}	4.61 ^{+0.02} _{-0.08}	0.25 ^{+0.20} _{-0.00}	9.21 ^{+0.41} _{-0.87}	4.32 ^{+0.11} _{-0.11}	0.64 ^{+0.90} _{-0.50}	I	0	2.79	595	446
AP1048	8.50 ^{+0.30} _{-0.00}	3.40 ^{+0.11} _{-0.04}	1.10 ^{+0.05} _{-0.50}	8.29 ^{+0.15} _{-0.18}	2.56 ^{+0.18} _{-0.16}	0.17 ^{+0.18} _{-0.16}	I	0	1.53	140	89
AP1049	8.30 ^{+0.00} _{-0.00}	3.32 ^{+0.05} _{-0.02}	0.55 ^{+0.15} _{-0.05}	8.46 ^{+0.08} _{-0.08}	3.22 ^{+0.09} _{-0.09}	0.14 ^{+0.17} _{-0.14}	I	0	1.59	168	135
AP1051	8.40 ^{+0.10} _{-0.00}	3.07 ^{+0.01} _{-0.03}	0.60 ^{+0.05} _{-0.15}	8.56 ^{+0.13} _{-0.14}	2.99 ^{+0.10} _{-0.11}	0.31 ^{+0.26} _{-0.26}	I	0	1.50	136	111
AP1052	8.40 ^{+0.80} _{-1.40}	2.17 ^{+0.03} _{-2.17}	0.35 ^{+1.90} _{-0.15}	0.00 ^{+0.00} _{-0.00}	0.00 ^{+0.00} _{-0.00}	0.00 ^{+0.00} _{-0.00}	I	0	3.41	170	1116
AP1053	8.50 ^{+0.00} _{-0.10}	3.26 ^{+0.02} _{-0.05}	0.50 ^{+0.10} _{-0.05}	8.38 ^{+0.14} _{-0.13}	2.89 ^{+0.14} _{-0.14}	0.37 ^{+0.28} _{-0.28}	I	0	1.42	122	99
AP1054	9.00 ^{+0.00} _{-0.10}	3.76 ^{+0.06} _{-0.03}	0.15 ^{+0.30} _{-0.00}	9.09 ^{+0.23} _{-0.19}	3.54 ^{+0.12} _{-0.11}	0.34 ^{+0.25} _{-0.27}	I	0	1.34	137	76
AP1055	7.70 ^{+0.00} _{-0.20}	3.21 ^{+0.01} _{-0.04}	1.45 ^{+0.15} _{-0.05}	6.87 ^{+0.10} _{-0.08}	3.14 ^{+0.24} _{-0.16}	1.30 ^{+0.07} _{-0.08}	I	0	2.08	147	84

Table 1 (cont'd)

AP ID ^a	CMD Best Fit Parameters ^b			Integrated Best Fit Parameters ^c			Best ^d Flag ^e	Rap ^f	N _{stars} ^g	N _{bg} ^h	
	log(<i>t</i> [Myr])	log(<i>M</i> [<i>M</i> _⊙])	<i>A_V</i> [mag]	log(<i>t</i> [Myr])	log(<i>M</i> [<i>M</i> _⊙])	<i>A_V</i> [mag]					
AP1058	8.50 ^{+0.10} _{-0.10}	3.20 ^{+0.00} _{-0.12}	0.80 ^{+0.10} _{-0.15}	8.07 ^{+0.25} _{-0.24}	3.09 ^{+0.23} _{-0.19}	0.89 ^{+0.54} _{-0.53}	I	0	1.54	153	118
AP1059	8.60 ^{+0.00} _{-0.10}	3.20 ^{+0.02} _{-0.04}	0.40 ^{+0.20} _{-0.00}	7.58 ^{+0.97} _{-0.93}	2.95 ^{+0.38} _{-0.41}	1.00 ^{+0.76} _{-0.73}	I	0	1.36	145	120
AP1061	9.10 ^{+0.00} _{-1.30}	3.80 ^{+0.16} _{-0.00}	0.00 ^{+2.45} _{-0.00}	9.00 ^{+0.13} _{-0.13}	3.76 ^{+0.08} _{-0.08}	0.37 ^{+0.22} _{-0.22}	I	0	1.62	245	153
AP1062	9.00 ^{+0.00} _{-0.00}	3.61 ^{+0.03} _{-0.05}	0.15 ^{+0.15} _{-0.05}	8.45 ^{+0.15} _{-0.13}	3.40 ^{+0.13} _{-0.13}	1.13 ^{+0.29} _{-0.33}	I	0	1.68	188	140
AP1064	8.40 ^{+0.00} _{-0.60}	3.26 ^{+0.03} _{-0.09}	0.55 ^{+0.35} _{-0.00}	8.64 ^{+0.20} _{-0.20}	3.34 ^{+0.11} _{-0.11}	0.29 ^{+0.30} _{-0.26}	I	0	1.86	302	273
AP1065	9.00 ^{+0.00} _{-0.00}	3.83 ^{+0.08} _{-0.00}	0.00 ^{+0.15} _{-0.00}	8.49 ^{+0.18} _{-0.21}	3.23 ^{+0.14} _{-0.14}	0.36 ^{+0.43} _{-0.34}	I	0	1.69	258	187
AP1067	8.20 ^{+0.00} _{-0.10}	3.19 ^{+0.01} _{-0.03}	0.55 ^{+0.10} _{-0.05}	8.24 ^{+0.20} _{-0.18}	3.27 ^{+0.16} _{-0.13}	0.54 ^{+0.38} _{-0.43}	I	0	1.45	149	116
AP1068	7.30 ^{+0.90} _{-0.20}	3.07 ^{+0.00} _{-0.21}	2.20 ^{+0.20} _{-0.35}	7.02 ^{+0.24} _{-0.24}	4.25 ^{+0.28} _{-0.47}	1.82 ^{+0.12} _{-0.11}	I	0	1.50	105	120
AP1070	8.80 ^{+0.00} _{-0.50}	3.02 ^{+0.02} _{-0.18}	0.35 ^{+0.80} _{-0.00}	8.61 ^{+0.15} _{-0.15}	2.56 ^{+0.16} _{-0.16}	0.51 ^{+0.33} _{-0.32}	I	0	1.15	45	29
AP1072	8.30 ^{+0.10} _{-0.10}	3.51 ^{+0.01} _{-0.07}	1.20 ^{+0.05} _{-0.10}	7.28 ^{+0.78} _{-0.76}	2.85 ^{+0.27} _{-0.31}	0.58 ^{+0.47} _{-0.46}	I	0	1.90	233	158
AP1078	7.70 ^{+0.00} _{-0.60}	2.88 ^{+0.00} _{-0.05}	0.50 ^{+0.15} _{-0.00}	7.53 ^{+0.26} _{-0.25}	3.10 ^{+0.09} _{-0.09}	0.90 ^{+0.29} _{-0.28}	I	0	1.57	119	90
AP1080	9.10 ^{+0.00} _{-0.00}	3.83 ^{+0.04} _{-0.04}	0.15 ^{+0.10} _{-0.00}	8.96 ^{+0.22} _{-0.21}	3.66 ^{+0.09} _{-0.09}	0.45 ^{+0.32} _{-0.33}	I	0	1.96	239	153
AP1081	8.00 ^{+0.10} _{-0.40}	3.70 ^{+0.00} _{-0.17}	2.20 ^{+0.20} _{-0.20}	9.04 ^{+0.56} _{-0.29}	4.07 ^{+0.10} _{-0.10}	0.84 ^{+0.35} _{-0.62}	I	0	1.61	234	124
AP1082	7.00 ^{+0.60} _{-0.20}	2.70 ^{+0.02} _{-0.05}	0.55 ^{+0.05} _{-0.15}	7.73 ^{+0.14} _{-0.11}	3.19 ^{+0.10} _{-0.11}	0.37 ^{+0.19} _{-0.19}	I	0	1.46	144	137
AP1083	8.20 ^{+0.00} _{-0.30}	3.50 ^{+0.03} _{-0.09}	1.65 ^{+0.10} _{-0.05}	8.68 ^{+0.17} _{-0.18}	3.26 ^{+0.15} _{-0.15}	0.60 ^{+0.30} _{-0.30}	I	0	1.50	165	97
AP1084	8.20 ^{+0.40} _{-0.00}	2.93 ^{+0.05} _{-0.05}	1.10 ^{+0.10} _{-0.20}	8.30 ^{+0.12} _{-0.11}	2.73 ^{+0.26} _{-0.29}	0.52 ^{+0.40} _{-0.42}	I	0	1.21	55	31
AP1088	6.70 ^{+0.40} _{-0.10}	2.83 ^{+0.04} _{-0.01}	1.10 ^{+0.05} _{-0.05}	7.18 ^{+0.17} _{-0.15}	3.34 ^{+0.09} _{-0.08}	0.98 ^{+0.12} _{-0.13}	I	0	1.38	130	113
AP1089	8.10 ^{+0.00} _{-0.40}	2.84 ^{+0.01} _{-0.07}	0.40 ^{+0.15} _{-0.05}	8.57 ^{+0.17} _{-0.16}	3.12 ^{+0.11} _{-0.10}	0.28 ^{+0.25} _{-0.24}	I	0	1.67	104	72
AP1090	8.40 ^{+0.00} _{-0.10}	3.35 ^{+0.00} _{-0.04}	0.75 ^{+0.10} _{-0.05}	7.85 ^{+0.04} _{-0.03}	2.23 ^{+0.02} _{-0.06}	0.41 ^{+0.07} _{-0.08}	I	0	1.39	125	85
AP1091	9.20 ^{+0.10} _{-0.10}	3.74 ^{+0.17} _{-0.21}	0.25 ^{+0.10} _{-0.15}	8.83 ^{+0.49} _{-0.65}	3.20 ^{+0.19} _{-0.17}	0.58 ^{+0.76} _{-0.52}	I	0	1.27	77	43
AP1092	8.90 ^{+0.00} _{-0.80}	3.26 ^{+0.00} _{-0.30}	0.60 ^{+1.20} _{-0.05}	7.65 ^{+0.38} _{-0.35}	2.97 ^{+0.15} _{-0.15}	1.25 ^{+0.45} _{-0.47}	I	0	1.63	117	61
AP1093	8.40 ^{+0.00} _{-0.00}	3.29 ^{+0.03} _{-0.06}	0.40 ^{+0.05} _{-0.10}	8.19 ^{+0.14} _{-0.13}	3.37 ^{+0.13} _{-0.13}	0.85 ^{+0.30} _{-0.30}	I	0	1.28	144	98
AP1096	7.90 ^{+0.00} _{-0.10}	3.17 ^{+0.14} _{-0.01}	0.85 ^{+0.35} _{-0.00}	8.59 ^{+0.29} _{-0.32}	3.46 ^{+0.14} _{-0.11}	0.47 ^{+0.60} _{-0.45}	I	0	1.41	158	108
AP1099	8.90 ^{+0.00} _{-0.10}	3.45 ^{+0.02} _{-0.07}	0.15 ^{+0.35} _{-0.00}	9.33 ^{+0.17} _{-0.15}	3.72 ^{+0.12} _{-0.13}	0.18 ^{+0.16} _{-0.17}	I	0	1.81	205	158
AP1100	7.10 ^{+0.40} _{-0.30}	3.00 ^{+0.02} _{-0.07}	0.80 ^{+0.00} _{-0.15}	7.89 ^{+0.12} _{-0.12}	3.07 ^{+0.07} _{-0.07}	0.54 ^{+0.17} _{-0.17}	I	0	1.50	126	89
AP1101	8.90 ^{+0.10} _{-0.00}	3.93 ^{+0.00} _{-0.20}	0.55 ^{+0.05} _{-0.45}	9.13 ^{+0.17} _{-0.18}	3.69 ^{+0.13} _{-0.13}	0.21 ^{+0.17} _{-0.17}	I	0	1.99	249	143
AP1102	9.10 ^{+0.90} _{-0.00}	3.54 ^{+0.75} _{-0.21}	0.65 ^{+0.00} _{-0.45}	8.79 ^{+0.61} _{-0.71}	3.33 ^{+0.22} _{-0.22}	0.79 ^{+0.83} _{-0.67}	I	0	1.62	102	39
AP1103	9.90 ^{+0.00} _{-0.30}	4.91 ^{+0.00} _{-0.23}	0.15 ^{+0.25} _{-0.00}	9.10 ^{+0.55} _{-0.95}	4.25 ^{+0.10} _{-0.10}	1.10 ^{+1.17} _{-0.67}	I	0	1.62	207	137
AP1104	9.20 ^{+0.10} _{-0.10}	3.68 ^{+0.15} _{-0.46}	0.30 ^{+0.20} _{-0.15}	7.79 ^{+0.97} _{-0.98}	3.05 ^{+0.22} _{-0.20}	1.26 ^{+0.73} _{-0.83}	I	0	1.34	80	31
AP1105	10.10 ^{+0.40} _{-2.90}	4.78 ^{+1.37} _{-4.78}	0.20 ^{+2.30} _{-0.10}	9.20 ^{+0.08} _{-0.12}	4.14 ^{+0.07} _{-0.10}	0.09 ^{+0.10} _{-0.09}	I	0	1.34	92	186
AP1106	9.10 ^{+0.00} _{-0.00}	3.80 ^{+0.00} _{-0.11}	0.35 ^{+0.05} _{-0.20}	8.69 ^{+0.16} _{-0.18}	3.36 ^{+0.10} _{-0.10}	0.76 ^{+0.25} _{-0.24}	I	0	1.70	178	111
AP1107	9.00 ^{+0.00} _{-1.40}	3.23 ^{+0.03} _{-0.51}	0.05 ^{+1.70} _{-0.10}	9.36 ^{+0.50} _{-0.58}	3.52 ^{+0.24} _{-0.22}	0.53 ^{+0.54} _{-0.45}	I	0	1.22	77	40
AP1108	9.10 ^{+0.00} _{-0.00}	3.58 ^{+0.04} _{-0.05}	0.30 ^{+0.15} _{-0.05}	8.48 ^{+0.10} _{-0.09}	2.92 ^{+0.11} _{-0.12}	0.29 ^{+0.21} _{-0.21}	I	0	1.98	181	96

Table 1 (cont'd)

AP ID ^a	CMD Best Fit Parameters ^b			Integrated Best Fit Parameters ^c			Best ^d Flag ^e	R _{ap} ^f	N _{stars} ^g	N _{bg} ^h	
	log(<i>t</i> [Myr])	log(<i>M</i> [<i>M</i> _⊙])	<i>A_V</i> [mag]	log(<i>t</i> [Myr])	log(<i>M</i> [<i>M</i> _⊙])	<i>A_V</i> [mag]					
AP1110	9.00 ^{+0.00} _{-0.00}	3.12 ^{+0.02} _{-0.00}	0.00 ^{+0.03} _{-0.00}	8.82 ^{+0.17} _{-0.20}	3.02 ^{+0.09} _{-0.10}	0.43 ^{+0.28} _{-0.27}	I	0	1.32	68	29
AP1111	8.20 ^{+0.60} _{-0.40}	3.15 ^{+0.21} _{-0.15}	1.30 ^{+0.15} _{-0.90}	8.35 ^{+0.54} _{-0.29}	3.38 ^{+0.17} _{-0.22}	1.21 ^{+0.56} _{-1.03}	I	0	1.41	119	75
AP1115	8.40 ^{+0.10} _{-0.20}	3.22 ^{+0.02} _{-0.13}	0.60 ^{+0.10} _{-0.15}	8.65 ^{+0.10} _{-0.10}	3.22 ^{+0.09} _{-0.10}	0.26 ^{+0.22} _{-0.22}	I	0	1.56	199	157
AP1116	8.60 ^{+0.10} _{-0.10}	2.91 ^{+0.01} _{-0.03}	0.45 ^{+0.05} _{-0.30}	8.58 ^{+0.14} _{-0.14}	2.52 ^{+0.16} _{-0.15}	0.20 ^{+0.22} _{-0.20}	I	0	1.35	54	24
AP1118	7.20 ^{+0.40} _{-0.30}	2.88 ^{+0.02} _{-0.04}	0.55 ^{+0.05} _{-0.15}	7.19 ^{+0.39} _{-0.45}	3.14 ^{+0.11} _{-0.09}	0.50 ^{+0.25} _{-0.27}	I	0	1.30	137	106
AP1120	9.10 ^{+0.10} _{-0.00}	3.90 ^{+0.25} _{-0.03}	0.10 ^{+0.05} _{-0.10}	8.73 ^{+0.11} _{-0.11}	3.55 ^{+0.08} _{-0.08}	0.25 ^{+0.21} _{-0.21}	I	0	2.21	348	219
AP1121	9.40 ^{+0.00} _{-0.00}	4.50 ^{+0.05} _{-0.00}	0.00 ^{+0.05} _{-0.00}	9.29 ^{+0.10} _{-0.11}	4.53 ^{+0.07} _{-0.07}	0.12 ^{+0.12} _{-0.11}	I	0	1.92	187	292
AP1122	8.80 ^{+0.10} _{-0.00}	3.53 ^{+0.00} _{-0.05}	0.50 ^{+0.00} _{-0.25}	8.66 ^{+0.13} _{-0.13}	2.98 ^{+0.10} _{-0.08}	0.22 ^{+0.21} _{-0.20}	I	0	1.41	167	113
AP1125	8.00 ^{+0.00} _{-1.00}	3.17 ^{+0.03} _{-0.25}	1.05 ^{+0.20} _{-0.10}	8.20 ^{+0.10} _{-0.10}	3.63 ^{+0.08} _{-0.08}	0.31 ^{+0.20} _{-0.22}	I	0	1.66	275	271
AP1128	8.40 ^{+0.00} _{-0.00}	3.10 ^{+0.02} _{-0.05}	0.45 ^{+0.05} _{-0.10}	8.56 ^{+0.11} _{-0.09}	2.92 ^{+0.11} _{-0.09}	0.17 ^{+0.18} _{-0.16}	I	0	1.31	154	125
AP1129	9.10 ^{+0.00} _{-0.10}	4.06 ^{+0.00} _{-0.09}	0.20 ^{+0.15} _{-0.00}	8.88 ^{+0.07} _{-0.07}	3.44 ^{+0.07} _{-0.07}	0.08 ^{+0.11} _{-0.08}	I	0	2.10	349	236
AP1130	7.70 ^{+0.00} _{-0.40}	3.07 ^{+0.01} _{-0.07}	1.95 ^{+0.15} _{-0.00}	7.41 ^{+0.03} _{-0.04}	3.58 ^{+0.08} _{-0.06}	1.93 ^{+0.12} _{-0.14}	I	0	1.20	69	59
AP1131	8.10 ^{+0.10} _{-0.60}	3.26 ^{+0.02} _{-0.05}	0.55 ^{+0.25} _{-0.00}	8.02 ^{+0.26} _{-0.38}	3.27 ^{+0.23} _{-0.17}	0.60 ^{+0.70} _{-0.47}	I	0	1.95	257	229
AP1132	6.60 ^{+0.10} _{-0.00}	3.11 ^{+0.00} _{-0.03}	0.55 ^{+0.00} _{-0.05}	6.92 ^{+0.13} _{-0.12}	3.00 ^{+0.17} _{-0.21}	0.26 ^{+0.11} _{-0.11}	I	0	3.52	360	225
AP1134	8.90 ^{+0.00} _{-1.20}	2.82 ^{+0.00} _{-0.24}	0.05 ^{+1.25} _{-0.15}	7.60 ^{+0.98} _{-0.95}	2.76 ^{+0.35} _{-0.40}	1.09 ^{+0.79} _{-0.79}	I	0	1.42	67	41
AP1135	8.40 ^{+0.00} _{-0.30}	3.10 ^{+0.02} _{-0.06}	0.30 ^{+0.20} _{-0.10}	8.43 ^{+0.15} _{-0.15}	3.11 ^{+0.12} _{-0.11}	0.41 ^{+0.31} _{-0.31}	I	0	1.75	238	238
AP1136	7.50 ^{+0.40} _{-0.20}	2.85 ^{+0.03} _{-0.03}	0.80 ^{+0.05} _{-0.10}	7.37 ^{+0.30} _{-0.26}	3.11 ^{+0.09} _{-0.07}	1.17 ^{+0.24} _{-0.20}	I	0	1.52	106	67
AP1137	7.20 ^{+0.10} _{-0.20}	3.52 ^{+0.05} _{-0.10}	2.95 ^{+0.05} _{-0.05}	0.00 ^{+0.00} _{-0.00}	0.00 ^{+0.00} _{-0.00}	0.00 ^{+0.00} _{-0.00}	I	0	3.15	263	801
AP1138	8.70 ^{+0.00} _{-0.60}	3.32 ^{+0.01} _{-0.19}	0.60 ^{+0.45} _{-0.15}	8.46 ^{+0.12} _{-0.11}	2.70 ^{+0.14} _{-0.15}	0.30 ^{+0.26} _{-0.24}	I	0	1.59	105	53
AP1141	8.30 ^{+0.10} _{-0.00}	2.99 ^{+0.03} _{-0.03}	0.45 ^{+0.05} _{-0.10}	8.35 ^{+0.11} _{-0.11}	2.94 ^{+0.12} _{-0.12}	0.21 ^{+0.22} _{-0.20}	I	0	1.43	150	130
AP1144	8.40 ^{+0.10} _{-0.00}	3.27 ^{+0.02} _{-0.11}	0.75 ^{+0.05} _{-0.30}	8.52 ^{+0.12} _{-0.12}	2.99 ^{+0.09} _{-0.09}	0.17 ^{+0.20} _{-0.17}	I	0	1.46	136	114
AP1146	10.10 ^{+0.00} _{-1.00}	4.86 ^{+0.03} _{-1.78}	0.15 ^{+0.50} _{-0.05}	8.71 ^{+0.18} _{-0.20}	3.25 ^{+0.11} _{-0.11}	0.83 ^{+0.30} _{-0.28}	I	0	1.22	103	60
AP1148	7.40 ^{+0.10} _{-0.30}	2.92 ^{+0.01} _{-0.05}	0.75 ^{+0.10} _{-0.05}	6.93 ^{+0.12} _{-0.11}	2.86 ^{+0.30} _{-0.38}	0.59 ^{+0.10} _{-0.10}	I	0	1.52	159	146
AP1149	9.20 ^{+0.10} _{-1.20}	3.52 ^{+0.10} _{-1.27}	0.15 ^{+1.65} _{-0.00}	0.00 ^{+0.00} _{-0.00}	0.00 ^{+0.00} _{-0.00}	0.00 ^{+0.00} _{-0.00}	I	0	1.51	146	77
AP1150	7.60 ^{+0.10} _{-0.60}	2.87 ^{+0.02} _{-0.04}	0.60 ^{+0.10} _{-0.05}	6.98 ^{+0.47} _{-0.59}	2.78 ^{+0.13} _{-0.13}	0.82 ^{+0.23} _{-0.23}	I	0	1.46	81	44
AP1151	9.10 ^{+0.10} _{-0.60}	3.59 ^{+0.04} _{-0.26}	0.20 ^{+1.25} _{-0.10}	8.74 ^{+0.12} _{-0.12}	3.02 ^{+0.08} _{-0.08}	0.21 ^{+0.18} _{-0.18}	I	0	1.17	131	73
AP1152	10.10 ^{+0.20} _{-1.40}	4.53 ^{+0.33} _{-1.31}	0.20 ^{+1.45} _{-0.20}	8.86 ^{+0.79} _{-0.83}	3.64 ^{+0.22} _{-0.21}	1.65 ^{+1.00} _{-0.84}	I	0	1.20	85	40
AP1153	9.30 ^{+0.30} _{-2.10}	4.30 ^{+0.54} _{-4.30}	0.50 ^{+1.95} _{-0.10}	9.53 ^{+0.70} _{-0.83}	4.62 ^{+0.17} _{-0.19}	1.15 ^{+0.86} _{-0.73}	I	0	1.32	147	199
AP1154	7.60 ^{+0.10} _{-0.10}	3.45 ^{+0.01} _{-0.02}	1.00 ^{+0.05} _{-0.05}	7.04 ^{+0.37} _{-0.38}	3.19 ^{+0.14} _{-0.12}	0.82 ^{+0.19} _{-0.19}	I	0	1.84	237	181
AP1155	8.40 ^{+0.00} _{-0.80}	3.23 ^{+0.02} _{-0.16}	0.55 ^{+0.25} _{-0.00}	7.91 ^{+0.09} _{-0.08}	2.96 ^{+0.10} _{-0.11}	0.56 ^{+0.17} _{-0.16}	I	0	1.31	122	101
AP1156	8.40 ^{+0.00} _{-0.60}	3.69 ^{+0.02} _{-0.13}	1.20 ^{+0.45} _{-0.05}	9.13 ^{+0.10} _{-0.10}	3.67 ^{+0.10} _{-0.12}	0.09 ^{+0.10} _{-0.09}	I	0	1.80	223	151
AP1158	9.00 ^{+0.00} _{-0.00}	3.37 ^{+0.00} _{-0.07}	0.25 ^{+0.00} _{-0.15}	9.07 ^{+0.23} _{-0.05}	3.21 ^{+0.12} _{-0.14}	0.21 ^{+0.03} _{-0.21}	I	0	1.54	99	44
AP1159	7.80 ^{+0.10} _{-0.30}	3.52 ^{+0.00} _{-0.09}	1.35 ^{+0.05} _{-0.05}	7.74 ^{+0.26} _{-0.15}	3.72 ^{+0.16} _{-0.12}	1.51 ^{+0.29} _{-0.31}	I	0	1.73	250	173

Table 1 (cont'd)

AP ID ^a	CMD Best Fit Parameters ^b			Integrated Best Fit Parameters ^c			Best ^d Flag ^e	Rap ^f	N _{stars} ^g	N _{bg} ^h	
	log(<i>t</i> [Myr])	log(<i>M</i> [<i>M</i> _⊙])	<i>A_V</i> [mag]	log(<i>t</i> [Myr])	log(<i>M</i> [<i>M</i> _⊙])	<i>A_V</i> [mag]					
AP1160	8.40 ^{+0.00} _{-0.20}	3.52 ^{+0.03} _{-0.04}	1.35 ^{+0.25} _{-0.05}	8.67 ^{+0.13} _{-0.14}	3.00 ^{+0.10} _{-0.09}	0.39 ^{+0.24} _{-0.24}	I	0	1.38	140	105
AP1161	8.10 ^{+0.00} _{-0.70}	3.15 ^{+0.01} _{-0.16}	1.60 ^{+0.20} _{-0.05}	9.17 ^{+0.12} _{-0.12}	3.38 ^{+0.13} _{-0.12}	0.04 ^{+0.08} _{-0.04}	I	0	1.36	127	60
AP1163	7.90 ^{+0.10} _{-0.10}	3.42 ^{+0.03} _{-0.03}	1.30 ^{+0.15} _{-0.00}	8.09 ^{+0.18} _{-0.16}	3.68 ^{+0.13} _{-0.13}	1.62 ^{+0.33} _{-0.33}	I	0	1.35	145	87
AP1164	8.30 ^{+0.10} _{-0.00}	3.27 ^{+0.02} _{-0.04}	0.95 ^{+0.05} _{-0.10}	7.51 ^{+0.44} _{-1.10}	3.51 ^{+0.26} _{-0.25}	1.93 ^{+0.51} _{-0.42}	I	0	1.75	185	135
AP1166	7.50 ^{+0.10} _{-0.20}	3.49 ^{+0.03} _{-0.03}	1.90 ^{+0.10} _{-0.10}	6.97 ^{+0.24} _{-0.22}	3.61 ^{+0.17} _{-0.14}	2.33 ^{+0.15} _{-0.11}	I	0	1.52	171	124
AP1168	9.10 ^{+0.00} _{-0.20}	3.45 ^{+0.22} _{-0.09}	0.00 ^{+1.65} _{-0.05}	7.55 ^{+0.67} _{-0.79}	3.20 ^{+0.23} _{-0.20}	1.43 ^{+0.70} _{-0.79}	I	0	1.33	138	83
AP1169	7.40 ^{+0.30} _{-0.10}	3.63 ^{+0.01} _{-0.30}	3.00 ^{+0.00} _{-0.75}	8.19 ^{+0.16} _{-0.21}	3.28 ^{+0.12} _{-0.09}	0.91 ^{+0.38} _{-0.27}	I	0	1.22	121	71
AP1170	8.40 ^{+0.00} _{-0.60}	3.41 ^{+0.03} _{-0.17}	0.65 ^{+0.25} _{-0.05}	8.54 ^{+0.07} _{-0.07}	3.02 ^{+0.09} _{-0.08}	0.07 ^{+0.11} _{-0.07}	I	0	1.70	238	202
AP1171	10.10 ^{+0.00} _{-0.00}	5.11 ^{+0.03} _{-0.01}	0.00 ^{+0.05} _{-0.00}	8.13 ^{+0.11} _{-0.13}	3.65 ^{+0.11} _{-0.10}	1.82 ^{+0.26} _{-0.21}	I	0	1.77	143	87
AP1172	8.30 ^{+0.20} _{-0.00}	3.25 ^{+0.02} _{-0.04}	0.85 ^{+0.05} _{-0.35}	8.79 ^{+0.13} _{-0.13}	3.19 ^{+0.11} _{-0.11}	0.38 ^{+0.23} _{-0.24}	I	0	1.44	139	111
AP1174	8.20 ^{+0.20} _{-0.10}	3.16 ^{+0.00} _{-0.09}	1.35 ^{+0.00} _{-0.30}	9.26 ^{+0.12} _{-0.10}	3.31 ^{+0.06} _{-0.05}	0.17 ^{+0.20} _{-0.16}	I	0	1.38	74	44
AP1175	8.70 ^{+0.00} _{-0.40}	3.35 ^{+0.00} _{-0.13}	0.35 ^{+0.50} _{-0.10}	7.75 ^{+0.08} _{-0.09}	3.48 ^{+0.09} _{-0.09}	1.66 ^{+0.18} _{-0.15}	I	0	1.58	186	137
AP1176	10.10 ^{+0.00} _{-0.20}	5.24 ^{+0.00} _{-0.60}	0.10 ^{+0.25} _{-0.00}	7.82 ^{+0.10} _{-0.09}	3.00 ^{+0.09} _{-0.08}	0.64 ^{+0.17} _{-0.18}	I	0	1.44	142	92
AP1177	9.00 ^{+0.00} _{-0.90}	3.59 ^{+0.00} _{-0.31}	0.30 ^{+1.60} _{-0.05}	8.68 ^{+0.25} _{-0.25}	3.07 ^{+0.16} _{-0.15}	0.55 ^{+0.36} _{-0.38}	I	0	1.29	125	76
AP1178	9.10 ^{+0.00} _{-0.00}	3.66 ^{+0.03} _{-0.09}	0.35 ^{+0.00} _{-0.15}	9.07 ^{+0.56} _{-0.78}	3.89 ^{+0.15} _{-0.14}	0.86 ^{+0.89} _{-0.64}	I	0	2.07	191	119
AP1179	7.10 ^{+0.60} _{-0.30}	2.72 ^{+0.08} _{-0.09}	1.15 ^{+0.05} _{-0.15}	7.87 ^{+0.20} _{-0.21}	2.97 ^{+0.11} _{-0.11}	0.73 ^{+0.28} _{-0.28}	I	0	1.27	131	99
AP1180	9.10 ^{+0.00} _{-0.10}	3.84 ^{+0.00} _{-0.25}	0.40 ^{+0.10} _{-0.10}	8.75 ^{+0.32} _{-0.34}	3.23 ^{+0.15} _{-0.15}	0.83 ^{+0.43} _{-0.46}	I	0	1.35	103	72
AP1181	7.40 ^{+0.10} _{-0.50}	2.96 ^{+0.03} _{-0.03}	1.10 ^{+0.15} _{-0.05}	6.77 ^{+0.47} _{-0.49}	3.13 ^{+0.20} _{-0.16}	1.51 ^{+0.15} _{-0.15}	I	0	1.35	138	125
AP1183	7.00 ^{+0.10} _{-0.10}	3.90 ^{+0.01} _{-0.07}	3.00 ^{+0.00} _{-0.05}	9.50 ^{+0.11} _{-0.09}	4.84 ^{+0.05} _{-0.06}	0.09 ^{+0.15} _{-0.09}	I	0	1.30	184	205
AP1184	7.10 ^{+0.00} _{-0.30}	3.56 ^{+0.00} _{-0.02}	0.95 ^{+0.10} _{-0.00}	6.52 ^{+0.12} _{-0.10}	3.63 ^{+0.27} _{-0.24}	0.59 ^{+0.11} _{-0.12}	I	0	4.99	740	485
AP1186	7.10 ^{+0.20} _{-0.40}	3.11 ^{+0.02} _{-0.07}	2.00 ^{+0.15} _{-0.10}	7.76 ^{+0.04} _{-0.04}	3.38 ^{+0.05} _{-0.04}	1.07 ^{+0.09} _{-0.09}	I	0	1.44	132	122
AP1187	8.30 ^{+0.10} _{-0.00}	2.81 ^{+0.01} _{-0.02}	0.45 ^{+0.05} _{-0.05}	8.18 ^{+0.11} _{-0.10}	2.56 ^{+0.18} _{-0.18}	0.26 ^{+0.24} _{-0.23}	I	0	1.39	70	40
AP1189	8.10 ^{+0.10} _{-0.30}	3.15 ^{+0.01} _{-0.11}	0.80 ^{+0.00} _{-0.20}	7.93 ^{+0.17} _{-0.18}	3.23 ^{+0.13} _{-0.13}	1.07 ^{+0.31} _{-0.29}	I	0	1.32	124	108
AP1190	8.50 ^{+0.20} _{-0.00}	3.03 ^{+0.00} _{-0.08}	0.85 ^{+0.00} _{-0.40}	8.68 ^{+0.16} _{-0.17}	2.75 ^{+0.14} _{-0.13}	0.35 ^{+0.31} _{-0.30}	I	0	1.44	97	52
AP1191	9.10 ^{+0.00} _{-0.10}	3.84 ^{+0.14} _{-0.06}	0.85 ^{+0.25} _{-0.00}	9.20 ^{+0.85} _{-0.65}	3.69 ^{+0.24} _{-0.16}	1.24 ^{+0.73} _{-0.80}	I	0	1.71	146	66
AP1197	8.30 ^{+0.00} _{-0.60}	2.97 ^{+0.00} _{-0.12}	0.55 ^{+0.40} _{-0.05}	9.16 ^{+0.18} _{-0.06}	3.37 ^{+0.11} _{-0.08}	0.09 ^{+0.05} _{-0.09}	I	0	1.42	131	105
AP1199	8.00 ^{+0.10} _{-0.20}	3.31 ^{+0.02} _{-0.05}	1.05 ^{+0.10} _{-0.05}	7.62 ^{+0.99} _{-1.06}	3.34 ^{+0.31} _{-0.32}	1.12 ^{+0.67} _{-0.69}	I	0	1.70	247	203
AP1200	6.60 ^{+0.60} _{-0.00}	3.01 ^{+0.00} _{-0.02}	1.15 ^{+0.00} _{-0.15}	7.51 ^{+0.03} _{-0.04}	3.23 ^{+0.09} _{-0.09}	0.19 ^{+0.07} _{-0.07}	I	0	2.68	231	188
AP1201	9.40 ^{+0.00} _{-0.00}	4.54 ^{+0.01} _{-0.00}	0.00 ^{+0.00} _{-0.00}	9.19 ^{+0.07} _{-0.08}	4.77 ^{+0.06} _{-0.06}	0.20 ^{+0.11} _{-0.11}	I	0	2.18	249	272
AP1206	8.10 ^{+0.00} _{-0.00}	3.10 ^{+0.02} _{-0.04}	0.60 ^{+0.10} _{-0.10}	8.08 ^{+0.17} _{-0.17}	2.99 ^{+0.17} _{-0.20}	0.57 ^{+0.28} _{-0.30}	I	0	1.42	130	101
AP1207	7.90 ^{+0.10} _{-0.20}	2.90 ^{+0.00} _{-0.05}	0.60 ^{+0.10} _{-0.05}	6.57 ^{+0.56} _{-0.48}	3.04 ^{+0.27} _{-0.20}	1.70 ^{+0.19} _{-0.13}	I	0	1.40	81	52
AP1212	9.20 ^{+0.00} _{-0.10}	4.04 ^{+0.05} _{-0.37}	0.15 ^{+0.25} _{-0.00}	8.29 ^{+0.68} _{-0.23}	3.68 ^{+0.13} _{-0.22}	1.27 ^{+0.45} _{-1.19}	I	0	1.39	172	89
AP1213	9.00 ^{+0.00} _{-0.00}	4.34 ^{+0.00} _{-0.03}	0.70 ^{+0.15} _{-0.00}	8.77 ^{+0.25} _{-0.27}	3.46 ^{+0.13} _{-0.13}	0.66 ^{+0.38} _{-0.41}	I	0	1.74	265	124

Table 1 (cont'd)

AP ID ^a	CMD Best Fit Parameters ^b			Integrated Best Fit Parameters ^c			Best ^d Flag ^e	R _{ap} ^f	N _{stars} ^g	N _{bg} ^h	
	log(<i>t</i> [Myr])	log(<i>M</i> [<i>M</i> _⊙])	<i>A_V</i> [mag]	log(<i>t</i> [Myr])	log(<i>M</i> [<i>M</i> _⊙])	<i>A_V</i> [mag]					
AP1214	8.40 ^{+0.00} _{-0.00}	3.24 ^{+0.00} _{-0.04}	0.85 ^{+0.00} _{-0.10}	8.51 ^{+0.15} _{-0.14}	3.13 ^{+0.14} _{-0.12}	0.70 ^{+0.33} _{-0.32}	I	0	1.27	103	70
AP1215	8.10 ^{+0.30} _{-0.20}	2.95 ^{+0.04} _{-0.06}	0.85 ^{+0.10} _{-0.15}	8.60 ^{+0.40} _{-0.38}	3.04 ^{+0.15} _{-0.14}	0.82 ^{+0.50} _{-0.57}	I	0	1.38	71	40
AP1217	8.80 ^{+0.00} _{-0.50}	3.56 ^{+0.04} _{-0.12}	0.35 ^{+0.70} _{-0.00}	7.80 ^{+0.07} _{-0.08}	2.27 ^{+0.19} _{-0.12}	0.42 ^{+0.29} _{-0.22}	I	0	1.70	208	156
AP1218	7.90 ^{+0.10} _{-0.40}	2.92 ^{+0.01} _{-0.05}	0.50 ^{+0.10} _{-0.05}	7.51 ^{+0.29} _{-0.27}	3.01 ^{+0.10} _{-0.10}	0.86 ^{+0.27} _{-0.26}	I	0	1.54	186	163
AP1219	7.60 ^{+0.40} _{-0.40}	3.06 ^{+0.10} _{-0.07}	0.85 ^{+0.10} _{-0.10}	7.64 ^{+0.41} _{-0.31}	3.13 ^{+0.18} _{-0.14}	1.22 ^{+0.48} _{-0.48}	I	0	1.47	154	123
AP1220	9.40 ^{+0.00} _{-0.10}	4.43 ^{+0.00} _{-0.22}	0.00 ^{+0.05} _{-0.00}	9.33 ^{+0.21} _{-0.19}	3.90 ^{+0.11} _{-0.12}	0.26 ^{+0.22} _{-0.22}	I	0	1.65	223	156
AP1221	6.80 ^{+0.40} _{-0.10}	2.92 ^{+0.02} _{-0.02}	0.85 ^{+0.05} _{-0.10}	6.76 ^{+0.42} _{-0.10}	3.00 ^{+0.12} _{-0.11}	0.82 ^{+0.13} _{-0.11}	I	0	1.18	104	78
AP1222	7.90 ^{+0.10} _{-0.00}	3.54 ^{+0.02} _{-0.07}	1.35 ^{+0.05} _{-0.15}	8.29 ^{+0.09} _{-0.12}	3.61 ^{+0.12} _{-0.10}	0.89 ^{+0.26} _{-0.20}	I	0	1.52	172	119
AP1224	7.10 ^{+0.10} _{-0.10}	2.97 ^{+0.00} _{-0.02}	0.50 ^{+0.00} _{-0.10}	7.03 ^{+0.12} _{-0.13}	2.88 ^{+0.24} _{-0.27}	0.27 ^{+0.10} _{-0.10}	I	0	1.35	140	115
AP1227	8.40 ^{+0.00} _{-1.20}	2.95 ^{+0.00} _{-0.18}	0.35 ^{+0.35} _{-0.05}	8.35 ^{+0.09} _{-0.09}	2.78 ^{+0.12} _{-0.10}	0.14 ^{+0.16} _{-0.14}	I	0	1.36	113	74
AP1229	7.90 ^{+0.10} _{-0.50}	2.71 ^{+0.01} _{-0.06}	0.45 ^{+0.15} _{-0.00}	6.73 ^{+0.33} _{-0.46}	3.03 ^{+0.21} _{-0.23}	1.98 ^{+0.21} _{-0.16}	I	0	1.47	112	90
AP1230	6.60 ^{+0.30} _{-0.00}	2.91 ^{+0.01} _{-0.02}	1.00 ^{+0.05} _{-0.10}	6.93 ^{+0.20} _{-0.16}	3.23 ^{+0.26} _{-0.26}	0.68 ^{+0.11} _{-0.12}	I	0	2.11	235	232
AP1231	8.20 ^{+0.00} _{-0.10}	3.22 ^{+0.02} _{-0.03}	0.40 ^{+0.15} _{-0.00}	8.10 ^{+0.14} _{-0.14}	3.27 ^{+0.11} _{-0.12}	0.44 ^{+0.26} _{-0.28}	I	0	1.63	255	227
AP1234	9.30 ^{+0.00} _{-0.00}	4.51 ^{+0.00} _{-0.07}	0.20 ^{+0.05} _{-0.05}	8.12 ^{+0.09} _{-0.15}	4.27 ^{+0.07} _{-0.07}	2.05 ^{+0.23} _{-0.17}	I	0	2.53	441	329
AP1235	9.10 ^{+0.00} _{-0.80}	3.33 ^{+0.06} _{-0.28}	0.10 ^{+2.00} _{-0.20}	9.65 ^{+0.03} _{-0.03}	3.48 ^{+0.05} _{-0.02}	0.27 ^{+0.09} _{-0.06}	I	0	1.34	83	39
AP1239	8.60 ^{+0.10} _{-0.00}	3.16 ^{+0.04} _{-0.03}	0.55 ^{+0.15} _{-0.25}	8.23 ^{+0.56} _{-0.31}	3.34 ^{+0.18} _{-0.19}	1.19 ^{+0.61} _{-1.03}	I	0	1.59	136	100
AP1242	8.00 ^{+0.00} _{-0.30}	3.27 ^{+0.01} _{-0.07}	1.50 ^{+0.15} _{-0.00}	8.78 ^{+0.10} _{-0.08}	3.03 ^{+0.08} _{-0.07}	0.19 ^{+0.16} _{-0.17}	I	0	1.45	148	98
AP1243	8.10 ^{+0.10} _{-0.20}	3.25 ^{+0.00} _{-0.09}	0.75 ^{+0.00} _{-0.10}	6.90 ^{+0.19} _{-0.17}	3.18 ^{+0.17} _{-0.14}	0.52 ^{+0.13} _{-0.12}	I	0	1.46	170	145
AP1244	9.60 ^{+0.10} _{-1.90}	4.66 ^{+0.11} _{-0.49}	0.00 ^{+2.95} _{-0.00}	9.85 ^{+0.19} _{-0.18}	4.92 ^{+0.10} _{-0.11}	0.16 ^{+0.10} _{-0.15}	I	0	1.90	197	129
AP1245	9.20 ^{+0.50} _{-0.00}	4.42 ^{+0.39} _{-0.01}	0.75 ^{+0.40} _{-0.15}	8.56 ^{+0.88} _{-0.66}	4.14 ^{+0.15} _{-0.08}	1.70 ^{+0.86} _{-1.05}	I	0	1.88	299	253
AP1246	9.40 ^{+0.00} _{-2.00}	3.91 ^{+0.05} _{-0.79}	0.00 ^{+2.95} _{-0.05}	8.48 ^{+0.79} _{-0.56}	3.46 ^{+0.15} _{-0.14}	1.05 ^{+0.79} _{-0.99}	I	0	1.48	109	37
AP1247	8.40 ^{+0.00} _{-0.50}	3.37 ^{+0.05} _{-0.09}	1.25 ^{+0.35} _{-0.15}	9.02 ^{+0.12} _{-0.10}	3.03 ^{+0.10} _{-0.10}	0.06 ^{+0.10} _{-0.06}	I	0	1.11	73	48
AP1251	6.70 ^{+0.10} _{-0.10}	3.38 ^{+0.02} _{-0.01}	1.45 ^{+0.05} _{-0.05}	6.65 ^{+0.17} _{-0.19}	3.71 ^{+0.28} _{-0.27}	1.26 ^{+0.09} _{-0.09}	I	0	2.87	517	447
AP1253	7.20 ^{+0.20} _{-0.20}	2.93 ^{+0.00} _{-0.03}	1.25 ^{+0.00} _{-0.10}	6.86 ^{+0.14} _{-0.13}	2.80 ^{+0.28} _{-0.28}	1.11 ^{+0.11} _{-0.11}	I	0	1.39	117	88
AP1254	8.80 ^{+0.00} _{-0.10}	3.20 ^{+0.03} _{-0.03}	0.05 ^{+0.30} _{-0.00}	8.80 ^{+0.04} _{-0.04}	2.73 ^{+0.06} _{-0.06}	0.01 ^{+0.07} _{-0.01}	I	0	1.36	95	61
AP1255	9.50 ^{+0.00} _{-0.00}	4.69 ^{+0.01} _{-0.00}	0.00 ^{+0.00} _{-0.00}	9.26 ^{+0.13} _{-0.10}	5.17 ^{+0.05} _{-0.05}	0.34 ^{+0.14} _{-0.15}	I	0	2.72	318	493
AP1256	9.10 ^{+0.00} _{-0.10}	3.58 ^{+0.02} _{-0.09}	0.05 ^{+0.25} _{-0.00}	9.12 ^{+0.20} _{-0.09}	3.44 ^{+0.14} _{-0.14}	0.29 ^{+0.11} _{-0.25}	I	0	1.66	128	60
AP1259	8.10 ^{+0.00} _{-0.30}	3.35 ^{+0.00} _{-0.08}	1.40 ^{+0.10} _{-0.00}	8.14 ^{+0.08} _{-0.10}	3.27 ^{+0.10} _{-0.09}	1.02 ^{+0.19} _{-0.17}	I	0	1.39	119	76
AP1260	9.40 ^{+0.10} _{-0.30}	4.44 ^{+0.07} _{-0.41}	0.05 ^{+0.45} _{-0.00}	8.04 ^{+0.48} _{-0.38}	2.90 ^{+0.81} _{-0.76}	0.85 ^{+0.48} _{-0.58}	I	0	1.63	240	156
AP1263	7.10 ^{+0.00} _{-0.10}	3.11 ^{+0.00} _{-0.02}	0.70 ^{+0.00} _{-0.05}	7.61 ^{+0.11} _{-0.08}	3.31 ^{+0.03} _{-0.04}	0.07 ^{+0.08} _{-0.07}	I	0	1.63	213	199
AP1268	7.90 ^{+0.00} _{-0.00}	3.89 ^{+0.04} _{-0.02}	2.00 ^{+0.05} _{-0.05}	8.26 ^{+0.06} _{-0.20}	4.74 ^{+0.06} _{-0.04}	1.24 ^{+0.30} _{-0.07}	I	1	1.44	251	253
AP1269	8.30 ^{+0.50} _{-0.10}	3.22 ^{+0.17} _{-0.02}	0.75 ^{+0.05} _{-0.65}	7.62 ^{+0.92} _{-0.83}	2.99 ^{+0.16} _{-0.17}	1.02 ^{+0.51} _{-0.70}	I	0	1.36	97	34
AP1270	8.00 ^{+0.00} _{-0.70}	2.93 ^{+0.00} _{-0.08}	0.65 ^{+0.20} _{-0.05}	8.28 ^{+0.34} _{-0.34}	3.33 ^{+0.19} _{-0.19}	0.84 ^{+0.68} _{-0.69}	I	0	1.54	153	118

Table 1 (cont'd)

AP ID ^a	CMD Best Fit Parameters ^b			Integrated Best Fit Parameters ^c			Best ^d Flag ^e	Rap ^f	N _{stars} ^g	N _{bg} ^h	
	log(<i>t</i> [Myr])	log(<i>M</i> [<i>M</i> _⊙])	<i>A_V</i> [mag]	log(<i>t</i> [Myr])	log(<i>M</i> [<i>M</i> _⊙])	<i>A_V</i> [mag]					
AP1271	8.20 ^{+0.00} _{-0.10}	3.66 ^{+0.02} _{-0.05}	1.55 ^{+0.10} _{-0.00}	8.73 ^{+0.43} _{-0.80}	3.35 ^{+0.18} _{-0.16}	0.44 ^{+1.20} _{-0.44}	I	0	1.42	179	129
AP1272	7.30 ^{+0.10} _{-0.40}	2.86 ^{+0.00} _{-0.06}	1.00 ^{+0.10} _{-0.05}	6.69 ^{+0.07} _{-0.07}	2.73 ^{+0.29} _{-0.33}	1.22 ^{+0.12} _{-0.11}	I	0	1.67	156	130
AP1274	7.40 ^{+0.10} _{-0.10}	3.96 ^{+0.06} _{-0.08}	2.90 ^{+0.10} _{-0.05}	9.62 ^{+0.09} _{-0.12}	4.28 ^{+0.07} _{-0.07}	0.05 ^{+0.09} _{-0.05}	I	0	1.63	227	166
AP1276	7.80 ^{+0.00} _{-0.30}	3.43 ^{+0.03} _{-0.10}	2.05 ^{+0.15} _{-0.00}	8.81 ^{+0.56} _{-0.74}	3.62 ^{+0.13} _{-0.12}	0.74 ^{+1.00} _{-0.70}	I	0	1.44	159	98
AP1278	8.90 ^{+0.00} _{-0.00}	3.71 ^{+0.01} _{-0.03}	0.50 ^{+0.10} _{-0.05}	9.64 ^{+0.24} _{-0.25}	3.52 ^{+0.18} _{-0.16}	0.07 ^{+0.11} _{-0.07}	I	0	1.48	119	68
AP1280	7.90 ^{+0.00} _{-0.40}	3.59 ^{+0.00} _{-0.21}	2.55 ^{+0.20} _{-0.10}	8.16 ^{+0.11} _{-0.26}	3.30 ^{+0.24} _{-0.23}	1.16 ^{+0.50} _{-0.57}	I	0	1.17	87	38
AP1282	9.50 ^{+0.10} _{-0.10}	5.00 ^{+0.07} _{-0.07}	0.25 ^{+0.20} _{-0.00}	10.21 ^{+0.04} _{-0.04}	5.47 ^{+0.04} _{-0.04}	0.18 ^{+0.08} _{-0.07}	I	0	2.58	500	458
AP1283	9.10 ^{+0.00} _{-0.00}	3.90 ^{+0.04} _{-0.05}	0.20 ^{+0.20} _{-0.05}	9.48 ^{+0.39} _{-0.28}	4.11 ^{+0.15} _{-0.13}	0.64 ^{+0.28} _{-0.42}	I	0	1.60	185	122
AP1284	9.10 ^{+0.00} _{-0.00}	3.69 ^{+0.04} _{-0.03}	0.15 ^{+0.10} _{-0.10}	9.19 ^{+0.25} _{-0.16}	3.62 ^{+0.14} _{-0.14}	0.35 ^{+0.18} _{-0.29}	I	0	1.73	158	82
AP1285	8.80 ^{+0.10} _{-0.00}	3.47 ^{+0.00} _{-0.11}	0.75 ^{+0.00} _{-0.30}	8.64 ^{+0.15} _{-0.18}	3.14 ^{+0.16} _{-0.15}	0.97 ^{+0.36} _{-0.31}	I	0	1.35	88	39
AP1286	7.50 ^{+0.10} _{-0.60}	2.77 ^{+0.03} _{-0.06}	0.40 ^{+0.20} _{-0.05}	6.50 ^{+0.31} _{-0.36}	2.97 ^{+0.19} _{-0.23}	0.83 ^{+0.12} _{-0.12}	I	0	1.36	115	101
AP1287	8.80 ^{+0.00} _{-0.10}	3.12 ^{+0.07} _{-0.01}	0.10 ^{+0.45} _{-0.05}	8.59 ^{+0.13} _{-0.12}	2.53 ^{+0.16} _{-0.15}	0.20 ^{+0.19} _{-0.18}	I	0	1.52	87	41
AP1289	8.00 ^{+0.00} _{-0.60}	2.89 ^{+0.00} _{-0.11}	0.75 ^{+0.20} _{-0.05}	7.38 ^{+0.43} _{-0.40}	3.17 ^{+0.14} _{-0.12}	1.50 ^{+0.36} _{-0.35}	I	0	1.36	111	94
AP1290	8.90 ^{+0.00} _{-0.00}	3.89 ^{+0.03} _{-0.00}	0.20 ^{+0.10} _{-0.00}	8.96 ^{+0.08} _{-0.09}	3.50 ^{+0.08} _{-0.08}	0.16 ^{+0.14} _{-0.15}	I	0	1.59	223	124
AP1291	9.50 ^{+0.00} _{-2.10}	4.91 ^{+0.00} _{-0.55}	0.00 ^{+3.00} _{-0.00}	9.11 ^{+0.09} _{-0.10}	4.32 ^{+0.07} _{-0.06}	0.36 ^{+0.12} _{-0.14}	I	0	1.26	183	163
AP1292	7.80 ^{+0.00} _{-0.50}	3.31 ^{+0.01} _{-0.04}	1.15 ^{+0.30} _{-0.05}	7.59 ^{+0.12} _{-0.13}	3.75 ^{+0.06} _{-0.05}	1.18 ^{+0.14} _{-0.11}	I	0	1.44	164	131
AP1294	9.10 ^{+0.10} _{-0.00}	3.94 ^{+0.12} _{-0.07}	0.50 ^{+0.10} _{-0.10}	8.22 ^{+1.19} _{-0.52}	4.27 ^{+0.08} _{-0.08}	2.23 ^{+0.67} _{-1.50}	I	0	1.66	225	158
AP1296	9.10 ^{+0.00} _{-0.00}	3.95 ^{+0.01} _{-0.11}	0.55 ^{+0.00} _{-0.20}	8.75 ^{+0.39} _{-0.39}	3.56 ^{+0.18} _{-0.17}	0.67 ^{+0.55} _{-0.51}	I	0	1.97	246	184
AP1298	9.10 ^{+0.10} _{-0.00}	4.09 ^{+0.20} _{-0.05}	0.55 ^{+0.00} _{-0.20}	8.95 ^{+0.30} _{-0.56}	3.80 ^{+0.11} _{-0.11}	1.06 ^{+0.82} _{-0.46}	I	0	1.60	204	136
AP1301	9.00 ^{+0.00} _{-0.10}	3.68 ^{+0.10} _{-0.01}	0.00 ^{+0.25} _{-0.00}	8.89 ^{+0.07} _{-0.03}	3.15 ^{+0.09} _{-0.07}	0.06 ^{+0.10} _{-0.06}	I	0	1.33	176	118
AP1302	9.10 ^{+0.00} _{-0.20}	3.46 ^{+0.03} _{-0.11}	0.20 ^{+0.30} _{-0.00}	8.83 ^{+0.50} _{-0.63}	3.22 ^{+0.22} _{-0.19}	0.54 ^{+0.70} _{-0.49}	I	0	1.48	86	38
AP1304	7.90 ^{+0.80} _{-0.00}	3.41 ^{+0.08} _{-0.05}	1.25 ^{+0.05} _{-0.80}	8.64 ^{+0.23} _{-0.23}	3.28 ^{+0.13} _{-0.15}	0.34 ^{+0.33} _{-0.31}	I	0	1.90	278	226
AP1305	9.00 ^{+0.00} _{-0.10}	3.77 ^{+0.02} _{-0.11}	0.20 ^{+0.25} _{-0.10}	8.81 ^{+0.35} _{-0.39}	3.63 ^{+0.12} _{-0.10}	0.61 ^{+0.51} _{-0.48}	I	0	1.95	314	246
AP1308	10.00 ^{+0.00} _{-0.70}	4.39 ^{+0.01} _{-0.59}	0.45 ^{+0.55} _{-0.10}	9.12 ^{+0.74} _{-0.78}	3.62 ^{+0.20} _{-0.17}	1.25 ^{+0.90} _{-0.77}	I	0	1.61	83	45
AP1309	10.00 ^{+0.10} _{-2.40}	4.62 ^{+0.14} _{-4.62}	0.00 ^{+2.45} _{-0.05}	9.90 ^{+0.14} _{-0.13}	4.87 ^{+0.06} _{-0.06}	0.23 ^{+0.14} _{-0.16}	I	0	1.26	61	141
AP1310	8.20 ^{+0.00} _{-0.10}	3.32 ^{+0.00} _{-0.08}	0.95 ^{+0.10} _{-0.05}	8.26 ^{+0.23} _{-0.21}	3.23 ^{+0.17} _{-0.16}	0.54 ^{+0.43} _{-0.45}	I	0	1.67	201	146
AP1311	7.50 ^{+1.50} _{-0.50}	2.55 ^{+0.95} _{-2.55}	1.40 ^{+0.95} _{-0.50}	7.18 ^{+0.04} _{-0.04}	3.60 ^{+0.03} _{-0.04}	1.57 ^{+0.09} _{-0.07}	I	0	1.71	90	92
AP1312	6.60 ^{+0.60} _{-0.00}	2.91 ^{+0.03} _{-0.01}	1.45 ^{+0.00} _{-0.15}	7.00 ^{+0.13} _{-0.12}	2.74 ^{+0.33} _{-0.37}	0.98 ^{+0.11} _{-0.11}	I	0	1.90	203	169
AP1313	9.40 ^{+0.00} _{-0.10}	4.70 ^{+0.00} _{-0.12}	0.30 ^{+0.05} _{-0.00}	0.00 ^{+0.00} _{-0.00}	0.00 ^{+0.00} _{-0.00}	0.00 ^{+0.00} _{-0.00}	I	0	3.40	654	686
AP1314	7.80 ^{+0.00} _{-0.50}	3.20 ^{+0.01} _{-0.08}	0.55 ^{+0.05} _{-0.05}	7.62 ^{+0.28} _{-0.02}	3.01 ^{+0.19} _{-0.14}	0.30 ^{+0.24} _{-0.26}	I	0	2.04	290	251
AP1315	9.20 ^{+0.60} _{-0.00}	4.37 ^{+0.44} _{-0.03}	1.10 ^{+0.00} _{-0.35}	7.59 ^{+0.04} _{-0.03}	2.28 ^{+0.05} _{-0.03}	0.02 ^{+0.07} _{-0.02}	I	0	1.68	195	167
AP1316	9.10 ^{+0.00} _{-0.00}	3.86 ^{+0.05} _{-0.10}	0.15 ^{+0.15} _{-0.05}	7.98 ^{+0.18} _{-0.20}	3.56 ^{+0.17} _{-0.14}	1.62 ^{+0.36} _{-0.33}	I	0	1.40	160	108
AP1318	9.70 ^{+0.00} _{-0.30}	4.96 ^{+0.00} _{-0.28}	0.00 ^{+0.10} _{-0.00}	9.89 ^{+0.10} _{-0.14}	5.00 ^{+0.06} _{-0.06}	0.19 ^{+0.10} _{-0.11}	I	0	1.92	190	267

Table 1 (cont'd)

AP ID ^a	CMD Best Fit Parameters ^b			Integrated Best Fit Parameters ^c			Best ^d Flag ^e	R _{ap} ^f	N _{stars} ^g	N _{bg} ^h	
	log(<i>t</i> [Myr])	log(<i>M</i> [<i>M</i> _⊙])	<i>A_V</i> [mag]	log(<i>t</i> [Myr])	log(<i>M</i> [<i>M</i> _⊙])	<i>A_V</i> [mag]					
AP1319	7.30 ^{+0.10} _{-0.30}	3.39 ^{+0.01} _{-0.05}	2.60 ^{+0.10} _{-0.05}	7.52 ^{+0.16} _{-0.15}	3.24 ^{+0.08} _{-0.08}	1.73 ^{+0.14} _{-0.14}	I	0	1.19	79	44
AP1320	8.50 ^{+0.10} _{-0.10}	2.96 ^{+0.01} _{-0.04}	0.30 ^{+0.15} _{-0.15}	8.13 ^{+0.05} _{-0.20}	3.27 ^{+0.06} _{-0.06}	1.27 ^{+0.28} _{-0.04}	I	0	1.17	82	53
AP1321	8.10 ^{+0.00} _{-0.20}	3.60 ^{+0.02} _{-0.04}	1.00 ^{+0.10} _{-0.05}	6.65 ^{+0.04} _{-0.09}	2.23 ^{+0.10} _{-0.14}	0.45 ^{+0.05} _{-0.11}	I	0	1.61	183	135
AP1322	7.70 ^{+0.30} _{-0.10}	3.49 ^{+0.02} _{-0.04}	2.05 ^{+0.05} _{-0.25}	8.11 ^{+0.58} _{-0.27}	3.61 ^{+0.17} _{-0.27}	1.54 ^{+0.52} _{-1.14}	I	0	1.46	155	78
AP1323	9.40 ^{+0.20} _{-0.10}	5.20 ^{+0.08} _{-0.09}	0.35 ^{+0.10} _{-0.10}	9.82 ^{+0.41} _{-0.89}	5.02 ^{+0.12} _{-0.20}	0.45 ^{+0.86} _{-0.42}	I	0	3.64	1121	668
AP1325	7.60 ^{+0.20} _{-0.60}	2.76 ^{+0.00} _{-0.06}	0.50 ^{+0.10} _{-0.05}	7.78 ^{+0.10} _{-0.08}	3.14 ^{+0.09} _{-0.10}	0.87 ^{+0.13} _{-0.13}	I	0	1.42	92	72
AP1326	8.40 ^{+0.00} _{-1.10}	2.82 ^{+0.15} _{-0.00}	0.20 ^{+1.10} _{-0.05}	8.53 ^{+0.16} _{-0.17}	3.10 ^{+0.12} _{-0.12}	0.43 ^{+0.35} _{-0.33}	I	0	1.30	138	121
AP1329	9.00 ^{+0.00} _{-0.10}	3.60 ^{+0.05} _{-0.06}	0.15 ^{+0.35} _{-0.00}	8.86 ^{+0.09} _{-0.09}	2.83 ^{+0.10} _{-0.11}	0.07 ^{+0.11} _{-0.07}	I	0	1.35	128	89
AP1330	9.90 ^{+0.00} _{-0.20}	5.11 ^{+0.00} _{-0.14}	0.00 ^{+0.10} _{-0.00}	9.73 ^{+0.14} _{-0.16}	5.32 ^{+0.08} _{-0.08}	0.14 ^{+0.11} _{-0.11}	I	0	2.44	284	346
AP1331	9.20 ^{+0.00} _{-0.06}	4.12 ^{+0.06} _{-0.08}	0.25 ^{+0.10} _{-0.00}	9.24 ^{+0.61} _{-0.69}	3.95 ^{+0.16} _{-0.14}	0.85 ^{+0.83} _{-0.63}	I	0	1.74	191	152
AP1332	9.60 ^{+0.20} _{-0.90}	4.66 ^{+0.05} _{-4.66}	0.40 ^{+0.85} _{-0.20}	7.63 ^{+1.10} _{-0.54}	3.24 ^{+1.01} _{-0.51}	2.39 ^{+0.40} _{-0.34}	I	0	1.36	181	135
AP1335	9.30 ^{+0.30} _{-0.00}	4.69 ^{+0.08} _{-4.69}	0.30 ^{+0.20} _{-0.20}	9.55 ^{+0.45} _{-0.46}	4.35 ^{+0.12} _{-0.12}	0.86 ^{+0.47} _{-0.43}	I	0	1.31	125	186
AP1336	8.40 ^{+0.00} _{-0.50}	2.99 ^{+0.03} _{-0.13}	0.75 ^{+0.40} _{-0.00}	9.75 ^{+0.39} _{-0.56}	3.99 ^{+0.15} _{-0.19}	0.40 ^{+0.49} _{-0.37}	I	0	1.30	125	96
AP1337	7.50 ^{+0.40} _{-0.60}	2.62 ^{+0.05} _{-0.06}	0.35 ^{+0.30} _{-0.00}	7.50 ^{+0.04} _{-0.03}	3.40 ^{+0.04} _{-0.03}	0.00 ^{+0.07} _{-0.00}	I	0	1.42	175	178
AP1338	8.70 ^{+0.10} _{-0.70}	3.78 ^{+0.08} _{-0.43}	1.50 ^{+0.70} _{-0.15}	7.99 ^{+0.14} _{-0.21}	2.55 ^{+0.23} _{-0.24}	0.38 ^{+0.29} _{-0.30}	I	0	1.58	180	114
AP1341	10.10 ^{+0.00} _{-0.00}	5.33 ^{+0.06} _{-0.01}	0.00 ^{+0.05} _{-0.00}	8.62 ^{+0.07} _{-0.06}	4.59 ^{+0.05} _{-0.04}	1.77 ^{+0.12} _{-0.13}	I	0	1.84	156	164
AP1343	9.10 ^{+0.00} _{-0.00}	3.84 ^{+0.08} _{-0.00}	0.15 ^{+0.15} _{-0.00}	8.94 ^{+0.16} _{-0.18}	3.91 ^{+0.08} _{-0.09}	0.92 ^{+0.22} _{-0.25}	I	0	2.23	275	150
AP1344	7.50 ^{+0.20} _{-0.40}	3.04 ^{+0.00} _{-0.07}	1.65 ^{+0.05} _{-0.15}	6.89 ^{+0.11} _{-0.10}	3.25 ^{+0.21} _{-0.22}	1.27 ^{+0.09} _{-0.07}	I	0	1.98	103	74
AP1345	8.70 ^{+0.10} _{-0.10}	3.44 ^{+0.03} _{-0.12}	0.65 ^{+0.25} _{-0.25}	8.31 ^{+0.11} _{-0.11}	2.76 ^{+0.15} _{-0.14}	0.22 ^{+0.22} _{-0.21}	I	0	1.56	160	121
AP1346	8.00 ^{+0.00} _{-0.30}	4.23 ^{+0.00} _{-0.31}	3.00 ^{+0.00} _{-0.15}	8.91 ^{+0.64} _{-1.07}	3.07 ^{+0.63} _{-1.02}	0.04 ^{+0.08} _{-0.04}	I	0	1.51	226	156
AP1351	9.80 ^{+0.10} _{-0.40}	4.76 ^{+0.07} _{-0.64}	0.45 ^{+0.15} _{-0.20}	9.55 ^{+0.25} _{-0.27}	4.35 ^{+0.10} _{-0.10}	0.71 ^{+0.31} _{-0.27}	I	0	1.58	217	130
AP1352	8.20 ^{+0.00} _{-0.60}	3.19 ^{+0.01} _{-0.08}	0.80 ^{+0.30} _{-0.05}	8.48 ^{+0.18} _{-0.16}	3.07 ^{+0.10} _{-0.10}	0.34 ^{+0.30} _{-0.30}	I	0	1.59	184	144
AP1353	9.10 ^{+0.10} _{-0.00}	3.85 ^{+0.28} _{-0.06}	0.40 ^{+0.20} _{-0.00}	8.62 ^{+0.75} _{-0.62}	3.65 ^{+0.16} _{-0.13}	1.10 ^{+0.86} _{-0.93}	I	0	1.60	207	104
AP1355	7.00 ^{+0.20} _{-0.30}	3.06 ^{+0.00} _{-0.03}	1.00 ^{+0.00} _{-0.05}	7.29 ^{+0.44} _{-0.49}	3.08 ^{+0.11} _{-0.09}	0.74 ^{+0.33} _{-0.33}	I	0	1.77	188	148
AP1356	8.80 ^{+0.10} _{-0.20}	3.01 ^{+0.06} _{-0.03}	0.20 ^{+0.50} _{-0.11}	8.68 ^{+0.15} _{-0.16}	2.94 ^{+0.10} _{-0.11}	0.63 ^{+0.26} _{-0.26}	I	0	1.41	69	32
AP1358	8.10 ^{+0.10} _{-0.50}	3.11 ^{+0.02} _{-0.16}	1.15 ^{+0.20} _{-0.20}	7.86 ^{+0.57} _{-0.55}	3.04 ^{+0.27} _{-0.25}	1.28 ^{+0.93} _{-0.86}	I	0	1.55	180	166
AP1360	7.30 ^{+0.10} _{-0.50}	2.76 ^{+0.03} _{-0.03}	0.45 ^{+0.15} _{-0.00}	7.60 ^{+0.06} _{-0.06}	2.96 ^{+0.14} _{-0.14}	0.22 ^{+0.19} _{-0.18}	I	0	1.50	153	137
AP1361	9.10 ^{+0.00} _{-1.80}	3.71 ^{+0.02} _{-0.60}	0.40 ^{+2.55} _{-0.05}	8.61 ^{+0.54} _{-0.41}	3.70 ^{+0.12} _{-0.13}	1.46 ^{+0.60} _{-0.74}	I	0	1.39	122	70
AP1364	7.90 ^{+0.20} _{-0.10}	3.37 ^{+0.05} _{-0.16}	1.90 ^{+0.15} _{-0.25}	9.30 ^{+0.38} _{-0.35}	3.70 ^{+0.15} _{-0.14}	0.39 ^{+0.36} _{-0.36}	I	0	1.53	179	120
AP1365	9.10 ^{+0.00} _{-0.00}	3.87 ^{+0.00} _{-0.06}	0.00 ^{+0.05} _{-0.00}	8.72 ^{+0.11} _{-0.12}	3.28 ^{+0.09} _{-0.09}	0.22 ^{+0.19} _{-0.19}	I	0	1.67	232	143
AP1367	9.40 ^{+0.00} _{-0.00}	5.31 ^{+0.00} _{-0.00}	0.00 ^{+0.00} _{-0.00}	9.94 ^{+0.06} _{-0.06}	5.49 ^{+0.04} _{-0.03}	0.14 ^{+0.10} _{-0.10}	I	0	1.59	317	284
AP1369	9.10 ^{+0.40} _{-1.90}	2.97 ^{+0.03} _{-2.97}	0.05 ^{+2.40} _{-0.20}	9.13 ^{+0.33} _{-0.27}	3.25 ^{+0.17} _{-0.16}	0.40 ^{+0.28} _{-0.34}	I	0	1.30	79	29
AP1370	9.00 ^{+0.00} _{-0.20}	3.35 ^{+0.08} _{-0.04}	0.00 ^{+0.45} _{-0.00}	8.67 ^{+0.11} _{-0.11}	3.06 ^{+0.08} _{-0.07}	0.66 ^{+0.20} _{-0.19}	I	0	1.20	83	50

Table 1 (cont'd)

AP ID ^a	CMD Best Fit Parameters ^b			Integrated Best Fit Parameters ^c			Best ^d Flag ^e	Rap ^f	N _{stars} ^g	N _{bg} ^h	
	log(<i>t</i> [Myr])	log(<i>M</i> [<i>M</i> _⊙])	<i>A_V</i> [mag]	log(<i>t</i> [Myr])	log(<i>M</i> [<i>M</i> _⊙])	<i>A_V</i> [mag]					
AP1371	8.40 ^{+0.00} _{-0.00}	2.91 ^{+0.02} _{-0.01}	0.65 ^{+0.05} _{-0.05}	9.05 ^{+0.09} _{-0.11}	3.01 ^{+0.10} _{-0.10}	0.07 ^{+0.11} _{-0.07}	I	0	1.14	43	16
AP1372	8.50 ^{+0.00} _{-0.20}	3.30 ^{+0.00} _{-0.11}	0.90 ^{+0.15} _{-0.10}	8.65 ^{+0.22} _{-0.22}	3.08 ^{+0.11} _{-0.10}	0.42 ^{+0.31} _{-0.32}	I	0	1.47	127	84
AP1373	8.70 ^{+0.10} _{-0.00}	3.42 ^{+0.02} _{-0.05}	0.65 ^{+0.15} _{-0.15}	9.10 ^{+0.04} _{-0.03}	3.94 ^{+0.05} _{-0.04}	0.01 ^{+0.07} _{-0.01}	I	0	1.50	105	32
AP1374	7.60 ^{+0.10} _{-0.80}	2.79 ^{+0.01} _{-0.12}	1.70 ^{+0.20} _{-0.10}	6.81 ^{+0.06} _{-0.06}	2.40 ^{+0.22} _{-0.25}	1.07 ^{+0.09} _{-0.07}	I	0	1.46	80	54
AP1375	9.60 ^{+0.00} _{-0.50}	4.04 ^{+0.00} _{-0.61}	0.05 ^{+0.25} _{-0.05}	7.89 ^{+0.09} _{-0.17}	2.39 ^{+0.10} _{-0.07}	0.10 ^{+0.07} _{-0.07}	I	0	1.79	122	36
AP1377	8.30 ^{+0.00} _{-0.00}	2.95 ^{+0.00} _{-0.09}	0.55 ^{+0.00} _{-0.20}	8.01 ^{+0.11} _{-0.12}	3.51 ^{+0.07} _{-0.08}	1.45 ^{+0.20} _{-0.20}	I	0	1.36	141	130
AP1378	7.70 ^{+0.10} _{-0.60}	3.01 ^{+0.01} _{-0.12}	1.55 ^{+0.20} _{-0.05}	8.46 ^{+0.25} _{-0.26}	2.94 ^{+0.15} _{-0.16}	0.44 ^{+0.49} _{-0.41}	I	0	1.24	111	75
AP1381	7.50 ^{+0.40} _{-0.10}	3.21 ^{+0.05} _{-0.02}	1.05 ^{+0.00} _{-0.10}	8.22 ^{+0.14} _{-0.15}	3.15 ^{+0.11} _{-0.10}	0.32 ^{+0.27} _{-0.27}	I	0	1.37	114	74
AP1382	8.10 ^{+0.20} _{-0.30}	3.58 ^{+0.03} _{-0.08}	1.60 ^{+0.15} _{-0.20}	8.46 ^{+0.09} _{-0.09}	3.15 ^{+0.11} _{-0.10}	0.26 ^{+0.22} _{-0.22}	I	0	1.67	240	183
AP1384	8.30 ^{+0.00} _{-0.20}	3.86 ^{+0.00} _{-0.11}	1.95 ^{+0.10} _{-0.00}	8.57 ^{+0.21} _{-0.16}	4.02 ^{+0.08} _{-0.09}	1.79 ^{+0.29} _{-0.33}	I	0	1.63	212	134
AP1385	9.10 ^{+0.00} _{-0.00}	3.97 ^{+0.01} _{-0.13}	0.60 ^{+0.20} _{-0.05}	9.27 ^{+0.71} _{-0.73}	4.20 ^{+0.21} _{-0.15}	1.50 ^{+0.91} _{-0.66}	I	0	1.63	205	156
AP1386	8.40 ^{+0.10} _{-1.40}	3.09 ^{+0.00} _{-0.22}	0.45 ^{+0.30} _{-0.05}	6.87 ^{+0.51} _{-0.58}	2.79 ^{+0.16} _{-0.16}	0.40 ^{+0.22} _{-0.24}	I	0	1.54	161	129
AP1388	8.80 ^{+0.00} _{-0.30}	3.50 ^{+0.04} _{-0.03}	0.30 ^{+0.75} _{-0.00}	9.02 ^{+0.24} _{-0.23}	3.49 ^{+0.15} _{-0.16}	0.40 ^{+0.23} _{-0.28}	I	0	1.50	167	108
AP1390	6.80 ^{+0.40} _{-0.10}	2.73 ^{+0.03} _{-0.02}	0.90 ^{+0.05} _{-0.05}	7.95 ^{+0.04} _{-0.03}	2.56 ^{+0.03} _{-0.04}	0.08 ^{+0.08} _{-0.07}	I	0	1.11	40	29
AP1391	9.40 ^{+0.20} _{-1.80}	3.91 ^{+0.75} _{-1.71}	0.10 ^{+1.35} _{-0.05}	7.95 ^{+0.18} _{-0.27}	3.73 ^{+0.16} _{-0.16}	2.08 ^{+0.46} _{-0.36}	I	0	1.56	125	66
AP1392	9.00 ^{+0.00} _{-0.80}	3.26 ^{+0.20} _{-0.28}	0.00 ^{+1.30} _{-0.15}	8.28 ^{+0.17} _{-0.16}	3.36 ^{+0.15} _{-0.17}	1.27 ^{+0.35} _{-0.39}	I	0	1.51	206	143
AP1393	8.70 ^{+0.10} _{-0.00}	3.54 ^{+0.03} _{-0.08}	0.70 ^{+0.15} _{-0.25}	8.06 ^{+0.16} _{-0.20}	3.39 ^{+0.16} _{-0.13}	1.57 ^{+0.44} _{-0.34}	I	0	1.15	110	81
AP1394	9.70 ^{+0.10} _{-0.20}	4.66 ^{+0.11} _{-0.13}	0.00 ^{+0.05} _{-0.00}	9.77 ^{+0.12} _{-0.11}	5.27 ^{+0.07} _{-0.07}	0.10 ^{+0.09} _{-0.09}	I	0	2.02	160	358
AP1398	7.10 ^{+0.60} _{-0.30}	2.84 ^{+0.07} _{-0.01}	0.80 ^{+0.10} _{-0.10}	7.99 ^{+0.05} _{-0.06}	2.87 ^{+0.13} _{-0.14}	0.40 ^{+0.18} _{-0.20}	I	0	1.71	108	54
AP1399	7.00 ^{+0.10} _{-0.30}	3.12 ^{+0.00} _{-0.02}	0.85 ^{+0.00} _{-0.05}	7.69 ^{+0.04} _{-0.03}	3.20 ^{+0.07} _{-0.08}	0.07 ^{+0.08} _{-0.07}	I	0	2.55	221	169
AP1400	8.50 ^{+0.40} _{-1.10}	2.72 ^{+0.39} _{-0.40}	0.60 ^{+0.70} _{-0.25}	8.44 ^{+0.46} _{-0.39}	3.03 ^{+0.22} _{-0.21}	0.75 ^{+0.63} _{-0.64}	I	0	1.51	132	106
AP1402	7.40 ^{+0.10} _{-0.30}	2.66 ^{+0.00} _{-0.05}	0.60 ^{+0.10} _{-0.10}	7.89 ^{+0.04} _{-0.03}	2.72 ^{+0.05} _{-0.05}	0.00 ^{+0.07} _{-0.00}	I	0	1.39	67	39
AP1404	6.90 ^{+0.30} _{-0.30}	2.70 ^{+0.01} _{-0.02}	1.15 ^{+0.10} _{-0.05}	6.89 ^{+0.06} _{-0.08}	2.58 ^{+0.16} _{-0.10}	0.96 ^{+0.09} _{-0.08}	I	0	1.61	73	38
AP1405	8.90 ^{+0.10} _{-0.00}	3.51 ^{+0.00} _{-0.09}	0.40 ^{+0.10} _{-0.25}	8.70 ^{+0.25} _{-0.29}	3.26 ^{+0.13} _{-0.15}	1.05 ^{+0.40} _{-0.40}	I	0	1.32	118	59
AP1406	8.80 ^{+0.00} _{-0.30}	3.18 ^{+0.00} _{-0.09}	0.05 ^{+0.55} _{-0.05}	8.68 ^{+0.15} _{-0.15}	2.95 ^{+0.11} _{-0.10}	0.48 ^{+0.24} _{-0.25}	I	0	1.35	95	63
AP1407	8.10 ^{+0.40} _{-0.00}	3.25 ^{+0.07} _{-0.13}	1.40 ^{+0.10} _{-0.55}	8.59 ^{+0.12} _{-0.11}	3.09 ^{+0.10} _{-0.08}	0.87 ^{+0.20} _{-0.21}	I	0	1.11	103	77
AP1408	8.30 ^{+0.10} _{-0.20}	3.27 ^{+0.02} _{-0.12}	0.75 ^{+0.10} _{-0.15}	8.48 ^{+0.15} _{-0.16}	3.00 ^{+0.10} _{-0.11}	0.22 ^{+0.30} _{-0.22}	I	0	1.39	138	118
AP1410	8.20 ^{+0.00} _{-0.70}	3.43 ^{+0.01} _{-0.11}	0.55 ^{+0.20} _{-0.10}	8.32 ^{+0.10} _{-0.09}	3.24 ^{+0.10} _{-0.11}	0.22 ^{+0.20} _{-0.20}	I	0	1.75	249	214
AP1411	8.60 ^{+0.20} _{-1.10}	3.89 ^{+0.23} _{-1.63}	2.25 ^{+0.40} _{-0.95}	8.78 ^{+0.39} _{-0.41}	3.20 ^{+0.15} _{-0.15}	0.63 ^{+0.49} _{-0.49}	I	0	1.36	152	108
AP1412	6.80 ^{+0.10} _{-0.10}	3.03 ^{+0.00} _{-0.03}	0.70 ^{+0.00} _{-0.05}	6.58 ^{+0.14} _{-0.14}	3.29 ^{+0.25} _{-0.20}	0.40 ^{+0.07} _{-0.07}	I	0	2.73	468	457
AP1414	9.10 ^{+0.00} _{-0.10}	3.93 ^{+0.06} _{-0.11}	0.20 ^{+0.30} _{-0.05}	8.67 ^{+0.26} _{-0.26}	3.26 ^{+0.20} _{-0.20}	0.63 ^{+0.45} _{-0.44}	I	0	1.41	185	136
AP1415	9.50 ^{+0.30} _{-0.00}	4.64 ^{+0.25} _{-0.03}	0.30 ^{+0.00} _{-0.30}	9.36 ^{+0.31} _{-0.26}	4.38 ^{+0.09} _{-0.09}	0.58 ^{+0.28} _{-0.34}	I	0	1.62	70	197
AP1416	8.40 ^{+0.10} _{-0.70}	2.50 ^{+0.02} _{-0.22}	0.40 ^{+0.30} _{-0.10}	0.00 ^{+0.00} _{-0.00}	0.00 ^{+0.00} _{-0.00}	0.00 ^{+0.00} _{-0.00}	I	0	2.04	129	330

Table 1 (cont'd)

AP ID ^a	CMD Best Fit Parameters ^b			Integrated Best Fit Parameters ^c			Best ^d Flag ^e	R _{ap} ^f	N _{stars} ^g	N _{bg} ^h	
	log(<i>t</i> [Myr])	log(<i>M</i> [<i>M</i> _⊙])	<i>A_V</i> [mag]	log(<i>t</i> [Myr])	log(<i>M</i> [<i>M</i> _⊙])	<i>A_V</i> [mag]					
AP1418	8.70 ^{+0.20} _{-0.00}	3.34 ^{+0.01} _{-0.19}	0.75 ^{+0.00} _{-0.60}	0.00 ^{+0.00} _{-0.00}	0.00 ^{+0.00} _{-0.00}	0.00 ^{+0.00} _{-0.00}	I	0	1.33	117	80
AP1419	9.00 ^{+0.00} _{-0.10}	3.42 ^{+0.03} _{-0.11}	0.10 ^{+0.15} _{-0.10}	9.52 ^{+0.17} _{-0.17}	3.67 ^{+0.12} _{-0.12}	0.19 ^{+0.20} _{-0.18}	I	0	1.56	127	70
AP1420	8.40 ^{+0.10} _{-0.30}	3.20 ^{+0.02} _{-0.06}	0.75 ^{+0.15} _{-0.10}	8.52 ^{+0.18} _{-0.19}	2.85 ^{+0.14} _{-0.14}	0.31 ^{+0.33} _{-0.29}	I	0	1.66	118	87
AP1421	7.80 ^{+0.10} _{-0.40}	2.89 ^{+0.02} _{-0.04}	0.65 ^{+0.10} _{-0.05}	7.29 ^{+0.38} _{-0.38}	3.07 ^{+0.13} _{-0.10}	1.13 ^{+0.32} _{-0.23}	I	0	1.63	118	92
AP1422	8.50 ^{+0.00} _{-0.10}	3.35 ^{+0.03} _{-0.07}	0.50 ^{+0.15} _{-0.05}	8.27 ^{+0.14} _{-0.15}	3.14 ^{+0.12} _{-0.11}	0.39 ^{+0.33} _{-0.32}	I	0	1.38	153	112
AP1423	7.70 ^{+0.00} _{-0.20}	3.19 ^{+0.00} _{-0.06}	1.30 ^{+0.10} _{-0.05}	7.24 ^{+0.04} _{-0.06}	3.54 ^{+0.07} _{-0.07}	1.19 ^{+0.10} _{-0.09}	I	0	1.57	168	91
AP1424	7.80 ^{+0.00} _{-0.10}	3.94 ^{+0.01} _{-0.08}	2.85 ^{+0.10} _{-0.00}	9.13 ^{+0.05} _{-0.05}	4.10 ^{+0.07} _{-0.07}	0.00 ^{+0.07} _{-0.00}	I	0	1.68	221	148
AP1425	9.10 ^{+0.00} _{-0.00}	3.72 ^{+0.02} _{-0.07}	0.15 ^{+0.10} _{-0.05}	8.81 ^{+0.37} _{-0.37}	3.53 ^{+0.11} _{-0.11}	0.72 ^{+0.51} _{-0.56}	I	0	1.49	158	60
AP1426	7.60 ^{+0.00} _{-0.20}	3.96 ^{+0.03} _{-0.07}	2.65 ^{+0.05} _{-0.00}	7.95 ^{+0.12} _{-0.17}	4.12 ^{+0.08} _{-0.07}	1.73 ^{+0.27} _{-0.20}	I	1	1.65	261	234
AP1428	8.10 ^{+0.00} _{-0.20}	3.35 ^{+0.01} _{-0.07}	1.00 ^{+0.10} _{-0.05}	8.60 ^{+0.10} _{-0.09}	3.12 ^{+0.09} _{-0.07}	0.13 ^{+0.14} _{-0.13}	I	0	1.34	125	90
AP1429	7.70 ^{+0.00} _{-0.30}	3.10 ^{+0.00} _{-0.07}	0.95 ^{+0.10} _{-0.06}	8.36 ^{+0.13} _{-0.00}	3.22 ^{+0.14} _{-0.01}	0.06 ^{+0.13} _{-0.06}	I	0	1.60	153	136
AP1430	8.20 ^{+0.30} _{-0.00}	3.25 ^{+0.02} _{-0.13}	1.40 ^{+0.05} _{-0.45}	8.41 ^{+0.15} _{-0.26}	2.89 ^{+0.24} _{-0.51}	0.69 ^{+0.28} _{-0.43}	I	0	1.41	124	83
AP1431	6.60 ^{+0.10} _{-0.00}	3.72 ^{+0.01} _{-0.01}	1.55 ^{+0.00} _{-0.05}	7.37 ^{+0.16} _{-0.20}	4.40 ^{+0.17} _{-0.17}	1.43 ^{+0.23} _{-0.23}	I	0	3.53	763	657
AP1432	10.10 ^{+0.10} _{-2.20}	4.73 ^{+0.07} _{-4.73}	0.10 ^{+2.40} _{-0.05}	9.47 ^{+0.32} _{-0.28}	4.17 ^{+0.14} _{-0.11}	1.27 ^{+0.28} _{-0.26}	I	0	1.84	106	56
AP1435	8.20 ^{+0.00} _{-0.00}	3.61 ^{+0.00} _{-0.04}	1.15 ^{+0.00} _{-0.05}	8.13 ^{+0.23} _{-0.29}	3.59 ^{+0.17} _{-0.17}	0.91 ^{+0.51} _{-0.47}	I	0	2.28	361	299
AP1436	7.60 ^{+0.20} _{-0.10}	3.65 ^{+0.05} _{-0.06}	2.20 ^{+0.10} _{-0.15}	8.44 ^{+0.26} _{-0.26}	3.39 ^{+0.19} _{-0.17}	0.84 ^{+0.56} _{-0.49}	I	0	1.15	131	87
AP1437	8.90 ^{+0.00} _{-0.80}	3.11 ^{+0.03} _{-0.14}	0.00 ^{+1.20} _{-0.05}	9.78 ^{+0.17} _{-0.18}	3.88 ^{+0.10} _{-0.11}	0.21 ^{+0.17} _{-0.18}	I	0	1.66	112	76
AP1438	7.90 ^{+0.00} _{-0.60}	3.03 ^{+0.01} _{-0.05}	0.80 ^{+0.20} _{-0.00}	8.19 ^{+0.07} _{-0.07}	2.69 ^{+0.10} _{-0.09}	0.09 ^{+0.11} _{-0.09}	I	0	1.24	122	98
AP1439	8.00 ^{+0.10} _{-0.40}	3.24 ^{+0.05} _{-0.05}	0.90 ^{+0.20} _{-0.00}	8.53 ^{+0.10} _{-0.08}	3.14 ^{+0.10} _{-0.08}	0.16 ^{+0.17} _{-0.16}	I	0	1.48	190	160
AP1440	8.20 ^{+0.00} _{-1.40}	2.92 ^{+0.00} _{-0.19}	0.55 ^{+0.30} _{-0.05}	8.18 ^{+0.15} _{-0.15}	3.18 ^{+0.14} _{-0.12}	0.69 ^{+0.35} _{-0.31}	I	0	1.20	101	80
AP1441	9.30 ^{+0.00} _{-0.10}	4.41 ^{+0.02} _{-0.08}	0.00 ^{+0.10} _{-0.00}	9.45 ^{+0.48} _{-0.42}	5.09 ^{+0.24} _{-0.20}	0.22 ^{+0.31} _{-0.22}	I	0	2.55	234	466
AP1442	7.40 ^{+0.40} _{-0.30}	2.90 ^{+0.00} _{-0.06}	0.85 ^{+0.05} _{-0.20}	7.84 ^{+0.13} _{-0.22}	3.11 ^{+0.08} _{-0.07}	0.50 ^{+0.25} _{-0.19}	I	0	1.63	217	197
AP1444	8.40 ^{+0.20} _{-0.50}	2.92 ^{+0.03} _{-0.14}	0.55 ^{+0.25} _{-0.25}	8.04 ^{+0.37} _{-0.41}	3.15 ^{+0.30} _{-0.25}	1.25 ^{+0.86} _{-0.80}	I	0	1.48	130	114
AP1445	6.80 ^{+0.90} _{-0.10}	2.53 ^{+0.05} _{-0.02}	0.40 ^{+0.00} _{-0.10}	7.05 ^{+0.28} _{-0.32}	2.35 ^{+0.19} _{-0.23}	0.19 ^{+0.13} _{-0.14}	I	0	1.25	42	24
AP1446	6.90 ^{+0.40} _{-0.20}	2.88 ^{+0.00} _{-0.07}	0.55 ^{+0.00} _{-0.15}	8.12 ^{+0.06} _{-0.04}	3.29 ^{+0.06} _{-0.05}	0.05 ^{+0.09} _{-0.05}	I	0	1.35	139	122
AP1448	9.30 ^{+0.00} _{-1.10}	3.78 ^{+0.04} _{-0.57}	0.15 ^{+1.65} _{-0.05}	7.93 ^{+0.19} _{-0.25}	3.23 ^{+0.23} _{-0.17}	1.57 ^{+0.57} _{-0.38}	I	0	1.42	106	60
AP1449	9.10 ^{+0.10} _{-0.20}	3.38 ^{+0.00} _{-0.68}	0.65 ^{+0.25} _{-0.45}	9.30 ^{+0.31} _{-0.25}	3.23 ^{+0.18} _{-0.19}	0.36 ^{+0.25} _{-0.30}	I	0	1.53	77	32
AP1452	9.10 ^{+0.10} _{-0.00}	3.70 ^{+0.19} _{-0.04}	0.40 ^{+0.00} _{-0.20}	8.73 ^{+0.15} _{-0.18}	3.53 ^{+0.10} _{-0.10}	1.15 ^{+0.29} _{-0.29}	I	0	1.67	150	99
AP1453	7.20 ^{+0.60} _{-0.30}	2.93 ^{+0.16} _{-0.04}	1.15 ^{+0.20} _{-0.05}	6.82 ^{+0.06} _{-0.06}	2.64 ^{+0.24} _{-0.18}	1.15 ^{+0.09} _{-0.09}	I	0	1.41	77	32
AP1454	8.30 ^{+0.00} _{-0.80}	2.86 ^{+0.01} _{-0.10}	0.25 ^{+0.35} _{-0.00}	7.91 ^{+0.11} _{-0.11}	3.03 ^{+0.09} _{-0.09}	0.92 ^{+0.22} _{-0.22}	I	0	1.25	133	94
AP1456	8.30 ^{+0.10} _{-0.00}	3.04 ^{+0.03} _{-0.04}	1.45 ^{+0.00} _{-0.25}	8.55 ^{+0.15} _{-0.14}	2.87 ^{+0.14} _{-0.13}	0.84 ^{+0.31} _{-0.30}	I	0	1.01	45	22
AP1458	9.40 ^{+0.10} _{-0.30}	4.32 ^{+0.08} _{-0.63}	0.00 ^{+0.45} _{-0.00}	8.95 ^{+0.20} _{-0.00}	3.54 ^{+0.13} _{-0.07}	0.18 ^{+0.01} _{-0.18}	I	0	1.56	243	180
AP1461	8.10 ^{+1.20} _{-0.80}	3.57 ^{+0.14} _{-3.57}	2.95 ^{+0.00} _{-2.40}	8.74 ^{+0.25} _{-0.28}	2.93 ^{+0.13} _{-0.13}	0.80 ^{+0.41} _{-0.45}	I	0	1.28	59	25

Table 1 (cont'd)

AP ID ^a	CMD Best Fit Parameters ^b			Integrated Best Fit Parameters ^c			Best ^d Flag ^e	Rap ^f	N _{stars} ^g	N _{bg} ^h	
	log(<i>t</i> [Myr])	log(<i>M</i> [<i>M</i> _⊙])	<i>A_V</i> [mag]	log(<i>t</i> [Myr])	log(<i>M</i> [<i>M</i> _⊙])	<i>A_V</i> [mag]					
AP1462	7.90 ^{+0.20} _{-0.50}	2.94 ^{+0.00} _{-0.11}	1.35 ^{+0.15} _{-0.10}	8.11 ^{+1.47} _{-1.46}	3.78 ^{+1.25} _{-1.18}	1.45 ^{+1.02} _{-1.02}	I	0	1.48	99	63
AP1463	8.00 ^{+0.00} _{-0.80}	3.07 ^{+0.02} _{-0.20}	0.60 ^{+0.13} _{-0.05}	7.53 ^{+0.53} _{-0.50}	3.06 ^{+0.14} _{-0.13}	0.79 ^{+0.47} _{-0.54}	I	0	1.86	205	126
AP1464	8.40 ^{+0.10} _{-0.30}	3.48 ^{+0.02} _{-0.06}	1.30 ^{+0.30} _{-0.10}	9.75 ^{+0.14} _{-0.14}	3.98 ^{+0.10} _{-0.10}	0.08 ^{+0.11} _{-0.08}	I	0	1.88	230	177
AP1465	8.90 ^{+0.10} _{-0.00}	4.02 ^{+0.17} _{-0.00}	1.10 ^{+0.25} _{-0.06}	7.93 ^{+1.04} _{-1.13}	2.93 ^{+0.47} _{-0.52}	1.32 ^{+1.00} _{-0.97}	I	0	1.39	146	70
AP1466	8.50 ^{+0.00} _{-0.10}	3.26 ^{+0.05} _{-0.03}	0.55 ^{+0.25} _{-0.05}	8.04 ^{+0.31} _{-0.22}	3.36 ^{+0.19} _{-0.21}	1.34 ^{+0.45} _{-0.54}	I	0	1.36	122	89
AP1467	8.40 ^{+0.10} _{-0.00}	3.30 ^{+0.03} _{-0.04}	0.55 ^{+0.05} _{-0.05}	7.84 ^{+0.04} _{-0.03}	2.07 ^{+0.03} _{-0.05}	0.03 ^{+0.07} _{-0.03}	I	0	1.56	148	97
AP1468	7.60 ^{+0.20} _{-0.30}	3.04 ^{+0.01} _{-0.05}	0.50 ^{+0.05} _{-0.10}	7.64 ^{+0.13} _{-0.13}	3.39 ^{+0.06} _{-0.06}	0.94 ^{+0.14} _{-0.14}	I	0	1.38	147	104
AP1469	9.10 ^{+0.00} _{-0.00}	3.64 ^{+0.12} _{-0.03}	0.10 ^{+0.20} _{-0.05}	9.28 ^{+0.15} _{-0.16}	3.61 ^{+0.12} _{-0.11}	0.24 ^{+0.19} _{-0.20}	I	0	1.57	190	134
AP1470	8.90 ^{+0.10} _{-0.10}	3.23 ^{+0.10} _{-0.00}	0.00 ^{+0.45} _{-0.00}	7.27 ^{+0.28} _{-0.26}	3.55 ^{+0.11} _{-0.08}	2.30 ^{+0.23} _{-0.24}	I	0	1.57	156	118
AP1471	9.20 ^{+0.10} _{-0.00}	4.05 ^{+0.22} _{-0.01}	0.25 ^{+0.20} _{-0.05}	9.26 ^{+0.66} _{-0.64}	3.91 ^{+0.19} _{-0.16}	0.77 ^{+0.64} _{-0.65}	I	0	1.75	197	155
AP1472	8.70 ^{+0.00} _{-0.00}	3.30 ^{+0.00} _{-0.06}	0.45 ^{+0.00} _{-0.20}	8.88 ^{+0.19} _{-0.22}	3.36 ^{+0.11} _{-0.10}	0.71 ^{+0.35} _{-0.38}	I	0	1.49	152	114
AP1474	8.80 ^{+0.00} _{-0.20}	2.90 ^{+0.03} _{-0.07}	0.10 ^{+0.45} _{-0.00}	7.81 ^{+0.99} _{-0.99}	3.05 ^{+0.20} _{-0.18}	1.31 ^{+0.73} _{-0.84}	I	0	1.50	77	45
AP1476	9.00 ^{+0.00} _{-0.10}	3.01 ^{+0.04} _{-0.06}	0.00 ^{+0.32} _{-0.00}	8.56 ^{+0.16} _{-0.16}	2.53 ^{+0.18} _{-0.17}	0.48 ^{+0.37} _{-0.35}	I	0	1.28	52	26
AP1477	9.30 ^{+0.30} _{-0.10}	3.98 ^{+0.24} _{-0.20}	0.20 ^{+0.10} _{-0.15}	7.66 ^{+0.16} _{-0.19}	3.59 ^{+0.20} _{-0.20}	2.28 ^{+0.38} _{-0.36}	I	0	1.70	118	66
AP1479	8.10 ^{+0.00} _{-0.50}	3.30 ^{+0.00} _{-0.08}	1.30 ^{+0.25} _{-0.05}	8.21 ^{+0.18} _{-0.23}	2.50 ^{+0.19} _{-0.22}	0.05 ^{+0.10} _{-0.05}	I	0	1.20	101	62
AP1482	8.80 ^{+0.10} _{-0.00}	3.33 ^{+0.07} _{-0.03}	0.25 ^{+0.15} _{-0.15}	8.64 ^{+0.14} _{-0.15}	2.64 ^{+0.13} _{-0.15}	0.27 ^{+0.24} _{-0.23}	I	0	1.22	104	88
AP1483	7.90 ^{+0.00} _{-0.30}	3.89 ^{+0.01} _{-0.25}	2.65 ^{+0.10} _{-0.10}	7.74 ^{+0.15} _{-0.13}	3.73 ^{+0.11} _{-0.11}	1.75 ^{+0.22} _{-0.23}	I	0	1.47	191	123
AP1484	8.00 ^{+0.00} _{-0.10}	3.69 ^{+0.22} _{-0.00}	2.15 ^{+0.45} _{-0.00}	9.10 ^{+0.13} _{-0.12}	3.47 ^{+0.12} _{-0.12}	0.25 ^{+0.16} _{-0.18}	I	0	1.46	156	72
AP1487	7.80 ^{+0.10} _{-0.10}	3.66 ^{+0.00} _{-0.06}	2.25 ^{+0.10} _{-0.05}	9.05 ^{+0.12} _{-0.12}	3.38 ^{+0.12} _{-0.11}	0.12 ^{+0.15} _{-0.12}	I	0	1.04	106	70
AP1489	9.10 ^{+0.00} _{-0.00}	3.65 ^{+0.03} _{-0.05}	0.40 ^{+0.10} _{-0.10}	8.43 ^{+0.22} _{-0.14}	2.86 ^{+0.17} _{-0.08}	0.85 ^{+0.21} _{-0.24}	I	0	1.48	118	67
AP1490	9.00 ^{+0.00} _{-0.00}	3.73 ^{+0.03} _{-0.03}	0.15 ^{+0.10} _{-0.10}	10.25 ^{+0.00} _{-0.03}	4.25 ^{+0.03} _{-0.03}	0.00 ^{+0.07} _{-0.00}	I	0	1.99	225	107
AP1492	9.30 ^{+0.10} _{-1.20}	3.90 ^{+0.10} _{-1.78}	0.10 ^{+0.30} _{-0.05}	9.10 ^{+0.19} _{-0.10}	3.23 ^{+0.15} _{-0.17}	0.10 ^{+0.01} _{-0.10}	I	0	1.37	131	92
AP1494	8.10 ^{+0.10} _{-0.60}	2.85 ^{+0.01} _{-0.11}	0.55 ^{+0.10} _{-0.10}	8.19 ^{+0.05} _{-0.06}	2.14 ^{+0.06} _{-0.07}	0.00 ^{+0.07} _{-0.00}	I	0	1.27	88	56
AP1496	7.50 ^{+0.40} _{-0.50}	2.67 ^{+0.01} _{-0.05}	0.50 ^{+0.05} _{-0.15}	6.85 ^{+0.46} _{-0.55}	2.59 ^{+0.19} _{-0.19}	0.74 ^{+0.22} _{-0.23}	I	0	1.78	82	43
AP1498	8.40 ^{+0.20} _{-0.50}	3.28 ^{+0.01} _{-0.18}	1.15 ^{+0.30} _{-0.25}	9.39 ^{+0.17} _{-0.20}	3.45 ^{+0.09} _{-0.11}	0.21 ^{+0.23} _{-0.19}	I	0	1.63	154	126
AP1499	8.60 ^{+0.00} _{-0.30}	3.24 ^{+0.01} _{-0.14}	0.60 ^{+0.35} _{-0.05}	8.69 ^{+0.19} _{-0.19}	2.99 ^{+0.10} _{-0.11}	0.40 ^{+0.28} _{-0.28}	I	0	1.37	81	53
AP1500	7.90 ^{+0.10} _{-0.00}	3.88 ^{+0.02} _{-0.14}	2.80 ^{+0.05} _{-0.20}	8.96 ^{+0.27} _{-0.22}	3.30 ^{+0.13} _{-0.14}	0.50 ^{+0.30} _{-0.34}	I	0	1.50	167	95
AP1502	7.60 ^{+0.30} _{-0.20}	3.23 ^{+0.04} _{-0.03}	1.15 ^{+0.10} _{-0.10}	8.22 ^{+0.18} _{-0.19}	2.87 ^{+0.12} _{-0.12}	0.21 ^{+0.22} _{-0.20}	I	0	1.56	221	164
AP1504	9.40 ^{+0.20} _{-0.10}	3.99 ^{+0.13} _{-0.08}	0.10 ^{+0.15} _{-0.05}	8.26 ^{+0.97} _{-0.71}	3.35 ^{+0.25} _{-0.25}	1.33 ^{+1.09} _{-1.11}	I	0	1.81	109	56
AP1506	8.90 ^{+0.00} _{-0.20}	3.40 ^{+0.04} _{-0.12}	0.15 ^{+0.55} _{-0.00}	9.02 ^{+0.14} _{-0.14}	3.23 ^{+0.16} _{-0.16}	0.27 ^{+0.20} _{-0.20}	I	0	1.12	86	64
AP1508	8.90 ^{+0.00} _{-0.70}	3.23 ^{+0.09} _{-0.24}	0.80 ^{+1.20} _{-0.00}	8.76 ^{+0.78} _{-0.62}	3.61 ^{+0.15} _{-0.16}	1.14 ^{+0.84} _{-0.88}	I	0	2.00	58	92
AP1510	9.60 ^{+0.40} _{-1.80}	4.22 ^{+0.37} _{-0.66}	0.00 ^{+2.90} _{-0.00}	8.02 ^{+0.01} _{-0.06}	2.15 ^{+0.03} _{-0.07}	0.29 ^{+0.08} _{-0.07}	I	0	1.45	137	90
AP1513	8.00 ^{+0.00} _{-0.10}	3.42 ^{+0.01} _{-0.05}	1.10 ^{+0.05} _{-0.05}	8.55 ^{+0.07} _{-0.04}	3.14 ^{+0.09} _{-0.05}	0.08 ^{+0.10} _{-0.08}	I	0	1.23	121	60

Table 1 (cont'd)

AP ID ^a	CMD Best Fit Parameters ^b			Integrated Best Fit Parameters ^c			Best ^d Flag ^e	R _{ap} ^f	N _{stars} ^g	N _{bg} ^h	
	log(<i>t</i> [Myr])	log(<i>M</i> [<i>M</i> _⊙])	<i>A_V</i> [mag]	log(<i>t</i> [Myr])	log(<i>M</i> [<i>M</i> _⊙])	<i>A_V</i> [mag]					
AP1514	7.80 ^{+0.10} _{-0.10}	3.11 ^{+0.00} _{-0.04}	0.80 ^{+0.05} _{-0.10}	8.02 ^{+0.17} _{-0.17}	2.95 ^{+0.15} _{-0.16}	0.36 ^{+0.35} _{-0.30}	I	0	1.65	157	128
AP1516	9.00 ^{+0.00} _{-0.10}	3.54 ^{+0.03} _{-0.13}	0.35 ^{+0.15} _{-0.15}	8.48 ^{+0.20} _{-0.19}	2.72 ^{+0.18} _{-0.18}	0.38 ^{+0.34} _{-0.33}	I	0	1.36	108	62
AP1518	9.00 ^{+0.10} _{-0.00}	3.74 ^{+0.03} _{-0.03}	0.35 ^{+0.10} _{-0.15}	8.04 ^{+0.10} _{-0.13}	2.95 ^{+0.14} _{-0.15}	1.47 ^{+0.27} _{-0.25}	I	0	1.17	108	75
AP1520	8.10 ^{+0.00} _{-0.40}	2.99 ^{+0.00} _{-0.07}	0.70 ^{+0.15} _{-0.05}	6.92 ^{+0.17} _{-0.16}	3.25 ^{+0.27} _{-0.28}	2.50 ^{+0.12} _{-0.12}	I	0	1.28	118	96
AP1521	8.40 ^{+0.10} _{-0.40}	3.54 ^{+0.00} _{-0.06}	0.90 ^{+0.35} _{-0.15}	8.90 ^{+0.07} _{-0.07}	3.51 ^{+0.07} _{-0.06}	0.11 ^{+0.13} _{-0.11}	I	0	1.34	152	103
AP1522	6.90 ^{+0.80} _{-0.20}	2.75 ^{+0.06} _{-0.02}	0.80 ^{+0.05} _{-0.10}	7.59 ^{+0.04} _{-0.04}	2.83 ^{+0.02} _{-0.06}	0.20 ^{+0.08} _{-0.07}	I	0	1.85	90	63
AP1523	6.90 ^{+0.20} _{-0.10}	3.21 ^{+0.00} _{-0.16}	3.00 ^{+0.00} _{-0.20}	10.07 ^{+0.05} _{-0.05}	4.70 ^{+0.04} _{-0.04}	0.05 ^{+0.09} _{-0.05}	I	0	1.16	114	146
AP1524	9.10 ^{+0.10} _{-0.50}	3.33 ^{+0.13} _{-0.68}	0.25 ^{+0.50} _{-0.10}	7.89 ^{+0.04} _{-0.12}	2.12 ^{+0.01} _{-0.12}	0.14 ^{+0.14} _{-0.12}	I	0	1.52	107	54
AP1525	8.00 ^{+0.10} _{-0.30}	3.00 ^{+0.03} _{-0.03}	0.55 ^{+0.10} _{-0.05}	8.22 ^{+0.07} _{-0.07}	2.57 ^{+0.12} _{-0.11}	0.07 ^{+0.11} _{-0.07}	I	0	1.03	67	42
AP1526	9.60 ^{+0.00} _{-2.00}	4.48 ^{+0.03} _{-1.21}	0.00 ^{+2.30} _{-0.00}	7.90 ^{+1.15} _{-1.38}	3.57 ^{+0.36} _{-0.44}	1.33 ^{+0.84} _{-0.95}	I	0	1.59	221	150
AP1527	7.40 ^{+0.20} _{-0.10}	3.69 ^{+0.01} _{-0.22}	3.00 ^{+0.00} _{-0.90}	9.11 ^{+0.09} _{-0.06}	3.38 ^{+0.10} _{-0.10}	0.11 ^{+0.11} _{-0.11}	I	0	1.17	119	72
AP1528	8.40 ^{+0.20} _{-0.60}	3.19 ^{+0.10} _{-0.18}	0.95 ^{+0.65} _{-0.45}	8.13 ^{+0.25} _{-0.27}	3.29 ^{+0.18} _{-0.18}	1.38 ^{+0.56} _{-0.48}	I	0	1.43	123	88
AP1529	9.10 ^{+0.00} _{-0.00}	3.73 ^{+0.03} _{-0.04}	0.05 ^{+0.10} _{-0.05}	8.77 ^{+0.07} _{-0.07}	2.99 ^{+0.08} _{-0.08}	0.08 ^{+0.11} _{-0.08}	I	0	1.59	172	128
AP1534	8.90 ^{+0.10} _{-0.00}	3.40 ^{+0.00} _{-0.07}	0.45 ^{+0.00} _{-0.35}	8.63 ^{+0.21} _{-0.21}	2.85 ^{+0.16} _{-0.15}	0.46 ^{+0.34} _{-0.34}	I	0	1.88	125	70
AP1535	9.00 ^{+0.00} _{-0.10}	3.75 ^{+0.06} _{-0.12}	0.50 ^{+0.25} _{-0.05}	8.52 ^{+0.21} _{-0.18}	3.46 ^{+0.13} _{-0.10}	1.04 ^{+0.37} _{-0.36}	I	0	1.44	139	89
AP1536	7.80 ^{+0.50} _{-0.10}	3.63 ^{+0.01} _{-0.11}	2.40 ^{+0.05} _{-0.80}	7.99 ^{+0.17} _{-0.26}	3.30 ^{+0.30} _{-0.27}	1.47 ^{+0.60} _{-0.56}	I	1	1.20	120	82
AP1539	7.90 ^{+0.00} _{-0.10}	3.40 ^{+0.00} _{-0.03}	0.70 ^{+0.05} _{-0.05}	7.74 ^{+0.13} _{-0.20}	3.41 ^{+0.15} _{-0.15}	0.81 ^{+0.31} _{-0.27}	I	0	1.85	252	185
AP1540	7.30 ^{+0.00} _{-0.50}	3.05 ^{+0.00} _{-0.12}	1.95 ^{+0.10} _{-0.10}	7.20 ^{+0.50} _{-0.67}	3.42 ^{+0.35} _{-0.53}	1.80 ^{+0.16} _{-0.18}	I	0	1.44	127	108
AP1542	8.20 ^{+0.00} _{-0.60}	2.91 ^{+0.02} _{-0.11}	0.30 ^{+0.20} _{-0.05}	8.21 ^{+0.37} _{-0.34}	3.21 ^{+0.25} _{-0.21}	0.83 ^{+0.63} _{-0.68}	I	0	1.78	192	156
AP1543	8.40 ^{+0.70} _{-0.00}	4.37 ^{+0.57} _{-0.09}	2.80 ^{+0.00} _{-1.00}	8.24 ^{+0.18} _{-0.15}	4.07 ^{+0.12} _{-0.13}	2.15 ^{+0.29} _{-0.35}	I	0	2.07	303	216
AP1548	9.30 ^{+0.30} _{-0.10}	4.08 ^{+0.29} _{-0.15}	0.35 ^{+0.05} _{-0.25}	7.82 ^{+0.06} _{-0.07}	2.20 ^{+0.15} _{-0.11}	1.01 ^{+0.29} _{-0.20}	I	0	1.34	128	92
AP1549	8.50 ^{+0.10} _{-0.90}	2.92 ^{+0.00} _{-0.11}	0.30 ^{+0.45} _{-0.10}	7.43 ^{+0.89} _{-0.84}	2.69 ^{+0.18} _{-0.19}	0.96 ^{+0.33} _{-0.45}	I	0	1.40	61	36
AP1550	8.20 ^{+0.00} _{-0.00}	3.04 ^{+0.01} _{-0.01}	1.00 ^{+0.05} _{-0.05}	9.22 ^{+0.12} _{-0.09}	3.27 ^{+0.11} _{-0.11}	0.05 ^{+0.06} _{-0.05}	I	0	1.37	66	35
AP1552	9.70 ^{+0.00} _{-0.20}	4.46 ^{+0.04} _{-0.16}	0.05 ^{+0.10} _{-0.05}	10.12 ^{+0.13} _{-0.09}	5.41 ^{+0.07} _{-0.01}	0.32 ^{+0.03} _{-0.19}	I	0	1.95	119	314
AP1553	6.80 ^{+0.40} _{-0.20}	3.25 ^{+0.06} _{-0.02}	1.90 ^{+0.10} _{-0.00}	7.07 ^{+0.19} _{-0.19}	3.01 ^{+0.28} _{-0.40}	1.09 ^{+0.15} _{-0.16}	I	0	1.63	164	138
AP1554	8.70 ^{+0.10} _{-0.00}	3.54 ^{+0.02} _{-0.05}	1.00 ^{+0.05} _{-0.25}	8.02 ^{+0.07} _{-0.09}	3.79 ^{+0.09} _{-0.10}	2.30 ^{+0.18} _{-0.19}	I	0	1.48	87	31
AP1555	8.90 ^{+0.00} _{-0.10}	3.66 ^{+0.02} _{-0.08}	0.45 ^{+0.25} _{-0.00}	9.56 ^{+0.22} _{-0.03}	3.76 ^{+0.18} _{-0.03}	0.06 ^{+0.03} _{-0.06}	I	0	1.46	158	87
AP1560	8.00 ^{+0.00} _{-0.00}	3.91 ^{+0.01} _{-0.23}	2.80 ^{+0.05} _{-0.25}	8.50 ^{+0.13} _{-0.14}	3.47 ^{+0.12} _{-0.13}	1.15 ^{+0.29} _{-0.30}	I	0	1.59	170	122
AP1561	8.60 ^{+1.20} _{-0.90}	5.27 ^{+0.59} _{-5.27}	2.90 ^{+0.15} _{-2.40}	9.10 ^{+0.60} _{-0.42}	4.15 ^{+0.14} _{-0.12}	1.16 ^{+0.52} _{-0.66}	I	0	1.90	271	166
AP1562	9.00 ^{+0.00} _{-1.10}	3.51 ^{+0.03} _{-0.09}	0.30 ^{+1.95} _{-0.00}	8.72 ^{+0.14} _{-0.12}	2.77 ^{+0.12} _{-0.11}	0.16 ^{+0.14} _{-0.16}	I	0	1.32	131	90
AP1563	7.60 ^{+0.10} _{-0.10}	3.69 ^{+0.05} _{-0.09}	2.35 ^{+0.25} _{-0.10}	7.79 ^{+0.10} _{-0.09}	4.37 ^{+0.08} _{-0.08}	1.85 ^{+0.15} _{-0.15}	I	0	1.37	117	100
AP1564	8.00 ^{+0.10} _{-0.80}	3.61 ^{+0.01} _{-0.22}	1.50 ^{+0.15} _{-0.20}	8.23 ^{+0.65} _{-0.45}	3.72 ^{+0.16} _{-0.12}	0.86 ^{+0.42} _{-0.61}	I	0	1.61	210	142
AP1566	7.30 ^{+0.20} _{-0.40}	3.14 ^{+0.00} _{-0.14}	1.95 ^{+0.10} _{-0.25}	7.63 ^{+0.07} _{-0.07}	3.09 ^{+0.06} _{-0.07}	0.48 ^{+0.12} _{-0.12}	I	0	1.56	145	113

Table 1 (cont'd)

AP ID ^a	CMD Best Fit Parameters ^b			Integrated Best Fit Parameters ^c			Best ^d Flag ^e	Rap ^f	N _{stars} ^g	N _{bg} ^h	
	log(<i>t</i> [Myr])	log(<i>M</i> [<i>M</i> _⊙])	<i>A_V</i> [mag]	log(<i>t</i> [Myr])	log(<i>M</i> [<i>M</i> _⊙])	<i>A_V</i> [mag]					
AP1567	8.20 ^{+0.00} _{-0.60}	3.06 ^{+0.01} _{-0.14}	1.10 ^{+0.20} _{-0.00}	8.02 ^{+0.14} _{-0.14}	2.89 ^{+0.11} _{-0.12}	0.79 ^{+0.25} _{-0.26}	I	0	1.40	59	26
AP1568	7.50 ^{+0.20} _{-0.40}	2.98 ^{+0.02} _{-0.04}	1.00 ^{+0.10} _{-0.05}	7.82 ^{+0.07} _{-0.07}	2.88 ^{+0.10} _{-0.09}	0.62 ^{+0.15} _{-0.13}	I	0	1.56	132	109
AP1569	8.60 ^{+0.10} _{-0.20}	3.47 ^{+0.01} _{-0.05}	0.45 ^{+0.25} _{-0.25}	8.45 ^{+0.26} _{-0.25}	3.32 ^{+0.16} _{-0.14}	0.52 ^{+0.51} _{-0.47}	I	0	1.46	182	124
AP1570	8.10 ^{+0.20} _{-0.60}	3.12 ^{+0.02} _{-0.16}	1.20 ^{+0.15} _{-0.15}	7.10 ^{+0.99} _{-0.80}	3.36 ^{+0.40} _{-0.44}	0.55 ^{+0.45} _{-0.43}	I	0	1.42	138	106
AP1571	9.20 ^{+0.00} _{-0.10}	3.91 ^{+0.04} _{-0.17}	0.05 ^{+0.20} _{-0.05}	6.33 ^{+0.29} _{-0.28}	2.64 ^{+0.29} _{-0.24}	0.79 ^{+0.11} _{-0.12}	I	0	1.62	197	130
AP1572	8.50 ^{+0.10} _{-0.10}	3.28 ^{+0.01} _{-0.06}	0.65 ^{+0.05} _{-0.15}	8.77 ^{+0.23} _{-0.26}	3.16 ^{+0.11} _{-0.11}	0.40 ^{+0.34} _{-0.32}	I	0	1.28	81	28
AP1574	8.40 ^{+0.10} _{-0.50}	2.74 ^{+0.00} _{-0.18}	0.50 ^{+0.15} _{-0.15}	10.12 ^{+0.11} _{-0.10}	3.86 ^{+0.09} _{-0.09}	0.06 ^{+0.10} _{-0.06}	I	0	1.52	81	51
AP1575	9.40 ^{+0.10} _{-0.10}	4.27 ^{+0.06} _{-0.09}	0.30 ^{+0.05} _{-0.15}	9.11 ^{+0.68} _{-0.50}	3.59 ^{+0.21} _{-0.14}	0.74 ^{+0.56} _{-0.65}	I	0	1.57	122	88
AP1576	9.10 ^{+0.00} _{-0.00}	3.92 ^{+0.04} _{-0.12}	0.40 ^{+0.00} _{-0.15}	8.52 ^{+0.38} _{-0.42}	3.10 ^{+0.18} _{-0.09}	0.65 ^{+0.65} _{-0.55}	I	0	1.54	160	106
AP1580	9.10 ^{+0.00} _{-0.00}	3.70 ^{+0.04} _{-0.07}	0.40 ^{+0.05} _{-0.15}	9.27 ^{+0.30} _{-0.28}	3.82 ^{+0.12} _{-0.12}	0.45 ^{+0.31} _{-0.35}	I	0	2.05	220	112
AP1581	8.30 ^{+0.00} _{-0.10}	3.23 ^{+0.01} _{-0.07}	0.95 ^{+0.10} _{-0.15}	8.72 ^{+0.31} _{-0.47}	3.36 ^{+0.16} _{-0.15}	0.54 ^{+0.80} _{-0.48}	I	0	1.28	146	119
AP1582	8.10 ^{+0.00} _{-0.70}	2.97 ^{+0.01} _{-0.11}	0.60 ^{+0.25} _{-0.05}	7.30 ^{+0.36} _{-0.35}	3.12 ^{+0.11} _{-0.08}	0.96 ^{+0.25} _{-0.21}	I	0	1.56	170	136
AP1586	8.50 ^{+0.10} _{-0.00}	3.41 ^{+0.02} _{-0.03}	0.55 ^{+0.10} _{-0.10}	8.37 ^{+0.18} _{-0.19}	3.26 ^{+0.14} _{-0.16}	0.57 ^{+0.40} _{-0.42}	I	0	2.18	291	223
AP1588	9.00 ^{+0.00} _{-0.10}	4.01 ^{+0.04} _{-0.04}	0.35 ^{+0.15} _{-0.05}	7.11 ^{+0.34} _{-0.31}	3.38 ^{+0.23} _{-0.26}	2.06 ^{+0.23} _{-0.25}	I	0	2.05	262	207
AP1594	8.10 ^{+0.00} _{-0.00}	3.16 ^{+0.04} _{-0.00}	0.50 ^{+0.10} _{-0.00}	8.13 ^{+0.09} _{-0.09}	3.13 ^{+0.10} _{-0.08}	0.43 ^{+0.22} _{-0.21}	I	0	1.33	133	103
AP1595	8.20 ^{+0.00} _{-0.10}	3.24 ^{+0.00} _{-0.06}	0.75 ^{+0.05} _{-0.10}	8.29 ^{+0.15} _{-0.16}	3.00 ^{+0.13} _{-0.14}	0.36 ^{+0.32} _{-0.31}	I	0	1.35	151	120
AP1596	8.80 ^{+0.50} _{-1.30}	3.23 ^{+0.08} _{-3.23}	0.95 ^{+1.10} _{-0.50}	7.63 ^{+0.10} _{-0.08}	2.93 ^{+0.08} _{-0.08}	0.71 ^{+0.16} _{-0.16}	I	0	1.21	74	86
AP1597	8.40 ^{+0.20} _{-1.30}	2.77 ^{+0.04} _{-0.08}	0.65 ^{+0.80} _{-0.10}	8.47 ^{+0.12} _{-0.11}	2.78 ^{+0.13} _{-0.12}	0.19 ^{+0.23} _{-0.19}	I	0	1.32	57	58
AP1599	9.00 ^{+0.00} _{-0.20}	3.58 ^{+0.24} _{-0.02}	0.05 ^{+0.70} _{-0.05}	9.08 ^{+0.10} _{-0.11}	3.35 ^{+0.10} _{-0.11}	0.05 ^{+0.10} _{-0.05}	I	0	1.40	151	92
AP1601	8.10 ^{+0.10} _{-0.00}	3.45 ^{+0.01} _{-0.03}	0.80 ^{+0.00} _{-0.05}	8.91 ^{+0.16} _{-0.16}	3.79 ^{+0.11} _{-0.12}	0.61 ^{+0.29} _{-0.33}	I	0	1.77	219	160
AP1602	8.30 ^{+0.00} _{-0.10}	2.85 ^{+0.01} _{-0.02}	0.45 ^{+0.10} _{-0.00}	8.30 ^{+0.07} _{-0.06}	2.41 ^{+0.20} _{-0.15}	0.08 ^{+0.13} _{-0.08}	I	0	1.34	40	24
AP1603	7.30 ^{+0.20} _{-0.50}	2.66 ^{+0.01} _{-0.05}	0.70 ^{+0.05} _{-0.10}	7.91 ^{+0.22} _{-0.22}	2.85 ^{+0.12} _{-0.12}	0.47 ^{+0.31} _{-0.30}	I	0	1.45	105	86
AP1604	8.80 ^{+0.00} _{-0.80}	3.38 ^{+0.02} _{-0.11}	0.20 ^{+1.20} _{-0.05}	8.89 ^{+0.10} _{-0.11}	3.18 ^{+0.10} _{-0.10}	0.12 ^{+0.15} _{-0.12}	I	0	1.18	86	28
AP1606	9.10 ^{+0.10} _{-0.00}	3.67 ^{+0.25} _{-0.18}	0.30 ^{+0.10} _{-0.15}	7.67 ^{+0.14} _{-0.15}	3.34 ^{+0.07} _{-0.07}	1.25 ^{+0.17} _{-0.17}	I	0	1.35	135	94
AP1607	8.90 ^{+0.10} _{-0.00}	3.88 ^{+0.03} _{-0.03}	0.45 ^{+0.05} _{-0.20}	8.72 ^{+0.62} _{-0.61}	3.60 ^{+0.17} _{-0.17}	0.84 ^{+0.81} _{-0.73}	I	0	2.12	302	201
AP1610	7.50 ^{+0.10} _{-0.00}	3.37 ^{+0.00} _{-0.03}	1.85 ^{+0.05} _{-0.05}	6.82 ^{+0.02} _{-0.10}	3.18 ^{+0.21} _{-0.29}	2.15 ^{+0.10} _{-0.10}	I	0	1.93	255	209
AP1611	8.60 ^{+0.00} _{-0.10}	3.53 ^{+0.01} _{-0.07}	0.85 ^{+0.15} _{-0.10}	8.26 ^{+0.17} _{-0.16}	2.86 ^{+0.21} _{-0.22}	0.73 ^{+0.36} _{-0.43}	I	0	1.54	137	92
AP1615	8.50 ^{+0.00} _{-0.90}	3.12 ^{+0.03} _{-0.13}	0.45 ^{+0.60} _{-0.00}	8.36 ^{+0.11} _{-0.10}	3.02 ^{+0.10} _{-0.10}	0.30 ^{+0.24} _{-0.24}	I	0	1.35	122	98
AP1617	9.10 ^{+0.00} _{-0.10}	3.61 ^{+0.03} _{-0.09}	0.60 ^{+0.30} _{-0.05}	8.64 ^{+0.32} _{-0.33}	2.62 ^{+0.26} _{-0.27}	0.70 ^{+0.54} _{-0.54}	I	0	1.13	57	28
AP1618	8.10 ^{+0.00} _{-0.30}	3.56 ^{+0.02} _{-0.08}	1.30 ^{+0.15} _{-0.05}	8.64 ^{+0.19} _{-0.19}	3.46 ^{+0.10} _{-0.10}	0.53 ^{+0.32} _{-0.33}	I	0	1.41	196	141
AP1620	8.40 ^{+0.10} _{-0.00}	3.36 ^{+0.18} _{-0.01}	0.85 ^{+0.35} _{-0.05}	8.67 ^{+0.14} _{-0.14}	2.93 ^{+0.11} _{-0.11}	0.21 ^{+0.19} _{-0.19}	I	0	1.34	102	68
AP1622	8.40 ^{+0.00} _{-0.00}	3.05 ^{+0.02} _{-0.04}	0.65 ^{+0.05} _{-0.15}	8.01 ^{+0.12} _{-0.14}	3.30 ^{+0.18} _{-0.20}	1.38 ^{+0.34} _{-0.32}	I	0	1.30	80	46
AP1623	8.10 ^{+0.00} _{-1.20}	3.04 ^{+0.00} _{-0.16}	0.65 ^{+0.20} _{-0.05}	7.92 ^{+0.13} _{-0.13}	2.89 ^{+0.10} _{-0.11}	0.62 ^{+0.19} _{-0.19}	I	0	1.43	87	44

Table 1 (cont'd)

AP ID ^a	CMD Best Fit Parameters ^b			Integrated Best Fit Parameters ^c			Best ^d	Flag ^e	R _{ap} ^f	N _{stars} ^g	N _{bg} ^h
	log(<i>t</i> [Myr])	log(<i>M</i> [<i>M</i> _⊙])	<i>A_V</i> [mag]	log(<i>t</i> [Myr])	log(<i>M</i> [<i>M</i> _⊙])	<i>A_V</i> [mag]					
AP1625	7.60 ^{+0.00} _{-0.20}	3.14 ^{+0.02} _{-0.04}	1.40 ^{+0.15} _{-0.00}	7.81 ^{+1.10} _{-1.27}	3.45 ^{+0.33} _{-0.38}	1.35 ^{+0.86} _{-0.91}	I	0	1.75	125	71
AP1626	7.80 ^{+0.40} _{-0.30}	2.86 ^{+0.04} _{-0.05}	0.55 ^{+0.05} _{-0.15}	7.93 ^{+0.11} _{-0.10}	3.17 ^{+0.10} _{-0.10}	0.90 ^{+0.19} _{-0.20}	I	0	1.40	158	135
AP1627	8.40 ^{+0.00} _{-0.10}	3.19 ^{+0.01} _{-0.02}	0.40 ^{+0.05} _{-0.05}	8.13 ^{+0.15} _{-0.15}	3.15 ^{+0.13} _{-0.11}	0.35 ^{+0.30} _{-0.29}	I	0	1.47	190	149
AP1628	7.90 ^{+0.50} _{-0.50}	2.84 ^{+0.03} _{-0.09}	0.80 ^{+0.05} _{-0.25}	8.27 ^{+0.07} _{-0.07}	2.51 ^{+0.15} _{-0.14}	0.04 ^{+0.08} _{-0.04}	I	0	1.57	130	99
AP1629	8.30 ^{+0.10} _{-0.00}	3.31 ^{+0.03} _{-0.02}	1.10 ^{+0.05} _{-0.10}	8.49 ^{+0.19} _{-0.19}	2.96 ^{+0.13} _{-0.14}	0.34 ^{+0.34} _{-0.31}	I	0	1.60	179	144
AP1632	7.60 ^{+0.20} _{-0.20}	3.31 ^{+0.02} _{-0.27}	1.90 ^{+0.06} _{-0.55}	7.68 ^{+0.11} _{-0.10}	3.47 ^{+0.08} _{-0.09}	1.66 ^{+0.17} _{-0.16}	I	0	1.36	141	108
AP1633	8.20 ^{+0.00} _{-0.70}	2.81 ^{+0.01} _{-0.06}	0.45 ^{+0.30} _{-0.05}	8.10 ^{+0.16} _{-0.25}	3.23 ^{+0.00} _{-0.11}	1.07 ^{+0.19} _{-0.04}	I	0	1.50	128	111
AP1634	8.80 ^{+0.00} _{-0.00}	3.44 ^{+0.03} _{-0.00}	0.05 ^{+0.15} _{-0.00}	8.40 ^{+1.31} _{-1.33}	2.74 ^{+0.42} _{-0.49}	1.57 ^{+0.94} _{-0.99}	I	0	1.10	88	54
AP1636	8.90 ^{+0.00} _{-0.10}	3.49 ^{+0.03} _{-0.03}	0.10 ^{+0.25} _{-0.05}	9.07 ^{+0.09} _{-0.11}	3.18 ^{+0.10} _{-0.11}	0.00 ^{+0.07} _{-0.00}	I	0	1.43	115	84
AP1638	7.10 ^{+0.30} _{-0.30}	3.24 ^{+0.08} _{-0.02}	2.20 ^{+0.15} _{-0.00}	6.71 ^{+0.28} _{-0.36}	3.08 ^{+0.20} _{-0.18}	2.03 ^{+0.15} _{-0.15}	I	0	1.17	81	68
AP1640	9.10 ^{+0.00} _{-0.30}	3.40 ^{+0.05} _{-0.11}	0.05 ^{+0.60} _{-0.00}	9.01 ^{+0.11} _{-0.10}	3.00 ^{+0.10} _{-0.09}	0.04 ^{+0.07} _{-0.04}	I	0	1.35	87	54
AP1642	6.90 ^{+0.10} _{-0.10}	4.16 ^{+0.03} _{-0.18}	3.00 ^{+0.00} _{-0.10}	9.32 ^{+0.10} _{-0.11}	5.08 ^{+0.05} _{-0.05}	0.12 ^{+0.14} _{-0.12}	I	0	1.56	274	300
AP1645	7.80 ^{+0.10} _{-0.00}	3.33 ^{+0.02} _{-0.02}	0.85 ^{+0.05} _{-0.05}	6.51 ^{+0.42} _{-0.44}	3.26 ^{+0.45} _{-0.48}	1.63 ^{+0.22} _{-0.21}	I	0	1.86	334	298
AP1646	8.30 ^{+0.00} _{-0.00}	3.47 ^{+0.00} _{-0.03}	0.85 ^{+0.00} _{-0.05}	8.58 ^{+0.11} _{-0.11}	3.06 ^{+0.08} _{-0.09}	0.15 ^{+0.16} _{-0.15}	I	0	1.35	140	99
AP1647	9.60 ^{+0.10} _{-0.00}	4.89 ^{+0.11} _{-0.01}	0.00 ^{+0.05} _{-0.00}	9.93 ^{+0.05} _{-0.05}	5.22 ^{+0.04} _{-0.04}	0.03 ^{+0.07} _{-0.03}	I	0	2.03	228	302
AP1651	9.10 ^{+0.10} _{-0.00}	3.47 ^{+0.26} _{-0.03}	0.25 ^{+0.05} _{-0.15}	8.42 ^{+0.86} _{-0.47}	3.36 ^{+0.20} _{-0.23}	1.25 ^{+0.78} _{-1.07}	I	0	1.23	106	86
AP1652	8.30 ^{+0.20} _{-0.90}	2.92 ^{+0.04} _{-0.31}	0.70 ^{+0.20} _{-0.35}	7.40 ^{+0.18} _{-0.18}	2.96 ^{+0.12} _{-0.08}	0.31 ^{+0.17} _{-0.18}	I	0	1.25	125	120
AP1653	8.40 ^{+0.00} _{-0.00}	3.19 ^{+0.02} _{-0.02}	0.80 ^{+0.10} _{-0.05}	9.20 ^{+0.04} _{-0.04}	3.17 ^{+0.05} _{-0.05}	0.02 ^{+0.07} _{-0.02}	I	0	1.20	84	47
AP1654	8.10 ^{+0.00} _{-0.60}	2.93 ^{+0.00} _{-0.06}	0.45 ^{+0.20} _{-0.05}	7.90 ^{+0.29} _{-0.28}	2.86 ^{+0.16} _{-0.16}	0.55 ^{+0.42} _{-0.44}	I	0	1.40	100	72
AP1655	7.80 ^{+0.20} _{-0.70}	2.70 ^{+0.01} _{-0.08}	0.35 ^{+0.10} _{-0.10}	7.96 ^{+0.03} _{-0.04}	2.38 ^{+0.11} _{-0.08}	0.04 ^{+0.10} _{-0.04}	I	0	1.40	70	42
AP1659	7.20 ^{+0.10} _{-0.00}	3.73 ^{+0.00} _{-0.01}	1.50 ^{+0.00} _{-0.10}	7.59 ^{+0.12} _{-0.15}	4.35 ^{+0.08} _{-0.08}	1.34 ^{+0.16} _{-0.18}	I	0	1.64	234	122
AP1660	8.20 ^{+0.00} _{-0.80}	3.25 ^{+0.04} _{-0.19}	1.15 ^{+0.25} _{-0.05}	9.00 ^{+0.17} _{-0.14}	3.19 ^{+0.15} _{-0.14}	0.11 ^{+0.13} _{-0.11}	I	0	1.33	133	109
AP1661	8.90 ^{+0.00} _{-0.00}	4.24 ^{+0.00} _{-0.04}	0.55 ^{+0.00} _{-0.10}	6.59 ^{+0.05} _{-0.05}	2.24 ^{+0.08} _{-0.13}	0.80 ^{+0.07} _{-0.07}	I	0	2.98	531	339
AP1662	7.60 ^{+0.00} _{-0.40}	3.35 ^{+0.02} _{-0.03}	1.55 ^{+0.20} _{-0.00}	7.49 ^{+0.19} _{-0.20}	3.48 ^{+0.07} _{-0.07}	1.45 ^{+0.21} _{-0.21}	I	0	1.28	145	120
AP1664	8.30 ^{+0.60} _{-0.10}	3.44 ^{+0.00} _{-0.12}	1.60 ^{+0.05} _{-1.40}	8.74 ^{+0.31} _{-0.39}	3.33 ^{+0.13} _{-0.13}	0.56 ^{+0.64} _{-0.47}	I	0	1.35	122	61
AP1665	7.00 ^{+0.20} _{-0.10}	3.19 ^{+0.06} _{-0.02}	1.50 ^{+0.10} _{-0.05}	7.40 ^{+0.08} _{-0.08}	3.47 ^{+0.12} _{-0.09}	0.96 ^{+0.11} _{-0.13}	I	0	1.55	138	97
AP1668	8.40 ^{+0.30} _{-1.10}	2.78 ^{+0.06} _{-0.18}	0.55 ^{+0.25} _{-0.25}	7.94 ^{+0.19} _{-0.17}	2.51 ^{+0.15} _{-0.15}	0.43 ^{+0.25} _{-0.26}	I	0	1.14	32	16
AP1672	8.20 ^{+0.00} _{-0.10}	3.31 ^{+0.00} _{-0.05}	1.50 ^{+0.05} _{-0.05}	8.00 ^{+0.03} _{-0.03}	3.19 ^{+0.05} _{-0.04}	1.70 ^{+0.08} _{-0.08}	I	0	1.29	108	84
AP1675	7.20 ^{+0.10} _{-0.50}	2.84 ^{+0.01} _{-0.04}	0.80 ^{+0.10} _{-0.05}	7.00 ^{+0.48} _{-0.57}	2.78 ^{+0.17} _{-0.17}	0.57 ^{+0.26} _{-0.28}	I	0	1.10	86	72
AP1676	7.50 ^{+0.00} _{-0.50}	2.68 ^{+0.02} _{-0.03}	0.30 ^{+0.15} _{-0.02}	6.42 ^{+0.29} _{-0.32}	2.89 ^{+0.24} _{-0.26}	0.79 ^{+0.12} _{-0.12}	I	0	1.21	97	67
AP1679	8.40 ^{+0.00} _{-0.90}	3.03 ^{+0.01} _{-0.15}	0.45 ^{+0.40} _{-0.05}	7.21 ^{+0.69} _{-0.76}	2.66 ^{+0.29} _{-0.29}	0.51 ^{+0.40} _{-0.40}	I	0	1.50	177	160
AP1680	9.70 ^{+0.00} _{-0.10}	4.74 ^{+0.00} _{-0.14}	0.20 ^{+0.00} _{-0.10}	9.62 ^{+0.11} _{-0.14}	5.18 ^{+0.06} _{-0.06}	0.07 ^{+0.12} _{-0.07}	I	0	2.10	174	288
AP1681	9.10 ^{+0.00} _{-0.10}	3.62 ^{+0.00} _{-0.13}	0.05 ^{+0.10} _{-0.05}	9.60 ^{+0.12} _{-0.11}	3.67 ^{+0.10} _{-0.10}	0.08 ^{+0.11} _{-0.08}	I	0	1.53	136	98

Table 1 (cont'd)

AP ID ^a	CMD Best Fit Parameters ^b			Integrated Best Fit Parameters ^c			Best ^d Flag ^e	Rap ^f	N _{stars} ^g	N _{bg} ^h	
	log(<i>t</i> [Myr])	log(<i>M</i> [<i>M</i> _⊙])	<i>A_V</i> [mag]	log(<i>t</i> [Myr])	log(<i>M</i> [<i>M</i> _⊙])	<i>A_V</i> [mag]					
AP1683	8.40 ^{+0.10} _{-0.00}	3.24 ^{+0.03} _{-0.05}	0.55 ^{+0.15} _{-0.10}	6.73 ^{+0.27} _{-0.27}	3.36 ^{+0.28} _{-0.31}	1.95 ^{+0.18} _{-0.19}	I	0	1.78	205	208
AP1686	7.90 ^{+0.10} _{-0.60}	2.98 ^{+0.04} _{-0.10}	0.65 ^{+0.20} _{-0.00}	7.71 ^{+0.11} _{-0.10}	3.10 ^{+0.08} _{-0.08}	1.03 ^{+0.15} _{-0.14}	I	0	1.66	139	133
AP1687	9.00 ^{+0.10} _{-0.00}	3.76 ^{+0.04} _{-0.07}	1.00 ^{+0.05} _{-0.20}	7.91 ^{+0.12} _{-0.24}	3.02 ^{+0.43} _{-0.56}	1.83 ^{+0.66} _{-0.86}	I	0	1.49	85	45
AP1688	6.70 ^{+0.40} _{-0.00}	2.86 ^{+0.03} _{-0.00}	0.60 ^{+0.00} _{-0.05}	6.79 ^{+0.10} _{-0.10}	2.66 ^{+0.29} _{-0.34}	0.53 ^{+0.09} _{-0.09}	I	0	2.65	160	138
AP1689	8.20 ^{+0.10} _{-0.90}	2.88 ^{+0.01} _{-0.13}	0.45 ^{+0.20} _{-0.10}	8.20 ^{+0.31} _{-0.27}	3.18 ^{+0.23} _{-0.20}	0.78 ^{+0.62} _{-0.67}	I	0	1.73	147	113
AP1691	8.00 ^{+0.00} _{-0.30}	3.42 ^{+0.01} _{-0.18}	2.50 ^{+0.15} _{-0.15}	8.15 ^{+0.26} _{-0.18}	2.21 ^{+0.16} _{-0.14}	0.12 ^{+0.15} _{-0.12}	I	1	1.58	107	72
AP1692	8.20 ^{+0.20} _{-0.10}	3.31 ^{+0.05} _{-0.02}	1.05 ^{+0.05} _{-0.15}	7.38 ^{+0.03} _{-0.06}	2.52 ^{+0.17} _{-0.18}	0.82 ^{+0.23} _{-0.34}	I	0	1.37	137	108
AP1693	6.90 ^{+0.30} _{-0.20}	2.79 ^{+0.02} _{-0.02}	1.65 ^{+0.05} _{-0.10}	7.84 ^{+0.06} _{-0.06}	2.54 ^{+0.09} _{-0.14}	0.34 ^{+0.12} _{-0.14}	I	0	1.62	53	31
AP1694	7.90 ^{+0.00} _{-0.60}	2.85 ^{+0.01} _{-0.06}	0.50 ^{+0.15} _{-0.00}	7.39 ^{+0.32} _{-0.30}	2.91 ^{+0.13} _{-0.13}	0.84 ^{+0.25} _{-0.24}	I	0	1.75	232	221
AP1695	7.40 ^{+0.20} _{-0.20}	3.73 ^{+0.03} _{-0.04}	2.05 ^{+0.05} _{-0.05}	7.03 ^{+0.02} _{-0.15}	3.83 ^{+0.09} _{-0.08}	1.49 ^{+0.17} _{-0.01}	I	0	1.50	113	111
AP1696	6.70 ^{+0.10} _{-0.00}	3.08 ^{+0.01} _{-0.01}	0.70 ^{+0.00} _{-0.00}	6.79 ^{+0.08} _{-0.07}	2.41 ^{+0.09} _{-0.19}	0.16 ^{+0.10} _{-0.10}	I	0	2.80	355	303
AP1697	8.40 ^{+0.30} _{-0.60}	3.23 ^{+0.03} _{-0.53}	1.20 ^{+0.05} _{-0.85}	8.64 ^{+0.16} _{-0.16}	2.95 ^{+0.12} _{-0.12}	0.26 ^{+0.24} _{-0.23}	I	0	1.44	127	84
AP1698	6.60 ^{+0.70} _{-0.00}	2.86 ^{+0.04} _{-0.01}	0.60 ^{+0.05} _{-0.05}	6.74 ^{+0.18} _{-0.17}	2.58 ^{+0.25} _{-0.28}	0.30 ^{+0.11} _{-0.12}	I	0	1.65	164	128
AP1699	9.20 ^{+0.00} _{-0.00}	4.41 ^{+0.00} _{-0.06}	0.20 ^{+0.00} _{-0.05}	8.88 ^{+0.57} _{-0.58}	3.95 ^{+0.16} _{-0.15}	0.86 ^{+0.69} _{-0.71}	I	0	2.50	436	327
AP1700	7.00 ^{+0.10} _{-0.10}	3.14 ^{+0.00} _{-0.01}	0.85 ^{+0.00} _{-0.05}	6.90 ^{+0.13} _{-0.13}	2.65 ^{+0.47} _{-0.48}	0.42 ^{+0.11} _{-0.10}	I	0	2.80	285	219
AP1701	8.50 ^{+0.00} _{-0.30}	3.46 ^{+0.12} _{-0.02}	0.75 ^{+0.55} _{-0.05}	8.64 ^{+0.28} _{-0.31}	3.20 ^{+0.18} _{-0.17}	0.37 ^{+0.46} _{-0.34}	I	0	1.38	163	108
AP1702	8.90 ^{+0.00} _{-0.50}	3.23 ^{+0.10} _{-0.18}	0.00 ^{+0.95} _{-0.05}	8.30 ^{+0.15} _{-0.14}	3.19 ^{+0.16} _{-0.14}	1.12 ^{+0.32} _{-0.33}	I	0	1.37	153	113
AP1703	8.40 ^{+0.00} _{-0.00}	3.49 ^{+0.00} _{-0.04}	1.00 ^{+0.05} _{-0.10}	8.67 ^{+0.15} _{-0.16}	3.11 ^{+0.13} _{-0.11}	0.53 ^{+0.28} _{-0.29}	I	0	1.29	134	80
AP1704	9.00 ^{+0.00} _{-0.00}	3.60 ^{+0.02} _{-0.03}	0.15 ^{+0.05} _{-0.05}	8.83 ^{+0.29} _{-0.30}	3.38 ^{+0.12} _{-0.11}	0.70 ^{+0.42} _{-0.47}	I	0	1.74	172	106
AP1707	10.00 ^{+0.10} _{-1.00}	4.45 ^{+0.33} _{-0.55}	0.70 ^{+0.65} _{-0.15}	9.16 ^{+0.80} _{-0.69}	3.45 ^{+0.20} _{-0.16}	1.28 ^{+0.81} _{-0.80}	I	0	1.34	72	36
AP1709	8.50 ^{+0.20} _{-0.00}	3.30 ^{+0.00} _{-0.10}	0.75 ^{+0.05} _{-0.45}	8.63 ^{+0.10} _{-0.10}	2.94 ^{+0.09} _{-0.08}	0.19 ^{+0.18} _{-0.18}	I	0	1.27	124	101
AP1710	9.60 ^{+0.00} _{-0.10}	4.60 ^{+0.00} _{-0.12}	0.00 ^{+0.10} _{-0.00}	9.70 ^{+0.55} _{-0.85}	5.02 ^{+0.20} _{-0.27}	0.47 ^{+0.74} _{-0.47}	I	0	1.35	88	157
AP1712	9.10 ^{+0.40} _{-0.20}	4.04 ^{+0.34} _{-0.02}	0.95 ^{+0.40} _{-0.10}	8.98 ^{+0.62} _{-0.90}	3.66 ^{+0.16} _{-0.14}	1.02 ^{+1.19} _{-0.79}	I	0	1.50	170	122
AP1714	8.80 ^{+0.60} _{-0.20}	3.87 ^{+0.21} _{-2.54}	1.50 ^{+0.35} _{-0.55}	10.13 ^{+0.12} _{-0.32}	3.89 ^{+0.04} _{-0.03}	0.08 ^{+0.20} _{-0.08}	I	0	1.24	126	73
AP1717	8.20 ^{+0.00} _{-0.00}	3.30 ^{+0.00} _{-0.03}	0.85 ^{+0.00} _{-0.05}	8.11 ^{+0.12} _{-0.11}	3.20 ^{+0.13} _{-0.12}	0.67 ^{+0.23} _{-0.24}	I	0	1.81	220	172
AP1718	10.10 ^{+0.00} _{-0.10}	5.02 ^{+0.00} _{-0.39}	0.15 ^{+0.05} _{-0.00}	9.14 ^{+0.87} _{-0.62}	3.90 ^{+0.19} _{-0.14}	1.35 ^{+0.77} _{-0.87}	I	0	2.04	149	80
AP1720	7.60 ^{+0.10} _{-0.40}	3.66 ^{+0.05} _{-0.48}	2.35 ^{+0.05} _{-0.45}	6.71 ^{+0.12} _{-0.12}	2.81 ^{+0.36} _{-0.38}	2.22 ^{+0.12} _{-0.11}	I	0	1.44	191	143
AP1722	9.00 ^{+0.10} _{-0.10}	3.37 ^{+0.04} _{-0.13}	0.15 ^{+0.25} _{-0.05}	10.20 ^{+0.04} _{-0.04}	4.00 ^{+0.05} _{-0.05}	0.11 ^{+0.08} _{-0.09}	I	0	1.40	85	46
AP1724	7.90 ^{+0.30} _{-0.50}	2.88 ^{+0.04} _{-0.11}	0.70 ^{+0.10} _{-0.20}	7.83 ^{+0.05} _{-0.05}	2.74 ^{+0.07} _{-0.07}	0.85 ^{+0.10} _{-0.10}	I	0	1.23	119	118
AP1725	8.00 ^{+0.00} _{-0.40}	3.30 ^{+0.00} _{-0.06}	0.85 ^{+0.15} _{-0.05}	7.71 ^{+0.20} _{-0.20}	3.59 ^{+0.08} _{-0.08}	1.42 ^{+0.25} _{-0.25}	I	0	1.45	188	154
AP1726	10.00 ^{+0.00} _{-0.50}	4.52 ^{+0.01} _{-0.48}	0.10 ^{+0.25} _{-0.00}	8.62 ^{+0.58} _{-0.54}	3.18 ^{+0.26} _{-0.23}	0.93 ^{+0.78} _{-0.75}	I	0	1.61	107	59
AP1727	7.00 ^{+0.50} _{-0.30}	2.83 ^{+0.01} _{-0.09}	0.80 ^{+0.00} _{-0.25}	6.79 ^{+0.45} _{-0.49}	2.75 ^{+0.19} _{-0.21}	0.80 ^{+0.16} _{-0.16}	I	0	1.21	114	105
AP1728	9.10 ^{+1.00} _{-0.00}	4.08 ^{+1.11} _{-0.05}	0.40 ^{+0.10} _{-0.30}	9.11 ^{+1.03} _{-0.53}	4.03 ^{+0.27} _{-0.09}	1.47 ^{+0.64} _{-1.00}	I	0	1.79	251	192

Table 1 (cont'd)

AP ID ^a	CMD Best Fit Parameters ^b			Integrated Best Fit Parameters ^c			Best ^d Flag ^e	R _{ap} ^f	N _{stars} ^g	N _{bg} ^h	
	log(<i>t</i> [Myr])	log(<i>M</i> [<i>M</i> _⊙])	<i>A_V</i> [mag]	log(<i>t</i> [Myr])	log(<i>M</i> [<i>M</i> _⊙])	<i>A_V</i> [mag]					
AP1730	7.60 ^{+1.20} _{-0.00}	3.82 ^{+0.00} _{-0.86}	2.90 ^{+0.05} _{-2.75}	9.17 ^{+0.11} _{-0.07}	3.62 ^{+0.11} _{-0.09}	0.08 ^{+0.10} _{-0.08}	I	0	1.42	164	137
AP1731	7.70 ^{+0.30} _{-0.30}	3.41 ^{+0.00} _{-0.17}	2.10 ^{+0.20} _{-0.30}	9.45 ^{+0.04} _{-0.05}	3.46 ^{+0.06} _{-0.05}	0.00 ^{+0.07} _{-0.00}	I	0	1.04	92	65
AP1733	8.50 ^{+0.11} _{-0.00}	3.38 ^{+0.01} _{-0.05}	0.70 ^{+0.00} _{-0.35}	8.65 ^{+0.17} _{-0.18}	3.11 ^{+0.10} _{-0.09}	0.20 ^{+0.21} _{-0.20}	I	0	1.22	99	73
AP1734	8.50 ^{+0.10} _{-0.20}	3.13 ^{+0.03} _{-0.11}	0.75 ^{+0.20} _{-0.20}	8.54 ^{+0.78} _{-0.64}	3.31 ^{+0.21} _{-0.22}	1.10 ^{+0.85} _{-0.98}	I	0	1.53	153	120
AP1735	9.00 ^{+0.00} _{-0.20}	3.36 ^{+0.11} _{-0.02}	0.00 ^{+0.54} _{-0.10}	8.24 ^{+0.15} _{-0.15}	2.33 ^{+0.17} _{-0.19}	0.17 ^{+0.18} _{-0.17}	I	0	1.15	93	78
AP1736	9.10 ^{+0.30} _{-0.00}	3.97 ^{+0.39} _{-0.06}	0.60 ^{+0.00} _{-0.50}	7.73 ^{+0.11} _{-0.10}	3.05 ^{+0.11} _{-0.13}	0.86 ^{+0.17} _{-0.17}	I	0	1.49	188	133
AP1738	9.40 ^{+0.10} _{-0.00}	4.88 ^{+0.07} _{-0.00}	0.05 ^{+0.00} _{-0.05}	9.51 ^{+0.17} _{-0.38}	5.10 ^{+0.09} _{-0.15}	0.09 ^{+0.22} _{-0.09}	I	0	2.57	482	475
AP1739	9.40 ^{+0.10} _{-0.10}	3.93 ^{+0.07} _{-0.22}	0.05 ^{+0.10} _{-0.05}	8.54 ^{+0.44} _{-0.38}	2.99 ^{+0.20} _{-0.20}	0.68 ^{+0.61} _{-0.57}	I	0	1.35	114	93
AP1740	8.50 ^{+0.10} _{-0.00}	3.09 ^{+0.02} _{-0.07}	0.75 ^{+0.10} _{-0.25}	8.51 ^{+0.36} _{-0.29}	2.90 ^{+0.17} _{-0.16}	0.61 ^{+0.44} _{-0.47}	I	0	1.23	80	50
AP1741	8.30 ^{+0.00} _{-0.70}	3.26 ^{+0.00} _{-0.10}	0.40 ^{+0.30} _{-0.05}	8.31 ^{+0.07} _{-0.06}	3.23 ^{+0.09} _{-0.08}	0.11 ^{+0.14} _{-0.11}	I	0	2.19	367	328
AP1743	8.70 ^{+0.00} _{-0.10}	2.97 ^{+0.04} _{-0.04}	0.05 ^{+0.25} _{-0.00}	8.65 ^{+0.14} _{-0.14}	2.72 ^{+0.13} _{-0.12}	0.35 ^{+0.25} _{-0.25}	I	0	1.28	83	56
AP1744	8.20 ^{+0.10} _{-0.00}	3.06 ^{+0.00} _{-0.07}	1.05 ^{+0.00} _{-0.20}	8.67 ^{+0.22} _{-0.21}	3.04 ^{+0.10} _{-0.11}	0.44 ^{+0.29} _{-0.29}	I	0	1.36	91	57
AP1747	8.00 ^{+0.00} _{-0.40}	3.11 ^{+0.00} _{-0.09}	1.25 ^{+0.15} _{-0.10}	8.34 ^{+0.15} _{-0.14}	3.14 ^{+0.17} _{-0.14}	0.76 ^{+0.34} _{-0.35}	I	0	1.39	120	76
AP1749	9.00 ^{+0.00} _{-0.00}	4.04 ^{+0.00} _{-0.08}	0.75 ^{+0.00} _{-0.15}	8.75 ^{+0.44} _{-0.44}	3.10 ^{+0.21} _{-0.18}	0.73 ^{+0.56} _{-0.52}	I	0	1.39	133	75
AP1752	8.10 ^{+0.00} _{-0.00}	4.60 ^{+0.00} _{-0.02}	1.70 ^{+0.00} _{-0.05}	9.48 ^{+0.09} _{-0.09}	5.39 ^{+0.05} _{-0.04}	0.12 ^{+0.16} _{-0.12}	I	0	2.01	337	439
AP1754	6.60 ^{+0.10} _{-0.00}	4.36 ^{+0.03} _{-0.00}	3.00 ^{+0.00} _{-0.00}	9.16 ^{+0.07} _{-0.07}	4.78 ^{+0.05} _{-0.05}	0.11 ^{+0.12} _{-0.11}	I	0	1.59	331	288
AP1756	7.60 ^{+0.10} _{-0.50}	3.02 ^{+0.01} _{-0.16}	1.65 ^{+0.10} _{-0.35}	7.16 ^{+0.17} _{-0.16}	2.72 ^{+0.23} _{-0.24}	1.08 ^{+0.15} _{-0.15}	I	0	1.77	129	112
AP1757	8.60 ^{+0.00} _{-0.10}	3.15 ^{+0.00} _{-0.05}	0.20 ^{+0.20} _{-0.00}	7.27 ^{+0.74} _{-0.78}	3.07 ^{+0.30} _{-0.29}	1.78 ^{+0.75} _{-0.92}	I	0	1.73	139	108
AP1759	7.60 ^{+0.00} _{-0.60}	2.97 ^{+0.01} _{-0.05}	0.80 ^{+0.15} _{-0.05}	7.98 ^{+0.16} _{-0.17}	3.34 ^{+0.11} _{-0.11}	0.99 ^{+0.29} _{-0.28}	I	0	1.33	102	84
AP1760	9.20 ^{+0.40} _{-1.80}	3.87 ^{+0.00} _{-3.87}	0.45 ^{+1.70} _{-0.15}	7.42 ^{+0.37} _{-0.33}	3.62 ^{+0.16} _{-0.15}	2.31 ^{+0.38} _{-0.50}	I	0	1.54	159	115
AP1762	8.40 ^{+0.40} _{-0.00}	3.38 ^{+0.01} _{-0.16}	1.35 ^{+0.00} _{-0.85}	9.33 ^{+0.04} _{-0.04}	3.33 ^{+0.09} _{-0.14}	0.07 ^{+0.09} _{-0.07}	I	0	1.28	116	73
AP1763	8.90 ^{+0.00} _{-0.20}	3.16 ^{+0.02} _{-0.06}	0.00 ^{+0.40} _{-0.05}	8.60 ^{+0.16} _{-0.15}	2.79 ^{+0.15} _{-0.13}	0.32 ^{+0.25} _{-0.25}	I	0	1.40	89	63
AP1766	7.50 ^{+0.10} _{-0.50}	2.81 ^{+0.02} _{-0.03}	0.90 ^{+0.15} _{-0.00}	7.16 ^{+0.46} _{-0.57}	2.69 ^{+0.13} _{-0.14}	0.53 ^{+0.21} _{-0.22}	I	0	1.50	67	42
AP1768	8.70 ^{+0.00} _{-0.00}	3.96 ^{+0.00} _{-0.06}	0.95 ^{+0.05} _{-0.15}	7.39 ^{+0.15} _{-0.16}	3.13 ^{+0.17} _{-0.15}	0.79 ^{+0.24} _{-0.23}	I	0	2.45	404	281
AP1769	9.00 ^{+0.60} _{-0.10}	4.24 ^{+0.20} _{-0.19}	1.30 ^{+0.35} _{-0.55}	8.82 ^{+0.97} _{-0.96}	3.88 ^{+0.30} _{-0.28}	1.79 ^{+0.85} _{-0.82}	I	0	1.39	126	62
AP1770	8.80 ^{+0.00} _{-0.50}	2.88 ^{+0.01} _{-0.07}	0.30 ^{+0.75} _{-0.05}	7.76 ^{+1.03} _{-1.02}	2.73 ^{+0.20} _{-0.22}	1.37 ^{+0.62} _{-0.91}	I	0	1.04	37	16
AP1773	9.40 ^{+0.20} _{-0.00}	4.55 ^{+0.23} _{-0.00}	0.00 ^{+0.05} _{-0.00}	9.65 ^{+0.03} _{-0.03}	5.45 ^{+0.03} _{-0.03}	0.00 ^{+0.07} _{-0.00}	I	0	3.16	468	506
AP1774	8.00 ^{+0.10} _{-1.10}	2.60 ^{+0.04} _{-0.19}	1.15 ^{+0.30} _{-0.15}	6.86 ^{+0.31} _{-0.36}	2.34 ^{+0.18} _{-0.20}	0.61 ^{+0.14} _{-0.15}	I	0	1.54	51	48
AP1775	7.80 ^{+0.00} _{-0.80}	2.75 ^{+0.00} _{-0.08}	0.50 ^{+0.15} _{-0.05}	7.41 ^{+0.36} _{-0.34}	2.71 ^{+0.15} _{-0.17}	0.43 ^{+0.24} _{-0.25}	I	0	1.38	129	100
AP1776	6.60 ^{+0.40} _{-0.00}	2.88 ^{+0.02} _{-0.01}	1.05 ^{+0.05} _{-0.05}	7.05 ^{+0.25} _{-0.20}	2.71 ^{+0.20} _{-0.21}	0.63 ^{+0.18} _{-0.19}	I	0	1.90	84	51
AP1778	8.70 ^{+0.10} _{-0.00}	3.56 ^{+0.03} _{-0.05}	0.50 ^{+0.15} _{-0.15}	8.84 ^{+0.14} _{-0.14}	3.31 ^{+0.10} _{-0.10}	0.38 ^{+0.27} _{-0.28}	I	0	1.41	159	93
AP1779	9.00 ^{+0.00} _{-0.10}	3.45 ^{+0.03} _{-0.07}	0.00 ^{+0.25} _{-0.00}	8.37 ^{+0.08} _{-0.06}	3.05 ^{+0.10} _{-0.11}	0.49 ^{+0.20} _{-0.21}	I	0	1.52	149	66
AP1782	8.30 ^{+0.30} _{-0.00}	3.67 ^{+0.07} _{-0.00}	1.15 ^{+0.00} _{-0.45}	8.57 ^{+0.13} _{-0.12}	3.19 ^{+0.11} _{-0.11}	0.21 ^{+0.21} _{-0.20}	I	0	1.75	237	140

Table 1 (cont'd)

AP ID ^a	CMD Best Fit Parameters ^b			Integrated Best Fit Parameters ^c			Best ^d Flag ^e	Rap ^f	N _{stars} ^g	N _{bg} ^h	
	log(<i>t</i> [Myr])	log(<i>M</i> [<i>M</i> _⊙])	<i>A_V</i> [mag]	log(<i>t</i> [Myr])	log(<i>M</i> [<i>M</i> _⊙])	<i>A_V</i> [mag]					
AP1783	8.70 ^{+0.30} _{-1.10}	3.32 ^{+0.00} _{-3.32}	1.60 ^{+1.00} _{-0.80}	8.39 ^{+0.56} _{-0.53}	2.84 ^{+0.26} _{-0.27}	0.85 ^{+0.98} _{-0.74}	I	0	1.33	78	34
AP1784	8.40 ^{+0.10} _{-0.20}	2.84 ^{+0.01} _{-0.07}	0.50 ^{+0.05} _{-0.20}	8.38 ^{+0.43} _{-0.37}	2.94 ^{+0.22} _{-0.22}	0.78 ^{+0.71} _{-0.71}	I	0	1.31	96	68
AP1786	7.50 ^{+0.20} _{-0.10}	3.36 ^{+0.01} _{-0.02}	1.60 ^{+0.00} _{-0.15}	7.67 ^{+0.17} _{-0.21}	3.25 ^{+0.15} _{-0.14}	0.99 ^{+0.30} _{-0.26}	I	0	1.33	121	90
AP1787	9.10 ^{+0.00} _{-0.00}	4.00 ^{+0.02} _{-0.05}	0.20 ^{+0.05} _{-0.05}	9.62 ^{+0.36} _{-0.35}	3.93 ^{+0.19} _{-0.18}	0.32 ^{+0.29} _{-0.29}	I	0	1.37	153	99
AP1788	8.10 ^{+1.20} _{-0.90}	2.89 ^{+0.17} _{-2.89}	1.00 ^{+1.25} _{-0.40}	8.95 ^{+0.04} _{-0.05}	4.28 ^{+0.05} _{-0.05}	0.05 ^{+0.09} _{-0.05}	I	1	1.23	186	181
AP1790	6.80 ^{+0.70} _{-0.10}	2.57 ^{+0.03} _{-0.15}	1.20 ^{+0.10} _{-0.10}	6.96 ^{+0.15} _{-0.11}	2.37 ^{+0.20} _{-0.22}	0.38 ^{+0.11} _{-0.11}	I	0	1.35	111	111
AP1791	7.70 ^{+0.30} _{-0.10}	3.51 ^{+0.04} _{-0.02}	1.45 ^{+0.05} _{-0.10}	7.62 ^{+0.42} _{-0.46}	3.67 ^{+0.27} _{-0.17}	1.67 ^{+0.65} _{-0.53}	I	0	1.56	197	136
AP1792	9.40 ^{+0.00} _{-0.00}	4.57 ^{+0.00} _{-0.00}	0.00 ^{+0.00} _{-0.00}	9.39 ^{+0.06} _{-0.06}	5.09 ^{+0.04} _{-0.03}	0.13 ^{+0.07} _{-0.09}	I	0	2.26	218	385
AP1794	9.40 ^{+0.20} _{-0.00}	4.59 ^{+0.15} _{-0.04}	0.20 ^{+0.10} _{-0.15}	10.25 ^{+0.00} _{-0.03}	5.45 ^{+0.04} _{-0.04}	0.18 ^{+0.08} _{-0.07}	I	0	2.36	238	340
AP1795	8.90 ^{+0.00} _{-0.10}	3.25 ^{+0.03} _{-0.03}	0.20 ^{+0.30} _{-0.05}	7.76 ^{+0.03} _{-0.04}	2.19 ^{+0.07} _{-0.08}	1.00 ^{+0.10} _{-0.07}	I	0	1.48	82	57
AP1797	7.30 ^{+2.20} _{-0.40}	2.17 ^{+0.21} _{-2.17}	1.55 ^{+1.00} _{-0.95}	0.00 ^{+0.00} _{-0.00}	0.00 ^{+0.00} _{-0.00}	0.00 ^{+0.00} _{-0.00}	I	0	2.86	191	833
AP1798	9.10 ^{+0.00} _{-0.20}	3.55 ^{+0.05} _{-0.11}	0.25 ^{+0.45} _{-0.05}	9.22 ^{+0.11} _{-0.14}	3.47 ^{+0.14} _{-0.14}	0.07 ^{+0.10} _{-0.07}	I	0	1.57	136	65
AP1799	8.20 ^{+0.00} _{-0.10}	3.06 ^{+0.00} _{-0.03}	0.40 ^{+0.05} _{-0.05}	7.98 ^{+0.15} _{-0.16}	3.06 ^{+0.15} _{-0.14}	0.57 ^{+0.28} _{-0.28}	I	0	1.85	206	164
AP1800	8.90 ^{+0.00} _{-0.50}	3.30 ^{+0.05} _{-0.05}	0.05 ^{+1.10} _{-0.05}	8.72 ^{+0.17} _{-0.21}	3.65 ^{+0.12} _{-0.10}	1.01 ^{+0.29} _{-0.27}	I	0	1.50	223	199
AP1801	8.10 ^{+0.10} _{-0.10}	3.29 ^{+0.03} _{-0.07}	1.45 ^{+0.05} _{-0.20}	8.68 ^{+0.17} _{-0.19}	3.31 ^{+0.12} _{-0.12}	0.74 ^{+0.30} _{-0.28}	I	0	1.44	150	112
AP1802	9.30 ^{+0.10} _{-0.00}	4.60 ^{+0.07} _{-0.00}	0.00 ^{+0.05} _{-0.05}	9.21 ^{+0.05} _{-0.05}	5.52 ^{+0.04} _{-0.04}	0.16 ^{+0.10} _{-0.10}	I	0	3.18	290	927
AP1803	6.90 ^{+0.10} _{-0.30}	3.13 ^{+0.03} _{-0.01}	1.40 ^{+0.15} _{-0.05}	6.85 ^{+0.11} _{-0.12}	3.12 ^{+0.27} _{-0.29}	0.91 ^{+0.09} _{-0.09}	I	0	1.46	135	98
AP1808	7.20 ^{+0.30} _{-0.10}	3.21 ^{+0.02} _{-0.01}	0.85 ^{+0.05} _{-0.05}	7.80 ^{+0.08} _{-0.07}	3.14 ^{+0.07} _{-0.08}	0.39 ^{+0.11} _{-0.11}	I	0	1.64	120	56
AP1810	8.20 ^{+0.10} _{-0.10}	3.46 ^{+0.03} _{-0.09}	1.55 ^{+0.15} _{-0.15}	9.03 ^{+0.12} _{-0.12}	3.38 ^{+0.10} _{-0.10}	0.22 ^{+0.19} _{-0.19}	I	0	1.57	176	148
AP1812	8.40 ^{+0.10} _{-0.00}	3.06 ^{+0.02} _{-0.07}	0.55 ^{+0.05} _{-0.15}	8.19 ^{+0.19} _{-0.17}	3.28 ^{+0.17} _{-0.20}	0.97 ^{+0.40} _{-0.45}	I	0	1.77	186	138
AP1813	8.00 ^{+0.40} _{-0.30}	3.34 ^{+0.27} _{-0.16}	2.45 ^{+0.40} _{-0.05}	0.00 ^{+0.00} _{-0.00}	0.00 ^{+0.00} _{-0.00}	0.00 ^{+0.00} _{-0.00}	I	0	1.14	37	14
AP1814	8.10 ^{+0.40} _{-0.30}	2.97 ^{+0.05} _{-0.11}	1.15 ^{+0.05} _{-0.45}	7.14 ^{+0.24} _{-0.21}	3.16 ^{+0.13} _{-0.10}	2.16 ^{+0.19} _{-0.15}	I	0	1.08	71	46
AP1816	7.50 ^{+0.20} _{-0.00}	3.67 ^{+0.08} _{-0.09}	3.00 ^{+0.00} _{-0.10}	9.60 ^{+0.09} _{-0.11}	4.90 ^{+0.04} _{-0.04}	0.06 ^{+0.11} _{-0.06}	I	0	2.15	87	351
AP1817	8.90 ^{+0.00} _{-0.00}	3.38 ^{+0.06} _{-0.02}	0.10 ^{+0.20} _{-0.00}	8.73 ^{+0.19} _{-0.21}	2.92 ^{+0.13} _{-0.14}	0.39 ^{+0.30} _{-0.32}	I	0	1.23	95	52
AP1818	8.80 ^{+0.00} _{-0.00}	3.50 ^{+0.02} _{-0.03}	0.45 ^{+0.05} _{-0.10}	9.06 ^{+0.11} _{-0.12}	3.21 ^{+0.12} _{-0.13}	0.04 ^{+0.09} _{-0.04}	I	0	1.53	109	68
AP1819	8.20 ^{+0.00} _{-0.40}	2.78 ^{+0.01} _{-0.06}	0.70 ^{+0.15} _{-0.05}	7.16 ^{+0.71} _{-0.77}	2.34 ^{+0.19} _{-0.21}	0.35 ^{+0.31} _{-0.29}	I	0	1.46	48	16
AP1820	6.80 ^{+0.10} _{-0.10}	3.44 ^{+0.01} _{-0.02}	0.65 ^{+0.00} _{-0.05}	7.09 ^{+0.29} _{-0.17}	4.26 ^{+0.09} _{-0.10}	0.79 ^{+0.21} _{-0.44}	I	0	2.62	255	161
AP1821	7.80 ^{+0.30} _{-0.60}	2.69 ^{+0.02} _{-0.07}	0.75 ^{+0.10} _{-0.10}	8.51 ^{+0.05} _{-0.05}	3.71 ^{+0.06} _{-0.06}	0.06 ^{+0.10} _{-0.06}	I	0	1.37	66	39
AP1822	9.20 ^{+0.00} _{-0.00}	3.63 ^{+0.08} _{-0.06}	0.10 ^{+0.10} _{-0.05}	7.85 ^{+0.03} _{-0.03}	2.80 ^{+0.03} _{-0.03}	0.00 ^{+0.07} _{-0.00}	I	0	2.12	124	98
AP1825	6.60 ^{+1.40} _{-0.10}	2.62 ^{+0.05} _{-0.10}	0.70 ^{+0.20} _{-0.20}	7.10 ^{+0.04} _{-0.04}	3.84 ^{+0.08} _{-0.07}	0.34 ^{+0.19} _{-0.20}	I	0	2.63	267	334
AP1826	7.80 ^{+0.30} _{-0.30}	2.96 ^{+0.04} _{-0.04}	0.65 ^{+0.10} _{-0.10}	6.90 ^{+0.49} _{-0.55}	2.78 ^{+0.23} _{-0.25}	1.24 ^{+0.28} _{-0.29}	I	0	1.66	174	169
AP1827	9.10 ^{+0.00} _{-0.00}	3.38 ^{+0.04} _{-0.11}	0.10 ^{+0.15} _{-0.05}	9.16 ^{+0.75} _{-0.59}	3.57 ^{+0.22} _{-0.16}	0.80 ^{+0.69} _{-0.70}	I	0	1.41	109	66
AP1828	7.10 ^{+0.00} _{-0.40}	2.76 ^{+0.02} _{-0.01}	1.15 ^{+0.15} _{-0.00}	6.74 ^{+0.11} _{-0.09}	2.90 ^{+0.22} _{-0.25}	1.11 ^{+0.11} _{-0.11}	I	0	1.36	102	77

Table 1 (cont'd)

AP ID ^a	CMD Best Fit Parameters ^b			Integrated Best Fit Parameters ^c			Best ^d Flag ^e	R _{ap} ^f	N _{stars} ^g	N _{bg} ^h	
	log(<i>t</i> [Myr])	log(<i>M</i> [<i>M</i> _⊙])	<i>A_V</i> [mag]	log(<i>t</i> [Myr])	log(<i>M</i> [<i>M</i> _⊙])	<i>A_V</i> [mag]					
AP1829	9.00 ^{+0.10} _{-0.00}	3.52 ^{+0.11} _{-0.11}	0.30 ^{+0.10} _{-0.20}	9.16 ^{+0.71} _{-0.77}	3.90 ^{+0.18} _{-0.17}	0.87 ^{+0.90} _{-0.72}	I	0	1.68	187	121
AP1831	9.00 ^{+0.00} _{-0.10}	3.67 ^{+0.03} _{-0.08}	0.15 ^{+0.20} _{-0.05}	8.79 ^{+0.21} _{-0.15}	3.12 ^{+0.13} _{-0.13}	0.28 ^{+0.15} _{-0.28}	I	0	1.82	192	160
AP1833	8.90 ^{+0.00} _{-0.00}	3.40 ^{+0.04} _{-0.03}	0.05 ^{+0.15} _{-0.05}	8.83 ^{+0.07} _{-0.07}	2.95 ^{+0.07} _{-0.07}	0.01 ^{+0.07} _{-0.01}	I	0	1.31	138	76
AP1834	8.10 ^{+0.30} _{-0.20}	3.08 ^{+0.02} _{-0.09}	0.85 ^{+0.05} _{-0.30}	7.85 ^{+0.27} _{-0.36}	3.38 ^{+0.27} _{-0.23}	1.12 ^{+0.70} _{-0.50}	I	0	1.30	145	117
AP1835	8.20 ^{+0.10} _{-0.10}	3.40 ^{+0.00} _{-0.13}	1.50 ^{+0.00} _{-0.15}	8.58 ^{+0.90} _{-0.84}	3.72 ^{+0.25} _{-0.24}	1.26 ^{+0.99} _{-0.97}	I	0	1.90	300	231
AP1836	6.90 ^{+0.10} _{-0.30}	2.70 ^{+0.01} _{-0.01}	0.50 ^{+0.05} _{-0.00}	6.89 ^{+0.13} _{-0.12}	2.58 ^{+0.27} _{-0.30}	0.44 ^{+0.10} _{-0.10}	I	0	2.06	244	236
AP1837	8.20 ^{+0.10} _{-0.90}	2.98 ^{+0.01} _{-0.12}	0.85 ^{+0.40} _{-0.05}	8.08 ^{+0.27} _{-0.26}	2.82 ^{+0.13} _{-0.12}	0.66 ^{+0.39} _{-0.43}	I	0	1.20	103	84
AP1838	9.10 ^{+0.00} _{-0.00}	3.32 ^{+0.02} _{-0.04}	0.05 ^{+0.10} _{-0.05}	8.61 ^{+0.55} _{-0.48}	3.15 ^{+0.21} _{-0.17}	0.77 ^{+0.65} _{-0.65}	I	0	1.35	102	71
AP1840	8.90 ^{+0.00} _{-0.10}	3.47 ^{+0.05} _{-0.04}	0.30 ^{+0.35} _{-0.00}	9.33 ^{+0.21} _{-0.22}	3.50 ^{+0.16} _{-0.17}	0.21 ^{+0.19} _{-0.19}	I	0	1.44	123	90
AP1841	8.80 ^{+0.00} _{-0.20}	3.08 ^{+0.03} _{-0.03}	0.05 ^{+0.35} _{-0.00}	8.99 ^{+0.11} _{-0.09}	3.05 ^{+0.10} _{-0.09}	0.05 ^{+0.10} _{-0.05}	I	0	1.62	119	83
AP1842	7.20 ^{+0.60} _{-0.40}	2.63 ^{+0.02} _{-0.10}	0.90 ^{+0.10} _{-0.30}	8.09 ^{+0.10} _{-0.09}	2.64 ^{+0.13} _{-0.13}	0.06 ^{+0.11} _{-0.06}	I	0	1.41	131	94
AP1843	9.90 ^{+0.10} _{-0.20}	4.82 ^{+0.06} _{-0.24}	0.25 ^{+0.30} _{-0.05}	9.46 ^{+0.48} _{-0.48}	4.06 ^{+0.17} _{-0.15}	0.62 ^{+0.53} _{-0.45}	I	0	1.95	258	161
AP1845	7.60 ^{+0.30} _{-0.20}	3.13 ^{+0.02} _{-0.03}	1.10 ^{+0.05} _{-0.10}	7.51 ^{+0.42} _{-0.38}	2.95 ^{+0.14} _{-0.14}	0.72 ^{+0.38} _{-0.38}	I	0	1.53	188	162
AP1846	8.60 ^{+0.00} _{-0.10}	3.39 ^{+0.00} _{-0.04}	0.35 ^{+0.20} _{-0.00}	8.52 ^{+0.16} _{-0.16}	3.15 ^{+0.12} _{-0.11}	0.31 ^{+0.29} _{-0.28}	I	0	1.47	158	98
AP1847	9.00 ^{+0.00} _{-0.00}	3.72 ^{+0.03} _{-0.02}	0.00 ^{+0.15} _{-0.00}	9.17 ^{+0.55} _{-0.58}	3.95 ^{+0.15} _{-0.14}	0.66 ^{+0.62} _{-0.57}	I	0	1.80	303	260
AP1848	8.90 ^{+0.00} _{-1.00}	2.95 ^{+0.00} _{-0.48}	0.60 ^{+1.25} _{-0.05}	7.48 ^{+0.34} _{-0.33}	3.10 ^{+0.12} _{-0.10}	2.23 ^{+0.37} _{-0.30}	I	0	1.09	44	24
AP1849	10.10 ^{+0.10} _{-2.50}	5.33 ^{+0.39} _{-5.33}	0.25 ^{+1.90} _{-0.05}	9.60 ^{+0.51} _{-0.66}	4.07 ^{+0.17} _{-0.17}	0.64 ^{+0.65} _{-0.50}	I	0	1.28	160	107
AP1850	8.10 ^{+0.00} _{-0.40}	3.17 ^{+0.00} _{-0.07}	1.00 ^{+0.20} _{-0.00}	7.05 ^{+0.52} _{-0.69}	3.11 ^{+0.16} _{-0.11}	1.67 ^{+0.26} _{-0.28}	I	0	1.52	164	146
AP1852	9.00 ^{+0.10} _{-0.10}	3.38 ^{+0.09} _{-0.03}	0.20 ^{+0.35} _{-0.10}	9.39 ^{+0.20} _{-0.24}	3.64 ^{+0.14} _{-0.16}	0.14 ^{+0.17} _{-0.14}	I	0	1.31	103	62
AP1854	7.20 ^{+0.50} _{-0.40}	2.69 ^{+0.04} _{-0.03}	0.45 ^{+0.05} _{-0.10}	7.90 ^{+0.07} _{-0.07}	2.70 ^{+0.09} _{-0.09}	0.05 ^{+0.09} _{-0.05}	I	0	1.39	143	137
AP1855	8.50 ^{+0.00} _{-0.10}	3.03 ^{+0.00} _{-0.06}	0.75 ^{+0.05} _{-0.10}	8.44 ^{+0.16} _{-0.16}	3.14 ^{+0.16} _{-0.14}	1.09 ^{+0.38} _{-0.37}	I	0	1.43	90	52
AP1856	10.00 ^{+0.40} _{-2.60}	4.07 ^{+0.38} _{-4.07}	0.05 ^{+2.55} _{-0.25}	6.48 ^{+0.37} _{-0.33}	2.79 ^{+0.22} _{-0.28}	1.62 ^{+0.13} _{-0.12}	I	0	1.47	61	28
AP1858	8.30 ^{+0.10} _{-1.00}	3.27 ^{+0.03} _{-0.16}	0.65 ^{+0.35} _{-0.05}	8.27 ^{+0.11} _{-0.11}	2.93 ^{+0.12} _{-0.12}	0.21 ^{+0.20} _{-0.19}	I	0	1.34	123	95
AP1859	9.00 ^{+0.10} _{-0.00}	3.50 ^{+0.09} _{-0.03}	0.30 ^{+0.10} _{-0.10}	8.65 ^{+0.26} _{-0.26}	2.96 ^{+0.12} _{-0.13}	0.66 ^{+0.39} _{-0.40}	I	0	1.41	92	35
AP1864	8.80 ^{+0.10} _{-0.00}	3.34 ^{+0.06} _{-0.03}	0.35 ^{+0.15} _{-0.20}	8.82 ^{+0.05} _{-0.05}	3.04 ^{+0.05} _{-0.04}	0.23 ^{+0.07} _{-0.09}	I	0	1.50	119	55
AP1865	8.20 ^{+0.10} _{-0.20}	3.45 ^{+0.02} _{-0.11}	1.35 ^{+0.10} _{-0.10}	8.69 ^{+0.26} _{-0.28}	3.11 ^{+0.15} _{-0.13}	0.38 ^{+0.39} _{-0.36}	I	0	1.35	145	105
AP1866	7.60 ^{+2.10} _{-0.40}	3.24 ^{+0.01} _{-3.24}	2.95 ^{+0.25} _{-2.65}	8.75 ^{+0.28} _{-0.37}	3.68 ^{+0.10} _{-0.11}	1.56 ^{+0.47} _{-0.52}	I	0	1.27	91	53
AP1867	9.10 ^{+0.20} _{-0.00}	5.22 ^{+0.36} _{-0.00}	1.75 ^{+0.00} _{-0.15}	0.00 ^{+0.00} _{-0.00}	0.00 ^{+0.00} _{-0.00}	0.00 ^{+0.00} _{-0.00}	I	0	2.47	115	325
AP1868	6.70 ^{+0.60} _{-0.00}	2.51 ^{+0.02} _{-0.03}	0.45 ^{+0.05} _{-0.10}	6.79 ^{+0.39} _{-0.49}	2.41 ^{+0.20} _{-0.24}	0.45 ^{+0.13} _{-0.13}	I	0	1.52	76	65
AP1869	8.90 ^{+0.10} _{-0.70}	3.23 ^{+0.07} _{-0.13}	0.20 ^{+1.45} _{-0.05}	8.81 ^{+0.17} _{-0.19}	3.02 ^{+0.08} _{-0.09}	0.24 ^{+0.24} _{-0.23}	I	0	1.42	106	61
AP1870	8.00 ^{+0.20} _{-0.10}	2.96 ^{+0.04} _{-0.02}	1.00 ^{+0.10} _{-0.05}	7.81 ^{+0.31} _{-0.36}	3.35 ^{+0.22} _{-0.24}	1.84 ^{+0.58} _{-0.57}	I	0	1.41	117	93
AP1871	8.10 ^{+0.40} _{-0.10}	3.10 ^{+0.03} _{-0.07}	1.10 ^{+0.05} _{-0.60}	9.01 ^{+0.20} _{-0.16}	3.23 ^{+0.13} _{-0.14}	0.22 ^{+0.21} _{-0.20}	I	0	1.59	214	183
AP1873	8.80 ^{+0.00} _{-0.00}	3.19 ^{+0.02} _{-0.02}	0.10 ^{+0.20} _{-0.00}	8.11 ^{+1.47} _{-1.46}	3.78 ^{+1.25} _{-1.18}	1.45 ^{+1.02} _{-1.02}	I	0	1.53	91	59

Table 1 (cont'd)

AP ID ^a	CMD Best Fit Parameters ^b			Integrated Best Fit Parameters ^c			Best ^d Flag ^e	R _{ap} ^f	N _{stars} ^g	N _{bg} ^h	
	log(<i>t</i> [Myr])	log(<i>M</i> [<i>M</i> _⊙])	<i>A_V</i> [mag]	log(<i>t</i> [Myr])	log(<i>M</i> [<i>M</i> _⊙])	<i>A_V</i> [mag]					
AP1875	8.30 ^{+0.00} _{-0.10}	3.39 ^{+0.03} _{-0.04}	1.45 ^{+0.10} _{-0.05}	8.21 ^{+0.17} _{-0.22}	2.74 ^{+0.28} _{-0.30}	0.46 ^{+0.34} _{-0.34}	I	0	1.20	128	88
AP1880	6.60 ^{+0.10} _{-0.00}	3.52 ^{+0.01} _{-0.00}	0.80 ^{+0.00} _{-0.00}	6.55 ^{+0.10} _{-0.11}	2.87 ^{+0.35} _{-0.46}	0.64 ^{+0.11} _{-0.11}	I	0	6.35	872	584
AP1881	8.90 ^{+0.10} _{-0.10}	3.18 ^{+0.12} _{-0.04}	0.30 ^{+0.40} _{-0.05}	8.27 ^{+0.13} _{-0.36}	2.37 ^{+0.11} _{-0.29}	0.35 ^{+0.28} _{-0.27}	I	0	1.32	113	91
AP1882	7.50 ^{+0.10} _{-0.20}	3.61 ^{+0.01} _{-0.07}	2.40 ^{+0.10} _{-0.05}	8.33 ^{+0.34} _{-0.31}	3.38 ^{+0.20} _{-0.20}	0.74 ^{+0.62} _{-0.68}	I	0	1.66	166	141
AP1885	10.10 ^{+0.00} _{-1.10}	5.19 ^{+0.00} _{-0.77}	0.00 ^{+1.00} _{-0.05}	8.54 ^{+0.22} _{-0.19}	3.49 ^{+0.14} _{-0.10}	1.15 ^{+0.38} _{-0.40}	I	0	1.69	219	136
AP1888	8.90 ^{+0.00} _{-0.10}	3.54 ^{+0.10} _{-0.00}	0.20 ^{+0.45} _{-0.00}	8.41 ^{+0.28} _{-0.26}	3.17 ^{+0.20} _{-0.17}	0.85 ^{+0.52} _{-0.58}	I	0	1.59	133	91
AP1889	8.20 ^{+0.00} _{-0.70}	3.33 ^{+0.04} _{-0.25}	1.80 ^{+0.25} _{-0.00}	9.59 ^{+0.20} _{-0.18}	3.58 ^{+0.13} _{-0.13}	0.24 ^{+0.19} _{-0.19}	I	0	1.35	62	30
AP1892	8.30 ^{+0.10} _{-0.00}	3.21 ^{+0.00} _{-0.13}	1.30 ^{+0.05} _{-0.20}	8.59 ^{+0.64} _{-0.87}	3.32 ^{+0.21} _{-0.20}	0.86 ^{+1.37} _{-0.83}	I	0	1.53	111	85
AP1893	8.10 ^{+0.10} _{-0.50}	3.18 ^{+0.03} _{-0.16}	0.80 ^{+0.20} _{-0.10}	7.95 ^{+0.13} _{-0.12}	3.33 ^{+0.11} _{-0.12}	0.77 ^{+0.21} _{-0.25}	I	0	1.45	147	112
AP1895	9.60 ^{+0.10} _{-0.00}	4.90 ^{+0.11} _{-0.01}	0.00 ^{+0.05} _{-0.00}	9.82 ^{+0.15} _{-0.17}	4.50 ^{+0.08} _{-0.08}	0.24 ^{+0.14} _{-0.14}	I	0	1.23	181	161
AP1896	9.00 ^{+0.00} _{-0.10}	4.07 ^{+0.15} _{-0.04}	0.95 ^{+0.40} _{-0.00}	8.25 ^{+0.12} _{-0.25}	3.37 ^{+0.28} _{-0.30}	1.70 ^{+0.50} _{-0.57}	I	0	1.66	154	104
AP1898	8.30 ^{+0.00} _{-0.50}	3.30 ^{+0.03} _{-0.10}	1.30 ^{+0.30} _{-0.00}	8.57 ^{+0.34} _{-0.35}	3.06 ^{+0.15} _{-0.15}	0.45 ^{+0.50} _{-0.43}	I	0	1.66	254	242
AP1899	8.20 ^{+0.20} _{-0.10}	3.37 ^{+0.05} _{-0.08}	1.15 ^{+0.05} _{-0.20}	8.96 ^{+0.03} _{-0.04}	4.20 ^{+0.04} _{-0.03}	0.00 ^{+0.07} _{-0.00}	I	0	1.64	114	82
AP1900	9.10 ^{+0.10} _{-0.00}	3.47 ^{+0.33} _{-0.02}	0.15 ^{+0.15} _{-0.00}	7.57 ^{+0.95} _{-0.91}	2.77 ^{+0.21} _{-0.21}	1.13 ^{+0.48} _{-0.69}	I	0	1.72	114	55
AP1901	8.00 ^{+0.10} _{-0.30}	3.44 ^{+0.01} _{-0.09}	1.45 ^{+0.20} _{-0.05}	8.79 ^{+0.42} _{-0.42}	3.62 ^{+0.13} _{-0.12}	0.79 ^{+0.50} _{-0.59}	I	0	1.36	142	110
AP1902	8.30 ^{+0.00} _{-0.60}	3.15 ^{+0.02} _{-0.12}	0.50 ^{+0.35} _{-0.05}	8.50 ^{+0.10} _{-0.09}	3.45 ^{+0.09} _{-0.08}	0.56 ^{+0.19} _{-0.19}	I	0	1.41	215	200
AP1903	8.20 ^{+0.00} _{-0.60}	3.45 ^{+0.02} _{-0.20}	1.30 ^{+0.15} _{-0.00}	8.80 ^{+0.13} _{-0.12}	3.33 ^{+0.09} _{-0.09}	0.43 ^{+0.24} _{-0.26}	I	0	1.17	121	86
AP1904	8.80 ^{+0.10} _{-0.40}	3.25 ^{+0.12} _{-0.04}	0.00 ^{+0.95} _{-0.05}	8.56 ^{+0.09} _{-0.10}	2.81 ^{+0.10} _{-0.10}	0.12 ^{+0.15} _{-0.12}	I	0	1.16	101	66
AP1905	8.80 ^{+0.00} _{-0.10}	3.16 ^{+0.04} _{-0.03}	0.05 ^{+0.30} _{-0.00}	8.67 ^{+0.17} _{-0.19}	2.96 ^{+0.13} _{-0.14}	0.61 ^{+0.31} _{-0.32}	I	0	1.45	106	76
AP1906	8.10 ^{+0.10} _{-0.00}	2.77 ^{+0.06} _{-0.00}	0.70 ^{+0.05} _{-0.10}	7.98 ^{+0.19} _{-0.17}	3.26 ^{+0.22} _{-0.19}	1.34 ^{+0.37} _{-0.40}	I	0	1.57	75	61
AP1907	9.00 ^{+0.00} _{-0.10}	3.71 ^{+0.04} _{-0.17}	0.65 ^{+0.25} _{-0.10}	9.48 ^{+0.48} _{-0.51}	3.72 ^{+0.20} _{-0.18}	0.63 ^{+0.50} _{-0.42}	I	0	1.40	105	55
AP1910	8.60 ^{+0.10} _{-0.00}	3.25 ^{+0.02} _{-0.05}	0.65 ^{+0.05} _{-0.25}	8.66 ^{+0.18} _{-0.18}	2.92 ^{+0.12} _{-0.12}	0.44 ^{+0.27} _{-0.27}	I	0	1.54	81	39
AP1915	8.10 ^{+0.20} _{-0.60}	3.08 ^{+0.05} _{-0.12}	0.85 ^{+0.15} _{-0.10}	8.79 ^{+0.05} _{-0.06}	3.16 ^{+0.08} _{-0.07}	0.07 ^{+0.10} _{-0.07}	I	0	1.22	128	95
AP1916	8.90 ^{+0.10} _{-0.20}	3.03 ^{+0.06} _{-0.06}	0.00 ^{+0.50} _{-0.05}	9.07 ^{+0.13} _{-0.14}	2.87 ^{+0.14} _{-0.14}	0.05 ^{+0.10} _{-0.05}	I	0	1.10	68	42
AP1917	7.40 ^{+0.20} _{-0.60}	2.59 ^{+0.01} _{-0.06}	0.70 ^{+0.10} _{-0.05}	6.98 ^{+0.17} _{-0.18}	2.26 ^{+0.22} _{-0.21}	1.18 ^{+0.10} _{-0.10}	I	0	1.10	50	42
AP1919	9.10 ^{+0.00} _{-0.90}	3.46 ^{+0.14} _{-3.46}	0.30 ^{+1.30} _{-0.10}	7.65 ^{+0.23} _{-0.21}	3.57 ^{+0.10} _{-0.11}	1.87 ^{+0.28} _{-0.34}	I	0	1.38	146	88
AP1920	9.70 ^{+0.00} _{-0.00}	5.09 ^{+0.01} _{-0.02}	0.00 ^{+0.00} _{-0.00}	0.00 ^{+0.00} _{-0.00}	0.00 ^{+0.00} _{-0.00}	0.00 ^{+0.00} _{-0.00}	I	0	3.48	555	586
AP1921	7.90 ^{+1.60} _{-0.70}	3.80 ^{+3.80} _{-3.80}	2.80 ^{+0.15} _{-2.30}	10.23 ^{+0.02} _{-0.03}	4.97 ^{+0.06} _{-0.06}	0.20 ^{+0.08} _{-0.08}	I	0	1.12	147	149
AP1923	8.20 ^{+0.10} _{-0.00}	3.12 ^{+0.02} _{-0.06}	0.60 ^{+0.05} _{-0.10}	8.34 ^{+0.10} _{-0.11}	2.99 ^{+0.11} _{-0.10}	0.23 ^{+0.23} _{-0.21}	I	0	1.15	90	67
AP1924	8.60 ^{+0.00} _{-1.10}	3.53 ^{+0.05} _{-0.27}	1.00 ^{+1.10} _{-0.10}	7.03 ^{+0.13} _{-0.12}	3.20 ^{+0.13} _{-0.12}	0.66 ^{+0.10} _{-0.11}	I	0	1.42	133	94
AP1925	8.80 ^{+0.00} _{-0.50}	3.23 ^{+0.07} _{-0.17}	0.60 ^{+0.95} _{-0.05}	9.15 ^{+0.77} _{-0.66}	3.82 ^{+0.18} _{-0.14}	1.22 ^{+0.79} _{-0.79}	I	0	1.50	83	39
AP1926	8.30 ^{+0.00} _{-0.10}	3.37 ^{+0.03} _{-0.03}	1.25 ^{+0.10} _{-0.05}	8.93 ^{+0.18} _{-0.16}	3.15 ^{+0.14} _{-0.13}	0.23 ^{+0.16} _{-0.20}	I	0	1.28	130	86
AP1927	8.80 ^{+0.00} _{-0.10}	3.47 ^{+0.04} _{-0.05}	0.10 ^{+0.30} _{-0.05}	8.80 ^{+0.40} _{-0.36}	3.41 ^{+0.13} _{-0.12}	0.71 ^{+0.52} _{-0.57}	I	0	1.36	141	94

Table 1 (cont'd)

AP ID ^a	CMD Best Fit Parameters ^b			Integrated Best Fit Parameters ^c			Best ^d Flag ^e	R _{ap} ^f	N _{stars} ^g	N _{bg} ^h	
	log(<i>t</i> [Myr])	log(<i>M</i> [<i>M</i> _⊙])	<i>A_V</i> [mag]	log(<i>t</i> [Myr])	log(<i>M</i> [<i>M</i> _⊙])	<i>A_V</i> [mag]					
AP1928	9.10 ^{+0.10} _{-1.30}	3.43 ^{+0.06} _{-3.43}	0.20 ^{+2.10} _{-0.00}	8.54 ^{+0.25} _{-0.23}	2.94 ^{+0.16} _{-0.17}	0.75 ^{+0.48} _{-0.51}	I	0	1.36	91	66
AP1929	8.20 ^{+0.20} _{-0.00}	3.14 ^{+0.03} _{-0.02}	0.55 ^{+0.05} _{-0.10}	6.80 ^{+0.43} _{-0.43}	3.19 ^{+0.27} _{-0.26}	2.39 ^{+0.28} _{-0.24}	I	0	1.86	164	125
AP1930	8.80 ^{+0.00} _{-1.10}	3.56 ^{+0.00} _{-0.31}	0.70 ^{+1.20} _{-0.00}	9.20 ^{+0.31} _{-0.22}	3.42 ^{+0.16} _{-0.16}	0.40 ^{+0.23} _{-0.33}	I	0	1.35	120	76
AP1931	8.50 ^{+0.00} _{-0.50}	3.39 ^{+0.00} _{-0.15}	1.00 ^{+0.25} _{-0.15}	6.83 ^{+0.19} _{-0.16}	2.94 ^{+0.24} _{-0.30}	2.51 ^{+0.17} _{-0.17}	I	0	1.13	80	43
AP1932	9.00 ^{+0.10} _{-0.00}	3.28 ^{+0.07} _{-0.07}	0.35 ^{+0.15} _{-0.10}	8.80 ^{+0.33} _{-0.36}	2.77 ^{+0.17} _{-0.15}	0.48 ^{+0.42} _{-0.40}	I	0	1.34	49	23
AP1933	7.50 ^{+0.30} _{-0.20}	3.25 ^{+0.02} _{-0.05}	1.20 ^{+0.05} _{-0.10}	7.88 ^{+0.41} _{-0.37}	3.30 ^{+0.22} _{-0.20}	0.93 ^{+0.70} _{-0.61}	I	0	1.85	262	205
AP1935	10.10 ^{+0.00} _{-0.50}	4.92 ^{+0.04} _{-0.73}	0.55 ^{+0.10} _{-0.25}	9.30 ^{+0.63} _{-0.88}	3.74 ^{+0.18} _{-0.18}	1.09 ^{+0.97} _{-0.66}	I	0	1.64	115	86
AP1936	7.40 ^{+0.10} _{-0.60}	3.54 ^{+0.05} _{-0.47}	2.35 ^{+0.05} _{-0.90}	6.70 ^{+0.09} _{-0.09}	2.75 ^{+0.35} _{-0.37}	1.13 ^{+0.10} _{-0.10}	I	0	1.98	273	239
AP1937	9.20 ^{+0.00} _{-1.50}	3.78 ^{+0.12} _{-0.90}	0.35 ^{+1.70} _{-0.05}	9.12 ^{+0.09} _{-0.10}	3.38 ^{+0.10} _{-0.12}	0.02 ^{+0.07} _{-0.02}	I	0	1.49	152	107
AP1939	8.80 ^{+0.00} _{-0.10}	3.51 ^{+0.07} _{-0.04}	0.25 ^{+0.35} _{-0.00}	8.28 ^{+0.15} _{-0.13}	3.07 ^{+0.12} _{-0.13}	0.42 ^{+0.31} _{-0.33}	I	0	1.92	267	226
AP1940	8.50 ^{+0.00} _{-0.10}	3.13 ^{+0.04} _{-0.01}	0.40 ^{+0.15} _{-0.05}	8.20 ^{+0.13} _{-0.18}	3.16 ^{+0.13} _{-0.10}	0.89 ^{+0.27} _{-0.23}	I	0	1.41	135	102
AP1941	9.20 ^{+0.10} _{-1.30}	3.70 ^{+0.01} _{-3.70}	0.20 ^{+2.10} _{-0.00}	8.57 ^{+0.87} _{-0.63}	3.39 ^{+0.21} _{-0.23}	1.30 ^{+0.86} _{-1.07}	I	0	1.61	142	116
AP1942	6.80 ^{+0.90} _{-0.00}	2.52 ^{+0.08} _{-0.02}	0.90 ^{+0.10} _{-0.10}	8.56 ^{+0.04} _{-0.05}	3.53 ^{+0.05} _{-0.06}	0.05 ^{+0.09} _{-0.05}	I	0	1.38	58	38
AP1943	9.10 ^{+0.00} _{-0.00}	3.88 ^{+0.04} _{-0.00}	0.00 ^{+0.15} _{-0.00}	9.99 ^{+0.08} _{-0.07}	4.27 ^{+0.07} _{-0.07}	0.02 ^{+0.07} _{-0.02}	I	0	1.84	208	84
AP1945	9.10 ^{+0.00} _{-0.00}	3.63 ^{+0.05} _{-0.03}	0.15 ^{+0.05} _{-0.10}	8.36 ^{+0.67} _{-0.32}	3.17 ^{+0.16} _{-0.15}	1.03 ^{+0.53} _{-0.89}	I	0	1.26	127	85
AP1949	8.10 ^{+0.10} _{-0.20}	3.25 ^{+0.00} _{-0.06}	0.95 ^{+0.05} _{-0.10}	8.26 ^{+0.17} _{-0.16}	3.05 ^{+0.15} _{-0.14}	0.53 ^{+0.37} _{-0.38}	I	0	1.47	141	105
AP1952	8.30 ^{+0.00} _{-0.10}	3.33 ^{+0.02} _{-0.07}	0.95 ^{+0.10} _{-0.05}	8.40 ^{+0.04} _{-0.08}	3.53 ^{+0.12} _{-0.12}	1.28 ^{+0.26} _{-0.24}	I	0	1.51	177	135
AP1953	7.50 ^{+0.10} _{-0.30}	2.86 ^{+0.01} _{-0.07}	1.25 ^{+0.10} _{-0.10}	6.87 ^{+0.36} _{-0.41}	2.75 ^{+0.24} _{-0.27}	0.98 ^{+0.16} _{-0.16}	I	0	1.47	99	90
AP1954	8.00 ^{+0.70} _{-0.00}	3.78 ^{+0.16} _{-0.19}	3.00 ^{+0.00} _{-0.80}	8.01 ^{+0.19} _{-0.19}	3.19 ^{+0.24} _{-0.20}	1.61 ^{+0.40} _{-0.41}	I	0	1.72	113	51
AP1956	6.60 ^{+0.70} _{-0.00}	2.92 ^{+0.02} _{-0.03}	0.65 ^{+0.05} _{-0.25}	7.35 ^{+0.04} _{-0.03}	4.30 ^{+0.03} _{-0.03}	1.11 ^{+0.07} _{-0.07}	I	0	1.66	191	147
AP1957	7.10 ^{+0.20} _{-0.40}	2.83 ^{+0.01} _{-0.04}	0.90 ^{+0.05} _{-0.05}	6.84 ^{+0.14} _{-0.14}	2.77 ^{+0.30} _{-0.37}	0.50 ^{+0.09} _{-0.09}	I	0	1.88	193	178
AP1960	8.00 ^{+0.00} _{-1.00}	2.50 ^{+0.01} _{-0.12}	0.40 ^{+0.15} _{-0.05}	7.28 ^{+0.52} _{-0.68}	2.37 ^{+0.14} _{-0.14}	0.26 ^{+0.25} _{-0.23}	I	0	1.15	111	102
AP1962	8.80 ^{+0.00} _{-0.20}	3.10 ^{+0.05} _{-0.28}	0.10 ^{+0.40} _{-0.00}	7.96 ^{+0.16} _{-0.17}	2.61 ^{+0.15} _{-0.15}	0.41 ^{+0.25} _{-0.25}	I	0	1.29	132	108
AP1968	7.90 ^{+0.10} _{-0.10}	3.44 ^{+0.01} _{-0.01}	0.80 ^{+0.05} _{-0.05}	8.11 ^{+0.39} _{-0.20}	3.89 ^{+0.09} _{-0.15}	0.81 ^{+0.36} _{-0.72}	I	0	1.76	134	78
AP1969	9.30 ^{+0.10} _{-0.00}	4.93 ^{+0.06} _{-0.00}	0.60 ^{+0.00} _{-0.05}	0.00 ^{+0.00} _{-0.00}	0.00 ^{+0.00} _{-0.00}	0.00 ^{+0.00} _{-0.00}	I	0	3.99	541	775
AP1973	7.10 ^{+0.30} _{-0.20}	2.61 ^{+0.01} _{-0.08}	0.60 ^{+0.05} _{-0.10}	6.76 ^{+0.07} _{-0.06}	2.32 ^{+0.22} _{-0.22}	0.59 ^{+0.11} _{-0.12}	I	0	1.42	99	86
AP1976	8.60 ^{+0.00} _{-0.30}	2.89 ^{+0.02} _{-0.05}	0.00 ^{+0.35} _{-0.00}	6.91 ^{+0.52} _{-0.57}	2.64 ^{+0.18} _{-0.20}	1.55 ^{+0.35} _{-0.39}	I	0	1.22	50	36
AP1978	7.90 ^{+0.00} _{-1.10}	2.76 ^{+0.00} _{-0.10}	1.00 ^{+0.10} _{-0.15}	7.00 ^{+0.08} _{-0.07}	2.32 ^{+0.21} _{-0.20}	0.79 ^{+0.08} _{-0.07}	I	0	1.36	43	18
AP1979	9.10 ^{+0.00} _{-0.00}	3.31 ^{+0.04} _{-0.04}	0.00 ^{+0.20} _{-0.00}	8.82 ^{+0.43} _{-0.40}	3.23 ^{+0.17} _{-0.17}	0.79 ^{+0.49} _{-0.56}	I	0	1.52	111	58
AP1980	6.90 ^{+0.40} _{-0.20}	2.67 ^{+0.01} _{-0.02}	0.50 ^{+0.05} _{-0.10}	7.73 ^{+0.10} _{-0.10}	3.25 ^{+0.08} _{-0.08}	0.08 ^{+0.11} _{-0.08}	I	0	2.46	181	114
AP1982	9.70 ^{+0.20} _{-0.10}	4.39 ^{+0.11} _{-0.13}	0.30 ^{+0.00} _{-0.15}	9.27 ^{+0.06} _{-0.06}	4.24 ^{+0.06} _{-0.06}	0.09 ^{+0.10} _{-0.09}	I	0	1.66	61	144
AP1984	8.00 ^{+0.10} _{-1.00}	3.06 ^{+0.04} _{-0.15}	0.75 ^{+0.20} _{-0.20}	7.87 ^{+0.24} _{-0.23}	3.16 ^{+0.12} _{-0.11}	0.60 ^{+0.34} _{-0.36}	I	0	1.53	174	150
AP1985	8.80 ^{+0.00} _{-0.00}	3.47 ^{+0.07} _{-0.04}	0.35 ^{+0.15} _{-0.05}	8.71 ^{+0.28} _{-0.29}	3.09 ^{+0.13} _{-0.12}	0.64 ^{+0.40} _{-0.39}	I	0	1.41	120	69

Table 1 (cont'd)

AP ID ^a	CMD Best Fit Parameters ^b			Integrated Best Fit Parameters ^c			Best ^d Flag ^e	Rap ^f	N _{stars} ^g	N _{bg} ^h	
	log(<i>t</i> [Myr])	log(<i>M</i> [<i>M</i> _⊙])	<i>A_V</i> [mag]	log(<i>t</i> [Myr])	log(<i>M</i> [<i>M</i> _⊙])	<i>A_V</i> [mag]					
AP1986	8.50 ^{+0.10} _{-0.00}	2.90 ^{+0.03} _{-0.01}	0.55 ^{+0.15} _{-0.10}	8.50 ^{+1.33} _{-1.44}	2.61 ^{+0.41} _{-0.43}	1.56 ^{+0.98} _{-1.02}	I	0	1.35	48	12
AP1987	8.90 ^{+0.00} _{-0.80}	3.82 ^{+0.03} _{-1.60}	1.25 ^{+0.85} _{-0.20}	8.37 ^{+1.74} _{-0.59}	3.26 ^{+0.76} _{-0.44}	1.41 ^{+0.59} _{-0.72}	I	0	1.38	106	60
AP1988	8.10 ^{+0.00} _{-0.60}	3.14 ^{+0.06} _{-0.12}	1.75 ^{+0.25} _{-0.05}	8.96 ^{+0.11} _{-0.14}	3.14 ^{+0.11} _{-0.10}	0.49 ^{+0.23} _{-0.26}	I	0	1.10	98	56
AP1989	8.30 ^{+0.20} _{-0.20}	3.29 ^{+0.03} _{-0.04}	0.95 ^{+0.05} _{-0.15}	8.48 ^{+0.15} _{-0.14}	3.06 ^{+0.10} _{-0.11}	0.43 ^{+0.27} _{-0.29}	I	0	1.48	109	40
AP1990	8.50 ^{+0.00} _{-0.10}	3.21 ^{+0.02} _{-0.02}	0.40 ^{+0.10} _{-0.05}	8.42 ^{+0.23} _{-0.23}	2.99 ^{+0.14} _{-0.15}	0.45 ^{+0.44} _{-0.42}	I	0	1.42	123	93
AP1994	8.10 ^{+0.10} _{-0.00}	3.30 ^{+0.02} _{-0.04}	1.40 ^{+0.05} _{-0.15}	8.93 ^{+0.16} _{-0.17}	3.54 ^{+0.10} _{-0.11}	0.71 ^{+0.21} _{-0.25}	I	0	1.39	127	82
AP1995	6.70 ^{+0.40} _{-0.00}	2.65 ^{+0.02} _{-0.02}	0.70 ^{+0.00} _{-0.15}	7.43 ^{+0.19} _{-0.18}	3.03 ^{+0.09} _{-0.08}	0.16 ^{+0.18} _{-0.16}	I	0	1.54	155	156
AP1996	6.60 ^{+0.30} _{-0.00}	3.13 ^{+0.01} _{-0.02}	0.75 ^{+0.00} _{-0.05}	6.85 ^{+0.65} _{-0.42}	2.74 ^{+0.57} _{-0.38}	0.44 ^{+0.31} _{-0.44}	I	0	2.27	317	280
AP1997	7.00 ^{+0.00} _{-0.20}	3.06 ^{+0.01} _{-0.05}	1.65 ^{+0.10} _{-0.05}	6.67 ^{+0.11} _{-0.10}	2.86 ^{+0.30} _{-0.23}	1.38 ^{+0.08} _{-0.07}	I	0	1.95	229	210
AP1998	8.10 ^{+0.10} _{-0.80}	3.02 ^{+0.01} _{-0.12}	0.90 ^{+0.30} _{-0.05}	8.48 ^{+0.46} _{-0.40}	3.11 ^{+0.22} _{-0.20}	0.69 ^{+0.65} _{-0.61}	I	0	1.46	132	120
AP2002	7.80 ^{+1.60} _{-0.30}	3.66 ^{+0.03} _{-3.66}	2.95 ^{+0.10} _{-2.55}	9.26 ^{+0.16} _{-0.10}	3.30 ^{+0.14} _{-0.14}	0.17 ^{+0.08} _{-0.17}	I	0	1.40	117	86
AP2004	6.70 ^{+0.20} _{-0.10}	2.85 ^{+0.00} _{-0.02}	0.80 ^{+0.10} _{-0.05}	6.84 ^{+0.11} _{-0.09}	2.59 ^{+0.28} _{-0.27}	0.34 ^{+0.09} _{-0.09}	I	0	1.79	201	194
AP2005	9.10 ^{+0.00} _{-0.20}	3.58 ^{+0.04} _{-0.11}	0.05 ^{+0.25} _{-0.00}	8.73 ^{+0.23} _{-0.24}	2.95 ^{+0.15} _{-0.16}	0.66 ^{+0.42} _{-0.44}	I	0	1.13	87	50
AP2007	8.70 ^{+0.00} _{-0.20}	3.01 ^{+0.02} _{-0.04}	0.30 ^{+0.45} _{-0.00}	7.19 ^{+0.61} _{-0.75}	2.49 ^{+0.15} _{-0.16}	0.78 ^{+0.41} _{-0.43}	I	0	1.28	71	57
AP2008	6.60 ^{+0.50} _{-0.00}	2.69 ^{+0.01} _{-0.03}	0.65 ^{+0.00} _{-0.10}	7.60 ^{+0.09} _{-0.10}	2.78 ^{+0.11} _{-0.11}	0.05 ^{+0.10} _{-0.05}	I	0	1.42	150	125
AP2009	6.60 ^{+0.40} _{-0.00}	2.69 ^{+0.02} _{-0.04}	0.50 ^{+0.00} _{-0.10}	7.24 ^{+0.13} _{-0.12}	2.58 ^{+0.21} _{-0.21}	0.30 ^{+0.12} _{-0.12}	I	0	1.20	94	68
AP2010	8.70 ^{+0.00} _{-0.10}	3.23 ^{+0.02} _{-0.05}	0.40 ^{+0.30} _{-0.05}	8.19 ^{+0.19} _{-0.20}	3.13 ^{+0.26} _{-0.23}	1.23 ^{+0.42} _{-0.42}	I	0	1.19	105	77
AP2012	9.60 ^{+0.00} _{-0.30}	4.66 ^{+0.00} _{-0.22}	0.15 ^{+0.05} _{-0.05}	9.81 ^{+0.09} _{-0.10}	5.20 ^{+0.06} _{-0.06}	0.19 ^{+0.09} _{-0.08}	I	0	1.53	76	226
AP2013	6.60 ^{+1.20} _{-0.20}	2.86 ^{+0.02} _{-0.04}	0.95 ^{+0.00} _{-0.40}	7.53 ^{+0.16} _{-0.18}	3.35 ^{+0.10} _{-0.09}	0.80 ^{+0.21} _{-0.21}	I	0	1.67	90	57
AP2016	9.40 ^{+0.10} _{-0.10}	4.15 ^{+0.02} _{-0.30}	0.05 ^{+0.30} _{-0.05}	9.46 ^{+0.04} _{-0.04}	5.55 ^{+0.03} _{-0.03}	0.09 ^{+0.08} _{-0.07}	I	0	2.44	198	420
AP2017	7.80 ^{+0.10} _{-0.80}	3.10 ^{+0.04} _{-0.11}	0.80 ^{+0.15} _{-0.00}	8.33 ^{+0.10} _{-0.09}	3.35 ^{+0.10} _{-0.10}	0.28 ^{+0.22} _{-0.23}	I	0	1.81	268	234
AP2019	9.10 ^{+0.00} _{-0.00}	4.15 ^{+0.00} _{-0.05}	0.75 ^{+0.00} _{-0.15}	9.40 ^{+0.66} _{-0.77}	4.28 ^{+0.17} _{-0.17}	1.10 ^{+0.80} _{-0.65}	I	0	2.32	311	202
AP2020	7.30 ^{+0.20} _{-0.30}	3.18 ^{+0.06} _{-0.02}	0.60 ^{+0.15} _{-0.04}	7.03 ^{+0.50} _{-0.61}	2.54 ^{+0.20} _{-0.19}	0.18 ^{+0.19} _{-0.17}	I	0	1.68	220	183
AP2023	8.80 ^{+0.00} _{-0.00}	3.78 ^{+0.00} _{-0.00}	0.00 ^{+0.05} _{-0.00}	0.00 ^{+0.00} _{-0.00}	0.00 ^{+0.00} _{-0.00}	0.00 ^{+0.00} _{-0.00}	I	0	2.38	479	450
AP2024	9.00 ^{+0.10} _{-0.00}	3.73 ^{+0.05} _{-0.09}	0.40 ^{+0.20} _{-0.25}	8.67 ^{+0.26} _{-0.42}	3.06 ^{+0.15} _{-0.13}	0.24 ^{+0.62} _{-0.24}	I	0	1.50	182	144
AP2025	8.80 ^{+0.10} _{-0.10}	3.37 ^{+0.03} _{-0.03}	0.35 ^{+0.35} _{-0.15}	8.06 ^{+0.21} _{-0.23}	2.88 ^{+0.22} _{-0.30}	1.09 ^{+0.53} _{-0.64}	I	0	1.17	72	38
AP2027	7.60 ^{+0.00} _{-0.70}	3.11 ^{+0.00} _{-0.07}	0.75 ^{+0.10} _{-0.05}	7.81 ^{+0.13} _{-0.12}	3.60 ^{+0.09} _{-0.09}	0.61 ^{+0.17} _{-0.18}	I	0	1.90	240	192
AP2028	8.90 ^{+0.00} _{-0.60}	3.66 ^{+0.00} _{-0.27}	0.40 ^{+0.95} _{-0.05}	8.29 ^{+0.36} _{-0.33}	2.91 ^{+0.24} _{-0.23}	0.76 ^{+0.69} _{-0.67}	I	0	1.33	136	111
AP2029	8.30 ^{+0.10} _{-0.00}	3.52 ^{+0.02} _{-0.07}	1.70 ^{+0.00} _{-0.15}	8.68 ^{+0.15} _{-0.16}	2.94 ^{+0.12} _{-0.12}	0.46 ^{+0.26} _{-0.26}	I	0	1.41	121	68
AP2030	9.20 ^{+0.50} _{-0.00}	3.90 ^{+0.41} _{-0.00}	1.05 ^{+0.10} _{-0.30}	9.17 ^{+0.81} _{-0.92}	3.96 ^{+0.34} _{-0.34}	2.00 ^{+0.68} _{-0.54}	I	0	1.25	66	34
AP2031	9.90 ^{+0.10} _{-0.60}	4.78 ^{+0.02} _{-0.48}	0.00 ^{+0.20} _{-0.00}	8.85 ^{+0.59} _{-0.76}	3.63 ^{+0.16} _{-0.16}	0.80 ^{+0.98} _{-0.73}	I	0	1.95	250	207
AP2033	8.20 ^{+0.00} _{-0.10}	3.33 ^{+0.02} _{-0.02}	0.35 ^{+0.10} _{-0.00}	8.24 ^{+0.08} _{-0.08}	3.53 ^{+0.08} _{-0.08}	0.51 ^{+0.18} _{-0.18}	I	0	1.52	192	151
AP2038	8.10 ^{+0.10} _{-0.40}	3.05 ^{+0.03} _{-0.05}	0.60 ^{+0.20} _{-0.05}	7.90 ^{+0.29} _{-0.28}	2.82 ^{+0.23} _{-0.23}	0.59 ^{+0.47} _{-0.46}	I	0	1.69	157	118

Table 1 (cont'd)

AP ID ^a	CMD Best Fit Parameters ^b			Integrated Best Fit Parameters ^c			Best ^d Flag ^e	R _{ap} ^f	N _{stars} ^g	N _{bg} ^h	
	log(<i>t</i> [Myr])	log(<i>M</i> [<i>M</i> _⊙])	<i>A_V</i> [mag]	log(<i>t</i> [Myr])	log(<i>M</i> [<i>M</i> _⊙])	<i>A_V</i> [mag]					
AP2039	8.80 ^{+0.10} _{-0.00}	3.16 ^{+0.03} _{-0.07}	0.35 ^{+0.05} _{-0.25}	8.20 ^{+0.17} _{-0.14}	2.73 ^{+0.24} _{-0.25}	0.50 ^{+0.33} _{-0.38}	I	0	1.57	127	69
AP2040	7.00 ^{+0.50} _{-0.20}	2.92 ^{+0.02} _{-0.03}	0.80 ^{+0.00} _{-0.15}	7.73 ^{+0.23} _{-0.22}	2.87 ^{+0.12} _{-0.12}	0.53 ^{+0.26} _{-0.26}	I	0	1.20	109	97
AP2043	7.90 ^{+0.40} _{-0.40}	2.94 ^{+0.12} _{-0.06}	0.65 ^{+0.15} _{-0.05}	8.40 ^{+0.12} _{-0.11}	3.01 ^{+0.11} _{-0.11}	0.29 ^{+0.24} _{-0.25}	I	0	1.59	168	141
AP2044	7.80 ^{+0.00} _{-0.40}	2.99 ^{+0.00} _{-0.05}	0.65 ^{+0.15} _{-0.05}	8.03 ^{+0.04} _{-0.04}	2.93 ^{+0.06} _{-0.05}	0.14 ^{+0.15} _{-0.14}	I	0	1.90	139	102
AP2045	8.40 ^{+0.00} _{-0.80}	2.90 ^{+0.02} _{-0.17}	0.40 ^{+0.15} _{-0.15}	8.08 ^{+0.19} _{-0.13}	2.27 ^{+0.14} _{-0.14}	0.10 ^{+0.14} _{-0.10}	I	0	1.01	45	26
AP2046	8.20 ^{+0.10} _{-0.70}	2.91 ^{+0.02} _{-0.20}	1.10 ^{+0.15} _{-0.25}	9.42 ^{+0.07} _{-0.07}	3.51 ^{+0.08} _{-0.08}	0.07 ^{+0.11} _{-0.07}	I	0	1.22	137	118
AP2047	7.40 ^{+0.70} _{-0.40}	2.81 ^{+0.07} _{-0.17}	0.80 ^{+0.00} _{-0.40}	6.75 ^{+0.13} _{-0.10}	2.99 ^{+0.23} _{-0.31}	0.28 ^{+0.08} _{-0.07}	I	0	1.54	170	143
AP2048	9.00 ^{+0.10} _{-0.00}	3.73 ^{+0.11} _{-0.05}	0.05 ^{+0.05} _{-0.05}	8.04 ^{+0.21} _{-0.31}	3.16 ^{+0.31} _{-0.37}	0.99 ^{+0.41} _{-0.42}	I	0	1.70	212	140
AP2050	8.80 ^{+0.00} _{-0.10}	3.32 ^{+0.04} _{-0.16}	0.30 ^{+0.15} _{-0.20}	7.74 ^{+0.10} _{-0.09}	3.08 ^{+0.07} _{-0.07}	1.40 ^{+0.14} _{-0.13}	I	0	1.32	99	64
AP2051	8.90 ^{+0.90} _{-1.10}	4.71 ^{+0.18} _{-4.71}	2.25 ^{+0.25} _{-1.45}	9.10 ^{+0.78} _{-0.87}	3.69 ^{+0.25} _{-0.24}	1.89 ^{+0.85} _{-0.76}	I	0	1.17	48	24
AP2052	8.20 ^{+0.00} _{-0.00}	3.77 ^{+0.01} _{-0.15}	2.55 ^{+0.10} _{-0.10}	9.27 ^{+0.85} _{-0.61}	4.18 ^{+0.23} _{-0.17}	1.55 ^{+0.65} _{-0.81}	I	0	1.48	136	82
AP2054	9.10 ^{+0.00} _{-0.10}	3.55 ^{+0.03} _{-0.16}	0.10 ^{+0.20} _{-0.00}	8.39 ^{+0.78} _{-0.43}	3.18 ^{+0.21} _{-0.19}	1.17 ^{+0.60} _{-0.87}	I	0	1.58	130	100
AP2056	8.20 ^{+0.00} _{-0.10}	3.58 ^{+0.00} _{-0.05}	0.95 ^{+0.05} _{-0.05}	7.66 ^{+0.27} _{-0.24}	3.90 ^{+0.09} _{-0.10}	1.73 ^{+0.31} _{-0.37}	I	0	2.32	331	285
AP2060	6.70 ^{+0.10} _{-0.10}	3.21 ^{+0.00} _{-0.01}	0.40 ^{+0.05} _{-0.00}	6.75 ^{+0.08} _{-0.09}	3.13 ^{+0.41} _{-0.29}	0.32 ^{+0.09} _{-0.09}	I	0	3.67	842	742
AP2063	7.80 ^{+0.10} _{-0.30}	2.86 ^{+0.01} _{-0.03}	0.50 ^{+0.10} _{-0.10}	8.03 ^{+0.05} _{-0.05}	2.48 ^{+0.06} _{-0.06}	0.05 ^{+0.12} _{-0.05}	I	0	1.50	87	44
AP2064	8.40 ^{+0.10} _{-0.00}	3.08 ^{+0.01} _{-0.03}	0.20 ^{+0.05} _{-0.10}	8.41 ^{+0.16} _{-0.16}	3.22 ^{+0.15} _{-0.13}	0.40 ^{+0.37} _{-0.34}	I	0	1.55	191	143
AP2066	7.50 ^{+0.80} _{-0.30}	3.23 ^{+0.00} _{-0.12}	1.80 ^{+0.05} _{-0.75}	8.67 ^{+0.14} _{-0.16}	3.19 ^{+0.11} _{-0.12}	0.62 ^{+0.34} _{-0.27}	I	0	1.27	98	75
AP2068	8.10 ^{+0.00} _{-0.60}	3.44 ^{+0.02} _{-0.17}	1.45 ^{+0.20} _{-0.05}	9.84 ^{+0.06} _{-0.06}	4.32 ^{+0.06} _{-0.06}	0.01 ^{+0.07} _{-0.01}	I	0	1.31	177	142
AP2069	7.80 ^{+0.70} _{-0.80}	3.04 ^{+0.07} _{-0.13}	0.60 ^{+0.10} _{-0.25}	7.81 ^{+0.13} _{-0.09}	3.05 ^{+0.10} _{-0.12}	0.47 ^{+0.20} _{-0.20}	I	0	1.30	66	33
AP2072	8.00 ^{+0.30} _{-0.40}	2.91 ^{+0.08} _{-0.07}	1.10 ^{+0.15} _{-0.10}	8.16 ^{+0.10} _{-0.10}	3.55 ^{+0.10} _{-0.12}	1.16 ^{+0.24} _{-0.24}	I	0	1.30	103	92
AP2074	8.80 ^{+0.00} _{-0.10}	3.16 ^{+0.05} _{-0.02}	0.25 ^{+0.35} _{-0.00}	8.17 ^{+0.20} _{-0.21}	3.08 ^{+0.12} _{-0.11}	1.03 ^{+0.33} _{-0.30}	I	0	1.76	96	44
AP2075	7.70 ^{+0.10} _{-0.60}	2.74 ^{+0.00} _{-0.10}	0.80 ^{+0.20} _{-0.15}	7.69 ^{+0.17} _{-0.13}	3.02 ^{+0.11} _{-0.12}	0.56 ^{+0.21} _{-0.21}	I	0	1.48	143	154
AP2079	7.70 ^{+0.10} _{-0.20}	3.87 ^{+0.03} _{-0.06}	2.75 ^{+0.15} _{-0.10}	8.89 ^{+0.04} _{-0.20}	3.96 ^{+0.09} _{-0.05}	1.24 ^{+0.30} _{-0.12}	I	0	1.30	168	117
AP2080	8.10 ^{+0.10} _{-1.10}	2.78 ^{+0.01} _{-0.33}	0.80 ^{+1.10} _{-0.05}	6.51 ^{+0.29} _{-0.32}	2.60 ^{+0.30} _{-0.30}	1.17 ^{+0.15} _{-0.16}	I	0	1.63	140	138
AP2082	10.10 ^{+0.00} _{-0.70}	4.94 ^{+0.01} _{-0.98}	0.10 ^{+0.40} _{-0.05}	8.60 ^{+0.51} _{-0.41}	3.52 ^{+0.16} _{-0.16}	1.33 ^{+0.73} _{-0.85}	I	0	1.19	99	53
AP2083	7.10 ^{+0.00} _{-0.40}	2.72 ^{+0.01} _{-0.06}	1.20 ^{+0.15} _{-0.00}	6.86 ^{+0.22} _{-0.25}	2.92 ^{+0.19} _{-0.20}	0.75 ^{+0.13} _{-0.13}	I	0	1.63	83	61
AP2086	8.30 ^{+0.30} _{-0.30}	3.36 ^{+0.09} _{-0.02}	0.80 ^{+0.60} _{-0.35}	8.18 ^{+0.70} _{-0.51}	3.73 ^{+0.27} _{-0.38}	1.55 ^{+0.96} _{-1.38}	I	0	1.21	147	118
AP2090	8.80 ^{+0.00} _{-0.10}	2.96 ^{+0.02} _{-0.14}	0.05 ^{+0.35} _{-0.00}	9.15 ^{+1.03} _{-0.82}	3.34 ^{+0.59} _{-0.48}	0.41 ^{+0.64} _{-0.41}	I	0	1.26	78	57
AP2091	8.50 ^{+0.00} _{-0.20}	2.64 ^{+0.02} _{-0.07}	0.00 ^{+0.20} _{-0.00}	7.51 ^{+0.31} _{-0.28}	2.82 ^{+0.12} _{-0.11}	1.16 ^{+0.27} _{-0.26}	I	0	1.36	60	25
AP2093	7.70 ^{+0.10} _{-0.30}	3.01 ^{+0.00} _{-0.05}	0.35 ^{+0.10} _{-0.05}	7.05 ^{+0.30} _{-0.26}	3.00 ^{+0.16} _{-0.15}	0.88 ^{+0.18} _{-0.17}	I	0	1.97	274	262
AP2095	8.50 ^{+0.10} _{-0.10}	3.26 ^{+0.03} _{-0.04}	0.45 ^{+0.25} _{-0.15}	8.75 ^{+0.15} _{-0.24}	3.70 ^{+0.09} _{-0.09}	1.05 ^{+0.31} _{-0.23}	I	0	1.83	212	170
AP2096	8.40 ^{+0.10} _{-0.20}	3.13 ^{+0.02} _{-0.11}	1.00 ^{+0.10} _{-0.20}	8.64 ^{+0.14} _{-0.14}	2.69 ^{+0.15} _{-0.16}	0.49 ^{+0.28} _{-0.28}	I	0	1.12	84	69
AP2098	8.80 ^{+0.00} _{-0.40}	3.19 ^{+0.03} _{-0.09}	0.40 ^{+0.60} _{-0.15}	8.85 ^{+0.47} _{-0.44}	3.39 ^{+0.13} _{-0.13}	0.83 ^{+0.55} _{-0.58}	I	0	1.46	123	83

Table 1 (cont'd)

AP ID ^a	CMD Best Fit Parameters ^b			Integrated Best Fit Parameters ^c			Best ^d Flag ^e	Rap ^f	N _{stars} ^g	N _{bg} ^h	
	log(<i>t</i> [Myr])	log(<i>M</i> [<i>M</i> _⊙])	<i>A_V</i> [mag]	log(<i>t</i> [Myr])	log(<i>M</i> [<i>M</i> _⊙])	<i>A_V</i> [mag]					
AP2100	9.10 ^{+0.00} _{-0.10}	3.49 ^{+0.01} _{-0.10}	0.15 ^{+0.20} _{-0.00}	9.29 ^{+0.51} _{-0.73}	3.39 ^{+0.25} _{-0.29}	0.46 ^{+0.55} _{-0.41}	I	0	1.40	92	50
AP2102	7.00 ^{+0.40} _{-0.10}	3.18 ^{+0.05} _{-0.03}	0.80 ^{+0.05} _{-0.00}	6.68 ^{+0.15} _{-0.12}	3.72 ^{+0.45} _{-0.24}	1.09 ^{+0.08} _{-0.07}	I	0	2.18	306	255
AP2103	8.60 ^{+0.10} _{-0.10}	2.87 ^{+0.01} _{-0.15}	0.85 ^{+0.15} _{-0.40}	8.51 ^{+0.13} _{-0.13}	2.45 ^{+0.26} _{-0.25}	0.74 ^{+0.36} _{-0.36}	I	0	1.21	45	24
AP2104	8.20 ^{+0.20} _{-0.10}	3.36 ^{+0.05} _{-0.16}	1.75 ^{+0.15} _{-0.30}	8.65 ^{+0.17} _{-0.17}	2.87 ^{+0.16} _{-0.16}	0.58 ^{+0.31} _{-0.32}	I	0	1.36	121	90
AP2105	8.50 ^{+0.10} _{-0.10}	3.37 ^{+0.02} _{-0.04}	1.00 ^{+0.15} _{-0.15}	8.46 ^{+0.17} _{-0.16}	2.74 ^{+0.18} _{-0.18}	0.47 ^{+0.36} _{-0.35}	I	0	1.37	98	66
AP2106	8.70 ^{+0.00} _{-0.10}	3.24 ^{+0.07} _{-0.07}	0.00 ^{+0.35} _{-0.05}	7.93 ^{+0.62} _{-0.68}	3.01 ^{+0.21} _{-0.22}	1.17 ^{+0.94} _{-0.95}	I	0	1.21	94	72
AP2109	9.10 ^{+0.30} _{-1.40}	3.62 ^{+0.30} _{-3.62}	0.50 ^{+1.77} _{-0.35}	10.11 ^{+0.14} _{-0.10}	3.91 ^{+0.13} _{-0.05}	0.01 ^{+0.07} _{-0.01}	I	0	1.48	181	158
AP2111	8.80 ^{+0.60} _{-1.30}	3.63 ^{+0.26} _{-0.44}	0.50 ^{+1.20} _{-0.80}	8.71 ^{+0.09} _{-0.09}	2.87 ^{+0.11} _{-0.11}	0.18 ^{+0.18} _{-0.17}	I	0	1.23	109	68
AP2112	8.70 ^{+0.10} _{-0.20}	3.21 ^{+0.03} _{-0.12}	0.60 ^{+0.40} _{-0.30}	8.55 ^{+0.30} _{-0.28}	2.84 ^{+0.20} _{-0.18}	0.49 ^{+0.44} _{-0.42}	I	0	1.45	123	105
AP2113	7.80 ^{+0.20} _{-0.50}	2.72 ^{+0.00} _{-0.09}	0.75 ^{+0.15} _{-0.05}	7.81 ^{+0.24} _{-0.19}	3.41 ^{+0.28} _{-0.27}	1.49 ^{+0.40} _{-0.39}	I	0	1.60	69	39
AP2115	9.70 ^{+0.10} _{-0.50}	4.32 ^{+0.09} _{-0.73}	0.05 ^{+0.20} _{-0.05}	6.68 ^{+0.32} _{-0.34}	3.36 ^{+0.34} _{-0.35}	2.55 ^{+0.24} _{-0.26}	I	0	1.41	147	94
AP2117	8.00 ^{+0.00} _{-1.00}	2.70 ^{+0.01} _{-0.10}	0.60 ^{+0.35} _{-0.00}	7.34 ^{+0.44} _{-0.40}	3.18 ^{+0.13} _{-0.13}	1.54 ^{+0.33} _{-0.32}	I	0	1.40	136	108
AP2119	8.30 ^{+0.10} _{-0.10}	3.32 ^{+0.02} _{-0.07}	0.90 ^{+0.10} _{-0.05}	8.77 ^{+0.18} _{-0.01}	3.34 ^{+0.04} _{-0.10}	0.25 ^{+0.07} _{-0.25}	I	0	1.11	148	126
AP2120	8.00 ^{+0.00} _{-0.00}	2.97 ^{+0.02} _{-0.02}	0.65 ^{+0.05} _{-0.05}	7.97 ^{+0.10} _{-0.10}	2.99 ^{+0.08} _{-0.08}	0.43 ^{+0.15} _{-0.16}	I	0	2.01	126	83
AP2121	8.20 ^{+0.00} _{-0.30}	2.97 ^{+0.02} _{-0.06}	0.55 ^{+0.10} _{-0.05}	8.02 ^{+1.13} _{-1.34}	3.38 ^{+0.29} _{-0.32}	1.45 ^{+0.97} _{-1.07}	I	0	1.17	84	56
AP2122	9.10 ^{+0.00} _{-0.00}	3.94 ^{+0.00} _{-0.00}	0.00 ^{+0.00} _{-0.00}	0.00 ^{+0.00} _{-0.00}	0.00 ^{+0.00} _{-0.00}	0.00 ^{+0.00} _{-0.00}	I	0	2.30	184	391
AP2123	7.50 ^{+0.20} _{-0.10}	3.46 ^{+0.04} _{-0.03}	1.35 ^{+0.10} _{-0.05}	8.25 ^{+0.15} _{-0.06}	3.33 ^{+0.20} _{-0.14}	0.55 ^{+0.22} _{-0.20}	I	0	1.93	269	222
AP2125	9.30 ^{+0.10} _{-1.90}	3.92 ^{+0.00} _{-3.92}	0.00 ^{+2.50} _{-0.00}	9.72 ^{+0.07} _{-0.08}	5.28 ^{+0.06} _{-0.05}	0.02 ^{+0.07} _{-0.02}	I	0	1.95	79	376
AP2126	6.70 ^{+0.20} _{-0.10}	3.42 ^{+0.01} _{-0.04}	1.90 ^{+0.00} _{-0.10}	6.96 ^{+0.43} _{-0.35}	3.59 ^{+0.35} _{-0.47}	0.87 ^{+0.27} _{-0.30}	I	0	4.19	814	699
AP2127	6.70 ^{+0.80} _{-0.10}	2.60 ^{+0.06} _{-0.00}	1.15 ^{+0.05} _{-0.10}	6.83 ^{+0.41} _{-0.50}	2.88 ^{+0.17} _{-0.17}	1.36 ^{+0.18} _{-0.17}	I	0	1.30	90	67
AP2128	8.70 ^{+0.00} _{-0.50}	3.09 ^{+0.02} _{-0.08}	0.00 ^{+0.55} _{-0.05}	8.02 ^{+0.24} _{-0.18}	2.39 ^{+0.13} _{-0.14}	0.11 ^{+0.14} _{-0.11}	I	0	1.36	83	73
AP2131	8.10 ^{+0.30} _{-0.10}	3.40 ^{+0.04} _{-0.09}	1.55 ^{+0.10} _{-0.35}	8.80 ^{+1.32} _{-1.06}	3.15 ^{+0.99} _{-0.85}	0.14 ^{+0.25} _{-0.14}	I	0	1.31	145	103
AP2132	7.80 ^{+0.00} _{-0.40}	2.94 ^{+0.00} _{-0.08}	0.60 ^{+0.15} _{-0.05}	6.94 ^{+0.90} _{-0.73}	3.08 ^{+0.31} _{-0.28}	1.41 ^{+0.47} _{-0.73}	I	0	1.67	201	176
AP2134	9.00 ^{+0.90} _{-0.10}	3.79 ^{+0.49} _{-0.04}	1.15 ^{+0.40} _{-0.40}	8.88 ^{+0.78} _{-0.62}	3.68 ^{+0.15} _{-0.14}	1.97 ^{+0.71} _{-0.92}	I	0	1.24	78	45
AP2136	8.20 ^{+0.70} _{-0.00}	3.24 ^{+0.14} _{-0.09}	1.45 ^{+0.05} _{-1.10}	8.52 ^{+0.15} _{-0.13}	3.18 ^{+0.15} _{-0.12}	0.97 ^{+0.29} _{-0.27}	I	0	1.36	117	77
AP2143	6.60 ^{+0.20} _{-0.00}	2.82 ^{+0.00} _{-0.03}	0.55 ^{+0.00} _{-0.10}	6.86 ^{+0.04} _{-0.06}	2.54 ^{+0.30} _{-0.23}	0.10 ^{+0.07} _{-0.07}	I	0	1.99	234	226
AP2145	6.80 ^{+0.40} _{-0.20}	2.84 ^{+0.01} _{-0.02}	0.55 ^{+0.05} _{-0.10}	7.68 ^{+0.05} _{-0.05}	2.68 ^{+0.06} _{-0.07}	0.02 ^{+0.07} _{-0.02}	I	0	1.83	199	168
AP2146	10.00 ^{+0.10} _{-0.60}	4.93 ^{+0.33} _{-0.66}	0.30 ^{+0.25} _{-0.05}	9.97 ^{+0.28} _{-0.07}	5.08 ^{+0.10} _{-0.07}	1.02 ^{+0.10} _{-0.28}	I	0	1.57	58	158
AP2147	9.10 ^{+0.00} _{-0.00}	3.82 ^{+0.06} _{-0.01}	0.10 ^{+0.15} _{-0.00}	8.27 ^{+0.16} _{-0.10}	3.35 ^{+0.24} _{-0.13}	1.15 ^{+0.31} _{-0.31}	I	0	1.98	220	139
AP2150	7.00 ^{+2.10} _{-0.20}	2.20 ^{+0.89} _{-0.17}	0.75 ^{+0.85} _{-0.35}	6.57 ^{+0.07} _{-0.05}	2.23 ^{+0.05} _{-0.06}	0.80 ^{+0.07} _{-0.07}	I	0	1.57	105	92
AP2151	8.30 ^{+0.10} _{-0.10}	3.17 ^{+0.02} _{-0.08}	0.85 ^{+0.10} _{-0.20}	7.82 ^{+0.06} _{-0.07}	2.19 ^{+0.05} _{-0.09}	0.65 ^{+0.28} _{-0.19}	I	0	1.25	143	126
AP2153	7.80 ^{+0.00} _{-0.60}	2.57 ^{+0.01} _{-0.07}	0.35 ^{+0.15} _{-0.05}	6.46 ^{+0.30} _{-0.33}	2.58 ^{+0.38} _{-0.36}	1.08 ^{+0.12} _{-0.13}	I	0	1.34	101	83
AP2154	9.10 ^{+0.10} _{-0.20}	4.05 ^{+0.08} _{-0.15}	0.75 ^{+0.45} _{-0.05}	8.82 ^{+0.19} _{-0.21}	3.93 ^{+0.10} _{-0.10}	1.20 ^{+0.28} _{-0.29}	I	0	1.75	230	190

Table 1 (cont'd)

AP ID ^a	CMD Best Fit Parameters ^b			Integrated Best Fit Parameters ^c			Best ^d Flag ^e	R _{ap} ^f	N _{stars} ^g	N _{bg} ^h	
	log(<i>t</i> [Myr])	log(<i>M</i> [<i>M</i> _⊙])	<i>A_V</i> [mag]	log(<i>t</i> [Myr])	log(<i>M</i> [<i>M</i> _⊙])	<i>A_V</i> [mag]					
AP2158	7.20 ^{+0.00} _{-0.00}	4.76 ^{+0.00} _{-0.03}	3.00 ^{+0.00} _{-0.05}	9.57 ^{+0.09} _{-0.13}	5.10 ^{+0.05} _{-0.05}	0.08 ^{+0.15} _{-0.08}	I	0	1.46	256	245
AP2160	8.70 ^{+0.10} _{-0.00}	3.25 ^{+0.04} _{-0.09}	0.65 ^{+0.10} _{-0.30}	8.59 ^{+0.30} _{-0.28}	2.91 ^{+0.16} _{-0.17}	0.54 ^{+0.44} _{-0.44}	I	0	1.50	113	95
AP2165	9.10 ^{+0.00} _{-0.00}	3.65 ^{+0.13} _{-0.06}	0.25 ^{+0.10} _{-0.10}	9.12 ^{+0.89} _{-0.55}	3.74 ^{+0.26} _{-0.16}	0.93 ^{+0.60} _{-0.83}	I	0	1.62	134	76
AP2170	9.00 ^{+0.00} _{-0.10}	3.52 ^{+0.05} _{-0.03}	0.10 ^{+0.40} _{-0.00}	8.94 ^{+0.26} _{-0.25}	3.26 ^{+0.14} _{-0.14}	0.42 ^{+0.34} _{-0.34}	I	0	1.32	112	66
AP2172	7.00 ^{+0.20} _{-0.20}	2.97 ^{+0.01} _{-0.03}	0.80 ^{+0.00} _{-0.15}	7.34 ^{+0.18} _{-0.16}	2.94 ^{+0.11} _{-0.11}	0.39 ^{+0.15} _{-0.15}	I	0	1.60	90	53
AP2174	7.70 ^{+0.20} _{-0.20}	3.40 ^{+0.03} _{-0.02}	1.60 ^{+0.10} _{-0.05}	8.75 ^{+0.04} _{-0.04}	3.01 ^{+0.05} _{-0.05}	0.00 ^{+0.07} _{-0.00}	I	0	0.96	101	81
AP2175	7.80 ^{+0.10} _{-0.60}	2.83 ^{+0.02} _{-0.05}	0.60 ^{+0.15} _{-0.00}	7.20 ^{+0.13} _{-0.13}	2.72 ^{+0.25} _{-0.29}	1.51 ^{+0.14} _{-0.14}	I	0	1.35	85	77
AP2176	7.30 ^{+0.20} _{-0.30}	3.01 ^{+0.03} _{-0.06}	1.75 ^{+0.15} _{-0.05}	7.16 ^{+0.21} _{-0.27}	3.23 ^{+0.21} _{-0.23}	1.89 ^{+0.16} _{-0.17}	I	0	1.25	91	50
AP2177	10.00 ^{+0.10} _{-0.30}	4.87 ^{+0.35} _{-0.27}	0.25 ^{+0.05} _{-0.20}	8.25 ^{+0.19} _{-0.19}	3.41 ^{+0.23} _{-0.23}	1.29 ^{+0.42} _{-0.46}	I	0	1.55	198	144
AP2179	8.20 ^{+0.00} _{-0.50}	3.24 ^{+0.02} _{-0.07}	0.30 ^{+0.25} _{-0.00}	8.08 ^{+0.13} _{-0.12}	3.38 ^{+0.10} _{-0.10}	0.33 ^{+0.23} _{-0.24}	I	0	1.57	235	212
AP2181	8.80 ^{+0.00} _{-0.50}	3.68 ^{+0.01} _{-0.12}	0.20 ^{+0.85} _{-0.02}	8.59 ^{+0.12} _{-0.11}	3.12 ^{+0.11} _{-0.09}	0.14 ^{+0.15} _{-0.14}	I	0	2.07	327	215
AP2183	9.60 ^{+0.10} _{-0.10}	4.69 ^{+0.06} _{-0.09}	0.25 ^{+0.00} _{-0.10}	9.38 ^{+0.18} _{-0.18}	3.83 ^{+0.10} _{-0.10}	0.24 ^{+0.21} _{-0.21}	I	0	1.74	262	202
AP2184	9.00 ^{+0.10} _{-0.10}	4.04 ^{+0.23} _{-0.15}	1.25 ^{+0.35} _{-0.10}	8.80 ^{+0.77} _{-0.71}	3.29 ^{+0.22} _{-0.22}	1.26 ^{+0.85} _{-0.89}	I	0	1.63	80	46
AP2186	7.50 ^{+0.30} _{-0.40}	2.90 ^{+0.03} _{-0.03}	0.80 ^{+0.10} _{-0.10}	8.12 ^{+0.15} _{-0.15}	2.98 ^{+0.11} _{-0.12}	0.38 ^{+0.30} _{-0.30}	I	0	1.35	131	104
AP2187	9.10 ^{+0.00} _{-0.00}	3.85 ^{+0.07} _{-0.00}	0.30 ^{+0.20} _{-0.00}	9.19 ^{+0.75} _{-0.63}	3.86 ^{+0.20} _{-0.15}	0.90 ^{+0.73} _{-0.73}	I	0	1.71	200	144
AP2188	9.10 ^{+0.00} _{-0.00}	3.57 ^{+0.15} _{-0.03}	0.15 ^{+0.20} _{-0.00}	8.68 ^{+0.20} _{-0.22}	3.01 ^{+0.12} _{-0.12}	0.59 ^{+0.31} _{-0.31}	I	0	1.31	93	54
AP2189	7.30 ^{+0.00} _{-0.40}	2.98 ^{+0.00} _{-0.03}	0.95 ^{+0.15} _{-0.00}	6.94 ^{+0.17} _{-0.23}	3.15 ^{+0.12} _{-0.10}	1.05 ^{+0.16} _{-0.05}	I	0	1.36	137	104
AP2190	8.30 ^{+0.10} _{-0.40}	3.24 ^{+0.04} _{-0.10}	1.20 ^{+0.30} _{-0.05}	8.78 ^{+0.13} _{-0.13}	3.03 ^{+0.08} _{-0.09}	0.16 ^{+0.17} _{-0.16}	I	0	1.38	118	87
AP2193	9.00 ^{+0.00} _{-0.00}	4.03 ^{+0.05} _{-0.05}	0.55 ^{+0.10} _{-0.10}	8.93 ^{+0.25} _{-0.21}	3.57 ^{+0.13} _{-0.11}	0.24 ^{+0.13} _{-0.24}	I	0	2.21	436	330
AP2194	9.10 ^{+0.00} _{-0.10}	3.34 ^{+0.06} _{-0.02}	0.00 ^{+0.40} _{-0.05}	7.79 ^{+0.04} _{-0.04}	2.06 ^{+0.11} _{-0.06}	0.12 ^{+0.07} _{-0.09}	I	0	1.48	135	84
AP2198	8.80 ^{+0.10} _{-0.70}	3.14 ^{+0.01} _{-0.21}	0.00 ^{+0.45} _{-0.05}	7.66 ^{+0.29} _{-0.28}	3.00 ^{+0.12} _{-0.12}	1.29 ^{+0.37} _{-0.37}	I	0	1.28	76	43
AP2202	7.00 ^{+0.20} _{-0.00}	3.31 ^{+0.01} _{-0.03}	1.15 ^{+0.00} _{-0.10}	6.71 ^{+0.04} _{-0.06}	2.75 ^{+0.08} _{-0.14}	0.59 ^{+0.07} _{-0.07}	I	0	2.73	459	394
AP2203	8.70 ^{+0.10} _{-0.10}	3.05 ^{+0.03} _{-0.02}	0.35 ^{+0.30} _{-0.15}	8.49 ^{+0.08} _{-0.07}	2.22 ^{+0.15} _{-0.15}	0.04 ^{+0.09} _{-0.04}	I	0	0.96	31	10
AP2205	9.10 ^{+0.00} _{-0.00}	3.68 ^{+0.02} _{-0.08}	0.15 ^{+0.10} _{-0.05}	8.35 ^{+0.09} _{-0.09}	2.71 ^{+0.13} _{-0.13}	0.15 ^{+0.18} _{-0.15}	I	0	1.99	187	148
AP2209	6.60 ^{+0.10} _{-0.00}	2.99 ^{+0.01} _{-0.02}	0.75 ^{+0.00} _{-0.05}	7.52 ^{+0.06} _{-0.06}	3.30 ^{+0.06} _{-0.06}	0.02 ^{+0.07} _{-0.02}	I	0	3.01	449	419
AP2210	8.20 ^{+0.10} _{-1.00}	2.41 ^{+0.01} _{-0.19}	0.60 ^{+0.30} _{-0.10}	9.08 ^{+0.33} _{-0.32}	3.29 ^{+0.15} _{-0.17}	0.43 ^{+0.35} _{-0.36}	I	0	1.68	109	56
AP2211	8.40 ^{+0.30} _{-0.50}	3.27 ^{+0.01} _{-0.11}	0.75 ^{+0.30} _{-0.55}	8.08 ^{+0.20} _{-0.15}	3.23 ^{+0.15} _{-0.15}	1.05 ^{+0.30} _{-0.36}	I	0	1.35	117	91
AP2214	8.00 ^{+0.10} _{-0.40}	2.97 ^{+0.01} _{-0.05}	0.85 ^{+0.15} _{-0.05}	8.18 ^{+0.13} _{-0.13}	2.66 ^{+0.12} _{-0.13}	0.27 ^{+0.23} _{-0.22}	I	0	1.33	73	45
AP2215	9.00 ^{+0.00} _{-0.90}	3.57 ^{+0.02} _{-0.24}	0.00 ^{+1.45} _{-0.05}	7.76 ^{+0.33} _{-0.33}	3.65 ^{+0.20} _{-0.21}	2.08 ^{+0.56} _{-0.59}	I	0	1.38	140	96
AP2217	9.00 ^{+0.00} _{-0.00}	3.30 ^{+0.02} _{-0.07}	0.30 ^{+0.05} _{-0.15}	6.93 ^{+0.47} _{-0.53}	2.86 ^{+0.23} _{-0.24}	2.13 ^{+0.36} _{-0.36}	I	0	1.41	77	45
AP2218	8.10 ^{+0.00} _{-0.00}	3.04 ^{+0.01} _{-0.10}	1.10 ^{+0.05} _{-0.20}	9.27 ^{+0.23} _{-0.22}	3.85 ^{+0.10} _{-0.10}	0.85 ^{+0.31} _{-0.32}	I	0	1.45	123	87
AP2219	6.90 ^{+0.20} _{-0.00}	4.32 ^{+0.05} _{-0.01}	2.95 ^{+0.05} _{-0.00}	9.10 ^{+0.03} _{-0.03}	4.50 ^{+0.03} _{-0.03}	0.20 ^{+0.07} _{-0.07}	I	1	1.51	265	266
AP2220	7.70 ^{+0.00} _{-0.40}	3.08 ^{+0.00} _{-0.03}	0.80 ^{+0.15} _{-0.00}	7.85 ^{+0.15} _{-0.16}	2.86 ^{+0.11} _{-0.10}	0.32 ^{+0.21} _{-0.21}	I	0	1.63	171	157

Table 1 (cont'd)

AP ID ^a	CMD Best Fit Parameters ^b			Integrated Best Fit Parameters ^c			Best ^d Flag ^e	Rap ^f	N _{stars} ^g	N _{bg} ^h	
	log(<i>t</i> [Myr])	log(<i>M</i> [<i>M</i> _⊙])	<i>A_V</i> [mag]	log(<i>t</i> [Myr])	log(<i>M</i> [<i>M</i> _⊙])	<i>A_V</i> [mag]					
AP2222	8.90 ^{+0.00} _{-0.80}	3.54 ^{+0.02} _{-0.33}	0.45 ^{+1.20} _{-0.00}	9.01 ^{+0.22} _{-0.18}	3.21 ^{+0.13} _{-0.14}	0.45 ^{+0.25} _{-0.29}	I	0	1.05	90	55
AP2223	9.10 ^{+0.10} _{-0.10}	3.57 ^{+0.12} _{-0.22}	0.35 ^{+0.30} _{-0.05}	9.55 ^{+0.70} _{-1.32}	3.67 ^{+0.37} _{-0.69}	0.38 ^{+0.56} _{-0.35}	I	0	1.29	90	57
AP2226	8.30 ^{+0.10} _{-0.70}	2.93 ^{+0.03} _{-0.18}	1.45 ^{+0.25} _{-0.10}	8.70 ^{+0.23} _{-0.23}	3.03 ^{+0.11} _{-0.11}	0.68 ^{+0.34} _{-0.37}	I	0	1.50	68	32
AP2230	8.40 ^{+0.40} _{-0.20}	3.08 ^{+0.07} _{-0.17}	0.90 ^{+0.15} _{-0.60}	8.65 ^{+0.13} _{-0.11}	2.89 ^{+0.11} _{-0.12}	0.21 ^{+0.19} _{-0.21}	I	0	1.40	153	114
AP2231	8.20 ^{+0.00} _{-0.10}	3.13 ^{+0.03} _{-0.15}	0.90 ^{+0.00} _{-0.25}	8.19 ^{+0.14} _{-0.17}	2.80 ^{+0.20} _{-0.14}	0.51 ^{+0.32} _{-0.40}	I	0	1.48	138	116
AP2234	9.20 ^{+0.10} _{-0.10}	4.05 ^{+0.07} _{-0.36}	0.50 ^{+0.00} _{-0.35}	8.89 ^{+0.38} _{-0.36}	3.24 ^{+0.16} _{-0.17}	0.74 ^{+0.46} _{-0.52}	I	0	1.52	149	116
AP2237	8.40 ^{+0.10} _{-0.30}	3.12 ^{+0.01} _{-0.17}	1.45 ^{+0.10} _{-0.35}	8.28 ^{+0.20} _{-0.16}	2.31 ^{+0.18} _{-0.20}	0.40 ^{+0.31} _{-0.31}	I	0	0.92	57	28
AP2240	9.90 ^{+0.10} _{-0.60}	4.70 ^{+0.03} _{-1.07}	0.00 ^{+0.50} _{-0.00}	8.38 ^{+0.29} _{-0.26}	3.81 ^{+0.16} _{-0.15}	1.93 ^{+0.43} _{-0.57}	I	0	1.47	188	121
AP2241	8.50 ^{+0.00} _{-1.00}	2.86 ^{+0.00} _{-0.19}	0.30 ^{+0.40} _{-0.05}	8.31 ^{+0.11} _{-0.12}	2.60 ^{+0.15} _{-0.16}	0.25 ^{+0.23} _{-0.22}	I	0	1.12	64	42
AP2242	9.10 ^{+0.00} _{-0.00}	3.78 ^{+0.03} _{-0.05}	0.50 ^{+0.10} _{-0.05}	8.87 ^{+0.42} _{-0.53}	3.22 ^{+0.17} _{-0.17}	0.58 ^{+0.61} _{-0.49}	I	0	1.54	123	90
AP2244	7.60 ^{+0.00} _{-0.70}	2.73 ^{+0.00} _{-0.06}	1.05 ^{+0.20} _{-0.00}	6.85 ^{+0.26} _{-0.25}	2.65 ^{+0.25} _{-0.28}	1.27 ^{+0.13} _{-0.14}	I	0	1.44	63	41
AP2245	8.30 ^{+0.60} _{-0.00}	3.50 ^{+0.11} _{-0.04}	1.75 ^{+0.05} _{-1.15}	8.10 ^{+0.34} _{-0.34}	2.85 ^{+0.25} _{-0.26}	0.96 ^{+0.70} _{-0.73}	I	0	1.13	112	73
AP2246	7.20 ^{+0.20} _{-0.20}	2.85 ^{+0.01} _{-0.03}	0.55 ^{+0.00} _{-0.05}	6.88 ^{+0.20} _{-0.17}	3.15 ^{+0.07} _{-0.06}	0.87 ^{+0.09} _{-0.08}	I	0	1.30	69	31
AP2247	8.50 ^{+0.10} _{-0.10}	3.14 ^{+0.00} _{-0.08}	0.70 ^{+0.05} _{-0.20}	8.52 ^{+0.09} _{-0.08}	2.43 ^{+0.14} _{-0.15}	0.07 ^{+0.11} _{-0.07}	I	0	1.29	109	82
AP2248	8.80 ^{+0.00} _{-0.10}	3.56 ^{+0.01} _{-0.14}	0.75 ^{+0.10} _{-0.25}	8.27 ^{+0.99} _{-0.98}	3.43 ^{+0.26} _{-0.27}	1.46 ^{+1.42} _{-1.44}	I	0	1.54	130	92
AP2253	8.10 ^{+0.10} _{-0.40}	2.77 ^{+0.02} _{-0.05}	0.45 ^{+0.15} _{-0.05}	7.89 ^{+0.14} _{-0.15}	3.07 ^{+0.07} _{-0.07}	1.02 ^{+0.20} _{-0.19}	I	0	1.48	76	41
AP2254	7.90 ^{+1.60} _{-0.80}	3.40 ^{+3.40} _{-3.40}	2.35 ^{+0.20} _{-1.85}	8.76 ^{+0.21} _{-0.04}	3.94 ^{+0.13} _{-0.02}	0.35 ^{+0.05} _{-0.26}	I	0	1.39	233	220
AP2256	8.00 ^{+0.20} _{-0.30}	2.84 ^{+0.02} _{-0.06}	0.60 ^{+0.10} _{-0.15}	8.40 ^{+0.26} _{-0.29}	3.05 ^{+0.15} _{-0.14}	0.46 ^{+0.56} _{-0.45}	I	0	1.36	89	69
AP2257	9.10 ^{+0.00} _{-0.20}	3.27 ^{+0.04} _{-0.14}	0.05 ^{+0.30} _{-0.05}	8.81 ^{+0.27} _{-0.30}	3.14 ^{+0.15} _{-0.14}	0.87 ^{+0.43} _{-0.49}	I	0	1.29	68	35
AP2258	9.10 ^{+0.00} _{-0.00}	3.72 ^{+0.02} _{-0.19}	0.30 ^{+0.05} _{-0.15}	7.99 ^{+0.15} _{-0.18}	3.27 ^{+0.24} _{-0.22}	1.49 ^{+0.44} _{-0.43}	I	0	1.72	129	75
AP2260	8.20 ^{+0.00} _{-0.70}	2.74 ^{+0.00} _{-0.15}	0.50 ^{+0.20} _{-0.05}	7.44 ^{+0.43} _{-0.44}	3.05 ^{+0.13} _{-0.12}	1.49 ^{+0.44} _{-0.42}	I	0	1.25	161	143
AP2261	9.10 ^{+0.00} _{-0.00}	3.63 ^{+0.06} _{-0.05}	0.45 ^{+0.10} _{-0.05}	8.90 ^{+0.61} _{-0.57}	3.31 ^{+0.25} _{-0.24}	0.91 ^{+0.67} _{-0.64}	I	0	1.50	107	74
AP2263	9.10 ^{+0.00} _{-0.10}	3.86 ^{+0.02} _{-0.06}	0.05 ^{+0.15} _{-0.00}	9.12 ^{+0.12} _{-0.12}	3.62 ^{+0.10} _{-0.09}	0.06 ^{+0.11} _{-0.06}	I	0	1.86	255	194
AP2264	8.90 ^{+0.00} _{-0.50}	3.72 ^{+0.03} _{-0.17}	0.45 ^{+1.10} _{-0.00}	9.40 ^{+0.05} _{-0.07}	3.47 ^{+0.07} _{-0.07}	0.06 ^{+0.10} _{-0.06}	I	0	1.30	123	77
AP2267	7.60 ^{+0.50} _{-0.10}	3.02 ^{+0.03} _{-0.04}	1.35 ^{+0.05} _{-0.20}	7.59 ^{+0.05} _{-0.05}	3.36 ^{+0.07} _{-0.06}	0.79 ^{+0.08} _{-0.07}	I	0	1.69	126	96
AP2273	9.10 ^{+0.10} _{-0.00}	3.89 ^{+0.07} _{-0.03}	0.55 ^{+0.00} _{-0.15}	9.16 ^{+0.89} _{-0.61}	3.90 ^{+0.19} _{-0.14}	1.30 ^{+0.68} _{-0.88}	I	0	1.63	139	102
AP2275	7.60 ^{+0.10} _{-0.50}	3.04 ^{+0.03} _{-0.03}	0.70 ^{+0.15} _{-0.00}	7.79 ^{+0.09} _{-0.09}	2.76 ^{+0.17} _{-0.19}	0.43 ^{+0.27} _{-0.26}	I	0	1.38	161	135
AP2281	7.30 ^{+0.20} _{-0.40}	2.83 ^{+0.01} _{-0.06}	0.75 ^{+0.10} _{-0.10}	8.08 ^{+0.11} _{-0.13}	3.48 ^{+0.14} _{-0.14}	1.43 ^{+0.31} _{-0.27}	I	0	2.02	238	200
AP2289	7.80 ^{+0.30} _{-0.60}	2.82 ^{+0.05} _{-0.04}	0.50 ^{+0.20} _{-0.05}	8.04 ^{+0.07} _{-0.27}	2.56 ^{+0.02} _{-0.23}	0.84 ^{+0.12} _{-0.12}	I	0	1.39	95	80
AP2291	9.10 ^{+0.00} _{-0.00}	3.93 ^{+0.02} _{-0.06}	0.35 ^{+0.05} _{-0.10}	7.49 ^{+0.23} _{-0.22}	3.10 ^{+0.08} _{-0.08}	1.42 ^{+0.24} _{-0.25}	I	0	1.66	230	162
AP2292	9.10 ^{+0.00} _{-0.00}	3.58 ^{+0.07} _{-0.03}	0.10 ^{+0.20} _{-0.00}	8.71 ^{+0.12} _{-0.12}	2.75 ^{+0.12} _{-0.10}	0.09 ^{+0.12} _{-0.09}	I	0	1.63	143	100
AP2293	8.30 ^{+0.10} _{-0.10}	2.85 ^{+0.06} _{-0.02}	0.50 ^{+0.05} _{-0.10}	9.21 ^{+0.09} _{-0.08}	3.08 ^{+0.12} _{-0.09}	0.04 ^{+0.08} _{-0.04}	I	0	1.22	88	71
AP2295	8.00 ^{+0.00} _{-0.50}	2.86 ^{+0.00} _{-0.06}	0.35 ^{+0.20} _{-0.05}	7.60 ^{+0.26} _{-0.24}	3.34 ^{+0.10} _{-0.09}	1.02 ^{+0.29} _{-0.29}	I	0	1.61	102	93

Table 1 (cont'd)

AP ID ^a	CMD Best Fit Parameters ^b			Integrated Best Fit Parameters ^c			Best ^d Flag ^e	R _{ap} ^f	N _{stars} ^g	N _{bg} ^h	
	log(<i>t</i> [Myr])	log(<i>M</i> [<i>M</i> _⊙])	<i>A_V</i> [mag]	log(<i>t</i> [Myr])	log(<i>M</i> [<i>M</i> _⊙])	<i>A_V</i> [mag]					
AP2296	8.40 ^{+0.20} _{-0.10}	3.28 ^{+0.07} _{-0.03}	0.60 ^{+0.20} _{-0.15}	8.14 ^{+0.16} _{-0.17}	3.41 ^{+0.16} _{-0.15}	1.21 ^{+0.41} _{-0.37}	I	0	1.70	190	174
AP2297	8.10 ^{+0.30} _{-0.00}	3.32 ^{+0.07} _{-0.00}	0.55 ^{+0.05} _{-0.14}	8.62 ^{+0.06} _{-0.07}	2.73 ^{+0.10} _{-0.11}	0.06 ^{+0.11} _{-0.06}	I	0	1.45	165	122
AP2298	9.70 ^{+0.10} _{-2.30}	4.43 ^{+0.21} _{-4.43}	0.10 ^{+2.25} _{-0.10}	9.34 ^{+0.08} _{-0.09}	3.47 ^{+0.08} _{-0.08}	0.11 ^{+0.13} _{-0.11}	I	0	1.42	168	127
AP2300	7.70 ^{+0.00} _{-0.50}	3.28 ^{+0.09} _{-0.17}	2.35 ^{+0.45} _{-0.15}	8.97 ^{+0.21} _{-0.26}	3.84 ^{+0.11} _{-0.12}	1.39 ^{+0.27} _{-0.26}	I	0	1.23	112	76
AP2303	8.40 ^{+0.30} _{-0.00}	3.27 ^{+0.09} _{-0.03}	1.00 ^{+0.00} _{-0.40}	8.62 ^{+0.16} _{-0.16}	2.63 ^{+0.16} _{-0.17}	0.34 ^{+0.30} _{-0.28}	I	0	1.21	90	46
AP2306	9.90 ^{+0.10} _{-0.60}	4.23 ^{+0.05} _{-0.66}	0.10 ^{+0.25} _{-0.05}	7.09 ^{+0.57} _{-0.67}	2.71 ^{+0.15} _{-0.17}	1.43 ^{+0.32} _{-0.33}	I	0	1.48	99	71
AP2308	9.00 ^{+0.00} _{-0.00}	3.55 ^{+0.05} _{-0.00}	0.05 ^{+0.15} _{-0.00}	8.48 ^{+0.17} _{-0.17}	2.84 ^{+0.16} _{-0.15}	0.56 ^{+0.38} _{-0.38}	I	0	1.56	148	72
AP2309	6.60 ^{+0.50} _{-0.00}	2.72 ^{+0.00} _{-0.03}	0.60 ^{+0.00} _{-0.15}	8.84 ^{+1.11} _{-1.26}	2.81 ^{+0.61} _{-0.61}	1.78 ^{+0.87} _{-0.95}	I	0	1.89	313	320
AP2310	8.40 ^{+0.10} _{-0.40}	3.78 ^{+0.04} _{-0.35}	2.50 ^{+0.30} _{-0.30}	7.59 ^{+0.16} _{-0.18}	3.78 ^{+0.19} _{-0.18}	2.10 ^{+0.33} _{-0.32}	I	0	1.02	42	18
AP2312	8.00 ^{+0.00} _{-1.00}	2.82 ^{+0.00} _{-0.12}	0.60 ^{+0.20} _{-0.05}	10.25 ^{+0.00} _{-0.03}	3.95 ^{+0.06} _{-0.06}	0.00 ^{+0.07} _{-0.00}	I	0	1.44	77	51
AP2313	9.80 ^{+0.20} _{-0.20}	4.44 ^{+0.15} _{-0.16}	0.15 ^{+0.05} _{-0.05}	6.69 ^{+0.07} _{-0.06}	2.71 ^{+0.29} _{-0.32}	0.59 ^{+0.09} _{-0.09}	I	0	1.80	140	79
AP2314	7.30 ^{+0.30} _{-0.40}	2.53 ^{+0.02} _{-0.02}	0.80 ^{+0.10} _{-0.10}	0.00 ^{+0.00} _{-0.00}	0.00 ^{+0.00} _{-0.00}	0.00 ^{+0.00} _{-0.00}	I	0	1.33	53	24
AP2316	9.00 ^{+0.00} _{-0.10}	3.93 ^{+0.04} _{-0.14}	0.25 ^{+0.30} _{-0.10}	6.97 ^{+0.41} _{-0.40}	3.08 ^{+0.15} _{-0.13}	2.49 ^{+0.30} _{-0.30}	I	0	2.10	228	174
AP2317	7.80 ^{+0.10} _{-0.10}	4.10 ^{+0.01} _{-0.15}	2.95 ^{+0.05} _{-0.35}	8.40 ^{+0.17} _{-0.17}	2.94 ^{+0.17} _{-0.18}	0.74 ^{+0.33} _{-0.32}	I	1	1.67	175	111
AP2319	8.80 ^{+0.10} _{-0.10}	3.47 ^{+0.05} _{-0.06}	0.75 ^{+0.50} _{-0.05}	8.63 ^{+0.62} _{-0.70}	3.53 ^{+0.17} _{-0.14}	0.76 ^{+0.91} _{-0.74}	I	0	1.42	130	78
AP2321	6.90 ^{+0.10} _{-0.10}	3.13 ^{+0.01} _{-0.02}	0.50 ^{+0.05} _{-0.00}	6.75 ^{+0.17} _{-0.17}	3.53 ^{+0.31} _{-0.39}	0.41 ^{+0.09} _{-0.09}	I	0	2.66	407	353
AP2324	6.90 ^{+0.10} _{-0.10}	2.91 ^{+0.00} _{-0.03}	1.20 ^{+0.00} _{-0.10}	6.92 ^{+0.12} _{-0.11}	3.05 ^{+0.16} _{-0.18}	1.03 ^{+0.11} _{-0.10}	I	0	1.40	149	127
AP2325	8.40 ^{+0.10} _{-0.50}	2.83 ^{+0.00} _{-0.10}	0.15 ^{+0.20} _{-0.05}	6.82 ^{+0.36} _{-0.44}	3.12 ^{+0.27} _{-0.25}	2.66 ^{+0.22} _{-0.15}	I	0	1.27	104	81
AP2327	9.20 ^{+0.50} _{-1.80}	3.81 ^{+0.04} _{-3.81}	0.95 ^{+1.30} _{-0.65}	9.24 ^{+0.51} _{-0.56}	3.72 ^{+0.16} _{-0.15}	0.77 ^{+0.60} _{-0.52}	I	0	1.58	144	119
AP2328	8.90 ^{+0.10} _{-1.10}	2.99 ^{+0.03} _{-0.21}	0.05 ^{+1.25} _{-0.25}	8.22 ^{+0.38} _{-0.40}	2.58 ^{+0.25} _{-0.25}	0.71 ^{+0.70} _{-0.62}	I	0	1.14	51	20
AP2330	9.00 ^{+0.10} _{-0.10}	3.13 ^{+0.12} _{-0.18}	0.35 ^{+0.16} _{-0.20}	8.87 ^{+0.51} _{-0.41}	3.10 ^{+0.17} _{-0.14}	0.89 ^{+0.49} _{-0.61}	I	0	1.50	70	31
AP2331	7.70 ^{+0.40} _{-0.30}	2.93 ^{+0.05} _{-0.03}	0.80 ^{+0.10} _{-0.10}	0.00 ^{+0.00} _{-0.00}	0.00 ^{+0.00} _{-0.00}	0.00 ^{+0.00} _{-0.00}	I	0	1.72	138	106
AP2333	9.10 ^{+0.00} _{-0.30}	3.23 ^{+0.00} _{-0.13}	0.15 ^{+0.70} _{-0.00}	8.36 ^{+0.14} _{-0.14}	2.38 ^{+0.15} _{-0.16}	0.27 ^{+0.26} _{-0.25}	I	0	1.19	60	40
AP2334	8.20 ^{+0.00} _{-0.30}	2.96 ^{+0.00} _{-0.07}	0.55 ^{+0.20} _{-0.00}	7.69 ^{+0.13} _{-0.11}	3.10 ^{+0.14} _{-0.13}	1.17 ^{+0.21} _{-0.20}	I	0	1.34	100	88
AP2335	8.50 ^{+0.00} _{-0.90}	2.61 ^{+0.02} _{-0.16}	0.15 ^{+0.40} _{-0.10}	8.10 ^{+0.02} _{-0.26}	2.28 ^{+0.06} _{-0.26}	0.37 ^{+0.18} _{-0.16}	I	0	1.26	58	41
AP2339	8.00 ^{+0.80} _{-0.10}	4.16 ^{+0.00} _{-4.16}	2.95 ^{+0.05} _{-1.75}	9.17 ^{+0.79} _{-0.69}	4.04 ^{+0.19} _{-0.15}	1.05 ^{+0.82} _{-0.80}	I	0	1.88	183	55
AP2341	7.40 ^{+0.60} _{-0.30}	3.12 ^{+0.08} _{-0.16}	1.10 ^{+0.00} _{-0.35}	6.99 ^{+0.14} _{-0.13}	2.70 ^{+0.32} _{-0.35}	0.30 ^{+0.11} _{-0.12}	I	0	1.55	161	133
AP2342	8.40 ^{+0.20} _{-0.00}	3.06 ^{+0.02} _{-0.05}	0.90 ^{+0.10} _{-0.35}	7.92 ^{+0.40} _{-0.43}	3.29 ^{+0.19} _{-0.23}	1.47 ^{+0.67} _{-0.84}	I	0	1.65	136	98
AP2343	9.40 ^{+0.10} _{-0.10}	4.49 ^{+0.07} _{-0.14}	0.10 ^{+0.10} _{-0.05}	9.72 ^{+0.25} _{-0.26}	4.18 ^{+0.13} _{-0.14}	0.21 ^{+0.18} _{-0.19}	I	0	1.88	296	229
AP2344	8.40 ^{+0.10} _{-0.00}	3.26 ^{+0.01} _{-0.04}	0.80 ^{+0.05} _{-0.15}	8.92 ^{+0.18} _{-0.18}	3.06 ^{+0.13} _{-0.12}	0.22 ^{+0.23} _{-0.21}	I	0	1.33	124	105
AP2345	8.30 ^{+0.00} _{-0.60}	3.11 ^{+0.00} _{-0.12}	1.15 ^{+0.30} _{-0.00}	8.55 ^{+0.17} _{-0.16}	2.68 ^{+0.15} _{-0.17}	0.29 ^{+0.27} _{-0.26}	I	0	1.11	86	71
AP2346	7.90 ^{+1.70} _{-0.80}	3.20 ^{+3.20} _{-3.20}	2.65 ^{+0.10} _{-2.20}	10.24 ^{+0.01} _{-0.03}	5.29 ^{+0.04} _{-0.04}	0.11 ^{+0.07} _{-0.08}	I	0	1.67	223	297
AP2347	8.40 ^{+0.10} _{-0.00}	3.03 ^{+0.03} _{-0.04}	0.50 ^{+0.10} _{-0.10}	8.56 ^{+0.21} _{-0.20}	3.02 ^{+0.13} _{-0.13}	0.35 ^{+0.30} _{-0.30}	I	0	2.14	257	216

Table 1 (cont'd)

AP ID ^a	CMD Best Fit Parameters ^b			Integrated Best Fit Parameters ^c			Best ^d Flag ^e	Rap ^f	N _{stars} ^g	N _{bg} ^h	
	log(<i>t</i> [Myr])	log(<i>M</i> [<i>M</i> _⊙])	<i>A_V</i> [mag]	log(<i>t</i> [Myr])	log(<i>M</i> [<i>M</i> _⊙])	<i>A_V</i> [mag]					
AP2348	9.60 ^{+0.00} _{-0.00}	4.93 ^{+0.00} _{-0.00}	0.10 ^{+0.00} _{-0.05}	9.20 ^{+0.10} _{-0.11}	5.20 ^{+0.05} _{-0.07}	0.33 ^{+0.13} _{-0.15}	I	0	2.77	318	413
AP2350	8.50 ^{+0.10} _{-0.00}	2.99 ^{+0.01} _{-0.07}	1.05 ^{+0.05} _{-0.25}	9.00 ^{+0.25} _{-0.22}	2.93 ^{+0.13} _{-0.14}	0.39 ^{+0.32} _{-0.32}	I	0	1.16	71	36
AP2352	8.80 ^{+0.10} _{-1.00}	2.95 ^{+0.01} _{-0.30}	0.70 ^{+0.85} _{-0.20}	7.36 ^{+0.82} _{-0.90}	2.23 ^{+0.17} _{-0.17}	0.63 ^{+0.42} _{-0.43}	I	0	0.88	39	20
AP2358	8.00 ^{+0.10} _{-0.90}	2.51 ^{+0.00} _{-0.09}	0.25 ^{+0.20} _{-0.05}	7.27 ^{+0.43} _{-0.45}	2.78 ^{+0.16} _{-0.16}	1.11 ^{+0.30} _{-0.31}	I	0	1.31	84	72
AP2359	8.00 ^{+0.10} _{-0.80}	2.91 ^{+0.00} _{-0.09}	0.35 ^{+0.20} _{-0.05}	6.87 ^{+0.50} _{-0.57}	2.75 ^{+0.20} _{-0.22}	1.08 ^{+0.25} _{-0.26}	I	0	1.33	97	60
AP2361	8.50 ^{+0.10} _{-0.20}	2.96 ^{+0.06} _{-0.08}	0.15 ^{+0.30} _{-0.05}	7.85 ^{+0.08} _{-0.09}	3.07 ^{+0.10} _{-0.10}	1.29 ^{+0.16} _{-0.16}	I	0	1.05	101	71
AP2362	8.80 ^{+0.10} _{-0.00}	3.26 ^{+0.03} _{-0.17}	0.60 ^{+0.10} _{-0.37}	8.49 ^{+0.13} _{-0.12}	3.12 ^{+0.14} _{-0.10}	1.18 ^{+0.27} _{-0.26}	I	0	1.15	80	54
AP2363	7.40 ^{+0.20} _{-0.40}	2.87 ^{+0.02} _{-0.04}	1.20 ^{+0.10} _{-0.05}	7.46 ^{+0.90} _{-0.85}	2.82 ^{+0.21} _{-0.21}	0.94 ^{+0.42} _{-0.54}	I	0	1.28	87	67
AP2365	8.90 ^{+0.00} _{-0.10}	3.50 ^{+0.04} _{-0.03}	0.10 ^{+0.35} _{-0.00}	8.26 ^{+0.12} _{-0.10}	3.45 ^{+0.16} _{-0.14}	1.29 ^{+0.28} _{-0.25}	I	0	1.32	98	45
AP2367	8.40 ^{+0.00} _{-0.50}	2.87 ^{+0.02} _{-0.12}	0.95 ^{+0.30} _{-0.05}	8.23 ^{+0.15} _{-0.14}	2.52 ^{+0.26} _{-0.26}	0.51 ^{+0.36} _{-0.37}	I	0	1.37	42	25
AP2368	8.60 ^{+0.10} _{-0.10}	3.09 ^{+0.07} _{-0.03}	0.45 ^{+0.15} _{-0.25}	8.46 ^{+0.48} _{-0.51}	3.16 ^{+0.14} _{-0.14}	0.62 ^{+0.81} _{-0.62}	I	0	1.22	95	57
AP2369	7.90 ^{+0.10} _{-0.30}	3.42 ^{+0.00} _{-0.16}	2.20 ^{+0.10} _{-0.15}	8.45 ^{+1.78} _{-0.84}	3.30 ^{+1.03} _{-1.00}	1.16 ^{+0.84} _{-0.67}	I	0	1.42	127	85
AP2370	9.10 ^{+0.90} _{-0.20}	3.88 ^{+0.78} _{-0.12}	1.15 ^{+0.15} _{-0.65}	7.89 ^{+0.12} _{-0.20}	2.26 ^{+0.20} _{-0.23}	0.57 ^{+0.32} _{-0.35}	I	0	1.26	91	72
AP2372	8.60 ^{+0.20} _{-0.10}	3.35 ^{+0.01} _{-0.13}	0.95 ^{+0.15} _{-0.50}	8.63 ^{+0.12} _{-0.13}	3.28 ^{+0.12} _{-0.14}	0.71 ^{+0.30} _{-0.28}	I	0	1.55	157	131
AP2373	6.80 ^{+0.30} _{-0.10}	2.66 ^{+0.01} _{-0.03}	0.50 ^{+0.00} _{-0.05}	7.25 ^{+0.17} _{-0.14}	2.54 ^{+0.20} _{-0.19}	0.16 ^{+0.11} _{-0.12}	I	0	1.31	57	33
AP2377	9.40 ^{+0.00} _{-2.30}	3.75 ^{+1.57} _{-3.75}	0.00 ^{+2.15} _{-0.35}	6.78 ^{+0.04} _{-0.04}	3.70 ^{+0.03} _{-0.03}	2.20 ^{+0.07} _{-0.07}	I	1	1.23	77	179
AP2378	7.40 ^{+0.20} _{-0.30}	3.46 ^{+0.02} _{-0.19}	2.70 ^{+0.10} _{-0.15}	9.15 ^{+0.67} _{-0.78}	3.98 ^{+0.17} _{-0.17}	1.04 ^{+0.99} _{-0.74}	I	0	1.27	161	87
AP2380	8.80 ^{+0.00} _{-0.20}	3.04 ^{+0.03} _{-0.08}	0.20 ^{+0.55} _{-0.05}	8.80 ^{+0.36} _{-0.42}	3.06 ^{+0.16} _{-0.14}	0.58 ^{+0.50} _{-0.43}	I	0	1.34	93	67
AP2381	8.80 ^{+0.00} _{-0.50}	3.35 ^{+0.06} _{-0.03}	0.20 ^{+0.95} _{-0.00}	8.62 ^{+0.26} _{-0.19}	3.11 ^{+0.17} _{-0.12}	0.44 ^{+0.22} _{-0.21}	I	0	1.57	162	142
AP2382	9.20 ^{+0.00} _{-0.20}	3.68 ^{+0.01} _{-0.39}	0.35 ^{+0.40} _{-0.15}	7.60 ^{+0.98} _{-0.97}	2.71 ^{+0.36} _{-0.39}	1.09 ^{+0.79} _{-0.79}	I	0	1.10	69	30
AP2383	8.30 ^{+0.10} _{-0.10}	3.31 ^{+0.07} _{-0.04}	1.15 ^{+0.15} _{-0.05}	8.38 ^{+0.26} _{-0.25}	2.97 ^{+0.17} _{-0.19}	0.85 ^{+0.48} _{-0.53}	I	0	1.24	98	64
AP2384	8.10 ^{+0.10} _{-0.00}	4.02 ^{+0.00} _{-0.10}	2.30 ^{+0.00} _{-0.15}	8.00 ^{+0.15} _{-0.18}	3.21 ^{+0.14} _{-0.13}	0.78 ^{+0.26} _{-0.25}	I	0	1.70	271	175
AP2386	8.00 ^{+0.20} _{-0.00}	2.96 ^{+0.01} _{-0.12}	0.90 ^{+0.00} _{-0.35}	8.68 ^{+0.13} _{-0.14}	3.27 ^{+0.08} _{-0.08}	0.74 ^{+0.24} _{-0.23}	I	0	1.25	128	124
AP2388	8.20 ^{+0.00} _{-0.40}	3.11 ^{+0.10} _{-0.07}	1.05 ^{+0.30} _{-0.00}	7.85 ^{+0.78} _{-0.82}	3.01 ^{+0.33} _{-0.33}	1.49 ^{+1.11} _{-1.14}	I	0	1.39	111	89
AP2389	7.70 ^{+0.00} _{-0.20}	3.04 ^{+0.07} _{-0.02}	1.00 ^{+0.25} _{-0.00}	7.74 ^{+0.10} _{-0.08}	3.37 ^{+0.10} _{-0.10}	1.55 ^{+0.14} _{-0.15}	I	0	1.23	117	88
AP2391	8.20 ^{+0.10} _{-0.50}	2.75 ^{+0.03} _{-0.08}	0.50 ^{+0.15} _{-0.10}	7.88 ^{+0.15} _{-0.15}	2.93 ^{+0.12} _{-0.09}	0.92 ^{+0.22} _{-0.16}	I	0	1.08	35	18
AP2392	8.80 ^{+0.00} _{-0.20}	3.30 ^{+0.06} _{-0.11}	0.30 ^{+0.30} _{-0.10}	8.66 ^{+0.52} _{-0.50}	3.36 ^{+0.18} _{-0.16}	0.80 ^{+0.59} _{-0.63}	I	0	1.44	188	138
AP2393	8.10 ^{+0.00} _{-0.60}	3.29 ^{+0.00} _{-0.08}	1.05 ^{+0.30} _{-0.05}	6.87 ^{+0.43} _{-0.44}	3.08 ^{+0.25} _{-0.24}	1.90 ^{+0.25} _{-0.24}	I	0	1.26	131	114
AP2395	7.80 ^{+0.00} _{-0.50}	3.30 ^{+0.08} _{-0.07}	1.50 ^{+0.25} _{-0.05}	8.67 ^{+0.10} _{-0.10}	3.01 ^{+0.08} _{-0.08}	0.17 ^{+0.18} _{-0.17}	I	0	1.11	83	62
AP2398	9.10 ^{+0.00} _{-0.00}	3.67 ^{+0.05} _{-0.02}	0.00 ^{+0.15} _{-0.00}	7.97 ^{+0.05} _{-0.06}	2.02 ^{+0.03} _{-0.02}	0.38 ^{+0.21} _{-0.14}	I	0	1.78	185	116
AP2399	8.30 ^{+0.10} _{-0.40}	3.46 ^{+0.00} _{-0.14}	1.40 ^{+0.05} _{-0.30}	9.24 ^{+0.10} _{-0.09}	3.49 ^{+0.08} _{-0.08}	0.15 ^{+0.14} _{-0.14}	I	0	1.16	130	97
AP2400	9.00 ^{+0.00} _{-0.90}	3.24 ^{+0.00} _{-0.22}	0.25 ^{+1.50} _{-0.05}	8.60 ^{+0.17} _{-0.18}	3.02 ^{+0.11} _{-0.12}	0.73 ^{+0.34} _{-0.33}	I	0	1.31	96	55
AP2401	6.70 ^{+0.40} _{-0.10}	2.66 ^{+0.01} _{-0.02}	0.65 ^{+0.00} _{-0.10}	6.76 ^{+0.35} _{-0.49}	3.10 ^{+0.09} _{-0.08}	0.51 ^{+0.10} _{-0.10}	I	0	2.00	132	82

Table 1 (cont'd)

AP ID ^a	CMD Best Fit Parameters ^b			Integrated Best Fit Parameters ^c			Best ^d Flag ^e	R _{ap} ^f	N _{stars} ^g	N _{bg} ^h	
	log(<i>t</i> [Myr])	log(<i>M</i> [<i>M</i> _⊙])	<i>A_V</i> [mag]	log(<i>t</i> [Myr])	log(<i>M</i> [<i>M</i> _⊙])	<i>A_V</i> [mag]					
AP2406	9.90 ^{+0.10} _{-0.60}	4.80 ^{+0.04} _{-0.54}	0.40 ^{+0.20} _{-0.15}	7.80 ^{+0.14} _{-0.19}	3.61 ^{+0.22} _{-0.23}	2.58 ^{+0.29} _{-0.27}	I	0	1.31	118	91
AP2407	7.80 ^{+0.90} _{-0.10}	3.63 ^{+0.05} _{-0.62}	2.70 ^{+0.00} _{-1.70}	8.76 ^{+0.28} _{-0.31}	3.00 ^{+0.19} _{-0.19}	0.87 ^{+0.46} _{-0.51}	I	0	1.19	111	78
AP2408	9.70 ^{+0.20} _{-1.00}	4.38 ^{+0.14} _{-1.97}	0.50 ^{+1.15} _{-0.15}	9.52 ^{+0.59} _{-0.53}	4.33 ^{+0.23} _{-0.15}	2.13 ^{+0.55} _{-0.43}	I	0	1.41	103	81
AP2409	7.70 ^{+0.20} _{-0.70}	2.67 ^{+0.01} _{-0.11}	0.80 ^{+0.15} _{-0.05}	8.50 ^{+0.10} _{-0.10}	2.70 ^{+0.10} _{-0.11}	0.12 ^{+0.15} _{-0.12}	I	0	1.25	98	72
AP2411	8.00 ^{+0.20} _{-0.00}	3.49 ^{+0.08} _{-0.06}	1.75 ^{+0.00} _{-0.15}	8.81 ^{+0.12} _{-0.13}	3.04 ^{+0.09} _{-0.09}	0.24 ^{+0.19} _{-0.20}	I	0	1.36	150	109
AP2412	7.90 ^{+0.20} _{-0.10}	2.83 ^{+0.03} _{-0.02}	0.50 ^{+0.05} _{-0.10}	7.88 ^{+0.17} _{-0.06}	3.05 ^{+0.15} _{-0.18}	0.77 ^{+0.22} _{-0.34}	I	0	1.52	78	39
AP2414	8.30 ^{+0.00} _{-0.50}	2.96 ^{+0.00} _{-0.09}	0.55 ^{+0.15} _{-0.05}	8.34 ^{+0.33} _{-0.15}	3.12 ^{+0.17} _{-0.15}	0.96 ^{+0.31} _{-0.36}	I	0	1.46	89	72
AP2415	7.30 ^{+0.20} _{-0.60}	3.11 ^{+0.01} _{-0.14}	1.30 ^{+0.05} _{-0.20}	6.69 ^{+0.17} _{-0.18}	2.73 ^{+0.33} _{-0.38}	0.72 ^{+0.15} _{-0.14}	I	0	1.59	185	159
AP2416	9.50 ^{+0.20} _{-0.10}	4.59 ^{+0.11} _{-0.08}	0.15 ^{+0.00} _{-0.15}	9.47 ^{+0.69} _{-0.70}	4.28 ^{+0.18} _{-0.17}	0.82 ^{+0.76} _{-0.66}	I	0	1.41	216	137
AP2417	6.60 ^{+3.00} _{-0.50}	0.00 ^{+0.00} _{-0.00}	0.00 ^{+2.55} _{-0.45}	9.85 ^{+0.38} _{-0.94}	4.84 ^{+0.12} _{-0.17}	0.74 ^{+0.98} _{-0.42}	I	0	1.75	146	286
AP2419	8.50 ^{+0.10} _{-0.10}	3.14 ^{+0.00} _{-0.15}	0.60 ^{+0.20} _{-0.20}	8.38 ^{+0.33} _{-0.34}	2.93 ^{+0.17} _{-0.18}	0.58 ^{+0.63} _{-0.53}	I	0	1.53	137	116
AP2420	8.20 ^{+0.10} _{-0.00}	3.26 ^{+0.06} _{-0.02}	0.95 ^{+0.15} _{-0.05}	8.40 ^{+0.17} _{-0.14}	3.49 ^{+0.18} _{-0.12}	1.02 ^{+0.36} _{-0.36}	I	0	1.32	183	156
AP2422	8.80 ^{+0.50} _{-1.30}	3.67 ^{+0.12} _{-3.67}	1.50 ^{+0.90} _{-1.05}	7.80 ^{+0.54} _{-0.62}	3.23 ^{+0.27} _{-0.22}	1.78 ^{+0.86} _{-0.77}	I	0	1.34	128	91
AP2424	8.80 ^{+0.00} _{-0.20}	3.00 ^{+0.03} _{-0.12}	0.15 ^{+0.20} _{-0.10}	8.73 ^{+0.48} _{-0.50}	2.72 ^{+0.30} _{-0.34}	0.29 ^{+0.32} _{-0.28}	I	0	1.11	67	48
AP2425	7.20 ^{+0.00} _{-0.50}	2.83 ^{+0.00} _{-0.19}	0.80 ^{+0.10} _{-0.25}	6.80 ^{+0.05} _{-0.06}	2.31 ^{+0.27} _{-0.20}	0.43 ^{+0.08} _{-0.09}	I	0	2.29	325	347
AP2427	8.40 ^{+0.00} _{-0.50}	3.48 ^{+0.06} _{-0.21}	1.40 ^{+0.30} _{-0.00}	9.56 ^{+0.51} _{-0.63}	3.88 ^{+0.25} _{-0.14}	0.40 ^{+0.58} _{-0.37}	I	0	1.55	180	145
AP2428	8.80 ^{+0.00} _{-0.30}	3.31 ^{+0.03} _{-0.13}	0.55 ^{+0.50} _{-0.05}	8.14 ^{+0.14} _{-0.13}	2.94 ^{+0.11} _{-0.13}	0.81 ^{+0.25} _{-0.27}	I	0	1.45	83	51
AP2430	0.00 ^{+0.00} _{-0.00}	0.00 ^{+0.00} _{-0.00}	0.00 ^{+0.00} _{-0.00}	0.00 ^{+0.00} _{-0.00}	0.00 ^{+0.00} _{-0.00}	0.00 ^{+0.00} _{-0.00}	I	0	2.41	0	0
AP2437	8.30 ^{+0.00} _{-0.70}	3.23 ^{+0.01} _{-0.18}	1.35 ^{+0.25} _{-0.05}	9.33 ^{+0.26} _{-0.22}	3.28 ^{+0.22} _{-0.23}	0.28 ^{+0.24} _{-0.26}	I	0	1.59	152	126
AP2439	8.60 ^{+0.00} _{-0.50}	2.91 ^{+0.02} _{-0.05}	0.15 ^{+0.55} _{-0.00}	8.46 ^{+0.12} _{-0.12}	2.72 ^{+0.13} _{-0.14}	0.23 ^{+0.23} _{-0.22}	I	0	1.16	96	77
AP2440	8.90 ^{+0.00} _{-0.00}	2.96 ^{+0.01} _{-0.01}	0.00 ^{+0.15} _{-0.00}	7.60 ^{+0.97} _{-0.94}	2.73 ^{+0.23} _{-0.24}	1.20 ^{+0.55} _{-0.71}	I	0	1.52	66	32
AP2441	7.70 ^{+0.10} _{-1.00}	3.02 ^{+0.00} _{-0.13}	0.80 ^{+0.15} _{-0.00}	7.77 ^{+0.14} _{-0.01}	2.85 ^{+0.15} _{-0.12}	0.16 ^{+0.12} _{-0.16}	I	0	2.01	260	252
AP2443	6.60 ^{+0.30} _{-0.00}	3.12 ^{+0.02} _{-0.00}	0.95 ^{+0.00} _{-0.05}	6.87 ^{+0.13} _{-0.13}	3.01 ^{+0.27} _{-0.26}	0.67 ^{+0.10} _{-0.11}	I	0	2.28	351	300
AP2444	8.30 ^{+0.10} _{-0.70}	2.90 ^{+0.02} _{-0.12}	0.55 ^{+0.25} _{-0.05}	6.62 ^{+0.33} _{-0.47}	2.79 ^{+0.31} _{-0.35}	1.41 ^{+0.26} _{-0.11}	I	0	1.53	115	95
AP2446	8.90 ^{+0.10} _{-0.20}	2.86 ^{+0.02} _{-0.20}	0.35 ^{+0.40} _{-0.20}	7.94 ^{+0.34} _{-0.28}	2.26 ^{+0.14} _{-0.15}	0.36 ^{+0.30} _{-0.29}	I	0	1.54	58	23
AP2447	8.20 ^{+0.00} _{-0.10}	3.20 ^{+0.03} _{-0.04}	0.35 ^{+0.15} _{-0.05}	8.31 ^{+0.36} _{-0.30}	3.18 ^{+0.16} _{-0.14}	0.47 ^{+0.41} _{-0.40}	I	0	1.37	147	116
AP2451	9.30 ^{+0.10} _{-0.20}	3.84 ^{+0.07} _{-0.61}	0.20 ^{+0.05} _{-0.20}	9.02 ^{+0.39} _{-0.25}	3.20 ^{+0.17} _{-0.16}	0.47 ^{+0.30} _{-0.37}	I	0	1.26	60	37
AP2452	7.80 ^{+0.00} _{-0.40}	3.07 ^{+0.02} _{-0.03}	0.65 ^{+0.25} _{-0.00}	7.93 ^{+0.16} _{-0.14}	3.14 ^{+0.13} _{-0.11}	0.67 ^{+0.26} _{-0.26}	I	0	1.51	157	132
AP2453	7.50 ^{+0.00} _{-0.40}	3.33 ^{+0.00} _{-0.15}	2.40 ^{+0.15} _{-0.05}	8.96 ^{+0.09} _{-0.09}	3.18 ^{+0.11} _{-0.11}	0.05 ^{+0.09} _{-0.05}	I	0	1.34	78	48
AP2454	7.50 ^{+0.40} _{-0.50}	2.67 ^{+0.09} _{-0.07}	1.00 ^{+0.15} _{-0.10}	7.54 ^{+0.01} _{-0.07}	3.10 ^{+0.04} _{-0.04}	0.57 ^{+0.09} _{-0.06}	I	0	1.67	121	92
AP2456	8.00 ^{+0.00} _{-0.70}	2.62 ^{+0.00} _{-0.06}	0.30 ^{+0.20} _{-0.00}	7.58 ^{+0.32} _{-0.26}	2.63 ^{+0.16} _{-0.16}	0.51 ^{+0.26} _{-0.27}	I	0	1.48	44	34
AP2458	7.20 ^{+0.00} _{-0.20}	2.85 ^{+0.01} _{-0.02}	1.10 ^{+0.10} _{-0.00}	8.81 ^{+0.05} _{-0.05}	3.76 ^{+0.04} _{-0.04}	0.01 ^{+0.07} _{-0.01}	I	0	1.86	263	251
AP2461	8.30 ^{+0.00} _{-0.50}	3.24 ^{+0.00} _{-0.17}	1.50 ^{+0.30} _{-0.05}	8.71 ^{+0.16} _{-0.17}	2.98 ^{+0.11} _{-0.12}	0.62 ^{+0.28} _{-0.28}	I	0	1.36	125	98

Table 1 (cont'd)

AP ID ^a	CMD Best Fit Parameters ^b			Integrated Best Fit Parameters ^c			Best ^d Flag ^e	Rap ^f	N _{stars} ^g	N _{bg} ^h	
	log(<i>t</i> [Myr])	log(<i>M</i> [<i>M</i> _⊙])	<i>A_V</i> [mag]	log(<i>t</i> [Myr])	log(<i>M</i> [<i>M</i> _⊙])	<i>A_V</i> [mag]					
AP2462	8.50 ^{+0.00} _{-0.10}	3.17 ^{+0.00} _{-0.12}	0.75 ^{+0.05} _{-0.20}	8.02 ^{+0.09} _{-0.07}	3.53 ^{+0.09} _{-0.07}	1.66 ^{+0.20} _{-0.15}	I	0	1.19	99	79
AP2463	8.10 ^{+0.00} _{-0.90}	3.09 ^{+0.01} _{-0.25}	1.30 ^{+0.30} _{-0.05}	8.33 ^{+0.68} _{-0.84}	3.08 ^{+0.25} _{-0.21}	0.94 ^{+1.29} _{-0.93}	I	0	1.40	114	94
AP2465	8.40 ^{+0.00} _{-0.60}	3.36 ^{+0.06} _{-0.11}	1.10 ^{+0.40} _{-0.05}	8.52 ^{+0.08} _{-0.08}	2.31 ^{+0.14} _{-0.14}	0.07 ^{+0.11} _{-0.07}	I	0	1.39	122	93
AP2466	9.20 ^{+0.00} _{-0.00}	4.83 ^{+0.00} _{-0.04}	0.00 ^{+0.00} _{-0.00}	0.00 ^{+0.00} _{-0.00}	0.00 ^{+0.00} _{-0.00}	0.00 ^{+0.00} _{-0.00}	I	0	2.15	333	465
AP2468	8.40 ^{+0.00} _{-0.50}	2.90 ^{+0.15} _{-0.14}	0.50 ^{+0.55} _{-0.05}	8.55 ^{+0.30} _{-0.26}	2.98 ^{+0.14} _{-0.15}	0.46 ^{+0.42} _{-0.40}	I	0	1.29	105	76
AP2470	8.20 ^{+0.20} _{-0.80}	2.93 ^{+0.02} _{-0.17}	0.50 ^{+0.25} _{-0.15}	7.90 ^{+0.45} _{-0.48}	3.02 ^{+0.14} _{-0.15}	0.77 ^{+0.62} _{-0.60}	I	0	1.62	192	141
AP2474	7.10 ^{+0.20} _{-0.40}	2.44 ^{+0.02} _{-0.03}	0.40 ^{+0.10} _{-0.05}	6.51 ^{+0.32} _{-0.39}	2.74 ^{+0.17} _{-0.18}	0.62 ^{+0.10} _{-0.10}	I	0	1.28	76	58
AP2475	8.90 ^{+0.00} _{-0.00}	3.40 ^{+0.05} _{-0.04}	0.35 ^{+0.20} _{-0.05}	8.56 ^{+0.18} _{-0.18}	2.79 ^{+0.15} _{-0.14}	0.29 ^{+0.27} _{-0.26}	I	0	1.55	155	92
AP2477	8.70 ^{+0.10} _{-0.00}	3.30 ^{+0.01} _{-0.09}	0.85 ^{+0.05} _{-0.40}	8.41 ^{+0.46} _{-0.48}	2.83 ^{+0.23} _{-0.23}	0.84 ^{+0.75} _{-0.66}	I	0	1.35	62	25
AP2478	6.60 ^{+0.60} _{-0.00}	2.88 ^{+0.01} _{-0.03}	0.70 ^{+0.00} _{-0.15}	6.90 ^{+0.26} _{-0.37}	2.65 ^{+0.18} _{-0.21}	0.75 ^{+0.11} _{-0.11}	I	0	1.06	65	20
AP2479	8.70 ^{+0.00} _{-0.60}	3.20 ^{+0.02} _{-0.21}	0.60 ^{+0.65} _{-0.00}	8.11 ^{+1.47} _{-1.46}	3.78 ^{+1.25} _{-1.18}	1.45 ^{+1.02} _{-1.02}	I	0	1.23	67	28
AP2480	8.10 ^{+0.40} _{-0.30}	3.21 ^{+0.07} _{-0.06}	1.45 ^{+0.20} _{-0.30}	8.67 ^{+0.15} _{-0.15}	2.88 ^{+0.13} _{-0.13}	0.52 ^{+0.27} _{-0.28}	I	0	1.08	95	55
AP2481	6.60 ^{+0.80} _{-0.00}	2.86 ^{+0.02} _{-0.08}	0.65 ^{+0.05} _{-0.25}	6.84 ^{+0.11} _{-0.13}	2.95 ^{+0.28} _{-0.53}	0.06 ^{+0.09} _{-0.06}	I	0	2.37	399	379
AP2482	7.90 ^{+0.10} _{-0.10}	3.39 ^{+0.01} _{-0.02}	1.30 ^{+0.10} _{-0.05}	8.74 ^{+0.16} _{-0.17}	3.40 ^{+0.08} _{-0.08}	0.48 ^{+0.25} _{-0.23}	I	0	1.31	155	119
AP2484	8.80 ^{+0.00} _{-0.10}	3.00 ^{+0.07} _{-0.02}	0.00 ^{+0.45} _{-0.05}	7.77 ^{+0.74} _{-0.82}	3.01 ^{+0.33} _{-0.32}	1.56 ^{+1.12} _{-1.22}	I	0	1.19	91	76
AP2485	7.20 ^{+1.10} _{-0.00}	2.98 ^{+0.13} _{-0.03}	1.45 ^{+0.00} _{-0.50}	6.67 ^{+0.11} _{-0.10}	2.64 ^{+0.37} _{-0.28}	0.80 ^{+0.08} _{-0.08}	I	0	1.77	187	168
AP2487	8.90 ^{+0.00} _{-0.10}	3.82 ^{+0.07} _{-0.06}	0.20 ^{+0.35} _{-0.05}	8.61 ^{+0.16} _{-0.14}	3.74 ^{+0.08} _{-0.07}	0.93 ^{+0.22} _{-0.24}	I	0	1.87	278	212
AP2488	6.80 ^{+1.40} _{-0.10}	2.79 ^{+0.13} _{-0.01}	1.10 ^{+0.05} _{-0.25}	8.01 ^{+0.10} _{-0.10}	3.23 ^{+0.08} _{-0.08}	0.37 ^{+0.17} _{-0.17}	I	0	1.29	99	82
AP2490	9.10 ^{+0.00} _{-0.00}	3.56 ^{+0.07} _{-0.05}	0.10 ^{+0.10} _{-0.05}	9.31 ^{+0.44} _{-0.43}	3.65 ^{+0.16} _{-0.15}	0.53 ^{+0.52} _{-0.45}	I	0	1.36	131	92
AP2491	8.80 ^{+0.00} _{-0.60}	3.13 ^{+0.02} _{-0.12}	0.40 ^{+0.90} _{-0.00}	8.80 ^{+0.09} _{-0.09}	2.89 ^{+0.09} _{-0.09}	0.06 ^{+0.09} _{-0.06}	I	0	1.34	89	49
AP2492	7.90 ^{+0.00} _{-0.30}	4.09 ^{+0.00} _{-0.18}	2.85 ^{+0.15} _{-0.00}	8.31 ^{+0.76} _{-0.44}	3.44 ^{+0.19} _{-0.17}	1.02 ^{+0.66} _{-0.94}	I	0	1.64	225	201
AP2496	9.10 ^{+0.00} _{-0.10}	3.66 ^{+0.04} _{-0.00}	0.05 ^{+0.20} _{-0.00}	8.70 ^{+0.18} _{-0.19}	3.12 ^{+0.12} _{-0.11}	0.67 ^{+0.29} _{-0.28}	I	0	1.43	112	81
AP2497	6.80 ^{+0.40} _{-0.10}	2.61 ^{+0.02} _{-0.01}	0.80 ^{+0.00} _{-0.05}	7.88 ^{+0.07} _{-0.09}	2.20 ^{+0.14} _{-0.16}	0.04 ^{+0.08} _{-0.04}	I	0	1.54	55	36
AP2498	6.60 ^{+0.30} _{-0.00}	2.68 ^{+0.02} _{-0.01}	0.70 ^{+0.05} _{-0.05}	6.72 ^{+0.07} _{-0.06}	2.64 ^{+0.22} _{-0.20}	0.62 ^{+0.11} _{-0.10}	I	0	2.35	336	312
AP2500	8.20 ^{+0.10} _{-0.00}	3.20 ^{+0.00} _{-0.04}	1.30 ^{+0.00} _{-0.10}	9.05 ^{+0.20} _{-0.17}	3.39 ^{+0.13} _{-0.13}	0.24 ^{+0.20} _{-0.20}	I	0	1.50	167	135
AP2501	9.50 ^{+0.10} _{-2.30}	3.80 ^{+0.49} _{-2.10}	0.00 ^{+2.55} _{-0.25}	8.70 ^{+0.15} _{-0.16}	3.12 ^{+0.11} _{-0.10}	0.90 ^{+0.26} _{-0.26}	I	0	1.36	94	55
AP2502	7.50 ^{+0.10} _{-0.60}	2.70 ^{+0.01} _{-0.05}	0.50 ^{+0.15} _{-0.00}	6.74 ^{+0.14} _{-0.10}	2.98 ^{+0.19} _{-0.19}	0.73 ^{+0.12} _{-0.11}	I	0	2.11	317	280
AP2508	8.10 ^{+0.00} _{-0.10}	3.40 ^{+0.02} _{-0.05}	1.30 ^{+0.10} _{-0.10}	8.81 ^{+0.25} _{-0.31}	3.73 ^{+0.10} _{-0.10}	0.90 ^{+0.38} _{-0.39}	I	0	1.58	220	172
AP2509	8.80 ^{+0.00} _{-0.30}	3.29 ^{+0.03} _{-0.07}	0.30 ^{+0.55} _{-0.05}	8.24 ^{+0.34} _{-0.34}	2.92 ^{+0.19} _{-0.20}	0.73 ^{+0.67} _{-0.64}	I	0	1.40	111	72
AP2510	9.40 ^{+0.20} _{-2.20}	3.44 ^{+0.63} _{-3.44}	0.00 ^{+2.60} _{-0.25}	8.96 ^{+0.65} _{-0.42}	3.47 ^{+0.16} _{-0.14}	0.85 ^{+0.49} _{-0.70}	I	0	1.80	97	50
AP2511	6.60 ^{+0.10} _{-0.00}	3.04 ^{+0.00} _{-0.04}	0.95 ^{+0.00} _{-0.05}	6.81 ^{+0.14} _{-0.13}	2.98 ^{+0.31} _{-0.32}	0.54 ^{+0.09} _{-0.09}	I	0	2.36	372	335
AP2513	8.30 ^{+0.10} _{-0.70}	2.82 ^{+0.00} _{-0.20}	0.80 ^{+0.25} _{-0.15}	8.16 ^{+0.71} _{-0.62}	2.97 ^{+0.32} _{-0.30}	1.31 ^{+1.16} _{-1.07}	I	0	1.29	88	70
AP2515	8.70 ^{+0.00} _{-0.30}	3.20 ^{+0.00} _{-0.07}	0.05 ^{+0.50} _{-0.05}	8.30 ^{+0.04} _{-0.03}	2.88 ^{+0.07} _{-0.08}	0.35 ^{+0.10} _{-0.12}	I	0	1.61	183	172

Table 1 (cont'd)

AP ID ^a	CMD Best Fit Parameters ^b			Integrated Best Fit Parameters ^c			Best ^d Flag ^e	R _{ap} ^f	N _{stars} ^g	N _{bg} ^h	
	log(<i>t</i> [Myr])	log(<i>M</i> [<i>M</i> _⊙])	<i>A_V</i> [mag]	log(<i>t</i> [Myr])	log(<i>M</i> [<i>M</i> _⊙])	<i>A_V</i> [mag]					
AP2519	9.00 ^{+0.00} _{-0.30}	3.59 ^{+0.04} _{-0.15}	0.55 ^{+0.95} _{-0.05}	7.38 ^{+0.85} _{-0.85}	2.63 ^{+0.36} _{-0.37}	1.37 ^{+0.75} _{-0.83}	I	0	1.56	155	123
AP2520	9.40 ^{+0.20} _{-0.00}	4.72 ^{+0.05} _{-0.06}	0.10 ^{+0.10} _{-0.05}	10.03 ^{+0.14} _{-0.12}	4.38 ^{+0.07} _{-0.07}	0.22 ^{+0.17} _{-0.18}	I	0	1.32	118	188
AP2521	9.00 ^{+0.00} _{-0.00}	3.91 ^{+0.00} _{-0.02}	0.65 ^{+0.00} _{-0.10}	9.04 ^{+0.19} _{-0.18}	3.32 ^{+0.15} _{-0.14}	0.26 ^{+0.15} _{-0.17}	I	0	1.51	156	109
AP2523	8.10 ^{+0.10} _{-0.00}	2.85 ^{+0.03} _{-0.01}	0.70 ^{+0.05} _{-0.05}	7.46 ^{+0.91} _{-0.86}	2.75 ^{+0.20} _{-0.21}	0.98 ^{+0.39} _{-0.55}	I	0	1.53	49	30
AP2524	9.10 ^{+0.00} _{-0.00}	3.43 ^{+0.02} _{-0.05}	0.05 ^{+0.10} _{-0.00}	8.66 ^{+0.42} _{-0.41}	3.02 ^{+0.15} _{-0.14}	0.59 ^{+0.57} _{-0.50}	I	0	1.80	85	34
AP2525	8.70 ^{+0.00} _{-0.10}	3.27 ^{+0.06} _{-0.06}	0.15 ^{+0.15} _{-0.10}	7.86 ^{+0.13} _{-0.20}	3.62 ^{+0.13} _{-0.10}	1.90 ^{+0.33} _{-0.18}	I	0	1.32	130	96
AP2528	7.70 ^{+0.06} _{-0.70}	3.37 ^{+0.04} _{-0.20}	1.95 ^{+0.10} _{-0.10}	8.62 ^{+0.06} _{-0.06}	3.15 ^{+0.07} _{-0.07}	0.04 ^{+0.07} _{-0.04}	I	0	1.71	202	169
AP2529	8.60 ^{+0.10} _{-0.10}	3.26 ^{+0.05} _{-0.05}	0.50 ^{+0.20} _{-0.15}	7.72 ^{+0.12} _{-0.12}	2.93 ^{+0.15} _{-0.16}	1.42 ^{+0.22} _{-0.21}	I	0	1.57	178	169
AP2530	9.10 ^{+0.00} _{-0.00}	3.62 ^{+0.01} _{-0.06}	0.55 ^{+0.00} _{-0.20}	8.26 ^{+0.18} _{-0.17}	2.98 ^{+0.20} _{-0.20}	1.00 ^{+0.39} _{-0.43}	I	0	1.37	86	49
AP2531	8.70 ^{+0.00} _{-0.20}	3.31 ^{+0.00} _{-0.10}	0.25 ^{+0.35} _{-0.00}	8.38 ^{+0.14} _{-0.13}	2.96 ^{+0.13} _{-0.13}	0.35 ^{+0.31} _{-0.30}	I	0	1.25	114	100
AP2533	7.50 ^{+0.10} _{-0.60}	2.69 ^{+0.00} _{-0.05}	1.05 ^{+0.10} _{-0.05}	6.94 ^{+0.09} _{-0.09}	2.24 ^{+0.18} _{-0.17}	1.21 ^{+0.08} _{-0.08}	I	0	1.26	47	28
AP2534	8.70 ^{+0.10} _{-0.03}	3.29 ^{+0.06} _{-0.00}	0.20 ^{+0.20} _{-0.15}	8.79 ^{+0.49} _{-0.63}	3.40 ^{+0.15} _{-0.14}	0.67 ^{+0.79} _{-0.60}	I	0	1.27	98	45
AP2536	8.10 ^{+0.00} _{-0.20}	3.30 ^{+0.06} _{-0.02}	1.40 ^{+0.25} _{-0.00}	8.76 ^{+0.10} _{-0.09}	3.10 ^{+0.10} _{-0.09}	0.32 ^{+0.19} _{-0.19}	I	0	1.06	81	42
AP2538	8.00 ^{+0.00} _{-0.20}	2.78 ^{+0.01} _{-0.05}	0.55 ^{+0.10} _{-0.10}	8.04 ^{+0.10} _{-0.09}	2.69 ^{+0.11} _{-0.13}	0.27 ^{+0.16} _{-0.16}	I	0	1.12	68	50
AP2542	8.40 ^{+0.10} _{-0.40}	2.91 ^{+0.00} _{-0.15}	0.35 ^{+0.15} _{-0.10}	8.19 ^{+0.14} _{-0.13}	2.88 ^{+0.14} _{-0.13}	0.25 ^{+0.25} _{-0.24}	I	0	1.29	158	98
AP2543	9.00 ^{+0.00} _{-0.10}	3.98 ^{+0.00} _{-0.11}	0.70 ^{+0.26} _{-0.00}	8.50 ^{+0.12} _{-0.10}	2.46 ^{+0.15} _{-0.15}	0.11 ^{+0.14} _{-0.11}	I	0	1.57	169	121
AP2546	9.10 ^{+0.00} _{-0.10}	3.37 ^{+0.03} _{-0.15}	0.25 ^{+0.15} _{-0.05}	8.76 ^{+0.33} _{-0.34}	2.86 ^{+0.17} _{-0.17}	0.37 ^{+0.39} _{-0.35}	I	0	1.41	73	36
AP2547	9.00 ^{+0.00} _{-0.10}	3.38 ^{+0.13} _{-0.05}	0.15 ^{+0.35} _{-0.00}	8.15 ^{+0.19} _{-0.22}	2.39 ^{+0.34} _{-0.29}	0.54 ^{+0.45} _{-0.41}	I	0	1.04	65	41
AP2548	7.40 ^{+0.10} _{-0.60}	2.80 ^{+0.01} _{-0.04}	0.80 ^{+0.20} _{-0.05}	6.70 ^{+0.11} _{-0.07}	3.36 ^{+0.12} _{-0.15}	0.94 ^{+0.09} _{-0.09}	I	0	2.93	187	149
AP2549	7.90 ^{+0.20} _{-0.20}	3.47 ^{+0.03} _{-0.08}	2.00 ^{+0.10} _{-0.10}	9.69 ^{+0.18} _{-0.17}	3.87 ^{+0.11} _{-0.10}	0.14 ^{+0.15} _{-0.14}	I	0	1.08	111	79
AP2550	9.20 ^{+0.00} _{-2.40}	3.63 ^{+0.00} _{-1.01}	0.00 ^{+0.80} _{-0.05}	6.75 ^{+0.13} _{-0.09}	2.93 ^{+0.22} _{-0.26}	0.18 ^{+0.11} _{-0.11}	I	0	2.12	260	267
AP2551	8.00 ^{+0.10} _{-0.60}	2.92 ^{+0.05} _{-0.08}	0.85 ^{+0.20} _{-0.00}	8.74 ^{+0.04} _{-0.04}	2.99 ^{+0.08} _{-0.07}	0.03 ^{+0.07} _{-0.03}	I	0	1.32	135	130
AP2552	9.10 ^{+0.00} _{-0.00}	3.83 ^{+0.01} _{-0.05}	0.25 ^{+0.05} _{-0.10}	9.06 ^{+0.35} _{-0.19}	3.65 ^{+0.16} _{-0.16}	0.58 ^{+0.20} _{-0.46}	I	0	1.96	230	187
AP2554	8.30 ^{+0.50} _{-0.80}	3.11 ^{+0.00} _{-0.79}	1.70 ^{+0.05} _{-1.00}	8.72 ^{+0.22} _{-0.25}	3.07 ^{+0.17} _{-0.16}	0.70 ^{+0.39} _{-0.41}	I	0	1.42	111	84
AP2555	8.20 ^{+0.67} _{-0.00}	3.43 ^{+0.23} _{-0.02}	1.55 ^{+0.25} _{-0.80}	8.80 ^{+0.34} _{-0.34}	3.64 ^{+0.11} _{-0.12}	1.04 ^{+0.44} _{-0.54}	I	0	1.70	226	158
AP2557	9.00 ^{+0.50} _{-0.10}	4.89 ^{+0.09} _{-0.10}	1.70 ^{+0.05} _{-0.35}	9.53 ^{+0.48} _{-0.46}	4.76 ^{+0.21} _{-0.14}	1.68 ^{+0.41} _{-0.35}	I	0	2.40	488	426
AP2559	9.10 ^{+0.00} _{-0.00}	3.22 ^{+0.17} _{-0.05}	0.25 ^{+0.15} _{-0.10}	9.21 ^{+0.41} _{-0.30}	3.14 ^{+0.20} _{-0.16}	0.42 ^{+0.32} _{-0.37}	I	0	1.43	87	45
AP2560	9.10 ^{+0.00} _{-0.10}	4.01 ^{+0.01} _{-0.04}	0.20 ^{+0.25} _{-0.05}	8.70 ^{+0.15} _{-0.16}	3.49 ^{+0.10} _{-0.09}	0.55 ^{+0.25} _{-0.25}	I	0	1.89	303	203
AP2562	8.00 ^{+0.10} _{-0.40}	2.63 ^{+0.00} _{-0.05}	0.40 ^{+0.10} _{-0.10}	7.83 ^{+0.21} _{-0.18}	2.35 ^{+0.16} _{-0.16}	0.58 ^{+0.26} _{-0.26}	I	0	1.13	72	67
AP2564	9.20 ^{+0.50} _{-0.00}	4.60 ^{+0.17} _{-0.00}	0.40 ^{+0.15} _{-0.25}	0.00 ^{+0.00} _{-0.00}	0.00 ^{+0.00} _{-0.00}	0.00 ^{+0.00} _{-0.00}	I	0	3.04	412	778
AP2565	8.70 ^{+0.10} _{-0.00}	3.57 ^{+0.05} _{-0.03}	1.35 ^{+0.10} _{-0.25}	8.12 ^{+1.14} _{-1.27}	3.20 ^{+0.24} _{-0.22}	1.53 ^{+1.04} _{-1.15}	I	0	1.27	89	47
AP2566	8.30 ^{+0.00} _{-0.10}	3.71 ^{+0.00} _{-0.13}	1.60 ^{+0.05} _{-0.15}	8.25 ^{+0.05} _{-0.08}	3.43 ^{+0.15} _{-0.13}	1.13 ^{+0.27} _{-0.19}	I	0	1.43	163	109
AP2570	8.10 ^{+0.70} _{-0.50}	3.40 ^{+0.02} _{-0.92}	2.10 ^{+0.30} _{-1.10}	9.15 ^{+0.71} _{-0.57}	3.79 ^{+0.18} _{-0.13}	0.93 ^{+0.71} _{-0.73}	I	0	1.41	139	83

Table 1 (cont'd)

AP ID ^a	CMD Best Fit Parameters ^b			Integrated Best Fit Parameters ^c			Best ^d Flag ^e	Rap ^f	N _{stars} ^g	N _{bg} ^h	
	log(<i>t</i> [Myr])	log(<i>M</i> [<i>M</i> _⊙])	<i>A_V</i> [mag]	log(<i>t</i> [Myr])	log(<i>M</i> [<i>M</i> _⊙])	<i>A_V</i> [mag]					
AP2571	9.20 ^{+0.00} _{-0.00}	4.19 ^{+0.08} _{-0.07}	0.30 ^{+0.10} _{-0.05}	10.13 ^{+0.11} _{-0.12}	4.31 ^{+0.08} _{-0.08}	0.11 ^{+0.14} _{-0.11}	I	0	2.09	294	224
AP2573	6.90 ^{+0.00} _{-0.20}	3.40 ^{+0.02} _{-0.01}	1.65 ^{+0.10} _{-0.00}	6.73 ^{+0.11} _{-0.11}	2.88 ^{+0.41} _{-0.54}	1.29 ^{+0.10} _{-0.10}	I	0	2.02	275	232
AP2574	8.20 ^{+0.30} _{-0.20}	2.99 ^{+0.00} _{-0.11}	0.65 ^{+0.05} _{-0.30}	7.84 ^{+0.06} _{-0.07}	2.89 ^{+0.11} _{-0.11}	0.86 ^{+0.17} _{-0.16}	I	0	1.30	93	80
AP2575	8.30 ^{+0.10} _{-0.00}	3.25 ^{+0.06} _{-0.03}	0.65 ^{+0.10} _{-0.10}	8.23 ^{+0.67} _{-0.77}	3.18 ^{+0.19} _{-0.17}	1.01 ^{+0.94} _{-0.75}	I	0	1.10	105	75
AP2577	7.50 ^{+0.10} _{-0.50}	2.91 ^{+0.00} _{-0.06}	0.35 ^{+0.10} _{-0.05}	7.67 ^{+0.10} _{-0.10}	3.05 ^{+0.10} _{-0.11}	0.40 ^{+0.19} _{-0.20}	I	0	2.09	289	255
AP2578	7.80 ^{+0.10} _{-0.80}	2.98 ^{+0.02} _{-0.08}	0.90 ^{+0.20} _{-0.05}	7.76 ^{+0.07} _{-0.07}	3.13 ^{+0.08} _{-0.08}	1.24 ^{+0.13} _{-0.13}	I	0	1.60	109	74
AP2581	0.00 ^{+0.00} _{-0.00}	0.00 ^{+0.00} _{-0.00}	0.00 ^{+0.00} _{-0.00}	0.00 ^{+0.00} _{-0.00}	0.00 ^{+0.00} _{-0.00}	0.00 ^{+0.00} _{-0.00}	I	0	1.20	0	0
AP2582	7.30 ^{+0.70} _{-0.40}	2.54 ^{+0.04} _{-0.09}	0.85 ^{+0.05} _{-0.25}	8.01 ^{+0.15} _{-0.15}	3.10 ^{+0.09} _{-0.08}	0.96 ^{+0.24} _{-0.24}	I	0	1.59	161	148
AP2583	7.70 ^{+0.10} _{-0.70}	2.65 ^{+0.02} _{-0.05}	0.50 ^{+0.20} _{-0.05}	7.25 ^{+0.16} _{-0.16}	2.76 ^{+0.19} _{-0.20}	0.42 ^{+0.16} _{-0.16}	I	0	1.42	167	170
AP2586	7.90 ^{+0.30} _{-0.90}	2.44 ^{+0.02} _{-0.12}	1.00 ^{+0.20} _{-0.15}	7.49 ^{+0.94} _{-0.95}	2.57 ^{+0.33} _{-0.33}	0.97 ^{+0.69} _{-0.70}	I	0	1.13	52	21
AP2587	7.70 ^{+0.50} _{-0.00}	2.92 ^{+0.05} _{-0.02}	1.00 ^{+0.10} _{-0.20}	8.55 ^{+0.07} _{-0.07}	3.87 ^{+0.06} _{-0.06}	1.32 ^{+0.12} _{-0.11}	I	0	1.42	74	39
AP2588	8.40 ^{+0.00} _{-0.50}	3.20 ^{+0.03} _{-0.15}	0.85 ^{+0.30} _{-0.10}	8.58 ^{+0.15} _{-0.15}	2.83 ^{+0.12} _{-0.12}	0.18 ^{+0.21} _{-0.18}	I	0	1.41	165	131
AP2589	9.10 ^{+0.00} _{-0.20}	3.86 ^{+0.00} _{-0.13}	0.45 ^{+0.40} _{-0.00}	9.25 ^{+0.73} _{-0.62}	3.82 ^{+0.21} _{-0.17}	0.97 ^{+0.73} _{-0.74}	I	0	1.57	163	121
AP2590	9.20 ^{+0.00} _{-0.00}	4.88 ^{+0.01} _{-0.01}	0.00 ^{+0.00} _{-0.00}	0.00 ^{+0.00} _{-0.00}	0.00 ^{+0.00} _{-0.00}	0.00 ^{+0.00} _{-0.00}	I	0	1.85	327	398
AP2591	8.00 ^{+0.30} _{-0.40}	2.94 ^{+0.05} _{-0.06}	0.65 ^{+0.15} _{-0.10}	8.50 ^{+0.16} _{-0.16}	3.02 ^{+0.11} _{-0.12}	0.35 ^{+0.32} _{-0.30}	I	0	1.42	141	102
AP2593	9.10 ^{+0.70} _{-1.60}	3.39 ^{+0.59} _{-3.39}	0.60 ^{+1.40} _{-0.10}	7.27 ^{+0.05} _{-0.05}	3.51 ^{+0.05} _{-0.05}	0.75 ^{+0.13} _{-0.12}	I	0	1.86	108	162
AP2594	7.20 ^{+0.20} _{-0.40}	3.04 ^{+0.01} _{-0.07}	1.15 ^{+0.05} _{-0.05}	7.25 ^{+0.26} _{-0.22}	2.57 ^{+0.21} _{-0.20}	0.31 ^{+0.20} _{-0.21}	I	0	1.52	144	121
AP2596	7.00 ^{+0.10} _{-0.40}	2.55 ^{+0.01} _{-0.01}	0.90 ^{+0.10} _{-0.05}	6.87 ^{+0.18} _{-0.15}	2.45 ^{+0.21} _{-0.23}	0.72 ^{+0.11} _{-0.11}	I	0	1.41	44	29
AP2597	8.50 ^{+0.10} _{-0.10}	2.82 ^{+0.04} _{-0.06}	0.20 ^{+0.10} _{-0.15}	7.86 ^{+0.12} _{-0.16}	3.23 ^{+0.19} _{-0.17}	1.46 ^{+0.32} _{-0.29}	I	0	1.57	190	175
AP2598	8.90 ^{+0.00} _{-0.10}	3.11 ^{+0.02} _{-0.03}	0.00 ^{+0.35} _{-0.00}	8.31 ^{+0.62} _{-0.56}	2.91 ^{+0.27} _{-0.27}	0.98 ^{+1.03} _{-0.84}	I	0	1.35	100	68
AP2599	8.80 ^{+0.10} _{-0.60}	3.66 ^{+0.02} _{-0.81}	1.05 ^{+0.05} _{-0.40}	6.69 ^{+0.10} _{-0.12}	2.66 ^{+0.19} _{-0.21}	0.49 ^{+0.07} _{-0.07}	I	0	1.89	181	142
AP2600	9.50 ^{+0.10} _{-0.00}	5.12 ^{+0.08} _{-0.00}	0.15 ^{+0.00} _{-0.05}	9.00 ^{+0.16} _{-0.13}	4.32 ^{+0.07} _{-0.06}	0.60 ^{+0.21} _{-0.24}	I	0	2.80	800	627
AP2601	8.90 ^{+0.00} _{-0.60}	3.57 ^{+0.00} _{-0.15}	0.25 ^{+1.10} _{-0.05}	9.36 ^{+0.08} _{-0.09}	3.49 ^{+0.09} _{-0.09}	0.11 ^{+0.13} _{-0.11}	I	0	1.17	119	78
AP2602	7.70 ^{+0.20} _{-0.10}	3.61 ^{+0.01} _{-0.07}	2.15 ^{+0.00} _{-0.15}	8.69 ^{+0.11} _{-0.08}	3.10 ^{+0.10} _{-0.07}	0.20 ^{+0.16} _{-0.17}	I	0	1.29	129	80
AP2603	6.70 ^{+1.80} _{-0.00}	2.45 ^{+0.23} _{-0.05}	1.00 ^{+0.35} _{-0.15}	6.88 ^{+0.10} _{-0.12}	2.58 ^{+0.30} _{-0.43}	0.56 ^{+0.09} _{-0.08}	I	0	1.43	148	131
AP2607	8.80 ^{+0.00} _{-1.30}	2.98 ^{+0.04} _{-0.53}	0.15 ^{+0.65} _{-0.05}	8.01 ^{+0.32} _{-0.28}	2.39 ^{+0.15} _{-0.16}	0.27 ^{+0.28} _{-0.25}	I	0	1.45	144	116
AP2608	7.80 ^{+0.40} _{-0.70}	2.69 ^{+0.03} _{-0.13}	0.95 ^{+0.20} _{-0.15}	7.41 ^{+0.06} _{-0.07}	3.37 ^{+0.10} _{-0.09}	1.35 ^{+0.13} _{-0.13}	I	0	1.40	121	110
AP2609	6.90 ^{+0.20} _{-0.20}	3.55 ^{+0.01} _{-0.09}	3.00 ^{+0.00} _{-0.10}	8.95 ^{+0.09} _{-0.09}	3.74 ^{+0.08} _{-0.08}	0.30 ^{+0.18} _{-0.18}	I	1	1.03	113	120
AP2610	8.10 ^{+0.00} _{-0.10}	3.28 ^{+0.03} _{-0.02}	1.10 ^{+0.15} _{-0.00}	9.14 ^{+0.12} _{-0.10}	3.43 ^{+0.11} _{-0.11}	0.08 ^{+0.10} _{-0.08}	I	0	1.20	118	80
AP2613	8.70 ^{+0.30} _{-1.60}	2.63 ^{+0.34} _{-2.63}	0.00 ^{+2.70} _{-0.20}	8.31 ^{+0.33} _{-0.24}	3.51 ^{+0.17} _{-0.19}	1.46 ^{+0.48} _{-0.68}	I	0	1.42	160	116
AP2614	7.00 ^{+0.30} _{-0.30}	2.90 ^{+0.02} _{-0.02}	0.40 ^{+0.05} _{-0.05}	6.66 ^{+0.14} _{-0.13}	2.84 ^{+0.27} _{-0.29}	0.62 ^{+0.11} _{-0.11}	I	0	1.45	142	128
AP2617	8.00 ^{+0.10} _{-0.50}	3.64 ^{+0.01} _{-0.20}	2.15 ^{+0.20} _{-0.30}	8.90 ^{+0.61} _{-0.39}	3.70 ^{+0.14} _{-0.13}	1.11 ^{+0.50} _{-0.78}	I	0	1.06	131	117
AP2618	7.40 ^{+0.00} _{-0.60}	3.03 ^{+0.00} _{-0.10}	1.55 ^{+0.05} _{-0.05}	6.75 ^{+0.17} _{-0.15}	2.86 ^{+0.74} _{-0.69}	2.54 ^{+0.10} _{-0.10}	I	0	1.79	213	195

Table 1 (cont'd)

AP ID ^a	CMD Best Fit Parameters ^b			Integrated Best Fit Parameters ^c			Best ^d Flag ^e	R _{ap} ^f	N _{stars} ^g	N _{bg} ^h	
	log(<i>t</i> [Myr])	log(<i>M</i> [<i>M</i> _⊙])	<i>A_V</i> [mag]	log(<i>t</i> [Myr])	log(<i>M</i> [<i>M</i> _⊙])	<i>A_V</i> [mag]					
AP2619	9.20 ^{+0.20} _{-1.90}	3.14 ^{+0.04} _{-3.14}	0.20 ^{+2.10} _{-0.00}	7.94 ^{+1.09} _{-1.11}	2.81 ^{+0.21} _{-0.22}	1.51 ^{+0.80} _{-1.07}	I	0	1.08	34	16
AP2620	8.30 ^{+0.00} _{-0.10}	3.43 ^{+0.01} _{-0.05}	1.20 ^{+0.10} _{-0.05}	8.61 ^{+0.10} _{-0.10}	2.98 ^{+0.09} _{-0.08}	0.36 ^{+0.20} _{-0.20}	I	0	1.05	112	63
AP2621	8.80 ^{+0.00} _{-0.20}	2.82 ^{+0.00} _{-0.04}	0.20 ^{+0.25} _{-0.15}	9.17 ^{+0.76} _{-0.88}	3.30 ^{+0.29} _{-0.25}	0.74 ^{+0.89} _{-0.64}	I	0	1.24	35	16
AP2623	9.00 ^{+0.00} _{-0.10}	4.19 ^{+0.02} _{-0.15}	1.00 ^{+0.25} _{-0.10}	9.01 ^{+1.04} _{-0.50}	3.75 ^{+0.18} _{-0.14}	1.42 ^{+0.60} _{-1.05}	I	0	1.82	215	152
AP2625	9.30 ^{+0.40} _{-1.10}	3.95 ^{+0.25} _{-3.95}	0.70 ^{+1.15} _{-0.20}	9.06 ^{+0.32} _{-0.24}	3.18 ^{+0.16} _{-0.15}	0.43 ^{+0.29} _{-0.33}	I	0	1.12	93	72
AP2627	7.90 ^{+0.00} _{-0.70}	3.28 ^{+0.00} _{-0.07}	0.60 ^{+0.20} _{-0.05}	7.67 ^{+0.33} _{-0.29}	3.49 ^{+0.16} _{-0.18}	0.81 ^{+0.43} _{-0.51}	I	0	2.06	310	244
AP2628	8.20 ^{+0.00} _{-0.80}	2.88 ^{+0.01} _{-0.13}	0.45 ^{+0.20} _{-0.05}	7.83 ^{+0.06} _{-0.08}	2.99 ^{+0.10} _{-0.08}	0.95 ^{+0.16} _{-0.17}	I	0	1.42	136	117
AP2629	9.10 ^{+0.00} _{-0.00}	3.66 ^{+0.03} _{-0.17}	0.20 ^{+0.10} _{-0.10}	7.87 ^{+0.09} _{-0.12}	2.71 ^{+0.25} _{-0.28}	0.84 ^{+0.34} _{-0.34}	I	0	1.30	121	97
AP2630	10.00 ^{+0.10} _{-0.60}	4.90 ^{+0.11} _{-0.52}	0.20 ^{+0.25} _{-0.10}	9.14 ^{+1.08} _{-0.57}	3.92 ^{+0.32} _{-0.10}	1.44 ^{+0.69} _{-1.02}	I	0	1.25	125	98
AP2631	8.40 ^{+0.00} _{-0.60}	3.30 ^{+0.03} _{-0.10}	0.95 ^{+0.50} _{-0.00}	8.25 ^{+0.49} _{-0.43}	3.00 ^{+0.24} _{-0.23}	0.87 ^{+0.81} _{-0.73}	I	0	1.19	91	71
AP2635	8.90 ^{+0.10} _{-0.00}	3.96 ^{+0.02} _{-0.07}	1.00 ^{+0.05} _{-0.20}	9.04 ^{+0.65} _{-0.95}	4.09 ^{+0.14} _{-0.13}	1.38 ^{+1.17} _{-0.75}	I	0	1.70	203	134
AP2636	8.60 ^{+0.40} _{-0.10}	4.76 ^{+0.35} _{-0.49}	2.65 ^{+0.20} _{-0.30}	9.22 ^{+0.77} _{-0.72}	3.88 ^{+0.21} _{-0.18}	1.44 ^{+0.83} _{-0.70}	I	0	1.25	144	103
AP2638	8.40 ^{+0.30} _{-0.20}	3.00 ^{+0.04} _{-0.10}	1.20 ^{+0.10} _{-0.40}	8.06 ^{+0.13} _{-0.15}	2.58 ^{+0.29} _{-0.30}	1.03 ^{+0.44} _{-0.39}	I	0	1.29	52	26
AP2639	8.20 ^{+0.10} _{-0.00}	2.95 ^{+0.01} _{-0.07}	0.60 ^{+0.00} _{-0.20}	8.20 ^{+0.13} _{-0.14}	2.77 ^{+0.13} _{-0.11}	0.23 ^{+0.20} _{-0.20}	I	0	1.14	97	68
AP2641	7.70 ^{+0.00} _{-0.70}	2.76 ^{+0.01} _{-0.06}	0.65 ^{+0.20} _{-0.00}	6.90 ^{+0.46} _{-0.69}	3.26 ^{+0.22} _{-0.24}	1.66 ^{+0.26} _{-0.15}	I	0	1.47	183	174
AP2642	7.50 ^{+0.20} _{-0.60}	2.64 ^{+0.00} _{-0.05}	0.85 ^{+0.10} _{-0.10}	6.87 ^{+0.35} _{-0.46}	2.61 ^{+0.18} _{-0.19}	0.83 ^{+0.14} _{-0.13}	I	0	1.70	110	86
AP2643	8.10 ^{+0.10} _{-0.70}	2.51 ^{+0.01} _{-0.09}	0.50 ^{+0.20} _{-0.05}	7.49 ^{+0.21} _{-0.21}	3.06 ^{+0.08} _{-0.05}	1.68 ^{+0.16} _{-0.10}	I	0	1.17	35	15
AP2644	8.70 ^{+0.00} _{-1.10}	2.62 ^{+0.03} _{-0.16}	0.50 ^{+0.80} _{-0.05}	8.33 ^{+0.67} _{-0.55}	2.49 ^{+0.23} _{-0.22}	0.86 ^{+0.87} _{-0.83}	I	0	1.03	44	15
AP2646	8.30 ^{+0.30} _{-0.00}	3.03 ^{+0.19} _{-0.00}	0.60 ^{+0.25} _{-0.30}	8.08 ^{+0.26} _{-0.22}	3.03 ^{+0.19} _{-0.20}	1.06 ^{+0.49} _{-0.51}	I	0	1.30	106	76
AP2649	9.10 ^{+0.90} _{-0.00}	4.12 ^{+0.73} _{-0.05}	1.10 ^{+0.10} _{-0.40}	7.86 ^{+0.25} _{-0.29}	2.81 ^{+0.17} _{-0.18}	1.01 ^{+0.42} _{-0.42}	I	0	1.65	121	92
AP2650	8.40 ^{+0.40} _{-0.00}	3.03 ^{+0.06} _{-0.07}	0.95 ^{+0.00} _{-0.70}	7.81 ^{+0.06} _{-0.08}	2.22 ^{+0.13} _{-0.11}	1.07 ^{+0.31} _{-0.20}	I	0	1.41	85	54
AP2651	9.10 ^{+0.00} _{-0.10}	3.39 ^{+0.16} _{-0.02}	0.00 ^{+0.50} _{-0.05}	8.65 ^{+0.15} _{-0.12}	3.02 ^{+0.12} _{-0.09}	0.89 ^{+0.23} _{-0.24}	I	0	1.70	133	87
AP2654	8.10 ^{+0.20} _{-0.10}	3.26 ^{+0.05} _{-0.03}	1.70 ^{+0.10} _{-0.10}	8.85 ^{+0.41} _{-0.40}	3.16 ^{+0.16} _{-0.14}	0.72 ^{+0.45} _{-0.50}	I	0	1.25	109	72
AP2655	7.00 ^{+0.10} _{-0.30}	2.97 ^{+0.00} _{-0.06}	0.95 ^{+0.05} _{-0.15}	6.71 ^{+0.04} _{-0.05}	2.37 ^{+0.58} _{-0.25}	0.83 ^{+0.13} _{-0.02}	I	0	2.30	365	328
AP2656	9.00 ^{+0.00} _{-0.00}	3.64 ^{+0.03} _{-0.01}	0.00 ^{+0.10} _{-0.00}	9.30 ^{+0.08} _{-0.08}	3.79 ^{+0.05} _{-0.04}	0.05 ^{+0.10} _{-0.05}	I	0	1.83	292	240
AP2658	8.40 ^{+0.50} _{-0.00}	3.21 ^{+0.08} _{-0.04}	1.10 ^{+0.00} _{-0.90}	9.58 ^{+0.41} _{-0.42}	3.49 ^{+0.26} _{-0.29}	0.20 ^{+0.19} _{-0.20}	I	0	1.27	106	83
AP2659	9.90 ^{+0.00} _{-0.30}	4.69 ^{+0.00} _{-0.26}	0.00 ^{+0.15} _{-0.00}	7.71 ^{+0.02} _{-0.05}	2.25 ^{+0.17} _{-0.14}	0.13 ^{+0.10} _{-0.10}	I	0	1.84	205	138
AP2660	7.80 ^{+0.10} _{-0.20}	3.05 ^{+0.01} _{-0.08}	0.90 ^{+0.00} _{-0.20}	7.81 ^{+0.14} _{-0.01}	2.93 ^{+0.13} _{-0.12}	0.63 ^{+0.14} _{-0.19}	I	0	1.19	118	71
AP2665	8.30 ^{+0.80} _{-0.00}	3.14 ^{+0.24} _{-0.27}	1.65 ^{+0.05} _{-1.40}	9.02 ^{+1.04} _{-0.46}	3.44 ^{+0.25} _{-0.17}	1.14 ^{+0.55} _{-0.97}	I	0	1.10	82	56
AP2666	7.20 ^{+0.30} _{-0.50}	3.01 ^{+0.07} _{-0.03}	1.30 ^{+0.20} _{-0.00}	6.99 ^{+0.14} _{-0.14}	3.04 ^{+0.26} _{-0.22}	1.00 ^{+0.10} _{-0.10}	I	0	1.24	87	56
AP2668	8.70 ^{+0.00} _{-0.50}	3.18 ^{+0.00} _{-0.15}	0.45 ^{+0.55} _{-0.05}	9.04 ^{+0.38} _{-0.39}	3.31 ^{+0.15} _{-0.16}	0.54 ^{+0.53} _{-0.47}	I	0	1.47	102	89
AP2670	8.80 ^{+0.00} _{-0.60}	2.73 ^{+0.02} _{-0.08}	0.10 ^{+0.85} _{-0.00}	8.56 ^{+0.12} _{-0.11}	2.31 ^{+0.16} _{-0.15}	0.40 ^{+0.22} _{-0.23}	I	0	1.15	36	19
AP2672	7.30 ^{+0.20} _{-0.50}	2.62 ^{+0.00} _{-0.07}	0.70 ^{+0.15} _{-0.10}	6.87 ^{+0.11} _{-0.11}	2.81 ^{+0.32} _{-0.37}	0.71 ^{+0.09} _{-0.09}	I	0	1.57	147	136

Table 1 (cont'd)

AP ID ^a	CMD Best Fit Parameters ^b			Integrated Best Fit Parameters ^c			Best ^d Flag ^e	Rap ^f	N _{stars} ^g	N _{bg} ^h	
	log(<i>t</i> [Myr])	log(<i>M</i> [<i>M</i> _⊙])	<i>A_V</i> [mag]	log(<i>t</i> [Myr])	log(<i>M</i> [<i>M</i> _⊙])	<i>A_V</i> [mag]					
AP2674	8.40 ^{+0.00} _{-0.10}	3.06 ^{+0.01} _{-0.05}	0.80 ^{+0.10} _{-0.10}	8.78 ^{+0.06} _{-0.06}	2.85 ^{+0.07} _{-0.07}	0.02 ^{+0.07} _{-0.02}	I	0	1.50	90	42
AP2675	8.30 ^{+0.20} _{-0.20}	2.84 ^{+0.01} _{-0.12}	0.80 ^{+0.10} _{-0.20}	7.93 ^{+0.17} _{-0.09}	3.00 ^{+0.14} _{-0.16}	1.32 ^{+0.23} _{-0.29}	I	0	1.10	79	59
AP2676	7.50 ^{+0.50} _{-0.40}	2.54 ^{+0.03} _{-0.08}	0.70 ^{+0.05} _{-0.30}	8.19 ^{+0.11} _{-0.11}	2.64 ^{+0.12} _{-0.13}	0.27 ^{+0.21} _{-0.21}	I	0	1.19	74	53
AP2677	8.20 ^{+0.00} _{-0.10}	2.83 ^{+0.07} _{-0.02}	0.35 ^{+0.20} _{-0.00}	8.21 ^{+0.11} _{-0.12}	2.76 ^{+0.18} _{-0.20}	0.47 ^{+0.31} _{-0.32}	I	0	0.96	53	33
AP2678	7.20 ^{+0.30} _{-0.50}	2.61 ^{+0.00} _{-0.05}	0.45 ^{+0.10} _{-0.05}	7.04 ^{+0.13} _{-0.12}	2.41 ^{+0.20} _{-0.16}	0.72 ^{+0.12} _{-0.12}	I	0	2.07	144	122
AP2681	8.60 ^{+0.00} _{-0.50}	3.48 ^{+0.07} _{-0.03}	0.55 ^{+0.80} _{-0.10}	6.81 ^{+0.81} _{-0.55}	3.40 ^{+0.40} _{-0.37}	1.82 ^{+0.44} _{-0.45}	I	0	1.85	224	165
AP2682	9.10 ^{+0.00} _{-0.00}	3.57 ^{+0.09} _{-0.07}	0.25 ^{+0.20} _{-0.00}	9.20 ^{+0.77} _{-0.71}	4.27 ^{+0.20} _{-0.15}	1.76 ^{+0.85} _{-0.75}	I	0	1.54	119	60
AP2683	10.00 ^{+0.40} _{-2.90}	4.42 ^{+4.42} _{-4.42}	0.25 ^{+2.30} _{-0.20}	10.13 ^{+0.07} _{-0.08}	5.22 ^{+0.05} _{-0.05}	0.07 ^{+0.13} _{-0.07}	I	0	1.60	238	294
AP2684	8.30 ^{+0.20} _{-0.10}	2.83 ^{+0.11} _{-0.18}	0.65 ^{+0.05} _{-0.25}	8.11 ^{+1.47} _{-1.46}	3.78 ^{+1.25} _{-1.18}	1.45 ^{+1.02} _{-1.02}	I	0	1.45	149	138
AP2687	8.90 ^{+0.10} _{-0.10}	3.53 ^{+0.09} _{-0.10}	0.40 ^{+0.50} _{-0.10}	8.05 ^{+0.14} _{-0.15}	3.24 ^{+0.12} _{-0.12}	0.30 ^{+0.23} _{-0.23}	I	0	2.65	591	620
AP2690	8.00 ^{+0.00} _{-0.40}	3.34 ^{+0.02} _{-0.21}	1.85 ^{+0.20} _{-0.20}	8.26 ^{+0.21} _{-0.23}	2.88 ^{+0.19} _{-0.18}	0.56 ^{+0.37} _{-0.38}	I	0	1.32	151	129
AP2691	9.20 ^{+0.10} _{-1.20}	3.45 ^{+0.15} _{-1.73}	0.10 ^{+1.45} _{-0.05}	8.87 ^{+0.23} _{-0.22}	2.83 ^{+0.17} _{-0.16}	0.32 ^{+0.27} _{-0.27}	I	0	1.43	86	55
AP2692	9.20 ^{+0.30} _{-0.10}	3.51 ^{+0.36} _{-0.17}	0.15 ^{+0.35} _{-0.05}	9.92 ^{+0.28} _{-0.08}	3.87 ^{+0.23} _{-0.03}	0.02 ^{+0.07} _{-0.02}	I	0	1.60	82	29
AP2694	9.10 ^{+0.00} _{-1.00}	3.89 ^{+0.00} _{-0.73}	0.35 ^{+0.50} _{-0.05}	6.78 ^{+0.04} _{-0.05}	2.95 ^{+0.13} _{-0.14}	1.89 ^{+0.09} _{-0.06}	I	0	2.38	429	389
AP2697	8.00 ^{+0.30} _{-0.20}	3.09 ^{+0.02} _{-0.07}	1.05 ^{+0.05} _{-0.25}	7.43 ^{+0.26} _{-0.26}	3.41 ^{+0.09} _{-0.09}	1.94 ^{+0.31} _{-0.30}	I	0	1.64	174	144
AP2698	8.90 ^{+0.00} _{-0.10}	3.49 ^{+0.01} _{-0.15}	0.50 ^{+0.10} _{-0.15}	8.18 ^{+0.83} _{-0.56}	3.17 ^{+0.23} _{-0.20}	1.31 ^{+0.92} _{-1.19}	I	0	1.45	105	69
AP2702	8.80 ^{+0.00} _{-0.30}	3.11 ^{+0.02} _{-0.08}	0.30 ^{+0.70} _{-0.00}	8.68 ^{+0.33} _{-0.32}	2.84 ^{+0.20} _{-0.19}	0.59 ^{+0.47} _{-0.43}	I	0	1.02	61	45
AP2707	10.00 ^{+0.00} _{-0.40}	4.74 ^{+0.03} _{-0.26}	0.00 ^{+0.20} _{-0.00}	7.75 ^{+0.10} _{-0.10}	3.29 ^{+0.10} _{-0.11}	1.82 ^{+0.20} _{-0.19}	I	0	1.71	175	131
AP2709	6.70 ^{+0.70} _{-0.10}	2.50 ^{+0.01} _{-0.04}	0.75 ^{+0.05} _{-0.10}	6.81 ^{+0.29} _{-0.35}	2.62 ^{+0.26} _{-0.29}	0.63 ^{+0.14} _{-0.14}	I	0	1.46	121	117
AP2710	9.70 ^{+0.00} _{-0.00}	5.56 ^{+0.00} _{-0.00}	0.00 ^{+0.00} _{-0.00}	0.00 ^{+0.00} _{-0.00}	0.00 ^{+0.00} _{-0.00}	0.00 ^{+0.00} _{-0.00}	I	0	3.16	708	721
AP2716	9.60 ^{+0.10} _{-0.70}	3.88 ^{+0.03} _{-0.65}	0.35 ^{+0.65} _{-0.15}	7.75 ^{+0.25} _{-0.30}	3.16 ^{+0.10} _{-0.09}	2.00 ^{+0.29} _{-0.14}	I	0	1.43	94	48
AP2719	8.70 ^{+0.10} _{-0.10}	3.02 ^{+0.04} _{-0.18}	0.45 ^{+0.15} _{-0.20}	8.48 ^{+0.14} _{-0.13}	2.41 ^{+0.18} _{-0.18}	0.34 ^{+0.28} _{-0.27}	I	0	1.22	91	65
AP2720	9.50 ^{+0.10} _{-2.40}	4.51 ^{+3.23} _{-4.51}	0.00 ^{+2.50} _{-0.40}	8.97 ^{+0.35} _{-0.29}	3.90 ^{+0.08} _{-0.08}	0.99 ^{+0.50} _{-0.54}	I	0	1.17	160	159
AP2721	8.40 ^{+0.30} _{-0.20}	3.21 ^{+0.07} _{-0.07}	1.20 ^{+0.15} _{-0.30}	9.41 ^{+0.54} _{-0.52}	3.55 ^{+0.25} _{-0.22}	0.45 ^{+0.47} _{-0.39}	I	0	1.15	101	77
AP2722	8.10 ^{+0.20} _{-0.10}	3.27 ^{+0.05} _{-0.07}	1.60 ^{+0.05} _{-0.15}	9.05 ^{+0.55} _{-0.37}	3.40 ^{+0.16} _{-0.15}	0.72 ^{+0.46} _{-0.60}	I	0	1.25	121	93
AP2723	7.60 ^{+0.10} _{-0.40}	3.04 ^{+0.01} _{-0.04}	0.75 ^{+0.10} _{-0.05}	7.87 ^{+0.12} _{-0.12}	2.88 ^{+0.11} _{-0.11}	0.24 ^{+0.17} _{-0.16}	I	0	1.56	153	128
AP2725	8.10 ^{+0.00} _{-1.10}	2.76 ^{+0.00} _{-0.11}	0.55 ^{+0.35} _{-0.00}	8.21 ^{+0.15} _{-0.15}	3.34 ^{+0.16} _{-0.17}	0.83 ^{+0.35} _{-0.36}	I	0	1.40	174	142
AP2727	8.40 ^{+0.10} _{-0.00}	2.81 ^{+0.02} _{-0.02}	0.50 ^{+0.05} _{-0.10}	8.52 ^{+0.14} _{-0.16}	2.61 ^{+0.14} _{-0.14}	0.21 ^{+0.27} _{-0.21}	I	0	1.18	40	14
AP2728	8.30 ^{+0.10} _{-1.20}	2.88 ^{+0.01} _{-0.11}	0.60 ^{+0.45} _{-0.05}	7.77 ^{+0.09} _{-0.09}	3.27 ^{+0.11} _{-0.11}	1.35 ^{+0.19} _{-0.19}	I	0	1.28	100	77
AP2729	8.20 ^{+0.20} _{-0.90}	2.46 ^{+0.01} _{-0.14}	0.65 ^{+0.20} _{-0.15}	8.21 ^{+0.23} _{-0.19}	2.39 ^{+0.14} _{-0.14}	0.52 ^{+0.33} _{-0.37}	I	0	1.19	40	24
AP2730	9.90 ^{+0.10} _{-0.10}	4.75 ^{+0.06} _{-0.07}	0.15 ^{+0.05} _{-0.10}	10.04 ^{+0.19} _{-0.17}	4.25 ^{+0.10} _{-0.10}	0.82 ^{+0.23} _{-0.22}	I	0	1.27	93	78
AP2731	9.10 ^{+0.00} _{-0.10}	3.84 ^{+0.00} _{-0.28}	0.25 ^{+0.25} _{-0.00}	9.02 ^{+0.69} _{-0.86}	4.31 ^{+0.15} _{-0.13}	1.65 ^{+0.97} _{-0.74}	I	0	1.88	228	165
AP2732	7.00 ^{+2.40} _{-0.00}	3.00 ^{+0.01} _{-3.00}	3.00 ^{+0.05} _{-2.45}	6.67 ^{+0.12} _{-0.13}	3.19 ^{+0.31} _{-0.30}	2.77 ^{+0.09} _{-0.08}	I	0	1.33	101	81

Table 1 (cont'd)

AP ID ^a	CMD Best Fit Parameters ^b			Integrated Best Fit Parameters ^c			Best ^d Flag ^e	R _{ap} ^f	N _{stars} ^g	N _{bg} ^h	
	log(<i>t</i> [Myr])	log(<i>M</i> [<i>M</i> _⊙])	<i>A_V</i> [mag]	log(<i>t</i> [Myr])	log(<i>M</i> [<i>M</i> _⊙])	<i>A_V</i> [mag]					
AP2734	8.50 ^{+0.20} _{-0.00}	3.04 ^{+0.04} _{-0.02}	0.75 ^{+0.05} _{-0.25}	8.44 ^{+0.12} _{-0.13}	2.47 ^{+0.24} _{-0.23}	0.42 ^{+0.31} _{-0.32}	I	0	1.19	71	38
AP2737	8.20 ^{+0.00} _{-0.00}	3.32 ^{+0.01} _{-0.03}	0.95 ^{+0.05} _{-0.05}	8.10 ^{+0.13} _{-0.15}	3.47 ^{+0.16} _{-0.15}	1.40 ^{+0.35} _{-0.30}	I	0	1.44	143	100
AP2738	8.90 ^{+0.00} _{-0.90}	3.26 ^{+0.04} _{-0.44}	0.40 ^{+0.95} _{-0.05}	7.91 ^{+0.05} _{-0.12}	2.43 ^{+0.10} _{-0.12}	0.84 ^{+0.13} _{-0.13}	I	0	1.10	52	26
AP2739	7.90 ^{+0.00} _{-0.50}	2.87 ^{+0.01} _{-0.04}	0.90 ^{+0.20} _{-0.00}	7.48 ^{+0.22} _{-0.21}	3.11 ^{+0.08} _{-0.08}	1.43 ^{+0.24} _{-0.23}	I	0	1.03	56	32
AP2741	8.40 ^{+0.10} _{-0.00}	3.12 ^{+0.04} _{-0.05}	0.50 ^{+0.10} _{-0.10}	8.71 ^{+0.12} _{-0.12}	2.74 ^{+0.12} _{-0.10}	0.09 ^{+0.12} _{-0.09}	I	0	1.66	167	167
AP2742	8.20 ^{+0.20} _{-1.10}	2.82 ^{+0.01} _{-0.23}	0.75 ^{+0.10} _{-0.15}	9.21 ^{+0.05} _{-0.06}	3.07 ^{+0.10} _{-0.07}	0.02 ^{+0.06} _{-0.02}	I	0	1.54	99	78
AP2745	7.70 ^{+0.10} _{-0.50}	2.86 ^{+0.01} _{-0.04}	0.40 ^{+0.15} _{-0.00}	7.60 ^{+0.26} _{-0.23}	3.35 ^{+0.10} _{-0.09}	1.02 ^{+0.29} _{-0.29}	I	0	1.66	181	153
AP2746	7.90 ^{+0.70} _{-0.00}	2.99 ^{+0.01} _{-0.11}	1.15 ^{+0.00} _{-0.85}	8.14 ^{+0.15} _{-0.16}	3.40 ^{+0.16} _{-0.15}	1.20 ^{+0.39} _{-0.36}	I	0	1.32	114	81
AP2747	8.00 ^{+0.30} _{-0.30}	2.88 ^{+0.07} _{-0.09}	0.70 ^{+0.20} _{-0.15}	8.62 ^{+0.07} _{-0.07}	2.75 ^{+0.09} _{-0.10}	0.05 ^{+0.10} _{-0.05}	I	0	1.24	93	57
AP2748	9.50 ^{+0.00} _{-1.70}	4.21 ^{+0.00} _{-0.67}	0.00 ^{+2.60} _{-0.00}	9.36 ^{+0.08} _{-0.09}	3.48 ^{+0.10} _{-0.10}	0.10 ^{+0.13} _{-0.10}	I	0	1.17	108	88
AP2749	9.30 ^{+0.00} _{-1.60}	4.15 ^{+0.19} _{-1.65}	0.45 ^{+1.80} _{-0.05}	8.97 ^{+0.28} _{-0.30}	3.84 ^{+0.13} _{-0.13}	1.39 ^{+0.30} _{-0.31}	I	0	1.42	197	165
AP2753	8.30 ^{+0.00} _{-0.10}	3.31 ^{+0.00} _{-0.06}	1.45 ^{+0.10} _{-0.05}	8.62 ^{+0.16} _{-0.16}	2.63 ^{+0.15} _{-0.16}	0.35 ^{+0.29} _{-0.28}	I	0	1.15	83	58
AP2755	8.10 ^{+0.10} _{-1.00}	2.60 ^{+0.01} _{-0.13}	0.50 ^{+0.10} _{-0.05}	7.09 ^{+0.56} _{-0.66}	2.71 ^{+0.14} _{-0.16}	1.43 ^{+0.32} _{-0.32}	I	0	1.16	44	29
AP2756	8.30 ^{+0.10} _{-0.70}	2.95 ^{+0.02} _{-0.12}	0.80 ^{+0.30} _{-0.05}	8.49 ^{+0.17} _{-0.17}	2.83 ^{+0.17} _{-0.15}	0.53 ^{+0.38} _{-0.37}	I	0	1.31	92	61
AP2758	8.50 ^{+0.00} _{-1.20}	2.37 ^{+0.00} _{-0.22}	0.40 ^{+0.35} _{-0.00}	8.85 ^{+1.10} _{-1.26}	2.81 ^{+0.61} _{-0.61}	1.78 ^{+0.87} _{-0.95}	I	0	1.20	35	26
AP2762	8.70 ^{+0.00} _{-1.10}	2.99 ^{+0.04} _{-0.29}	0.30 ^{+0.85} _{-0.05}	7.59 ^{+0.17} _{-0.19}	3.77 ^{+0.18} _{-0.18}	2.08 ^{+0.35} _{-0.32}	I	0	1.79	244	232
AP2766	8.40 ^{+0.10} _{-0.00}	2.88 ^{+0.04} _{-0.04}	0.30 ^{+0.10} _{-0.10}	10.25 ^{+0.00} _{-0.03}	3.91 ^{+0.03} _{-0.04}	0.00 ^{+0.07} _{-0.00}	I	0	1.22	103	100
AP2769	6.70 ^{+0.10} _{-0.10}	2.90 ^{+0.01} _{-0.01}	0.70 ^{+0.05} _{-0.05}	6.68 ^{+0.07} _{-0.07}	2.69 ^{+0.31} _{-0.36}	0.59 ^{+0.09} _{-0.09}	I	0	1.58	173	157
AP2771	6.70 ^{+1.50} _{-0.00}	2.55 ^{+0.09} _{-0.04}	0.70 ^{+0.00} _{-0.25}	0.00 ^{+0.00} _{-0.00}	0.00 ^{+0.00} _{-0.00}	0.00 ^{+0.00} _{-0.00}	I	0	1.80	154	164
AP2772	8.60 ^{+0.00} _{-0.10}	2.78 ^{+0.02} _{-0.02}	0.10 ^{+0.20} _{-0.05}	6.97 ^{+0.41} _{-0.40}	3.08 ^{+0.15} _{-0.12}	2.50 ^{+0.30} _{-0.30}	I	0	1.11	55	46
AP2777	8.50 ^{+0.07} _{-0.60}	3.12 ^{+0.05} _{-0.13}	0.65 ^{+0.40} _{-0.05}	8.39 ^{+0.18} _{-0.18}	2.93 ^{+0.18} _{-0.18}	0.74 ^{+0.34} _{-0.33}	I	0	1.23	103	59
AP2778	9.40 ^{+0.00} _{-0.30}	4.18 ^{+0.00} _{-0.63}	0.00 ^{+0.20} _{-0.00}	8.62 ^{+0.61} _{-0.68}	3.52 ^{+0.17} _{-0.14}	0.76 ^{+0.91} _{-0.74}	I	0	1.38	132	91
AP2779	8.80 ^{+0.00} _{-0.20}	3.34 ^{+0.05} _{-0.03}	0.15 ^{+0.40} _{-0.05}	7.79 ^{+0.73} _{-0.73}	3.11 ^{+0.31} _{-0.27}	1.57 ^{+1.04} _{-1.04}	I	0	1.41	142	111
AP2782	7.40 ^{+0.00} _{-0.60}	2.67 ^{+0.01} _{-0.05}	0.95 ^{+0.20} _{-0.05}	7.20 ^{+0.41} _{-0.47}	2.97 ^{+0.10} _{-0.10}	0.95 ^{+0.22} _{-0.22}	I	0	1.32	105	94
AP2783	9.10 ^{+0.00} _{-0.00}	3.98 ^{+0.07} _{-0.02}	0.25 ^{+0.15} _{-0.00}	9.44 ^{+0.16} _{-0.16}	3.90 ^{+0.11} _{-0.11}	0.17 ^{+0.19} _{-0.17}	I	0	2.42	363	261
AP2786	9.10 ^{+0.00} _{-0.10}	3.59 ^{+0.08} _{-0.08}	0.25 ^{+0.25} _{-0.00}	9.08 ^{+0.54} _{-0.69}	3.38 ^{+0.18} _{-0.17}	0.84 ^{+0.76} _{-0.60}	I	0	1.26	95	54
AP2790	8.90 ^{+0.10} _{-0.20}	3.54 ^{+0.23} _{-0.11}	0.70 ^{+0.85} _{-0.10}	8.58 ^{+0.14} _{-0.14}	2.42 ^{+0.16} _{-0.16}	0.25 ^{+0.23} _{-0.22}	I	0	1.16	91	59
AP2791	8.90 ^{+0.00} _{-0.10}	3.13 ^{+0.02} _{-0.11}	0.05 ^{+0.30} _{-0.05}	8.93 ^{+0.12} _{-0.09}	2.83 ^{+0.13} _{-0.11}	0.03 ^{+0.07} _{-0.03}	I	0	1.35	105	75
AP2793	6.60 ^{+0.40} _{-0.00}	2.60 ^{+0.00} _{-0.05}	0.90 ^{+0.00} _{-0.15}	7.56 ^{+0.18} _{-0.17}	3.04 ^{+0.08} _{-0.08}	0.15 ^{+0.15} _{-0.14}	I	0	1.62	150	139
AP2795	8.00 ^{+0.20} _{-0.20}	3.13 ^{+0.02} _{-0.12}	1.65 ^{+0.10} _{-0.35}	7.38 ^{+0.52} _{-0.76}	3.39 ^{+0.37} _{-0.34}	2.20 ^{+0.64} _{-0.64}	I	0	1.25	115	97
AP2798	6.70 ^{+0.10} _{-0.10}	2.60 ^{+0.02} _{-0.07}	0.40 ^{+0.05} _{-0.05}	6.84 ^{+0.07} _{-0.07}	2.72 ^{+0.25} _{-0.22}	0.11 ^{+0.09} _{-0.09}	I	0	1.96	237	216
AP2800	7.80 ^{+0.20} _{-0.30}	3.83 ^{+0.11} _{-0.01}	2.15 ^{+0.30} _{-0.10}	8.43 ^{+0.44} _{-0.26}	3.59 ^{+0.13} _{-0.15}	0.89 ^{+0.48} _{-0.75}	I	0	1.72	237	159
AP2801	9.10 ^{+0.00} _{-0.00}	3.46 ^{+0.06} _{-0.00}	0.05 ^{+0.15} _{-0.00}	8.64 ^{+0.13} _{-0.13}	2.67 ^{+0.12} _{-0.13}	0.21 ^{+0.22} _{-0.20}	I	0	1.82	144	88

Table 1 (cont'd)

AP ID ^a	CMD Best Fit Parameters ^b			Integrated Best Fit Parameters ^c			Best ^d Flag ^e	Rap ^f	N _{stars} ^g	N _{bg} ^h	
	log(<i>t</i> [Myr])	log(<i>M</i> [<i>M</i> _⊙])	<i>A_V</i> [mag]	log(<i>t</i> [Myr])	log(<i>M</i> [<i>M</i> _⊙])	<i>A_V</i> [mag]					
AP2803	9.10 ^{+0.20} _{-0.00}	3.90 ^{+0.26} _{-0.00}	0.50 ^{+0.20} _{-0.05}	8.95 ^{+0.61} _{-0.60}	3.40 ^{+0.18} _{-0.17}	0.87 ^{+0.70} _{-0.70}	I	0	1.43	165	126
AP2804	8.60 ^{+0.00} _{-0.60}	2.91 ^{+0.01} _{-0.18}	0.40 ^{+0.40} _{-0.10}	8.54 ^{+0.10} _{-0.09}	2.39 ^{+0.15} _{-0.15}	0.11 ^{+0.14} _{-0.11}	I	0	1.06	104	98
AP2805	6.70 ^{+1.20} _{-0.00}	2.99 ^{+0.15} _{-0.04}	1.70 ^{+0.10} _{-0.10}	7.35 ^{+0.04} _{-0.04}	3.61 ^{+0.06} _{-0.06}	1.42 ^{+0.13} _{-0.14}	I	0	1.27	109	89
AP2806	8.50 ^{+0.00} _{-0.70}	2.92 ^{+0.00} _{-0.19}	0.55 ^{+0.30} _{-0.00}	9.25 ^{+0.12} _{-0.12}	3.17 ^{+0.13} _{-0.14}	0.09 ^{+0.11} _{-0.09}	I	0	1.42	75	49
AP2807	7.80 ^{+0.10} _{-0.90}	2.49 ^{+0.00} _{-0.08}	0.75 ^{+0.15} _{-0.05}	7.44 ^{+0.52} _{-0.58}	2.65 ^{+0.16} _{-0.17}	0.73 ^{+0.40} _{-0.41}	I	0	1.21	96	76
AP2810	7.30 ^{+0.00} _{-0.40}	2.76 ^{+0.02} _{-0.01}	0.40 ^{+0.10} _{-0.00}	6.66 ^{+0.16} _{-0.19}	2.49 ^{+0.21} _{-0.21}	0.52 ^{+0.10} _{-0.10}	I	0	1.97	238	212
AP2811	8.90 ^{+0.10} _{-0.10}	3.42 ^{+0.07} _{-0.04}	0.15 ^{+0.35} _{-0.10}	8.28 ^{+0.74} _{-0.46}	2.64 ^{+0.58} _{-0.49}	0.21 ^{+0.15} _{-0.20}	I	0	2.09	227	163
AP2812	8.10 ^{+0.10} _{-0.10}	3.82 ^{+0.00} _{-0.12}	1.25 ^{+0.05} _{-0.15}	8.20 ^{+0.08} _{-0.08}	3.65 ^{+0.08} _{-0.08}	0.64 ^{+0.19} _{-0.18}	I	0	1.67	229	174
AP2813	8.70 ^{+0.10} _{-0.10}	3.36 ^{+0.03} _{-0.10}	0.35 ^{+0.05} _{-0.25}	8.90 ^{+0.05} _{-0.05}	3.02 ^{+0.06} _{-0.06}	0.02 ^{+0.07} _{-0.02}	I	0	1.01	74	41
AP2815	7.80 ^{+0.10} _{-0.00}	3.45 ^{+0.05} _{-0.14}	2.45 ^{+0.10} _{-0.20}	7.14 ^{+0.43} _{-0.42}	3.26 ^{+0.17} _{-0.15}	2.29 ^{+0.30} _{-0.30}	I	0	1.36	121	103
AP2816	7.30 ^{+0.10} _{-0.40}	2.89 ^{+0.00} _{-0.03}	0.60 ^{+0.10} _{-0.05}	6.95 ^{+0.52} _{-0.57}	2.88 ^{+0.23} _{-0.27}	0.44 ^{+0.24} _{-0.26}	I	0	1.65	191	167
AP2818	9.10 ^{+0.00} _{-0.00}	3.43 ^{+0.06} _{-0.08}	0.20 ^{+0.15} _{-0.10}	9.08 ^{+0.74} _{-0.62}	3.45 ^{+0.21} _{-0.19}	1.07 ^{+0.78} _{-0.78}	I	0	1.45	118	85
AP2819	8.90 ^{+0.00} _{-0.20}	3.15 ^{+0.03} _{-0.06}	0.00 ^{+0.50} _{-0.05}	8.76 ^{+0.27} _{-0.30}	2.95 ^{+0.14} _{-0.16}	0.37 ^{+0.36} _{-0.33}	I	0	1.73	124	71
AP2820	8.50 ^{+0.00} _{-0.10}	3.04 ^{+0.09} _{-0.01}	0.75 ^{+0.35} _{-0.05}	8.06 ^{+0.08} _{-0.10}	2.99 ^{+0.13} _{-0.11}	1.28 ^{+0.22} _{-0.21}	I	0	1.12	63	30
AP2821	8.10 ^{+0.30} _{-0.30}	3.36 ^{+0.00} _{-0.26}	1.70 ^{+0.10} _{-0.55}	8.66 ^{+0.42} _{-0.41}	3.22 ^{+0.21} _{-0.19}	0.54 ^{+0.58} _{-0.49}	I	0	1.46	181	138
AP2822	8.20 ^{+0.00} _{-0.20}	3.38 ^{+0.00} _{-0.06}	1.25 ^{+0.10} _{-0.05}	8.27 ^{+0.16} _{-0.14}	3.07 ^{+0.16} _{-0.18}	0.79 ^{+0.37} _{-0.43}	I	0	1.46	108	40
AP2823	8.30 ^{+0.10} _{-0.70}	3.16 ^{+0.05} _{-0.21}	1.45 ^{+0.30} _{-0.00}	8.79 ^{+0.47} _{-0.50}	3.20 ^{+0.24} _{-0.21}	0.77 ^{+0.67} _{-0.58}	I	0	1.22	99	79
AP2825	6.60 ^{+0.60} _{-0.00}	2.80 ^{+0.01} _{-0.05}	1.25 ^{+0.00} _{-0.20}	6.64 ^{+0.21} _{-0.25}	2.52 ^{+0.27} _{-0.23}	0.78 ^{+0.13} _{-0.14}	I	0	1.50	103	89
AP2826	8.50 ^{+0.20} _{-0.10}	3.13 ^{+0.03} _{-0.14}	0.95 ^{+0.00} _{-0.50}	8.40 ^{+0.03} _{-0.03}	2.00 ^{+0.03} _{-0.00}	0.00 ^{+0.07} _{-0.00}	I	0	1.15	56	39
AP2828	8.60 ^{+0.10} _{-0.30}	2.96 ^{+0.08} _{-0.14}	0.30 ^{+0.35} _{-0.15}	9.23 ^{+0.06} _{-0.06}	3.25 ^{+0.07} _{-0.08}	0.00 ^{+0.07} _{-0.00}	I	0	1.21	107	92
AP2829	9.50 ^{+0.20} _{-1.60}	4.12 ^{+0.14} _{-4.12}	0.00 ^{+2.55} _{-0.00}	8.70 ^{+0.22} _{-0.23}	3.15 ^{+0.16} _{-0.15}	0.57 ^{+0.32} _{-0.34}	I	0	1.43	163	130
AP2830	9.00 ^{+0.00} _{-0.70}	3.48 ^{+0.10} _{-0.15}	0.15 ^{+1.50} _{-0.10}	8.59 ^{+0.24} _{-0.23}	2.92 ^{+0.15} _{-0.17}	0.44 ^{+0.34} _{-0.35}	I	0	1.43	130	97
AP2831	8.00 ^{+0.00} _{-0.10}	2.98 ^{+0.04} _{-0.02}	0.80 ^{+0.05} _{-0.05}	8.16 ^{+0.07} _{-0.06}	3.44 ^{+0.10} _{-0.08}	0.92 ^{+0.18} _{-0.16}	I	0	1.10	50	15
AP2832	8.00 ^{+0.10} _{-0.00}	3.59 ^{+0.03} _{-0.05}	1.85 ^{+0.15} _{-0.05}	9.12 ^{+0.82} _{-0.76}	3.78 ^{+0.26} _{-0.20}	1.49 ^{+0.89} _{-0.86}	I	0	1.25	139	89
AP2833	9.10 ^{+0.00} _{-0.00}	3.62 ^{+0.04} _{-0.08}	0.15 ^{+0.15} _{-0.05}	8.54 ^{+0.19} _{-0.18}	2.59 ^{+0.18} _{-0.18}	0.34 ^{+0.31} _{-0.29}	I	0	1.40	120	90
AP2834	8.90 ^{+0.10} _{-0.00}	3.26 ^{+0.04} _{-0.11}	0.55 ^{+0.10} _{-0.40}	8.09 ^{+0.32} _{-0.36}	2.80 ^{+0.32} _{-0.43}	1.27 ^{+0.84} _{-0.83}	I	0	1.00	63	41
AP2835	8.40 ^{+0.30} _{-0.10}	3.22 ^{+0.03} _{-0.05}	1.20 ^{+0.05} _{-0.50}	9.11 ^{+0.19} _{-0.10}	3.30 ^{+0.13} _{-0.14}	0.19 ^{+0.10} _{-0.19}	I	0	1.93	120	56
AP2839	8.30 ^{+0.20} _{-0.10}	3.12 ^{+0.01} _{-0.11}	0.85 ^{+0.10} _{-0.35}	8.75 ^{+0.13} _{-0.12}	3.15 ^{+0.10} _{-0.10}	0.09 ^{+0.12} _{-0.09}	I	0	1.73	154	114
AP2841	8.30 ^{+0.00} _{-1.00}	3.33 ^{+0.02} _{-0.26}	1.15 ^{+0.25} _{-0.00}	8.39 ^{+0.17} _{-0.20}	2.89 ^{+0.15} _{-0.14}	0.34 ^{+0.41} _{-0.33}	I	0	1.08	100	80
AP2843	9.40 ^{+0.50} _{-0.00}	4.11 ^{+0.33} _{-0.01}	0.25 ^{+0.00} _{-0.20}	7.82 ^{+0.03} _{-0.19}	2.40 ^{+0.09} _{-0.40}	0.41 ^{+0.25} _{-0.32}	I	0	1.54	118	57
AP2845	8.10 ^{+0.00} _{-0.60}	2.72 ^{+0.01} _{-0.12}	0.35 ^{+0.20} _{-0.05}	7.55 ^{+0.27} _{-0.27}	3.08 ^{+0.09} _{-0.08}	1.58 ^{+0.27} _{-0.26}	I	0	1.35	100	78
AP2848	8.40 ^{+0.40} _{-0.90}	3.79 ^{+0.03} _{-0.91}	2.60 ^{+0.15} _{-1.30}	6.80 ^{+0.07} _{-0.08}	3.04 ^{+0.16} _{-0.08}	1.31 ^{+0.07} _{-0.08}	I	0	1.32	126	69
AP2849	8.90 ^{+1.00} _{-0.10}	5.57 ^{+0.14} _{-1.83}	2.60 ^{+0.30} _{-1.30}	8.84 ^{+0.47} _{-0.47}	3.22 ^{+0.17} _{-0.17}	0.77 ^{+0.56} _{-0.62}	I	0	1.33	103	75

Table 1 (cont'd)

AP ID ^a	CMD Best Fit Parameters ^b			Integrated Best Fit Parameters ^c			Best ^d Flag ^e	R _{ap} ^f	N _{stars} ^g	N _{bg} ^h	
	log(<i>t</i> [Myr])	log(<i>M</i> [<i>M</i> _⊙])	<i>A_V</i> [mag]	log(<i>t</i> [Myr])	log(<i>M</i> [<i>M</i> _⊙])	<i>A_V</i> [mag]					
AP2850	7.30 ^{+0.00} _{-0.20}	3.92 ^{+0.03} _{-0.05}	2.60 ^{+0.10} _{-0.00}	7.71 ^{+1.20} _{-1.20}	4.43 ^{+0.46} _{-0.53}	1.25 ^{+0.60} _{-0.72}	I	1	1.55	236	283
AP2851	9.90 ^{+0.00} _{-0.60}	4.62 ^{+0.01} _{-0.44}	0.55 ^{+0.40} _{-0.00}	8.82 ^{+1.02} _{-1.04}	4.07 ^{+0.32} _{-0.30}	1.85 ^{+0.83} _{-0.81}	I	0	2.21	153	92
AP2852	8.80 ^{+0.30} _{-0.00}	4.46 ^{+0.26} _{-0.15}	2.05 ^{+0.15} _{-0.45}	8.71 ^{+0.22} _{-0.25}	3.77 ^{+0.12} _{-0.12}	2.04 ^{+0.29} _{-0.29}	I	0	1.47	103	76
AP2853	8.30 ^{+0.00} _{-0.80}	2.75 ^{+0.02} _{-0.11}	0.40 ^{+0.25} _{-0.05}	7.53 ^{+0.35} _{-0.32}	2.76 ^{+0.13} _{-0.12}	0.39 ^{+0.26} _{-0.27}	I	0	1.30	44	26
AP2855	9.10 ^{+0.10} _{-0.00}	3.91 ^{+0.04} _{-0.13}	0.40 ^{+0.00} _{-0.25}	9.34 ^{+0.16} _{-0.17}	3.36 ^{+0.13} _{-0.13}	0.43 ^{+0.29} _{-0.28}	I	0	1.48	128	97
AP2857	7.90 ^{+0.10} _{-1.00}	2.77 ^{+0.02} _{-0.13}	0.70 ^{+0.25} _{-0.10}	7.97 ^{+0.12} _{-0.11}	2.79 ^{+0.19} _{-0.19}	0.24 ^{+0.23} _{-0.21}	I	0	1.06	110	103
AP2858	8.90 ^{+0.00} _{-0.30}	2.63 ^{+0.05} _{-0.21}	0.10 ^{+0.55} _{-0.05}	8.20 ^{+0.24} _{-0.19}	2.27 ^{+0.16} _{-0.16}	0.46 ^{+0.36} _{-0.36}	I	0	1.12	32	11
AP2859	7.30 ^{+0.10} _{-0.20}	2.83 ^{+0.00} _{-0.02}	0.90 ^{+0.05} _{-0.05}	6.63 ^{+0.23} _{-0.25}	2.69 ^{+0.25} _{-0.25}	0.96 ^{+0.13} _{-0.13}	I	0	2.12	99	73
AP2860	7.80 ^{+1.20} _{-0.00}	3.77 ^{+0.07} _{-0.52}	2.80 ^{+0.10} _{-2.35}	8.66 ^{+0.15} _{-0.15}	2.86 ^{+0.13} _{-0.12}	0.37 ^{+0.25} _{-0.25}	I	0	1.32	121	53
AP2862	6.90 ^{+0.30} _{-0.20}	3.24 ^{+0.05} _{-0.10}	1.85 ^{+0.05} _{-0.40}	7.65 ^{+0.13} _{-0.10}	3.40 ^{+0.08} _{-0.08}	0.95 ^{+0.15} _{-0.17}	I	0	1.13	140	143
AP2863	8.80 ^{+0.10} _{-0.00}	2.91 ^{+0.03} _{-0.03}	0.40 ^{+0.10} _{-0.15}	7.28 ^{+0.80} _{-0.87}	2.22 ^{+0.17} _{-0.16}	0.46 ^{+0.36} _{-0.36}	I	0	1.47	61	26
AP2864	8.60 ^{+0.10} _{-0.10}	3.01 ^{+0.07} _{-0.03}	0.45 ^{+0.15} _{-0.30}	8.60 ^{+0.18} _{-0.18}	2.75 ^{+0.18} _{-0.18}	0.40 ^{+0.31} _{-0.30}	I	0	1.27	123	97
AP2865	9.00 ^{+0.10} _{-0.10}	4.07 ^{+0.06} _{-0.20}	1.40 ^{+0.20} _{-0.25}	9.20 ^{+0.74} _{-0.58}	3.88 ^{+0.26} _{-0.14}	1.95 ^{+0.73} _{-0.63}	I	0	1.13	63	45
AP2867	8.00 ^{+0.00} _{-0.30}	2.80 ^{+0.01} _{-0.05}	0.30 ^{+0.10} _{-0.00}	7.41 ^{+0.41} _{-0.42}	2.88 ^{+0.14} _{-0.13}	0.67 ^{+0.32} _{-0.33}	I	0	1.89	159	142
AP2868	7.50 ^{+0.30} _{-0.50}	2.90 ^{+0.01} _{-0.07}	0.90 ^{+0.10} _{-0.10}	8.54 ^{+0.08} _{-0.09}	3.79 ^{+0.05} _{-0.06}	0.09 ^{+0.14} _{-0.09}	I	0	2.01	230	205
AP2871	7.40 ^{+0.20} _{-0.50}	2.67 ^{+0.05} _{-0.06}	0.40 ^{+0.15} _{-0.05}	7.08 ^{+0.28} _{-0.24}	2.94 ^{+0.14} _{-0.13}	0.43 ^{+0.16} _{-0.16}	I	0	1.15	104	83
AP2875	8.20 ^{+0.10} _{-1.00}	2.70 ^{+0.01} _{-0.17}	0.45 ^{+0.30} _{-0.05}	8.38 ^{+0.12} _{-0.18}	2.55 ^{+0.18} _{-0.23}	0.02 ^{+0.07} _{-0.02}	I	0	1.32	117	55
AP2876	10.10 ^{+0.10} _{-0.50}	5.18 ^{+0.37} _{-0.71}	0.05 ^{+0.35} _{-0.00}	9.07 ^{+0.61} _{-0.48}	3.16 ^{+0.22} _{-0.18}	0.73 ^{+0.58} _{-0.61}	I	0	1.30	138	107
AP2880	9.10 ^{+0.00} _{-0.10}	3.15 ^{+0.05} _{-0.10}	0.05 ^{+0.30} _{-0.00}	9.26 ^{+0.36} _{-0.22}	3.27 ^{+0.20} _{-0.21}	0.45 ^{+0.29} _{-0.39}	I	0	1.41	69	46
AP2881	7.80 ^{+0.10} _{-0.70}	2.75 ^{+0.00} _{-0.10}	1.20 ^{+0.15} _{-0.05}	9.64 ^{+0.04} _{-0.03}	3.44 ^{+0.04} _{-0.03}	0.13 ^{+0.07} _{-0.08}	I	0	1.16	37	24
AP2884	8.30 ^{+0.00} _{-0.10}	3.41 ^{+0.02} _{-0.05}	1.65 ^{+0.10} _{-0.05}	7.81 ^{+0.06} _{-0.08}	2.20 ^{+0.05} _{-0.09}	1.35 ^{+0.32} _{-0.20}	I	0	1.00	60	37
AP2885	8.60 ^{+0.00} _{-0.40}	3.02 ^{+0.02} _{-0.14}	0.25 ^{+0.50} _{-0.05}	8.17 ^{+0.16} _{-0.17}	2.80 ^{+0.18} _{-0.15}	0.32 ^{+0.34} _{-0.30}	I	0	1.60	185	166
AP2887	9.00 ^{+0.10} _{-0.10}	3.56 ^{+0.07} _{-0.10}	0.40 ^{+0.35} _{-0.15}	9.38 ^{+0.15} _{-0.13}	3.67 ^{+0.12} _{-0.11}	0.21 ^{+0.19} _{-0.18}	I	0	1.54	148	100
AP2888	9.00 ^{+0.00} _{-0.20}	3.38 ^{+0.01} _{-0.25}	0.35 ^{+0.40} _{-0.10}	9.31 ^{+0.56} _{-0.50}	3.51 ^{+0.21} _{-0.18}	0.55 ^{+0.56} _{-0.50}	I	0	1.54	126	97
AP2889	8.50 ^{+0.10} _{-0.20}	3.03 ^{+0.02} _{-0.15}	0.70 ^{+0.15} _{-0.15}	7.21 ^{+0.72} _{-0.75}	3.05 ^{+0.26} _{-0.27}	2.13 ^{+0.63} _{-0.73}	I	0	1.13	66	40
AP2891	9.10 ^{+0.00} _{-0.00}	3.67 ^{+0.00} _{-0.06}	0.25 ^{+0.00} _{-0.15}	8.76 ^{+0.62} _{-0.55}	3.50 ^{+0.18} _{-0.18}	0.93 ^{+0.71} _{-0.76}	I	0	2.55	259	166
AP2893	6.60 ^{+0.80} _{-0.10}	2.66 ^{+0.03} _{-0.01}	0.75 ^{+0.00} _{-0.15}	6.86 ^{+0.41} _{-0.49}	2.54 ^{+0.22} _{-0.23}	0.45 ^{+0.19} _{-0.20}	I	0	1.33	135	124
AP2894	6.70 ^{+0.10} _{-0.10}	3.09 ^{+0.04} _{-0.01}	0.25 ^{+0.10} _{-0.00}	8.11 ^{+1.47} _{-1.46}	3.78 ^{+1.25} _{-1.18}	1.45 ^{+1.03} _{-1.02}	I	0	4.31	1354	1236
AP2898	8.90 ^{+0.00} _{-0.00}	3.42 ^{+0.02} _{-0.02}	0.40 ^{+0.10} _{-0.05}	8.71 ^{+0.20} _{-0.23}	3.02 ^{+0.13} _{-0.13}	0.84 ^{+0.36} _{-0.38}	I	0	1.35	73	34
AP2900	8.40 ^{+0.00} _{-0.60}	3.09 ^{+0.00} _{-0.12}	0.40 ^{+0.30} _{-0.00}	7.72 ^{+0.46} _{-0.47}	3.56 ^{+0.16} _{-0.17}	1.77 ^{+0.60} _{-0.64}	I	0	1.96	252	207
AP2901	7.70 ^{+0.40} _{-0.30}	3.16 ^{+0.05} _{-0.05}	1.60 ^{+0.20} _{-0.15}	8.76 ^{+0.08} _{-0.08}	2.90 ^{+0.09} _{-0.11}	0.02 ^{+0.07} _{-0.02}	I	0	1.28	128	109
AP2903	9.90 ^{+0.10} _{-2.65}	4.65 ^{+0.62} _{-4.65}	0.30 ^{+2.15} _{-0.05}	8.38 ^{+1.20} _{-1.48}	3.36 ^{+0.29} _{-0.31}	1.51 ^{+1.10} _{-1.12}	I	0	1.37	125	108
AP2906	7.90 ^{+0.10} _{-0.50}	2.70 ^{+0.01} _{-0.05}	0.70 ^{+0.20} _{-0.05}	9.19 ^{+0.11} _{-0.10}	3.37 ^{+0.12} _{-0.11}	0.02 ^{+0.07} _{-0.02}	I	0	1.59	143	119

Table 1 (cont'd)

AP ID ^a	CMD Best Fit Parameters ^b			Integrated Best Fit Parameters ^c			Best ^d Flag ^e	Rap ^f	N _{stars} ^g	N _{bg} ^h	
	log(<i>t</i> [Myr])	log(<i>M</i> [<i>M</i> _⊙])	<i>A_V</i> [mag]	log(<i>t</i> [Myr])	log(<i>M</i> [<i>M</i> _⊙])	<i>A_V</i> [mag]					
AP2907	8.00 ^{+0.00} _{-0.60}	2.78 ^{+0.00} _{-0.13}	0.50 ^{+0.15} _{-0.10}	7.83 ^{+0.07} _{-0.07}	3.19 ^{+0.14} _{-0.15}	0.33 ^{+0.14} _{-0.14}	I	0	1.20	102	67
AP2909	8.70 ^{+0.00} _{-0.10}	3.02 ^{+0.02} _{-0.05}	0.20 ^{+0.30} _{-0.05}	7.57 ^{+0.87} _{-0.95}	2.92 ^{+0.38} _{-0.43}	1.58 ^{+0.94} _{-1.03}	I	0	1.38	142	136
AP2911	8.80 ^{+0.00} _{-0.10}	3.01 ^{+0.06} _{-0.01}	0.05 ^{+0.45} _{-0.05}	8.92 ^{+0.20} _{-0.14}	2.91 ^{+0.14} _{-0.14}	0.15 ^{+0.08} _{-0.15}	I	0	1.30	72	46
AP2912	8.40 ^{+0.30} _{-0.10}	3.21 ^{+0.06} _{-0.07}	1.05 ^{+0.20} _{-0.45}	9.04 ^{+0.70} _{-0.38}	3.32 ^{+0.20} _{-0.18}	0.82 ^{+0.45} _{-0.68}	I	0	1.33	121	96
AP2914	9.10 ^{+0.00} _{-0.20}	3.52 ^{+0.03} _{-0.15}	0.30 ^{+0.40} _{-0.10}	9.14 ^{+0.57} _{-0.83}	3.22 ^{+0.22} _{-0.20}	1.02 ^{+0.89} _{-0.65}	I	0	1.24	93	62
AP2916	8.30 ^{+0.04} _{-0.10}	3.09 ^{+0.05} _{-0.03}	0.65 ^{+0.15} _{-0.00}	8.51 ^{+0.51} _{-0.54}	3.33 ^{+0.22} _{-0.22}	0.69 ^{+0.90} _{-0.67}	I	0	1.51	207	194
AP2919	8.80 ^{+0.00} _{-0.10}	3.32 ^{+0.03} _{-0.09}	0.25 ^{+0.30} _{-0.10}	8.93 ^{+0.10} _{-0.10}	3.37 ^{+0.12} _{-0.12}	0.72 ^{+0.24} _{-0.25}	I	0	1.45	169	137
AP2921	8.00 ^{+0.20} _{-1.00}	2.52 ^{+0.03} _{-0.35}	1.40 ^{+0.20} _{-0.60}	8.05 ^{+0.07} _{-0.07}	2.66 ^{+0.15} _{-0.16}	1.32 ^{+0.19} _{-0.21}	I	0	1.03	40	34
AP2922	7.20 ^{+0.00} _{-0.50}	2.76 ^{+0.01} _{-0.04}	0.60 ^{+0.10} _{-0.05}	6.85 ^{+0.20} _{-0.16}	2.84 ^{+0.26} _{-0.31}	0.41 ^{+0.14} _{-0.13}	I	0	2.00	274	247
AP2926	8.00 ^{+1.10} _{-0.70}	3.65 ^{+0.12} _{-1.73}	3.00 ^{+0.45} _{-2.55}	7.96 ^{+0.14} _{-0.17}	2.58 ^{+0.16} _{-0.18}	0.51 ^{+0.28} _{-0.27}	I	1	1.44	79	55
AP2927	9.20 ^{+0.30} _{-0.20}	4.33 ^{+0.01} _{-4.33}	0.25 ^{+1.60} _{-0.05}	0.00 ^{+0.00} _{-0.00}	0.00 ^{+0.00} _{-0.00}	0.00 ^{+0.00} _{-0.00}	I	0	2.44	79	561
AP2928	9.10 ^{+0.00} _{-0.00}	3.53 ^{+0.03} _{-0.04}	0.10 ^{+0.10} _{-0.00}	8.33 ^{+0.17} _{-0.17}	2.47 ^{+0.18} _{-0.17}	0.32 ^{+0.31} _{-0.28}	I	0	1.52	95	44
AP2932	6.80 ^{+0.20} _{-0.20}	2.71 ^{+0.01} _{-0.02}	0.70 ^{+0.05} _{-0.05}	7.64 ^{+0.08} _{-0.08}	2.80 ^{+0.10} _{-0.09}	0.13 ^{+0.11} _{-0.11}	I	0	1.14	134	121
AP2933	7.20 ^{+0.30} _{-0.40}	2.95 ^{+0.16} _{-0.04}	1.25 ^{+0.35} _{-0.00}	7.14 ^{+0.18} _{-0.16}	2.77 ^{+0.20} _{-0.22}	1.11 ^{+0.15} _{-0.15}	I	0	0.93	58	41
AP2934	9.00 ^{+0.00} _{-0.10}	3.28 ^{+0.02} _{-0.08}	0.00 ^{+0.25} _{-0.00}	7.71 ^{+0.15} _{-0.14}	3.04 ^{+0.07} _{-0.07}	1.26 ^{+0.14} _{-0.14}	I	0	1.40	91	71
AP2935	8.00 ^{+0.00} _{-0.60}	3.08 ^{+0.02} _{-0.10}	1.45 ^{+0.20} _{-0.05}	8.47 ^{+0.12} _{-0.12}	2.63 ^{+0.16} _{-0.17}	0.31 ^{+0.26} _{-0.25}	I	0	1.23	107	78
AP2936	8.80 ^{+0.00} _{-0.20}	3.16 ^{+0.04} _{-0.01}	0.05 ^{+0.50} _{-0.05}	8.44 ^{+0.10} _{-0.09}	2.53 ^{+0.17} _{-0.15}	0.20 ^{+0.19} _{-0.18}	I	0	1.49	123	109
AP2938	8.20 ^{+0.50} _{-0.00}	2.80 ^{+0.06} _{-0.06}	0.70 ^{+0.10} _{-0.45}	7.92 ^{+0.22} _{-0.27}	2.85 ^{+0.30} _{-0.35}	1.19 ^{+0.63} _{-0.63}	I	0	1.15	67	44
AP2943	9.10 ^{+0.00} _{-0.00}	3.94 ^{+0.03} _{-0.05}	0.25 ^{+0.10} _{-0.05}	8.87 ^{+0.39} _{-0.41}	3.89 ^{+0.12} _{-0.12}	0.85 ^{+0.46} _{-0.45}	I	0	1.81	241	184
AP2945	8.10 ^{+0.00} _{-1.10}	2.75 ^{+0.05} _{-0.19}	1.05 ^{+0.35} _{-0.05}	7.83 ^{+0.21} _{-0.19}	2.46 ^{+0.14} _{-0.14}	0.53 ^{+0.24} _{-0.22}	I	0	1.22	87	68
AP2947	8.90 ^{+0.00} _{-0.70}	3.40 ^{+0.01} _{-0.18}	0.60 ^{+1.40} _{-0.00}	0.00 ^{+0.00} _{-0.00}	0.00 ^{+0.00} _{-0.00}	0.00 ^{+0.00} _{-0.00}	I	0	1.71	122	71
AP2949	8.80 ^{+0.00} _{-0.80}	2.92 ^{+0.02} _{-0.18}	0.25 ^{+0.90} _{-0.10}	8.50 ^{+0.18} _{-0.18}	2.48 ^{+0.18} _{-0.18}	0.35 ^{+0.35} _{-0.31}	I	0	1.35	74	40
AP2952	9.10 ^{+0.80} _{-0.00}	3.38 ^{+0.71} _{-0.02}	0.70 ^{+0.00} _{-0.50}	8.44 ^{+1.10} _{-0.70}	3.58 ^{+0.26} _{-0.26}	1.69 ^{+0.84} _{-1.05}	I	0	1.63	70	38
AP2953	9.70 ^{+0.10} _{-0.30}	4.73 ^{+0.07} _{-0.19}	0.25 ^{+0.20} _{-0.10}	8.98 ^{+0.98} _{-0.41}	3.71 ^{+0.23} _{-0.13}	1.07 ^{+0.45} _{-0.90}	I	0	1.39	185	146
AP2959	7.50 ^{+0.10} _{-0.30}	3.21 ^{+0.02} _{-0.06}	1.20 ^{+0.10} _{-0.05}	7.28 ^{+0.55} _{-0.57}	3.09 ^{+0.15} _{-0.13}	1.00 ^{+0.41} _{-0.47}	I	0	1.69	176	130
AP2960	8.10 ^{+0.60} _{-0.10}	3.76 ^{+0.16} _{-0.03}	0.65 ^{+0.05} _{-0.50}	7.13 ^{+0.68} _{-0.28}	3.40 ^{+0.12} _{-0.13}	0.96 ^{+0.29} _{-0.72}	I	0	1.38	120	36
AP2967	7.20 ^{+0.20} _{-0.40}	2.87 ^{+0.02} _{-0.07}	1.85 ^{+0.10} _{-0.15}	7.55 ^{+0.12} _{-0.19}	3.34 ^{+0.17} _{-0.20}	1.63 ^{+0.25} _{-0.19}	I	0	1.41	125	125
AP2971	7.30 ^{+0.30} _{-0.20}	3.14 ^{+0.04} _{-0.07}	1.40 ^{+0.00} _{-0.10}	7.50 ^{+0.14} _{-0.14}	3.45 ^{+0.13} _{-0.11}	1.17 ^{+0.19} _{-0.19}	I	0	1.59	187	179
AP2972	8.30 ^{+0.10} _{-0.10}	2.89 ^{+0.07} _{-0.28}	0.75 ^{+0.45} _{-0.15}	8.85 ^{+0.09} _{-0.09}	3.03 ^{+0.08} _{-0.08}	0.10 ^{+0.12} _{-0.10}	I	0	1.25	108	84
AP2973	8.40 ^{+0.20} _{-0.10}	3.42 ^{+0.02} _{-0.07}	1.30 ^{+0.10} _{-0.35}	8.90 ^{+0.09} _{-0.11}	3.42 ^{+0.10} _{-0.10}	0.60 ^{+0.17} _{-0.17}	I	0	1.39	156	130
AP2977	8.70 ^{+0.30} _{-1.00}	3.39 ^{+0.05} _{-3.39}	1.25 ^{+1.10} _{-0.50}	8.87 ^{+0.77} _{-0.72}	3.48 ^{+0.20} _{-0.17}	1.06 ^{+0.77} _{-0.85}	I	0	1.85	164	107
AP2978	8.70 ^{+0.00} _{-0.10}	2.86 ^{+0.02} _{-0.04}	0.10 ^{+0.30} _{-0.05}	8.25 ^{+0.03} _{-0.34}	2.42 ^{+0.07} _{-0.32}	0.11 ^{+0.13} _{-0.11}	I	0	1.42	104	82
AP2979	7.40 ^{+0.20} _{-0.30}	3.29 ^{+0.03} _{-0.06}	1.75 ^{+0.10} _{-0.10}	8.35 ^{+0.21} _{-0.17}	3.60 ^{+0.15} _{-0.13}	0.50 ^{+0.39} _{-0.44}	I	0	1.63	183	159

Table 1 (cont'd)

AP ID ^a	CMD Best Fit Parameters ^b			Integrated Best Fit Parameters ^c			Best ^d Flag ^e	R _{ap} ^f	N _{stars} ^g	N _{bg} ^h	
	log(<i>t</i> [Myr])	log(<i>M</i> [<i>M</i> _⊙])	<i>A_V</i> [mag]	log(<i>t</i> [Myr])	log(<i>M</i> [<i>M</i> _⊙])	<i>A_V</i> [mag]					
AP2981	8.00 ^{+0.10} _{-0.60}	2.80 ^{+0.01} _{-0.07}	0.55 ^{+0.15} _{-0.05}	7.77 ^{+0.30} _{-0.27}	2.98 ^{+0.14} _{-0.16}	0.98 ^{+0.38} _{-0.39}	I	0	1.18	99	81
AP2984	7.80 ^{+0.00} _{-0.10}	3.74 ^{+0.01} _{-0.06}	1.55 ^{+0.05} _{-0.10}	8.86 ^{+0.06} _{-0.06}	3.58 ^{+0.06} _{-0.06}	0.01 ^{+0.07} _{-0.01}	I	0	1.74	273	220
AP2986	8.80 ^{+0.10} _{-0.00}	3.18 ^{+0.03} _{-0.07}	0.35 ^{+0.10} _{-0.20}	8.58 ^{+0.61} _{-0.47}	3.06 ^{+0.20} _{-0.19}	1.17 ^{+0.57} _{-0.72}	I	0	1.03	68	29
AP2987	6.90 ^{+0.30} _{-0.20}	2.72 ^{+0.08} _{-0.02}	0.65 ^{+0.15} _{-0.05}	6.95 ^{+0.20} _{-0.15}	2.90 ^{+0.22} _{-0.27}	0.62 ^{+0.15} _{-0.14}	I	0	3.18	207	183
AP2988	9.00 ^{+0.00} _{-0.10}	3.72 ^{+0.00} _{-0.10}	0.75 ^{+0.10} _{-0.10}	8.94 ^{+0.89} _{-0.96}	3.44 ^{+0.31} _{-0.34}	1.35 ^{+0.92} _{-0.88}	I	0	1.32	72	53
AP2989	9.00 ^{+0.10} _{-0.00}	3.49 ^{+0.06} _{-0.04}	0.35 ^{+0.10} _{-0.15}	8.15 ^{+0.69} _{-0.69}	2.82 ^{+0.29} _{-0.33}	1.20 ^{+1.12} _{-1.01}	I	0	1.37	93	68
AP2990	7.00 ^{+0.00} _{-0.20}	3.04 ^{+0.00} _{-0.03}	1.25 ^{+0.05} _{-0.05}	6.63 ^{+0.13} _{-0.10}	2.84 ^{+0.28} _{-0.28}	0.93 ^{+0.14} _{-0.13}	I	0	1.81	226	190
AP2991	9.10 ^{+0.00} _{-0.20}	3.54 ^{+0.02} _{-0.03}	0.10 ^{+0.50} _{-0.05}	9.30 ^{+0.13} _{-0.15}	3.28 ^{+0.17} _{-0.18}	0.20 ^{+0.18} _{-0.18}	I	0	1.30	101	63
AP2992	0.00 ^{+0.00} _{-0.00}	0.00 ^{+0.00} _{-0.00}	0.00 ^{+0.00} _{-0.00}	0.00 ^{+0.00} _{-0.00}	0.00 ^{+0.00} _{-0.00}	0.00 ^{+0.00} _{-0.00}	I	0	1.40	0	0
AP2993	7.90 ^{+0.40} _{-0.20}	2.95 ^{+0.05} _{-0.06}	1.20 ^{+0.05} _{-0.20}	6.91 ^{+0.16} _{-0.14}	2.93 ^{+0.24} _{-0.33}	2.62 ^{+0.17} _{-0.17}	I	0	1.15	52	34
AP2996	9.00 ^{+0.40} _{-1.70}	3.19 ^{+0.12} _{-3.19}	0.20 ^{+2.35} _{-0.15}	9.07 ^{+0.55} _{-0.47}	3.52 ^{+0.17} _{-0.15}	0.74 ^{+0.60} _{-0.60}	I	0	1.25	118	81
AP2997	9.10 ^{+0.00} _{-0.20}	3.46 ^{+0.17} _{-0.10}	0.05 ^{+0.70} _{-0.00}	8.94 ^{+0.62} _{-0.59}	3.63 ^{+0.16} _{-0.15}	0.88 ^{+0.70} _{-0.71}	I	0	1.43	169	126
AP2998	8.60 ^{+0.00} _{-0.70}	2.80 ^{+0.01} _{-0.14}	0.25 ^{+0.50} _{-0.10}	8.33 ^{+0.09} _{-0.09}	2.83 ^{+0.11} _{-0.11}	0.14 ^{+0.15} _{-0.14}	I	0	1.39	147	120
AP3001	8.70 ^{+0.10} _{-0.00}	3.79 ^{+0.04} _{-0.03}	0.75 ^{+0.05} _{-0.30}	7.71 ^{+0.03} _{-0.04}	2.94 ^{+0.06} _{-0.06}	0.12 ^{+0.08} _{-0.09}	I	0	1.49	106	41
AP3002	8.30 ^{+0.60} _{-0.50}	3.29 ^{+0.04} _{-0.18}	1.60 ^{+0.50} _{-1.45}	8.71 ^{+0.11} _{-0.12}	3.20 ^{+0.10} _{-0.10}	0.95 ^{+0.20} _{-0.19}	I	0	1.23	90	69
AP3009	6.90 ^{+0.40} _{-0.20}	2.71 ^{+0.01} _{-0.03}	0.70 ^{+0.05} _{-0.05}	7.54 ^{+0.05} _{-0.05}	2.90 ^{+0.13} _{-0.11}	0.18 ^{+0.13} _{-0.14}	I	0	1.71	98	62
AP3011	9.10 ^{+0.00} _{-1.30}	3.39 ^{+0.03} _{-0.78}	0.20 ^{+1.70} _{-0.05}	7.23 ^{+0.21} _{-0.25}	3.42 ^{+0.17} _{-0.23}	2.50 ^{+0.29} _{-0.03}	I	0	1.20	76	33
AP3013	9.00 ^{+0.00} _{-1.80}	3.14 ^{+0.00} _{-3.14}	0.00 ^{+2.90} _{-0.40}	8.74 ^{+0.22} _{-0.22}	3.04 ^{+0.09} _{-0.10}	0.34 ^{+0.32} _{-0.33}	I	0	1.11	93	51
AP3014	6.60 ^{+0.90} _{-0.10}	2.32 ^{+0.01} _{-0.12}	0.75 ^{+0.00} _{-0.30}	6.73 ^{+0.42} _{-0.48}	2.45 ^{+0.21} _{-0.24}	0.52 ^{+0.14} _{-0.14}	I	0	1.50	104	99
AP3015	9.00 ^{+0.10} _{-1.20}	3.66 ^{+0.12} _{-0.47}	0.40 ^{+1.70} _{-0.20}	9.39 ^{+0.28} _{-0.26}	3.79 ^{+0.15} _{-0.14}	0.30 ^{+0.26} _{-0.26}	I	0	1.93	235	158
AP3016	8.10 ^{+0.00} _{-0.10}	3.31 ^{+0.01} _{-0.23}	1.70 ^{+0.05} _{-0.50}	8.34 ^{+0.26} _{-0.23}	3.40 ^{+0.17} _{-0.15}	1.33 ^{+0.42} _{-0.46}	I	0	1.28	110	80
AP3019	8.70 ^{+0.10} _{-0.20}	3.52 ^{+0.04} _{-0.16}	0.80 ^{+0.30} _{-0.20}	7.51 ^{+0.76} _{-0.85}	2.91 ^{+0.29} _{-0.35}	1.72 ^{+0.94} _{-1.16}	I	0	1.40	132	106
AP3020	9.00 ^{+0.00} _{-0.10}	3.51 ^{+0.07} _{-0.06}	0.20 ^{+0.25} _{-0.05}	8.60 ^{+0.16} _{-0.15}	2.68 ^{+0.15} _{-0.16}	0.32 ^{+0.27} _{-0.26}	I	0	1.61	137	93
AP3021	8.30 ^{+0.50} _{-1.30}	2.78 ^{+0.03} _{-2.78}	1.05 ^{+0.85} _{-0.30}	6.69 ^{+0.06} _{-0.06}	2.63 ^{+0.18} _{-0.23}	0.50 ^{+0.07} _{-0.07}	I	0	1.76	186	184
AP3024	8.40 ^{+0.00} _{-0.10}	3.12 ^{+0.03} _{-0.04}	0.95 ^{+0.10} _{-0.05}	8.34 ^{+0.18} _{-0.17}	2.81 ^{+0.17} _{-0.15}	0.51 ^{+0.37} _{-0.39}	I	0	1.04	90	74
AP3025	8.20 ^{+0.40} _{-1.00}	3.09 ^{+0.02} _{-1.86}	1.60 ^{+0.65} _{-0.65}	7.56 ^{+1.54} _{-0.81}	3.04 ^{+1.06} _{-0.88}	1.55 ^{+0.74} _{-1.36}	I	1	1.49	229	212
AP3026	8.50 ^{+0.00} _{-0.80}	2.67 ^{+0.01} _{-0.14}	0.20 ^{+0.25} _{-0.10}	8.35 ^{+1.25} _{-1.22}	3.32 ^{+0.74} _{-0.64}	1.59 ^{+0.93} _{-0.98}	I	0	1.45	72	53
AP3027	8.20 ^{+0.00} _{-0.10}	2.87 ^{+0.01} _{-0.04}	0.55 ^{+0.10} _{-0.05}	8.07 ^{+0.23} _{-0.23}	2.67 ^{+0.27} _{-0.24}	0.43 ^{+0.26} _{-0.28}	I	0	1.26	121	96
AP3028	9.10 ^{+0.00} _{-0.00}	3.56 ^{+0.07} _{-0.00}	0.10 ^{+0.15} _{-0.00}	10.21 ^{+0.04} _{-0.03}	3.99 ^{+0.10} _{-0.08}	0.31 ^{+0.12} _{-0.14}	I	0	1.30	78	37
AP3029	7.30 ^{+0.30} _{-0.50}	2.55 ^{+0.01} _{-0.07}	0.95 ^{+0.10} _{-0.15}	6.89 ^{+0.14} _{-0.10}	2.90 ^{+0.21} _{-0.24}	1.61 ^{+0.11} _{-0.11}	I	0	1.46	85	62
AP3030	8.00 ^{+0.10} _{-0.60}	2.50 ^{+0.00} _{-0.06}	0.60 ^{+0.15} _{-0.10}	8.16 ^{+0.17} _{-0.15}	2.54 ^{+0.15} _{-0.13}	0.58 ^{+0.32} _{-0.35}	I	0	1.04	32	15
AP3032	9.20 ^{+0.00} _{-0.00}	3.65 ^{+0.06} _{-0.07}	0.05 ^{+0.15} _{-0.00}	8.29 ^{+0.22} _{-0.24}	2.83 ^{+0.18} _{-0.15}	0.48 ^{+0.47} _{-0.42}	I	0	1.55	140	92
AP3034	8.50 ^{+0.10} _{-0.50}	2.80 ^{+0.01} _{-0.20}	0.35 ^{+0.30} _{-0.20}	8.27 ^{+0.18} _{-0.23}	2.40 ^{+0.18} _{-0.23}	0.39 ^{+0.35} _{-0.33}	I	0	1.10	92	71

Table 1 (cont'd)

AP ID ^a	CMD Best Fit Parameters ^b			Integrated Best Fit Parameters ^c			Best ^d Flag ^e	Rap ^f	Nstars ^g	Nbg ^h	
	log(<i>t</i> [Myr])	log(<i>M</i> [<i>M</i> _⊙])	<i>A_V</i> [mag]	log(<i>t</i> [Myr])	log(<i>M</i> [<i>M</i> _⊙])	<i>A_V</i> [mag]					
AP3035	7.20 ^{+0.20} _{-0.50}	2.80 ^{+0.01} _{-0.09}	1.45 ^{+0.10} _{-0.20}	6.94 ^{+0.14} _{-0.10}	2.98 ^{+0.16} _{-0.19}	1.07 ^{+0.10} _{-0.11}	I	0	1.12	73	59
AP3038	8.50 ^{+0.10} _{-0.30}	2.75 ^{+0.02} _{-0.06}	0.30 ^{+0.25} _{-0.10}	8.59 ^{+0.14} _{-0.13}	2.52 ^{+0.16} _{-0.16}	0.21 ^{+0.20} _{-0.18}	I	0	1.17	70	57
AP3039	6.90 ^{+0.20} _{-0.20}	3.04 ^{+0.01} _{-0.01}	0.90 ^{+0.05} _{-0.05}	7.53 ^{+0.06} _{-0.07}	3.46 ^{+0.05} _{-0.05}	0.09 ^{+0.09} _{-0.08}	I	0	3.25	377	346
AP3041	8.30 ^{+0.00} _{-0.90}	2.89 ^{+0.02} _{-0.17}	0.80 ^{+0.30} _{-0.05}	8.62 ^{+0.13} _{-0.12}	2.66 ^{+0.13} _{-0.14}	0.20 ^{+0.20} _{-0.19}	I	0	1.10	57	49
AP3043	8.40 ^{+0.20} _{-0.10}	3.20 ^{+0.01} _{-0.11}	0.95 ^{+0.10} _{-0.35}	8.24 ^{+0.22} _{-0.25}	3.15 ^{+0.23} _{-0.19}	1.00 ^{+0.55} _{-0.50}	I	0	1.59	175	142
AP3044	6.90 ^{+0.30} _{-0.20}	2.93 ^{+0.01} _{-0.01}	0.55 ^{+0.05} _{-0.05}	7.01 ^{+0.33} _{-0.36}	2.98 ^{+0.15} _{-0.14}	0.19 ^{+0.17} _{-0.17}	I	0	2.26	309	312
AP3046	9.10 ^{+0.70} _{-0.00}	3.99 ^{+0.64} _{-0.02}	0.70 ^{+0.20} _{-0.10}	9.35 ^{+0.68} _{-0.63}	4.11 ^{+0.23} _{-0.14}	1.80 ^{+0.77} _{-0.60}	I	0	1.62	158	146
AP3047	8.70 ^{+0.10} _{-1.90}	2.93 ^{+0.08} _{-0.45}	0.45 ^{+0.85} _{-0.10}	6.62 ^{+0.06} _{-0.06}	2.64 ^{+0.41} _{-0.22}	0.89 ^{+0.07} _{-0.07}	I	0	1.49	125	134
AP3048	6.90 ^{+0.30} _{-0.10}	3.21 ^{+0.01} _{-0.06}	1.25 ^{+0.00} _{-0.10}	8.04 ^{+0.05} _{-0.03}	4.80 ^{+0.03} _{-0.03}	1.01 ^{+0.07} _{-0.08}	I	0	2.47	344	266
AP3049	8.10 ^{+0.00} _{-0.20}	3.09 ^{+0.00} _{-0.11}	1.05 ^{+0.10} _{-0.05}	7.09 ^{+0.33} _{-0.31}	3.37 ^{+0.17} _{-0.19}	2.43 ^{+0.23} _{-0.20}	I	0	1.25	107	65
AP3050	7.80 ^{+0.00} _{-0.90}	2.55 ^{+0.03} _{-0.12}	0.30 ^{+0.30} _{-0.00}	7.45 ^{+0.37} _{-0.28}	3.19 ^{+0.13} _{-0.13}	0.85 ^{+0.30} _{-0.32}	I	0	1.12	102	81
AP3053	8.50 ^{+0.10} _{-0.20}	3.23 ^{+0.05} _{-0.04}	0.95 ^{+0.30} _{-0.10}	8.32 ^{+0.18} _{-0.20}	2.28 ^{+0.17} _{-0.19}	0.20 ^{+0.20} _{-0.19}	I	0	1.02	74	44
AP3054	8.20 ^{+0.00} _{-1.10}	2.77 ^{+0.00} _{-0.24}	1.05 ^{+0.35} _{-0.00}	8.26 ^{+0.31} _{-0.34}	2.73 ^{+0.20} _{-0.20}	0.64 ^{+0.62} _{-0.56}	I	0	1.15	81	79
AP3055	7.50 ^{+0.00} _{-0.70}	2.70 ^{+0.00} _{-0.05}	0.65 ^{+0.20} _{-0.05}	7.00 ^{+0.21} _{-0.14}	2.50 ^{+0.27} _{-0.28}	0.69 ^{+0.14} _{-0.14}	I	0	1.46	147	144
AP3057	7.70 ^{+0.10} _{-0.30}	3.31 ^{+0.02} _{-0.04}	0.95 ^{+0.05} _{-0.10}	8.37 ^{+0.42} _{-0.35}	3.49 ^{+0.17} _{-0.16}	0.64 ^{+0.40} _{-0.46}	I	0	2.13	417	365
AP3059	6.90 ^{+0.20} _{-0.20}	2.55 ^{+0.00} _{-0.02}	0.80 ^{+0.05} _{-0.00}	6.99 ^{+0.23} _{-0.22}	2.40 ^{+0.22} _{-0.26}	0.59 ^{+0.13} _{-0.14}	I	0	1.70	45	29
AP3064	9.10 ^{+0.00} _{-0.00}	3.81 ^{+0.04} _{-0.04}	0.35 ^{+0.05} _{-0.10}	9.49 ^{+0.15} _{-0.13}	3.56 ^{+0.11} _{-0.08}	0.49 ^{+0.18} _{-0.15}	I	0	1.70	131	73
AP3065	7.70 ^{+0.10} _{-0.70}	2.72 ^{+0.01} _{-0.06}	0.55 ^{+0.10} _{-0.10}	6.92 ^{+0.54} _{-0.61}	2.69 ^{+0.16} _{-0.18}	0.93 ^{+0.26} _{-0.28}	I	0	1.55	158	133
AP3070	7.30 ^{+0.40} _{-0.30}	2.83 ^{+0.01} _{-0.06}	0.85 ^{+0.00} _{-0.25}	7.96 ^{+0.32} _{-0.29}	3.21 ^{+0.10} _{-0.11}	0.76 ^{+0.35} _{-0.68}	I	0	1.19	122	113
AP3075	7.10 ^{+0.20} _{-0.30}	2.98 ^{+0.05} _{-0.03}	1.25 ^{+0.10} _{-0.05}	6.55 ^{+0.26} _{-0.35}	2.90 ^{+0.27} _{-0.31}	1.27 ^{+0.16} _{-0.17}	I	0	1.25	101	76
AP3076	8.20 ^{+0.10} _{-0.50}	3.18 ^{+0.00} _{-0.13}	0.85 ^{+0.15} _{-0.10}	8.69 ^{+0.16} _{-0.16}	3.05 ^{+0.10} _{-0.10}	0.18 ^{+0.19} _{-0.18}	I	0	1.43	176	148
AP3077	8.40 ^{+0.00} _{-0.50}	2.92 ^{+0.02} _{-0.10}	0.70 ^{+0.30} _{-0.00}	9.12 ^{+0.66} _{-0.66}	3.59 ^{+0.18} _{-0.16}	0.95 ^{+0.76} _{-0.67}	I	0	1.34	84	63
AP3078	8.20 ^{+0.00} _{-0.00}	3.27 ^{+0.00} _{-0.02}	0.80 ^{+0.05} _{-0.05}	8.34 ^{+0.14} _{-0.16}	2.85 ^{+0.14} _{-0.13}	0.27 ^{+0.30} _{-0.26}	I	0	1.36	153	134
AP3079	8.50 ^{+0.20} _{-0.00}	3.21 ^{+0.03} _{-0.03}	0.85 ^{+0.00} _{-0.35}	8.92 ^{+0.18} _{-0.11}	2.95 ^{+0.12} _{-0.13}	0.17 ^{+0.10} _{-0.17}	I	0	1.20	109	82
AP3080	9.10 ^{+0.80} _{-0.10}	3.32 ^{+0.95} _{-0.22}	0.35 ^{+0.35} _{-0.20}	9.67 ^{+0.16} _{-0.16}	3.30 ^{+0.14} _{-0.14}	0.04 ^{+0.08} _{-0.04}	I	0	1.25	79	46
AP3084	7.50 ^{+0.20} _{-0.60}	2.59 ^{+0.01} _{-0.07}	0.85 ^{+0.15} _{-0.10}	8.14 ^{+0.16} _{-0.15}	2.94 ^{+0.13} _{-0.14}	0.40 ^{+0.31} _{-0.32}	I	0	1.52	146	132
AP3085	7.30 ^{+0.50} _{-0.36}	2.85 ^{+0.03} _{-0.10}	1.70 ^{+0.10} _{-0.25}	7.90 ^{+0.03} _{-0.03}	3.40 ^{+0.03} _{-0.03}	0.00 ^{+0.07} _{-0.00}	I	0	1.51	128	137
AP3087	8.80 ^{+0.10} _{-0.20}	3.12 ^{+0.04} _{-0.10}	0.25 ^{+0.45} _{-0.10}	7.54 ^{+0.65} _{-0.72}	2.90 ^{+0.24} _{-0.27}	1.52 ^{+0.78} _{-0.86}	I	0	1.79	112	93
AP3088	9.40 ^{+0.10} _{-0.00}	4.08 ^{+0.15} _{-0.05}	0.05 ^{+0.05} _{-0.05}	9.30 ^{+0.06} _{-0.06}	4.73 ^{+0.05} _{-0.05}	0.30 ^{+0.09} _{-0.10}	I	0	1.71	78	262
AP3089	7.20 ^{+0.30} _{-0.20}	2.93 ^{+0.03} _{-0.04}	1.90 ^{+0.05} _{-0.15}	8.19 ^{+0.20} _{-0.19}	2.80 ^{+0.17} _{-0.17}	0.64 ^{+0.38} _{-0.45}	I	0	1.05	29	9
AP3091	9.00 ^{+0.00} _{-0.00}	3.34 ^{+0.05} _{-0.07}	0.15 ^{+0.15} _{-0.10}	9.15 ^{+0.25} _{-0.03}	3.28 ^{+0.16} _{-0.15}	0.31 ^{+0.02} _{-0.31}	I	0	1.30	94	62
AP3093	8.30 ^{+0.00} _{-0.70}	3.09 ^{+0.00} _{-0.14}	0.90 ^{+0.30} _{-0.00}	8.54 ^{+0.12} _{-0.12}	2.68 ^{+0.14} _{-0.15}	0.33 ^{+0.24} _{-0.26}	I	0	1.10	80	50
AP3096	8.70 ^{+0.00} _{-1.10}	2.97 ^{+0.01} _{-0.25}	0.00 ^{+0.55} _{-0.05}	8.56 ^{+0.08} _{-0.06}	2.56 ^{+0.12} _{-0.11}	0.05 ^{+0.09} _{-0.05}	I	0	0.97	81	62

Table 1 (cont'd)

AP ID ^a	CMD Best Fit Parameters ^b			Integrated Best Fit Parameters ^c			Best ^d Flag ^e	R _{ap} ^f	N _{stars} ^g	N _{bg} ^h	
	log(<i>t</i> [Myr])	log(<i>M</i> [<i>M</i> _⊙])	<i>A_V</i> [mag]	log(<i>t</i> [Myr])	log(<i>M</i> [<i>M</i> _⊙])	<i>A_V</i> [mag]					
AP3097	8.80 ^{+0.00} _{-0.10}	3.09 ^{+0.03} _{-0.07}	0.25 ^{+0.35} _{-0.00}	8.74 ^{+0.26} _{-0.29}	3.02 ^{+0.17} _{-0.18}	0.77 ^{+0.43} _{-0.47}	I	0	1.36	107	86
AP3100	8.90 ^{+0.10} _{-0.00}	3.82 ^{+0.22} _{-0.14}	1.35 ^{+0.10} _{-0.40}	6.64 ^{+0.25} _{-0.27}	2.23 ^{+0.18} _{-0.18}	0.53 ^{+0.10} _{-0.10}	I	0	1.66	118	64
AP3102	7.40 ^{+0.20} _{-0.10}	3.32 ^{+0.02} _{-0.02}	1.60 ^{+0.05} _{-0.05}	7.71 ^{+0.36} _{-0.36}	3.22 ^{+0.16} _{-0.16}	1.08 ^{+0.51} _{-0.54}	I	0	1.59	191	151
AP3105	9.00 ^{+0.00} _{-0.10}	3.07 ^{+0.04} _{-0.03}	0.35 ^{+0.30} _{-0.05}	7.00 ^{+0.03} _{-0.03}	2.00 ^{+0.03} _{-0.00}	0.71 ^{+0.07} _{-0.07}	I	0	1.03	39	21
AP3106	8.30 ^{+0.00} _{-0.10}	2.92 ^{+0.01} _{-0.07}	0.55 ^{+0.15} _{-0.10}	8.02 ^{+0.24} _{-0.22}	2.58 ^{+0.16} _{-0.16}	0.27 ^{+0.28} _{-0.25}	I	0	1.52	173	168
AP3109	8.80 ^{+0.10} _{-0.10}	2.86 ^{+0.04} _{-0.06}	0.15 ^{+0.25} _{-0.10}	9.32 ^{+0.07} _{-0.08}	3.14 ^{+0.06} _{-0.09}	0.12 ^{+0.10} _{-0.10}	I	0	1.00	25	13
AP3110	8.30 ^{+0.00} _{-1.40}	2.92 ^{+0.03} _{-0.26}	0.55 ^{+0.25} _{-0.00}	7.80 ^{+0.09} _{-0.11}	3.24 ^{+0.10} _{-0.09}	1.16 ^{+0.19} _{-0.17}	I	0	1.71	260	217
AP3111	7.00 ^{+0.10} _{-0.30}	2.99 ^{+0.01} _{-0.03}	1.00 ^{+0.05} _{-0.05}	7.74 ^{+0.20} _{-0.20}	3.21 ^{+0.09} _{-0.09}	0.55 ^{+0.23} _{-0.22}	I	0	1.95	263	201
AP3112	8.20 ^{+0.00} _{-0.00}	3.69 ^{+0.04} _{-0.05}	2.30 ^{+0.10} _{-0.05}	9.95 ^{+0.29} _{-0.13}	3.90 ^{+0.13} _{-0.14}	0.27 ^{+0.11} _{-0.27}	I	0	1.66	172	126
AP3113	8.70 ^{+0.00} _{-0.20}	3.71 ^{+0.03} _{-0.17}	0.80 ^{+0.30} _{-0.10}	8.53 ^{+1.30} _{-1.41}	2.65 ^{+0.42} _{-0.45}	1.59 ^{+0.96} _{-1.00}	I	0	1.40	120	91
AP3114	7.90 ^{+0.00} _{-1.00}	2.79 ^{+0.01} _{-0.18}	0.65 ^{+0.60} _{-0.10}	6.89 ^{+0.43} _{-0.53}	3.09 ^{+0.22} _{-0.22}	1.57 ^{+0.20} _{-0.19}	I	0	1.42	105	99
AP3117	8.10 ^{+0.50} _{-0.10}	3.06 ^{+0.11} _{-0.11}	0.75 ^{+0.25} _{-0.40}	8.60 ^{+0.15} _{-0.16}	3.42 ^{+0.09} _{-0.09}	0.31 ^{+0.28} _{-0.27}	I	0	1.40	171	120
AP3118	9.00 ^{+0.00} _{-0.10}	3.25 ^{+0.06} _{-0.05}	0.35 ^{+0.35} _{-0.00}	7.81 ^{+0.80} _{-0.88}	2.46 ^{+0.25} _{-0.24}	0.95 ^{+0.68} _{-0.70}	I	0	1.20	59	32
AP3119	9.10 ^{+0.04} _{-0.00}	4.05 ^{+0.11} _{-0.03}	0.50 ^{+0.15} _{-0.10}	9.24 ^{+0.75} _{-0.69}	4.04 ^{+0.19} _{-0.16}	1.01 ^{+0.79} _{-0.75}	I	0	2.15	292	229
AP3121	8.90 ^{+0.10} _{-0.00}	3.57 ^{+0.03} _{-0.06}	0.45 ^{+0.11} _{-0.20}	8.41 ^{+0.16} _{-0.15}	2.77 ^{+0.18} _{-0.17}	0.47 ^{+0.34} _{-0.35}	I	0	1.39	122	86
AP3122	8.50 ^{+0.20} _{-0.10}	3.20 ^{+0.05} _{-0.04}	0.85 ^{+0.10} _{-0.35}	8.61 ^{+0.13} _{-0.12}	2.79 ^{+0.11} _{-0.10}	0.12 ^{+0.16} _{-0.12}	I	0	1.41	95	53
AP3123	9.00 ^{+0.00} _{-0.00}	3.79 ^{+0.07} _{-0.03}	0.35 ^{+0.15} _{-0.05}	8.86 ^{+0.14} _{-0.14}	3.03 ^{+0.10} _{-0.11}	0.18 ^{+0.18} _{-0.18}	I	0	1.88	199	125
AP3126	8.80 ^{+0.10} _{-0.00}	3.29 ^{+0.03} _{-0.03}	0.15 ^{+0.15} _{-0.10}	9.48 ^{+0.15} _{-0.13}	3.44 ^{+0.13} _{-0.13}	0.06 ^{+0.11} _{-0.06}	I	0	1.14	70	28
AP3127	9.10 ^{+0.00} _{-0.10}	3.90 ^{+0.06} _{-0.01}	0.40 ^{+0.15} _{-0.15}	6.48 ^{+0.06} _{-0.06}	2.21 ^{+0.10} _{-0.17}	1.50 ^{+0.07} _{-0.07}	I	0	2.10	261	212
AP3129	6.80 ^{+0.10} _{-0.10}	2.55 ^{+0.02} _{-0.03}	0.70 ^{+0.05} _{-0.05}	6.83 ^{+0.11} _{-0.09}	2.53 ^{+0.29} _{-0.22}	0.55 ^{+0.09} _{-0.09}	I	0	1.99	123	94
AP3130	9.10 ^{+0.60} _{-0.00}	3.69 ^{+0.75} _{-0.04}	0.45 ^{+0.10} _{-0.35}	8.83 ^{+0.12} _{-0.27}	3.62 ^{+0.10} _{-0.08}	0.99 ^{+0.34} _{-0.24}	I	0	1.63	169	79
AP3131	8.10 ^{+0.60} _{-0.00}	3.37 ^{+0.08} _{-0.02}	1.15 ^{+0.05} _{-0.55}	7.80 ^{+0.99} _{-1.24}	3.33 ^{+0.33} _{-0.27}	1.55 ^{+1.16} _{-1.38}	I	0	1.85	252	198
AP3136	7.80 ^{+0.40} _{-0.50}	2.59 ^{+0.02} _{-0.10}	0.55 ^{+0.05} _{-0.20}	8.32 ^{+0.10} _{-0.10}	3.06 ^{+0.09} _{-0.08}	0.17 ^{+0.18} _{-0.17}	I	0	1.55	84	79
AP3138	8.20 ^{+0.00} _{-0.60}	2.88 ^{+0.01} _{-0.08}	0.65 ^{+0.20} _{-0.00}	9.92 ^{+0.33} _{-0.34}	3.80 ^{+0.12} _{-0.12}	0.40 ^{+0.24} _{-0.25}	I	0	1.25	92	74
AP3139	8.30 ^{+0.10} _{-1.00}	2.78 ^{+0.08} _{-0.26}	0.70 ^{+0.60} _{-0.05}	9.19 ^{+0.38} _{-0.20}	3.62 ^{+0.22} _{-0.14}	0.40 ^{+0.21} _{-0.32}	I	0	1.57	155	151
AP3140	9.30 ^{+0.00} _{-0.00}	5.13 ^{+0.00} _{-0.00}	0.00 ^{+0.00} _{-0.00}	0.00 ^{+0.00} _{-0.00}	0.00 ^{+0.00} _{-0.00}	0.00 ^{+0.00} _{-0.00}	I	0	1.64	305	290
AP3143	7.80 ^{+0.20} _{-0.00}	2.93 ^{+0.03} _{-0.03}	1.05 ^{+0.05} _{-0.10}	7.95 ^{+0.06} _{-0.06}	3.09 ^{+0.06} _{-0.07}	1.26 ^{+0.12} _{-0.13}	I	0	1.27	98	70
AP3144	8.40 ^{+0.10} _{-0.10}	3.08 ^{+0.03} _{-0.04}	0.65 ^{+0.05} _{-0.20}	7.24 ^{+0.05} _{-0.05}	3.51 ^{+0.24} _{-0.24}	2.44 ^{+0.33} _{-0.34}	I	0	1.36	96	66
AP3146	6.60 ^{+0.20} _{-0.00}	2.73 ^{+0.00} _{-0.06}	0.95 ^{+0.00} _{-0.10}	6.89 ^{+0.10} _{-0.10}	2.51 ^{+0.17} _{-0.13}	0.49 ^{+0.09} _{-0.08}	I	0	1.96	267	255
AP3148	9.00 ^{+0.00} _{-1.50}	3.16 ^{+0.03} _{-0.47}	0.05 ^{+1.75} _{-0.10}	8.58 ^{+0.44} _{-0.40}	3.03 ^{+0.18} _{-0.18}	0.66 ^{+0.62} _{-0.56}	I	0	1.54	115	63
AP3151	8.10 ^{+0.00} _{-1.00}	2.76 ^{+0.03} _{-0.14}	0.60 ^{+0.20} _{-0.05}	7.42 ^{+0.48} _{-0.53}	2.70 ^{+0.14} _{-0.16}	0.83 ^{+0.34} _{-0.34}	I	0	1.35	107	101
AP3155	6.60 ^{+0.20} _{-0.00}	2.97 ^{+0.01} _{-0.01}	0.60 ^{+0.00} _{-0.05}	6.59 ^{+0.16} _{-0.15}	3.31 ^{+0.26} _{-0.22}	0.36 ^{+0.12} _{-0.12}	I	0	3.44	1114	1123
AP3156	9.10 ^{+0.00} _{-0.00}	4.18 ^{+0.02} _{-0.02}	0.40 ^{+0.10} _{-0.05}	8.26 ^{+1.22} _{-1.52}	3.53 ^{+0.35} _{-0.40}	1.43 ^{+0.97} _{-1.06}	I	0	1.90	300	237

Table 1 (cont'd)

AP ID ^a	CMD Best Fit Parameters ^b			Integrated Best Fit Parameters ^c			Best ^d Flag ^e	Rap ^f	N _{stars} ^g	N _{bg} ^h	
	log(<i>t</i> [Myr])	log(<i>M</i> [<i>M</i> _⊙])	<i>A_V</i> [mag]	log(<i>t</i> [Myr])	log(<i>M</i> [<i>M</i> _⊙])	<i>A_V</i> [mag]					
AP3161	8.30 ^{+0.50} _{-0.50}	3.11 ^{+0.16} _{-0.33}	1.30 ^{+0.15} _{-1.00}	7.42 ^{+0.10} _{-0.08}	3.51 ^{+0.07} _{-0.05}	0.55 ^{+0.09} _{-0.10}	I	0	1.27	65	60
AP3163	8.40 ^{+0.30} _{-0.20}	3.10 ^{+0.01} _{-0.12}	1.35 ^{+0.15} _{-0.50}	8.11 ^{+1.47} _{-1.46}	3.78 ^{+1.25} _{-1.18}	1.45 ^{+1.02} _{-1.02}	I	0	1.26	63	26
AP3165	8.30 ^{+0.10} _{-0.40}	3.19 ^{+0.01} _{-0.07}	0.75 ^{+0.15} _{-0.05}	8.73 ^{+0.16} _{-0.12}	3.05 ^{+0.09} _{-0.09}	0.14 ^{+0.11} _{-0.14}	I	0	1.28	97	61
AP3166	7.10 ^{+0.10} _{-0.30}	2.84 ^{+0.01} _{-0.03}	1.05 ^{+0.10} _{-0.05}	7.77 ^{+0.10} _{-0.11}	2.76 ^{+0.04} _{-0.05}	0.10 ^{+0.19} _{-0.10}	I	0	1.50	154	140
AP3168	8.50 ^{+0.10} _{-0.40}	2.99 ^{+0.00} _{-0.07}	0.45 ^{+0.25} _{-0.15}	8.88 ^{+0.09} _{-0.10}	2.97 ^{+0.09} _{-0.09}	0.03 ^{+0.07} _{-0.03}	I	0	1.37	139	121
AP3172	8.90 ^{+0.00} _{-0.10}	3.65 ^{+0.04} _{-0.04}	0.30 ^{+0.35} _{-0.10}	7.67 ^{+0.32} _{-0.30}	3.57 ^{+0.14} _{-0.17}	1.73 ^{+0.41} _{-0.52}	I	0	1.27	145	96
AP3173	8.50 ^{+0.00} _{-0.70}	2.99 ^{+0.02} _{-0.17}	0.50 ^{+0.40} _{-0.05}	8.19 ^{+0.84} _{-0.45}	3.30 ^{+0.20} _{-0.21}	1.40 ^{+0.71} _{-1.18}	I	0	1.17	108	71
AP3174	8.80 ^{+0.00} _{-0.60}	3.58 ^{+0.02} _{-0.16}	0.70 ^{+1.00} _{-0.10}	9.22 ^{+0.66} _{-0.79}	3.98 ^{+0.17} _{-0.16}	1.26 ^{+0.88} _{-0.67}	I	0	1.41	158	112
AP3179	8.70 ^{+0.00} _{-0.20}	2.93 ^{+0.17} _{-0.02}	0.00 ^{+0.65} _{-0.10}	7.86 ^{+0.83} _{-0.83}	2.98 ^{+0.31} _{-0.32}	1.56 ^{+1.05} _{-1.18}	I	0	1.34	126	118
AP3182	9.80 ^{+0.00} _{-0.40}	4.95 ^{+0.00} _{-0.51}	0.00 ^{+0.20} _{-0.00}	10.21 ^{+0.04} _{-0.06}	5.32 ^{+0.05} _{-0.05}	0.10 ^{+0.08} _{-0.09}	I	0	1.75	84	238
AP3183	7.90 ^{+0.10} _{-0.30}	2.76 ^{+0.01} _{-0.02}	0.45 ^{+0.10} _{-0.05}	9.80 ^{+0.04} _{-0.03}	3.65 ^{+0.04} _{-0.03}	0.00 ^{+0.07} _{-0.00}	I	0	1.38	87	76
AP3184	9.80 ^{+0.00} _{-1.30}	4.37 ^{+0.01} _{-2.40}	0.15 ^{+1.10} _{-0.10}	8.72 ^{+0.10} _{-0.10}	2.97 ^{+0.09} _{-0.08}	0.23 ^{+0.22} _{-0.20}	I	0	1.25	127	95
AP3187	7.60 ^{+0.20} _{-0.50}	2.74 ^{+0.01} _{-0.05}	0.80 ^{+0.05} _{-0.10}	7.72 ^{+0.30} _{-0.26}	2.63 ^{+0.15} _{-0.15}	0.75 ^{+0.30} _{-0.30}	I	0	1.37	66	42
AP3188	8.40 ^{+0.10} _{-0.10}	2.97 ^{+0.04} _{-0.04}	0.05 ^{+0.15} _{-0.05}	8.22 ^{+0.08} _{-0.08}	2.55 ^{+0.13} _{-0.12}	0.07 ^{+0.11} _{-0.07}	I	0	1.20	95	74
AP3189	8.10 ^{+0.10} _{-0.10}	3.06 ^{+0.03} _{-0.05}	0.55 ^{+0.05} _{-0.10}	7.70 ^{+0.47} _{-0.45}	2.89 ^{+0.14} _{-0.14}	0.88 ^{+0.45} _{-0.48}	I	0	1.33	128	113
AP3190	8.10 ^{+0.40} _{-0.50}	2.91 ^{+0.05} _{-0.17}	1.30 ^{+0.10} _{-0.30}	7.56 ^{+0.17} _{-0.18}	3.25 ^{+0.08} _{-0.08}	2.17 ^{+0.14} _{-0.13}	I	0	1.00	50	25
AP3191	8.00 ^{+0.50} _{-0.00}	3.04 ^{+0.07} _{-0.02}	0.65 ^{+0.00} _{-0.35}	7.84 ^{+0.11} _{-0.11}	3.05 ^{+0.10} _{-0.10}	0.75 ^{+0.21} _{-0.22}	I	0	1.33	108	96
AP3194	9.20 ^{+0.00} _{-1.70}	3.63 ^{+0.00} _{-3.63}	0.25 ^{+1.70} _{-0.05}	7.43 ^{+0.50} _{-0.40}	3.46 ^{+0.17} _{-0.20}	2.28 ^{+0.43} _{-0.66}	I	0	1.60	121	77
AP3195	8.30 ^{+0.30} _{-0.00}	2.83 ^{+0.07} _{-0.02}	0.55 ^{+0.10} _{-0.30}	8.39 ^{+0.24} _{-0.25}	2.77 ^{+0.24} _{-0.21}	0.63 ^{+0.56} _{-0.52}	I	0	1.05	49	33
AP3196	8.10 ^{+0.00} _{-0.10}	3.20 ^{+0.06} _{-0.03}	1.90 ^{+0.30} _{-0.00}	8.17 ^{+0.12} _{-0.12}	2.39 ^{+0.26} _{-0.24}	0.57 ^{+0.36} _{-0.35}	I	0	1.15	67	38
AP3203	8.40 ^{+0.00} _{-0.80}	2.67 ^{+0.01} _{-0.12}	0.35 ^{+0.30} _{-0.00}	10.17 ^{+0.08} _{-0.10}	3.50 ^{+0.09} _{-0.09}	0.20 ^{+0.08} _{-0.13}	I	0	1.17	84	78
AP3204	7.00 ^{+0.10} _{-0.40}	2.64 ^{+0.02} _{-0.03}	0.80 ^{+0.10} _{-0.05}	6.90 ^{+0.11} _{-0.11}	2.47 ^{+0.25} _{-0.22}	0.77 ^{+0.11} _{-0.11}	I	0	1.77	163	158
AP3205	8.90 ^{+0.00} _{-0.10}	3.52 ^{+0.01} _{-0.13}	0.50 ^{+0.35} _{-0.10}	8.11 ^{+1.47} _{-1.46}	3.78 ^{+1.25} _{-1.18}	1.45 ^{+1.02} _{-1.02}	I	0	1.41	104	55
AP3209	8.00 ^{+0.20} _{-0.00}	3.09 ^{+0.04} _{-0.02}	1.00 ^{+0.10} _{-0.05}	8.83 ^{+0.10} _{-0.09}	2.88 ^{+0.09} _{-0.09}	0.02 ^{+0.07} _{-0.02}	I	0	1.44	129	122
AP3210	9.00 ^{+0.10} _{-0.00}	3.89 ^{+0.07} _{-0.02}	0.80 ^{+0.10} _{-0.05}	7.85 ^{+0.08} _{-0.08}	2.08 ^{+0.05} _{-0.08}	0.15 ^{+0.13} _{-0.14}	I	0	2.36	219	115
AP3212	8.30 ^{+0.00} _{-0.10}	2.96 ^{+0.02} _{-0.04}	0.45 ^{+0.10} _{-0.05}	7.12 ^{+0.54} _{-0.63}	3.01 ^{+0.15} _{-0.14}	1.53 ^{+0.33} _{-0.34}	I	0	1.16	106	102
AP3213	7.70 ^{+0.00} _{-0.40}	2.95 ^{+0.01} _{-0.09}	0.75 ^{+0.05} _{-0.10}	7.73 ^{+0.11} _{-0.09}	3.05 ^{+0.09} _{-0.09}	0.79 ^{+0.16} _{-0.16}	I	0	1.63	164	135
AP3215	6.60 ^{+1.00} _{-0.00}	2.50 ^{+0.12} _{-0.07}	0.95 ^{+0.15} _{-0.15}	6.78 ^{+0.44} _{-0.50}	2.51 ^{+0.20} _{-0.21}	0.72 ^{+0.17} _{-0.18}	I	0	1.64	146	139
AP3216	9.00 ^{+0.00} _{-0.10}	3.85 ^{+0.00} _{-0.22}	0.75 ^{+0.10} _{-0.15}	8.35 ^{+0.96} _{-0.67}	3.34 ^{+0.24} _{-0.27}	1.44 ^{+0.93} _{-1.16}	I	0	1.43	126	86
AP3219	9.10 ^{+0.10} _{-1.10}	3.36 ^{+0.45} _{-0.06}	0.25 ^{+2.35} _{-0.15}	9.60 ^{+0.26} _{-0.27}	3.41 ^{+0.17} _{-0.18}	0.31 ^{+0.31} _{-0.28}	I	0	1.04	64	34
AP3220	7.80 ^{+0.20} _{-0.50}	2.90 ^{+0.02} _{-0.05}	0.70 ^{+0.10} _{-0.10}	8.10 ^{+0.19} _{-0.18}	2.55 ^{+0.17} _{-0.16}	0.26 ^{+0.28} _{-0.24}	I	0	1.21	79	57
AP3221	9.10 ^{+0.00} _{-0.00}	3.52 ^{+0.06} _{-0.15}	0.40 ^{+0.05} _{-0.20}	8.11 ^{+1.47} _{-1.46}	3.78 ^{+1.25} _{-1.18}	1.45 ^{+1.02} _{-1.02}	I	0	1.36	89	52
AP3222	7.90 ^{+0.00} _{-0.40}	2.81 ^{+0.00} _{-0.05}	0.40 ^{+0.15} _{-0.05}	7.47 ^{+0.63} _{-0.58}	2.96 ^{+0.18} _{-0.20}	1.13 ^{+0.57} _{-0.71}	I	0	1.05	105	70

Table 1 (cont'd)

AP ID ^a	CMD Best Fit Parameters ^b			Integrated Best Fit Parameters ^c			Best ^d Flag ^e	R _{ap} ^f	N _{stars} ^g	N _{bg} ^h	
	log(<i>t</i> [Myr])	log(<i>M</i> [<i>M</i> _⊙])	<i>A_V</i> [mag]	log(<i>t</i> [Myr])	log(<i>M</i> [<i>M</i> _⊙])	<i>A_V</i> [mag]					
AP3223	9.10 ^{+0.00} _{-1.30}	3.55 ^{+0.02} _{-0.37}	0.20 ^{+1.85} _{-0.05}	9.37 ^{+0.42} _{-0.38}	3.66 ^{+0.18} _{-0.17}	0.43 ^{+0.36} _{-0.36}	I	0	1.26	103	66
AP3224	9.10 ^{+0.00} _{-0.00}	3.83 ^{+0.11} _{-0.02}	0.15 ^{+0.15} _{-0.00}	8.64 ^{+0.11} _{-0.11}	3.42 ^{+0.09} _{-0.09}	0.45 ^{+0.21} _{-0.22}	I	0	2.09	319	198
AP3225	8.40 ^{+0.10} _{-0.00}	3.28 ^{+0.01} _{-0.10}	0.85 ^{+0.00} _{-0.30}	8.65 ^{+0.10} _{-0.09}	2.65 ^{+0.10} _{-0.11}	0.05 ^{+0.09} _{-0.05}	I	0	1.35	108	87
AP3230	8.40 ^{+0.20} _{-0.00}	3.05 ^{+0.04} _{-0.04}	0.85 ^{+0.05} _{-0.25}	9.02 ^{+0.15} _{-0.11}	3.19 ^{+0.13} _{-0.16}	0.44 ^{+0.28} _{-0.27}	I	0	1.39	95	68
AP3232	7.00 ^{+0.20} _{-0.40}	2.74 ^{+0.03} _{-0.03}	1.45 ^{+0.15} _{-0.05}	6.58 ^{+0.20} _{-0.15}	3.18 ^{+0.28} _{-0.30}	1.87 ^{+0.09} _{-0.07}	I	0	1.52	142	135
AP3235	8.40 ^{+0.10} _{-1.00}	3.03 ^{+0.02} _{-0.23}	0.95 ^{+0.60} _{-0.15}	8.23 ^{+0.63} _{-0.41}	3.55 ^{+0.23} _{-0.28}	1.71 ^{+0.77} _{-1.18}	I	0	1.36	136	122
AP3236	8.70 ^{+0.10} _{-0.10}	2.96 ^{+0.07} _{-0.03}	0.25 ^{+0.20} _{-0.15}	8.63 ^{+0.16} _{-0.17}	2.67 ^{+0.17} _{-0.19}	0.51 ^{+0.31} _{-0.31}	I	0	1.05	72	66
AP3237	9.10 ^{+0.00} _{-0.20}	3.63 ^{+0.04} _{-0.17}	0.10 ^{+0.55} _{-0.00}	8.27 ^{+0.44} _{-0.37}	3.52 ^{+0.18} _{-0.15}	1.37 ^{+0.59} _{-0.70}	I	0	1.19	128	91
AP3238	8.40 ^{+0.00} _{-0.10}	2.75 ^{+0.22} _{-0.00}	0.10 ^{+0.30} _{-0.00}	7.68 ^{+1.05} _{-1.09}	3.47 ^{+0.30} _{-0.29}	1.79 ^{+1.01} _{-1.29}	I	0	1.04	106	91
AP3239	8.10 ^{+0.30} _{-0.50}	3.12 ^{+0.09} _{-0.19}	1.20 ^{+0.15} _{-0.10}	8.97 ^{+0.38} _{-0.89}	3.42 ^{+0.17} _{-0.16}	0.60 ^{+1.42} _{-0.56}	I	0	1.34	111	61
AP3243	7.70 ^{+0.00} _{-0.00}	2.96 ^{+0.02} _{-0.03}	1.10 ^{+0.05} _{-0.05}	8.16 ^{+0.20} _{-0.23}	3.68 ^{+0.14} _{-0.15}	1.10 ^{+0.45} _{-0.43}	I	0	1.68	152	82
AP3244	7.80 ^{+0.00} _{-0.40}	3.15 ^{+0.01} _{-0.04}	1.25 ^{+0.15} _{-0.05}	7.91 ^{+0.02} _{-0.09}	2.56 ^{+0.02} _{-0.09}	0.07 ^{+0.08} _{-0.07}	I	0	1.44	143	121
AP3246	9.30 ^{+0.30} _{-2.10}	3.60 ^{+0.31} _{-3.60}	0.65 ^{+1.85} _{-0.20}	8.20 ^{+0.21} _{-0.21}	2.82 ^{+0.27} _{-0.37}	1.33 ^{+0.49} _{-0.63}	I	0	1.26	55	25
AP3247	7.40 ^{+0.60} _{-0.30}	2.81 ^{+0.05} _{-0.06}	1.05 ^{+0.10} _{-0.30}	7.98 ^{+0.18} _{-0.20}	3.54 ^{+0.16} _{-0.13}	1.04 ^{+0.35} _{-0.33}	I	0	1.78	224	213
AP3249	8.10 ^{+0.10} _{-0.20}	3.18 ^{+0.00} _{-0.13}	1.25 ^{+0.10} _{-0.15}	7.74 ^{+0.10} _{-0.09}	2.97 ^{+0.16} _{-0.18}	0.89 ^{+0.25} _{-0.26}	I	0	1.38	143	117
AP3250	9.20 ^{+0.00} _{-0.10}	4.03 ^{+0.00} _{-0.27}	0.30 ^{+0.20} _{-0.00}	9.96 ^{+0.18} _{-0.19}	3.74 ^{+0.13} _{-0.12}	0.13 ^{+0.15} _{-0.13}	I	0	1.38	137	92
AP3251	8.10 ^{+0.00} _{-0.90}	3.01 ^{+0.03} _{-0.16}	0.85 ^{+0.25} _{-0.00}	7.79 ^{+0.07} _{-0.08}	2.59 ^{+0.15} _{-0.14}	0.14 ^{+0.15} _{-0.14}	I	0	1.33	129	113
AP3252	7.00 ^{+0.60} _{-0.20}	2.39 ^{+0.02} _{-0.04}	0.60 ^{+0.00} _{-0.15}	7.16 ^{+0.39} _{-0.45}	2.58 ^{+0.19} _{-0.20}	0.93 ^{+0.24} _{-0.24}	I	0	1.00	42	17
AP3256	8.20 ^{+0.00} _{-0.60}	3.34 ^{+0.02} _{-0.28}	1.40 ^{+0.15} _{-0.10}	7.76 ^{+0.06} _{-0.15}	3.09 ^{+0.10} _{-0.10}	1.53 ^{+0.23} _{-0.17}	I	0	1.36	129	86
AP3258	8.10 ^{+0.20} _{-0.90}	2.64 ^{+0.07} _{-0.13}	0.90 ^{+0.25} _{-0.10}	8.24 ^{+0.17} _{-0.19}	2.55 ^{+0.32} _{-0.32}	0.52 ^{+0.43} _{-0.42}	I	0	1.03	62	63
AP3260	7.60 ^{+0.30} _{-0.10}	2.97 ^{+0.03} _{-0.02}	1.00 ^{+0.05} _{-0.10}	8.35 ^{+0.12} _{-0.12}	2.90 ^{+0.14} _{-0.14}	0.32 ^{+0.29} _{-0.27}	I	0	1.23	108	81
AP3264	8.20 ^{+0.10} _{-0.30}	3.17 ^{+0.01} _{-0.08}	0.70 ^{+0.10} _{-0.10}	8.39 ^{+0.11} _{-0.10}	3.11 ^{+0.10} _{-0.09}	0.16 ^{+0.15} _{-0.16}	I	0	2.03	259	233
AP3267	9.50 ^{+0.30} _{-0.10}	4.56 ^{+0.24} _{-0.11}	0.35 ^{+0.05} _{-0.25}	8.76 ^{+0.03} _{-0.17}	3.64 ^{+0.16} _{-0.01}	1.25 ^{+0.29} _{-0.05}	I	0	1.73	251	231
AP3269	8.70 ^{+0.00} _{-0.10}	3.49 ^{+0.02} _{-0.08}	0.75 ^{+0.35} _{-0.00}	8.81 ^{+1.09} _{-1.14}	3.03 ^{+0.75} _{-0.75}	1.72 ^{+0.91} _{-0.98}	I	0	1.55	145	110
AP3271	8.00 ^{+0.10} _{-0.30}	3.27 ^{+0.02} _{-0.11}	1.65 ^{+0.10} _{-0.05}	8.25 ^{+0.14} _{-0.14}	2.47 ^{+0.16} _{-0.16}	0.23 ^{+0.22} _{-0.21}	I	0	1.19	115	96
AP3273	8.80 ^{+0.10} _{-1.20}	3.08 ^{+0.00} _{-0.22}	0.00 ^{+0.75} _{-0.20}	7.22 ^{+0.55} _{-0.70}	2.78 ^{+0.15} _{-0.15}	0.93 ^{+0.36} _{-0.36}	I	0	1.27	104	82
AP3275	8.30 ^{+0.00} _{-0.10}	3.12 ^{+0.00} _{-0.05}	0.55 ^{+0.10} _{-0.05}	8.40 ^{+0.10} _{-0.10}	2.79 ^{+0.13} _{-0.11}	0.16 ^{+0.19} _{-0.16}	I	0	1.31	92	63
AP3277	7.20 ^{+0.20} _{-0.30}	2.97 ^{+0.01} _{-0.03}	0.55 ^{+0.05} _{-0.05}	7.70 ^{+0.15} _{-0.13}	3.23 ^{+0.17} _{-0.16}	0.45 ^{+0.28} _{-0.28}	I	0	2.31	336	310
AP3281	8.20 ^{+0.00} _{-0.00}	2.75 ^{+0.02} _{-0.02}	0.50 ^{+0.05} _{-0.10}	8.88 ^{+0.27} _{-0.31}	2.95 ^{+0.13} _{-0.14}	0.38 ^{+0.34} _{-0.31}	I	0	1.14	32	16
AP3283	9.00 ^{+0.00} _{-0.00}	3.89 ^{+0.03} _{-0.03}	0.60 ^{+0.10} _{-0.10}	8.45 ^{+0.46} _{-0.40}	3.24 ^{+0.17} _{-0.17}	0.80 ^{+0.50} _{-0.57}	I	0	1.99	239	161
AP3286	6.70 ^{+0.30} _{-0.10}	3.01 ^{+0.01} _{-0.04}	1.75 ^{+0.00} _{-0.15}	6.93 ^{+0.54} _{-0.62}	2.89 ^{+0.16} _{-0.14}	0.73 ^{+0.25} _{-0.29}	I	0	1.77	166	129
AP3288	8.20 ^{+0.00} _{-1.30}	2.84 ^{+0.01} _{-0.17}	0.70 ^{+0.25} _{-0.05}	8.35 ^{+0.09} _{-0.09}	2.77 ^{+0.12} _{-0.11}	0.15 ^{+0.18} _{-0.15}	I	0	1.32	109	90
AP3289	6.90 ^{+0.20} _{-0.10}	3.12 ^{+0.01} _{-0.07}	2.10 ^{+0.00} _{-0.15}	7.57 ^{+0.07} _{-0.10}	3.33 ^{+0.08} _{-0.08}	0.58 ^{+0.18} _{-0.16}	I	0	2.06	223	211

Table 1 (cont'd)

AP ID ^a	CMD Best Fit Parameters ^b			Integrated Best Fit Parameters ^c			Best ^d Flag ^e	Rap ^f	N _{stars} ^g	N _{bg} ^h	
	log(<i>t</i> [Myr])	log(<i>M</i> [<i>M</i> _⊙])	<i>A_V</i> [mag]	log(<i>t</i> [Myr])	log(<i>M</i> [<i>M</i> _⊙])	<i>A_V</i> [mag]					
AP3291	9.00 ^{+0.00} _{-0.20}	3.30 ^{+0.00} _{-0.24}	0.40 ^{+0.60} _{-0.05}	8.17 ^{+0.44} _{-0.45}	2.55 ^{+0.22} _{-0.23}	0.63 ^{+0.57} _{-0.52}	I	0	1.20	81	50
AP3292	9.30 ^{+0.10} _{-2.10}	3.50 ^{+0.32} _{-3.50}	0.25 ^{+2.00} _{-0.05}	8.63 ^{+0.26} _{-0.26}	2.98 ^{+0.15} _{-0.16}	1.07 ^{+0.50} _{-0.53}	I	0	1.16	73	54
AP3294	6.70 ^{+0.50} _{-0.10}	2.59 ^{+0.01} _{-0.04}	1.45 ^{+0.00} _{-0.20}	7.85 ^{+0.03} _{-0.03}	2.93 ^{+0.04} _{-0.04}	0.00 ^{+0.07} _{-0.00}	I	0	1.50	120	72
AP3295	8.00 ^{+0.30} _{-0.20}	2.63 ^{+0.02} _{-0.08}	0.55 ^{+0.10} _{-0.15}	7.81 ^{+0.03} _{-0.04}	2.12 ^{+0.15} _{-0.09}	0.16 ^{+0.19} _{-0.16}	I	0	1.48	71	43
AP3298	8.20 ^{+0.00} _{-0.20}	3.21 ^{+0.02} _{-0.12}	0.80 ^{+0.05} _{-0.30}	8.44 ^{+0.14} _{-0.15}	3.04 ^{+0.11} _{-0.11}	0.27 ^{+0.34} _{-0.27}	I	0	1.24	103	84
AP3299	8.20 ^{+0.10} _{-0.70}	3.23 ^{+0.04} _{-0.32}	1.00 ^{+0.05} _{-0.55}	7.98 ^{+0.37} _{-0.31}	3.34 ^{+0.22} _{-0.22}	0.97 ^{+0.59} _{-0.65}	I	0	1.81	254	246
AP3300	9.50 ^{+0.20} _{-0.10}	5.04 ^{+0.04} _{-0.10}	0.55 ^{+0.05} _{-0.45}	8.85 ^{+0.03} _{-0.14}	4.72 ^{+0.03} _{-0.05}	1.69 ^{+0.19} _{-0.07}	I	0	1.54	241	193
AP3303	8.10 ^{+0.20} _{-0.50}	2.82 ^{+0.02} _{-0.14}	0.75 ^{+0.10} _{-0.15}	8.60 ^{+0.26} _{-0.25}	2.78 ^{+0.17} _{-0.16}	0.41 ^{+0.41} _{-0.36}	I	0	1.41	121	107
AP3304	7.30 ^{+0.10} _{-0.20}	2.67 ^{+0.02} _{-0.01}	0.40 ^{+0.10} _{-0.00}	6.80 ^{+0.35} _{-0.42}	2.71 ^{+0.23} _{-0.27}	0.71 ^{+0.17} _{-0.17}	I	0	1.46	140	152
AP3306	8.00 ^{+0.00} _{-0.20}	3.49 ^{+0.00} _{-0.08}	1.90 ^{+0.10} _{-0.05}	8.25 ^{+0.12} _{-0.13}	2.77 ^{+0.13} _{-0.11}	0.13 ^{+0.16} _{-0.13}	I	0	2.09	210	146
AP3308	8.70 ^{+0.00} _{-0.00}	3.04 ^{+0.04} _{-0.01}	0.10 ^{+0.05} _{-0.10}	7.38 ^{+0.85} _{-0.88}	2.56 ^{+0.31} _{-0.31}	0.79 ^{+0.58} _{-0.59}	I	0	1.79	84	43
AP3309	8.20 ^{+0.00} _{-1.30}	2.63 ^{+0.01} _{-0.16}	0.80 ^{+0.50} _{-0.10}	7.85 ^{+0.03} _{-0.03}	2.18 ^{+0.05} _{-0.06}	0.20 ^{+0.07} _{-0.07}	I	0	1.40	72	44
AP3310	8.20 ^{+0.10} _{-0.90}	2.66 ^{+0.01} _{-0.07}	0.30 ^{+0.25} _{-0.05}	8.00 ^{+0.25} _{-0.21}	2.49 ^{+0.15} _{-0.15}	0.28 ^{+0.27} _{-0.25}	I	0	1.08	58	36
AP3311	8.40 ^{+0.00} _{-0.10}	3.65 ^{+0.07} _{-0.10}	2.40 ^{+0.15} _{-0.10}	8.55 ^{+0.28} _{-0.23}	3.62 ^{+0.11} _{-0.05}	1.76 ^{+0.30} _{-0.32}	I	0	1.17	104	55
AP3312	8.70 ^{+0.10} _{-0.30}	3.02 ^{+0.02} _{-0.07}	0.00 ^{+0.60} _{-0.15}	7.09 ^{+0.74} _{-0.72}	3.34 ^{+0.33} _{-0.30}	2.25 ^{+0.55} _{-0.57}	I	0	2.04	353	331
AP3319	7.60 ^{+0.30} _{-0.50}	2.75 ^{+0.06} _{-0.04}	0.95 ^{+0.15} _{-0.05}	6.92 ^{+0.23} _{-0.23}	2.48 ^{+0.25} _{-0.25}	1.58 ^{+0.14} _{-0.14}	I	0	1.32	62	38
AP3320	8.00 ^{+0.00} _{-0.40}	2.58 ^{+0.00} _{-0.09}	0.70 ^{+0.20} _{-0.05}	7.14 ^{+0.96} _{-0.77}	3.33 ^{+0.33} _{-0.34}	0.63 ^{+0.41} _{-0.49}	I	0	1.58	46	31
AP3322	9.20 ^{+0.00} _{-0.10}	4.14 ^{+0.00} _{-0.22}	0.40 ^{+0.00} _{-0.20}	8.90 ^{+0.10} _{-0.25}	3.83 ^{+0.09} _{-0.12}	1.06 ^{+0.31} _{-0.24}	I	0	1.82	226	164
AP3325	9.10 ^{+0.00} _{-0.00}	3.79 ^{+0.06} _{-0.01}	0.25 ^{+0.15} _{-0.00}	7.78 ^{+0.13} _{-0.13}	3.66 ^{+0.13} _{-0.13}	1.66 ^{+0.25} _{-0.24}	I	0	1.99	244	196
AP3327	6.60 ^{+0.40} _{-0.00}	2.73 ^{+0.00} _{-0.03}	0.95 ^{+0.00} _{-0.10}	6.76 ^{+0.05} _{-0.05}	2.48 ^{+0.23} _{-0.15}	0.84 ^{+0.11} _{-0.11}	I	0	2.44	118	92
AP3331	8.70 ^{+0.10} _{-0.60}	3.13 ^{+0.00} _{-0.20}	0.55 ^{+0.25} _{-0.20}	8.29 ^{+1.33} _{-1.32}	3.39 ^{+0.85} _{-0.79}	1.49 ^{+1.00} _{-1.00}	I	0	1.54	121	98
AP3332	8.50 ^{+0.00} _{-1.00}	2.61 ^{+0.01} _{-0.18}	0.05 ^{+0.35} _{-0.00}	8.65 ^{+0.66} _{-0.77}	3.64 ^{+0.16} _{-0.13}	0.86 ^{+1.03} _{-0.83}	I	0	1.49	144	143
AP3333	7.40 ^{+0.40} _{-0.30}	2.73 ^{+0.04} _{-0.03}	0.60 ^{+0.10} _{-0.10}	8.12 ^{+0.08} _{-0.08}	2.89 ^{+0.10} _{-0.10}	0.10 ^{+0.14} _{-0.10}	I	0	1.13	87	74
AP3338	9.10 ^{+0.70} _{-0.00}	4.01 ^{+0.69} _{-0.00}	0.65 ^{+0.10} _{-0.30}	9.65 ^{+0.42} _{-0.70}	4.14 ^{+0.17} _{-0.18}	0.43 ^{+0.68} _{-0.40}	I	0	2.36	372	295
AP3339	9.00 ^{+0.00} _{-0.10}	3.45 ^{+0.07} _{-0.06}	0.15 ^{+0.35} _{-0.00}	9.49 ^{+0.41} _{-0.51}	3.34 ^{+0.21} _{-0.21}	0.30 ^{+0.41} _{-0.29}	I	0	1.07	88	54
AP3342	6.80 ^{+2.60} _{-0.10}	2.00 ^{+1.22} _{-2.00}	1.00 ^{+0.85} _{-0.40}	7.54 ^{+0.45} _{-0.57}	2.48 ^{+0.13} _{-0.15}	0.18 ^{+0.18} _{-0.17}	I	0	1.41	41	31
AP3345	8.40 ^{+0.40} _{-0.60}	3.21 ^{+0.40} _{-0.26}	1.85 ^{+0.80} _{-0.35}	9.31 ^{+0.37} _{-0.28}	3.75 ^{+0.14} _{-0.14}	0.44 ^{+0.31} _{-0.37}	I	0	1.39	93	54
AP3346	8.80 ^{+0.00} _{-0.70}	3.34 ^{+0.03} _{-0.18}	0.50 ^{+1.00} _{-0.10}	8.83 ^{+0.57} _{-0.49}	3.36 ^{+0.26} _{-0.25}	0.93 ^{+0.62} _{-0.61}	I	0	1.48	145	84
AP3350	8.10 ^{+0.50} _{-0.00}	3.45 ^{+0.09} _{-0.02}	1.60 ^{+0.00} _{-0.65}	9.22 ^{+0.23} _{-0.18}	3.60 ^{+0.15} _{-0.13}	0.62 ^{+0.26} _{-0.29}	I	0	1.39	134	100
AP3351	9.10 ^{+0.00} _{-1.40}	3.76 ^{+0.04} _{-1.39}	0.40 ^{+0.55} _{-0.05}	7.51 ^{+0.52} _{-0.57}	2.82 ^{+0.17} _{-0.16}	0.84 ^{+0.46} _{-0.48}	I	0	1.43	151	129
AP3352	9.10 ^{+0.10} _{-0.20}	3.92 ^{+0.00} _{-0.46}	0.75 ^{+0.50} _{-0.55}	8.79 ^{+0.28} _{-0.24}	4.08 ^{+0.11} _{-0.11}	1.98 ^{+0.39} _{-0.56}	I	0	1.63	176	115
AP3356	9.50 ^{+0.10} _{-0.30}	4.15 ^{+0.03} _{-0.36}	0.05 ^{+0.25} _{-0.05}	8.58 ^{+0.16} _{-0.16}	2.57 ^{+0.14} _{-0.14}	0.25 ^{+0.25} _{-0.22}	I	0	1.10	75	54
AP3357	7.20 ^{+0.30} _{-0.40}	2.70 ^{+0.07} _{-0.04}	0.60 ^{+0.15} _{-0.10}	7.85 ^{+0.04} _{-0.03}	2.55 ^{+0.08} _{-0.08}	0.03 ^{+0.07} _{-0.03}	I	0	1.60	200	168

Table 1 (cont'd)

AP ID ^a	CMD Best Fit Parameters ^b			Integrated Best Fit Parameters ^c			Best ^d Flag ^e	R _{ap} ^f	N _{stars} ^g	N _{bg} ^h	
	log(<i>t</i> [Myr])	log(<i>M</i> [<i>M</i> _⊙])	<i>A_V</i> [mag]	log(<i>t</i> [Myr])	log(<i>M</i> [<i>M</i> _⊙])	<i>A_V</i> [mag]					
AP3359	9.90 ^{+0.00} _{-0.20}	4.59 ^{+0.01} _{-0.16}	0.20 ^{+0.10} _{-0.05}	9.39 ^{+0.67} _{-0.71}	3.85 ^{+0.20} _{-0.18}	1.18 ^{+0.84} _{-0.63}	I	0	1.67	116	87
AP3360	7.20 ^{+0.00} _{-0.30}	2.73 ^{+0.00} _{-0.04}	0.65 ^{+0.10} _{-0.00}	7.00 ^{+0.09} _{-0.09}	2.58 ^{+0.33} _{-0.32}	0.51 ^{+0.09} _{-0.09}	I	0	1.75	185	175
AP3361	8.80 ^{+0.10} _{-0.70}	2.98 ^{+0.11} _{-0.08}	0.00 ^{+1.15} _{-0.25}	8.62 ^{+0.12} _{-0.12}	2.53 ^{+0.15} _{-0.14}	0.29 ^{+0.22} _{-0.22}	I	0	1.08	66	63
AP3363	9.10 ^{+0.00} _{-1.10}	3.28 ^{+0.01} _{-0.16}	0.00 ^{+1.70} _{-0.00}	9.08 ^{+0.26} _{-0.13}	3.19 ^{+0.16} _{-0.16}	0.31 ^{+0.13} _{-0.29}	I	0	1.10	84	53
AP3364	9.10 ^{+0.00} _{-0.70}	3.89 ^{+0.11} _{-1.42}	0.40 ^{+1.05} _{-0.10}	8.46 ^{+0.29} _{-0.25}	2.85 ^{+0.17} _{-0.15}	0.50 ^{+0.45} _{-0.43}	I	0	1.55	175	157
AP3365	8.10 ^{+0.10} _{-0.40}	3.12 ^{+0.01} _{-0.29}	1.20 ^{+0.05} _{-0.40}	8.78 ^{+0.19} _{-0.22}	3.17 ^{+0.12} _{-0.12}	0.33 ^{+0.31} _{-0.29}	I	0	1.56	165	140
AP3366	8.10 ^{+0.10} _{-0.00}	3.25 ^{+0.00} _{-0.08}	1.80 ^{+0.05} _{-0.20}	8.43 ^{+0.13} _{-0.10}	3.23 ^{+0.15} _{-0.12}	1.29 ^{+0.28} _{-0.29}	I	0	1.04	79	45
AP3367	7.60 ^{+0.10} _{-0.20}	3.58 ^{+0.00} _{-0.06}	2.05 ^{+0.05} _{-0.05}	7.56 ^{+0.13} _{-0.12}	3.78 ^{+0.08} _{-0.08}	1.28 ^{+0.18} _{-0.19}	I	0	1.86	245	188
AP3371	8.20 ^{+0.20} _{-0.00}	3.33 ^{+0.04} _{-0.03}	1.05 ^{+0.05} _{-0.30}	8.74 ^{+0.44} _{-0.41}	3.62 ^{+0.14} _{-0.12}	0.89 ^{+0.52} _{-0.64}	I	0	2.20	294	230
AP3372	8.80 ^{+0.10} _{-1.70}	2.96 ^{+0.22} _{-1.52}	0.85 ^{+0.80} _{-0.15}	8.11 ^{+1.47} _{-1.46}	3.78 ^{+1.25} _{-1.18}	1.45 ^{+1.03} _{-1.02}	I	0	1.29	62	33
AP3375	6.60 ^{+0.40} _{-0.00}	2.79 ^{+0.03} _{-0.03}	2.05 ^{+0.00} _{-0.15}	6.84 ^{+0.23} _{-0.21}	2.72 ^{+0.24} _{-0.25}	1.65 ^{+0.14} _{-0.15}	I	0	1.19	60	57
AP3377	8.00 ^{+0.20} _{-0.80}	2.80 ^{+0.01} _{-0.13}	0.55 ^{+0.65} _{-0.15}	7.75 ^{+0.08} _{-0.07}	3.27 ^{+0.09} _{-0.09}	0.97 ^{+0.12} _{-0.13}	I	0	1.56	131	106
AP3378	8.20 ^{+0.70} _{-0.00}	3.25 ^{+0.12} _{-0.04}	1.70 ^{+0.00} _{-1.25}	9.35 ^{+0.27} _{-0.25}	3.32 ^{+0.17} _{-0.17}	0.31 ^{+0.26} _{-0.27}	I	0	1.15	79	65
AP3379	7.50 ^{+0.40} _{-0.40}	2.86 ^{+0.02} _{-0.05}	0.60 ^{+0.05} _{-0.10}	9.59 ^{+0.09} _{-0.01}	3.56 ^{+0.08} _{-0.04}	0.15 ^{+0.13} _{-0.15}	I	0	1.65	117	95
AP3380	8.80 ^{+0.00} _{-1.10}	2.61 ^{+0.01} _{-0.48}	0.15 ^{+1.05} _{-0.10}	9.51 ^{+0.28} _{-0.25}	3.28 ^{+0.16} _{-0.16}	0.26 ^{+0.25} _{-0.22}	I	0	1.06	55	37
AP3382	8.60 ^{+0.00} _{-1.40}	2.72 ^{+0.03} _{-0.27}	0.00 ^{+0.45} _{-0.05}	8.05 ^{+0.26} _{-0.30}	2.78 ^{+0.26} _{-0.26}	0.59 ^{+0.61} _{-0.51}	I	0	2.02	127	97
AP3383	7.50 ^{+0.20} _{-0.30}	2.99 ^{+0.01} _{-0.06}	1.30 ^{+0.05} _{-0.10}	7.04 ^{+0.18} _{-0.16}	2.86 ^{+0.26} _{-0.30}	1.96 ^{+0.16} _{-0.16}	I	0	1.36	146	128
AP3384	7.80 ^{+0.10} _{-0.70}	2.88 ^{+0.01} _{-0.05}	0.50 ^{+0.15} _{-0.00}	7.50 ^{+0.18} _{-0.13}	2.52 ^{+0.19} _{-0.18}	0.05 ^{+0.09} _{-0.05}	I	0	2.11	215	199
AP3386	8.30 ^{+0.00} _{-0.50}	3.25 ^{+0.02} _{-0.18}	1.50 ^{+0.15} _{-0.10}	7.93 ^{+0.09} _{-0.14}	3.11 ^{+0.13} _{-0.12}	1.55 ^{+0.27} _{-0.23}	I	0	1.50	113	76
AP3387	7.30 ^{+0.30} _{-0.20}	3.30 ^{+0.06} _{-0.05}	2.35 ^{+0.10} _{-0.10}	7.79 ^{+0.07} _{-0.24}	3.36 ^{+0.21} _{-0.24}	1.88 ^{+0.47} _{-0.29}	I	1	1.15	100	77
AP3388	9.00 ^{+0.00} _{-0.10}	3.77 ^{+0.00} _{-0.08}	0.35 ^{+0.20} _{-0.15}	6.76 ^{+0.06} _{-0.07}	2.41 ^{+0.17} _{-0.14}	1.53 ^{+0.08} _{-0.09}	I	0	1.45	121	88
AP3389	8.00 ^{+0.00} _{-0.00}	3.44 ^{+0.01} _{-0.02}	1.50 ^{+0.00} _{-0.05}	7.82 ^{+0.03} _{-0.05}	2.36 ^{+0.03} _{-0.09}	0.14 ^{+0.05} _{-0.10}	I	0	1.68	103	32
AP3391	8.60 ^{+0.00} _{-0.10}	3.20 ^{+0.03} _{-0.03}	0.70 ^{+0.15} _{-0.10}	8.66 ^{+0.20} _{-0.21}	2.81 ^{+0.17} _{-0.16}	0.65 ^{+0.35} _{-0.38}	I	0	1.30	65	51
AP3393	8.00 ^{+0.10} _{-0.10}	3.39 ^{+0.37} _{-0.15}	2.10 ^{+0.70} _{-0.05}	8.88 ^{+0.35} _{-0.49}	3.31 ^{+0.20} _{-0.21}	0.57 ^{+0.48} _{-0.42}	I	0	1.27	139	107
AP3394	8.30 ^{+0.00} _{-0.40}	3.19 ^{+0.00} _{-0.09}	0.80 ^{+0.20} _{-0.00}	8.99 ^{+0.12} _{-0.10}	3.19 ^{+0.12} _{-0.11}	0.03 ^{+0.07} _{-0.03}	I	0	1.22	98	57
AP3395	6.70 ^{+0.40} _{-0.10}	2.85 ^{+0.00} _{-0.03}	0.45 ^{+0.00} _{-0.05}	6.85 ^{+0.12} _{-0.10}	2.80 ^{+0.27} _{-0.27}	0.06 ^{+0.09} _{-0.06}	I	0	2.06	182	120
AP3396	7.00 ^{+1.90} _{-0.20}	2.29 ^{+0.10} _{-0.06}	0.90 ^{+0.10} _{-0.30}	6.67 ^{+0.10} _{-0.07}	2.63 ^{+0.29} _{-0.29}	1.38 ^{+0.15} _{-0.15}	I	0	2.14	227	233
AP3398	8.50 ^{+0.00} _{-0.30}	3.13 ^{+0.01} _{-0.11}	0.75 ^{+0.15} _{-0.15}	8.37 ^{+0.20} _{-0.21}	2.71 ^{+0.14} _{-0.15}	0.26 ^{+0.28} _{-0.24}	I	0	1.31	120	93
AP3399	7.80 ^{+0.00} _{-0.60}	3.11 ^{+0.00} _{-0.10}	1.05 ^{+0.15} _{-0.00}	8.32 ^{+0.11} _{-0.11}	3.37 ^{+0.11} _{-0.11}	0.50 ^{+0.25} _{-0.28}	I	0	1.15	130	117
AP3404	8.20 ^{+0.00} _{-0.00}	2.91 ^{+0.01} _{-0.02}	0.50 ^{+0.05} _{-0.05}	8.11 ^{+0.09} _{-0.26}	2.36 ^{+0.02} _{-0.26}	0.05 ^{+0.10} _{-0.05}	I	0	1.37	96	79
AP3405	8.30 ^{+0.10} _{-0.00}	3.45 ^{+0.04} _{-0.16}	2.15 ^{+0.15} _{-0.30}	9.65 ^{+0.03} _{-0.03}	3.45 ^{+0.03} _{-0.03}	0.20 ^{+0.07} _{-0.07}	I	0	1.15	85	52
AP3406	8.20 ^{+0.20} _{-0.50}	2.93 ^{+0.02} _{-0.09}	1.30 ^{+0.15} _{-0.20}	8.49 ^{+0.07} _{-0.07}	2.17 ^{+0.11} _{-0.11}	0.20 ^{+0.16} _{-0.16}	I	0	1.00	30	16
AP3407	9.10 ^{+0.20} _{-0.10}	3.12 ^{+0.40} _{-0.57}	0.25 ^{+0.35} _{-0.15}	8.79 ^{+0.46} _{-0.45}	3.01 ^{+0.20} _{-0.20}	0.76 ^{+0.58} _{-0.56}	I	0	1.10	61	27

Table 1 (cont'd)

AP ID ^a	CMD Best Fit Parameters ^b			Integrated Best Fit Parameters ^c			Best ^d Flag ^e	Rap ^f	N _{stars} ^g	N _{bg} ^h	
	log(<i>t</i> [Myr])	log(<i>M</i> [<i>M</i> _⊙])	<i>A_V</i> [mag]	log(<i>t</i> [Myr])	log(<i>M</i> [<i>M</i> _⊙])	<i>A_V</i> [mag]					
AP3415	7.90 ^{+0.10} _{-0.50}	2.90 ^{+0.02} _{-0.09}	1.00 ^{+0.15} _{-0.05}	7.90 ^{+0.04} _{-0.14}	2.54 ^{+0.18} _{-0.24}	0.48 ^{+0.24} _{-0.27}	I	0	1.10	74	61
AP3417	8.00 ^{+0.10} _{-0.00}	2.95 ^{+0.00} _{-0.05}	0.80 ^{+0.05} _{-0.15}	8.39 ^{+0.51} _{-0.43}	3.34 ^{+0.24} _{-0.25}	0.82 ^{+0.68} _{-0.69}	I	0	2.02	184	148
AP3419	7.90 ^{+0.60} _{-0.00}	3.68 ^{+0.00} _{-0.83}	2.80 ^{+0.00} _{-0.95}	8.99 ^{+0.74} _{-0.50}	3.37 ^{+0.25} _{-0.26}	0.94 ^{+0.61} _{-0.71}	I	0	1.31	123	89
AP3421	8.80 ^{+0.00} _{-0.10}	3.16 ^{+0.01} _{-0.19}	0.25 ^{+0.35} _{-0.05}	6.70 ^{+0.14} _{-0.16}	2.53 ^{+0.30} _{-0.37}	0.83 ^{+0.11} _{-0.10}	I	0	1.72	90	54
AP3424	7.60 ^{+0.10} _{-0.60}	2.82 ^{+0.02} _{-0.15}	1.15 ^{+0.25} _{-0.05}	7.76 ^{+0.24} _{-0.20}	3.41 ^{+0.10} _{-0.10}	1.19 ^{+0.25} _{-0.34}	I	0	1.28	85	80
AP3427	9.10 ^{+0.00} _{-1.40}	3.37 ^{+0.01} _{-0.98}	0.00 ^{+1.55} _{-0.05}	8.85 ^{+0.14} _{-0.14}	2.98 ^{+0.10} _{-0.11}	0.54 ^{+0.25} _{-0.28}	I	0	1.30	110	88
AP3429	9.00 ^{+0.10} _{-0.00}	3.75 ^{+0.07} _{-0.04}	0.30 ^{+0.15} _{-0.10}	9.01 ^{+0.95} _{-0.46}	3.73 ^{+0.23} _{-0.14}	1.08 ^{+0.53} _{-0.90}	I	0	1.55	177	117
AP3430	7.30 ^{+0.00} _{-0.30}	3.26 ^{+0.00} _{-0.08}	1.10 ^{+0.10} _{-0.20}	7.14 ^{+0.29} _{-0.32}	3.66 ^{+0.17} _{-0.12}	1.45 ^{+0.23} _{-0.21}	I	0	2.51	471	413
AP3432	8.90 ^{+0.00} _{-0.40}	3.32 ^{+0.05} _{-0.14}	0.10 ^{+0.90} _{-0.00}	7.72 ^{+0.72} _{-0.79}	3.21 ^{+0.23} _{-0.21}	1.69 ^{+0.85} _{-1.05}	I	0	1.33	119	81
AP3433	8.30 ^{+0.00} _{-1.10}	2.79 ^{+0.02} _{-0.15}	0.45 ^{+0.35} _{-0.05}	8.31 ^{+0.13} _{-0.13}	2.64 ^{+0.16} _{-0.18}	0.30 ^{+0.28} _{-0.26}	I	0	1.03	71	64
AP3434	8.80 ^{+0.00} _{-0.10}	3.30 ^{+0.01} _{-0.11}	0.25 ^{+0.15} _{-0.10}	8.61 ^{+0.09} _{-0.09}	2.73 ^{+0.09} _{-0.08}	0.11 ^{+0.15} _{-0.11}	I	0	1.22	81	68
AP3435	8.50 ^{+0.00} _{-0.50}	3.02 ^{+0.03} _{-0.19}	0.65 ^{+0.45} _{-0.00}	9.00 ^{+0.22} _{-0.12}	3.00 ^{+0.20} _{-0.13}	0.02 ^{+0.07} _{-0.02}	I	0	1.67	141	114
AP3436	8.00 ^{+0.00} _{-0.90}	2.66 ^{+0.03} _{-0.12}	0.50 ^{+0.20} _{-0.00}	8.44 ^{+0.09} _{-0.07}	2.62 ^{+0.12} _{-0.11}	0.03 ^{+0.07} _{-0.03}	I	0	1.15	40	26
AP3437	8.70 ^{+0.00} _{-0.90}	2.81 ^{+0.01} _{-0.18}	0.00 ^{+0.55} _{-0.10}	7.59 ^{+0.98} _{-0.95}	2.77 ^{+0.34} _{-0.39}	1.04 ^{+0.77} _{-0.76}	I	0	1.12	63	48
AP3442	8.70 ^{+0.10} _{-0.10}	3.06 ^{+0.00} _{-0.11}	0.55 ^{+0.05} _{-0.40}	8.55 ^{+0.11} _{-0.11}	3.11 ^{+0.11} _{-0.10}	0.57 ^{+0.24} _{-0.24}	I	0	1.25	87	59
AP3444	6.80 ^{+1.10} _{-0.00}	2.68 ^{+0.13} _{-0.08}	1.20 ^{+0.05} _{-0.35}	6.96 ^{+0.08} _{-0.09}	2.39 ^{+0.20} _{-0.25}	0.85 ^{+0.10} _{-0.10}	I	0	1.22	82	69
AP3446	8.30 ^{+0.40} _{-0.60}	3.11 ^{+0.00} _{-0.58}	1.30 ^{+0.45} _{-0.40}	0.00 ^{+0.00} _{-0.00}	0.00 ^{+0.00} _{-0.00}	0.00 ^{+0.00} _{-0.00}	I	0	1.20	111	112
AP3450	7.60 ^{+0.10} _{-0.40}	3.05 ^{+0.02} _{-0.03}	0.50 ^{+0.15} _{-0.05}	7.95 ^{+0.12} _{-0.13}	3.61 ^{+0.08} _{-0.09}	0.48 ^{+0.19} _{-0.22}	I	0	1.61	154	127
AP3451	8.80 ^{+0.00} _{-1.90}	2.80 ^{+0.00} _{-0.32}	0.00 ^{+0.90} _{-0.00}	8.10 ^{+1.47} _{-1.46}	3.78 ^{+1.25} _{-1.18}	1.45 ^{+1.02} _{-1.02}	I	0	1.12	36	24
AP3452	7.20 ^{+0.10} _{-0.40}	2.67 ^{+0.00} _{-0.02}	0.35 ^{+0.10} _{-0.00}	7.06 ^{+0.54} _{-0.62}	2.79 ^{+0.24} _{-0.26}	0.23 ^{+0.22} _{-0.21}	I	0	1.78	100	80
AP3453	8.20 ^{+0.10} _{-0.50}	2.55 ^{+0.03} _{-0.10}	0.50 ^{+0.15} _{-0.05}	8.29 ^{+0.11} _{-0.12}	2.27 ^{+0.17} _{-0.16}	0.13 ^{+0.15} _{-0.13}	I	0	1.04	64	36
AP3454	8.30 ^{+0.10} _{-0.60}	2.69 ^{+0.02} _{-0.08}	0.45 ^{+0.15} _{-0.10}	8.34 ^{+0.05} _{-0.05}	2.20 ^{+0.11} _{-0.11}	0.03 ^{+0.07} _{-0.03}	I	0	0.96	30	13
AP3455	7.10 ^{+0.00} _{-0.20}	2.74 ^{+0.00} _{-0.04}	1.15 ^{+0.10} _{-0.05}	6.73 ^{+0.08} _{-0.07}	2.39 ^{+0.39} _{-0.37}	0.84 ^{+0.11} _{-0.11}	I	0	1.30	109	93
AP3456	8.50 ^{+0.00} _{-0.10}	2.65 ^{+0.27} _{-0.00}	0.05 ^{+0.85} _{-0.00}	8.70 ^{+0.12} _{-0.11}	2.89 ^{+0.10} _{-0.10}	0.32 ^{+0.19} _{-0.20}	I	0	1.15	53	36
AP3457	7.80 ^{+0.20} _{-0.30}	2.77 ^{+0.01} _{-0.07}	0.95 ^{+0.05} _{-0.20}	7.09 ^{+0.67} _{-0.71}	2.52 ^{+0.25} _{-0.24}	1.12 ^{+0.51} _{-0.56}	I	0	1.21	93	73
AP3458	9.60 ^{+0.00} _{-1.60}	4.35 ^{+0.00} _{-0.74}	0.00 ^{+2.65} _{-0.00}	10.20 ^{+0.05} _{-0.06}	4.43 ^{+0.07} _{-0.07}	0.30 ^{+0.13} _{-0.13}	I	0	1.58	216	176
AP3462	8.90 ^{+0.00} _{-0.60}	3.04 ^{+0.00} _{-0.28}	0.25 ^{+1.00} _{-0.05}	8.05 ^{+0.47} _{-0.21}	2.27 ^{+0.64} _{-0.27}	0.88 ^{+0.21} _{-0.27}	I	0	1.27	83	62
AP3463	9.00 ^{+0.00} _{-0.00}	3.47 ^{+0.05} _{-0.04}	0.10 ^{+0.05} _{-0.10}	8.68 ^{+0.19} _{-0.21}	2.98 ^{+0.15} _{-0.17}	0.73 ^{+0.34} _{-0.35}	I	0	1.13	115	86
AP3464	0.00 ^{+0.00} _{-0.00}	0.00 ^{+0.00} _{-0.00}	0.00 ^{+0.00} _{-0.00}	0.00 ^{+0.00} _{-0.00}	0.00 ^{+0.00} _{-0.00}	0.00 ^{+0.00} _{-0.00}	I	0	1.24	0	0
AP3469	8.40 ^{+0.10} _{-0.40}	3.08 ^{+0.03} _{-0.09}	0.85 ^{+0.35} _{-0.10}	9.03 ^{+0.72} _{-0.59}	3.54 ^{+0.20} _{-0.17}	0.90 ^{+0.65} _{-0.72}	I	0	1.18	106	89
AP3470	8.20 ^{+0.20} _{-0.50}	2.92 ^{+0.03} _{-0.10}	1.15 ^{+0.15} _{-0.10}	8.08 ^{+0.28} _{-0.28}	2.55 ^{+0.22} _{-0.21}	0.57 ^{+0.51} _{-0.47}	I	0	1.16	65	31
AP3472	9.40 ^{+0.20} _{-0.60}	4.44 ^{+0.14} _{-1.35}	0.00 ^{+0.80} _{-0.00}	8.44 ^{+0.10} _{-0.11}	3.99 ^{+0.09} _{-0.08}	1.83 ^{+0.23} _{-0.20}	I	0	1.12	128	114
AP3474	7.30 ^{+0.40} _{-0.30}	3.11 ^{+0.08} _{-0.02}	1.25 ^{+0.15} _{-0.00}	7.73 ^{+0.12} _{-0.09}	3.34 ^{+0.10} _{-0.13}	0.99 ^{+0.18} _{-0.20}	I	0	1.32	136	98

Table 1 (cont'd)

AP ID ^a	CMD Best Fit Parameters ^b			Integrated Best Fit Parameters ^c			Best ^d Flag ^e	R _{ap} ^f	N _{stars} ^g	N _{bg} ^h	
	log(<i>t</i> [Myr])	log(<i>M</i> [<i>M</i> _⊙])	<i>A_V</i> [mag]	log(<i>t</i> [Myr])	log(<i>M</i> [<i>M</i> _⊙])	<i>A_V</i> [mag]					
AP3478	8.20 ^{+0.10} _{-1.00}	3.12 ^{+0.07} _{-0.44}	1.60 ^{+0.00} _{-0.50}	8.53 ^{+0.28} _{-0.26}	2.84 ^{+0.19} _{-0.17}	0.46 ^{+0.42} _{-0.39}	I	0	1.38	104	95
AP3480	8.80 ^{+0.10} _{-0.10}	3.28 ^{+0.07} _{-0.06}	0.40 ^{+0.45} _{-0.10}	8.05 ^{+0.18} _{-0.21}	3.44 ^{+0.17} _{-0.18}	1.67 ^{+0.37} _{-0.31}	I	0	1.35	153	121
AP3481	9.10 ^{+0.00} _{-0.10}	3.28 ^{+0.07} _{-0.15}	0.25 ^{+0.35} _{-0.00}	8.14 ^{+0.09} _{-0.10}	2.34 ^{+0.19} _{-0.22}	0.85 ^{+0.30} _{-0.33}	I	0	1.06	58	29
AP3482	8.10 ^{+0.20} _{-1.20}	2.69 ^{+0.01} _{-0.16}	0.40 ^{+0.25} _{-0.05}	7.79 ^{+0.07} _{-0.07}	2.68 ^{+0.11} _{-0.14}	0.11 ^{+0.12} _{-0.11}	I	0	1.72	265	246
AP3483	8.80 ^{+0.10} _{-0.00}	3.47 ^{+0.03} _{-0.06}	0.50 ^{+0.00} _{-0.30}	9.04 ^{+0.32} _{-0.23}	3.47 ^{+0.13} _{-0.10}	0.42 ^{+0.31} _{-0.34}	I	0	1.21	101	52
AP3484	7.10 ^{+0.10} _{-0.20}	3.09 ^{+0.03} _{-0.01}	1.45 ^{+0.20} _{-0.00}	8.12 ^{+1.39} _{-1.32}	2.97 ^{+0.46} _{-0.53}	1.38 ^{+0.98} _{-0.95}	I	0	1.30	93	90
AP3488	6.80 ^{+0.40} _{-0.30}	2.46 ^{+0.02} _{-0.02}	0.85 ^{+0.05} _{-0.10}	7.81 ^{+0.19} _{-0.19}	2.93 ^{+0.11} _{-0.12}	0.45 ^{+0.24} _{-0.23}	I	0	1.03	84	79
AP3489	7.90 ^{+0.50} _{-0.30}	2.94 ^{+0.08} _{-0.13}	1.50 ^{+0.10} _{-0.40}	9.20 ^{+0.67} _{-0.73}	3.77 ^{+0.18} _{-0.17}	0.91 ^{+0.84} _{-0.71}	I	0	1.27	118	93
AP3490	7.30 ^{+0.40} _{-0.50}	2.89 ^{+0.04} _{-0.23}	2.10 ^{+0.20} _{-0.70}	7.09 ^{+0.13} _{-0.12}	2.38 ^{+0.20} _{-0.20}	0.56 ^{+0.12} _{-0.13}	I	0	1.20	68	68
AP3492	7.30 ^{+0.30} _{-0.00}	3.47 ^{+0.07} _{-0.11}	3.00 ^{+0.00} _{-0.20}	7.61 ^{+0.03} _{-0.04}	2.03 ^{+0.04} _{-0.03}	0.42 ^{+0.08} _{-0.10}	I	1	1.36	106	66
AP3493	9.20 ^{+0.00} _{-0.00}	3.97 ^{+0.04} _{-0.06}	0.30 ^{+0.10} _{-0.05}	9.05 ^{+0.62} _{-0.59}	3.47 ^{+0.19} _{-0.15}	0.78 ^{+0.65} _{-0.64}	I	0	1.80	128	80
AP3496	8.80 ^{+0.10} _{-0.30}	3.26 ^{+0.08} _{-0.04}	0.40 ^{+0.80} _{-0.10}	8.72 ^{+0.79} _{-0.70}	3.81 ^{+0.16} _{-0.13}	1.74 ^{+0.86} _{-0.94}	I	0	1.20	109	84
AP3498	8.80 ^{+0.00} _{-0.00}	3.05 ^{+0.02} _{-0.01}	0.50 ^{+0.10} _{-0.10}	8.21 ^{+0.83} _{-0.71}	2.85 ^{+0.30} _{-0.36}	1.37 ^{+1.17} _{-1.12}	I	0	1.35	44	24
AP3499	10.10 ^{+0.50} _{-2.90}	4.83 ^{+1.78} _{-4.83}	0.00 ^{+2.50} _{-0.35}	7.79 ^{+0.04} _{-0.03}	2.05 ^{+0.04} _{-0.03}	0.02 ^{+0.07} _{-0.02}	I	0	1.24	131	74
AP3500	8.80 ^{+0.10} _{-0.80}	2.58 ^{+0.01} _{-0.23}	0.00 ^{+0.60} _{-0.05}	7.73 ^{+1.03} _{-1.04}	2.77 ^{+0.37} _{-0.43}	1.18 ^{+0.86} _{-0.86}	I	0	1.35	63	43
AP3501	8.30 ^{+0.00} _{-0.00}	3.08 ^{+0.01} _{-0.03}	0.95 ^{+0.05} _{-0.10}	8.62 ^{+0.13} _{-0.14}	2.75 ^{+0.11} _{-0.09}	0.26 ^{+0.24} _{-0.23}	I	0	1.31	95	66
AP3503	7.20 ^{+0.30} _{-0.20}	2.91 ^{+0.00} _{-0.03}	0.85 ^{+0.05} _{-0.10}	6.84 ^{+0.21} _{-0.17}	2.74 ^{+0.25} _{-0.25}	1.21 ^{+0.16} _{-0.16}	I	0	1.43	109	79
AP3504	8.20 ^{+0.10} _{-0.60}	2.78 ^{+0.03} _{-0.09}	0.70 ^{+0.20} _{-0.10}	7.23 ^{+0.48} _{-0.46}	3.18 ^{+0.18} _{-0.14}	2.20 ^{+0.40} _{-0.43}	I	0	1.13	79	61
AP3507	9.10 ^{+0.20} _{-1.00}	3.44 ^{+0.17} _{-3.44}	0.30 ^{+1.95} _{-0.05}	9.43 ^{+0.39} _{-0.35}	3.47 ^{+0.18} _{-0.16}	0.57 ^{+0.35} _{-0.38}	I	0	1.29	115	95
AP3508	8.90 ^{+0.30} _{-1.20}	3.42 ^{+0.12} _{-3.42}	0.95 ^{+1.40} _{-0.35}	8.69 ^{+0.10} _{-0.11}	2.53 ^{+0.14} _{-0.14}	0.22 ^{+0.22} _{-0.20}	I	0	1.31	121	82
AP3509	9.10 ^{+0.10} _{-0.00}	4.01 ^{+0.25} _{-0.01}	0.40 ^{+0.05} _{-0.10}	6.73 ^{+0.09} _{-0.10}	2.79 ^{+0.34} _{-0.27}	0.46 ^{+0.09} _{-0.08}	I	0	3.68	796	780
AP3510	0.00 ^{+0.00} _{-0.00}	0.00 ^{+0.00} _{-0.00}	0.00 ^{+0.00} _{-0.00}	0.00 ^{+0.00} _{-0.00}	0.00 ^{+0.00} _{-0.00}	0.00 ^{+0.00} _{-0.00}	I	0	1.98	0	0
AP3513	7.90 ^{+0.00} _{-0.50}	3.03 ^{+0.00} _{-0.09}	0.85 ^{+0.20} _{-0.05}	8.05 ^{+0.29} _{-0.29}	3.01 ^{+0.13} _{-0.14}	0.72 ^{+0.48} _{-0.48}	I	0	1.27	110	89
AP3515	7.90 ^{+1.90} _{-0.00}	3.65 ^{+0.41} _{-3.65}	3.00 ^{+0.50} _{-2.80}	9.40 ^{+0.74} _{-0.73}	3.72 ^{+0.23} _{-0.17}	1.05 ^{+0.80} _{-0.68}	I	0	1.26	95	50
AP3516	8.90 ^{+0.00} _{-1.60}	3.44 ^{+0.02} _{-0.67}	0.45 ^{+0.75} _{-0.05}	7.63 ^{+0.31} _{-0.30}	2.93 ^{+0.12} _{-0.12}	1.07 ^{+0.30} _{-0.31}	I	0	1.39	144	96
AP3517	8.00 ^{+0.10} _{-0.40}	2.99 ^{+0.02} _{-0.06}	0.45 ^{+0.10} _{-0.05}	8.04 ^{+0.07} _{-0.06}	2.55 ^{+0.14} _{-0.11}	0.30 ^{+0.19} _{-0.16}	I	0	1.14	55	12
AP3518	8.00 ^{+0.00} _{-0.10}	2.73 ^{+0.01} _{-0.05}	0.55 ^{+0.10} _{-0.05}	8.05 ^{+0.14} _{-0.17}	3.34 ^{+0.18} _{-0.15}	1.27 ^{+0.41} _{-0.34}	I	0	1.12	52	28
AP3519	7.70 ^{+0.00} _{-0.30}	3.08 ^{+0.00} _{-0.03}	0.70 ^{+0.10} _{-0.05}	6.90 ^{+0.11} _{-0.11}	2.51 ^{+0.32} _{-0.23}	0.79 ^{+0.10} _{-0.10}	I	0	1.75	180	170
AP3522	7.60 ^{+0.20} _{-0.30}	3.09 ^{+0.02} _{-0.04}	1.35 ^{+0.10} _{-0.05}	7.98 ^{+0.17} _{-0.14}	2.49 ^{+0.14} _{-0.14}	0.17 ^{+0.19} _{-0.17}	I	0	1.52	105	85
AP3524	0.00 ^{+0.00} _{-0.00}	0.00 ^{+0.00} _{-0.00}	0.00 ^{+0.00} _{-0.00}	0.00 ^{+0.00} _{-0.00}	0.00 ^{+0.00} _{-0.00}	0.00 ^{+0.00} _{-0.00}	I	0	1.25	0	0
AP3526	8.10 ^{+0.00} _{-1.10}	2.37 ^{+0.01} _{-0.17}	0.55 ^{+0.25} _{-0.00}	8.63 ^{+0.17} _{-0.16}	2.68 ^{+0.15} _{-0.16}	0.36 ^{+0.28} _{-0.28}	I	0	1.20	57	41
AP3530	7.70 ^{+0.00} _{-0.50}	2.98 ^{+0.00} _{-0.07}	1.45 ^{+0.10} _{-0.05}	7.75 ^{+0.22} _{-0.21}	3.09 ^{+0.08} _{-0.08}	1.45 ^{+0.24} _{-0.24}	I	0	1.16	93	68
AP3534	7.70 ^{+0.20} _{-0.50}	2.71 ^{+0.05} _{-0.05}	0.95 ^{+0.20} _{-0.05}	6.95 ^{+0.12} _{-0.11}	2.92 ^{+0.28} _{-0.42}	1.90 ^{+0.09} _{-0.09}	I	0	1.30	69	54

Table 1 (cont'd)

AP ID ^a	CMD Best Fit Parameters ^b			Integrated Best Fit Parameters ^c			Best ^d Flag ^e	Rap ^f	N _{stars} ^g	N _{bg} ^h	
	log(<i>t</i> [Myr])	log(<i>M</i> [<i>M</i> _⊙])	<i>A_V</i> [mag]	log(<i>t</i> [Myr])	log(<i>M</i> [<i>M</i> _⊙])	<i>A_V</i> [mag]					
AP3536	8.40 ^{+0.10} _{-0.00}	3.14 ^{+0.02} _{-0.02}	0.35 ^{+0.05} _{-0.15}	8.34 ^{+0.10} _{-0.08}	3.09 ^{+0.10} _{-0.11}	0.50 ^{+0.19} _{-0.24}	I	0	1.34	126	100
AP3537	7.70 ^{+0.00} _{-0.80}	2.58 ^{+0.01} _{-0.08}	0.60 ^{+0.15} _{-0.05}	7.83 ^{+0.06} _{-0.08}	2.50 ^{+0.13} _{-0.09}	0.29 ^{+0.15} _{-0.15}	I	0	1.36	120	108
AP3540	7.10 ^{+0.10} _{-0.10}	3.59 ^{+0.02} _{-0.05}	2.50 ^{+0.00} _{-0.15}	6.62 ^{+0.06} _{-0.07}	2.69 ^{+0.09} _{-0.12}	1.29 ^{+0.08} _{-0.07}	I	0	1.88	178	137
AP3541	9.20 ^{+0.20} _{-1.20}	3.81 ^{+0.02} _{-3.81}	0.45 ^{+1.60} _{-0.25}	9.29 ^{+0.51} _{-0.40}	3.56 ^{+0.21} _{-0.17}	0.56 ^{+0.46} _{-0.49}	I	0	1.45	128	74
AP3544	9.10 ^{+0.03} _{-0.00}	3.58 ^{+0.04} _{-0.09}	0.45 ^{+0.15} _{-0.05}	7.42 ^{+0.89} _{-0.91}	2.52 ^{+0.31} _{-0.30}	0.87 ^{+0.62} _{-0.64}	I	0	1.45	108	68
AP3547	8.10 ^{+0.00} _{-0.40}	3.26 ^{+0.00} _{-0.27}	1.60 ^{+0.20} _{-0.10}	6.66 ^{+0.16} _{-0.59}	2.71 ^{+0.22} _{-0.23}	1.12 ^{+0.33} _{-0.62}	I	0	1.25	112	81
AP3549	9.10 ^{+0.10} _{-0.00}	3.80 ^{+0.14} _{-0.04}	0.35 ^{+0.05} _{-0.05}	7.74 ^{+0.24} _{-0.23}	3.10 ^{+0.09} _{-0.09}	0.87 ^{+0.31} _{-0.30}	I	0	1.79	189	152
AP3551	8.40 ^{+0.10} _{-0.00}	3.55 ^{+0.04} _{-0.03}	1.00 ^{+0.05} _{-0.15}	8.67 ^{+0.15} _{-0.16}	3.34 ^{+0.11} _{-0.10}	0.76 ^{+0.27} _{-0.27}	I	0	1.32	140	88
AP3558	8.80 ^{+0.10} _{-1.20}	3.23 ^{+0.04} _{-0.88}	0.70 ^{+1.30} _{-0.05}	8.13 ^{+1.08} _{-0.40}	3.06 ^{+0.17} _{-0.18}	1.53 ^{+0.58} _{-1.29}	I	0	1.03	88	53
AP3559	8.80 ^{+0.00} _{-0.50}	3.10 ^{+0.00} _{-0.17}	0.20 ^{+0.70} _{-0.00}	8.11 ^{+0.24} _{-0.22}	2.51 ^{+0.18} _{-0.17}	0.36 ^{+0.35} _{-0.31}	I	0	1.31	125	106
AP3563	8.80 ^{+0.40} _{-1.40}	3.25 ^{+0.19} _{-3.25}	0.90 ^{+1.40} _{-0.50}	8.61 ^{+0.18} _{-0.18}	2.68 ^{+0.16} _{-0.17}	0.34 ^{+0.30} _{-0.29}	I	0	1.31	97	74
AP3567	9.10 ^{+0.10} _{-0.00}	3.22 ^{+0.15} _{-0.05}	0.10 ^{+0.20} _{-0.05}	7.59 ^{+0.42} _{-0.36}	2.92 ^{+0.16} _{-0.13}	1.71 ^{+0.40} _{-0.34}	I	0	0.96	45	24
AP3569	8.10 ^{+0.00} _{-0.60}	2.65 ^{+0.01} _{-0.09}	0.30 ^{+0.25} _{-0.05}	8.62 ^{+0.20} _{-0.19}	3.00 ^{+0.10} _{-0.11}	0.35 ^{+0.29} _{-0.29}	I	0	1.41	104	90
AP3572	9.10 ^{+0.00} _{-0.00}	4.08 ^{+0.02} _{-0.03}	0.15 ^{+0.10} _{-0.05}	8.23 ^{+0.29} _{-0.23}	3.42 ^{+0.18} _{-0.17}	0.79 ^{+0.45} _{-0.53}	I	0	1.76	284	192
AP3574	9.10 ^{+0.00} _{-0.00}	3.50 ^{+0.14} _{-0.09}	0.15 ^{+0.20} _{-0.05}	9.74 ^{+0.17} _{-0.17}	3.53 ^{+0.14} _{-0.13}	0.04 ^{+0.07} _{-0.04}	I	0	1.40	133	89
AP3578	6.70 ^{+0.40} _{-0.00}	2.82 ^{+0.00} _{-0.02}	0.75 ^{+0.00} _{-0.15}	6.93 ^{+0.11} _{-0.11}	2.81 ^{+0.37} _{-0.35}	0.78 ^{+0.08} _{-0.07}	I	0	1.13	124	110
AP3582	8.90 ^{+0.00} _{-1.40}	3.20 ^{+0.00} _{-0.42}	0.35 ^{+1.30} _{-0.05}	7.90 ^{+0.05} _{-0.20}	3.45 ^{+0.22} _{-0.29}	1.72 ^{+0.37} _{-0.32}	I	0	1.64	163	121
AP3583	8.90 ^{+0.00} _{-0.60}	3.28 ^{+0.02} _{-0.30}	0.50 ^{+1.00} _{-0.15}	8.70 ^{+0.34} _{-0.33}	2.92 ^{+0.17} _{-0.18}	0.67 ^{+0.49} _{-0.47}	I	0	1.19	95	63
AP3584	8.00 ^{+0.00} _{-0.60}	2.86 ^{+0.04} _{-0.06}	0.65 ^{+0.50} _{-0.05}	8.70 ^{+0.06} _{-0.06}	3.10 ^{+0.31} _{-0.26}	0.50 ^{+0.62} _{-0.50}	I	0	1.12	87	68
AP3586	8.80 ^{+0.00} _{-0.10}	3.01 ^{+0.02} _{-0.03}	0.25 ^{+0.30} _{-0.06}	7.83 ^{+0.20} _{-0.19}	2.88 ^{+0.08} _{-0.08}	1.26 ^{+0.16} _{-0.14}	I	0	1.22	61	27
AP3590	8.40 ^{+0.10} _{-0.50}	3.17 ^{+0.01} _{-0.15}	1.10 ^{+0.20} _{-0.10}	8.63 ^{+0.17} _{-0.17}	2.85 ^{+0.13} _{-0.13}	0.28 ^{+0.26} _{-0.25}	I	0	1.15	109	77
AP3593	8.00 ^{+0.00} _{-0.30}	2.84 ^{+0.08} _{-0.12}	0.75 ^{+0.35} _{-0.05}	7.45 ^{+0.36} _{-0.23}	3.46 ^{+0.17} _{-0.28}	2.02 ^{+0.34} _{-0.67}	I	0	1.28	104	67
AP3594	7.70 ^{+0.10} _{-0.60}	2.64 ^{+0.01} _{-0.08}	0.55 ^{+0.10} _{-0.10}	7.29 ^{+0.63} _{-0.42}	3.04 ^{+0.15} _{-0.21}	1.12 ^{+0.33} _{-0.65}	I	0	1.41	108	89
AP3595	7.70 ^{+0.20} _{-0.20}	3.06 ^{+0.03} _{-0.07}	1.25 ^{+0.30} _{-0.00}	8.08 ^{+0.21} _{-0.22}	3.67 ^{+0.17} _{-0.12}	1.29 ^{+0.29} _{-0.29}	I	0	1.64	210	200
AP3596	8.50 ^{+0.10} _{-0.00}	3.04 ^{+0.03} _{-0.06}	0.45 ^{+0.15} _{-0.20}	7.79 ^{+0.51} _{-1.14}	2.57 ^{+0.36} _{-0.32}	0.67 ^{+1.01} _{-0.59}	I	0	1.22	93	78
AP3597	8.80 ^{+0.10} _{-0.30}	2.78 ^{+0.03} _{-0.10}	0.35 ^{+0.70} _{-0.15}	8.88 ^{+0.21} _{-0.18}	2.36 ^{+0.17} _{-0.17}	0.17 ^{+0.20} _{-0.17}	I	0	1.03	33	18
AP3603	7.70 ^{+0.60} _{-0.70}	2.40 ^{+0.05} _{-0.09}	0.75 ^{+0.10} _{-0.25}	7.93 ^{+0.12} _{-0.11}	2.56 ^{+0.13} _{-0.12}	0.86 ^{+0.13} _{-0.13}	I	0	1.06	32	11
AP3604	8.30 ^{+0.10} _{-0.90}	3.00 ^{+0.02} _{-0.17}	0.75 ^{+0.30} _{-0.10}	7.24 ^{+0.66} _{-0.64}	3.34 ^{+0.25} _{-0.25}	2.19 ^{+0.48} _{-0.69}	I	0	1.28	123	70
AP3606	8.00 ^{+0.40} _{-0.40}	2.83 ^{+0.07} _{-0.08}	0.60 ^{+0.10} _{-0.20}	6.83 ^{+0.28} _{-0.28}	2.81 ^{+0.26} _{-0.31}	2.09 ^{+0.17} _{-0.17}	I	0	1.14	85	80
AP3607	6.90 ^{+0.60} _{-0.10}	2.54 ^{+0.04} _{-0.03}	1.10 ^{+0.05} _{-0.10}	8.13 ^{+0.12} _{-0.12}	2.58 ^{+0.13} _{-0.12}	0.32 ^{+0.25} _{-0.25}	I	0	1.17	45	24
AP3611	8.90 ^{+0.00} _{-0.70}	3.03 ^{+0.00} _{-0.85}	0.45 ^{+0.60} _{-0.10}	8.67 ^{+0.18} _{-0.18}	2.80 ^{+0.17} _{-0.15}	0.72 ^{+0.33} _{-0.34}	I	0	1.18	62	37
AP3613	8.70 ^{+0.10} _{-0.30}	3.46 ^{+0.03} _{-0.10}	0.65 ^{+0.40} _{-0.20}	9.08 ^{+0.11} _{-0.10}	3.35 ^{+0.09} _{-0.10}	0.16 ^{+0.16} _{-0.15}	I	0	1.17	92	54
AP3615	7.90 ^{+0.20} _{-0.30}	3.09 ^{+0.03} _{-0.04}	0.80 ^{+0.10} _{-0.10}	9.00 ^{+0.15} _{-0.11}	3.32 ^{+0.14} _{-0.12}	0.13 ^{+0.14} _{-0.13}	I	0	1.99	194	157

Table 1 (cont'd)

AP ID ^a	CMD Best Fit Parameters ^b			Integrated Best Fit Parameters ^c			Best ^d Flag ^e	R _{ap} ^f	N _{stars} ^g	N _{bg} ^h	
	log(<i>t</i> [Myr])	log(<i>M</i> [<i>M</i> _⊙])	<i>A</i> _V [mag]	log(<i>t</i> [Myr])	log(<i>M</i> [<i>M</i> _⊙])	<i>A</i> _V [mag]					
AP3620	8.90 ^{+0.10} _{-0.04}	3.49 ^{+0.00} _{-0.09}	0.60 ^{+0.15} _{-0.35}	7.70 ^{+0.74} _{-0.77}	2.87 ^{+0.30} _{-0.37}	1.67 ^{+1.04} _{-1.30}	I	0	1.16	96	71
AP3622	7.50 ^{+0.20} _{-0.70}	2.65 ^{+0.01} _{-0.04}	0.95 ^{+0.10} _{-0.10}	6.67 ^{+0.31} _{-0.35}	2.51 ^{+0.21} _{-0.20}	0.98 ^{+0.11} _{-0.12}	I	0	1.27	75	58
AP3628	9.00 ^{+0.10} _{-0.00}	3.00 ^{+0.08} _{-0.00}	0.00 ^{+0.20} _{-0.00}	8.39 ^{+0.12} _{-0.12}	2.27 ^{+0.17} _{-0.18}	0.28 ^{+0.24} _{-0.23}	I	0	1.31	75	36
AP3629	6.90 ^{+0.20} _{-0.20}	3.00 ^{+0.01} _{-0.01}	1.55 ^{+0.10} _{-0.05}	7.56 ^{+0.20} _{-0.17}	3.60 ^{+0.09} _{-0.04}	1.30 ^{+0.17} _{-0.18}	I	0	1.64	163	135
AP3630	8.40 ^{+0.00} _{-0.10}	2.78 ^{+0.00} _{-0.04}	0.60 ^{+0.05} _{-0.10}	8.74 ^{+0.26} _{-0.32}	2.95 ^{+0.12} _{-0.12}	0.49 ^{+0.44} _{-0.37}	I	0	1.03	40	17
AP3631	8.40 ^{+0.10} _{-0.50}	2.80 ^{+0.05} _{-0.06}	0.20 ^{+0.35} _{-0.00}	8.85 ^{+0.11} _{-0.11}	2.81 ^{+0.12} _{-0.12}	0.08 ^{+0.11} _{-0.08}	I	0	1.07	84	79
AP3632	7.90 ^{+0.20} _{-0.70}	2.71 ^{+0.00} _{-0.11}	0.70 ^{+0.15} _{-0.10}	8.10 ^{+0.14} _{-0.23}	2.41 ^{+0.11} _{-0.18}	0.08 ^{+0.11} _{-0.08}	I	0	1.10	90	83
AP3633	9.10 ^{+0.00} _{-0.30}	3.41 ^{+0.11} _{-0.20}	0.05 ^{+0.90} _{-0.05}	7.73 ^{+0.35} _{-0.35}	3.18 ^{+0.17} _{-0.16}	1.61 ^{+0.52} _{-0.52}	I	0	1.48	150	110
AP3637	7.50 ^{+0.30} _{-0.70}	2.46 ^{+0.02} _{-0.04}	0.65 ^{+0.10} _{-0.05}	7.69 ^{+0.91} _{-0.84}	2.95 ^{+0.16} _{-0.16}	1.15 ^{+0.51} _{-0.76}	I	0	1.10	36	17
AP3639	7.70 ^{+0.00} _{-0.60}	3.40 ^{+0.13} _{-0.25}	2.25 ^{+0.25} _{-0.05}	9.21 ^{+0.57} _{-0.63}	3.82 ^{+0.21} _{-0.21}	0.62 ^{+0.75} _{-0.56}	I	0	1.88	256	192
AP3640	8.00 ^{+0.10} _{-0.50}	2.71 ^{+0.02} _{-0.09}	0.30 ^{+0.15} _{-0.05}	7.81 ^{+0.20} _{-0.17}	2.69 ^{+0.10} _{-0.12}	0.79 ^{+0.20} _{-0.19}	I	0	1.29	60	42
AP3650	7.80 ^{+0.00} _{-0.90}	2.48 ^{+0.01} _{-0.14}	0.80 ^{+0.20} _{-0.10}	6.65 ^{+0.36} _{-0.44}	2.19 ^{+0.15} _{-0.15}	0.88 ^{+0.11} _{-0.12}	I	0	1.21	36	25
AP3651	7.70 ^{+2.00} _{-0.40}	3.54 ^{+0.06} _{-3.54}	3.00 ^{+0.40} _{-2.85}	8.79 ^{+0.43} _{-0.39}	3.31 ^{+0.22} _{-0.23}	0.80 ^{+0.53} _{-0.56}	I	0	1.22	114	59
AP3652	8.40 ^{+0.10} _{-0.00}	3.47 ^{+0.03} _{-0.07}	1.45 ^{+0.05} _{-0.15}	8.26 ^{+1.22} _{-1.53}	3.38 ^{+0.30} _{-0.32}	1.51 ^{+1.09} _{-1.15}	I	0	1.39	125	88
AP3654	7.90 ^{+0.30} _{-0.70}	2.44 ^{+0.02} _{-0.09}	0.65 ^{+0.15} _{-0.10}	9.11 ^{+0.13} _{-0.14}	2.83 ^{+0.14} _{-0.15}	0.07 ^{+0.10} _{-0.07}	I	0	1.12	29	15
AP3658	8.30 ^{+0.20} _{-0.60}	2.76 ^{+0.03} _{-0.16}	0.50 ^{+0.15} _{-0.20}	8.73 ^{+0.18} _{-0.25}	3.28 ^{+0.14} _{-0.15}	0.97 ^{+0.34} _{-0.31}	I	0	1.23	148	124
AP3659	9.20 ^{+0.10} _{-0.40}	3.40 ^{+0.21} _{-0.64}	0.25 ^{+0.65} _{-0.00}	9.03 ^{+0.18} _{-0.14}	2.73 ^{+0.16} _{-0.15}	0.21 ^{+0.15} _{-0.19}	I	0	1.05	41	17
AP3661	9.20 ^{+0.00} _{-0.10}	3.56 ^{+0.06} _{-0.20}	0.10 ^{+0.30} _{-0.00}	7.87 ^{+1.08} _{-1.13}	2.89 ^{+0.43} _{-0.48}	1.25 ^{+0.92} _{-0.91}	I	0	1.68	149	128
AP3663	8.30 ^{+0.20} _{-0.50}	2.92 ^{+0.04} _{-0.12}	0.75 ^{+0.21} _{-0.10}	7.55 ^{+0.70} _{-0.77}	2.68 ^{+0.27} _{-0.27}	1.23 ^{+0.73} _{-0.81}	I	0	1.55	145	121
AP3665	8.60 ^{+0.10} _{-0.20}	3.20 ^{+0.03} _{-0.11}	0.60 ^{+0.30} _{-0.25}	7.78 ^{+0.10} _{-0.10}	3.08 ^{+0.09} _{-0.09}	1.39 ^{+0.19} _{-0.18}	I	0	1.45	178	138
AP3666	8.20 ^{+0.10} _{-0.00}	2.64 ^{+0.03} _{-0.02}	0.30 ^{+0.10} _{-0.05}	8.00 ^{+0.35} _{-0.37}	2.99 ^{+0.13} _{-0.11}	1.07 ^{+0.55} _{-0.54}	I	0	1.36	105	81
AP3671	6.80 ^{+0.20} _{-0.20}	3.00 ^{+0.00} _{-0.05}	0.55 ^{+0.00} _{-0.10}	6.58 ^{+0.05} _{-0.05}	3.04 ^{+0.08} _{-0.06}	0.28 ^{+0.08} _{-0.07}	I	0	3.04	611	570
AP3672	8.40 ^{+0.10} _{-0.00}	3.21 ^{+0.04} _{-0.07}	1.20 ^{+0.10} _{-0.20}	8.42 ^{+0.27} _{-0.29}	2.72 ^{+0.16} _{-0.17}	0.50 ^{+0.45} _{-0.41}	I	0	1.36	104	81
AP3673	8.20 ^{+0.20} _{-0.20}	2.99 ^{+0.01} _{-0.12}	1.00 ^{+0.10} _{-0.25}	8.71 ^{+0.41} _{-0.39}	3.08 ^{+0.23} _{-0.21}	0.81 ^{+0.55} _{-0.57}	I	0	1.18	74	59
AP3676	8.70 ^{+0.00} _{-0.30}	3.08 ^{+0.13} _{-0.06}	0.30 ^{+0.70} _{-0.15}	9.10 ^{+1.14} _{-0.80}	3.53 ^{+0.61} _{-0.46}	0.53 ^{+0.45} _{-0.48}	I	0	1.43	161	142
AP3677	8.80 ^{+0.00} _{-0.40}	3.29 ^{+0.04} _{-0.12}	0.15 ^{+0.75} _{-0.05}	8.44 ^{+0.18} _{-0.17}	3.03 ^{+0.12} _{-0.13}	0.47 ^{+0.36} _{-0.35}	I	0	1.74	226	178
AP3680	8.40 ^{+0.00} _{-0.10}	2.99 ^{+0.03} _{-0.05}	0.70 ^{+0.15} _{-0.10}	7.94 ^{+0.12} _{-0.13}	2.37 ^{+0.17} _{-0.30}	0.16 ^{+0.16} _{-0.13}	I	0	1.12	92	72
AP3684	8.80 ^{+0.00} _{-0.70}	3.00 ^{+0.05} _{-0.08}	0.05 ^{+0.90} _{-0.00}	8.61 ^{+0.19} _{-0.20}	2.90 ^{+0.13} _{-0.13}	0.47 ^{+0.37} _{-0.35}	I	0	1.04	69	53
AP3685	8.70 ^{+0.00} _{-0.40}	3.45 ^{+0.00} _{-0.16}	0.70 ^{+0.65} _{-0.00}	8.58 ^{+0.36} _{-0.34}	3.12 ^{+0.21} _{-0.19}	0.69 ^{+0.47} _{-0.52}	I	0	1.49	144	106
AP3686	7.10 ^{+0.70} _{-0.30}	2.67 ^{+0.05} _{-0.04}	1.25 ^{+0.10} _{-0.20}	8.58 ^{+0.06} _{-0.06}	3.72 ^{+0.12} _{-0.12}	1.33 ^{+0.21} _{-0.20}	I	0	1.52	163	146
AP3687	9.10 ^{+0.10} _{-1.30}	3.45 ^{+0.21} _{-3.45}	0.15 ^{+2.30} _{-0.00}	8.47 ^{+0.23} _{-0.23}	2.99 ^{+0.13} _{-0.13}	0.48 ^{+0.47} _{-0.41}	I	0	1.48	144	98
AP3689	7.90 ^{+0.30} _{-0.30}	3.07 ^{+0.06} _{-0.10}	1.60 ^{+0.15} _{-0.20}	9.03 ^{+0.13} _{-0.12}	3.06 ^{+0.12} _{-0.12}	0.06 ^{+0.10} _{-0.06}	I	0	1.09	69	50
AP3692	7.00 ^{+0.20} _{-0.30}	2.51 ^{+0.01} _{-0.02}	0.55 ^{+0.10} _{-0.05}	6.86 ^{+0.23} _{-0.18}	2.85 ^{+0.24} _{-0.28}	0.57 ^{+0.12} _{-0.13}	I	0	1.58	217	222

Table 1 (cont'd)

AP ID ^a	CMD Best Fit Parameters ^b			Integrated Best Fit Parameters ^c			Best ^d Flag ^e	Rap ^f	N _{stars} ^g	N _{bg} ^h	
	log(<i>t</i> [Myr])	log(<i>M</i> [<i>M</i> _⊙])	<i>A_V</i> [mag]	log(<i>t</i> [Myr])	log(<i>M</i> [<i>M</i> _⊙])	<i>A_V</i> [mag]					
AP3694	8.30 ^{+0.30} _{-0.00}	2.84 ^{+0.03} _{-0.03}	0.65 ^{+0.00} _{-0.30}	7.97 ^{+0.20} _{-0.19}	2.63 ^{+0.15} _{-0.15}	0.59 ^{+0.30} _{-0.32}	I	0	1.34	52	25
AP3695	8.00 ^{+0.20} _{-0.80}	2.73 ^{+0.02} _{-0.13}	1.00 ^{+0.20} _{-0.10}	6.97 ^{+0.44} _{-0.58}	2.99 ^{+0.08} _{-0.08}	1.34 ^{+0.16} _{-0.15}	I	0	1.17	41	24
AP3696	8.20 ^{+0.10} _{-0.50}	2.59 ^{+0.03} _{-0.09}	0.30 ^{+0.20} _{-0.05}	8.04 ^{+0.11} _{-0.08}	2.52 ^{+0.20} _{-0.19}	0.16 ^{+0.18} _{-0.16}	I	0	1.66	149	117
AP3697	9.70 ^{+0.10} _{-0.30}	4.37 ^{+0.10} _{-0.55}	0.20 ^{+0.20} _{-0.10}	9.47 ^{+0.59} _{-0.64}	4.32 ^{+0.18} _{-0.18}	1.30 ^{+0.62} _{-0.53}	I	0	1.84	180	153
AP3698	9.10 ^{+0.00} _{-1.20}	3.51 ^{+0.02} _{-0.30}	0.20 ^{+1.65} _{-0.00}	7.98 ^{+0.09} _{-0.24}	3.20 ^{+0.20} _{-0.21}	1.68 ^{+0.49} _{-0.37}	I	0	1.04	83	49
AP3702	8.60 ^{+0.10} _{-1.20}	2.58 ^{+0.00} _{-0.15}	0.00 ^{+0.55} _{-0.20}	7.00 ^{+0.61} _{-0.65}	2.50 ^{+0.19} _{-0.18}	1.28 ^{+0.42} _{-0.46}	I	0	1.24	100	83
AP3703	8.50 ^{+0.00} _{-0.10}	3.13 ^{+0.03} _{-0.02}	0.45 ^{+0.10} _{-0.05}	8.60 ^{+0.19} _{-0.19}	2.79 ^{+0.16} _{-0.14}	0.33 ^{+0.31} _{-0.29}	I	0	1.30	101	79
AP3704	0.00 ^{+0.00} _{-0.00}	0.00 ^{+0.00} _{-0.00}	0.00 ^{+0.00} _{-0.00}	0.00 ^{+0.00} _{-0.00}	0.00 ^{+0.00} _{-0.00}	0.00 ^{+0.00} _{-0.00}	I	0	2.05	0	0
AP3706	9.10 ^{+0.10} _{-0.40}	3.56 ^{+0.07} _{-0.11}	0.25 ^{+1.20} _{-0.15}	9.33 ^{+0.62} _{-0.60}	3.68 ^{+0.21} _{-0.16}	0.75 ^{+0.73} _{-0.60}	I	0	1.36	136	87
AP3707	8.70 ^{+0.00} _{-0.20}	3.19 ^{+0.03} _{-0.05}	0.45 ^{+0.40} _{-0.00}	7.90 ^{+1.29} _{-1.39}	3.10 ^{+0.28} _{-0.23}	1.58 ^{+1.26} _{-1.52}	I	0	1.27	117	93
AP3708	9.10 ^{+0.00} _{-0.20}	3.19 ^{+0.09} _{-0.01}	0.05 ^{+0.50} _{-0.00}	8.02 ^{+1.06} _{-0.50}	3.00 ^{+0.11} _{-0.09}	1.59 ^{+0.57} _{-1.27}	I	0	1.14	58	33
AP3709	9.10 ^{+0.00} _{-0.00}	3.80 ^{+0.03} _{-0.05}	0.40 ^{+0.10} _{-0.05}	0.00 ^{+0.00} _{-0.00}	0.00 ^{+0.00} _{-0.00}	0.00 ^{+0.00} _{-0.00}	I	0	2.36	287	276
AP3711	7.50 ^{+0.00} _{-0.20}	3.04 ^{+0.01} _{-0.01}	0.75 ^{+0.10} _{-0.00}	7.61 ^{+0.05} _{-0.05}	3.50 ^{+0.04} _{-0.04}	0.64 ^{+0.11} _{-0.11}	I	0	2.20	148	100
AP3712	8.90 ^{+0.00} _{-0.60}	3.44 ^{+0.06} _{-0.11}	0.60 ^{+1.30} _{-0.00}	7.93 ^{+0.15} _{-0.40}	3.56 ^{+0.13} _{-0.13}	2.31 ^{+0.55} _{-0.36}	I	0	1.38	160	114
AP3713	8.70 ^{+0.00} _{-0.40}	2.96 ^{+0.02} _{-0.10}	0.25 ^{+0.45} _{-0.05}	7.25 ^{+0.79} _{-0.85}	2.14 ^{+0.13} _{-0.12}	0.75 ^{+0.46} _{-0.48}	I	0	1.21	63	48
AP3714	6.80 ^{+2.20} _{-0.00}	2.51 ^{+0.02} _{-2.51}	0.90 ^{+1.15} _{-0.30}	7.75 ^{+0.15} _{-0.15}	3.50 ^{+0.23} _{-0.24}	0.92 ^{+0.33} _{-0.34}	I	0	1.68	162	163
AP3716	8.50 ^{+0.10} _{-0.10}	3.00 ^{+0.02} _{-0.05}	0.90 ^{+0.15} _{-0.20}	7.94 ^{+0.27} _{-0.21}	2.51 ^{+0.14} _{-0.14}	0.61 ^{+0.27} _{-0.29}	I	0	1.38	49	26
AP3718	8.90 ^{+0.00} _{-1.60}	3.72 ^{+0.04} _{-3.72}	1.05 ^{+1.25} _{-0.10}	8.76 ^{+1.02} _{-0.99}	3.66 ^{+0.32} _{-0.32}	1.38 ^{+0.99} _{-0.97}	I	0	1.40	158	102
AP3719	7.20 ^{+1.00} _{-0.00}	2.88 ^{+0.12} _{-0.06}	1.35 ^{+0.00} _{-0.55}	7.17 ^{+0.53} _{-0.75}	3.15 ^{+0.19} _{-0.14}	1.15 ^{+0.29} _{-0.31}	I	0	1.69	249	224
AP3722	9.00 ^{+0.00} _{-0.10}	3.27 ^{+0.04} _{-0.07}	0.10 ^{+0.35} _{-0.05}	7.58 ^{+0.37} _{-0.32}	3.51 ^{+0.12} _{-0.14}	2.30 ^{+0.38} _{-0.50}	I	0	1.42	108	84
AP3726	8.50 ^{+0.10} _{-0.10}	3.18 ^{+0.01} _{-0.09}	0.60 ^{+0.20} _{-0.15}	9.21 ^{+0.11} _{-0.10}	3.34 ^{+0.06} _{-0.12}	0.07 ^{+0.10} _{-0.07}	I	0	1.20	96	59
AP3727	8.40 ^{+0.10} _{-0.50}	3.04 ^{+0.01} _{-0.11}	1.15 ^{+0.25} _{-0.15}	7.49 ^{+0.99} _{-0.95}	2.50 ^{+0.20} _{-0.20}	1.16 ^{+0.43} _{-0.59}	I	0	0.99	42	20
AP3728	9.10 ^{+0.00} _{-0.10}	3.72 ^{+0.03} _{-0.16}	0.20 ^{+0.20} _{-0.00}	7.93 ^{+1.25} _{-1.50}	3.09 ^{+0.30} _{-0.25}	1.52 ^{+1.32} _{-1.48}	I	0	1.63	149	110
AP3729	9.10 ^{+0.00} _{-2.20}	3.50 ^{+0.00} _{-1.30}	0.45 ^{+1.45} _{-0.00}	7.00 ^{+0.14} _{-0.11}	2.42 ^{+0.22} _{-0.22}	0.52 ^{+0.11} _{-0.11}	I	0	1.13	92	85
AP3732	8.80 ^{+0.10} _{-0.00}	3.50 ^{+0.09} _{-0.10}	0.65 ^{+0.00} _{-0.45}	9.08 ^{+0.83} _{-0.80}	3.75 ^{+0.67} _{-0.64}	1.59 ^{+0.96} _{-0.96}	I	0	1.14	117	89
AP3734	8.30 ^{+0.50} _{-1.00}	3.23 ^{+0.03} _{-0.89}	1.60 ^{+0.35} _{-0.85}	7.63 ^{+0.36} _{-0.33}	2.91 ^{+0.13} _{-0.13}	0.98 ^{+0.34} _{-0.34}	I	0	1.17	87	80
AP3735	7.90 ^{+0.00} _{-0.80}	2.72 ^{+0.04} _{-0.24}	0.85 ^{+0.25} _{-0.10}	8.17 ^{+0.14} _{-0.14}	3.37 ^{+0.18} _{-0.18}	0.99 ^{+0.31} _{-0.33}	I	0	1.25	103	81
AP3737	8.00 ^{+0.10} _{-0.37}	3.35 ^{+0.03} _{-0.08}	1.60 ^{+0.20} _{-0.10}	8.44 ^{+0.12} _{-0.12}	2.93 ^{+0.14} _{-0.15}	0.40 ^{+0.25} _{-0.26}	I	0	1.83	149	129
AP3741	7.70 ^{+0.10} _{-0.60}	2.67 ^{+0.00} _{-0.06}	0.50 ^{+0.10} _{-0.10}	7.29 ^{+0.38} _{-0.39}	2.95 ^{+0.12} _{-0.13}	1.01 ^{+0.25} _{-0.26}	I	0	1.14	110	101
AP3743	8.10 ^{+0.20} _{-0.70}	3.13 ^{+0.02} _{-0.23}	1.25 ^{+0.15} _{-0.10}	8.56 ^{+0.09} _{-0.08}	2.76 ^{+0.11} _{-0.10}	0.13 ^{+0.15} _{-0.13}	I	0	1.65	166	133
AP3744	6.80 ^{+0.40} _{-0.20}	2.41 ^{+0.00} _{-0.03}	0.55 ^{+0.10} _{-0.10}	7.17 ^{+0.14} _{-0.11}	2.33 ^{+0.19} _{-0.19}	0.40 ^{+0.11} _{-0.10}	I	0	1.46	54	38
AP3745	9.30 ^{+0.10} _{-0.10}	3.93 ^{+0.08} _{-0.36}	0.25 ^{+0.20} _{-0.10}	9.09 ^{+0.37} _{-0.32}	2.99 ^{+0.16} _{-0.17}	0.50 ^{+0.43} _{-0.43}	I	0	1.12	86	66
AP3747	8.90 ^{+0.30} _{-1.40}	3.29 ^{+0.02} _{-3.29}	0.70 ^{+1.45} _{-0.25}	9.34 ^{+0.38} _{-0.32}	3.53 ^{+0.18} _{-0.16}	0.46 ^{+0.34} _{-0.38}	I	0	1.15	98	74

Table 1 (cont'd)

AP ID ^a	CMD Best Fit Parameters ^b			Integrated Best Fit Parameters ^c			Best ^d Flag ^e	R _{ap} ^f	N _{stars} ^g	N _{bg} ^h	
	log(<i>t</i> [Myr])	log(<i>M</i> [<i>M</i> _⊙])	<i>A_V</i> [mag]	log(<i>t</i> [Myr])	log(<i>M</i> [<i>M</i> _⊙])	<i>A_V</i> [mag]					
AP3749	8.90 ^{+0.10} _{-0.00}	3.83 ^{+0.05} _{-0.16}	1.20 ^{+0.15} _{-0.30}	8.98 ^{+0.75} _{-0.60}	3.27 ^{+0.29} _{-0.28}	1.16 ^{+0.77} _{-0.77}	I	0	1.21	91	68
AP3753	8.00 ^{+0.20} _{-0.60}	2.69 ^{+0.02} _{-0.09}	0.75 ^{+0.15} _{-0.15}	8.49 ^{+0.27} _{-0.25}	2.82 ^{+0.19} _{-0.18}	0.49 ^{+0.43} _{-0.41}	I	0	1.43	113	91
AP3756	8.80 ^{+0.10} _{-1.10}	3.11 ^{+0.04} _{-0.59}	0.55 ^{+0.30} _{-0.30}	7.03 ^{+0.56} _{-0.61}	2.84 ^{+0.24} _{-0.26}	2.19 ^{+0.48} _{-0.48}	I	0	1.05	58	38
AP3757	9.00 ^{+0.00} _{-0.00}	3.28 ^{+0.03} _{-0.04}	0.05 ^{+0.10} _{-0.05}	10.08 ^{+0.17} _{-0.33}	3.40 ^{+0.13} _{-0.16}	0.06 ^{+0.14} _{-0.06}	I	0	1.50	103	62
AP3759	8.40 ^{+0.00} _{-0.60}	3.17 ^{+0.04} _{-0.15}	0.80 ^{+0.40} _{-0.00}	8.82 ^{+0.09} _{-0.09}	3.42 ^{+0.07} _{-0.07}	0.21 ^{+0.16} _{-0.17}	I	0	1.54	126	109
AP3760	7.50 ^{+0.30} _{-0.20}	3.19 ^{+0.04} _{-0.10}	1.85 ^{+0.05} _{-0.15}	9.27 ^{+0.27} _{-0.31}	3.62 ^{+0.12} _{-0.10}	0.26 ^{+0.35} _{-0.26}	I	0	1.08	121	93
AP3761	10.10 ^{+0.00} _{-0.00}	5.34 ^{+0.00} _{-0.01}	0.00 ^{+0.10} _{-0.00}	8.48 ^{+0.95} _{-0.60}	4.10 ^{+0.16} _{-0.09}	1.93 ^{+0.79} _{-1.13}	I	0	2.61	301	227
AP3763	9.10 ^{+0.40} _{-0.00}	3.57 ^{+0.49} _{-0.11}	0.10 ^{+0.15} _{-0.05}	8.97 ^{+0.14} _{-0.13}	2.87 ^{+0.13} _{-0.13}	0.15 ^{+0.14} _{-0.14}	I	0	1.10	91	64
AP3769	8.70 ^{+0.00} _{-0.20}	3.22 ^{+0.03} _{-0.07}	0.35 ^{+0.35} _{-0.00}	8.68 ^{+0.25} _{-0.25}	3.03 ^{+0.12} _{-0.12}	0.62 ^{+0.43} _{-0.42}	I	0	1.22	115	81
AP3772	9.30 ^{+0.20} _{-0.00}	3.72 ^{+0.18} _{-0.01}	0.30 ^{+0.00} _{-0.20}	8.67 ^{+0.58} _{-0.54}	3.10 ^{+0.20} _{-0.17}	0.91 ^{+0.54} _{-0.68}	I	0	1.61	64	33
AP3776	8.40 ^{+0.10} _{-0.00}	2.85 ^{+0.02} _{-0.05}	0.45 ^{+0.10} _{-0.15}	8.64 ^{+0.12} _{-0.12}	3.35 ^{+0.08} _{-0.08}	0.97 ^{+0.20} _{-0.20}	I	0	1.19	112	89
AP3778	6.90 ^{+0.10} _{-0.20}	2.20 ^{+0.01} _{-0.10}	0.35 ^{+0.10} _{-0.00}	7.01 ^{+0.43} _{-0.46}	3.06 ^{+0.18} _{-0.16}	0.14 ^{+0.12} _{-0.12}	I	0	1.59	63	56
AP3779	9.00 ^{+0.00} _{-0.10}	3.42 ^{+0.06} _{-0.04}	0.20 ^{+0.30} _{-0.00}	9.31 ^{+0.53} _{-0.49}	3.78 ^{+0.18} _{-0.16}	0.60 ^{+0.57} _{-0.50}	I	0	1.76	132	68
AP3780	9.40 ^{+0.20} _{-2.30}	4.08 ^{+4.08} _{-4.08}	0.00 ^{+2.60} _{-0.45}	8.85 ^{+0.09} _{-0.06}	3.69 ^{+0.09} _{-0.05}	0.20 ^{+0.14} _{-0.15}	I	1	1.19	133	160
AP3783	8.40 ^{+0.00} _{-1.40}	3.06 ^{+0.01} _{-0.72}	1.20 ^{+0.60} _{-0.15}	8.27 ^{+0.16} _{-0.17}	2.81 ^{+0.28} _{-0.38}	0.62 ^{+0.40} _{-0.47}	I	0	1.21	89	74
AP3784	7.90 ^{+0.80} _{-0.30}	3.30 ^{+0.16} _{-1.30}	2.55 ^{+0.25} _{-1.10}	9.11 ^{+0.77} _{-0.72}	3.83 ^{+0.17} _{-0.15}	1.62 ^{+0.86} _{-0.80}	I	0	1.33	82	60
AP3785	8.70 ^{+0.00} _{-0.40}	2.79 ^{+0.04} _{-0.11}	0.05 ^{+0.60} _{-0.05}	8.67 ^{+0.20} _{-0.20}	3.05 ^{+0.10} _{-0.10}	0.45 ^{+0.31} _{-0.31}	I	0	1.27	107	91
AP3790	8.30 ^{+0.10} _{-0.40}	3.11 ^{+0.01} _{-0.14}	1.10 ^{+0.15} _{-0.15}	7.99 ^{+0.15} _{-0.15}	2.59 ^{+0.24} _{-0.25}	0.46 ^{+0.31} _{-0.30}	I	0	1.48	164	122
AP3792	7.40 ^{+1.10} _{-0.50}	2.98 ^{+0.04} _{-2.98}	2.70 ^{+0.15} _{-1.45}	9.12 ^{+0.04} _{-0.04}	4.50 ^{+0.05} _{-0.05}	0.00 ^{+0.07} _{-0.00}	I	0	1.84	198	213
AP3795	6.70 ^{+2.90} _{-0.40}	2.75 ^{+2.75} _{-2.75}	2.95 ^{+0.40} _{-2.50}	8.11 ^{+1.47} _{-1.46}	3.78 ^{+1.25} _{-1.18}	1.45 ^{+1.02} _{-1.02}	I	1	2.04	276	267
AP3796	7.00 ^{+0.10} _{-0.10}	3.01 ^{+0.03} _{-0.04}	1.45 ^{+0.05} _{-0.05}	6.85 ^{+0.13} _{-0.12}	2.81 ^{+0.30} _{-0.31}	1.28 ^{+0.10} _{-0.10}	I	0	1.70	143	119
AP3797	9.10 ^{+0.00} _{-0.00}	3.77 ^{+0.05} _{-0.00}	0.15 ^{+0.20} _{-0.00}	8.77 ^{+0.19} _{-0.21}	2.90 ^{+0.15} _{-0.16}	0.44 ^{+0.36} _{-0.36}	I	0	1.42	136	96
AP3799	8.20 ^{+0.00} _{-0.10}	2.91 ^{+0.03} _{-0.05}	0.65 ^{+0.15} _{-0.00}	8.12 ^{+0.18} _{-0.18}	2.50 ^{+0.23} _{-0.23}	0.30 ^{+0.33} _{-0.28}	I	0	1.61	139	114
AP3801	0.00 ^{+0.00} _{-0.00}	0.00 ^{+0.00} _{-0.00}	0.00 ^{+0.00} _{-0.00}	0.00 ^{+0.00} _{-0.00}	0.00 ^{+0.00} _{-0.00}	0.00 ^{+0.00} _{-0.00}	I	0	1.35	0	0
AP3802	8.80 ^{+0.10} _{-0.10}	3.12 ^{+0.06} _{-0.05}	0.35 ^{+0.20} _{-0.25}	8.74 ^{+0.48} _{-0.47}	3.20 ^{+0.18} _{-0.16}	0.76 ^{+0.59} _{-0.57}	I	0	1.32	113	92
AP3803	7.90 ^{+1.40} _{-0.90}	2.47 ^{+0.00} _{-2.47}	1.00 ^{+1.35} _{-0.25}	9.14 ^{+0.04} _{-0.03}	3.06 ^{+0.03} _{-0.04}	0.00 ^{+0.07} _{-0.00}	I	0	0.99	47	32
AP3805	8.80 ^{+0.00} _{-0.10}	3.36 ^{+0.11} _{-0.17}	0.60 ^{+0.30} _{-0.10}	8.97 ^{+0.89} _{-0.82}	3.74 ^{+0.69} _{-0.66}	1.59 ^{+0.97} _{-1.00}	I	0	1.39	139	103
AP3808	7.90 ^{+0.10} _{-0.70}	3.03 ^{+0.03} _{-0.05}	0.75 ^{+0.30} _{-0.00}	8.39 ^{+0.08} _{-0.07}	2.67 ^{+0.11} _{-0.11}	0.07 ^{+0.11} _{-0.07}	I	0	1.20	106	96
AP3809	9.00 ^{+0.10} _{-0.10}	3.18 ^{+0.07} _{-0.12}	0.40 ^{+0.30} _{-0.20}	7.88 ^{+0.16} _{-0.28}	3.04 ^{+0.34} _{-0.27}	1.72 ^{+0.90} _{-0.50}	I	0	1.47	94	51
AP3810	8.50 ^{+0.20} _{-0.20}	2.93 ^{+0.09} _{-0.10}	0.85 ^{+0.40} _{-0.30}	8.30 ^{+0.16} _{-0.17}	2.87 ^{+0.21} _{-0.21}	0.96 ^{+0.40} _{-0.42}	I	0	1.14	75	54
AP3811	7.50 ^{+1.10} _{-0.30}	3.16 ^{+0.00} _{-0.57}	1.90 ^{+0.40} _{-0.60}	7.92 ^{+0.98} _{-0.33}	2.70 ^{+1.02} _{-0.50}	0.49 ^{+0.17} _{-0.30}	I	0	1.03	79	72
AP3812	8.90 ^{+0.00} _{-0.10}	3.63 ^{+0.08} _{-0.09}	0.40 ^{+0.40} _{-0.05}	8.75 ^{+0.31} _{-0.25}	3.28 ^{+0.15} _{-0.16}	0.62 ^{+0.27} _{-0.30}	I	0	1.82	224	200
AP3813	8.10 ^{+0.60} _{-0.10}	2.81 ^{+0.04} _{-0.05}	0.90 ^{+0.05} _{-0.40}	7.99 ^{+0.06} _{-0.07}	2.48 ^{+0.14} _{-0.18}	0.46 ^{+0.14} _{-0.16}	I	0	1.52	69	47

Table 1 (cont'd)

AP ID ^a	CMD Best Fit Parameters ^b			Integrated Best Fit Parameters ^c			Best ^d Flag ^e	Rap ^f	N _{stars} ^g	N _{bg} ^h	
	log(<i>t</i> [Myr])	log(<i>M</i> [<i>M</i> _⊙])	<i>A</i> _V [mag]	log(<i>t</i> [Myr])	log(<i>M</i> [<i>M</i> _⊙])	<i>A</i> _V [mag]					
AP3814	8.20 ^{+0.10} _{-0.00}	3.11 ^{+0.03} _{-0.03}	0.85 ^{+0.05} _{-0.05}	8.22 ^{+0.26} _{-0.28}	2.79 ^{+0.20} _{-0.19}	0.52 ^{+0.52} _{-0.44}	I	0	1.80	164	150
AP3816	8.70 ^{+0.10} _{-0.20}	2.90 ^{+0.02} _{-0.08}	0.60 ^{+0.45} _{-0.35}	8.55 ^{+0.28} _{-0.27}	2.70 ^{+0.22} _{-0.21}	0.50 ^{+0.49} _{-0.43}	I	0	1.20	55	34
AP3817	7.20 ^{+0.40} _{-0.20}	3.02 ^{+0.01} _{-0.04}	1.05 ^{+0.05} _{-0.20}	8.37 ^{+0.16} _{-0.16}	2.93 ^{+0.14} _{-0.14}	0.31 ^{+0.30} _{-0.29}	I	0	1.38	143	148
AP3820	8.30 ^{+0.10} _{-0.20}	2.94 ^{+0.06} _{-0.03}	0.45 ^{+0.25} _{-0.00}	8.39 ^{+0.44} _{-0.37}	2.99 ^{+0.22} _{-0.22}	0.75 ^{+0.66} _{-0.66}	I	0	1.15	82	59
AP3822	9.20 ^{+0.00} _{-0.10}	3.93 ^{+0.05} _{-0.26}	0.20 ^{+0.15} _{-0.05}	8.03 ^{+0.20} _{-0.35}	3.32 ^{+0.26} _{-0.28}	1.16 ^{+0.33} _{-0.34}	I	0	1.84	211	176
AP3823	8.00 ^{+0.00} _{-0.80}	2.73 ^{+0.03} _{-0.09}	1.00 ^{+0.25} _{-0.05}	7.84 ^{+0.22} _{-0.20}	2.97 ^{+0.12} _{-0.09}	1.46 ^{+0.31} _{-0.26}	I	0	1.00	37	18
AP3824	7.70 ^{+0.10} _{-0.10}	3.18 ^{+0.01} _{-0.01}	1.40 ^{+0.10} _{-0.05}	7.05 ^{+0.17} _{-0.16}	3.57 ^{+0.10} _{-0.10}	2.13 ^{+0.14} _{-0.10}	I	0	1.54	145	121
AP3826	8.70 ^{+0.00} _{-1.40}	2.99 ^{+0.08} _{-0.40}	0.80 ^{+0.80} _{-0.10}	8.75 ^{+0.18} _{-0.24}	3.20 ^{+0.14} _{-0.14}	0.96 ^{+0.36} _{-0.36}	I	0	1.71	88	52
AP3828	7.90 ^{+0.30} _{-0.60}	2.70 ^{+0.02} _{-0.11}	0.70 ^{+0.15} _{-0.25}	7.98 ^{+0.56} _{-0.65}	3.07 ^{+0.23} _{-0.22}	1.15 ^{+0.96} _{-0.90}	I	0	1.06	84	65
AP3829	8.20 ^{+0.19} _{-0.30}	2.98 ^{+0.00} _{-0.08}	1.00 ^{+0.05} _{-0.20}	8.66 ^{+0.11} _{-0.09}	2.45 ^{+0.13} _{-0.14}	0.04 ^{+0.08} _{-0.04}	I	0	1.05	48	21
AP3831	7.90 ^{+0.00} _{-0.20}	3.31 ^{+0.02} _{-0.07}	1.80 ^{+0.15} _{-0.00}	8.19 ^{+0.14} _{-0.14}	2.98 ^{+0.24} _{-0.26}	1.00 ^{+0.39} _{-0.42}	I	0	1.11	77	59
AP3832	8.40 ^{+0.20} _{-0.30}	2.69 ^{+0.06} _{-0.13}	0.50 ^{+0.25} _{-0.25}	8.45 ^{+0.49} _{-0.50}	3.03 ^{+0.22} _{-0.21}	0.98 ^{+0.93} _{-0.79}	I	0	1.08	60	60
AP3833	8.10 ^{+0.10} _{-0.80}	2.79 ^{+0.01} _{-0.12}	0.55 ^{+0.15} _{-0.05}	7.46 ^{+0.73} _{-0.73}	2.97 ^{+0.17} _{-0.17}	1.13 ^{+0.53} _{-0.63}	I	0	1.25	98	78
AP3837	7.60 ^{+0.10} _{-0.50}	2.73 ^{+0.01} _{-0.05}	0.30 ^{+0.10} _{-0.00}	6.56 ^{+0.13} _{-0.11}	2.60 ^{+0.34} _{-0.33}	0.76 ^{+0.13} _{-0.14}	I	0	3.55	271	236
AP3839	8.90 ^{+0.00} _{-0.20}	3.13 ^{+0.04} _{-0.15}	0.15 ^{+0.60} _{-0.05}	7.97 ^{+0.06} _{-0.15}	2.95 ^{+0.18} _{-0.18}	1.58 ^{+0.37} _{-0.32}	I	0	1.10	72	46
AP3840	9.10 ^{+0.00} _{-0.20}	3.31 ^{+0.08} _{-1.27}	0.55 ^{+0.50} _{-0.10}	9.01 ^{+0.66} _{-0.79}	3.33 ^{+0.20} _{-0.20}	1.00 ^{+0.95} _{-0.74}	I	0	1.47	75	41
AP3841	8.90 ^{+0.70} _{-1.30}	3.73 ^{+0.43} _{-3.73}	1.60 ^{+1.00} _{-0.75}	9.51 ^{+0.29} _{-0.30}	3.51 ^{+0.17} _{-0.17}	0.22 ^{+0.27} _{-0.22}	I	0	1.40	62	31
AP3845	7.70 ^{+1.50} _{-0.80}	2.55 ^{+0.07} _{-2.55}	1.00 ^{+1.55} _{-0.40}	7.46 ^{+0.38} _{-0.86}	3.11 ^{+0.23} _{-0.20}	1.41 ^{+0.60} _{-0.45}	I	0	1.84	176	152
AP3846	7.60 ^{+0.20} _{-0.30}	3.02 ^{+0.02} _{-0.05}	0.90 ^{+0.05} _{-0.13}	8.00 ^{+0.13} _{-0.13}	2.75 ^{+0.11} _{-0.11}	0.18 ^{+0.18} _{-0.16}	I	0	1.44	148	125
AP3848	6.60 ^{+0.90} _{-0.10}	2.79 ^{+0.03} _{-0.02}	0.55 ^{+0.05} _{-0.10}	7.42 ^{+0.24} _{-0.21}	2.30 ^{+0.19} _{-0.22}	0.14 ^{+0.14} _{-0.13}	I	0	1.21	63	39
AP3850	9.40 ^{+0.40} _{-1.50}	4.38 ^{+0.11} _{-4.38}	0.30 ^{+1.60} _{-0.20}	7.80 ^{+1.16} _{-0.67}	2.50 ^{+0.27} _{-0.33}	1.97 ^{+0.80} _{-1.40}	I	0	1.32	167	142
AP3853	9.20 ^{+0.00} _{-0.10}	3.98 ^{+0.04} _{-0.30}	0.40 ^{+0.20} _{-0.05}	7.63 ^{+0.41} _{-1.04}	3.03 ^{+0.25} _{-0.25}	1.66 ^{+0.75} _{-0.51}	I	0	1.49	124	90
AP3854	8.40 ^{+0.30} _{-0.10}	3.04 ^{+0.06} _{-0.07}	0.95 ^{+0.10} _{-0.55}	8.50 ^{+0.30} _{-0.33}	2.69 ^{+0.21} _{-0.21}	0.64 ^{+0.68} _{-0.56}	I	0	1.26	96	76
AP3856	8.30 ^{+0.00} _{-0.90}	2.73 ^{+0.02} _{-0.21}	0.45 ^{+0.25} _{-0.00}	8.26 ^{+0.17} _{-0.18}	2.79 ^{+0.17} _{-0.14}	0.40 ^{+0.32} _{-0.31}	I	0	1.42	123	118
AP3857	8.30 ^{+0.30} _{-0.60}	2.90 ^{+0.13} _{-0.29}	1.20 ^{+0.45} _{-0.55}	6.75 ^{+0.09} _{-0.08}	2.39 ^{+0.37} _{-0.39}	2.76 ^{+0.10} _{-0.09}	I	0	1.39	142	122
AP3858	8.00 ^{+0.00} _{-0.60}	3.32 ^{+0.02} _{-0.19}	1.70 ^{+0.30} _{-0.10}	8.73 ^{+0.40} _{-0.93}	3.27 ^{+0.15} _{-0.32}	0.45 ^{+0.38} _{-0.21}	I	0	1.45	115	110
AP3860	8.20 ^{+0.00} _{-0.50}	2.76 ^{+0.02} _{-0.13}	0.75 ^{+0.20} _{-0.05}	8.56 ^{+0.09} _{-0.09}	2.77 ^{+0.11} _{-0.10}	0.13 ^{+0.15} _{-0.13}	I	0	1.35	111	93
AP3861	8.60 ^{+0.10} _{-0.10}	2.94 ^{+0.01} _{-0.10}	0.50 ^{+0.20} _{-0.20}	8.08 ^{+0.25} _{-0.27}	3.38 ^{+0.20} _{-0.20}	2.02 ^{+0.45} _{-0.37}	I	0	1.17	111	94
AP3864	8.90 ^{+0.00} _{-1.10}	2.73 ^{+0.02} _{-0.36}	0.05 ^{+0.85} _{-0.00}	8.77 ^{+0.08} _{-0.07}	2.41 ^{+0.13} _{-0.13}	0.36 ^{+0.16} _{-0.15}	I	0	1.16	36	20
AP3866	7.80 ^{+0.00} _{-0.60}	2.90 ^{+0.01} _{-0.06}	0.80 ^{+0.20} _{-0.05}	8.18 ^{+0.13} _{-0.14}	2.79 ^{+0.11} _{-0.10}	0.25 ^{+0.23} _{-0.22}	I	0	1.44	151	130
AP3869	8.10 ^{+0.20} _{-0.30}	3.26 ^{+0.04} _{-0.38}	1.70 ^{+0.00} _{-0.55}	7.95 ^{+0.33} _{-0.50}	3.83 ^{+0.15} _{-0.14}	2.07 ^{+0.50} _{-0.42}	I	0	1.31	120	77
AP3870	6.70 ^{+0.20} _{-0.10}	2.91 ^{+0.00} _{-0.04}	0.90 ^{+0.00} _{-0.10}	6.97 ^{+0.10} _{-0.12}	2.44 ^{+0.29} _{-0.26}	0.45 ^{+0.11} _{-0.11}	I	0	1.95	225	186
AP3873	8.90 ^{+0.00} _{-0.16}	3.19 ^{+0.05} _{-0.09}	0.10 ^{+0.35} _{-0.05}	8.62 ^{+0.16} _{-0.15}	2.68 ^{+0.13} _{-0.14}	0.28 ^{+0.26} _{-0.25}	I	0	1.13	98	77

Table 1 (cont'd)

AP ID ^a	CMD Best Fit Parameters ^b			Integrated Best Fit Parameters ^c			Best ^d Flag ^e	R _{ap} ^f	N _{stars} ^g	N _{bg} ^h	
	log(<i>t</i> [Myr])	log(<i>M</i> [<i>M</i> _⊙])	<i>A_V</i> [mag]	log(<i>t</i> [Myr])	log(<i>M</i> [<i>M</i> _⊙])	<i>A_V</i> [mag]					
AP3876	9.10 ^{+0.00} _{-0.00}	3.82 ^{+0.03} _{-0.05}	0.45 ^{+0.10} _{-0.10}	9.15 ^{+0.32} _{-0.30}	3.53 ^{+0.15} _{-0.14}	0.42 ^{+0.35} _{-0.35}	I	0	1.74	196	136
AP3879	8.70 ^{+0.10} _{-0.20}	3.40 ^{+0.00} _{-0.16}	0.80 ^{+0.30} _{-0.50}	8.42 ^{+0.16} _{-0.15}	2.65 ^{+0.24} _{-0.26}	0.55 ^{+0.38} _{-0.38}	I	0	1.06	107	63
AP3881	7.60 ^{+0.30} _{-0.50}	2.65 ^{+0.03} _{-0.05}	0.70 ^{+0.10} _{-0.10}	7.82 ^{+0.29} _{-0.27}	2.68 ^{+0.15} _{-0.16}	0.63 ^{+0.36} _{-0.37}	I	0	1.20	95	80
AP3882	7.80 ^{+0.30} _{-0.60}	2.81 ^{+0.04} _{-0.07}	0.70 ^{+0.15} _{-0.05}	7.52 ^{+0.64} _{-0.60}	2.83 ^{+0.21} _{-0.23}	1.21 ^{+0.57} _{-0.72}	I	0	1.25	76	40
AP3883	7.70 ^{+0.00} _{-0.40}	2.67 ^{+0.01} _{-0.03}	0.50 ^{+0.15} _{-0.05}	7.98 ^{+0.09} _{-0.09}	2.47 ^{+0.13} _{-0.12}	0.12 ^{+0.14} _{-0.12}	I	0	1.59	110	96
AP3884	6.60 ^{+3.00} _{-0.10}	2.76 ^{+1.05} _{-0.11}	2.65 ^{+0.05} _{-2.30}	8.34 ^{+0.39} _{-0.27}	2.69 ^{+0.09} _{-0.10}	0.63 ^{+0.43} _{-0.59}	I	0	0.85	50	34
AP3890	8.80 ^{+0.10} _{-0.00}	3.37 ^{+0.00} _{-0.08}	0.45 ^{+0.00} _{-0.25}	7.71 ^{+0.10} _{-0.11}	3.36 ^{+0.12} _{-0.12}	1.84 ^{+0.24} _{-0.22}	I	0	1.45	123	103
AP3895	9.10 ^{+0.00} _{-0.00}	3.81 ^{+0.04} _{-0.06}	0.25 ^{+0.10} _{-0.05}	8.52 ^{+0.17} _{-0.17}	2.99 ^{+0.14} _{-0.14}	0.59 ^{+0.34} _{-0.35}	I	0	1.84	190	138
AP3903	9.50 ^{+0.10} _{-2.50}	3.98 ^{+0.28} _{-2.91}	0.80 ^{+0.70} _{-0.30}	7.64 ^{+0.11} _{-0.18}	3.30 ^{+0.23} _{-0.22}	1.47 ^{+0.33} _{-0.31}	I	0	1.11	88	82
AP3904	7.90 ^{+0.20} _{-0.30}	3.02 ^{+0.03} _{-0.06}	1.10 ^{+0.20} _{-0.05}	0.00 ^{+0.00} _{-0.00}	0.00 ^{+0.00} _{-0.00}	0.00 ^{+0.00} _{-0.00}	I	0	1.05	66	60
AP3906	8.70 ^{+0.10} _{-0.90}	3.33 ^{+0.07} _{-0.32}	0.65 ^{+0.75} _{-0.15}	8.79 ^{+0.41} _{-0.90}	2.98 ^{+0.28} _{-0.75}	0.36 ^{+0.30} _{-0.31}	I	0	1.00	95	61
AP3907	8.70 ^{+0.00} _{-0.50}	2.84 ^{+0.00} _{-0.18}	0.30 ^{+0.55} _{-0.05}	8.01 ^{+0.46} _{-0.47}	2.88 ^{+0.24} _{-0.24}	1.04 ^{+0.80} _{-0.81}	I	0	1.44	75	46
AP3909	6.80 ^{+0.00} _{-0.20}	3.31 ^{+0.01} _{-0.01}	0.70 ^{+0.05} _{-0.00}	6.92 ^{+0.57} _{-0.62}	3.55 ^{+0.31} _{-0.39}	0.31 ^{+0.35} _{-0.29}	I	0	3.81	973	885
AP3912	9.10 ^{+0.00} _{-0.00}	3.62 ^{+0.03} _{-0.13}	0.25 ^{+0.10} _{-0.15}	9.71 ^{+0.17} _{-0.16}	3.64 ^{+0.13} _{-0.12}	0.07 ^{+0.11} _{-0.07}	I	0	1.46	149	116
AP3913	8.30 ^{+0.10} _{-0.10}	3.05 ^{+0.03} _{-0.06}	1.35 ^{+0.10} _{-0.05}	7.02 ^{+0.31} _{-0.27}	3.09 ^{+0.14} _{-0.11}	2.34 ^{+0.18} _{-0.18}	I	0	1.56	75	46
AP3914	9.70 ^{+0.00} _{-2.40}	3.78 ^{+0.42} _{-3.78}	0.00 ^{+2.55} _{-0.10}	9.04 ^{+0.51} _{-0.74}	3.11 ^{+0.22} _{-0.18}	0.66 ^{+0.71} _{-0.52}	I	0	1.15	35	14
AP3915	9.10 ^{+0.00} _{-0.00}	3.54 ^{+0.07} _{-0.08}	0.20 ^{+0.05} _{-0.15}	8.04 ^{+0.17} _{-0.21}	3.35 ^{+0.22} _{-0.24}	1.75 ^{+0.38} _{-0.34}	I	0	1.95	179	152
AP3917	7.60 ^{+0.10} _{-0.10}	3.94 ^{+0.00} _{-0.46}	2.95 ^{+0.05} _{-0.55}	7.59 ^{+0.12} _{-0.13}	4.15 ^{+0.10} _{-0.10}	2.56 ^{+0.22} _{-0.21}	I	0	1.06	90	63
AP3920	9.60 ^{+0.10} _{-2.40}	3.97 ^{+0.25} _{-3.97}	0.15 ^{+2.20} _{-0.10}	9.26 ^{+0.75} _{-0.30}	4.39 ^{+0.43} _{-0.00}	2.33 ^{+0.45} _{-0.40}	I	0	1.10	76	85
AP3923	8.40 ^{+0.20} _{-0.20}	2.90 ^{+0.04} _{-0.09}	0.40 ^{+0.20} _{-0.25}	6.78 ^{+0.27} _{-0.26}	3.12 ^{+0.25} _{-0.22}	2.73 ^{+0.16} _{-0.17}	I	0	1.46	155	133
AP3924	6.60 ^{+0.50} _{-0.00}	3.05 ^{+0.03} _{-0.02}	0.80 ^{+0.05} _{-0.10}	6.42 ^{+0.17} _{-0.24}	2.66 ^{+0.39} _{-0.35}	0.43 ^{+0.13} _{-0.12}	I	0	2.12	272	239
AP3927	7.90 ^{+0.20} _{-0.20}	3.15 ^{+0.03} _{-0.18}	1.95 ^{+0.10} _{-0.20}	8.28 ^{+0.22} _{-0.26}	2.50 ^{+0.43} _{-0.37}	0.46 ^{+0.48} _{-0.40}	I	0	1.03	77	56
AP3928	7.80 ^{+0.00} _{-0.80}	2.87 ^{+0.00} _{-0.11}	1.40 ^{+0.15} _{-0.05}	7.82 ^{+0.22} _{-0.18}	2.90 ^{+0.14} _{-0.12}	1.00 ^{+0.27} _{-0.18}	I	0	1.26	51	37
AP3931	9.20 ^{+0.00} _{-0.10}	3.88 ^{+0.05} _{-0.34}	0.30 ^{+0.15} _{-0.05}	8.76 ^{+0.16} _{-0.18}	2.95 ^{+0.13} _{-0.13}	0.32 ^{+0.29} _{-0.28}	I	0	1.63	174	122
AP3934	6.80 ^{+2.40} _{-0.00}	1.89 ^{+0.02} _{-1.89}	0.60 ^{+1.55} _{-0.15}	6.82 ^{+0.06} _{-0.08}	2.87 ^{+0.06} _{-0.05}	0.81 ^{+0.07} _{-0.07}	I	0	1.10	35	23
AP3936	8.20 ^{+0.00} _{-0.00}	3.12 ^{+0.01} _{-0.03}	0.45 ^{+0.05} _{-0.05}	7.80 ^{+0.14} _{-0.16}	3.30 ^{+0.13} _{-0.14}	0.89 ^{+0.27} _{-0.28}	I	0	2.15	230	182
AP3937	7.00 ^{+0.20} _{-0.30}	2.92 ^{+0.07} _{-0.01}	1.35 ^{+0.15} _{-0.00}	7.25 ^{+0.76} _{-0.73}	2.93 ^{+0.26} _{-0.29}	0.57 ^{+0.47} _{-0.45}	I	0	1.09	102	106
AP3938	6.70 ^{+0.50} _{-0.10}	2.27 ^{+0.02} _{-0.06}	0.85 ^{+0.05} _{-0.15}	7.73 ^{+0.06} _{-0.06}	2.85 ^{+0.09} _{-0.09}	0.46 ^{+0.14} _{-0.14}	I	0	1.14	133	122
AP3939	8.90 ^{+0.30} _{-1.10}	3.12 ^{+0.23} _{-3.12}	1.05 ^{+1.25} _{-0.35}	8.57 ^{+0.20} _{-0.20}	2.62 ^{+0.16} _{-0.17}	1.01 ^{+0.40} _{-0.40}	I	0	1.22	51	39
AP3940	8.50 ^{+0.10} _{-0.00}	2.86 ^{+0.05} _{-0.04}	0.50 ^{+0.15} _{-0.15}	8.70 ^{+0.19} _{-0.22}	3.14 ^{+0.11} _{-0.11}	0.83 ^{+0.29} _{-0.29}	I	0	1.64	153	122
AP3941	7.20 ^{+0.50} _{-0.40}	2.49 ^{+0.01} _{-0.03}	0.40 ^{+0.05} _{-0.15}	6.58 ^{+0.32} _{-0.36}	2.61 ^{+0.23} _{-0.25}	0.55 ^{+0.12} _{-0.12}	I	0	1.37	128	103
AP3942	7.60 ^{+0.70} _{-0.40}	2.79 ^{+0.06} _{-0.07}	0.60 ^{+0.05} _{-0.20}	7.98 ^{+0.06} _{-0.22}	2.54 ^{+0.11} _{-0.27}	0.37 ^{+0.17} _{-0.15}	I	0	1.21	129	119
AP3943	8.50 ^{+0.10} _{-0.10}	2.95 ^{+0.02} _{-0.06}	0.60 ^{+0.15} _{-0.10}	8.12 ^{+0.20} _{-0.20}	2.76 ^{+0.18} _{-0.18}	0.53 ^{+0.39} _{-0.37}	I	0	1.22	77	53

Table 1 (cont'd)

AP ID ^a	CMD Best Fit Parameters ^b			Integrated Best Fit Parameters ^c			Best ^d Flag ^e	Rap ^f	N _{stars} ^g	N _{bg} ^h	
	log(<i>t</i> [Myr])	log(<i>M</i> [<i>M</i> _⊙])	<i>A_V</i> [mag]	log(<i>t</i> [Myr])	log(<i>M</i> [<i>M</i> _⊙])	<i>A_V</i> [mag]					
AP3946	8.10 ^{+0.00} _{-0.70}	2.83 ^{+0.00} _{-0.10}	1.00 ^{+0.30} _{-0.00}	9.98 ^{+0.27} _{-0.35}	3.77 ^{+0.20} _{-0.24}	0.24 ^{+0.08} _{-0.09}	I	0	1.24	83	61
AP3947	8.70 ^{+0.00} _{-0.00}	3.54 ^{+0.03} _{-0.06}	0.70 ^{+0.10} _{-0.15}	7.61 ^{+0.70} _{-0.79}	2.96 ^{+0.26} _{-0.28}	1.49 ^{+0.88} _{-0.95}	I	0	1.49	140	96
AP3949	6.60 ^{+0.40} _{-0.00}	2.81 ^{+0.00} _{-0.02}	0.45 ^{+0.00} _{-0.05}	6.89 ^{+0.22} _{-0.20}	2.22 ^{+0.17} _{-0.17}	0.00 ^{+0.07} _{-0.00}	I	0	2.51	192	174
AP3950	9.10 ^{+0.20} _{-2.10}	3.21 ^{+0.28} _{-3.21}	0.00 ^{+2.30} _{-0.40}	7.71 ^{+0.41} _{-0.37}	2.94 ^{+0.16} _{-0.17}	0.81 ^{+0.48} _{-0.53}	I	0	1.30	128	90
AP3952	8.90 ^{+0.10} _{-0.70}	2.97 ^{+0.12} _{-0.23}	0.00 ^{+1.35} _{-0.12}	8.12 ^{+0.57} _{-0.53}	2.93 ^{+0.19} _{-0.21}	1.05 ^{+0.85} _{-0.94}	I	0	1.26	109	98
AP3953	9.10 ^{+0.10} _{-0.00}	3.34 ^{+0.25} _{-0.09}	0.35 ^{+0.00} _{-0.20}	8.69 ^{+0.09} _{-0.09}	3.33 ^{+0.08} _{-0.07}	0.62 ^{+0.17} _{-0.18}	I	0	1.84	81	36
AP3955	8.90 ^{+0.00} _{-0.10}	3.06 ^{+0.09} _{-0.03}	0.10 ^{+0.50} _{-0.00}	8.24 ^{+1.17} _{-1.34}	3.22 ^{+0.26} _{-0.23}	1.55 ^{+1.10} _{-1.17}	I	0	1.54	122	90
AP3956	8.40 ^{+0.10} _{-0.20}	3.16 ^{+0.00} _{-0.10}	0.70 ^{+0.15} _{-0.10}	7.60 ^{+0.98} _{-0.94}	2.87 ^{+0.35} _{-0.41}	1.02 ^{+0.77} _{-0.76}	I	0	1.92	198	170
AP3963	9.00 ^{+0.00} _{-0.10}	3.36 ^{+0.02} _{-0.07}	0.35 ^{+0.35} _{-0.00}	8.84 ^{+0.07} _{-0.06}	2.93 ^{+0.05} _{-0.04}	0.69 ^{+0.17} _{-0.21}	I	0	1.10	52	28
AP3966	6.60 ^{+0.50} _{-0.00}	2.63 ^{+0.02} _{-0.04}	0.70 ^{+0.05} _{-0.10}	6.84 ^{+0.30} _{-0.37}	2.91 ^{+0.16} _{-0.16}	0.58 ^{+0.12} _{-0.13}	I	0	2.17	251	220
AP3972	8.80 ^{+0.10} _{-0.00}	3.63 ^{+0.07} _{-0.08}	0.60 ^{+0.00} _{-0.30}	6.77 ^{+0.05} _{-0.13}	2.96 ^{+0.34} _{-0.26}	2.16 ^{+0.12} _{-0.11}	I	0	1.57	148	130
AP3975	8.50 ^{+0.00} _{-1.00}	2.96 ^{+0.01} _{-0.45}	0.60 ^{+0.25} _{-0.20}	8.69 ^{+0.11} _{-0.11}	2.99 ^{+0.08} _{-0.08}	0.17 ^{+0.18} _{-0.17}	I	0	1.20	74	54
AP3976	8.00 ^{+0.30} _{-1.10}	2.53 ^{+0.01} _{-0.15}	0.80 ^{+0.15} _{-0.25}	6.70 ^{+0.29} _{-0.37}	2.52 ^{+0.15} _{-0.16}	0.76 ^{+0.10} _{-0.11}	I	0	1.10	39	25
AP3978	9.10 ^{+0.00} _{-0.00}	3.44 ^{+0.06} _{-0.02}	0.15 ^{+0.10} _{-0.05}	9.08 ^{+0.32} _{-0.25}	3.19 ^{+0.22} _{-0.20}	0.39 ^{+0.20} _{-0.33}	I	0	1.43	132	87
AP3980	8.90 ^{+0.00} _{-0.80}	2.75 ^{+0.01} _{-0.19}	0.20 ^{+1.15} _{-0.05}	8.10 ^{+1.47} _{-1.46}	3.78 ^{+1.25} _{-1.18}	1.45 ^{+1.02} _{-1.02}	I	0	1.12	42	26
AP3983	6.60 ^{+3.00} _{-0.50}	0.00 ^{+0.00} _{-0.00}	0.00 ^{+2.55} _{-0.45}	0.00 ^{+0.00} _{-0.00}	0.00 ^{+0.00} _{-0.00}	0.00 ^{+0.00} _{-0.00}	I	0	1.74	214	347
AP3984	8.50 ^{+0.00} _{-0.40}	3.09 ^{+0.01} _{-0.15}	0.75 ^{+0.30} _{-0.00}	7.93 ^{+0.39} _{-0.38}	2.53 ^{+0.25} _{-0.25}	0.59 ^{+0.54} _{-0.49}	I	0	1.37	135	99
AP3986	8.60 ^{+0.10} _{-0.10}	2.92 ^{+0.00} _{-0.16}	0.45 ^{+0.15} _{-0.30}	8.08 ^{+0.18} _{-0.20}	3.08 ^{+0.15} _{-0.17}	1.28 ^{+0.35} _{-0.27}	I	0	1.20	84	66
AP3988	7.40 ^{+0.40} _{-0.30}	2.99 ^{+0.03} _{-0.12}	1.65 ^{+0.10} _{-0.20}	7.33 ^{+0.79} _{-0.82}	2.74 ^{+0.40} _{-0.45}	1.46 ^{+0.83} _{-0.87}	I	0	1.01	74	52
AP3993	9.00 ^{+0.10} _{-0.00}	3.35 ^{+0.06} _{-0.11}	0.30 ^{+0.05} _{-0.20}	7.75 ^{+0.09} _{-0.10}	2.84 ^{+0.16} _{-0.16}	1.55 ^{+0.26} _{-0.27}	I	0	1.32	96	60
AP3995	6.60 ^{+0.30} _{-0.00}	2.87 ^{+0.01} _{-0.00}	0.80 ^{+0.05} _{-0.05}	6.64 ^{+0.41} _{-0.45}	2.95 ^{+0.21} _{-0.27}	0.48 ^{+0.13} _{-0.14}	I	0	2.29	210	202
AP3996	8.40 ^{+0.00} _{-0.10}	3.01 ^{+0.00} _{-0.06}	0.65 ^{+0.05} _{-0.10}	8.37 ^{+0.11} _{-0.12}	2.56 ^{+0.18} _{-0.17}	0.22 ^{+0.22} _{-0.21}	I	0	1.49	123	104
AP3997	8.90 ^{+0.30} _{-1.30}	3.57 ^{+0.02} _{-3.57}	1.10 ^{+1.20} _{-0.45}	7.68 ^{+0.13} _{-0.12}	2.93 ^{+0.32} _{-0.33}	1.91 ^{+0.43} _{-0.40}	I	0	1.21	93	66
AP3998	7.90 ^{+0.30} _{-0.20}	2.82 ^{+0.06} _{-0.04}	0.75 ^{+0.05} _{-0.15}	7.35 ^{+0.33} _{-0.30}	3.23 ^{+0.11} _{-0.11}	1.63 ^{+0.31} _{-0.32}	I	0	1.43	98	83
AP3999	7.60 ^{+0.10} _{-0.30}	2.61 ^{+0.01} _{-0.02}	0.75 ^{+0.09} _{-0.10}	8.00 ^{+0.03} _{-0.03}	2.45 ^{+0.03} _{-0.04}	0.30 ^{+0.07} _{-0.07}	I	0	1.33	47	23
AP4000	6.80 ^{+1.00} _{-0.10}	2.61 ^{+0.02} _{-0.04}	0.55 ^{+0.05} _{-0.20}	6.94 ^{+0.20} _{-0.16}	3.09 ^{+0.22} _{-0.21}	0.17 ^{+0.13} _{-0.14}	I	0	1.74	198	192
AP4002	8.60 ^{+0.10} _{-0.20}	2.80 ^{+0.07} _{-0.06}	0.25 ^{+0.25} _{-0.15}	9.00 ^{+0.41} _{-1.04}	3.25 ^{+0.12} _{-0.12}	0.45 ^{+1.13} _{-0.45}	I	0	1.05	42	30
AP4003	8.00 ^{+0.20} _{-0.30}	2.81 ^{+0.03} _{-0.06}	0.55 ^{+0.10} _{-0.15}	8.23 ^{+0.14} _{-0.14}	2.65 ^{+0.13} _{-0.14}	0.29 ^{+0.26} _{-0.24}	I	0	1.10	73	49
AP4008	7.50 ^{+1.10} _{-0.20}	3.24 ^{+0.02} _{-1.02}	3.00 ^{+0.05} _{-2.00}	9.44 ^{+0.12} _{-0.19}	3.48 ^{+0.06} _{-0.07}	0.51 ^{+0.35} _{-0.20}	I	0	1.03	50	34
AP4013	8.30 ^{+0.10} _{-0.70}	2.67 ^{+0.03} _{-0.19}	0.45 ^{+0.30} _{-0.05}	9.06 ^{+0.07} _{-0.10}	3.09 ^{+0.06} _{-0.07}	0.04 ^{+0.08} _{-0.04}	I	0	1.19	56	36
AP4017	8.90 ^{+0.00} _{-0.80}	3.05 ^{+0.02} _{-0.47}	0.60 ^{+0.95} _{-0.05}	8.62 ^{+1.20} _{-1.27}	2.73 ^{+0.46} _{-0.51}	1.69 ^{+0.92} _{-0.99}	I	0	1.18	69	46
AP4019	8.80 ^{+0.30} _{-1.70}	2.74 ^{+0.13} _{-0.31}	0.00 ^{+0.75} _{-0.35}	7.72 ^{+0.48} _{-0.52}	2.37 ^{+0.17} _{-0.18}	0.59 ^{+0.44} _{-0.43}	I	0	1.03	58	49
AP4021	8.50 ^{+0.10} _{-0.00}	2.82 ^{+0.03} _{-0.04}	0.45 ^{+0.05} _{-0.15}	8.24 ^{+0.56} _{-0.39}	2.38 ^{+0.54} _{-0.36}	1.07 ^{+0.30} _{-0.26}	I	0	1.28	54	32

Table 1 (cont'd)

AP ID ^a	CMD Best Fit Parameters ^b			Integrated Best Fit Parameters ^c			Best ^d Flag ^e	R _{ap} ^f	N _{stars} ^g	N _{bg} ^h	
	log(<i>t</i> [Myr])	log(<i>M</i> [<i>M</i> _⊙])	<i>A_V</i> [mag]	log(<i>t</i> [Myr])	log(<i>M</i> [<i>M</i> _⊙])	<i>A_V</i> [mag]					
AP4025	7.50 ^{+0.00} _{-0.50}	2.69 ^{+0.00} _{-0.04}	0.55 ^{+0.20} _{-0.05}	7.80 ^{+0.05} _{-0.05}	2.76 ^{+0.05} _{-0.05}	0.02 ^{+0.07} _{-0.02}	I	0	1.63	204	184
AP4027	8.90 ^{+0.10} _{-0.40}	2.98 ^{+0.01} _{-0.13}	0.00 ^{+0.80} _{-0.05}	8.33 ^{+0.15} _{-0.15}	2.47 ^{+0.21} _{-0.19}	0.30 ^{+0.28} _{-0.27}	I	0	1.57	117	96
AP4028	8.10 ^{+0.00} _{-1.00}	2.81 ^{+0.04} _{-0.17}	0.70 ^{+0.30} _{-0.05}	8.09 ^{+0.22} _{-0.14}	3.10 ^{+0.09} _{-0.11}	0.95 ^{+0.30} _{-0.36}	I	0	1.50	131	96
AP4034	9.10 ^{+0.00} _{-0.10}	3.14 ^{+0.01} _{-0.09}	0.15 ^{+0.25} _{-0.00}	8.55 ^{+0.14} _{-0.14}	2.39 ^{+0.15} _{-0.16}	0.25 ^{+0.23} _{-0.22}	I	0	1.67	66	34
AP4038	7.60 ^{+1.40} _{-0.50}	3.49 ^{+0.28} _{-3.49}	3.00 ^{+0.10} _{-2.65}	8.64 ^{+0.26} _{-0.27}	2.85 ^{+0.18} _{-0.17}	0.49 ^{+0.39} _{-0.38}	I	0	1.40	107	73
AP4039	7.50 ^{+0.00} _{-0.60}	2.66 ^{+0.00} _{-0.03}	0.40 ^{+0.15} _{-0.00}	7.61 ^{+0.07} _{-0.13}	3.13 ^{+0.04} _{-0.06}	0.20 ^{+0.23} _{-0.15}	I	0	1.33	157	147
AP4042	8.80 ^{+0.00} _{-0.00}	2.71 ^{+0.03} _{-0.02}	0.10 ^{+0.20} _{-0.05}	6.95 ^{+0.40} _{-0.47}	2.36 ^{+0.19} _{-0.22}	1.71 ^{+0.21} _{-0.20}	I	0	1.18	35	17
AP4043	6.60 ^{+1.30} _{-0.00}	2.57 ^{+0.08} _{-0.04}	0.80 ^{+0.05} _{-0.20}	6.79 ^{+0.10} _{-0.07}	2.44 ^{+0.12} _{-0.13}	0.41 ^{+0.12} _{-0.11}	I	0	1.72	109	100
AP4046	8.30 ^{+0.10} _{-0.40}	3.31 ^{+0.07} _{-0.19}	1.70 ^{+0.25} _{-0.20}	9.15 ^{+0.16} _{-0.16}	3.11 ^{+0.16} _{-0.14}	0.09 ^{+0.13} _{-0.09}	I	0	1.36	136	89
AP4048	8.70 ^{+0.10} _{-0.10}	3.19 ^{+0.02} _{-0.05}	0.50 ^{+0.05} _{-0.25}	8.60 ^{+0.46} _{-0.42}	3.30 ^{+0.23} _{-0.25}	1.02 ^{+0.52} _{-0.46}	I	0	1.41	92	50
AP4049	6.90 ^{+0.50} _{-0.20}	2.50 ^{+0.01} _{-0.03}	0.75 ^{+0.10} _{-0.15}	7.06 ^{+0.09} _{-0.09}	2.17 ^{+0.14} _{-0.13}	0.38 ^{+0.10} _{-0.11}	I	0	1.45	103	100
AP4056	8.20 ^{+0.10} _{-0.10}	2.85 ^{+0.03} _{-0.04}	0.25 ^{+0.15} _{-0.10}	6.57 ^{+0.41} _{-0.42}	3.11 ^{+0.37} _{-0.38}	2.40 ^{+0.26} _{-0.21}	I	0	1.85	263	203
AP4057	8.60 ^{+0.10} _{-0.30}	2.95 ^{+0.03} _{-0.21}	0.70 ^{+0.35} _{-0.20}	8.73 ^{+0.82} _{-0.68}	3.31 ^{+0.24} _{-0.25}	1.25 ^{+0.74} _{-0.93}	I	0	1.71	79	52
AP4060	8.10 ^{+0.20} _{-0.20}	3.10 ^{+0.07} _{-0.03}	0.85 ^{+0.10} _{-0.10}	7.62 ^{+0.14} _{-0.13}	3.52 ^{+0.14} _{-0.15}	2.02 ^{+0.27} _{-0.29}	I	0	1.24	91	62
AP4066	9.00 ^{+0.70} _{-1.80}	2.82 ^{+0.12} _{-2.82}	0.55 ^{+1.80} _{-0.20}	9.57 ^{+0.47} _{-0.31}	3.24 ^{+0.18} _{-0.20}	0.54 ^{+0.29} _{-0.49}	I	0	0.92	25	13
AP4067	9.10 ^{+0.00} _{-0.10}	3.97 ^{+0.00} _{-0.27}	0.40 ^{+0.15} _{-0.10}	9.27 ^{+0.27} _{-0.24}	3.77 ^{+0.16} _{-0.15}	0.78 ^{+0.32} _{-0.37}	I	0	1.68	196	147
AP4069	8.40 ^{+0.00} _{-0.20}	3.26 ^{+0.00} _{-0.07}	0.80 ^{+0.15} _{-0.00}	8.74 ^{+0.34} _{-0.33}	3.46 ^{+0.14} _{-0.13}	0.68 ^{+0.49} _{-0.51}	I	0	1.47	199	153
AP4075	6.60 ^{+0.80} _{-0.00}	2.89 ^{+0.03} _{-0.04}	1.75 ^{+0.00} _{-0.20}	6.27 ^{+0.28} _{-0.20}	2.57 ^{+0.23} _{-0.21}	0.70 ^{+0.11} _{-0.12}	I	0	1.14	51	17
AP4077	9.00 ^{+0.50} _{-1.60}	3.80 ^{+0.03} _{-3.80}	1.05 ^{+1.55} _{-0.45}	8.86 ^{+0.49} _{-0.39}	3.05 ^{+0.21} _{-0.20}	0.97 ^{+0.51} _{-0.65}	I	0	1.39	132	106
AP4083	8.00 ^{+0.10} _{-0.00}	3.26 ^{+0.03} _{-0.14}	1.95 ^{+0.10} _{-0.25}	8.11 ^{+1.47} _{-1.46}	3.78 ^{+1.25} _{-1.18}	1.45 ^{+1.02} _{-1.02}	I	0	1.66	85	32
AP4088	8.40 ^{+0.00} _{-0.90}	3.07 ^{+0.03} _{-0.20}	0.90 ^{+0.40} _{-0.05}	8.95 ^{+0.16} _{-0.10}	2.99 ^{+0.13} _{-0.12}	0.12 ^{+0.08} _{-0.12}	I	0	1.14	86	67
AP4095	9.10 ^{+0.00} _{-0.00}	3.40 ^{+0.02} _{-0.07}	0.15 ^{+0.15} _{-0.05}	8.03 ^{+0.17} _{-0.15}	2.97 ^{+0.22} _{-0.25}	1.13 ^{+0.37} _{-0.45}	I	0	1.30	94	66
AP4098	8.20 ^{+0.20} _{-1.30}	2.47 ^{+0.01} _{-0.08}	0.25 ^{+0.45} _{-0.10}	6.42 ^{+0.30} _{-0.32}	2.68 ^{+0.37} _{-0.35}	1.78 ^{+0.17} _{-0.14}	I	0	1.15	85	77
AP4101	6.60 ^{+0.20} _{-0.00}	2.74 ^{+0.01} _{-0.03}	1.25 ^{+0.00} _{-0.05}	6.73 ^{+0.07} _{-0.07}	2.68 ^{+0.31} _{-0.24}	1.09 ^{+0.11} _{-0.12}	I	0	1.69	189	179
AP4103	8.20 ^{+0.20} _{-1.30}	2.43 ^{+0.00} _{-0.12}	0.05 ^{+0.50} _{-0.05}	8.09 ^{+0.14} _{-0.17}	2.91 ^{+0.13} _{-0.13}	0.17 ^{+0.17} _{-0.16}	I	0	1.04	83	69
AP4104	8.00 ^{+0.20} _{-1.10}	2.73 ^{+0.02} _{-0.13}	0.40 ^{+0.25} _{-0.10}	7.79 ^{+0.12} _{-0.15}	3.39 ^{+0.11} _{-0.11}	0.62 ^{+0.20} _{-0.19}	I	0	1.50	181	189
AP4105	8.50 ^{+0.00} _{-1.40}	3.29 ^{+0.01} _{-0.43}	0.80 ^{+0.20} _{-0.15}	7.41 ^{+0.35} _{-0.33}	2.85 ^{+0.13} _{-0.12}	0.59 ^{+0.25} _{-0.26}	I	0	1.35	113	98
AP4106	7.30 ^{+0.60} _{-0.30}	2.67 ^{+0.03} _{-0.03}	0.50 ^{+0.10} _{-0.10}	7.84 ^{+0.04} _{-0.03}	2.65 ^{+0.09} _{-0.10}	0.07 ^{+0.09} _{-0.07}	I	0	1.16	68	53
AP4111	9.10 ^{+0.00} _{-0.00}	3.31 ^{+0.10} _{-0.00}	0.00 ^{+0.10} _{-0.00}	8.36 ^{+0.27} _{-0.24}	2.35 ^{+0.16} _{-0.17}	0.42 ^{+0.36} _{-0.34}	I	0	1.27	84	42
AP4117	8.00 ^{+0.00} _{-0.90}	2.66 ^{+0.02} _{-0.12}	0.70 ^{+0.20} _{-0.05}	7.60 ^{+0.51} _{-0.50}	2.82 ^{+0.22} _{-0.22}	1.08 ^{+0.63} _{-0.65}	I	0	1.09	60	46
AP4118	8.90 ^{+0.00} _{-0.80}	3.18 ^{+0.02} _{-0.45}	0.20 ^{+1.25} _{-0.05}	8.46 ^{+0.38} _{-0.35}	3.10 ^{+0.19} _{-0.19}	0.78 ^{+0.65} _{-0.66}	I	0	1.32	106	75
AP4123	7.80 ^{+0.00} _{-0.40}	3.46 ^{+0.01} _{-0.14}	2.35 ^{+0.15} _{-0.05}	7.92 ^{+0.41} _{-0.41}	3.35 ^{+0.22} _{-0.25}	1.45 ^{+0.71} _{-0.72}	I	0	1.17	134	125
AP4124	6.60 ^{+0.50} _{-0.00}	2.80 ^{+0.02} _{-0.02}	0.80 ^{+0.05} _{-0.05}	6.78 ^{+0.12} _{-0.08}	2.48 ^{+0.30} _{-0.29}	0.38 ^{+0.11} _{-0.12}	I	0	2.09	202	200

Table 1 (cont'd)

AP ID ^a	CMD Best Fit Parameters ^b			Integrated Best Fit Parameters ^c			Best ^d Flag ^e	Rap ^f	N _{stars} ^g	N _{bg} ^h	
	log(<i>t</i> [Myr])	log(<i>M</i> [<i>M</i> _⊙])	<i>A_V</i> [mag]	log(<i>t</i> [Myr])	log(<i>M</i> [<i>M</i> _⊙])	<i>A_V</i> [mag]					
AP4125	7.20 ^{+0.40} _{-0.20}	2.54 ^{+0.01} _{-0.02}	0.75 ^{+0.05} _{-0.10}	6.97 ^{+0.11} _{-0.09}	2.25 ^{+0.19} _{-0.18}	0.73 ^{+0.11} _{-0.10}	I	0	1.24	80	82
AP4127	9.10 ^{+0.00} _{-0.20}	3.68 ^{+0.00} _{-0.29}	0.35 ^{+0.40} _{-0.05}	8.68 ^{+0.49} _{-0.56}	2.96 ^{+0.20} _{-0.21}	0.64 ^{+0.86} _{-0.60}	I	0	1.22	107	76
AP4129	9.20 ^{+0.10} _{-0.10}	3.81 ^{+0.10} _{-0.22}	0.45 ^{+0.05} _{-0.20}	8.76 ^{+0.47} _{-0.43}	3.19 ^{+0.24} _{-0.22}	0.81 ^{+0.55} _{-0.59}	I	0	1.61	152	113
AP4131	8.30 ^{+0.40} _{-1.10}	2.62 ^{+0.16} _{-0.17}	0.30 ^{+0.25} _{-0.05}	8.03 ^{+0.12} _{-0.14}	2.85 ^{+0.21} _{-0.20}	1.26 ^{+0.33} _{-0.34}	I	0	1.12	42	30
AP4132	8.80 ^{+0.00} _{-0.80}	2.68 ^{+0.00} _{-0.10}	0.00 ^{+0.70} _{-0.00}	9.06 ^{+0.13} _{-0.09}	3.13 ^{+0.13} _{-0.12}	0.07 ^{+0.06} _{-0.07}	I	0	1.08	33	14
AP4134	7.80 ^{+0.30} _{-0.50}	2.96 ^{+0.05} _{-0.09}	0.90 ^{+0.15} _{-0.15}	8.34 ^{+0.06} _{-0.06}	2.20 ^{+0.13} _{-0.13}	0.02 ^{+0.07} _{-0.02}	I	0	1.13	93	78
AP4138	8.10 ^{+0.20} _{-0.30}	3.33 ^{+0.00} _{-0.17}	1.65 ^{+0.05} _{-0.35}	9.11 ^{+0.54} _{-0.78}	3.55 ^{+0.17} _{-0.15}	0.68 ^{+0.88} _{-0.57}	I	0	1.17	121	103
AP4139	8.90 ^{+0.10} _{-0.30}	3.08 ^{+0.10} _{-0.12}	0.10 ^{+0.80} _{-0.00}	7.54 ^{+0.13} _{-0.12}	3.68 ^{+0.21} _{-0.20}	2.58 ^{+0.26} _{-0.26}	I	0	1.46	108	127
AP4142	8.00 ^{+0.22} _{-0.60}	2.38 ^{+0.02} _{-0.12}	0.35 ^{+0.15} _{-0.15}	8.17 ^{+0.04} _{-0.05}	2.20 ^{+0.10} _{-0.07}	0.07 ^{+0.08} _{-0.07}	I	0	1.31	62	32
AP4145	8.10 ^{+0.20} _{-0.50}	3.10 ^{+0.00} _{-0.24}	1.40 ^{+0.20} _{-0.25}	8.77 ^{+0.20} _{-0.23}	2.88 ^{+0.14} _{-0.14}	0.41 ^{+0.30} _{-0.29}	I	0	1.40	150	130
AP4150	8.70 ^{+0.30} _{-1.40}	3.02 ^{+0.03} _{-3.02}	0.60 ^{+2.05} _{-0.30}	6.64 ^{+0.14} _{-0.09}	3.02 ^{+0.25} _{-0.40}	2.49 ^{+0.08} _{-0.07}	I	0	1.45	93	76
AP4153	8.50 ^{+0.30} _{-0.90}	2.70 ^{+1.08} _{-0.56}	0.65 ^{+1.70} _{-0.25}	8.48 ^{+0.14} _{-0.13}	2.59 ^{+0.19} _{-0.20}	0.41 ^{+0.31} _{-0.30}	I	0	1.31	109	80
AP4157	8.80 ^{+0.00} _{-0.00}	2.93 ^{+0.03} _{-0.01}	0.25 ^{+0.15} _{-0.10}	10.15 ^{+0.03} _{-0.03}	2.45 ^{+0.03} _{-0.03}	0.00 ^{+0.07} _{-0.00}	I	0	1.03	34	13
AP4161	8.10 ^{+0.10} _{-0.00}	3.15 ^{+0.00} _{-0.05}	1.25 ^{+0.05} _{-0.15}	8.44 ^{+0.19} _{-0.20}	2.85 ^{+0.17} _{-0.15}	0.37 ^{+0.39} _{-0.33}	I	0	1.48	142	122
AP4163	8.80 ^{+0.00} _{-0.00}	3.39 ^{+0.02} _{-0.03}	0.25 ^{+0.10} _{-0.06}	8.62 ^{+0.18} _{-0.19}	2.97 ^{+0.12} _{-0.13}	0.52 ^{+0.35} _{-0.34}	I	0	1.51	158	144
AP4167	8.80 ^{+0.10} _{-0.20}	3.17 ^{+0.12} _{-0.13}	0.65 ^{+0.70} _{-0.15}	7.49 ^{+0.78} _{-0.84}	2.74 ^{+0.32} _{-0.35}	1.83 ^{+0.88} _{-1.15}	I	0	1.04	47	40
AP4169	8.30 ^{+0.00} _{-0.10}	3.13 ^{+0.03} _{-0.15}	1.45 ^{+0.10} _{-0.20}	8.65 ^{+0.25} _{-0.25}	2.79 ^{+0.18} _{-0.17}	0.50 ^{+0.39} _{-0.39}	I	0	1.31	76	51
AP4171	0.00 ^{+0.00} _{-0.00}	0.00 ^{+0.00} _{-0.00}	0.00 ^{+0.00} _{-0.00}	0.00 ^{+0.00} _{-0.00}	0.00 ^{+0.00} _{-0.00}	0.00 ^{+0.00} _{-0.00}	I	0	1.52	0	0
AP4173	8.00 ^{+0.50} _{-0.10}	3.12 ^{+0.12} _{-0.12}	1.50 ^{+0.10} _{-0.40}	9.32 ^{+0.87} _{-0.72}	4.06 ^{+0.21} _{-0.16}	1.06 ^{+0.81} _{-0.88}	I	0	1.28	150	119
AP4174	7.60 ^{+0.40} _{-0.60}	2.57 ^{+0.03} _{-0.06}	1.05 ^{+0.15} _{-0.15}	7.05 ^{+0.51} _{-0.62}	3.20 ^{+0.19} _{-0.20}	1.80 ^{+0.29} _{-0.21}	I	0	1.32	68	39
AP4175	8.00 ^{+0.10} _{-0.60}	2.59 ^{+0.00} _{-0.16}	0.40 ^{+0.20} _{-0.10}	7.81 ^{+0.09} _{-0.11}	2.86 ^{+0.12} _{-0.12}	0.71 ^{+0.21} _{-0.21}	I	0	1.42	132	116
AP4177	7.40 ^{+0.00} _{-0.60}	2.52 ^{+0.00} _{-0.05}	0.65 ^{+0.20} _{-0.10}	6.85 ^{+0.06} _{-0.06}	2.37 ^{+0.20} _{-0.20}	1.08 ^{+0.09} _{-0.07}	I	0	1.24	98	71
AP4179	8.80 ^{+0.10} _{-0.30}	3.21 ^{+0.02} _{-0.26}	0.55 ^{+0.55} _{-0.20}	10.21 ^{+0.03} _{-0.04}	3.68 ^{+0.04} _{-0.04}	0.00 ^{+0.07} _{-0.00}	I	0	1.39	117	72
AP4185	8.30 ^{+0.20} _{-0.70}	2.59 ^{+0.06} _{-0.17}	0.35 ^{+0.30} _{-0.10}	7.61 ^{+0.43} _{-0.43}	2.62 ^{+0.16} _{-0.16}	0.58 ^{+0.36} _{-0.36}	I	0	1.32	86	71
AP4187	8.70 ^{+0.10} _{-0.10}	2.85 ^{+0.02} _{-0.02}	0.35 ^{+0.35} _{-0.15}	8.74 ^{+1.06} _{-0.94}	3.60 ^{+0.32} _{-0.37}	1.60 ^{+0.96} _{-0.91}	I	0	1.49	48	25
AP4190	7.90 ^{+0.30} _{-0.70}	2.78 ^{+0.04} _{-0.31}	1.05 ^{+0.20} _{-0.20}	8.76 ^{+0.05} _{-0.05}	3.41 ^{+0.06} _{-0.06}	0.05 ^{+0.10} _{-0.05}	I	0	1.13	74	62
AP4193	7.90 ^{+0.00} _{-0.20}	3.55 ^{+0.00} _{-0.07}	1.95 ^{+0.15} _{-0.05}	8.00 ^{+0.18} _{-0.28}	3.23 ^{+0.24} _{-0.22}	1.29 ^{+0.48} _{-0.49}	I	0	1.48	165	120
AP4195	7.20 ^{+0.70} _{-0.30}	2.36 ^{+0.05} _{-0.06}	0.70 ^{+0.10} _{-0.20}	7.76 ^{+0.38} _{-0.36}	2.72 ^{+0.16} _{-0.17}	0.67 ^{+0.40} _{-0.41}	I	0	1.22	103	90
AP4197	8.90 ^{+0.00} _{-0.20}	3.50 ^{+0.00} _{-0.25}	0.30 ^{+0.45} _{-0.10}	8.01 ^{+0.46} _{-0.42}	2.79 ^{+0.22} _{-0.23}	1.05 ^{+0.68} _{-0.79}	I	0	1.14	78	65
AP4199	9.10 ^{+0.00} _{-0.10}	3.50 ^{+0.09} _{-0.06}	0.30 ^{+0.25} _{-0.00}	8.95 ^{+0.73} _{-0.47}	3.17 ^{+0.23} _{-0.20}	1.09 ^{+0.59} _{-0.76}	I	0	1.33	88	52
AP4202	9.10 ^{+0.00} _{-0.00}	3.62 ^{+0.06} _{-0.05}	0.15 ^{+0.15} _{-0.05}	9.80 ^{+0.03} _{-0.04}	3.65 ^{+0.04} _{-0.03}	0.60 ^{+0.07} _{-0.07}	I	0	1.26	118	100
AP4204	7.20 ^{+0.10} _{-0.30}	2.67 ^{+0.01} _{-0.03}	0.85 ^{+0.10} _{-0.10}	7.31 ^{+0.28} _{-0.23}	2.62 ^{+0.18} _{-0.20}	0.60 ^{+0.20} _{-0.20}	I	0	1.61	145	135
AP4207	7.80 ^{+1.50} _{-0.40}	3.32 ^{+0.52} _{-3.32}	3.00 ^{+0.50} _{-2.80}	8.86 ^{+0.53} _{-0.44}	3.13 ^{+0.21} _{-0.17}	0.92 ^{+0.50} _{-0.56}	I	0	1.25	65	41

Table 1 (cont'd)

AP ID ^a	CMD Best Fit Parameters ^b			Integrated Best Fit Parameters ^c			Best ^d Flag ^e	R _{ap} ^f	N _{stars} ^g	N _{bg} ^h	
	log(<i>t</i> [Myr])	log(<i>M</i> [<i>M</i> _⊙])	<i>A_V</i> [mag]	log(<i>t</i> [Myr])	log(<i>M</i> [<i>M</i> _⊙])	<i>A_V</i> [mag]					
AP4209	8.80 ^{+0.10} _{-0.00}	3.25 ^{+0.06} _{-0.03}	0.65 ^{+0.15} _{-0.17}	8.68 ^{+0.26} _{-0.28}	2.56 ^{+0.23} _{-0.24}	0.67 ^{+0.45} _{-0.46}	I	0	1.04	60	32
AP4211	8.20 ^{+0.00} _{-0.60}	3.10 ^{+0.02} _{-0.13}	0.70 ^{+0.20} _{-0.00}	10.20 ^{+0.03} _{-0.03}	3.95 ^{+0.03} _{-0.03}	0.10 ^{+0.07} _{-0.07}	I	0	1.28	111	75
AP4215	8.20 ^{+0.00} _{-0.00}	2.88 ^{+0.03} _{-0.02}	0.85 ^{+0.20} _{-0.05}	8.94 ^{+0.81} _{-0.78}	3.48 ^{+0.23} _{-0.20}	1.07 ^{+0.82} _{-0.83}	I	0	1.37	77	59
AP4223	8.00 ^{+0.10} _{-0.80}	3.11 ^{+0.07} _{-0.14}	1.40 ^{+0.25} _{-0.05}	8.18 ^{+0.14} _{-0.14}	3.40 ^{+0.15} _{-0.12}	1.52 ^{+0.31} _{-0.30}	I	0	1.18	100	65
AP4224	8.80 ^{+0.00} _{-0.90}	2.90 ^{+0.10} _{-0.12}	0.00 ^{+0.85} _{-0.05}	8.11 ^{+0.20} _{-0.17}	2.45 ^{+0.14} _{-0.15}	0.30 ^{+0.28} _{-0.26}	I	0	1.25	55	36
AP4225	8.10 ^{+0.00} _{-0.80}	2.72 ^{+0.00} _{-0.15}	1.05 ^{+0.25} _{-0.10}	7.93 ^{+0.23} _{-0.18}	2.42 ^{+0.14} _{-0.15}	0.53 ^{+0.29} _{-0.30}	I	0	0.92	40	28
AP4226	6.70 ^{+0.60} _{-0.00}	2.71 ^{+0.02} _{-0.01}	0.80 ^{+0.05} _{-0.10}	7.75 ^{+0.20} _{-0.33}	3.22 ^{+0.15} _{-0.24}	0.04 ^{+0.07} _{-0.04}	I	0	2.54	388	294
AP4234	0.00 ^{+0.00} _{-0.00}	0.00 ^{+0.00} _{-0.00}	0.00 ^{+0.00} _{-0.00}	0.00 ^{+0.00} _{-0.00}	0.00 ^{+0.00} _{-0.00}	0.00 ^{+0.00} _{-0.00}	I	0	1.05	0	0
AP4237	8.40 ^{+0.10} _{-0.00}	2.97 ^{+0.01} _{-0.09}	0.60 ^{+0.00} _{-0.25}	7.04 ^{+0.56} _{-0.62}	3.02 ^{+0.22} _{-0.23}	2.34 ^{+0.45} _{-0.43}	I	0	1.21	109	86
AP4242	9.10 ^{+0.00} _{-1.00}	3.80 ^{+0.04} _{-0.56}	0.50 ^{+1.55} _{-0.05}	8.43 ^{+0.68} _{-0.50}	2.12 ^{+0.03} _{-0.12}	0.45 ^{+0.35} _{-0.29}	I	0	1.46	167	134
AP4245	8.80 ^{+0.00} _{-0.10}	3.32 ^{+0.02} _{-0.13}	0.50 ^{+0.15} _{-0.22}	7.96 ^{+0.39} _{-0.34}	3.03 ^{+0.18} _{-0.18}	0.99 ^{+0.66} _{-0.59}	I	0	1.34	139	108
AP4246	7.90 ^{+0.00} _{-0.80}	2.83 ^{+0.03} _{-0.09}	0.80 ^{+0.30} _{-0.05}	7.35 ^{+0.59} _{-0.71}	2.49 ^{+0.17} _{-0.17}	0.52 ^{+0.37} _{-0.38}	I	0	1.20	110	88
AP4247	9.10 ^{+0.10} _{-0.10}	3.01 ^{+0.13} _{-0.24}	0.10 ^{+0.30} _{-0.10}	9.20 ^{+0.46} _{-0.49}	3.03 ^{+0.28} _{-0.25}	0.40 ^{+0.36} _{-0.34}	I	0	1.17	45	14
AP4248	7.40 ^{+0.20} _{-0.50}	2.82 ^{+0.06} _{-0.05}	0.55 ^{+0.20} _{-0.05}	6.28 ^{+0.16} _{-0.16}	2.44 ^{+0.23} _{-0.24}	0.73 ^{+0.07} _{-0.09}	I	0	1.65	141	120
AP4249	8.10 ^{+0.10} _{-0.00}	2.99 ^{+0.03} _{-0.05}	1.25 ^{+0.05} _{-0.05}	7.90 ^{+0.08} _{-0.08}	2.98 ^{+0.07} _{-0.07}	1.55 ^{+0.10} _{-0.10}	I	0	1.08	35	16
AP4252	7.20 ^{+0.20} _{-0.40}	2.65 ^{+0.02} _{-0.03}	0.50 ^{+0.10} _{-0.05}	6.95 ^{+0.59} _{-0.64}	2.46 ^{+0.23} _{-0.23}	0.14 ^{+0.15} _{-0.14}	I	0	1.09	75	61
AP4254	8.50 ^{+0.10} _{-0.10}	3.30 ^{+0.02} _{-0.08}	0.70 ^{+0.10} _{-0.10}	7.99 ^{+0.34} _{-0.30}	2.45 ^{+0.18} _{-0.18}	0.43 ^{+0.39} _{-0.36}	I	0	1.27	98	77
AP4255	7.60 ^{+0.20} _{-0.50}	2.75 ^{+0.00} _{-0.13}	1.20 ^{+0.05} _{-0.15}	7.66 ^{+0.02} _{-0.09}	2.61 ^{+0.02} _{-0.09}	0.01 ^{+0.07} _{-0.01}	I	0	1.57	148	144
AP4256	8.10 ^{+0.20} _{-0.40}	3.22 ^{+0.08} _{-0.27}	1.90 ^{+0.20} _{-0.30}	9.22 ^{+0.12} _{-0.11}	3.08 ^{+0.13} _{-0.11}	0.07 ^{+0.10} _{-0.07}	I	0	1.17	87	66
AP4259	8.20 ^{+0.10} _{-0.20}	2.77 ^{+0.00} _{-0.05}	0.75 ^{+0.05} _{-0.10}	7.12 ^{+0.72} _{-0.77}	2.25 ^{+0.17} _{-0.17}	0.24 ^{+0.24} _{-0.22}	I	0	1.22	43	18
AP4261	8.20 ^{+0.10} _{-0.70}	2.77 ^{+0.02} _{-0.12}	0.55 ^{+0.20} _{-0.10}	8.40 ^{+0.89} _{-0.66}	3.26 ^{+0.12} _{-0.13}	1.13 ^{+0.91} _{-1.13}	I	0	1.20	104	84
AP4262	0.00 ^{+0.00} _{-0.00}	0.00 ^{+0.00} _{-0.00}	0.00 ^{+0.00} _{-0.00}	0.00 ^{+0.00} _{-0.00}	0.00 ^{+0.00} _{-0.00}	0.00 ^{+0.00} _{-0.00}	I	0	1.72	0	0
AP4265	9.00 ^{+0.10} _{-0.90}	3.49 ^{+0.01} _{-0.17}	0.25 ^{+1.45} _{-0.15}	8.13 ^{+0.15} _{-0.10}	3.03 ^{+0.11} _{-0.22}	0.94 ^{+0.23} _{-0.44}	I	0	1.35	131	93
AP4270	6.90 ^{+0.10} _{-0.10}	3.25 ^{+0.02} _{-0.01}	1.00 ^{+0.05} _{-0.00}	7.63 ^{+0.05} _{-0.06}	3.49 ^{+0.05} _{-0.04}	0.10 ^{+0.09} _{-0.09}	I	0	3.71	840	770
AP4271	8.10 ^{+0.00} _{-0.20}	2.94 ^{+0.01} _{-0.17}	1.05 ^{+0.15} _{-0.05}	7.91 ^{+0.10} _{-0.13}	2.65 ^{+0.15} _{-0.19}	0.54 ^{+0.27} _{-0.29}	I	0	1.30	112	84
AP4273	9.00 ^{+0.00} _{-0.10}	3.65 ^{+0.02} _{-0.11}	0.45 ^{+0.30} _{-0.05}	7.11 ^{+0.59} _{-0.59}	3.03 ^{+0.18} _{-0.19}	2.01 ^{+0.42} _{-0.45}	I	0	1.77	206	172
AP4277	7.80 ^{+1.70} _{-0.60}	3.04 ^{+0.19} _{-3.04}	2.60 ^{+0.05} _{-2.15}	8.70 ^{+0.23} _{-0.26}	2.83 ^{+0.21} _{-0.22}	0.83 ^{+0.46} _{-0.49}	I	0	1.11	72	53
AP4278	8.40 ^{+0.00} _{-0.20}	2.61 ^{+0.02} _{-0.05}	0.15 ^{+0.30} _{-0.00}	7.48 ^{+0.61} _{-0.76}	2.25 ^{+0.13} _{-0.14}	0.13 ^{+0.15} _{-0.13}	I	0	1.09	71	72
AP4279	7.00 ^{+0.70} _{-0.20}	2.30 ^{+0.05} _{-0.02}	0.70 ^{+0.10} _{-0.10}	7.90 ^{+0.05} _{-0.07}	2.69 ^{+0.12} _{-0.15}	0.69 ^{+0.15} _{-0.15}	I	0	1.70	84	68
AP4280	6.90 ^{+0.60} _{-0.10}	2.67 ^{+0.06} _{-0.01}	0.80 ^{+0.10} _{-0.10}	6.81 ^{+0.50} _{-0.54}	2.48 ^{+0.18} _{-0.18}	0.81 ^{+0.23} _{-0.24}	I	0	1.39	103	102
AP4283	7.30 ^{+0.00} _{-0.20}	2.97 ^{+0.01} _{-0.02}	1.25 ^{+0.05} _{-0.00}	7.60 ^{+0.19} _{-0.21}	2.68 ^{+0.13} _{-0.14}	0.30 ^{+0.24} _{-0.23}	I	0	1.38	114	116
AP4285	9.20 ^{+0.00} _{-0.20}	3.33 ^{+0.07} _{-0.42}	0.10 ^{+0.35} _{-0.00}	9.38 ^{+0.41} _{-0.37}	3.23 ^{+0.22} _{-0.19}	0.35 ^{+0.33} _{-0.31}	I	0	1.19	40	14
AP4286	8.50 ^{+0.00} _{-0.60}	3.23 ^{+0.01} _{-0.22}	1.15 ^{+0.40} _{-0.10}	8.48 ^{+0.13} _{-0.12}	2.42 ^{+0.14} _{-0.15}	0.21 ^{+0.22} _{-0.20}	I	0	1.20	96	76

Table 1 (cont'd)

AP ID ^a	CMD Best Fit Parameters ^b			Integrated Best Fit Parameters ^c			Best ^d Flag ^e	Rap ^f	N _{stars} ^g	N _{bg} ^h	
	log(<i>t</i> [Myr])	log(<i>M</i> [<i>M</i> _⊙])	<i>A_V</i> [mag]	log(<i>t</i> [Myr])	log(<i>M</i> [<i>M</i> _⊙])	<i>A_V</i> [mag]					
AP4287	7.40 ^{+0.10} _{-0.40}	2.75 ^{+0.01} _{-0.06}	1.10 ^{+0.10} _{-0.10}	7.30 ^{+0.42} _{-0.42}	3.11 ^{+0.12} _{-0.10}	1.19 ^{+0.34} _{-0.34}	I	0	1.43	168	143
AP4292	8.20 ^{+0.10} _{-0.00}	3.05 ^{+0.03} _{-0.19}	1.25 ^{+0.05} _{-0.40}	8.76 ^{+0.38} _{-0.53}	3.18 ^{+0.18} _{-0.17}	0.70 ^{+0.94} _{-0.62}	I	0	1.14	96	71
AP4294	8.90 ^{+0.10} _{-0.10}	3.28 ^{+0.04} _{-0.04}	0.10 ^{+0.35} _{-0.10}	9.12 ^{+0.28} _{-0.25}	3.11 ^{+0.15} _{-0.14}	0.33 ^{+0.29} _{-0.29}	I	0	1.08	81	46
AP4296	8.50 ^{+0.10} _{-0.60}	2.85 ^{+0.02} _{-0.14}	0.25 ^{+0.25} _{-0.10}	7.91 ^{+0.31} _{-0.30}	2.94 ^{+0.13} _{-0.13}	1.11 ^{+0.40} _{-0.40}	I	0	1.35	130	110
AP4298	7.80 ^{+1.80} _{-0.40}	3.22 ^{+0.20} _{-3.22}	3.00 ^{+0.40} _{-2.80}	7.87 ^{+0.11} _{-0.12}	2.08 ^{+0.07} _{-0.08}	0.17 ^{+0.19} _{-0.17}	I	1	1.19	61	34
AP4303	7.60 ^{+0.90} _{-0.10}	3.01 ^{+0.05} _{-0.11}	1.30 ^{+0.05} _{-0.70}	8.58 ^{+0.05} _{-0.04}	3.45 ^{+0.05} _{-0.05}	0.01 ^{+0.07} _{-0.01}	I	0	1.32	137	111
AP4305	8.20 ^{+0.10} _{-0.00}	2.94 ^{+0.00} _{-0.11}	0.70 ^{+0.05} _{-0.45}	8.14 ^{+0.18} _{-0.35}	2.97 ^{+0.35} _{-0.19}	0.55 ^{+0.90} _{-0.49}	I	0	1.37	136	108
AP4307	6.90 ^{+0.90} _{-0.10}	2.76 ^{+0.01} _{-0.10}	0.80 ^{+0.10} _{-0.35}	7.55 ^{+0.03} _{-0.03}	3.08 ^{+0.04} _{-0.04}	0.00 ^{+0.07} _{-0.00}	I	0	1.52	162	153
AP4309	8.90 ^{+0.00} _{-0.10}	3.27 ^{+0.04} _{-0.04}	0.25 ^{+0.30} _{-0.05}	8.87 ^{+0.59} _{-0.88}	3.45 ^{+0.18} _{-0.18}	0.89 ^{+1.19} _{-0.79}	I	0	1.32	97	82
AP4314	7.90 ^{+0.40} _{-0.50}	3.04 ^{+0.03} _{-0.39}	2.00 ^{+0.40} _{-0.65}	8.95 ^{+0.59} _{-0.87}	3.47 ^{+0.17} _{-0.16}	0.95 ^{+1.22} _{-0.78}	I	0	1.05	94	76
AP4315	8.70 ^{+0.00} _{-0.10}	3.70 ^{+0.03} _{-0.08}	1.15 ^{+0.30} _{-0.05}	7.84 ^{+0.04} _{-0.03}	2.20 ^{+0.05} _{-0.09}	1.21 ^{+0.08} _{-0.13}	I	0	1.44	144	94
AP4319	9.80 ^{+0.00} _{-0.40}	4.83 ^{+0.01} _{-0.33}	0.05 ^{+0.40} _{-0.05}	7.76 ^{+0.05} _{-0.05}	2.34 ^{+0.07} _{-0.07}	0.09 ^{+0.08} _{-0.07}	I	0	1.54	239	214
AP4320	8.60 ^{+0.10} _{-0.10}	2.81 ^{+0.04} _{-0.06}	0.55 ^{+0.20} _{-0.20}	10.22 ^{+0.03} _{-0.04}	3.34 ^{+0.08} _{-0.07}	0.04 ^{+0.08} _{-0.04}	I	0	1.22	54	35
AP4327	7.70 ^{+0.40} _{-0.70}	2.48 ^{+0.07} _{-0.09}	0.70 ^{+0.25} _{-0.15}	9.80 ^{+0.42} _{-0.19}	3.55 ^{+0.28} _{-0.20}	0.32 ^{+0.14} _{-0.23}	I	0	1.59	94	88
AP4331	7.50 ^{+0.00} _{-0.30}	3.23 ^{+0.04} _{-0.03}	1.85 ^{+0.25} _{-0.00}	7.61 ^{+0.18} _{-0.17}	4.02 ^{+0.16} _{-0.06}	2.02 ^{+0.26} _{-0.22}	I	0	1.52	108	77
AP4334	8.30 ^{+0.00} _{-0.10}	3.10 ^{+0.04} _{-0.03}	0.85 ^{+0.15} _{-0.00}	7.87 ^{+0.06} _{-0.08}	3.23 ^{+0.11} _{-0.12}	1.17 ^{+0.18} _{-0.18}	I	0	1.44	135	108
AP4335	9.50 ^{+0.20} _{-2.30}	3.86 ^{+0.27} _{-3.86}	0.25 ^{+2.22} _{-0.05}	9.08 ^{+0.84} _{-0.56}	3.29 ^{+0.29} _{-0.27}	1.06 ^{+0.67} _{-0.75}	I	0	1.20	131	103
AP4339	8.00 ^{+0.00} _{-0.90}	2.72 ^{+0.00} _{-0.18}	0.70 ^{+0.25} _{-0.05}	7.61 ^{+0.57} _{-0.62}	2.72 ^{+0.20} _{-0.21}	0.88 ^{+0.54} _{-0.58}	I	0	1.36	104	78
AP4340	7.00 ^{+0.20} _{-0.20}	2.89 ^{+0.02} _{-0.01}	0.70 ^{+0.05} _{-0.05}	6.79 ^{+0.42} _{-0.49}	2.74 ^{+0.22} _{-0.25}	0.30 ^{+0.18} _{-0.19}	I	0	2.73	370	314
AP4343	8.20 ^{+0.00} _{-0.50}	2.91 ^{+0.00} _{-0.21}	1.15 ^{+0.30} _{-0.05}	8.91 ^{+0.40} _{-0.49}	3.10 ^{+0.17} _{-0.14}	0.55 ^{+0.52} _{-0.44}	I	0	0.91	52	27
AP4347	8.80 ^{+0.00} _{-1.14}	2.85 ^{+0.03} _{-0.58}	0.10 ^{+1.20} _{-0.05}	7.86 ^{+0.17} _{-0.18}	3.55 ^{+0.15} _{-0.15}	1.44 ^{+0.33} _{-0.28}	I	0	1.86	245	178
AP4352	8.10 ^{+0.30} _{-1.10}	2.37 ^{+0.02} _{-0.21}	0.75 ^{+0.65} _{-0.05}	8.18 ^{+0.09} _{-0.17}	2.22 ^{+0.10} _{-0.14}	0.16 ^{+0.17} _{-0.15}	I	0	1.05	70	52
AP4355	8.00 ^{+0.00} _{-1.00}	2.59 ^{+0.03} _{-0.11}	0.40 ^{+0.30} _{-0.05}	7.92 ^{+0.15} _{-0.15}	3.00 ^{+0.09} _{-0.09}	0.26 ^{+0.23} _{-0.22}	I	0	2.04	194	164
AP4365	8.40 ^{+0.10} _{-1.00}	3.11 ^{+0.00} _{-0.24}	0.60 ^{+0.30} _{-0.15}	7.92 ^{+0.37} _{-0.41}	3.06 ^{+0.19} _{-0.18}	0.76 ^{+0.67} _{-0.59}	I	0	1.95	257	244
AP4366	8.10 ^{+0.10} _{-0.50}	3.07 ^{+0.03} _{-0.13}	1.35 ^{+0.20} _{-0.10}	8.82 ^{+0.09} _{-0.09}	2.99 ^{+0.09} _{-0.08}	0.17 ^{+0.17} _{-0.16}	I	0	1.26	127	119
AP4369	8.90 ^{+0.10} _{-0.10}	3.32 ^{+0.05} _{-0.09}	0.70 ^{+0.15} _{-0.25}	7.75 ^{+1.08} _{-1.05}	2.67 ^{+0.35} _{-0.38}	1.56 ^{+1.01} _{-1.13}	I	0	1.15	59	36
AP4370	8.10 ^{+0.60} _{-1.00}	2.93 ^{+0.00} _{-1.18}	1.20 ^{+0.80} _{-0.20}	8.90 ^{+0.07} _{-0.07}	3.08 ^{+0.07} _{-0.07}	0.07 ^{+0.11} _{-0.07}	I	0	1.15	102	74
AP4373	8.70 ^{+0.10} _{-1.50}	2.75 ^{+0.04} _{-0.34}	0.15 ^{+0.65} _{-0.15}	7.77 ^{+0.14} _{-0.18}	3.68 ^{+0.16} _{-0.18}	2.47 ^{+0.35} _{-0.30}	I	0	1.45	73	64
AP4374	8.80 ^{+0.00} _{-0.10}	3.27 ^{+0.02} _{-0.13}	0.35 ^{+0.40} _{-0.05}	8.58 ^{+0.17} _{-0.18}	3.11 ^{+0.12} _{-0.13}	0.76 ^{+0.32} _{-0.34}	I	0	1.39	134	107
AP4377	9.10 ^{+0.00} _{-0.10}	3.28 ^{+0.05} _{-0.14}	0.40 ^{+0.20} _{-0.00}	8.06 ^{+0.01} _{-0.23}	2.82 ^{+0.26} _{-0.30}	1.71 ^{+0.57} _{-0.49}	I	0	0.98	36	16
AP4385	7.70 ^{+0.00} _{-0.80}	2.64 ^{+0.02} _{-0.11}	0.70 ^{+0.15} _{-0.15}	8.02 ^{+0.20} _{-0.20}	3.03 ^{+0.12} _{-0.12}	0.53 ^{+0.32} _{-0.31}	I	0	1.73	268	248
AP4387	8.60 ^{+0.10} _{-1.00}	2.62 ^{+0.00} _{-0.28}	0.50 ^{+0.60} _{-0.10}	7.68 ^{+0.48} _{-0.66}	2.11 ^{+0.10} _{-0.10}	0.17 ^{+0.18} _{-0.16}	I	0	1.07	35	21
AP4391	9.10 ^{+0.10} _{-1.60}	3.43 ^{+0.09} _{-1.62}	0.35 ^{+1.00} _{-0.15}	7.76 ^{+0.07} _{-0.07}	3.12 ^{+0.17} _{-0.14}	1.73 ^{+0.23} _{-0.22}	I	0	1.26	80	64

Table 1 (cont'd)

AP ID ^a	CMD Best Fit Parameters ^b			Integrated Best Fit Parameters ^c			Best ^d Flag ^e	R _{ap} ^f	N _{stars} ^g	N _{bg} ^h	
	log(<i>t</i> [Myr])	log(<i>M</i> [<i>M</i> _⊙])	<i>A_V</i> [mag]	log(<i>t</i> [Myr])	log(<i>M</i> [<i>M</i> _⊙])	<i>A_V</i> [mag]					
AP4393	7.10 ^{+0.10} _{-0.40}	3.01 ^{+0.01} _{-0.02}	0.80 ^{+0.15} _{-0.00}	7.60 ^{+0.10} _{-0.10}	2.94 ^{+0.12} _{-0.11}	0.16 ^{+0.14} _{-0.15}	I	0	1.96	205	174
AP4398	7.70 ^{+0.10} _{-0.80}	2.41 ^{+0.02} _{-0.05}	0.45 ^{+0.30} _{-0.05}	7.98 ^{+0.25} _{-0.25}	2.94 ^{+0.17} _{-0.18}	0.63 ^{+0.46} _{-0.47}	I	0	1.40	124	94
AP4399	7.20 ^{+1.00} _{-0.30}	2.55 ^{+0.19} _{-0.05}	0.75 ^{+0.10} _{-0.20}	7.44 ^{+0.41} _{-0.46}	2.52 ^{+0.17} _{-0.17}	0.44 ^{+0.27} _{-0.28}	I	0	0.99	69	52
AP4400	8.30 ^{+0.10} _{-0.30}	3.21 ^{+0.05} _{-0.06}	0.90 ^{+0.15} _{-0.10}	8.86 ^{+0.10} _{-0.10}	3.19 ^{+0.09} _{-0.10}	0.09 ^{+0.10} _{-0.09}	I	0	1.29	131	105
AP4409	7.60 ^{+0.10} _{-0.40}	2.57 ^{+0.01} _{-0.05}	0.80 ^{+0.15} _{-0.05}	6.84 ^{+0.23} _{-0.18}	2.89 ^{+0.24} _{-0.29}	1.91 ^{+0.14} _{-0.14}	I	0	1.60	131	127
AP4412	9.10 ^{+0.00} _{-0.00}	3.91 ^{+0.03} _{-0.07}	0.35 ^{+0.10} _{-0.05}	9.23 ^{+0.57} _{-0.79}	3.71 ^{+0.20} _{-0.18}	0.76 ^{+0.77} _{-0.56}	I	0	1.74	196	127
AP4414	9.30 ^{+0.20} _{-0.00}	4.46 ^{+0.14} _{-0.07}	0.70 ^{+0.10} _{-0.10}	8.64 ^{+0.15} _{-0.09}	3.76 ^{+0.16} _{-0.01}	1.20 ^{+0.20} _{-0.16}	I	0	2.79	482	387
AP4417	8.30 ^{+0.00} _{-1.10}	3.09 ^{+0.02} _{-0.23}	0.65 ^{+0.20} _{-0.05}	7.69 ^{+0.25} _{-0.23}	2.99 ^{+0.11} _{-0.11}	0.67 ^{+0.27} _{-0.28}	I	0	1.04	85	60
AP4418	9.10 ^{+0.30} _{-0.00}	3.44 ^{+0.50} _{-0.05}	0.15 ^{+0.10} _{-0.10}	8.09 ^{+0.18} _{-0.19}	3.09 ^{+0.22} _{-0.17}	1.08 ^{+0.51} _{-0.41}	I	0	1.59	154	127
AP4420	8.90 ^{+0.10} _{-0.00}	3.73 ^{+0.05} _{-0.07}	0.85 ^{+0.05} _{-0.35}	8.71 ^{+0.23} _{-0.24}	2.96 ^{+0.14} _{-0.16}	0.59 ^{+0.34} _{-0.35}	I	0	1.36	101	53
AP4431	8.70 ^{+0.10} _{-0.10}	3.08 ^{+0.01} _{-0.08}	0.35 ^{+0.15} _{-0.20}	8.59 ^{+0.27} _{-0.25}	2.97 ^{+0.13} _{-0.15}	0.40 ^{+0.39} _{-0.35}	I	0	1.32	84	49
AP4434	6.60 ^{+0.40} _{-0.00}	2.89 ^{+0.02} _{-0.03}	0.90 ^{+0.05} _{-0.10}	7.25 ^{+0.03} _{-0.03}	3.31 ^{+0.03} _{-0.04}	0.70 ^{+0.07} _{-0.07}	I	0	2.14	246	230
AP4437	8.30 ^{+1.00} _{-0.90}	2.60 ^{+1.39} _{-0.80}	0.65 ^{+1.60} _{-0.15}	7.41 ^{+0.43} _{-0.39}	2.99 ^{+0.14} _{-0.14}	1.58 ^{+0.43} _{-0.44}	I	0	1.19	60	40
AP4438	9.10 ^{+0.60} _{-2.10}	3.07 ^{+0.83} _{-1.02}	0.00 ^{+0.55} _{-0.15}	7.70 ^{+1.01} _{-0.98}	2.74 ^{+0.20} _{-0.22}	1.30 ^{+0.58} _{-0.85}	I	0	1.03	48	29
AP4453	6.70 ^{+0.50} _{-0.10}	2.87 ^{+0.04} _{-0.01}	1.05 ^{+0.15} _{-0.10}	7.85 ^{+0.03} _{-0.03}	2.58 ^{+0.08} _{-0.06}	0.00 ^{+0.07} _{-0.00}	I	0	1.90	194	178
AP4466	9.00 ^{+0.10} _{-0.20}	3.71 ^{+0.52} _{-0.10}	1.10 ^{+0.70} _{-0.20}	9.34 ^{+0.51} _{-0.55}	3.54 ^{+0.22} _{-0.22}	0.75 ^{+0.45} _{-0.56}	I	0	1.35	113	60
AP4470	0.00 ^{+0.00} _{-0.00}	0.00 ^{+0.00} _{-0.00}	0.00 ^{+0.00} _{-0.00}	0.00 ^{+0.00} _{-0.00}	0.00 ^{+0.00} _{-0.00}	0.00 ^{+0.00} _{-0.00}	I	0	1.59	0	0
AP4474	7.90 ^{+0.10} _{-0.40}	3.19 ^{+0.00} _{-0.12}	1.55 ^{+0.05} _{-0.10}	9.60 ^{+0.03} _{-0.03}	3.65 ^{+0.03} _{-0.03}	0.20 ^{+0.07} _{-0.07}	I	0	1.17	86	72
AP4475	6.90 ^{+0.30} _{-0.20}	2.92 ^{+0.04} _{-0.04}	1.70 ^{+0.05} _{-0.10}	6.72 ^{+0.11} _{-0.08}	2.40 ^{+0.24} _{-0.22}	1.30 ^{+0.14} _{-0.16}	I	0	1.13	101	77
AP4481	8.70 ^{+0.20} _{-0.50}	3.19 ^{+0.03} _{-0.61}	0.85 ^{+0.30} _{-0.50}	8.24 ^{+0.04} _{-0.05}	2.00 ^{+0.03} _{-0.00}	0.28 ^{+0.09} _{-0.06}	I	0	1.27	93	68
AP4490	7.90 ^{+1.10} _{-0.00}	3.93 ^{+0.00} _{-0.32}	3.00 ^{+0.00} _{-2.40}	9.37 ^{+0.07} _{-0.09}	2.98 ^{+0.08} _{-0.09}	0.05 ^{+0.09} _{-0.05}	I	0	1.39	109	56
AP4491	8.90 ^{+0.20} _{-0.10}	3.47 ^{+0.02} _{-0.48}	0.70 ^{+0.40} _{-0.50}	9.05 ^{+0.82} _{-0.62}	3.60 ^{+0.27} _{-0.26}	1.30 ^{+0.81} _{-0.81}	I	0	1.46	130	101
AP4494	6.80 ^{+0.80} _{-0.00}	2.67 ^{+0.23} _{-0.05}	2.35 ^{+0.40} _{-0.20}	6.50 ^{+0.25} _{-0.25}	2.24 ^{+0.21} _{-0.17}	1.43 ^{+0.10} _{-0.10}	I	0	1.15	39	14
AP4497	7.80 ^{+0.10} _{-0.90}	2.98 ^{+0.02} _{-0.12}	0.60 ^{+0.05} _{-0.10}	7.74 ^{+0.08} _{-0.07}	2.88 ^{+0.10} _{-0.10}	0.43 ^{+0.12} _{-0.11}	I	0	1.28	152	143
AP4501	10.10 ^{+0.40} _{-2.80}	4.83 ^{+1.02} _{-4.83}	0.00 ^{+2.30} _{-0.15}	8.42 ^{+0.93} _{-0.60}	3.45 ^{+0.24} _{-0.27}	1.50 ^{+0.75} _{-1.06}	I	0	1.42	121	98
AP4504	8.40 ^{+0.18} _{-0.10}	3.37 ^{+0.01} _{-0.08}	0.80 ^{+0.05} _{-0.25}	6.94 ^{+0.88} _{-0.78}	3.17 ^{+0.34} _{-0.33}	1.87 ^{+0.49} _{-0.62}	I	0	2.24	300	263
AP4506	8.40 ^{+0.70} _{-0.70}	3.11 ^{+0.74} _{-3.11}	1.55 ^{+0.80} _{-0.45}	8.77 ^{+0.19} _{-0.27}	3.19 ^{+0.15} _{-0.15}	0.92 ^{+0.38} _{-0.40}	I	0	1.28	95	62
AP4507	7.70 ^{+0.00} _{-0.50}	3.23 ^{+0.03} _{-0.07}	1.55 ^{+0.25} _{-0.00}	8.50 ^{+0.10} _{-0.10}	2.96 ^{+0.11} _{-0.10}	0.29 ^{+0.23} _{-0.22}	I	0	1.13	106	70
AP4508	8.90 ^{+0.00} _{-0.10}	3.17 ^{+0.06} _{-0.02}	0.15 ^{+0.25} _{-0.10}	9.44 ^{+0.15} _{-0.10}	3.32 ^{+0.14} _{-0.13}	0.11 ^{+0.13} _{-0.11}	I	0	1.13	98	92
AP4518	8.40 ^{+0.00} _{-1.30}	2.37 ^{+0.04} _{-0.14}	0.05 ^{+0.50} _{-0.10}	7.82 ^{+0.21} _{-0.13}	3.12 ^{+0.27} _{-0.25}	1.19 ^{+0.42} _{-0.45}	I	0	1.41	92	79
AP4519	7.90 ^{+0.20} _{-0.20}	2.98 ^{+0.01} _{-0.05}	0.90 ^{+0.05} _{-0.15}	7.80 ^{+0.25} _{-0.26}	3.21 ^{+0.11} _{-0.10}	0.67 ^{+0.33} _{-0.32}	I	0	1.75	171	156
AP4520	8.70 ^{+0.00} _{-0.80}	3.08 ^{+0.03} _{-0.19}	0.55 ^{+0.65} _{-0.05}	7.26 ^{+0.68} _{-0.76}	2.63 ^{+0.27} _{-0.27}	1.38 ^{+0.64} _{-0.71}	I	0	1.33	81	58
AP4525	8.10 ^{+0.00} _{-1.20}	2.65 ^{+0.08} _{-0.15}	0.65 ^{+0.70} _{-0.15}	7.54 ^{+0.05} _{-0.05}	3.12 ^{+0.06} _{-0.05}	0.61 ^{+0.09} _{-0.09}	I	0	1.21	92	84

Table 1 (cont'd)

AP ID ^a	CMD Best Fit Parameters ^b			Integrated Best Fit Parameters ^c			Best ^d Flag ^e	Rap ^f	N _{stars} ^g	N _{bg} ^h	
	log(<i>t</i> [Myr])	log(<i>M</i> [<i>M</i> _⊙])	<i>A_V</i> [mag]	log(<i>t</i> [Myr])	log(<i>M</i> [<i>M</i> _⊙])	<i>A_V</i> [mag]					
AP4526	8.10 ^{+0.00} _{-0.20}	3.25 ^{+0.00} _{-0.10}	1.50 ^{+0.05} _{-0.15}	8.36 ^{+0.29} _{-0.32}	2.79 ^{+0.18} _{-0.16}	0.54 ^{+0.59} _{-0.49}	I	0	1.02	75	62
AP4528	8.10 ^{+0.00} _{-0.90}	2.65 ^{+0.01} _{-0.15}	0.60 ^{+0.10} _{-0.10}	8.07 ^{+0.18} _{-0.19}	3.00 ^{+0.12} _{-0.12}	1.02 ^{+0.35} _{-0.34}	I	0	1.05	75	61
AP4529	7.40 ^{+0.10} _{-0.50}	2.81 ^{+0.00} _{-0.07}	1.05 ^{+0.10} _{-0.10}	6.73 ^{+0.14} _{-0.12}	3.06 ^{+0.27} _{-0.26}	0.96 ^{+0.12} _{-0.13}	I	0	1.45	210	205
AP4530	8.40 ^{+0.00} _{-0.70}	2.65 ^{+0.02} _{-0.25}	0.45 ^{+0.40} _{-0.15}	8.18 ^{+0.21} _{-0.21}	2.88 ^{+0.24} _{-0.31}	0.61 ^{+0.38} _{-0.40}	I	0	1.48	129	82
AP4533	9.10 ^{+0.50} _{-0.00}	3.46 ^{+0.40} _{-0.35}	0.20 ^{+0.25} _{-0.05}	7.95 ^{+0.09} _{-0.09}	2.75 ^{+0.23} _{-0.25}	1.34 ^{+0.32} _{-0.32}	I	0	1.21	73	60
AP4536	9.10 ^{+0.00} _{-0.00}	4.11 ^{+0.00} _{-0.05}	0.20 ^{+0.00} _{-0.10}	8.89 ^{+0.53} _{-0.63}	3.78 ^{+0.15} _{-0.15}	0.74 ^{+0.78} _{-0.62}	I	0	2.91	511	412
AP4537	8.40 ^{+0.00} _{-0.10}	2.47 ^{+0.02} _{-0.03}	0.45 ^{+0.10} _{-0.10}	8.62 ^{+0.22} _{-0.22}	2.64 ^{+0.17} _{-0.18}	0.41 ^{+0.36} _{-0.34}	I	0	0.96	54	44
AP4543	8.00 ^{+0.70} _{-0.80}	3.71 ^{+0.00} _{-1.47}	2.80 ^{+0.05} _{-1.65}	7.56 ^{+0.51} _{-0.46}	3.07 ^{+0.22} _{-0.25}	1.99 ^{+0.59} _{-0.83}	I	0	1.23	109	90
AP4549	8.30 ^{+0.00} _{-1.00}	3.08 ^{+0.04} _{-0.25}	0.90 ^{+0.15} _{-0.20}	8.70 ^{+0.03} _{-0.03}	2.85 ^{+0.05} _{-0.05}	0.50 ^{+0.07} _{-0.07}	I	0	1.18	72	43
AP4550	8.90 ^{+0.00} _{-1.50}	3.10 ^{+0.03} _{-0.60}	0.25 ^{+0.70} _{-0.10}	7.71 ^{+0.55} _{-0.60}	2.71 ^{+0.29} _{-0.29}	1.06 ^{+0.83} _{-0.80}	I	0	1.27	91	67
AP4555	8.20 ^{+0.00} _{-0.60}	3.51 ^{+0.00} _{-0.35}	2.10 ^{+0.40} _{-0.10}	10.25 ^{+0.00} _{-0.03}	4.65 ^{+0.07} _{-0.07}	0.52 ^{+0.12} _{-0.12}	I	0	1.66	196	154
AP4556	8.90 ^{+0.10} _{-0.10}	3.25 ^{+0.06} _{-0.15}	0.30 ^{+0.25} _{-0.10}	8.70 ^{+0.14} _{-0.20}	2.99 ^{+0.13} _{-0.14}	1.11 ^{+0.33} _{-0.31}	I	0	1.63	130	93
AP4558	8.80 ^{+0.00} _{-0.70}	2.95 ^{+0.02} _{-0.12}	0.10 ^{+0.95} _{-0.00}	8.46 ^{+0.24} _{-0.27}	2.60 ^{+0.18} _{-0.18}	0.44 ^{+0.51} _{-0.40}	I	0	0.89	41	23
AP4565	7.40 ^{+0.30} _{-0.60}	2.44 ^{+0.00} _{-0.04}	0.65 ^{+0.10} _{-0.10}	7.22 ^{+0.25} _{-0.30}	2.46 ^{+0.18} _{-0.21}	0.74 ^{+0.11} _{-0.11}	I	0	1.03	22	17
AP4569	8.40 ^{+0.10} _{-0.80}	2.88 ^{+0.00} _{-0.20}	0.90 ^{+0.30} _{-0.10}	7.97 ^{+0.44} _{-0.44}	2.47 ^{+0.24} _{-0.22}	0.79 ^{+0.64} _{-0.62}	I	0	1.23	78	61
AP4571	7.70 ^{+0.10} _{-0.90}	2.71 ^{+0.00} _{-0.15}	1.05 ^{+0.25} _{-0.00}	6.90 ^{+0.26} _{-0.27}	3.28 ^{+0.15} _{-0.15}	2.04 ^{+0.14} _{-0.13}	I	0	1.10	71	73
AP4575	8.20 ^{+0.10} _{-0.60}	2.78 ^{+0.01} _{-0.08}	0.55 ^{+0.10} _{-0.15}	8.33 ^{+0.08} _{-0.08}	2.48 ^{+0.10} _{-0.10}	0.24 ^{+0.14} _{-0.14}	I	0	0.89	36	11
AP4577	0.00 ^{+0.00} _{-0.00}	0.00 ^{+0.00} _{-0.00}	0.00 ^{+0.00} _{-0.00}	0.00 ^{+0.00} _{-0.00}	0.00 ^{+0.00} _{-0.00}	0.00 ^{+0.00} _{-0.00}	I	0	1.14	0	0
AP4578	8.50 ^{+0.10} _{-0.00}	3.08 ^{+0.01} _{-0.03}	0.50 ^{+0.05} _{-0.20}	8.75 ^{+0.14} _{-0.13}	2.97 ^{+0.12} _{-0.11}	0.53 ^{+0.27} _{-0.29}	I	0	1.23	82	62
AP4581	9.10 ^{+0.10} _{-0.00}	3.51 ^{+0.36} _{-0.11}	0.30 ^{+0.20} _{-0.05}	10.20 ^{+0.03} _{-0.04}	3.92 ^{+0.05} _{-0.05}	0.31 ^{+0.07} _{-0.07}	I	0	1.25	88	56
AP4582	8.50 ^{+0.10} _{-1.20}	2.79 ^{+0.06} _{-0.28}	0.70 ^{+0.35} _{-0.05}	8.45 ^{+0.10} _{-0.09}	2.04 ^{+0.05} _{-0.04}	0.03 ^{+0.07} _{-0.03}	I	0	1.17	43	29
AP4584	8.80 ^{+0.10} _{-0.00}	3.28 ^{+0.00} _{-0.12}	0.60 ^{+0.10} _{-0.30}	8.06 ^{+0.13} _{-0.31}	3.11 ^{+0.22} _{-0.21}	1.61 ^{+0.56} _{-0.63}	I	0	1.32	76	46
AP4589	7.40 ^{+0.60} _{-0.30}	3.09 ^{+0.02} _{-0.29}	1.80 ^{+0.10} _{-0.85}	8.62 ^{+0.18} _{-0.17}	2.99 ^{+0.11} _{-0.12}	0.30 ^{+0.25} _{-0.25}	I	0	1.23	125	112
AP4593	8.90 ^{+0.00} _{-0.00}	3.29 ^{+0.04} _{-0.09}	0.10 ^{+0.20} _{-0.00}	8.54 ^{+0.48} _{-0.45}	3.05 ^{+0.25} _{-0.22}	0.80 ^{+0.71} _{-0.65}	I	0	1.56	150	154
AP4600	7.90 ^{+0.20} _{-0.70}	2.88 ^{+0.00} _{-0.13}	0.70 ^{+0.10} _{-0.15}	6.94 ^{+0.60} _{-0.64}	2.47 ^{+0.20} _{-0.20}	0.84 ^{+0.34} _{-0.37}	I	0	1.53	135	99
AP4603	7.00 ^{+0.20} _{-0.30}	2.89 ^{+0.00} _{-0.04}	0.65 ^{+0.00} _{-0.05}	6.90 ^{+0.18} _{-0.14}	2.80 ^{+0.28} _{-0.35}	0.65 ^{+0.15} _{-0.15}	I	0	2.36	293	279
AP4607	7.40 ^{+0.40} _{-0.30}	2.64 ^{+0.01} _{-0.05}	0.50 ^{+0.15} _{-0.20}	6.95 ^{+0.23} _{-0.23}	2.56 ^{+0.21} _{-0.19}	0.88 ^{+0.13} _{-0.14}	I	0	1.36	105	97
AP4613	7.50 ^{+0.20} _{-0.50}	2.72 ^{+0.02} _{-0.08}	0.80 ^{+0.10} _{-0.10}	7.71 ^{+0.39} _{-0.35}	2.75 ^{+0.18} _{-0.19}	0.90 ^{+0.47} _{-0.52}	I	0	1.26	60	33
AP4614	8.90 ^{+0.00} _{-0.40}	3.21 ^{+0.06} _{-0.10}	0.05 ^{+0.90} _{-0.05}	8.16 ^{+0.19} _{-0.23}	2.74 ^{+0.34} _{-0.39}	0.83 ^{+0.53} _{-0.57}	I	0	1.25	105	72
AP4616	8.60 ^{+0.10} _{-0.00}	3.18 ^{+0.01} _{-0.06}	0.45 ^{+0.05} _{-0.30}	9.23 ^{+0.16} _{-0.16}	3.60 ^{+0.12} _{-0.12}	0.33 ^{+0.22} _{-0.22}	I	0	1.43	143	127
AP4618	9.60 ^{+0.20} _{-1.00}	3.78 ^{+0.06} _{-3.78}	0.20 ^{+1.09} _{-0.10}	8.85 ^{+0.42} _{-0.37}	2.89 ^{+0.21} _{-0.22}	1.12 ^{+0.56} _{-0.70}	I	0	1.38	59	36
AP4628	7.90 ^{+0.40} _{-0.00}	2.93 ^{+0.10} _{-0.05}	1.45 ^{+0.10} _{-0.25}	8.10 ^{+0.20} _{-0.19}	2.94 ^{+0.21} _{-0.25}	1.14 ^{+0.43} _{-0.45}	I	0	1.23	78	56
AP4633	6.70 ^{+0.70} _{-0.10}	2.46 ^{+0.01} _{-0.06}	0.50 ^{+0.10} _{-0.10}	6.74 ^{+0.06} _{-0.06}	2.40 ^{+0.16} _{-0.20}	0.25 ^{+0.13} _{-0.13}	I	0	2.01	167	141

Table 1 (cont'd)

AP ID ^a	CMD Best Fit Parameters ^b			Integrated Best Fit Parameters ^c			Best ^d Flag ^e	R _{ap} ^f	N _{stars} ^g	N _{bg} ^h	
	log(<i>t</i> [Myr])	log(<i>M</i> [<i>M</i> _⊙])	<i>A_V</i> [mag]	log(<i>t</i> [Myr])	log(<i>M</i> [<i>M</i> _⊙])	<i>A_V</i> [mag]					
AP4635	7.50 ^{+0.30} _{-0.40}	3.02 ^{+0.08} _{-0.06}	1.65 ^{+0.27} _{-0.00}	8.81 ^{+0.06} _{-0.04}	3.00 ^{+0.09} _{-0.07}	0.30 ^{+0.10} _{-0.10}	I	0	1.20	114	97
AP4636	8.50 ^{+0.10} _{-0.60}	3.05 ^{+0.00} _{-0.25}	0.75 ^{+0.30} _{-0.15}	8.05 ^{+0.36} _{-0.33}	2.38 ^{+0.16} _{-0.16}	0.46 ^{+0.39} _{-0.38}	I	0	1.20	82	72
AP4637	7.80 ^{+0.00} _{-0.60}	3.07 ^{+0.00} _{-0.13}	1.70 ^{+0.25} _{-0.00}	7.43 ^{+0.65} _{-0.67}	2.83 ^{+0.24} _{-0.26}	1.40 ^{+0.68} _{-0.77}	I	0	1.12	91	76
AP4642	8.20 ^{+0.50} _{-0.10}	3.14 ^{+0.10} _{-0.05}	1.10 ^{+0.25} _{-0.55}	7.37 ^{+0.78} _{-0.82}	2.59 ^{+0.26} _{-0.27}	1.47 ^{+0.59} _{-0.71}	I	0	1.06	85	67
AP4644	8.80 ^{+0.00} _{-1.60}	3.02 ^{+0.00} _{-0.53}	0.05 ^{+0.80} _{-0.00}	7.72 ^{+0.36} _{-0.32}	2.93 ^{+0.14} _{-0.15}	0.80 ^{+0.42} _{-0.46}	I	0	1.38	141	118
AP4647	7.90 ^{+1.10} _{-0.70}	2.90 ^{+0.04} _{-2.90}	2.25 ^{+0.30} _{-1.40}	9.88 ^{+0.36} _{-0.39}	4.07 ^{+0.15} _{-0.18}	1.08 ^{+0.25} _{-0.36}	I	0	1.35	68	46
AP4654	6.60 ^{+0.80} _{-0.10}	2.81 ^{+0.09} _{-0.00}	2.20 ^{+0.00} _{-0.25}	7.62 ^{+0.27} _{-0.27}	3.16 ^{+0.11} _{-0.10}	1.62 ^{+0.32} _{-0.31}	I	0	1.10	87	65
AP4657	7.80 ^{+0.40} _{-0.60}	2.76 ^{+0.03} _{-0.10}	0.85 ^{+0.15} _{-0.20}	8.11 ^{+0.17} _{-0.17}	2.61 ^{+0.17} _{-0.17}	0.25 ^{+0.23} _{-0.22}	I	0	1.45	132	104
AP4658	8.80 ^{+0.00} _{-0.14}	3.12 ^{+0.00} _{-0.18}	0.45 ^{+0.15} _{-0.15}	9.04 ^{+0.73} _{-0.67}	3.18 ^{+0.25} _{-0.20}	1.04 ^{+0.73} _{-0.72}	I	0	1.20	53	29
AP4659	9.10 ^{+0.10} _{-0.00}	3.83 ^{+0.26} _{-0.22}	0.70 ^{+0.05} _{-0.20}	9.53 ^{+0.72} _{-1.69}	3.53 ^{+0.56} _{-1.25}	0.46 ^{+0.15} _{-0.14}	I	0	1.21	110	83
AP4670	10.10 ^{+0.00} _{-1.10}	5.19 ^{+0.01} _{-5.19}	0.00 ^{+0.95} _{-0.00}	8.34 ^{+0.16} _{-0.25}	3.77 ^{+0.11} _{-0.12}	1.76 ^{+0.36} _{-0.32}	I	0	1.50	196	193
AP4674	8.80 ^{+0.00} _{-1.30}	2.75 ^{+0.11} _{-0.33}	0.00 ^{+1.45} _{-0.20}	8.64 ^{+0.13} _{-0.13}	2.59 ^{+0.14} _{-0.14}	0.41 ^{+0.26} _{-0.25}	I	0	1.31	103	89
AP4676	9.50 ^{+0.20} _{-2.10}	3.75 ^{+0.00} _{-3.75}	0.00 ^{+2.45} _{-0.15}	7.92 ^{+0.05} _{-0.19}	2.27 ^{+0.16} _{-0.25}	0.42 ^{+0.23} _{-0.26}	I	0	1.15	49	46
AP4677	0.00 ^{+0.00} _{-0.00}	0.00 ^{+0.00} _{-0.00}	0.00 ^{+0.00} _{-0.00}	0.00 ^{+0.00} _{-0.00}	0.00 ^{+0.00} _{-0.00}	0.00 ^{+0.00} _{-0.00}	I	0	1.20	0	0
AP4685	9.00 ^{+0.00} _{-0.00}	3.40 ^{+0.04} _{-0.08}	0.30 ^{+0.05} _{-0.10}	8.36 ^{+0.99} _{-0.55}	3.17 ^{+0.21} _{-0.19}	1.37 ^{+0.78} _{-1.19}	I	0	1.13	86	49
AP4686	7.50 ^{+0.50} _{-0.30}	2.83 ^{+0.06} _{-0.05}	1.00 ^{+0.10} _{-0.15}	7.25 ^{+0.64} _{-0.72}	2.84 ^{+0.21} _{-0.20}	1.28 ^{+0.52} _{-0.58}	I	0	1.37	109	103
AP4693	7.40 ^{+0.90} _{-0.40}	2.37 ^{+0.05} _{-0.09}	0.65 ^{+0.05} _{-0.30}	8.11 ^{+0.00} _{-0.18}	2.50 ^{+0.20} _{-0.24}	0.80 ^{+0.24} _{-0.23}	I	0	1.07	54	37
AP4700	8.40 ^{+0.00} _{-0.10}	2.92 ^{+0.00} _{-0.10}	1.15 ^{+0.10} _{-0.10}	8.75 ^{+0.26} _{-0.29}	2.93 ^{+0.14} _{-0.15}	0.77 ^{+0.41} _{-0.45}	I	0	1.18	59	37
AP4703	7.60 ^{+0.30} _{-0.70}	2.44 ^{+0.05} _{-0.04}	0.30 ^{+0.20} _{-0.05}	6.75 ^{+0.35} _{-0.42}	2.33 ^{+0.17} _{-0.20}	0.37 ^{+0.13} _{-0.14}	I	0	1.59	109	100
AP4705	7.50 ^{+0.30} _{-0.60}	2.84 ^{+0.17} _{-0.06}	0.60 ^{+0.25} _{-0.00}	7.92 ^{+0.07} _{-0.08}	2.78 ^{+0.11} _{-0.13}	0.59 ^{+0.16} _{-0.19}	I	0	1.19	114	82
AP4712	9.10 ^{+0.10} _{-1.60}	2.72 ^{+0.03} _{-0.79}	0.00 ^{+2.00} _{-0.50}	8.63 ^{+0.14} _{-0.12}	2.77 ^{+0.15} _{-0.10}	1.29 ^{+0.26} _{-0.24}	I	0	0.95	32	12
AP4718	7.50 ^{+0.40} _{-0.50}	2.58 ^{+0.04} _{-0.08}	0.80 ^{+0.10} _{-0.15}	9.82 ^{+0.28} _{-0.19}	3.64 ^{+0.16} _{-0.12}	0.52 ^{+0.10} _{-0.10}	I	0	1.32	85	83
AP4725	8.30 ^{+0.10} _{-0.80}	2.49 ^{+0.01} _{-0.10}	0.35 ^{+0.25} _{-0.00}	8.12 ^{+0.12} _{-0.07}	2.13 ^{+0.11} _{-0.10}	0.22 ^{+0.16} _{-0.17}	I	0	0.86	19	13
AP4729	8.30 ^{+0.10} _{-0.80}	2.56 ^{+0.00} _{-0.13}	0.35 ^{+0.30} _{-0.05}	8.27 ^{+0.09} _{-0.11}	2.23 ^{+0.14} _{-0.14}	0.02 ^{+0.07} _{-0.02}	I	0	1.06	59	43
AP4733	9.00 ^{+0.30} _{-1.50}	3.48 ^{+0.03} _{-3.48}	0.50 ^{+1.75} _{-0.15}	7.81 ^{+0.42} _{-0.41}	2.54 ^{+0.22} _{-0.22}	0.77 ^{+0.57} _{-0.57}	I	0	1.15	108	93
AP4737	10.00 ^{+0.20} _{-2.70}	4.23 ^{+0.88} _{-4.23}	0.00 ^{+2.50} _{-0.15}	8.16 ^{+0.46} _{-0.45}	2.69 ^{+0.27} _{-0.26}	1.04 ^{+0.82} _{-0.86}	I	0	1.23	50	41
AP4738	6.60 ^{+1.90} _{-0.10}	2.35 ^{+0.30} _{-0.08}	0.55 ^{+0.70} _{-0.15}	8.22 ^{+0.12} _{-0.11}	3.85 ^{+0.09} _{-0.09}	0.52 ^{+0.22} _{-0.24}	I	0	2.05	273	286
AP4747	8.30 ^{+1.10} _{-1.20}	2.21 ^{+0.04} _{-2.21}	0.15 ^{+1.90} _{-0.05}	7.22 ^{+0.09} _{-0.05}	4.05 ^{+0.04} _{-0.03}	0.82 ^{+0.12} _{-0.12}	I	0	1.67	95	138
AP4749	8.70 ^{+0.00} _{-1.50}	2.78 ^{+0.10} _{-0.23}	0.15 ^{+2.00} _{-0.20}	8.65 ^{+0.17} _{-0.17}	2.90 ^{+0.13} _{-0.14}	0.48 ^{+0.31} _{-0.33}	I	0	1.10	98	93
AP4757	8.20 ^{+0.01} _{-0.40}	2.89 ^{+0.01} _{-0.06}	0.35 ^{+0.15} _{-0.05}	8.36 ^{+0.08} _{-0.09}	2.54 ^{+0.14} _{-0.12}	0.10 ^{+0.13} _{-0.10}	I	0	1.17	59	32
AP4759	9.20 ^{+0.00} _{-2.10}	3.60 ^{+0.22} _{-3.60}	0.25 ^{+1.50} _{-0.05}	8.48 ^{+0.00} _{-0.34}	2.97 ^{+0.13} _{-0.24}	0.59 ^{+0.42} _{-0.36}	I	0	1.30	104	74
AP4767	7.00 ^{+0.30} _{-0.30}	2.37 ^{+0.01} _{-0.03}	0.40 ^{+0.05} _{-0.10}	7.55 ^{+0.03} _{-0.03}	3.06 ^{+0.03} _{-0.04}	0.00 ^{+0.07} _{-0.00}	I	0	1.40	120	118
AP4768	9.00 ^{+0.00} _{-0.90}	3.68 ^{+0.05} _{-0.15}	0.50 ^{+2.00} _{-0.00}	8.82 ^{+0.31} _{-0.30}	2.95 ^{+0.15} _{-0.17}	0.49 ^{+0.42} _{-0.43}	I	0	1.38	127	96

Table 1 (cont'd)

AP ID ^a	CMD Best Fit Parameters ^b			Integrated Best Fit Parameters ^c			Best ^d Flag ^e	Rap ^f	Nstars ^g	Nbg ^h	
	log(<i>t</i> [Myr])	log(<i>M</i> [<i>M</i> _⊙])	<i>A_V</i> [mag]	log(<i>t</i> [Myr])	log(<i>M</i> [<i>M</i> _⊙])	<i>A_V</i> [mag]					
AP4769	8.30 ^{+0.00} _{-1.00}	2.70 ^{+0.04} _{-0.18}	0.50 ^{+0.25} _{-0.06}	8.72 ^{+1.51} _{-0.72}	2.60 ^{+1.10} _{-0.57}	0.07 ^{+0.10} _{-0.07}	I	0	1.28	103	83
AP4770	8.40 ^{+0.10} _{-0.60}	2.81 ^{+0.01} _{-0.18}	0.40 ^{+0.20} _{-0.15}	8.10 ^{+0.29} _{-0.27}	2.53 ^{+0.20} _{-0.19}	0.58 ^{+0.47} _{-0.46}	I	0	1.00	61	48
AP4775	6.60 ^{+0.10} _{-0.00}	3.40 ^{+0.00} _{-0.02}	0.75 ^{+0.00} _{-0.05}	7.10 ^{+0.03} _{-0.03}	4.25 ^{+0.03} _{-0.03}	0.40 ^{+0.07} _{-0.07}	I	0	4.67	1364	1135
AP4779	8.40 ^{+0.50} _{-0.00}	3.21 ^{+0.31} _{-0.00}	0.80 ^{+0.15} _{-0.50}	7.78 ^{+0.01} _{-0.11}	2.34 ^{+0.08} _{-0.15}	0.10 ^{+0.09} _{-0.09}	I	0	1.72	190	144
AP4780	8.80 ^{+0.00} _{-0.80}	3.12 ^{+0.05} _{-0.21}	0.20 ^{+1.00} _{-0.10}	10.17 ^{+0.07} _{-0.00}	3.70 ^{+0.05} _{-0.03}	0.14 ^{+0.05} _{-0.10}	I	0	1.20	105	86
AP4782	8.80 ^{+0.70} _{-1.60}	2.95 ^{+0.32} _{-2.95}	0.40 ^{+2.05} _{-0.05}	9.16 ^{+0.71} _{-0.74}	3.53 ^{+0.20} _{-0.17}	1.27 ^{+0.85} _{-0.72}	I	0	1.03	56	37
AP4785	8.90 ^{+0.00} _{-0.10}	3.58 ^{+0.03} _{-0.08}	0.50 ^{+0.20} _{-0.10}	9.21 ^{+0.84} _{-0.64}	3.72 ^{+0.22} _{-0.17}	1.06 ^{+0.70} _{-0.80}	I	0	1.41	118	88
AP4788	8.20 ^{+0.10} _{-0.80}	2.55 ^{+0.03} _{-0.17}	0.45 ^{+0.35} _{-0.05}	8.71 ^{+0.56} _{-0.80}	3.44 ^{+0.22} _{-0.22}	1.04 ^{+1.14} _{-0.73}	I	0	1.22	113	106
AP4791	9.10 ^{+0.00} _{-0.10}	3.54 ^{+0.03} _{-0.09}	0.20 ^{+0.05} _{-0.10}	9.38 ^{+0.20} _{-0.20}	3.40 ^{+0.15} _{-0.15}	0.23 ^{+0.25} _{-0.22}	I	0	1.43	98	60
AP4805	8.00 ^{+0.10} _{-0.20}	2.81 ^{+0.01} _{-0.07}	0.70 ^{+0.10} _{-0.05}	7.68 ^{+0.15} _{-0.20}	3.92 ^{+0.12} _{-0.11}	2.26 ^{+0.29} _{-0.25}	I	0	1.71	202	210
AP4806	9.20 ^{+0.00} _{-1.20}	3.60 ^{+0.23} _{-0.92}	0.35 ^{+1.45} _{-0.05}	7.82 ^{+0.09} _{-0.10}	2.89 ^{+0.15} _{-0.14}	1.37 ^{+0.26} _{-0.24}	I	0	1.13	92	58
AP4811	7.90 ^{+0.40} _{-0.30}	2.87 ^{+0.04} _{-0.12}	1.10 ^{+0.05} _{-0.25}	8.27 ^{+0.16} _{-0.16}	2.40 ^{+0.14} _{-0.15}	0.30 ^{+0.29} _{-0.27}	I	0	1.01	61	44
AP4815	9.00 ^{+0.40} _{-1.40}	3.08 ^{+0.27} _{-3.08}	0.75 ^{+1.85} _{-0.25}	8.61 ^{+0.13} _{-0.12}	2.31 ^{+0.16} _{-0.16}	0.42 ^{+0.23} _{-0.22}	I	0	1.17	50	35
AP4827	7.60 ^{+0.60} _{-0.60}	2.64 ^{+0.07} _{-0.15}	1.10 ^{+0.10} _{-0.35}	6.90 ^{+0.51} _{-0.57}	2.52 ^{+0.23} _{-0.22}	1.33 ^{+0.32} _{-0.33}	I	0	1.23	75	76
AP4830	9.00 ^{+0.00} _{-0.10}	3.26 ^{+0.06} _{-0.04}	0.05 ^{+0.30} _{-0.00}	7.91 ^{+1.09} _{-1.18}	3.06 ^{+0.51} _{-0.53}	1.23 ^{+0.94} _{-0.90}	I	0	1.97	213	171
AP4835	9.10 ^{+0.20} _{-1.30}	3.56 ^{+0.00} _{-3.56}	0.40 ^{+1.75} _{-0.05}	9.27 ^{+0.42} _{-0.30}	3.30 ^{+0.19} _{-0.20}	0.59 ^{+0.36} _{-0.45}	I	0	1.11	59	34
AP4836	8.10 ^{+0.00} _{-0.40}	3.61 ^{+0.01} _{-0.14}	1.90 ^{+0.25} _{-0.15}	8.63 ^{+0.88} _{-0.75}	3.68 ^{+0.20} _{-0.17}	1.21 ^{+0.91} _{-0.97}	I	0	1.63	177	124
AP4842	8.50 ^{+0.20} _{-0.10}	2.93 ^{+0.04} _{-0.10}	1.10 ^{+0.15} _{-0.40}	7.96 ^{+0.71} _{-0.66}	2.77 ^{+0.28} _{-0.33}	1.39 ^{+0.94} _{-1.13}	I	0	1.12	66	55
AP4845	8.30 ^{+0.00} _{-0.80}	2.82 ^{+0.00} _{-0.13}	0.40 ^{+0.30} _{-0.00}	7.28 ^{+0.42} _{-0.41}	3.03 ^{+0.11} _{-0.11}	1.67 ^{+0.35} _{-0.35}	I	0	1.29	65	65
AP4846	6.70 ^{+0.40} _{-0.10}	2.38 ^{+0.02} _{-0.03}	0.85 ^{+0.05} _{-0.10}	6.70 ^{+0.12} _{-0.14}	2.35 ^{+0.33} _{-0.27}	0.90 ^{+0.12} _{-0.12}	I	0	1.17	106	102
AP4858	8.30 ^{+0.30} _{-1.00}	2.61 ^{+0.00} _{-0.30}	1.05 ^{+0.15} _{-0.40}	8.20 ^{+0.25} _{-0.20}	2.09 ^{+0.09} _{-0.09}	0.11 ^{+0.15} _{-0.11}	I	0	1.00	45	29
AP4860	8.80 ^{+0.00} _{-0.70}	3.11 ^{+0.05} _{-0.07}	0.00 ^{+1.10} _{-0.05}	7.75 ^{+0.11} _{-0.11}	4.00 ^{+0.11} _{-0.11}	2.81 ^{+0.09} _{-0.11}	I	0	1.24	109	79
AP4862	0.00 ^{+0.00} _{-0.00}	0.00 ^{+0.00} _{-0.00}	0.00 ^{+0.00} _{-0.00}	0.00 ^{+0.00} _{-0.00}	0.00 ^{+0.00} _{-0.00}	0.00 ^{+0.00} _{-0.00}	I	0	1.15	0	0
AP4870	8.30 ^{+0.00} _{-0.80}	2.90 ^{+0.00} _{-0.17}	0.65 ^{+0.30} _{-0.00}	8.25 ^{+0.12} _{-0.13}	2.70 ^{+0.21} _{-0.24}	0.51 ^{+0.36} _{-0.38}	I	0	1.57	90	62
AP4890	7.90 ^{+0.00} _{-0.50}	2.79 ^{+0.02} _{-0.04}	0.25 ^{+0.20} _{-0.00}	7.56 ^{+0.28} _{-0.22}	2.59 ^{+0.16} _{-0.15}	0.20 ^{+0.18} _{-0.18}	I	0	1.09	80	64
AP4896	8.40 ^{+0.10} _{-0.00}	3.11 ^{+0.03} _{-0.05}	0.85 ^{+0.10} _{-0.15}	8.26 ^{+0.13} _{-0.14}	2.69 ^{+0.24} _{-0.26}	0.69 ^{+0.40} _{-0.42}	I	0	1.12	84	67
AP4911	7.20 ^{+0.30} _{-0.30}	3.07 ^{+0.06} _{-0.07}	2.05 ^{+0.10} _{-0.05}	7.67 ^{+0.10} _{-0.09}	3.62 ^{+0.10} _{-0.10}	1.95 ^{+0.16} _{-0.18}	I	0	1.42	146	127
AP4912	8.80 ^{+0.00} _{-0.20}	3.19 ^{+0.01} _{-0.10}	0.30 ^{+0.40} _{-0.05}	8.70 ^{+0.36} _{-0.34}	3.29 ^{+0.16} _{-0.17}	0.72 ^{+0.47} _{-0.48}	I	0	1.58	163	135
AP4917	8.50 ^{+1.30} _{-0.10}	4.45 ^{+0.21} _{-0.99}	3.00 ^{+0.40} _{-1.75}	7.25 ^{+0.03} _{-0.03}	3.20 ^{+0.03} _{-0.04}	0.01 ^{+0.06} _{-0.01}	I	0	1.75	60	85
AP4921	8.30 ^{+0.10} _{-0.50}	2.80 ^{+0.01} _{-0.12}	0.40 ^{+0.20} _{-0.10}	6.89 ^{+0.51} _{-0.59}	2.73 ^{+0.19} _{-0.21}	1.52 ^{+0.25} _{-0.26}	I	0	0.97	67	58
AP4932	8.40 ^{+0.10} _{-0.40}	3.18 ^{+0.02} _{-0.35}	1.35 ^{+0.25} _{-0.20}	8.56 ^{+0.44} _{-0.41}	2.92 ^{+0.23} _{-0.25}	0.85 ^{+0.64} _{-0.65}	I	0	1.14	91	56
AP4936	9.20 ^{+0.00} _{-0.10}	3.98 ^{+0.00} _{-0.43}	0.25 ^{+0.10} _{-0.15}	8.48 ^{+0.50} _{-1.77}	3.41 ^{+0.37} _{-1.26}	0.25 ^{+0.90} _{-0.25}	I	0	1.46	175	164
AP4950	7.80 ^{+0.20} _{-0.70}	2.74 ^{+0.03} _{-0.10}	0.90 ^{+0.20} _{-0.10}	7.84 ^{+0.19} _{-0.17}	2.63 ^{+0.14} _{-0.14}	0.23 ^{+0.22} _{-0.20}	I	0	1.25	119	120

Table 1 (cont'd)

AP ID ^a	CMD Best Fit Parameters ^b			Integrated Best Fit Parameters ^c			Best ^d Flag ^e	R _{ap} ^f	N _{stars} ^g	N _{bg} ^h	
	log(<i>t</i> [Myr])	log(<i>M</i> [<i>M</i> _⊙])	<i>A_V</i> [mag]	log(<i>t</i> [Myr])	log(<i>M</i> [<i>M</i> _⊙])	<i>A_V</i> [mag]					
AP4956	8.90 ^{+0.20} _{-0.30}	3.52 ^{+0.06} _{-3.52}	0.60 ^{+0.65} _{-0.35}	7.89 ^{+0.09} _{-0.08}	2.11 ^{+0.15} _{-0.11}	0.85 ^{+0.14} _{-0.28}	I	0	1.22	120	81
AP4957	8.90 ^{+0.10} _{-0.50}	3.34 ^{+0.01} _{-0.62}	0.65 ^{+0.10} _{-0.35}	6.37 ^{+0.30} _{-0.31}	2.57 ^{+0.29} _{-0.31}	0.93 ^{+0.11} _{-0.10}	I	0	1.03	49	26
AP4967	9.90 ^{+0.10} _{-1.80}	4.37 ^{+0.02} _{-4.37}	0.15 ^{+1.70} _{-0.05}	9.36 ^{+0.71} _{-0.80}	4.20 ^{+0.20} _{-0.17}	1.40 ^{+0.97} _{-0.65}	I	0	2.06	192	143
AP4968	9.20 ^{+0.10} _{-0.00}	3.86 ^{+0.10} _{-0.06}	0.25 ^{+0.10} _{-0.10}	9.38 ^{+0.24} _{-0.20}	3.31 ^{+0.18} _{-0.19}	0.28 ^{+0.24} _{-0.24}	I	0	1.01	67	48
AP4970	9.10 ^{+0.00} _{-0.10}	3.40 ^{+0.03} _{-0.09}	0.25 ^{+0.30} _{-0.05}	7.91 ^{+0.08} _{-0.07}	2.32 ^{+0.10} _{-0.11}	0.11 ^{+0.13} _{-0.11}	I	0	2.05	150	86
AP4983	8.50 ^{+0.10} _{-0.00}	2.94 ^{+0.01} _{-0.06}	0.45 ^{+0.00} _{-0.25}	8.39 ^{+0.10} _{-0.10}	2.52 ^{+0.16} _{-0.14}	0.18 ^{+0.20} _{-0.18}	I	0	1.13	78	54
AP5001	9.00 ^{+0.20} _{-1.00}	3.12 ^{+0.00} _{-3.12}	0.45 ^{+1.35} _{-0.10}	8.95 ^{+0.69} _{-0.44}	2.95 ^{+0.17} _{-0.17}	1.00 ^{+0.56} _{-0.81}	I	0	1.08	37	16
AP5002	0.00 ^{+0.00} _{-0.00}	0.00 ^{+0.00} _{-0.00}	0.00 ^{+0.00} _{-0.00}	0.00 ^{+0.00} _{-0.00}	0.00 ^{+0.00} _{-0.00}	0.00 ^{+0.00} _{-0.00}	I	0	1.78	0	0
AP5014	7.60 ^{+0.40} _{-0.40}	2.77 ^{+0.03} _{-0.07}	0.80 ^{+0.10} _{-0.15}	7.21 ^{+0.46} _{-0.50}	2.71 ^{+0.16} _{-0.18}	1.18 ^{+0.33} _{-0.34}	I	0	1.36	96	86
AP5021	9.10 ^{+0.00} _{-0.00}	3.30 ^{+0.04} _{-0.13}	0.50 ^{+0.15} _{-0.05}	8.78 ^{+0.60} _{-0.53}	2.73 ^{+0.25} _{-0.26}	0.79 ^{+0.60} _{-0.64}	I	0	1.10	41	18
AP5023	9.10 ^{+0.10} _{-2.30}	3.99 ^{+1.03} _{-2.19}	0.75 ^{+1.00} _{-0.45}	7.02 ^{+0.06} _{-0.05}	2.19 ^{+0.14} _{-0.13}	0.00 ^{+0.07} _{-0.00}	I	0	1.32	148	140
AP5032	9.10 ^{+0.00} _{-0.40}	3.60 ^{+0.09} _{-0.58}	0.35 ^{+1.05} _{-0.05}	8.66 ^{+0.20} _{-0.21}	2.70 ^{+0.16} _{-0.17}	0.64 ^{+0.36} _{-0.37}	I	0	1.21	95	81
AP5046	8.20 ^{+0.00} _{-0.80}	2.89 ^{+0.03} _{-0.16}	0.80 ^{+0.40} _{-0.00}	7.34 ^{+0.81} _{-0.95}	3.11 ^{+0.31} _{-0.30}	2.04 ^{+0.76} _{-0.96}	I	0	1.37	131	119
AP5047	8.90 ^{+0.20} _{-0.40}	3.32 ^{+0.09} _{-0.28}	0.50 ^{+0.75} _{-0.15}	8.82 ^{+0.13} _{-0.12}	2.86 ^{+0.12} _{-0.12}	0.08 ^{+0.10} _{-0.08}	I	0	1.66	175	125
AP5099	9.00 ^{+0.00} _{-0.30}	3.35 ^{+0.03} _{-0.20}	0.25 ^{+0.60} _{-0.00}	8.40 ^{+0.28} _{-0.27}	2.94 ^{+0.18} _{-0.19}	0.72 ^{+0.57} _{-0.58}	I	0	1.74	155	113
AP5102	9.00 ^{+0.00} _{-0.10}	3.16 ^{+0.08} _{-0.08}	0.20 ^{+0.45} _{-0.00}	9.16 ^{+1.00} _{-0.56}	3.49 ^{+0.26} _{-0.17}	1.08 ^{+0.62} _{-0.95}	I	0	1.48	94	58
AP5105	0.00 ^{+0.00} _{-0.00}	0.00 ^{+0.00} _{-0.00}	0.00 ^{+0.00} _{-0.00}	0.00 ^{+0.00} _{-0.00}	0.00 ^{+0.00} _{-0.00}	0.00 ^{+0.00} _{-0.00}	I	0	1.14	0	0
AP5116	6.60 ^{+0.10} _{-0.00}	3.03 ^{+0.00} _{-0.04}	0.90 ^{+0.00} _{-0.05}	6.52 ^{+0.11} _{-0.10}	3.06 ^{+0.24} _{-0.20}	0.58 ^{+0.16} _{-0.18}	I	0	3.59	778	726
AP5117	0.00 ^{+0.00} _{-0.00}	0.00 ^{+0.00} _{-0.00}	0.00 ^{+0.00} _{-0.00}	0.00 ^{+0.00} _{-0.00}	0.00 ^{+0.00} _{-0.00}	0.00 ^{+0.00} _{-0.00}	I	0	1.53	272	275
AP5131	6.80 ^{+0.60} _{-0.10}	2.53 ^{+0.04} _{-0.08}	1.05 ^{+0.05} _{-0.20}	7.90 ^{+0.17} _{-0.16}	3.08 ^{+0.10} _{-0.10}	0.44 ^{+0.25} _{-0.26}	I	0	1.56	233	261
AP5135	8.30 ^{+0.10} _{-0.20}	3.08 ^{+0.06} _{-0.09}	1.25 ^{+0.15} _{-0.10}	8.65 ^{+0.13} _{-0.11}	3.13 ^{+0.11} _{-0.08}	1.08 ^{+0.20} _{-0.20}	I	0	1.18	71	38
AP5137	7.40 ^{+0.00} _{-0.40}	2.96 ^{+0.00} _{-0.04}	0.50 ^{+0.15} _{-0.00}	6.87 ^{+0.42} _{-0.48}	3.05 ^{+0.19} _{-0.18}	0.52 ^{+0.20} _{-0.20}	I	0	2.81	479	437
AP5138	0.00 ^{+0.00} _{-0.00}	0.00 ^{+0.00} _{-0.00}	0.00 ^{+0.00} _{-0.00}	0.00 ^{+0.00} _{-0.00}	0.00 ^{+0.00} _{-0.00}	0.00 ^{+0.00} _{-0.00}	I	0	1.51	0	0
AP5149	7.70 ^{+1.00} _{-0.70}	2.54 ^{+0.04} _{-2.54}	1.25 ^{+0.45} _{-0.50}	6.86 ^{+0.51} _{-0.56}	2.39 ^{+0.15} _{-0.16}	0.81 ^{+0.29} _{-0.32}	I	0	1.10	73	65
AP5201	7.10 ^{+0.00} _{-0.40}	2.63 ^{+0.00} _{-0.02}	1.05 ^{+0.10} _{-0.00}	7.68 ^{+0.04} _{-0.04}	2.52 ^{+0.04} _{-0.05}	0.00 ^{+0.07} _{-0.00}	I	0	1.41	92	91
AP5206	7.60 ^{+0.20} _{-0.60}	2.58 ^{+0.03} _{-0.06}	0.65 ^{+0.20} _{-0.05}	7.42 ^{+0.52} _{-0.62}	2.64 ^{+0.15} _{-0.16}	0.56 ^{+0.32} _{-0.32}	I	0	1.23	93	86
AP5216	7.50 ^{+0.00} _{-0.70}	2.94 ^{+0.03} _{-0.18}	2.30 ^{+0.20} _{-0.10}	8.11 ^{+1.47} _{-1.46}	3.78 ^{+1.25} _{-1.18}	1.45 ^{+1.02} _{-1.02}	I	0	1.12	40	22
AP5226	9.10 ^{+0.10} _{-1.10}	3.49 ^{+0.17} _{-0.53}	0.20 ^{+2.15} _{-0.05}	9.18 ^{+0.22} _{-0.22}	3.30 ^{+0.20} _{-0.20}	0.20 ^{+0.18} _{-0.17}	I	0	1.45	164	140
AP5274	7.70 ^{+0.40} _{-0.50}	2.96 ^{+0.04} _{-0.08}	0.80 ^{+0.15} _{-0.10}	7.20 ^{+0.14} _{-0.13}	3.60 ^{+0.08} _{-0.07}	1.70 ^{+0.13} _{-0.12}	I	0	1.45	161	138
AP5277	6.60 ^{+0.60} _{-0.00}	2.55 ^{+0.03} _{-0.03}	0.55 ^{+0.05} _{-0.10}	6.91 ^{+0.34} _{-0.40}	2.42 ^{+0.20} _{-0.24}	0.43 ^{+0.15} _{-0.15}	I	0	1.52	125	119
AP5313	8.00 ^{+0.20} _{-1.10}	3.02 ^{+0.08} _{-0.22}	1.25 ^{+0.15} _{-0.15}	7.66 ^{+0.08} _{-0.08}	3.00 ^{+0.11} _{-0.13}	1.07 ^{+0.18} _{-0.19}	I	0	1.00	67	61
AP5316	8.90 ^{+0.00} _{-0.10}	3.21 ^{+0.03} _{-0.08}	0.00 ^{+0.35} _{-0.05}	7.05 ^{+0.32} _{-0.62}	2.98 ^{+0.22} _{-0.23}	2.49 ^{+0.40} _{-0.07}	I	0	1.21	82	64
AP5348	8.30 ^{+0.00} _{-0.00}	3.65 ^{+0.03} _{-0.06}	1.80 ^{+0.10} _{-0.05}	9.68 ^{+0.25} _{-0.26}	3.83 ^{+0.14} _{-0.13}	0.20 ^{+0.21} _{-0.20}	I	0	1.09	117	46

Table 1 (cont'd)

AP ID ^a	CMD Best Fit Parameters ^b			Integrated Best Fit Parameters ^c			Best ^d Flag ^e	Rap ^f	N _{stars} ^g	N _{bg} ^h	
	log(<i>t</i> [Myr])	log(<i>M</i> [<i>M</i> _⊙])	<i>A_V</i> [mag]	log(<i>t</i> [Myr])	log(<i>M</i> [<i>M</i> _⊙])	<i>A_V</i> [mag]					
AP5349	9.20 ^{+0.00} _{-0.10}	3.61 ^{+0.04} _{-0.17}	0.10 ^{+0.25} _{-0.00}	8.90 ^{+1.04} _{-1.13}	2.58 ^{+0.40} _{-0.42}	1.73 ^{+0.91} _{-0.99}	I	0	1.10	60	32
AP5350	6.80 ^{+0.30} _{-0.10}	2.89 ^{+0.00} _{-0.04}	1.00 ^{+0.05} _{-0.10}	6.45 ^{+0.19} _{-0.24}	2.80 ^{+0.31} _{-0.34}	0.57 ^{+0.14} _{-0.14}	I	0	2.78	460	428
AP5355	0.00 ^{+0.00} _{-0.00}	0.00 ^{+0.00} _{-0.00}	0.00 ^{+0.00} _{-0.00}	0.00 ^{+0.00} _{-0.00}	0.00 ^{+0.00} _{-0.00}	0.00 ^{+0.00} _{-0.00}	I	0	1.09	0	0
AP5391	7.60 ^{+0.40} _{-0.40}	2.69 ^{+0.04} _{-0.05}	0.60 ^{+0.05} _{-0.20}	8.27 ^{+0.05} _{-0.05}	2.17 ^{+0.11} _{-0.11}	0.00 ^{+0.07} _{-0.00}	I	0	1.06	66	47
AP5404	9.50 ^{+0.50} _{-0.40}	4.09 ^{+0.28} _{-0.59}	0.30 ^{+0.80} _{-0.15}	9.04 ^{+0.72} _{-0.61}	3.47 ^{+0.21} _{-0.18}	0.94 ^{+0.71} _{-0.74}	I	0	1.21	93	69
AP5412	8.70 ^{+0.00} _{-0.80}	2.82 ^{+0.06} _{-0.23}	0.35 ^{+0.80} _{-0.05}	8.39 ^{+0.17} _{-0.18}	2.52 ^{+0.27} _{-0.28}	0.60 ^{+0.41} _{-0.40}	I	0	1.19	86	69
AP5428	8.80 ^{+0.00} _{-0.10}	3.80 ^{+0.00} _{-0.14}	0.85 ^{+0.30} _{-0.10}	7.70 ^{+0.65} _{-0.76}	2.56 ^{+0.27} _{-0.27}	1.16 ^{+0.78} _{-0.80}	I	0	1.07	81	60
AP5460	7.00 ^{+0.40} _{-0.30}	2.38 ^{+0.02} _{-0.04}	0.70 ^{+0.05} _{-0.15}	9.10 ^{+0.03} _{-0.03}	3.15 ^{+0.03} _{-0.03}	0.00 ^{+0.07} _{-0.00}	I	0	1.20	125	129
AP5466	8.80 ^{+0.10} _{-0.40}	3.43 ^{+0.02} _{-0.33}	0.95 ^{+0.60} _{-0.30}	8.68 ^{+0.54} _{-0.86}	3.10 ^{+0.25} _{-0.21}	0.72 ^{+1.37} _{-0.70}	I	0	1.27	135	115
AP5477	8.30 ^{+0.30} _{-0.10}	3.12 ^{+0.06} _{-0.05}	1.30 ^{+0.15} _{-0.35}	8.00 ^{+0.36} _{-0.37}	2.41 ^{+0.22} _{-0.22}	0.57 ^{+0.50} _{-0.45}	I	0	1.06	76	61
AP5482	8.80 ^{+0.00} _{-0.20}	3.01 ^{+0.01} _{-0.17}	0.10 ^{+0.35} _{-0.00}	8.50 ^{+0.11} _{-0.11}	2.55 ^{+0.17} _{-0.16}	0.34 ^{+0.26} _{-0.25}	I	0	1.13	63	42
AP5496	0.00 ^{+0.00} _{-0.00}	0.00 ^{+0.00} _{-0.00}	0.00 ^{+0.00} _{-0.00}	0.00 ^{+0.00} _{-0.00}	0.00 ^{+0.00} _{-0.00}	0.00 ^{+0.00} _{-0.00}	I	0	2.28	0	0
AP5515	9.10 ^{+0.20} _{-2.10}	3.53 ^{+0.75} _{-3.53}	0.60 ^{+1.65} _{-0.00}	7.08 ^{+0.34} _{-0.30}	3.10 ^{+0.13} _{-0.10}	2.08 ^{+0.21} _{-0.22}	I	0	1.06	83	62
AP5519	8.80 ^{+0.00} _{-0.10}	3.51 ^{+0.02} _{-0.08}	0.70 ^{+0.25} _{-0.15}	8.75 ^{+0.33} _{-0.35}	3.10 ^{+0.23} _{-0.21}	0.81 ^{+0.52} _{-0.54}	I	0	1.24	104	79
AP5535	9.00 ^{+0.00} _{-0.10}	3.28 ^{+0.14} _{-0.05}	0.20 ^{+0.56} _{-0.05}	9.13 ^{+0.76} _{-0.88}	3.56 ^{+0.24} _{-0.23}	1.07 ^{+0.99} _{-0.79}	I	0	1.28	100	62
AP5575	8.20 ^{+0.10} _{-0.50}	2.89 ^{+0.02} _{-0.09}	0.65 ^{+0.20} _{-0.10}	7.81 ^{+0.27} _{-0.43}	3.30 ^{+0.16} _{-0.19}	1.74 ^{+0.57} _{-0.50}	I	0	1.19	82	46
AP5579	8.30 ^{+0.10} _{-0.10}	3.06 ^{+0.00} _{-0.09}	0.70 ^{+0.05} _{-0.10}	8.65 ^{+0.24} _{-0.24}	2.92 ^{+0.13} _{-0.14}	0.39 ^{+0.38} _{-0.35}	I	0	1.30	94	46
AP5610	8.80 ^{+0.10} _{-0.20}	3.53 ^{+0.02} _{-0.32}	0.75 ^{+0.40} _{-0.50}	8.98 ^{+0.24} _{-0.22}	2.85 ^{+0.17} _{-0.17}	0.28 ^{+0.28} _{-0.26}	I	0	1.30	130	112
AP5623	7.10 ^{+0.60} _{-0.30}	2.63 ^{+0.02} _{-0.08}	1.15 ^{+0.05} _{-0.20}	7.45 ^{+0.27} _{-0.23}	3.06 ^{+0.08} _{-0.09}	1.29 ^{+0.25} _{-0.24}	I	0	1.23	65	58
AP5704	8.00 ^{+0.20} _{-1.10}	2.68 ^{+0.02} _{-0.13}	1.00 ^{+0.60} _{-0.10}	7.22 ^{+0.73} _{-0.75}	2.69 ^{+0.39} _{-0.41}	1.47 ^{+0.80} _{-0.88}	I	0	1.29	120	123
AP5726	8.30 ^{+0.00} _{-0.40}	3.11 ^{+0.00} _{-0.20}	0.95 ^{+0.10} _{-0.10}	8.69 ^{+0.21} _{-0.23}	3.05 ^{+0.11} _{-0.12}	0.25 ^{+0.28} _{-0.25}	I	0	1.35	118	97
AP5808	0.00 ^{+0.00} _{-0.00}	0.00 ^{+0.00} _{-0.00}	0.00 ^{+0.00} _{-0.00}	0.00 ^{+0.00} _{-0.00}	0.00 ^{+0.00} _{-0.00}	0.00 ^{+0.00} _{-0.00}	I	0	1.05	0	0
AP5823	8.50 ^{+0.00} _{-0.10}	3.32 ^{+0.00} _{-0.08}	1.30 ^{+0.15} _{-0.05}	8.57 ^{+0.18} _{-0.18}	2.31 ^{+0.16} _{-0.16}	0.34 ^{+0.29} _{-0.28}	I	0	1.11	73	54
AP5915	6.80 ^{+0.90} _{-0.00}	2.65 ^{+0.08} _{-0.03}	1.35 ^{+0.00} _{-0.20}	7.72 ^{+0.02} _{-0.06}	3.00 ^{+0.24} _{-0.20}	1.33 ^{+0.26} _{-0.22}	I	0	0.96	61	51
AP5933	9.10 ^{+0.10} _{-1.30}	3.74 ^{+0.02} _{-0.92}	0.30 ^{+1.45} _{-0.05}	8.88 ^{+0.89} _{-0.83}	3.72 ^{+0.63} _{-0.61}	1.55 ^{+1.03} _{-1.05}	I	0	1.54	181	152
AP5980	8.10 ^{+0.00} _{-0.90}	2.51 ^{+0.00} _{-0.09}	0.35 ^{+0.25} _{-0.00}	7.92 ^{+0.04} _{-0.06}	2.71 ^{+0.08} _{-0.07}	0.98 ^{+0.11} _{-0.08}	I	0	0.95	78	65
AP6039	0.00 ^{+0.00} _{-0.00}	0.00 ^{+0.00} _{-0.00}	0.00 ^{+0.00} _{-0.00}	0.00 ^{+0.00} _{-0.00}	0.00 ^{+0.00} _{-0.00}	0.00 ^{+0.00} _{-0.00}	I	0	0.88	0	0
AP6182	7.70 ^{+0.30} _{-0.70}	2.57 ^{+0.03} _{-0.08}	0.75 ^{+0.15} _{-0.10}	8.00 ^{+0.06} _{-0.05}	2.62 ^{+0.12} _{-0.11}	0.80 ^{+0.13} _{-0.14}	I	0	0.92	63	47
AP6284	0.00 ^{+0.00} _{-0.00}	0.00 ^{+0.00} _{-0.00}	0.00 ^{+0.00} _{-0.00}	0.00 ^{+0.00} _{-0.00}	0.00 ^{+0.00} _{-0.00}	0.00 ^{+0.00} _{-0.00}	I	0	1.48	0	0
AP6501	0.00 ^{+0.00} _{-0.00}	0.00 ^{+0.00} _{-0.00}	0.00 ^{+0.00} _{-0.00}	0.00 ^{+0.00} _{-0.00}	0.00 ^{+0.00} _{-0.00}	0.00 ^{+0.00} _{-0.00}	I	0	1.45	0	0
AP6564	0.00 ^{+0.00} _{-0.00}	0.00 ^{+0.00} _{-0.00}	0.00 ^{+0.00} _{-0.00}	0.00 ^{+0.00} _{-0.00}	0.00 ^{+0.00} _{-0.00}	0.00 ^{+0.00} _{-0.00}	I	0	1.60	0	0
AP6947	0.00 ^{+0.00} _{-0.00}	0.00 ^{+0.00} _{-0.00}	0.00 ^{+0.00} _{-0.00}	0.00 ^{+0.00} _{-0.00}	0.00 ^{+0.00} _{-0.00}	0.00 ^{+0.00} _{-0.00}	I	0	1.74	0	0
AP7231	0.00 ^{+0.00} _{-0.00}	0.00 ^{+0.00} _{-0.00}	0.00 ^{+0.00} _{-0.00}	0.00 ^{+0.00} _{-0.00}	0.00 ^{+0.00} _{-0.00}	0.00 ^{+0.00} _{-0.00}	I	0	0.98	0	0

Table 1 (cont'd)

AP ID ^a	CMD Best Fit Parameters ^b			Integrated Best Fit Parameters ^c			Best ^d Flag ^e	R _{ap} ^f	N _{stars} ^g	N _{bg} ^h	
	log(<i>t</i> [Myr])	log(<i>M</i> [<i>M</i> _⊙])	<i>A_V</i> [mag]	log(<i>t</i> [Myr])	log(<i>M</i> [<i>M</i> _⊙])	<i>A_V</i> [mag]					
AP7632	0.00 ^{+0.00} _{-0.00}	0.00 ^{+0.00} _{-0.00}	0.00 ^{+0.00} _{-0.00}	0.00 ^{+0.00} _{-0.00}	0.00 ^{+0.00} _{-0.00}	0.00 ^{+0.00} _{-0.00}	I	0	0.70	0	0
AP7980	0.00 ^{+0.00} _{-0.00}	0.00 ^{+0.00} _{-0.00}	0.00 ^{+0.00} _{-0.00}	0.00 ^{+0.00} _{-0.00}	0.00 ^{+0.00} _{-0.00}	0.00 ^{+0.00} _{-0.00}	I	0	1.19	0	0
AP8052	0.00 ^{+0.00} _{-0.00}	0.00 ^{+0.00} _{-0.00}	0.00 ^{+0.00} _{-0.00}	0.00 ^{+0.00} _{-0.00}	0.00 ^{+0.00} _{-0.00}	0.00 ^{+0.00} _{-0.00}	I	0	0.79	0	0
AP8593	0.00 ^{+0.00} _{-0.00}	0.00 ^{+0.00} _{-0.00}	0.00 ^{+0.00} _{-0.00}	0.00 ^{+0.00} _{-0.00}	0.00 ^{+0.00} _{-0.00}	0.00 ^{+0.00} _{-0.00}	I	0	0.92	0	0
AP8764	0.00 ^{+0.00} _{-0.00}	0.00 ^{+0.00} _{-0.00}	0.00 ^{+0.00} _{-0.00}	0.00 ^{+0.00} _{-0.00}	0.00 ^{+0.00} _{-0.00}	0.00 ^{+0.00} _{-0.00}	I	0	0.98	0	0
AP8925	0.00 ^{+0.00} _{-0.00}	0.00 ^{+0.00} _{-0.00}	0.00 ^{+0.00} _{-0.00}	0.00 ^{+0.00} _{-0.00}	0.00 ^{+0.00} _{-0.00}	0.00 ^{+0.00} _{-0.00}	I	0	0.89	0	0
AP9766	0.00 ^{+0.00} _{-0.00}	0.00 ^{+0.00} _{-0.00}	0.00 ^{+0.00} _{-0.00}	0.00 ^{+0.00} _{-0.00}	0.00 ^{+0.00} _{-0.00}	0.00 ^{+0.00} _{-0.00}	I	0	0.80	0	0
AP12519	0.00 ^{+0.00} _{-0.00}	0.00 ^{+0.00} _{-0.00}	0.00 ^{+0.00} _{-0.00}	0.00 ^{+0.00} _{-0.00}	0.00 ^{+0.00} _{-0.00}	0.00 ^{+0.00} _{-0.00}	I	0	1.23	0	0
AP15121	0.00 ^{+0.00} _{-0.00}	0.00 ^{+0.00} _{-0.00}	0.00 ^{+0.00} _{-0.00}	0.00 ^{+0.00} _{-0.00}	0.00 ^{+0.00} _{-0.00}	0.00 ^{+0.00} _{-0.00}	I	0	2.80	0	0
AP54265	0.00 ^{+0.00} _{-0.00}	0.00 ^{+0.00} _{-0.00}	0.00 ^{+0.00} _{-0.00}	0.00 ^{+0.00} _{-0.00}	0.00 ^{+0.00} _{-0.00}	0.00 ^{+0.00} _{-0.00}	I	0	2.29	0	0
AP54266	0.00 ^{+0.00} _{-0.00}	0.00 ^{+0.00} _{-0.00}	0.00 ^{+0.00} _{-0.00}	0.00 ^{+0.00} _{-0.00}	0.00 ^{+0.00} _{-0.00}	0.00 ^{+0.00} _{-0.00}	I	0	1.81	0	0
AP54267	0.00 ^{+0.00} _{-0.00}	0.00 ^{+0.00} _{-0.00}	0.00 ^{+0.00} _{-0.00}	0.00 ^{+0.00} _{-0.00}	0.00 ^{+0.00} _{-0.00}	0.00 ^{+0.00} _{-0.00}	I	0	2.02	0	0
AP54268	0.00 ^{+0.00} _{-0.00}	0.00 ^{+0.00} _{-0.00}	0.00 ^{+0.00} _{-0.00}	0.00 ^{+0.00} _{-0.00}	0.00 ^{+0.00} _{-0.00}	0.00 ^{+0.00} _{-0.00}	I	0	2.02	0	0
AP54269	0.00 ^{+0.00} _{-0.00}	0.00 ^{+0.00} _{-0.00}	0.00 ^{+0.00} _{-0.00}	0.00 ^{+0.00} _{-0.00}	0.00 ^{+0.00} _{-0.00}	0.00 ^{+0.00} _{-0.00}	I	0	1.22	0	0

^aAndromeda Project ID (Johnson et al., 2015)

^bBest fit parameter results from CMD fitting using the MATCH package (Dolphin, 2002).

^cWeighted mean of the PDF results from fitting the integrated light using Pegase.2n (Fouesneau et al., 2014).

^dMethod that produces the most accurate results. The default is CMD fitting for clusters < 300 Myr and integrated fitting for clusters older than 300 Myr, but in individual cases the alternative method is adopted based on a by-eye quality check.

^eFlag set to 1 indicates best fit is not acceptable based on by eye quality check.

^fAperture radius in arcseconds.

^gNumber of stars in the cluster CMD.

^hNumber of predicted background stars in the aperture.

BIBLIOGRAPHY

- Adamo, A., Zackrisson, E., Östlin, G., & Hayes, M. 2010, *Astroph. J.*, 725, 1620
- Anders, P., Bissantz, N., Fritze-v. Alvensleben, U., & de Grijs, R. 2004, *MNRAS*, 347, 196
- Barbaro, C., & Bertelli, C. 1977, *A&A*, 54, 243
- Barnby, P., Ashby, M. L. N., Bianchi, L., et al. 2006, *ApJ*, 650, L45
- Bastian, N., & Goodwin, S. P. 2006, *MNRAS*, 369, L9
- Bastian, N., & Strader, J. 2014, *MNRAS*, 443, 3594
- Bastian, N., Adamo, A., Gieles, M., et al. 2011, *MNRAS*, 417, L6
- . 2012, *MNRAS*, 419, 2606
- Beerman, L. C., Johnson, L. C., Fouesneau, M., et al. 2012, *Astroph. J.*, 760, 104
- Bica, E., Claria, J. J., Dottori, H., Santos, Jr., J. F. C., & Piatti, A. E. 1996, *Astroph. J. Suppl.*, 102, 57
- Blitz, L. 1991, in *NATO Advanced Science Institutes (ASI) Series C*, Vol. 342, NATO Advanced Science Institutes (ASI) Series C, ed. C. J. Lada & N. D. Kylafis, 3
- Blitz, L. 1993, in *Protostars and Planets III*, ed. E. H. Levy & J. I. Lunine, 125–161
- Blitz, L., Fukui, Y., Kawamura, A., et al. 2007, *Protostars and Planets V*, 81
- Blitz, L., & Shu, F. H. 1980, *Astroph. J.*, 238, 148
- Bolato, A. D., Wolfire, M., & Leroy, A. K. 2013, *ARA&A*, 51, 207
- Brocato, E., Castellani, V., Raimondo, G., & Romaniello, M. 1999, *A&AS*, 136, 65

- Bruzual, G. 2002, in IAU Symposium, Vol. 207, Extragalactic Star Clusters, ed. D. P. Geisler, E. K. Grebel, & D. Minniti, 616
- Caldwell, N., Harding, P., Morrison, H., et al. 2009, *Astron. J.*, 137, 94
- Calzetti, D., Lee, J. C., Sabbi, E., et al. 2015, *Astron. J.*, 149, 51
- Cardelli, J. A., Clayton, G. C., & Mathis, J. S. 1989, *Astroph. J.*, 345, 245
- Cerviño, M., & Luridiana, V. 2004, *A&A*, 413, 145
- . 2006, *A&A*, 451, 475
- Cerviño, M., & Valls-Gabaud, D. 2003, *MNRAS*, 338, 481
- Chabrier, G. 2003, *PASP*, 115, 763
- Chandar, R., Whitmore, B. C., Calzetti, D., et al. 2011, *Astroph. J.*, 727, 88
- Chiar, J. E., Kutner, M. L., Verter, F., & Leous, J. 1994, *Astroph. J.*, 431, 658
- Chiosi, C., Bertelli, G., & Bressan, A. 1988, *A&A*, 196, 84
- Corbelli, E., Lorenzoni, S., Walterbos, R., Braun, R., & Thilker, D. 2010, *A&A*, 511, A89
- da Silva, R. L., Fumagalli, M., & Krumholz, M. 2012, *Astroph. J.*, 745, 145
- Dalcanton, J. J., Williams, B. F., Lang, D., et al. 2012, *Astroph. J. Suppl.*, 200, 18
- Dame, T. M., Hartmann, D., & Thaddeus, P. 2001, *Astroph. J.*, 547, 792
- Deveikis, V., Narbutis, D., Stonkutė, R., Bridžius, A., & Vansevičius, V. 2008, *Baltic Astronomy*, 17, 351
- Dohm-Palmer, R. C., & Skillman, E. D. 2002, *Astron. J.*, 123, 1433
- Dolphin, A. E. 2000, *PASP*, 112, 1383
- . 2002, *MNRAS*, 332, 91
- Draine, B. T., Dale, D. A., Bendo, G., et al. 2007, *Astroph. J.*, 663, 866

- Elmegreen, B. G. 2000, *Astroph. J.*, 530, 277
- Elson, R. A., & Fall, S. M. 1988, *Astron. J.*, 96, 1383
- Engargiola, G., Plambeck, R. L., Rosolowsky, E., & Blitz, L. 2003, *Astroph. J. Suppl.*, 149, 343
- Evans, II, N. J., Dunham, M. M., Jørgensen, J. K., et al. 2009, *Astroph. J. Suppl.*, 181, 321
- Fall, S. M., & Chandar, R. 2012, *Astroph. J.*, 752, 96
- Ferrière, K. M. 2001, *Reviews of Modern Physics*, 73, 1031
- Fioc, M., & Rocca-Volmerange, B. 1997, *A&A*, 326, 950
- Fouesneau, M., & Lançon, A. 2010, *A&A*, 521, A22
- Fouesneau, M., Lançon, A., Chandar, R., & Whitmore, B. C. 2012, *Astroph. J.*, 750, 60
- Fouesneau, M., Johnson, L. C., Weisz, D. R., et al. 2014, *Astroph. J.*, 786, 117
- Fukui, Y., & Kawamura, A. 2010, *ARA&A*, 48, 547
- Fukui, Y., Mizuno, N., Yamaguchi, R., Mizuno, A., & Onishi, T. 2001, *PASJ*, 53, L41
- Fukui, Y., Mizuno, N., Yamaguchi, R., et al. 1999, *PASJ*, 51, 745
- Gieles, M., Hogg, D. C., & Zhao, H. 2011, *MNRAS*, 413, 2509
- Girardi, L., & Bica, E. 1993, *A&A*, 274, 279
- Girardi, L., Chiosi, C., Bertelli, G., & Bressan, A. 1995, *A&A*, 298, 87
- Girardi, L., Williams, B. F., Gilbert, K. M., et al. 2010, *Astroph. J.*, 724, 1030
- Gordon, K. D., Bailin, J., Engelbracht, C. W., et al. 2006, *ApJ*, 638, L87
- Gratier, P., Braine, J., Rodríguez-Fernández, N. J., et al. 2012, *A&A*, 542, A108
- Hancock, M., Smith, B. J., Giroux, M. L., & Struck, C. 2008, *MNRAS*, 389, 1470

- Hartmann, L., Ballesteros-Paredes, J., & Bergin, E. A. 2001, *Astroph. J.*, 562, 852
- Hirota, A., Kuno, N., Sato, N., et al. 2011, *Astroph. J.*, 737, 40
- Hodge, P. W. 1983, *Astroph. J.*, 264, 470
- Hughes, A., Wong, T., Ott, J., et al. 2010, *MNRAS*, 406, 2065
- Humphreys, R. M., Massey, P., & Freedman, W. L. 1990, *Astron. J.*, 99, 84
- Hunter, D. A., Elmegreen, B. G., Dupuy, T. J., & Mortonson, M. 2003, *Astron. J.*, 126, 1836
- Israel, F. P., Johansson, L. E. B., Lequeux, J., et al. 1993, *A&A*, 276, 25
- Johnson, L. C., Seth, A. C., Dalcanton, J. J., et al. 2012, *Astroph. J.*, 752, 95
- . 2015, *Astroph. J.*, 802, 127
- Kawamura, A., Mizuno, Y., Minamidani, T., et al. 2009, *Astroph. J. Suppl.*, 184, 1
- Kennicutt, R. C., & Evans, N. J. 2012, *ARA&A*, 50, 531
- King, I. 1962, *Astron. J.*, 67, 471
- Kirk, J. M., Gear, W. K., Fritz, J., et al. 2013, *ArXiv e-prints*, arXiv:1306.2913
- Koda, J., Scoville, N., Sawada, T., et al. 2009, *ApJ*, 700, L132
- Kroupa, P. 2001, *MNRAS*, 322, 231
- Lada, C. J., & Lada, E. A. 2003, *ARA&A*, 41, 57
- Lançon, A., Gallagher, III, J. S., Mouhcine, M., et al. 2008, *A&A*, 486, 165
- Lançon, A., & Mouhcine, M. 2000, in *Astronomical Society of the Pacific Conference Series*, Vol. 211, *Massive Stellar Clusters*, ed. A. Lançon & C. M. Boily, 34
- Larsen, S. S. 2009, *A&A*, 494, 539
- Larsen, S. S., de Mink, S. E., Eldridge, J. J., et al. 2011, *A&A*, 532, A147

- Leisawitz, D., Bash, F. N., & Thaddeus, P. 1989, *Astroph. J. Suppl.*, 70, 731
- Leroy, A., Bolatto, A., Stanimirovic, S., et al. 2007, *Astroph. J.*, 658, 1027
- Lewis, A. R., Dolphin, A. E., Dalcanton, J. J., et al. 2015, ArXiv e-prints, arXiv:1504.03338
- Longmore, S. N., Bally, J., Testi, L., et al. 2013, *MNRAS*, 429, 987
- Maddalena, R. J., & Thaddeus, P. 1985, *Astroph. J.*, 294, 231
- Maíz Apellániz, J. 2009, *Astroph. J.*, 699, 1938
- Marigo, P., Girardi, L., Bressan, A., et al. 2008, *A&A*, 482, 883
- Massey, P., Olsen, K. A. G., Hodge, P. W., et al. 2006, *Astron. J.*, 131, 2478
- McConnachie, A. W., Irwin, M. J., Ferguson, A. M. N., et al. 2005, *MNRAS*, 356, 979
- McKee, C. F., & Ostriker, E. C. 2007, *ARA&A*, 45, 565
- McQuinn, K. B. W., Skillman, E. D., Dalcanton, J. J., et al. 2011, *Astroph. J.*, 740, 48
- Meidt, S. E., Hughes, A., Dobbs, C. L., et al. 2015, ArXiv e-prints, arXiv:1504.04528
- Miura, R. E., Kohno, K., Tosaki, T., et al. 2012, *Astroph. J.*, 761, 37
- Mizuno, N., Rubio, M., Mizuno, A., et al. 2001, *PASJ*, 53, L45
- Murray, N. 2011, *Astroph. J.*, 729, 133
- Nieten, C., Neininger, N., Guélin, M., et al. 2006, *A&A*, 453, 459
- Pasquali, A., de Grijs, R., & Gallagher, J. S. 2003, *MNRAS*, 345, 161
- Piatti, A. E., Sarajedini, A., Geisler, D., Clark, D., & Seguel, J. 2007, *MNRAS*, 377, 300
- Piskunov, A. E., Kharchenko, N. V., Schilbach, E., et al. 2009, *A&A*, 507, L5
- . 2011, *A&A*, 525, A122
- Popescu, B., & Hanson, M. M. 2009, *Astron. J.*, 138, 1724

- . 2010a, *Astroph. J.*, 724, 296
- . 2010b, *ApJ*, 713, L21
- Popescu, B., Hanson, M. M., & Elmegreen, B. G. 2012, *Astroph. J.*, 751, 122
- Raimondo, G., Brocato, E., Cantiello, M., & Capaccioli, M. 2005, *Astron. J.*, 130, 2625
- Rosolowsky, E. 2005, *PASP*, 117, 1403
- . 2007, *Astroph. J.*, 654, 240
- Rosolowsky, E., & Leroy, A. 2006, *PASP*, 118, 590
- Salpeter, E. E. 1955, *Astroph. J.*, 121, 161
- San Roman, I., Sarajedini, A., & Aparicio, A. 2010, *Astroph. J.*, 720, 1674
- Sanders, N. E., Caldwell, N., McDowell, J., & Harding, P. 2012, *Astroph. J.*, 758, 133
- Santos, Jr., J. F. C., & Frogel, J. A. 1997, *Astroph. J.*, 479, 764
- Silva-Villa, E., Adamo, A., & Bastian, N. 2013, *MNRAS*, 436, L69
- Soderblom, D. R. 2010, *ARA&A*, 48, 581
- Tabatabaei, F. S., & Berkhuijsen, E. M. 2010, *A&A*, 517, A77
- Tan, J. C., Krumholz, M. R., & McKee, C. F. 2006, *ApJ*, 641, L121
- Tassis, K., & Mouschovias, T. C. 2004, *Astroph. J.*, 616, 283
- Weidner, C., & Kroupa, P. 2004, *MNRAS*, 348, 187
- . 2006, *MNRAS*, 365, 1333
- Whitmore, B. C., Chandar, R., Schweizer, F., et al. 2010, *Astron. J.*, 140, 75
- Williams, B. F., Lang, D., Dalcanton, J. J., et al. 2014, *Astroph. J. Suppl.*, 215, 9
- Williams, J. P., & McKee, C. F. 1997, *Astroph. J.*, 476, 166

Wong, T., Hughes, A., Ott, J., et al. 2011, *Astroph. J. Suppl.*, 197, 16

Yamaguchi, R., Mizuno, N., Mizuno, A., et al. 2001, *PASJ*, 53, 985

Zasov, A., & Kasparova, A. 2014, *Ap&SS*, arXiv:1407.3356

Zhang, Q., & Fall, S. M. 1999, *ApJ*, 527, L81

Zurita, A., & Bresolin, F. 2012, *MNRAS*, 427, 1463

VITA

Lori is originally from Cincinnati, Ohio. Her Bachelors degree is actually not in Physics or Astronomy, but in Finance and Marketing. After working for a year in Finance, she decided to go back to school at the University of Cincinnati to study Astrophysics. While at UC she had the opportunity to do a summer program at the University of Hawaii and observe with telescopes on Mauna Kea. In the summer of 2009 Lori started graduate school at UW. While in graduate school, she worked on the PHAT survey with advisor Julianne Dalcanton and studied star clusters and their relation to molecular clouds in the Andromeda Galaxy. One of the highlights of grad school was spending a month studying at the Vatican Observatory in Rome. Lori has grown to love the Pacific Northwest, and has decided to stay in Seattle after graduation and put her skills to use in industry.